frontiers | Research Topics

Prevention and treatment of infectious diseases by herbal medicine

Edited by
Quansheng Feng, Qingquan Liu and Marcello Iriti

Published in
Frontiers in Pharmacology



FRONTIERS EBOOK COPYRIGHT STATEMENT

The copyright in the text of individual articles in this ebook is the property of their respective authors or their respective institutions or funders. The copyright in graphics and images within each article may be subject to copyright of other parties. In both cases this is subject to a license granted to Frontiers.

The compilation of articles constituting this ebook is the property of Frontiers.

Each article within this ebook, and the ebook itself, are published under the most recent version of the Creative Commons CC-BY licence. The version current at the date of publication of this ebook is CC-BY 4.0. If the CC-BY licence is updated, the licence granted by Frontiers is automatically updated to the new version.

When exercising any right under the CC-BY licence, Frontiers must be attributed as the original publisher of the article or ebook, as applicable.

Authors have the responsibility of ensuring that any graphics or other materials which are the property of others may be included in the CC-BY licence, but this should be checked before relying on the CC-BY licence to reproduce those materials. Any copyright notices relating to those materials must be complied with.

Copyright and source acknowledgement notices may not be removed and must be displayed in any copy, derivative work or partial copy which includes the elements in question.

All copyright, and all rights therein, are protected by national and international copyright laws. The above represents a summary only. For further information please read Frontiers' Conditions for Website Use and Copyright Statement, and the applicable CC-BY licence.

ISSN 1664-8714
ISBN 978-2-8325-7342-6
DOI 10.3389/978-2-8325-7342-6

Generative AI statement
Any alternative text (Alt text) provided alongside figures in the articles in this ebook has been generated by Frontiers with the support of artificial intelligence and reasonable efforts have been made to ensure accuracy, including review by the authors wherever possible. If you identify any issues, please contact us.

About Frontiers

Frontiers is more than just an open access publisher of scholarly articles: it is a pioneering approach to the world of academia, radically improving the way scholarly research is managed. The grand vision of Frontiers is a world where all people have an equal opportunity to seek, share and generate knowledge. Frontiers provides immediate and permanent online open access to all its publications, but this alone is not enough to realize our grand goals.

Frontiers journal series

The Frontiers journal series is a multi-tier and interdisciplinary set of open-access, online journals, promising a paradigm shift from the current review, selection and dissemination processes in academic publishing. All Frontiers journals are driven by researchers for researchers; therefore, they constitute a service to the scholarly community. At the same time, the *Frontiers journal series* operates on a revolutionary invention, the tiered publishing system, initially addressing specific communities of scholars, and gradually climbing up to broader public understanding, thus serving the interests of the lay society, too.

Dedication to quality

Each Frontiers article is a landmark of the highest quality, thanks to genuinely collaborative interactions between authors and review editors, who include some of the world's best academicians. Research must be certified by peers before entering a stream of knowledge that may eventually reach the public - and shape society; therefore, Frontiers only applies the most rigorous and unbiased reviews. Frontiers revolutionizes research publishing by freely delivering the most outstanding research, evaluated with no bias from both the academic and social point of view. By applying the most advanced information technologies, Frontiers is catapulting scholarly publishing into a new generation.

What are Frontiers Research Topics?

Frontiers Research Topics are very popular trademarks of the *Frontiers journals series*: they are collections of at least ten articles, all centered on a particular subject. With their unique mix of varied contributions from Original Research to Review Articles, Frontiers Research Topics unify the most influential researchers, the latest key findings and historical advances in a hot research area.

Find out more on how to host your own Frontiers Research Topic or contribute to one as an author by contacting the Frontiers editorial office: frontiersin.org/about/contact

Prevention and treatment of infectious diseases by herbal medicine

Topic editors

Quansheng Feng — Chengdu University of Traditional Chinese Medicine, China

Qingquan Liu — Capital Medical University, China

Marcello Iriti — University of Milan, Italy

Citation

Feng, Q., Liu, Q., Iriti, M., eds. (2026). *Prevention and treatment of infectious diseases by herbal medicine*. Lausanne: Frontiers Media SA.

doi: 10.3389/978-2-8325-7342-6

Table of contents

05 Yinqin Qingfei granules alleviate *Mycoplasma pneumoniae* pneumonia via inhibiting NLRP3 inflammasome-mediated macrophage pyroptosis
Zhe Song, Chengen Han, Guangzhi Luo, Guangyuan Jia, Xiao Wang and Baoqing Zhang

27 Medicinal plants diversity among the oromo community in heban-arsi district of Ethiopia used to manage human and livestock ailments
Geritu Nuro, Ketema Tolossa, Mahlet Arage and Mirutse Giday

40 Fei-Yan-Qing-Hua decoction attenuates influenza virus infection by enhancing host antiviral response through microbiota-derived acetate
Biao Dou, Xiao Wu, Yurong He, Guihua Xu, Huan Zhang, Qilin Huang, Xuan Chen, Naifan Duan, Linqiong Zhou, Wei Zhang, Huazhang An and Yuejuan Zheng

59 Efficacy and safety of Shenmai injection in the treatment of viral myocarditis: a systematic review and meta-analysis
Qianhe Yang, Jie Qin, Ziyue Li, Yue He and Yabin Zhou

76 Unveiling the therapeutic role of Dachaihu decoction in acute cholecystitis: a comprehensive systematic review and meta-analysis of its efficacy and safety
Xin-xin Liu, Ying-qi Ma, Ling-yao Kong, You-zhu Su, Nicola Robinson and Jian-ping Liu

99 Combination of *Vitex pseudo-negundo* methanolic-extract with cisplatin can induce antioxidant activity and apoptosis in HeLa and Caski cells
Parisa Shiri Aghbash, Javid Sadri Nahand, Omid Rahbar Farzam, Seyed Mohammad Reza Hosseini, Mobina Bayat, Taher Entezari Maleki and Hossein Bannazadeh Baghi

116 *Panzerina lanata* accelerates methicillin-resistant *Staphylococcus aureus* eradication by promoting migration and activation of neutrophils
Shuai Dong, Xingyuan Bai, Bin Chen, Minzhe Fan, Qi Liu, Yubo Zhao, Linsen Li and Dan Zhu

132 Hexane extract from *Lindera communis* roots: wound healing properties and membrane-disruptive activities against methicillin-resistant *Staphylococcus aureus*
Miaomiao Wang, Xian Hu, Liya Liu, Yi Zhong, Wanlin Li, Qing Zhang, Congli Xu and Chunlin Long

144 Potential activity of *Ferula macrecolea* essential oil for treating *Giardia lamblia* infection through modulating electrolytes and suppressing NF-κB p65 pathway
Iraj Salimikia, Seyed Ehsan Yaghoubi, Amal Khudair Khalaf, Leila Masoori, Javad Ghasemian Yadegari and Hossein Mahmoudvand

153 Exploring the antimicrobial, anti-inflammatory, antioxidant, and immunomodulatory properties of *Chrysanthemum morifolium* and *Chrysanthemum indicum*: a narrow review
Yuqing Liang, Tengwen Liu, Dong Wang and Qingquan Liu

174 Steamed panax notoginseng mitigates CA-MRSA USA300-induced necroptosis in human neutrophils
Lulu Zhang, Xiaoyu Feng, Hongsa An, Weifeng Yang, Yuwen Xia, Bo Wen, Haoran Zheng, Yihuan Chen, Yungchi Cheng, Chunyan Jiang, Cheng Lu and Yong Tan

187 Exploring the pathogenesis of acute lung injury and its treatment through Traditional Chinese Medicine: a state-of-the-art review
Jiayun Wang, Zhiqiang Yan, Xinxin Zhang, Shun Wang, Liangbo Jiao, Binghua Zhu, Bo Tan and Aidong Yang

208 Ethnobotanical survey of herbal medicines for anti-COVID-19 used by traditional Chinese medicine pharmacies in Taiwan
Min-Han Chi, Chien-Yu Ko, Ting-Wei Chi, Chi-Ruei Huang, Jaung-Geng Lin, Jung Chao and Shyh-Shyun Huang

226 Oral commercial Chinese polyherbal preparations combined with conventional biomedicine for pulmonary tuberculosis: network meta-analysis
Jiankang Jiang, Siqi Zhang, Hui Wang, Lu Zhang, Zegeng Li, Jiabing Tong and Fan Wu

frontiers | Frontiers in Pharmacology

TYPE Original Research
PUBLISHED 27 August 2024
DOI 10.3389/fphar.2024.1437475

Check for updates

OPEN ACCESS

EDITED BY
Qingquan Liu,
Beijing Hospital of Traditional Chinese Medicine, Capital Medical University, China

REVIEWED BY
Xiaolong Xu,
Capital Medical University, China
Shanshan Guo,
China Academy of Chinese Medical Sciences, China
Jingxia Zhao,
Capital Medical University, China

*CORRESPONDENCE
Xiao Wang,
2017101069@sdutcm.edu.cn
Baoqing Zhang,
71000923@sdutcm.edu.cn

†These authors have contributed equally to this work

RECEIVED 23 May 2024
ACCEPTED 15 August 2024
PUBLISHED 27 August 2024

CITATION
Song Z, Han C, Luo G, Jia G, Wang X and Zhang B (2024) Yinqin Qingfei granules alleviate *Mycoplasma pneumoniae* pneumonia via inhibiting NLRP3 inflammasome-mediated macrophage pyroptosis.
Front. Pharmacol. 15:1437475.
doi: 10.3389/fphar.2024.1437475

COPYRIGHT
© 2024 Song, Han, Luo, Jia, Wang and Zhang. This is an open-access article distributed under the terms of the Creative Commons Attribution License (CC BY). The use, distribution or reproduction in other forums is permitted, provided the original author(s) and the copyright owner(s) are credited and that the original publication in this journal is cited, in accordance with accepted academic practice. No use, distribution or reproduction is permitted which does not comply with these terms.

Yinqin Qingfei granules alleviate *Mycoplasma pneumoniae* pneumonia via inhibiting NLRP3 inflammasome-mediated macrophage pyroptosis

Zhe Song[1†], Chengen Han[1†], Guangzhi Luo[2], Guangyuan Jia[1], Xiao Wang[1*] and Baoqing Zhang[1*]

[1]Department of Pediatrics, Affiliated Hospital of Shandong University of Traditional Chinese Medicine, Jinan, China, [2]College of Traditional Chinese Medicine, Shandong University of Traditional Chinese Medicine, Jinan, China

Background: *Mycoplasma pneumoniae* pneumonia (MPP) is a prevalent respiratory infectious disease in children. Given the increasing resistance of *M. pneumoniae* (MP) to macrolide antibiotics, the identification of new therapeutic agents is critical. Yinqin Qingfei granules (YQQFG), a Chinese patent medicine formulated specifically for pediatric MPP, lacks a clear explanation of its mechanism.

Methods: The primary components of YQQFG were identified using LC-MS/MS. *In vitro*, RAW264.7 cells infected with MP underwent morphological examination via scanning electron microscopy. Drug-containing serum was prepared, and its intervention concentration was determined using the CCK-8 assay. The active components of YQQFG were molecularly docked with NLRP3 protein using Autodock Vina software. A RAW264.7 cell line overexpressing NLRP3 was created using lentivirus to pinpoint the target of YQQFG. *In vivo*, MPP model mice were established via nasal instillation of MP. Lung damage was assessed by lung index and H&E staining. Pyroptosis-associated protein levels in cells and lung tissue were measured by western blot, while interleukin (IL)-1β and IL-18 levels in cell supernatants and mouse serum were quantified using ELISA. Immunofluorescence double staining of lung tissue sections was conducted to assess the correlation between NLRP3 protein expression and macrophages. The expression of the community-acquired respiratory distress syndrome toxin (CARDS TX) was evaluated by qPCR.

Results: 25 effective components with favorable oral bioavailability were identified in YQQFG. Both *in vitro* and *in vivo* studies demonstrated that YQQFG substantially reduced the expression of the NLRP3/Caspase-1/GSDMD pathway, decreasing the release of IL-1β and IL-18, and inhibited MP exotoxin. Molecular docking indicated strong affinity between most YQQFG components and NLRP3 protein. Lentivirus transfection and immunofluorescence double staining confirmed that YQQFG significantly suppressed NLRP3 expression in macrophages, outperforming azithromycin (AZM). The combination of YQQFG and AZM yielded the optimal therapeutic effect for MPP.

Conclusion: YQQFG mitigates inflammatory responses by suppressing NLRP3 inflammasome-mediated macrophage pyroptosis, thereby ameliorating MP-induced acute lung injury. YQQFG serves as an effective adjunct and alternative medication for pediatric MPP treatment.

KEYWORDS

Yinqin Qingfei granules, *Mycoplasma pneumoniae* pneumonia, macrophage, pyroptosis, NLRP3 inflammasome

1 Introduction

Mycoplasma pneumoniae (MP) is the smallest prokaryote capable of independent survival (Kumar and Kumar, 2023). It spreads through respiratory droplets, leading to periodic outbreaks every 3–7 years. Children are predominantly susceptible (Jacobs et al., 2015). During epidemic years, *M. pneumoniae* pneumonia (MPP) accounts for over 40% of pediatric community-acquired pneumonia (CAP) cases (Kumar, 2018). Currently, macrolide antibiotics, notably azithromycin (AZM), are the first-line treatment for MPP in children (Tsai et al., 2021). However, the extensive use of these antibiotics has led to escalating rates of MP resistance (Kim et al., 2022). Developing new therapeutic agents for MPP is thus critically urgent.

An excessive immune inflammatory response triggered by MP is identified as the primary pathological mechanism of MPP (Deng et al., 2023). Macrophages, the most abundant immune cells in the lungs, are the first to respond to pathogens with phagocytic and pro-inflammatory actions (Byrne et al., 2015). Recent research indicates that MP's membrane lipoprotein components can activate the NLRP3 inflammasome via the TLRs/NF-κB signaling pathway (Luo et al., 2021). Furthermore, the community-acquired respiratory distress syndrome toxin (CARDS TX) produced by MP possesses ADP-ribosyltransferase (ADPRT) activity, enabling it to catalyze inflammasome assembly directly via NLRP3 protein (Bose et al., 2014). Activation of the NLRP3 inflammasome leads to the conversion of interleukin (IL)-1β and IL-18 precursors into mature forms and the cleavage of the pyroptosis execution protein gasdermin D (GSDMD), which generates N-terminal active fragments (GSDMD-NT) to perforate the cell membrane, resulting in cell death (Yin et al., 2023). The process of pyroptosis not only exacerbates the inflammatory response (Fan and Fan, 2018); it also causes pathogen antigens previously engulfed by macrophages to be released extracellularly, perpetuating infection (Ding et al., 2021). Thus, targeting NLRP3 inflammasome-mediated macrophage pyroptosis offers a promising strategy to mitigate the inflammatory damage associated with MPP.

The use of traditional Chinese medicine (TCM) in treating respiratory tract infections boasts a long-standing history and distinct advantages. Chinese herbal compounds effectively combat pathogens, enhance symptom relief, suppress inflammatory response, and modulate immune function through the strategic combination of various herbs. When used alongside antibiotics, these compounds often yield a synergistic effect (Li et al., 2017; Sun et al., 2020). The primary clinical symptoms of MP infection include fever and cough, often characterized by a prolonged course and the potential to affect multiple organs (Narita, 2010; Wang et al., 2016). This aligns with the TCM concept of "damp-heat evil", traditionally linked to prolonged inflammatory states marked by intense consumption of body fluids, leading to phlegm and blood stasis accumulation. In TCM theory, dampness, heat, phlegm, and blood stasis are identified as the principal pathological factors in pediatric MPP, with treatments aimed at eliminating dampness and heat, resolving phlegm, and dispelling blood stasis. Yinqin Qingfei granules (YQQFG) are specifically formulated for treating MPP in children, based on these principles. The formulation comprises nine kinds of medicinal materials and has demonstrated effective clinical results. Currently, YQQFG is endorsed as a proprietary blend by the Affiliated Hospital of Shandong University of Traditional Chinese Medicine. However, the mechanism by which YQQFG treats MPP remains to be fully understood. Considering the significant role of NLRP3 inflammasome-mediated macrophage pyroptosis in MP-induced acute lung injury, we postulated that YQQFG possesses the potential to alleviate MPP by inhibiting the activation of the NLRP3 inflammasome and macrophage pyroptosis, and verified this by constructing cellular and murine experimental models in this research.

2 Materials and methods

2.1 Preparation and component identification of YQQFG

The nine herbs were sourced from the Affiliated Hospital of Shandong University of Traditional Chinese Medicine and verified as authentic by the Pharmacology Laboratory of Traditional Chinese Medicine at Shandong University of Traditional Chinese Medicine. They conformed to the standards outlined in the 2020 edition of the "Pharmacopoeia of the People's Republic of China". These herbs were mixed according to the proportions listed in Table 1, subjected to two boiling cycles of 30 min each, and the resulting decoctions were filtered and merged. The mixture was then concentrated under reduced pressure, followed by the addition of dextrin. From each Gram of the original compound preparation, 0.24 g was extracted. The extraction rate of YQQFG was 24%.

Adding methanol containing 4 ppm of 2-Amino-3-(2-chloro-phenyl)-propionic acid, we prepared samples from six different production batches of YQQFG. Then, we subjected them to vortexing, grinding, ultrasonication, and centrifugation in sequence, and collected the supernatants for testing. LC analysis was carried out with the use of an ACQUITY UPLC® HSS T3 column (2.1 × 100 mm, 1.8 μm) and a Thermo Vanquish UPLC system. We used acetonitrile and ammonium formate (5 mM) for gradient elution in the negative ion mode, and for the positive ion mode, we used 0.1% formic acid in

TABLE 1 Herbal formula of YQQFG.

Chinese name	Latin name	Medicinal part	Weight (g)
Yinchen	*Artemisia scoparia Waldst. et Kit*	dry overground parts	15
Huangqin	*Scutellaria sieversii Bge*	dry roots	9
Huzhang	*Polygonum cuspidatum Sieb. et Zucc*	dry roots and rhizomes	12
Guanghuoxiang	*Pogostemon cablin (Blanco) Benth*	dry overground parts	9
Shichangpu	*Acorus tatarinowii Schott*	dry rhizomes	9
Zhebeimu	*Fritillaria thunbergii Miq*	dry bulbs	9
Houpo	*Magnolia officinalis Rehd. et wils*	dry barks, root barks, and branch barks	9
Taoren	*Prunus davidiana (Carr.) Franch*	dry mature seeds	9
Gancao	*Glycyrrhiza aspera Pall*	dry roots	6

acetonitrile (v/v) and 0.1% formic acid in water (v/v). Thermo Q Exactive mass spectrometers equipped with electrospray ionization were used for MS detection. Concurrent acquisition of MS1 and MS/MS data was carried out in both ion modes. Supplementary Data Sheet S1 details the elution procedure and experimental parameters.

The R XCMS software package was used for feature detection, retention time (RT) correction and alignment. The MS identification of substances was achieved by public spectral databases including HMDB (http://www.hmdb.ca), massbank (http://www.massbank.jp/), LipidMaps (http://www.lipidmaps.org), mzclound (https://www.mzcloud.org), and KEGG (https://www.genome.jp/kegg/). At the same time, the MS/MS data were matched with the fragment ions in the database to achieved the MS/MS identification of the substances. Finally, the TCMSP database (https://old.tcmsp-e.com/tcmsp.php) was employed to screen the identified substances, yielding the active components of YQQFG.

2.2 Preparation of drug-containing serum

Forty female 7-week-old Wistar rats, weighing 180–200 g, were acquired from Beijing Weitonglihua Laboratory Animal Co., Ltd. (Beijing, China) and housed in the SPF animal facility at the Experimental Center of Shandong University of Traditional Chinese Medicine. Following a week of acclimatization, the rats were randomly assigned to four groups: drug-free serum, YQQFG serum, AZM serum, and YQQFG + AZM serum, with 10 rats per group. The average weight of rat's post-acclimatization was 210 g. The dosage of rats was converted according to the dosage of 6-year-old children (standard weight 20 kg). According to product guidelines, the daily oral dosage of YQQFG for 6-year-old children is 12 g, equivalent to 600 mg/kg. Consequently, the dosage for rats was calculated as 6.3 × 600 mg/kg × 0.21 kg ≈ 794 mg. Similarly, the children's oral dosage of AZM (Pfizer Inc., specification: 100mg/bag, approval number: Z20220088000) is 10 mg/kg, leading to a rat dosage of 6.3 × 10 mg/kg × 0.21 kg ≈ 13.2 mg. The administration regimen was as follows: the YQQFG serum group received 2 mL of YQQFG solution (397 mg/mL) intragastrically daily; the AZM serum group received 2 mL of AZM solution (6.6 mg/mL) daily; the YQQFG + AZM serum group was administered YQQFG by gavage daily, followed by AZM 6 h later; the drug-free serum group received 2 mL of distilled water daily for 7 days. Blood was collected from the abdominal aorta of rats sedated with pentobarbital sodium 2 h after the final gavage. The serum underwent separation, inactivation at 56°C for 30 min, filtration, sterile packaging, and storage at −80°C. The above operations have been approved by the Animal Ethics Committee of Shandong University of Traditional Chinese Medicine (approval number: SDUTCM20220524001).

2.3 MP culture and concentration determination

The MP standard strain (ATCC-15531) was sourced from the American Type Culture Collection (Manassas, Virginia, United States). Firstly, MP medium was prepared. In short, 2.04 g *Mycoplasma* broth base (Oxoid, CM1166) was dissolved in 79 mL ultrapure water, and 2 mL 50% glucose injection (Hubei Kelun Pharmaceutical Co., Ltd., approval number: H42021188) and 1 mL 0.5% phenol red sterile solution (Solarbio, G1230) were added. After autoclaving, 50 g of *Mycoplasma* supplement G (Oxoid, SR0059C) was incorporated, thoroughly mixed, and stored at 4°C for future use. The MP strain was revived in the prepared medium and cultured in an incubator at 37°C with 50% humidity. The medium was monitored until the color transitioned from red to yellow, indicating a need for subculturing at a ratio of 1:10.

Due to the minuscule size of MP, conventional turbidimetric methods are unsuitable for quantification. Thus, color change units (CCU) were employed to estimate MP concentration (Calus et al., 2010). The procedure involved labeling dilutions: 10^1, 10^2, . . . 10^{12} on a 96-well plate, adding 180 μL of MP medium to each well. 20 μL of MP bacterial solution was added to the 10^1 well, followed by serial transfer of 20 μL from 10^1 to 10^2 well after thorough mixing, and so forth, achieving gradient dilution. To prevent evaporation, two to three drops of glycerol (Solarbio, G8190) were added to each well. After continuous observation for 1 month, the color change of the medium was recorded. The concentration of MP was calculated according to 1×10^x CCU/200 μL, which is, 5×10^x CCU/mL. Here, "x" represents the maximum dilution factor at which the color change occurs (Calus et al., 2010). The MP concentration established in this study was 5×10^8 CCU/mL (Supplementary Data Sheet S2).

2.4 Cell culture

Mouse monocyte-macrophage leukemia cells (RAW264.7) were procured from the Cell Resource Center of Peking Union Medical College. The cells were cultured in DMEM High Glucose Medium (BasalMedia, L110KJ) containing 10% fetal bovine serum (FBS) (Gibco, A3161002C) and 1% penicillin-streptomycin solution (BasalMedia, S110JV). Upon reaching 90% confluency, the cells were subcultured at a ratio of 1:3.

2.5 Screening for the optimal intervention time of MP

The MP bacterial solution was sub-packed into 2 mL EP tubes, centrifuged at 12,000 rpm for 20 min, and the supernatant was discarded. In each EP tube, 1 mL of cell complete medium was added to resuspend the precipitated bacteria. The cells, in their logarithmic growth phase, were seeded into 6-well plates with a cell density of 5×10^5 cells/mL and a volume of 2 mL. The plates were then incubated in a CO_2 incubator. The following day, cells were randomly assigned to either a control group or one that underwent MP infection at 2/4/6/12/24-h intervals. For all groups except the control, the medium was replaced with cell culture medium containing MP. Supernatants collected at various intervals post-MP infection were analyzed for IL-1β and tumor necrosis factor-α (TNF-α) levels using ELISA kits (Elabscience, E-EL-M0037 for IL-1β and E-EL-M3063 for TNF-α).

2.6 Scanning electron microscope (SEM) observation

Cells were cultured in 24-well plates (cell density: 5×10^5 cells/mL, volume: 0.5 mL). Following 12 h of MP infection, the medium was removed. Each well was then treated with 0.5 mL of electron microscope fixative (Servicebio, G1102) and placed at 4°C for 12 h. The samples underwent fixation, dehydration, drying, and conductive treatment sequentially. SEM was used to observe the morphological alterations in cells post-MP treatment.

2.7 Screening the intervention concentration of drug-containing serum by CCK-8 method

Cells in logarithmic growth phase were seeded into 96-well plates (cell density: 2×10^5 cells/mL, volume: 100 μL) and cultured in a CO_2 incubator. The following day, various concentrations of rat serum were added to the FBS-free cell culture medium. The cells were organized into 18 groups: drug-free serum group (2.5%, 5%, 10%, 20%), YQQFG serum group (2.5%, 5%, 10%, 20%), AZM serum group (2.5%, 5%, 10%, 20%), YQQFG + AZM serum group (2.5%, 5%, 10%, 20%), a positive control group (cells + medium, without rat serum), and a negative control group (medium only). After 12 h of intervention with rat serum, the medium was discarded and 100 μL of CCK-8 solution (Elabscience, E-CK-A362) was introduced to every well. Following this, the 96-well plates were dark-incubated for another 2 h. A microplate reader was used to measure the optical density (OD) of each well at a wavelength of 450 nm. Cell viability $= \frac{\text{dosing group OD} - \text{negative control group OD}}{\text{positive control group OD} - \text{negative control group OD}}$.

2.8 Cell grouping and treatment

Cells were plated in 10 × 10 mm culture dishes (cell density: 2×10^5 cells/mL, volume: 10 mL). On the subsequent day, the cells were divided into five groups: Control group (cell culture medium containing drug-free serum), Model group (MP + cell culture medium containing drug-free serum), YQQFG group (MP + cell culture medium containing YQQFG serum), AZM group (MP + cell culture medium containing AZM serum), and YQQFG + AZM group (MP + cell culture medium containing combined serum). The concentration of drug-containing serum in the cell culture medium was determined based on the results from the CCK-8 assay. Following the intervention, cells and cell supernatants from each group were collected.

2.9 Molecular docking analysis

Given that NLRP3 protein activation is pivotal in inflammasome assembly and central to the process of pyroptosis (Fu and Wu, 2023), molecular docking was employed to predict the binding ability of YQQFG's main active components with NLRP3 protein. These chemicals' molecular structures were obtained from the PubChem database (https://pubchem.ncbi.nlm.nih.gov/). The three-dimensional crystal structure of NLRP3 protein (PDB ID: 8WSM) was obtained from the Protein Data Bank database (https://www.rcsb.org/). Autodock Vina software was used to perform the docking calculations, and Discovery Studio software was used for visualization.

2.10 Cell transfection

In this study, the synthesis of the *NLRP3* gene, construction of the plasmid vector and packaging of the lentivirus were entrusted to Hanbio Biotechnology Co., Ltd. (Shanghai, China). The second generation of RAW264.7 cells were seeded into 6-well plates and divided into the NLRP3 overexpression ($NLRP3^{-OE}$) group and the empty vector lentivirus (LV^{-Con}) group. Upon reaching 60% cell density, the culture medium was supplemented with the virus solution at an MOI of 20 for transfection. After 72 h of transfection, puromycin (30 μg/mL) (MCE, HY-K1057) was applied to select successfully transfected cells. Transfection efficiency was assessed using quantitative real-time PCR (qPCR).

2.11 Animal modeling and administration

Sixty male 5-week-old BALB/c mice, weighing 12–14 g, were acquired from Beijing Weitonglihua Laboratory Animal Co., Ltd., and housed in the biosafety level-2 (BSL-2) animal room. Mice were randomly allocated into five groups: Control, Model, YQQFG, AZM, and YQQFG + AZM, with each group further subdivided

into two subgroups based on gavage duration: 3 and 7 days. Following a week of acclimatization, the mice were anesthetized with isoflurane (RWD Life Science Co., Ltd., R510-22-10). The Control group received 100 μL of normal saline intranasally, while the other groups were administered 100 μL of MP bacterial solution (5×10^8 CCU/mL) nasally for three consecutive days. Subsequent gavage of the designated drugs commenced the following day. Dosages for the mice were adapted from those for 6-year-old children (standard weight 20 kg), using a mouse-to-human dose conversion factor of 9.01 (Dou et al., 2024). The calculated doses were 86 mg/d for YQQFG and 1.4 mg/d for AZM for mice averaging 16 g in weight. The gavage regimen was structured as follows: (1) the Control and Model groups received 0.2 mL of distilled water for either 3 or 7 days; (2) the YQQFG group was administered 0.2 mL of YQQFG solution (430 mg/mL) for either 3 or 7 days; (3) the AZM group received 0.2 mL of AZM solution (7 mg/mL) for 3 days, followed by 0.2 mL of distilled water daily for the remaining 4 days; (4) the YQQFG + AZM-3d group received 0.2 mL of YQQFG solution administered via gavage, followed 6 h later by 0.2 mL of AZM solution for 3 days. In the YQQFG + AZM-7d group, for the first 3 days, the mice received the same treatment as the YQQFG + AZM-3d group. However, for the remaining 4 days, the mice were administered 0.2 mL of YQQFG solution daily, followed by 0.2 mL of distilled water 6 h later. The next day after the end of administration, the mice were anesthetized with isoflurane, and blood was collected from the orbital venous plexus. Serum was then separated and stored at −80°C. The left lung was preserved in tissue fixative, and the right lung was cryopreserved. These procedures received approval from the Animal Ethics Committee of Shandong University of Traditional Chinese Medicine (approval number: SDUTCM20220516002).

2.12 Calculate the lung index in mice

The body weight of the mice was recorded daily. During dissection, the lung tissue was rinsed with normal saline and then weighed after blotting with filter paper. Lung index = lung weight (mg)/body weight (g).

2.13 Histological evaluation

Following a 24-h fixation in tissue fixative, the lung tissue was dehydrated and embedded in paraffin. H&E staining was performed on Sections 5 μm thick. An upright microscope was used to examine the pathological conditions of lung tissue in each group.

2.14 qPCR detection

Total RNA was extracted from cells and lung tissues using the SPARKeasy Improved Tissue/Cell RNA Kit (SparkJade, AC0202) and quantified with an ultra-micro spectrophotometer. RNA was reverse transcribed to cDNA using the SPARKscript II RT Plus Kit (With gDNA Eraser) (SparkJade, AG0304). The qPCR reactions were set up according to the manufacturer's instructions using 2 × SYBR Green qPCR Mix (SparkJade, AH0104) and performed on a Roche LightCycler 480 II instrument. The qPCR primers were synthesized by Sangon Biotech Co., Ltd. (Shanghai, China) (Table 2). The relative expression of target genes was calculated by the $2^{-\Delta\Delta Ct}$ method with GAPDH serving as the internal reference gene.

TABLE 2 Primers for qPCR.

Genes	Primers (5′→3′)
CARDS TX	F: CATGATTGCCAACACCAGGAATAGC
	R: AAACGATAGCGAAGCGGAAGTACC
NLRP3	F: GCTGCGATCAACAGGCGAGAC
	R: CCATCCACTCTTCTTCAAGGCTGTC
GAPDH	F: GGTTGTCTCCTGCGACTTCA
	R: TGGTCCAGGGTTTCTTACTCC

2.15 Western blot (WB)

Total protein was extracted from cells and lung tissues using RIPA lysis buffer (Beyotime, P0013B), and protein concentration was determined using a BCA Protein Assay Kit (Beyotime, P0010). Proteins were separated by SDS-PAGE gel electrophoresis and transferred to a PVDF membrane. The membrane was incubated overnight at 4°C with primary antibodies including NLRP3 (abcam, ab270449), ASC (Cohesion, CPA7120), proCaspase-1 (abcam, ab179515), cleaved Caspase-1 (Proteintech, 22915-1-AP), GSDMD (abcam, ab219800), GSDMD-NT (ABclonal, A22523), and GAPDH (Proteintech, HRP-60004). The following day, the membrane was incubated with secondary antibodies at room temperature for 1 h. Detection was performed using ECL chemiluminescence substrate (Millipore, WBULS0100). Band intensities were analyzed using ImageJ software. The relative expression of the target proteins was calculated with GAPDH as the internal reference.

2.16 Immunofluorescence detection

Immunofluorescence double staining was performed on lung tissue sections from mice in the 3-day gavage group using the tyramide signal amplification (TSA) method. Paraffin sections underwent sequential dewaxing, hydration, antigen retrieval, and blocking. Sections were first incubated with NLRP3 primary antibody (Servicebio, GB114320) followed by the appropriate fluorescent secondary antibody. Then the TSA staining solution was added dropwise for signal amplification. After a second antigen retrieval, sections were treated with F4/80 primary antibody (Proteintech, 28463-1-AP) and corresponding fluorescent secondary antibody. Nuclei were stained with DAPI (Servicebio, G1012). A fluorescence microscope was used for imaging. The fluorescence intensity of NLRP3 and F4/80, along with their Pearson's correlation coefficient (PCC), were quantified using ImageJ software.

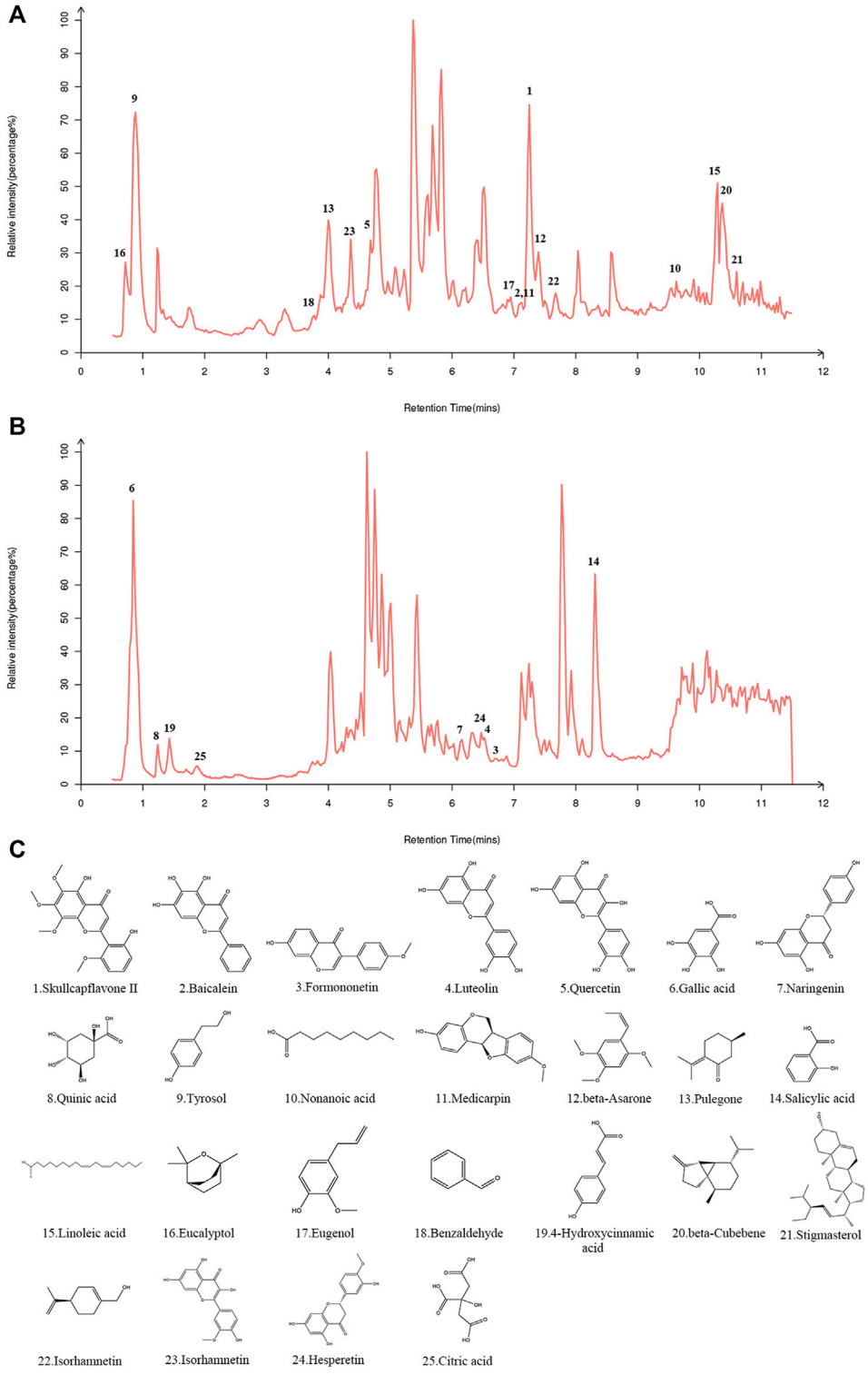


FIGURE 1
Identification of components in YQQFG. **(A)** Representative TIC in positive ion mode. **(B)** Representative TIC in negative ion mode. **(C)** Molecular structure of components in YQQFG. The molecular structures of the compounds were downloaded from the PubChem database (https://pubchem.ncbi.nlm.nih.gov/) and drawn using the Chem3D software.

TABLE 3 25 components with favorable oral bioavailability in YQQFG.

No.	Components	RT (min)	m/z	Error (ppm)	Precursor type	OB (%)	Source
1	Skullcapflavone II	7.27	375.107	1.5356	[M + H]+	69.51	*Scutellaria sieversii Bge*
2	Baicalein	7.15	271.059	3.9696	[M + H]+	33.52	*Scutellaria sieversii Bge*
3	Formononetin	6.72	267.067	0.3181	[M-H]-	69.67	*Glycyrrhiza aspera Pall*
4	Luteolin	6.53	285.04	2.5400	[M-H]-	36.16	*Polygonum cuspidatum Sieb. et Zucc.; Scutellaria sieversii Bge.; Prunus davidiana (Carr.) Franch*
5	Quercetin	4.59	303.049	3.8806	[M + H]+	46.43	*Glycyrrhiza aspera Pall.; Pogostemon cablin (Blanco) Benth.; Polygonum cuspidatum Sieb. et Zucc.; Artemisia scoparia Waldst. et Kit.; Scutellaria sieversii Bge*
6	Gallic acid	0.83	169.014	2.5087	[M-H]-	31.69	*Polygonum cuspidatum Sieb. et Zucc*
7	Naringenin	6.16	271.061	0.2791	[M-H]-	59.29	*Glycyrrhiza aspera Pall.; Magnolia officinalis Rehd. et wils*
8	Quinic acid	1.15	191.056	0.1256	[M-H]-	55.92	*Glycyrrhiza aspera Pall*
9	Tyrosol	0.96	121.066	6.1467	[M + H-H_2O]+	33.81	*Scutellaria sieversii Bge*
10	Nonanoic acid	9.68	158.153	1.7069	[M]+	40.51	*Scutellaria sieversii Bge.; Acorus tatarinowii Schott*
11	Medicarpin	7.15	271.097	0.8263	[M + H]+	49.22	*Glycyrrhiza aspera Pall*
12	beta-Asarone	7.34	209.117	0.5930	[M + H]+	35.61	*Acorus tatarinowii Schott*
13	Pulegone	4.16	153.127	0.0948	[M + H]+	51.60	*Pogostemon cablin (Blanco) Benth.; Scutellaria sieversii Bge*
14	Salicylic acid	8.50	137.025	4.9334	[M-H]-	32.13	*Artemisia scoparia Waldst. et Kit*
15	Linoleic acid	10.20	263.236	10.7660	[M + H-H_2O]+	41.90	*Magnolia officinalis Rehd. et wils.; Scutellaria sieversii Bge.; Prunus davidiana (Carr.) Franch*
16	Eucalyptol	0.80	154.134	12.3269	[M]+	39.73	*Magnolia officinalis Rehd. et wils.; Scutellaria sieversii Bge*
17	Eugenol	7.09	165.091	0.0146	[M + H]+	56.24	*Pogostemon cablin (Blanco) Benth.; Magnolia officinalis Rehd. et wils.; Scutellaria sieversii Bge.; Acorus tatarinowii Schott; Artemisia scoparia Waldst. et Kit*
18	Benzaldehyde	3.80	107.049	0.0010	[M + H]+	32.63	*Pogostemon cablin (Blanco) Benth.; Acorus tatarinowii Schott*
19	4-Hydroxycinnamic acid	1.30	164.04	1.5158	[M−H]-	43.29	*Scutellaria sieversii Bge.; Acorus tatarinowii Schott*
20	beta-Cubebene	10.40	205.196	3.5790	[M + H]+	32.81	*Acorus tatarinowii Schott*
21	Stigmasterol	10.62	395.366	5.5645	[M + H-H_2O]+	43.83	*Scutellaria sieversii Bge*
22	Perillyl alcohol	7.50	135.117	2.2203	[M + H-H_2O]+	46.24	*Pogostemon cablin (Blanco) Benth*
23	Isorhamnetin	4.55	317.066	0.0610	[M + H]+	49.60	*Glycyrrhiza aspera Pall.; Artemisia scoparia Waldst. et Kit*
24	Hesperetin	6.50	302.075	2.5420	[M]-	70.31	*Magnolia officinalis Rehd. et wils*
25	Citric acid	1.86	191.02	1.9684	[M−H]-	56.22	*Polygonum cuspidatum Sieb. et Zucc.; Fritillaria thunbergii Miq*

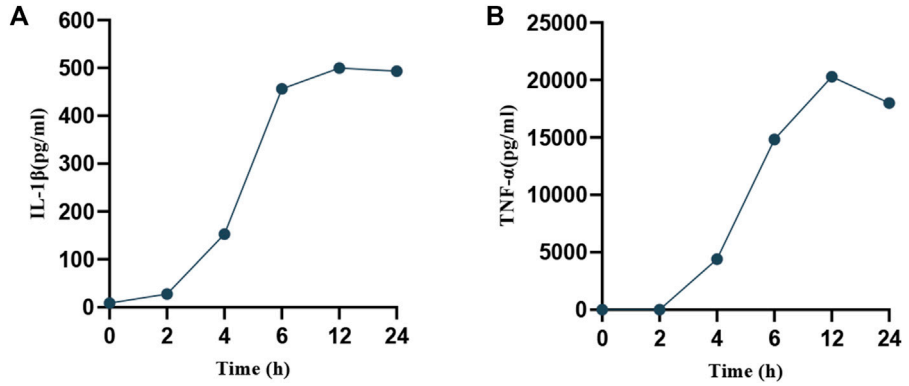


FIGURE 2
Temporal expression of pro-inflammatory factors in cell supernatants post-MP intervention. **(A)** IL-1β. **(B)** TNF-α.

2.17 Detection of the concentrations of pro-inflammatory factors

Mouse IL-1β ELISA Kit (Elabscience, E-EL-M0037) and Mouse IL-18 ELISA Kit (Elabscience, E-EL-M0730) were used to detect the levels of IL-1β and IL-18 in cell supernatants and mouse serum.

2.18 Statistical analysis

The GraphPad Prism 9.0 software was used for statistical analysis and graphical representation. Data were presented as mean ± standard deviation. A one-way ANOVA was employed to assess significant differences between the groups, with a significance level set at $P < 0.05$.

3 Results

3.1 Identification of components in YQQFG

In both the positive and negative ion modes, the LC-MS/MS method was used to create the total ion chromatogram (TIC) of YQQFG (Figure 1). Database matching led to the identification of 52 components, comprising 19 flavonoids, 18 organic acids, 6 terpenoids, and 9 other substances (Supplementary Data Sheet S3). Given that oral bioavailability (OB) is a critical pharmacokinetic index reflecting the proportion of an orally administered drug that reaches systemic circulation and exerts pharmacological effects (Xu et al., 2012). Therefore, a criterion of OB ≥ 30% (Zheng et al., 2016; Huo et al., 2022; Ji et al., 2023) was used to select 25 substances in YQQFG with good oral bioavailability from the TCMSP database (Table 3).

3.2 Screening for the optimal intervention time of MP

To ascertain the optimal timing for MP intervention, RAW264.7 cells were infected with MP for periods of 2, 4, 6, 12, and 24 h. Supernatants were collected at each time point to measure the expression of pro-inflammatory factors (IL-1β, TNF-α). As depicted in Figure 2, a rapid increase in the levels of IL-1β and TNF-α was observed starting at 6 h, peaking at 12 h, and subsequently declining. This suggests that the macrophage inflammatory response is most intense at 12 h post-infection, during which pyroptosis likely occurs. To confirm this hypothesis, SEM was utilized to examine changes in cell morphology post-MP infection. Normal RAW264.7 cells appeared round or oval, with a continuous, intact membrane and numerous small pseudopods aiding in phagocytosis (Figure 3A). MP displayed an elongated shape with a attachment organelle at one end (Figures 3B, C). Following 12 h of MP infection, notable changes included increased cell volume, the formation of pyroptotic bodies on the surface, and rupturing of the cell membrane to form pores (Figures 3C, D). These alterations align with the classic morphological features of pyroptosis, indicating that a 12 h MP infection can indeed induce substantial production of pro-inflammatory factors and pyroptosis. Consequently, 12 h was selected as the intervention point for MP in subsequent experiments.

3.3 Serum containing YQQFG shows promise in reducing the release of pro-inflammatory factors, inhibiting MP-induced NLRP3 inflammasome activation and pyroptosis

We began by using the CCK-8 assay to determine the effect of various concentrations of drug-containing serum on cell survival. Figure 4A shows that the medium containing 10% drug-carrying serum had the highest survival rate, thus this was the concentration chosen for subsequent *in vitro* drug intervention treatments. See the WB results in Figures 4B, C. In the Model group, the expression levels of the NLRP3/Caspase-1/GSDMD pathway were significantly elevated ($P < 0.001$), and there was a marked increase in the concentrations of IL-1β and IL-18 in the cell supernatants ($P < 0.001$) (Figure 4D). Serum containing YQQFG, serum containing AZM, and combination serum were all able to successfully reverse these alterations. Protein expression levels along the NLRP3/

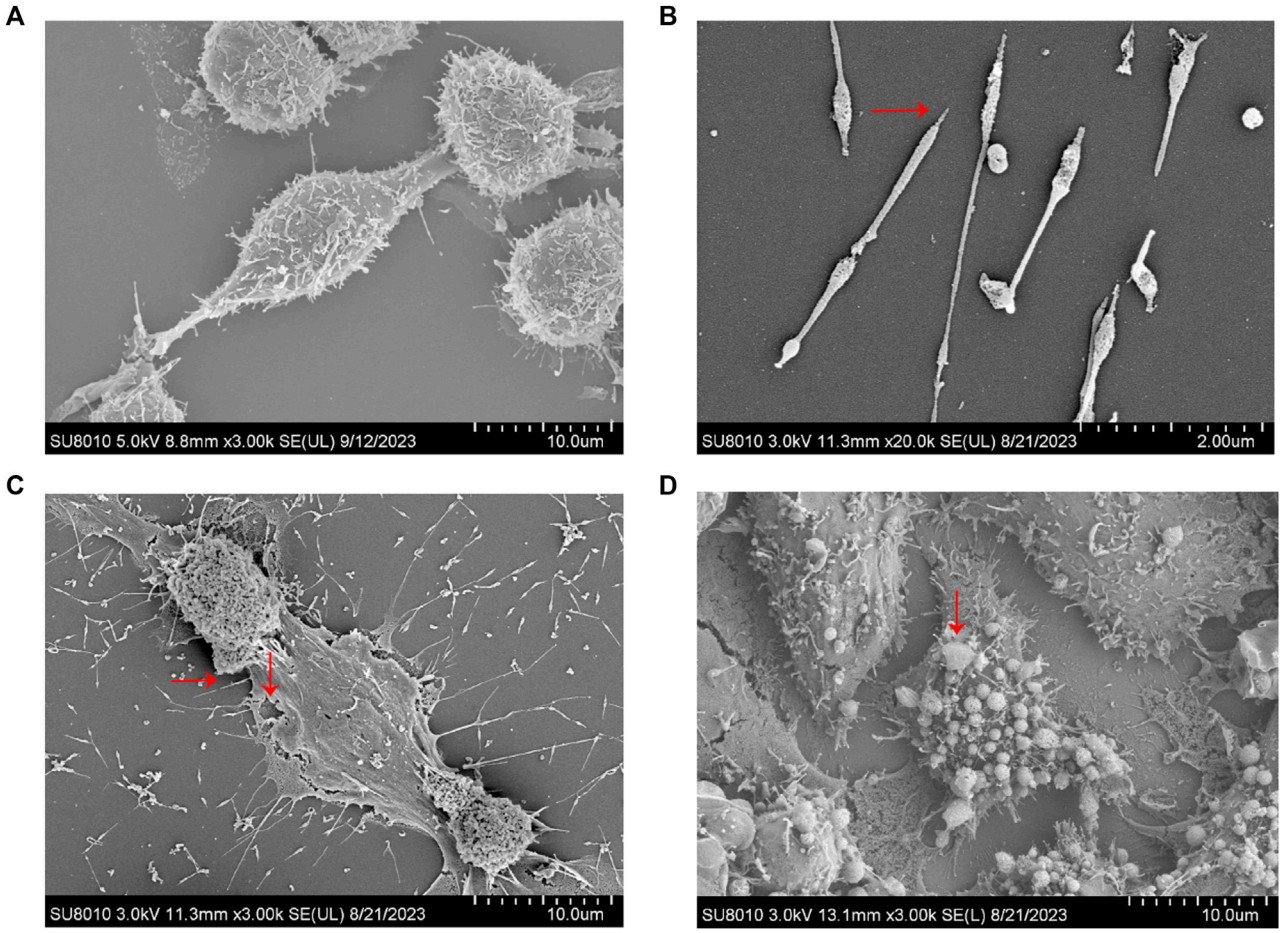


FIGURE 3
Electron microscopic examination of MP and RAW264.7 cell morphology. **(A)** Normal RAW264.7 cells. **(B)** MP. **(C–D)** Changes in RAW264.7 cells infected with MP for 12 h. →: MP and its attachments; ↓: Cell membrane rupture and pyroptosis bodies.

Caspase-1/GSDMD pathway did not differ significantly between the YQQFG and AZM groups. Crucially, when contrasted with the YQQFG and AZM groups, the YQQFG + AZM group exhibited significantly decreased levels of NLRP3, proCaspase-1, cleaved Caspase-1, GSDMD, and GSDMD-NT protein expression in the cells, as well as a reduction in the content of pro-inflammatory components in the cell supernatants ($P < 0.05$). This suggests that the combined use of YQQFG and AZM can have a synergistic effect.

3.4 Molecular docking analysis

To elucidate the potential of YQQFG in regulating NLRP3, we performed molecular docking of 25 active components from YQQFG with the NLRP3 protein. Typically, if the binding energy of a compound to a target protein is less than −4.25 kcal mol^{-1}, this indicates some binding activity and the ability to form a stable complex. A binding energy less than −5.0 kal·mol^{-1} indicates strong binding activity (Ji et al., 2023). As detailed in Table 4, the binding energies of most YQQFG components to NLRP3 were below −4.25 kal·mol^{-1}, with 17 components displaying binding energies below −5.0 kal·mol^{-1}. To illustrate this interaction, the five compounds with the lowest binding energies were selected for detailed visualization of their binding modes with NLRP3 (Figure 5).

3.5 NLRP3 overexpression exacerbates MP-induced pyroptosis and inflammatory responses, whereas YQQFG potently inhibits the expression of NLRP3 protein to exert therapeutic effects

Subsequently, we engineered RAW264.7 cells to overexpress NLRP3 via lentiviral transfection (referred to as $NLRP3^{-OE}$). qPCR results demonstrated that NLRP3 expression in $NLRP3^{-OE}$ cells was over threefold higher than in wild-type RAW264.7 cells, confirming successful establishment of a stable NLRP3-overexpressing cell line (Figure 6A). We then examined the impact of YQQFG-containing and AZM-containing sera on the NLRP3/Caspase-1/GSDMD pathway and the levels of IL-1β and IL-18 under conditions of NLRP3 overexpression. WB and ELISA analyses indicated no statistically significant differences in the levels of NLRP3, ASC, proCaspase-1, cleaved Caspase-1, GSDMD, GSDMD-NT, IL-1β,

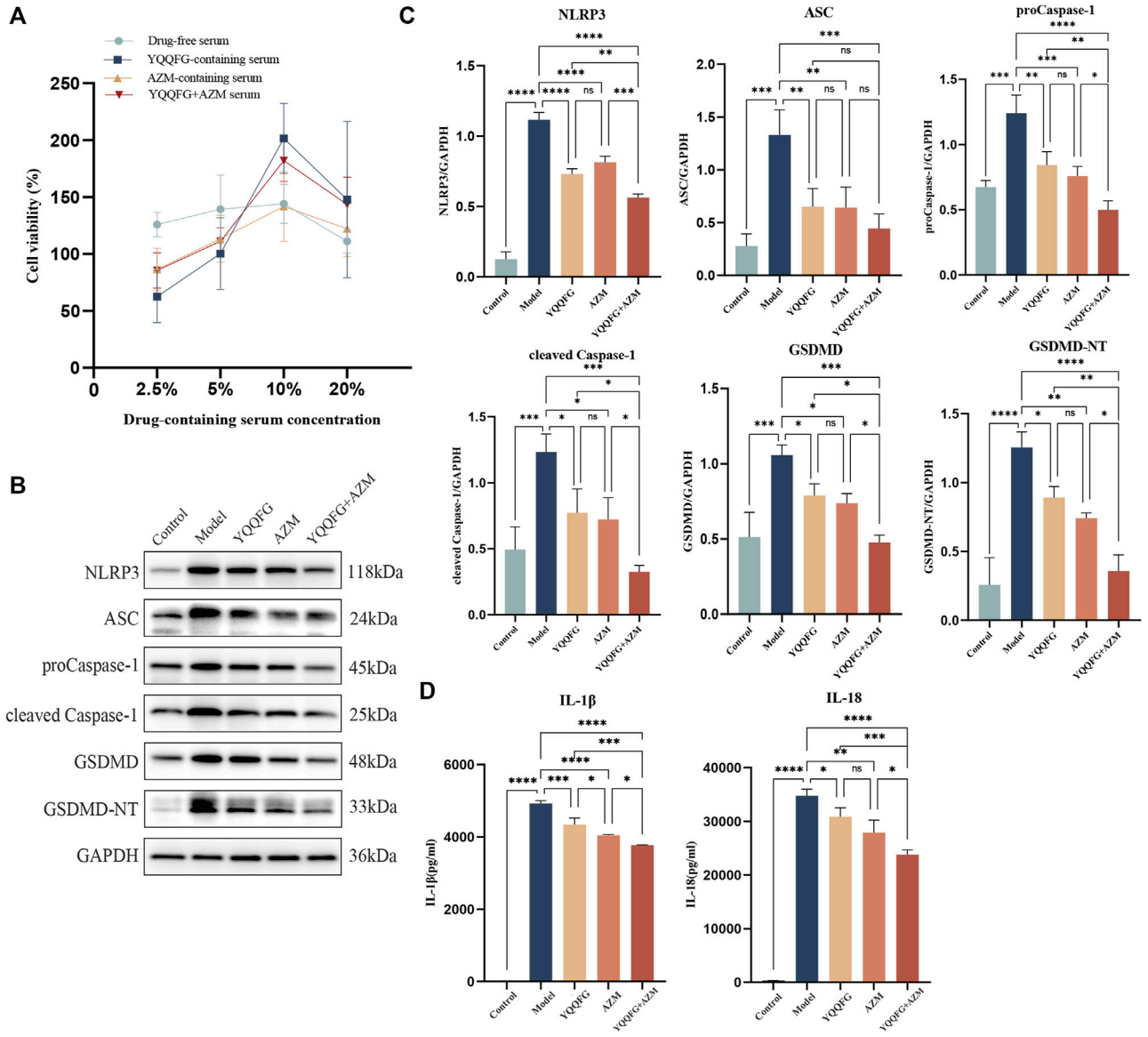


FIGURE 4
The effect of YQQFG-containing serum on the expression of the NLRP3/Caspase-1/GSDMD pyroptosis pathway induced by MP. **(A)** Effect of different concentrations of drug-containing serum on cell viability. **(B)** Representative WB bands of each protein. **(C)** Statistics on the gray values for each protein. **(D)** Statistics on the expression levels of IL-1β and IL-18 in cell supernatants. Values are the mean ± SD (n = 3). ns $P > 0.05$, * $P < 0.05$, ** $P < 0.01$, *** $P < 0.001$, **** $P < 0.0001$.

and IL-18 between the LV^{-Con} group and the Control group ($p > 0.05$), suggesting that the vector virus did not alter the pathway's expression or increase the release of pro-inflammatory factors (Figures 6B–J). However, levels of NLRP3, GSDMD, and GSDMD-NT, as well as the concentrations of IL-1β and IL-18 in the cell supernatants, were significantly elevated in the MP + $NLRP3^{-OE}$ group compared to the MP group ($P < 0.05$), signifying that NLRP3 overexpression exacerbated MP-induced pyroptosis and inflammatory responses. Furthermore, we observed that YQQFG-containing serum still inhibited the activation of the NLRP3/Caspase-1/GSDMD pathway and the release of pro-inflammatory factors following NLRP3 overexpression, but the effect of AZM-containing serum was notably reversed. These findings confirm that YQQFG can specifically modulate the expression of NLRP3 protein, thereby inhibiting inflammasome activation and pyroptosis, and ultimately mitigating MP-induced inflammatory responses.

3.6 YQQFG enhances weight recovery in MPP mice, reduces lung index, and alleviates acute lung injury

Figures 7A, B displays the daily weight changes of mice in each group. The body weight of mice in the Control group slightly decreased on days 2–3 post-modeling but then gradually increased, indicating that inhalation of isoflurane and saline nasal drops did not have a long-term impact on their health. The weight of mice exposed to MP nasal drip decreased significantly. Drug-treated

TABLE 4 Binding energy of YQQFG active components to NLRP3.

No.	Components	Binding energy (kal·mol^{-1})	No.	Components	Binding energy (kal·mol^{-1})
1	Stigmasterol	−8.59	14	Quercetin	−5.18
2	Formononetin	−6.99	15	Gallic acid	−5.07
3	beta-Cubebene	−6.96	16	Isorhamnetin	−5.04
4	Baicalein	−6.53	17	Perillyl alcohol	−5.03
5	Hesperetin	−6.34	18	Eucalyptol	−4.98
6	Citric acid	−6.18	19	Salicylic acid	−4.97
7	Naringenin	−6.09	20	Nonanoic acid	−4.50
8	4-Hydroxycinnamic acid	−5.85	21	Benzaldehyde	−4.43
9	Pulegone	−5.81	22	Linoleic acid	−4.42
10	Skullcapflavone II	−5.72	23	Eugenol	−4.35
11	beta-Asarone	−5.64	24	Tyrosol	−4.22
12	Luteolin	−5.58	25	Quinic acid	−3.79
13	Medicarpin	−5.53			

mice began to gain weight on the 5th day (i.e., the second day of gavage). The weight recovery rate of the YQQFG + AZM group was marginally better than that of the YQQFG group and the AZM group. The weight of the Model group exhibited a slight upward trend on the 8th day. The lung index, a common metric for evaluating pathological changes in lung tissue in animal models, showed a significant increase in the Model group ($P < 0.0001$) (Figures 7C, D). YQQFG administration for 3 days had no significant impact on the lung index, but the lung index of the YQQFG + AZM group was significantly lower than that of the AZM group ($P < 0.05$). After 7 days of gavage, compared to the Model group, the lung index in the three drug treatment groups decreased, with no statistical differences between the YQQFG and AZM groups. Figures 7E, F shows H&E staining results indicating that the lung tissue structure of the Control group was clear and intact, with consistent alveolar wall thickness and no hemorrhage, edema, or exudation in the alveoli, nor any inflammatory cell infiltration around the trachea. The lungs of mice in the Model group exhibited severe inflammatory changes, characterized by alveolar loss, lung consolidation, and extensive inflammatory cell infiltration around the alveoli and trachea. As the disease progressed, the extent of inflammatory cell infiltration in the Model-7d group was significantly greater than in the Model-3d group, with some airways completely blocked. The lung tissue of the YQQFG-3d group, the AZM-3d group, and the YQQFG + AZM-3d group showed limited consolidation, disappearance of some alveolar regions, and lower levels of inflammatory cell infiltration compared to the Model-3d group. The YQQFG + AZM-3d group exhibited the best lung ventilation. Longitudinal comparisons across the treatment durations revealed that the lung condition in the 7-day administration groups was significantly improved compared to the 3-day groups. Notably, the lung tissue of mice in the YQQFG + AZM-7d group returned to normal, reaffirming the synergistic effect of combining YQQFG and AZM.

3.7 *In vivo* experiments indicate that YQQFG mitigates MPP by suppressing NLRP3 inflammasome activation and macrophage pyroptosis

Compared to the Control-3d and Control-7d groups, the NLRP3/Caspase-1/GSDMD pathway proteins in the lung tissues of the Model-3d and Model-7d groups were significantly upregulated (Figures 8A, B), and the levels of IL-1β and IL-18 in peripheral serum increased significantly ($P < 0.01$) (Figures 8C, D). This suggests that the NLRP3 inflammasome-mediated pyroptosis pathway was activated during the acute phase of MPP, enhancing the release of IL-1β and IL-18. Administration of YQQFG or AZM for 3 days effectively reduced the expression of the NLRP3/Caspase-1/GSDMD pathway and the content of IL-18. However, a reduction in IL-1β required 7 days of treatment. Aligning with *in vitro* findings, the results indicate that both YQQFG and AZM are equally effective, but their combination provides the most substantial therapeutic benefit.

To explore the relationship between NLRP3 protein expression in lung tissue and macrophages, we conducted immunofluorescence double staining of NLRP3 and mouse macrophage-specific markers (F4/80) on lung tissue sections from the 3-day gavage group. The fluorescence intensity of NLRP3 and F4/80 was significantly enhanced in the Model-3d group ($P < 0.0001$) (Figures 9A–C), indicating NLRP3 protein activation and macrophage infiltration in the lungs of MPP mice. In contrast, the fluorescence intensity of NLRP3 in the YQQFG-3d group, the AZM-3d group, and the YQQFG + AZM-3d group was significantly reduced. PCC, a metric utilized to quantify the extent of protein co-localization, spans a range from −1 to 1, where values approaching 1 signify a stronger degree of co-localization (Dunn et al., 2011). As demonstrated in Figure 9D, the PCC values in the Model-3d group were significantly elevated ($P < 0.0001$). In comparison to the Model-3d group, the PCC values in both the YQQFG-3d and

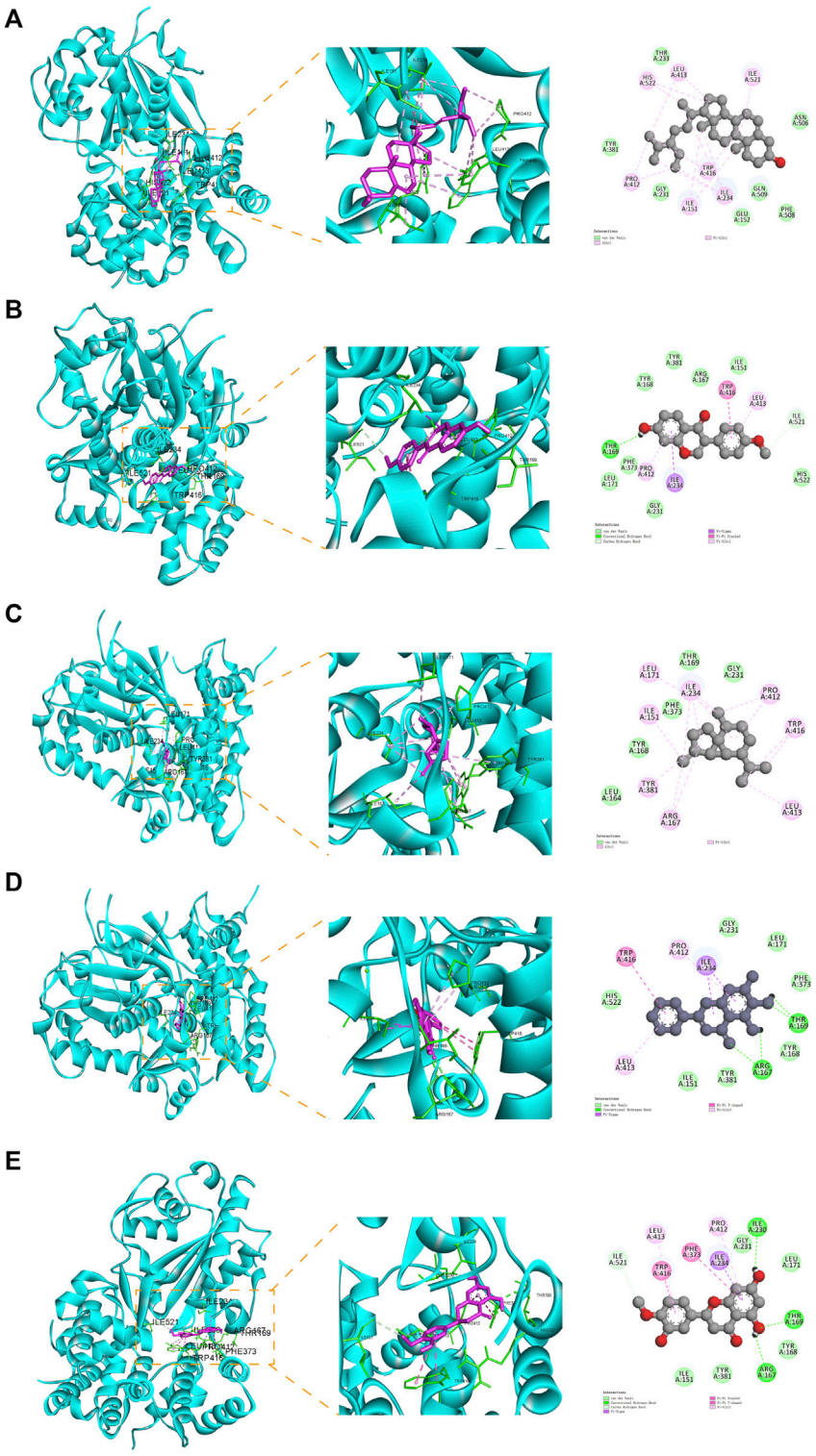


FIGURE 5
Molecular docking pattern diagram (the five compounds with the strongest affinity to NLRP3). **(A)** Stigmasterol and NLRP3 (binding energy: -8.59). **(B)** Formononetin and NLRP3 (binding energy: -6.99). **(C)** beta-Cubebene and NLRP3 (binding energy: -6.96). **(D)** Baicalein and NLRP3 (binding energy: -6.53). **(E)** Hesperetin and NLRP3 (binding energy: -6.34).

YQQFG + AZM-3d groups exhibited significant decreases ($P < 0.001$), whereas no statistical difference was observed between the AZM-3d and Model-3d groups. This suggests that MP predominantly activates NLRP3 protein in macrophages, leading to inflammasome assembly and macrophage pyroptosis, thereby causing acute lung injury. YQQFG effectively inhibits NLRP3 protein activation in macrophages, demonstrating a significant advantage over AZM in this regard.

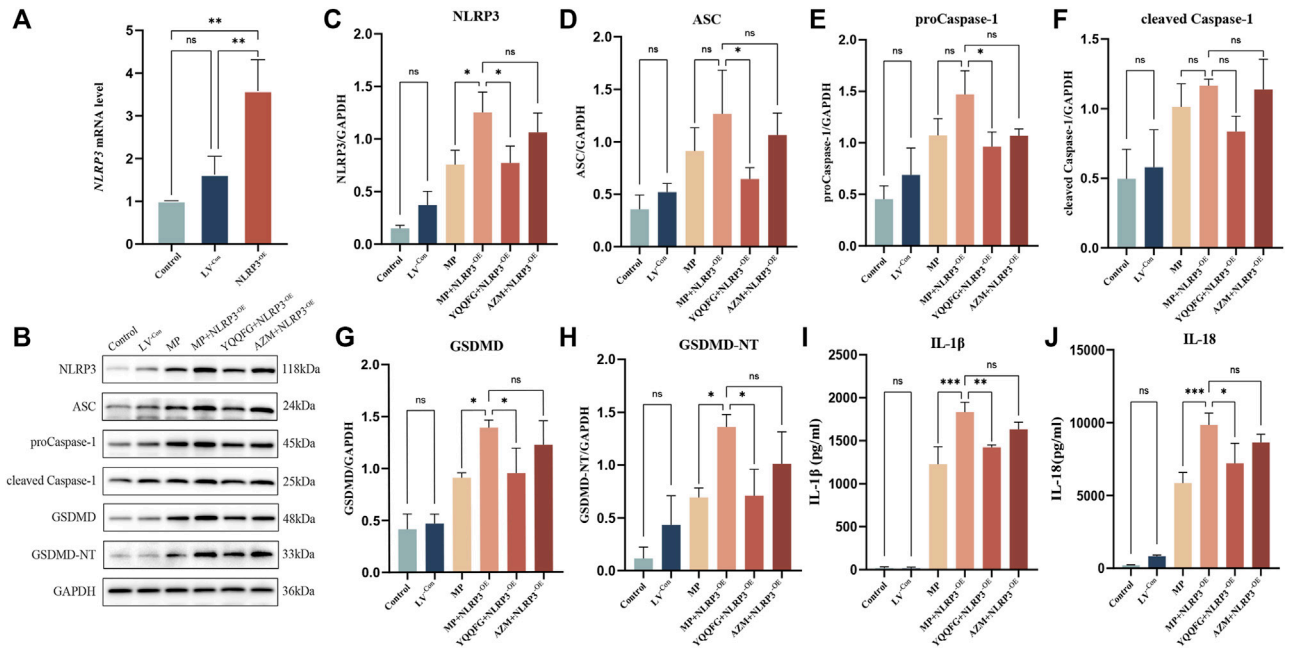


FIGURE 6
Effects of NLRP3 overexpression on the expression levels of NLRP3/Caspase-1/GSDMD pathway across different cell groups. **(A)** qPCR verification of transfection efficiency. **(B)** Representative WB bands for each protein. **(C–H)** Statistics on the gray values for each protein. **(I–J)** Statistics on the expression levels of IL-1β and IL-18 in cell supernatants. Values are the mean ± SD ($n = 3$). ns $P > 0.05$, * $P < 0.05$, ** $P < 0.01$, *** $P < 0.001$, **** $P < 0.0001$.

3.8 YQQFG moderately reduces the release of MP exotoxin

CARDS TX is currently the only identified MP exotoxin (Li et al., 2019). Studies have shown that after endocytosis into cells, CARDS TX transfers the ADP ribose groups to specific amino acids of NLRP3, thereby directly initiating the assembly of the NLRP3 inflammasome (Bose et al., 2014). Consequently, we employed qPCR to assess the relative expression of CARDS TX mRNA in MP-infected RAW264.7 cells and MPP model mice (Figure 10). In the *in vitro* model, CARDS TX expression was not detected in the Control group. Compared with the Model group, the expression of CARDS TX in the drug intervention groups was significantly reduced ($P < 0.0001$). However, the inhibitory effect of YQQFG on CARDS TX was less pronounced than that of AZM. In the *in vivo* model, similar results were observed. The expression of CARDS TX in the lung tissue of mice decreased following 3 days of treatment with YQQFG, AZM, or their combination ($P < 0.05$). After 7 days of treatment, CARDS TX was undetectable in the AZM-7d group and the YQQFG + AZM-7d group, while a trace amount of CARDS TX expression was still observable in the YQQFG-7d group.

4 Discussion

MPP is a prevalent form of childhood CAP and frequently causes outbreaks among student populations, thereby posing a significant public health challenge worldwide (Song et al., 2023). Currently, the treatment of MPP in children primarily involves symptomatic care and the use of macrolide antibiotics (Tsai et al., 2021). Nevertheless, in recent years, the resistance of MP to macrolide antibiotics has been increasing. This is especially true in East Asian nations like Japan and China, where the resistance rate in children is above 70% (Tanaka et al., 2017; Hsiung et al., 2022). This resistance often delays treatment, increasing the risk of progression from common to severe MPP (Lee et al., 2021). Clinically, tetracyclines and fluoroquinolones are considered alternative treatments (Tong et al., 2022). Unfortunately, the hazards of enamel hypoplasia and permanent tooth discolouration make tetracyclines unsafe for children under the age of eight. Patients under the age of 18 should exercise caution when prescribed fluoroquinolones due to the risk of musculoskeletal toxicity (Okubo et al., 2018). These challenges underline the urgent need for developing new therapeutic agents for MPP in children.

Pyroptosis, a form of programmed cell death, is characterized by the rupture of the cell membrane and the subsequent release of substantial inflammatory mediators (Liu et al., 2021). It is governed by both classical pathway (Caspase-1-dependent) and non-classical pathway (non-Caspase-1-dependent) mechanisms. (1) The classical pathway involves inflammasome activation of Caspase-1 (Dai et al., 2023). Inflammasomes, multiprotein complexes, consist of pattern recognition receptors (PRRs), an adaptor protein (ASC), and the precursor molecule (proCaspase-1) (Li et al., 2021). The human innate immune system mainly encompasses six types of PRRs, among which NOD-like receptors (NLRs) and absent in melanoma 2 (AIM2)-like receptors (ALRs) possess the capability to assemble inflammasomes (Man and Kanneganti, 2015; Isazadeh et al., 2023). Upon recognizing pathogen-associated molecular patterns (PAMPs) and damage-associated molecular patterns (DAMPs), NLRs or ALRs recruit ASC and proCaspase-1 via homotypic domain interactions to assemble the canonical

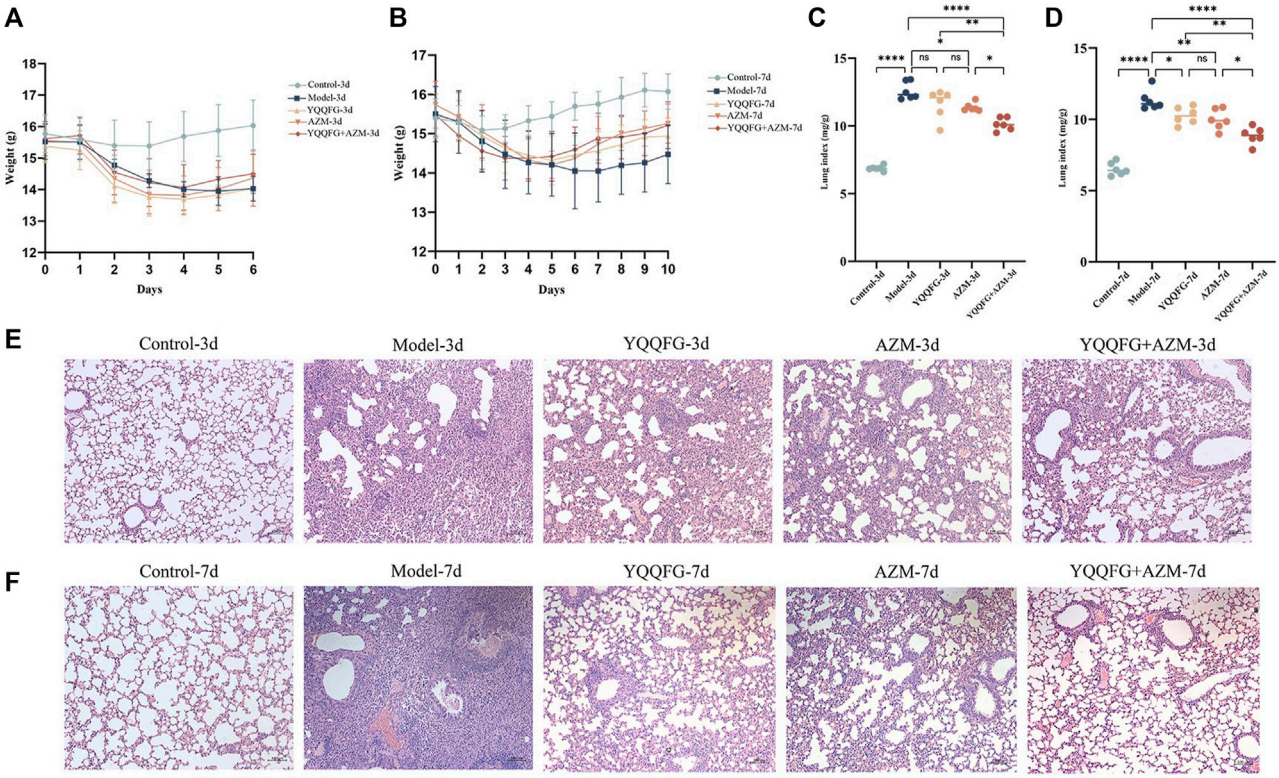


FIGURE 7
Effect of YQQFG on body weight, lung index, and lung pathology in MPP model mice. **(A)** Body weight change line chart for the 3-day gavage group. **(B)** Body weight change line chart for the 7-day gavage group. **(C)** Lung index for the 3-day gavage group. **(D)** Lung index for the 7-day gavage group. **(E–F)** H&E staining of lung tissue sections for the 3-day and 7-day gavage groups, respectively (Scale: 100 μm). Values are the mean ± SD (n = 6). ns $P > 0.05$, * $P < 0.05$, ** $P < 0.01$, *** $P < 0.001$, **** $P < 0.0001$.

inflammasome complexes, thereby converting proCaspase-1 into active Caspase-1 (Dick et al., 2016; Malik and Kanneganti, 2017). Caspase-1 not only converts the precursors of IL-1β and IL-18 into their mature forms but also cleaves GSDMD, producing the GSDMD-NT fragment that inserts into the lipid bilayer of the cell membrane, resulting in pyroptosis (Shi et al., 2015). (2) In the non-classical pathway, the bacterial endotoxin component lipopolysaccharide (LPS) commonly serves as the direct activator of Caspase-4, Caspase-5, or Caspase-11, which then cleave GSDMD to mediate pyroptosis (Kayagaki et al., 2013; Dai et al., 2023). Notably, this pathway does not directly augment the synthesis and release of IL-1β and IL-18, but rather promotes the release of ATP via the pannexin-1/P2X7 axis. Subsequently, ATP activates the NLRP3 inflammasome, thereby indirectly amplifying the inflammatory response (Yang et al., 2015; Li et al., 2023).

Among the various inflammasomes identified, the NLRP3 inflammasome attracts the most attention (Zhao and Zhao, 2020). A number of studies have shown that the classical pyroptosis pathway mediated by NLRP3 inflammasome plays an important role in acute lung injury induced by respiratory pathogens such as influenza and SARS-CoV-2 (Pan et al., 2021; Liu et al., 2022; You et al., 2023). The NLRP3 protein is a PRR found in the cytoplasm and is made up of three domains: an N-terminal pyrin domain, a central NACHT domain, and a C-terminal LRR domain (Seoane et al., 2020). At rest, NLRP3 is inactivated through binding with HSP90 and SGT1 in the cytoplasm (Yin et al., 2023). Upon pathogen invasion, the LRR domain senses danger signals, prompting NLRP3 to dissociate from HSP90 and SGT1, undergo oligomerization, expose its pyrin domain, and start recruiting ASC to assemble the inflammasome (Jo et al., 2016). IL-1β and IL-18, both characterized by their potent pro-inflammatory proFperties, are downstream products of the NLRP3 inflammasome and members of the IL-1 family. Due to the absence of signal peptides and leader sequences, IL-1β and IL-18 cannot be directly released into the extracellular environment via the Golgi vesicle transport pathway. Instead, their release necessitates cellular death mechanisms, such as pyroptosis (Lopez-Castejon and Brough, 2011). IL-1β is an important cytokine that mediates inflammatory damage in lung tissue. It can bind to the IL-1 receptor (IL-1R) on the surface of immune cells to promote the transcriptional expression of NF-κB, resulting in increased synthesis of pro-IL-1β, forming a positive feedback loop that escalates the inflammatory response (Vora et al., 2021). When IL-1β binds to IL-1R on lung vascular endothelial cells, it suppresses the transcription of VE-cadherin, compromising vascular integrity and causing lung vascular damage (Xiong et al., 2020). IL-18, initially identified as an interferon-γ (IFN-γ) inducing factor, targets T cells to induce IFN-γ production, promoting a Th1-type immune response (Yang et al., 2004). Furthermore, Narita M and colleagues have identified elevated levels of IL-18 in patients with MPP accompanied by pleural

10.3389/fphar.2024.1437475

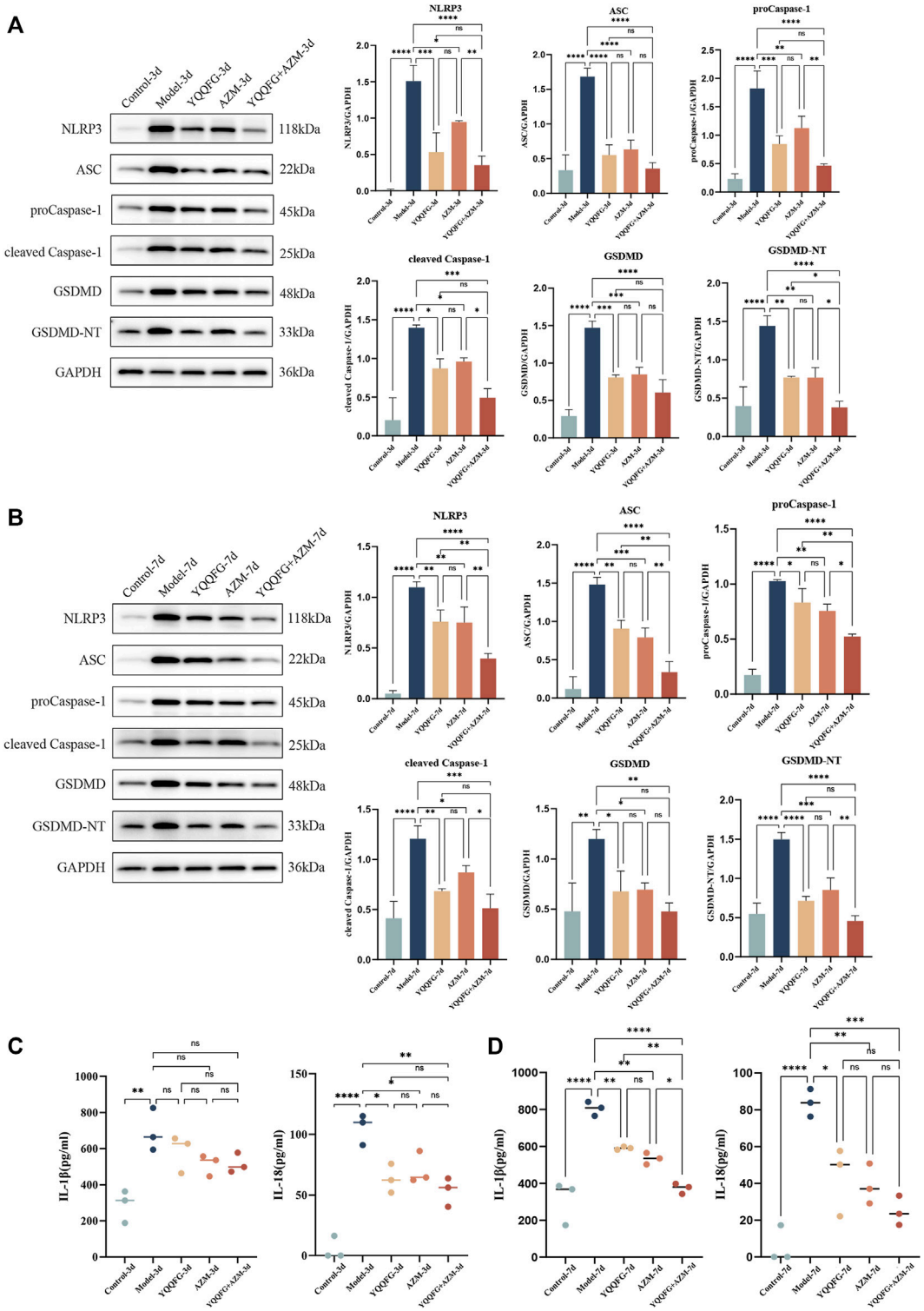


FIGURE 8
Effects of YQQFG on the NLRP3/Caspase-1/GSDMD pathway in lung tissue and pro-inflammatory factors expression in peripheral serum of mice. **(A, B)** Representative WB bands and statistics on the gray values for proteins in the NLRP3/Caspase-1/GSDMD pathway from the 3-day gavage group and the 7-day gavage group of mice. **(C)** Statistics on the expression levels of IL-1β and IL-18 in peripheral serum of mice in the 3-day gavage group. **(D)** Statistics on the expression levels of IL-1β and IL-18 in peripheral serum of mice in the 7-day gavage group. Values are the mean ± SD ($n = 3$). ns $P > 0.05$, * $P < 0.05$, ** $P < 0.01$, *** $P < 0.001$, **** $P < 0.0001$.

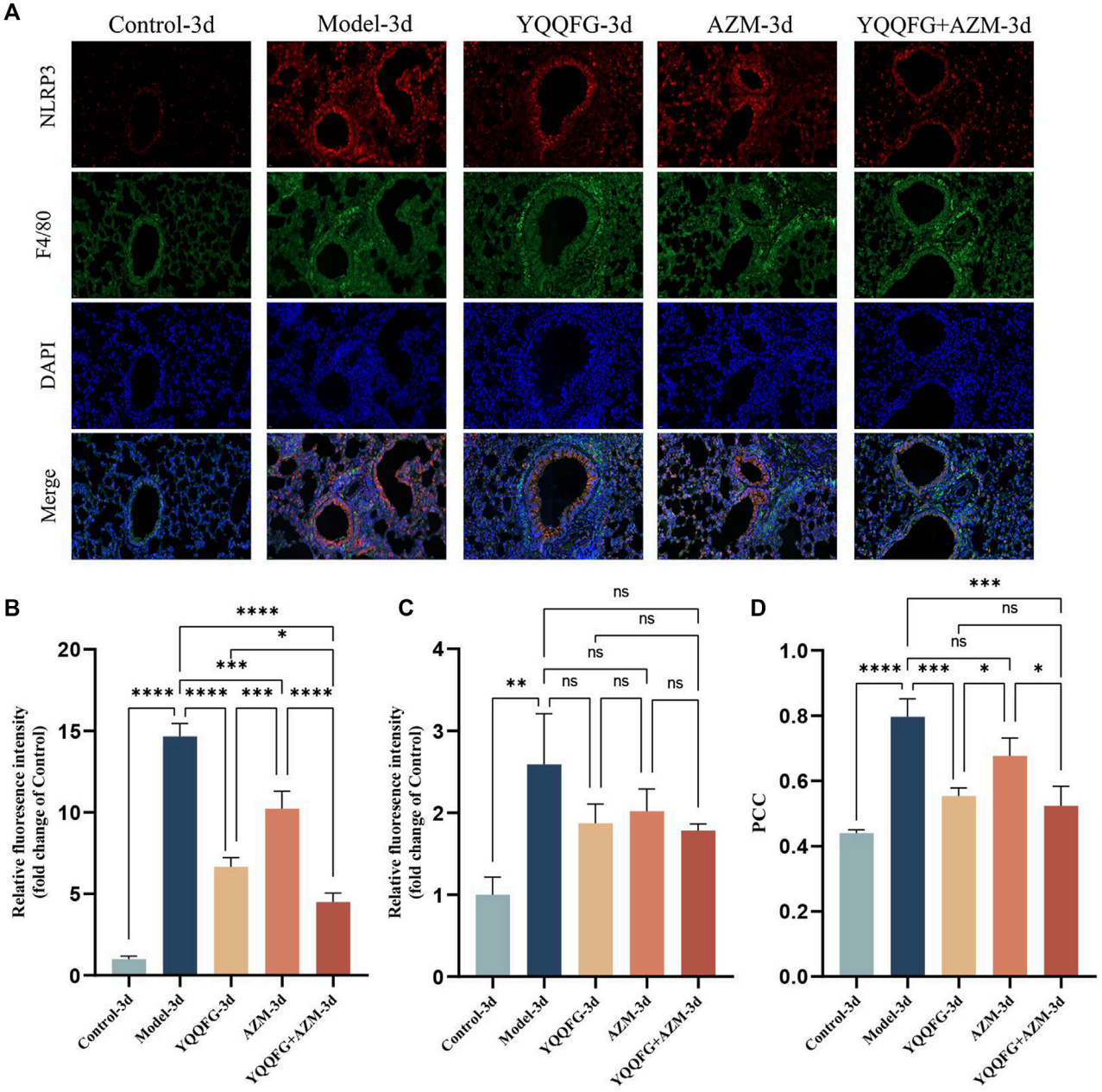


FIGURE 9
YQQFG can significantly inhibit the expression of NLRP3 protein in macrophages in the lungs of MPP model mice. **(A)** Representative immunofluorescence staining of the 3-day gavage group: red fluorescence indicates NLRP3, green represents F4/80, and blue denotes DAPI (Scale: 20 μm). **(B)** Statistics on relative fluorescence intensity for NLRP3. **(C)** Statistics on relative fluorescence intensity for F4/80. **(D)** Co-localization analysis of NLRP3 and F4/80. Values are the mean ± SD (n = 3). ns $P > 0.05$, * $P < 0.05$, ** $P < 0.01$, *** $P < 0.001$, **** $P < 0.0001$.

effusion or central nervous system complications, emphasizing the association between this cytokine and the severity of MPP disease (Narita et al., 2000). Hence, inhibiting NLRP3 inflammasome-mediated pyroptosis and reducing excessive levels of IL-1β and IL-18 constitute effective strategies for preventing and treating acute lung injury caused by MP.

Current studies have identified the pathogenesis of MP to primarily encompass direct adhesion damage, exotoxin release, immune inflammatory damage, and immune escape (Jiang et al., 2021). The most critical pathogenic mechanism is believed to be the intense immune inflammatory response triggered by the interaction between MP and the host (He et al., 2016). Given that macrophages are critical participants in the body's inflammatory response (Knoll et al., 2021), this study confirms the therapeutic pathways and targets of YQQFG in treating MPP from the perspective of macrophage pyroptosis mediated by NLRP3 inflammasome, offering new insights into the prevention and treatment of MPP in children.

Initially, LC-MS/MS was utilized to identify compounds in YQQFG, from which 25 compounds with favorable oral

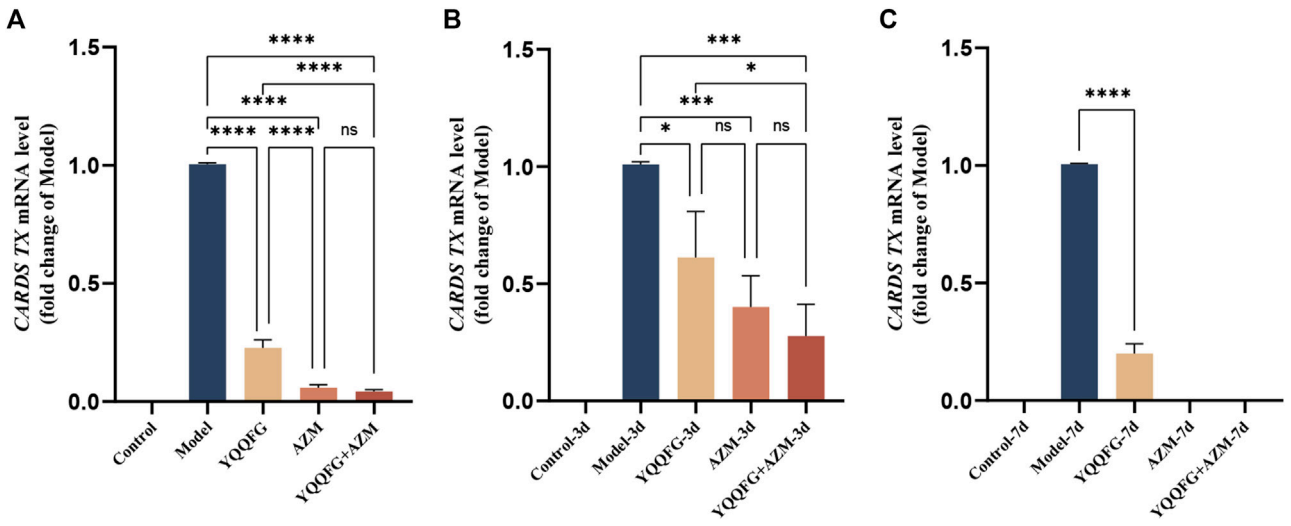


FIGURE 10
YQQFG can inhibit the release of MP exotoxin to a certain extent. **(A)** Comparison of CARDS TX expression in cells of each group. **(B)** Comparison of CARDS TX expression in lung tissue of mice in the 3-day gavage group. **(C)** Comparison of CARDS TX expression in lung tissue of mice in the 7-day gavage group. Values are the mean ± SD (n = 3). ns $P > 0.05$, * $P < 0.05$, ** $P < 0.01$, *** $P < 0.001$, **** $P < 0.0001$.

bioavailability were selected. Notably, compounds such as Baicalein (Zhang et al., 2019; Zhang et al., 2020; Song et al., 2021), Quercetin (Colunga Biancatelli et al., 2020; Zheng et al., 2021; Sun et al., 2023), Eucalyptol (Zhao et al., 2014; Kennedy-Feitosa et al., 2016), Eugenol (Bittencourt-Mernak et al., 2021; Elken et al., 2022), Isorhamnetin (Zou et al., 2023), Luteolin (Kuo et al., 2011; Zhang et al., 2021), Gallic acid (Chosa et al., 1992; Haute et al., 2020), Naringenin (Lin et al., 2018; Zhang et al., 2022), 4-Hydroxycinnamic acid (Chen et al., 2019; Souza et al., 2021), and Hesperetin (Kaya et al., 2019; Wang et al., 2019) are recognized for their strong anti-inflammatory, antioxidant, and antimicrobial properties. The protective effects of these components against infectious lung injuries are well-documented. In MP-related studies, Chosa H et al. demonstrated significant bactericidal activity of Gallic Acid against MP (Chosa et al., 1992), while Lin Y et al. established that Naringenin prevents MP-induced pulmonary fibrosis by inhibiting autophagy in airway epithelial cells and reducing the inflammatory response in MPP model mice (Lin et al., 2018). These pharmacological findings provide support for verifying the mechanism of YQQFG in treating MPP.

Next, we utilized RAW264.7 cells and BALB/c mice to develop MP-infected cell and animal models, respectively. *In vitro*, peak production of IL-1β and TNF-α in RAW264.7 cells occurred 12 h post-MP infection, after which expression levels decreased. We speculated that 12 h post-MP intervention represents the peak of the pyroptotic effect, after which a significant number of cells have died. To test this hypothesis, we examined changes in cell morphology post-MP infection using SEM. MP is 1–2 μm in length and 0.1–0.2 μm in width, making it the smallest self-replicating organism currently identified, invisible to ordinary optical microscopes (Atkinson et al., 2008; Razin and Hayflick, 2010). We successfully captured the microscopic morphology of MP using SEM (Figure 3B). MP possesses a slender shape with a sharp structure at the top, which serves as its attachment organelle. This region harbors adhesion proteins and genomes that facilitate gliding, enabling MP to adhere to and colonize the cell surface (Krause, 1998; Balish, 2006). 12 h post-MP infection, we observed an increase in cell volume, cell membrane rupture, and the formation of numerous surface bubbles (Figures 3C, D), which are characteristic morphological features of pyroptosis (Xu et al., 2021). During the initial stage of pyroptosis, GSDMD inserts into the cell membrane, creating small pores. The osmotic pressure differential between the intracellular and extracellular environments allows only sodium ions and water from the extracellular matrix to enter, leading to cell enlargement and the appearance of bulging bubbles at the pores. As the cells continue to expand, the complete rupture of the cell membrane occurs, resulting in the release of cell contents and cell death (Dai et al., 2023). Subsequent WB and ELISA results indicated that in the Model group, the expression levels of NLRP3/Caspase-1/GSDMD pathway proteins and the concentrations of IL-1β and IL-18 were significantly increased, demonstrating that MP activates the NLRP3 inflammasome, triggering macrophage pyroptosis and the release of pro-inflammatory cytokines. Treatment with YQQFG-containing serum and AZM-containing serum reversed these changes, with no significant differences in the inhibition of the NLRP3/Caspase-1/GSDMD pathway. However, following NLRP3 overexpression, the lentivirus expressing NLRP3 neutralized the effect of AZM, whereas YQQFG-containing serum continued to suppress the levels of pyroptosis and the release of pro-inflammatory factors. This indicates that YQQFG's therapeutic action is mediated through the regulation of NLRP3. It is well established that macrolide antibiotics function by binding to the 23S rRNA of MP ribosomes, thereby disrupting MP protein synthesis (Vázquez-Laslop and Mankin, 2018). However, mutations at specific sites on the 23S rRNA can prevent macrolides from binding effectively, leading to therapeutic failure (Leng et al., 2023). Different from the single-site mechanism of antibiotics against pathogens, TCM focuses on the overall regulation of the human body, so it is not easy to develop pathogen resistance, which fully reflects the significant potential of TCM in the prevention and treatment of infectious diseases.

Similar results were obtained *in vivo*. The lung index in MPP model mice increased, and H&E staining revealed acute

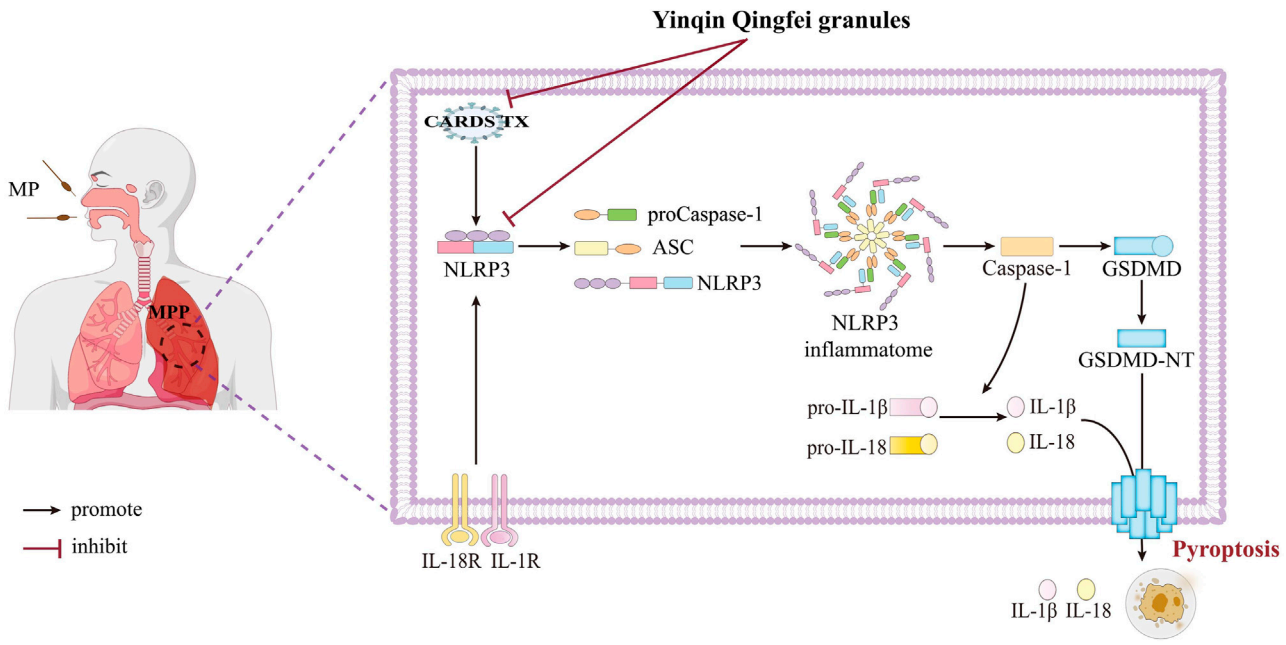


FIGURE 11
YQQFG treats MPP by inhibiting NLRP3 inflammasome-mediated macrophage pyroptosis. Some of the materials in this figure were sourced from Figdraw 2.0 (https://www.figdraw.com).

inflammatory changes in lung tissue, such as extensive inflammatory cell infiltration, alveolar loss, and airway obstruction. WB and ELISA analyses indicated a significant increase in the expression levels of NLRP3/Caspase-1/GSDMD pathway proteins in the Model group, along with elevated levels of IL-1β and IL-18 in peripheral serum, and a strong co-localization of NLRP3 and F4/80. These results suggest that MP primarily activates the NLRP3 protein in macrophages, and this activation triggers macrophage pyroptosis, a key pathological mechanism in MP-induced acute lung injury. The expression of NLRP3 protein in macrophages significantly decreased after 3 days of YQQFG treatment. Following 7 days of treatment, there were marked improvements in lung index, inflammatory cell infiltration, and peripheral blood inflammation levels in mice treated with YQQFG. Thus, YQQFG appears to mitigate the inflammatory response by inhibiting NLRP3 inflammasome-mediated macrophage pyroptosis, effectively alleviating MP-induced acute lung injury. Importantly, our findings demonstrate that combining YQQFG with AZM yields the most effective therapeutic outcome for MPP, with synergistic effects observed. Moving forward, greater emphasis should be placed on integrating traditional Chinese and Western medicine in the treatment of MPP in children.

In 2005, Kannan TR et al. first identified the MP pathogenic factor MPN372, also known as CARDS TX (Kannan et al., 2005). Its structure closely resembles the S1 subunit of pertussis toxin and exhibits ADPRT activity and cell vacuolation activity (Hardy et al., 2009). CARDS TX is currently the only known exotoxin of MP and is strongly associated with MP's pathogenicity and persistent infection (Techasaensiri et al., 2010). Given that CARDS TX can directly mediate the post-translational modification and activation of the NLRP3 protein (Bose et al., 2014), we assessed the relative expression of CARDS TX in various cell groups and mouse lung tissues using qPCR. The results indicated that YQQFG could reduce the release of CARDS TX to some extent, though not as effectively as AZM. This suggests that YQQFG not only targets the NLRP3 protein directly but also indirectly influences NLRP3 expression by inhibiting the effects of MP toxin (Figure 11).

Our research, however, has some limitations. First, while we have identified the main components of YQQFG, the key active components against MPP remain unclear. Second, the ability to treat diseases through a "multi-component, multi-target, and multi-pathway" approach is a distinctive advantage of TCM (Lou et al., 2022). Beyond NLRP3, other potential targets of YQQFG require further exploration and validation. Lastly, the interaction between YQQFG and AZM *in vivo* should be elucidated through pharmacokinetic studies to ensure the safety and efficacy of clinical use.

5 Conclusion

In summary, our study confirms that YQQFG mitigates the inflammatory response by inhibiting NLRP3 inflammasome-mediated macrophage pyroptosis, thereby alleviating MP-induced acute lung injury. This provides novel insights and approaches for the prevention and treatment of MPP in children.

Data availability statement

The raw data presented in the study are deposited in the Figshare repository (https://doi.org/10.6084/m9.figshare.26784610.v2).

Ethics statement

The animal study was approved by Animal Ethics Committee of Shandong University of Traditional Chinese Medicine. The study was conducted in accordance with the local legislation and institutional requirements.

Author contributions

ZS: Methodology, Validation, Writing–original draft. CH: Methodology, Validation, Writing–original draft. GL: Data curation, Software, Writing–review and editing. GJ: Supervision, Writing–review and editing, Validation. XW: Conceptualization, Project administration, Writing–review and editing. BZ: Conceptualization, Funding acquisition, Project administration, Writing–review and editing.

Funding

The author(s) declare that financial support was received for the research, authorship, and/or publication of this article. This study was supported by Shandong Province Integrated Traditional Chinese and Western Medicine Professional Disease Prevention and Control Project (No. YXH2019ZXY010).

Acknowledgments

We would like to thank Experimental Center of Shandong University of Traditional Chinese Medicine for the technical support and assistance.

Conflict of interest

The authors declare that the research was conducted in the absence of any commercial or financial relationships that could be construed as a potential conflict of interest.

Publisher's note

All claims expressed in this article are solely those of the authors and do not necessarily represent those of their affiliated organizations, or those of the publisher, the editors and the reviewers. Any product that may be evaluated in this article, or claim that may be made by its manufacturer, is not guaranteed or endorsed by the publisher.

Supplementary material

The Supplementary Material for this article can be found online at: https://www.frontiersin.org/articles/10.3389/fphar.2024.1437475/full#supplementary-material

References

Atkinson, T. P., Balish, M. F., and Waites, K. B. (2008). Epidemiology, clinical manifestations, pathogenesis and laboratory detection of Mycoplasma pneumoniae infections. *FEMS Microbiol. Rev.* 32 (6), 956–973. doi:10.1111/j.1574-6976.2008.00129.x

Balish, M. F. (2006). Subcellular structures of mycoplasmas. *Front. Biosci.* 11, 2017–2027. doi:10.2741/1943

Bittencourt-Mernak, M. I., Pinheiro, N. M., da Silva, R. C., Ponci, V., Banzato, R., Pinheiro, A., et al. (2021). Effects of Eugenol and dehydrodieugenol B from nectandra leucantha against lipopolysaccharide (LPS)-Induced experimental acute lung inflammation. *J. Nat. Prod.* 84 (8), 2282–2294. doi:10.1021/acs.jnatprod.1c00386

Bose, S., Segovia, J. A., Somarajan, S. R., Chang, T. H., Kannan, T. R., and Baseman, J. B. (2014). ADP-ribosylation of NLRP3 by Mycoplasma pneumoniae CARDS toxin regulates inflammasome activity. *mBio* 5 (6). doi:10.1128/mBio.02186-14

Byrne, A. J., Mathie, S. A., Gregory, L. G., and Lloyd, C. M. (2015). Pulmonary macrophages: key players in the innate defence of the airways. *Thorax* 70 (12), 1189–1196. doi:10.1136/thoraxjnl-2015-207020

Calus, D., Maes, D., Vranckx, K., Villareal, I., Pasmans, F., and Haesebrouck, F. (2010). Validation of ATP luminometry for rapid and accurate titration of Mycoplasma hyopneumoniae in Friis medium and a comparison with the color changing units assay. *J. Microbiol. Methods* 83 (3), 335–340. doi:10.1016/j.mimet.2010.09.001

Chen, J. J., Deng, J. S., Huang, C. C., Li, P. Y., Liang, Y. C., Chou, C. Y., et al. (2019). p-Coumaric-Acid-Containing adenostemma lavenia ameliorates acute lung injury by activating AMPK/Nrf2/HO-1 signaling and improving the anti-oxidant response. *Am. J. Chin. Med.* 47 (7), 1483–1506. doi:10.1142/s0192415x19500769

Chosa, H., Toda, M., Okubo, S., Hara, Y., and Shimamura, T. (1992). Antimicrobial and microbicidal activities of tea and catechins against Mycoplasma. *Kansenshogaku Zasshi* 66 (5), 606–611. doi:10.11150/kansenshogakuzasshi1970.66.606

Colunga Biancatelli, R. M. L., Berrill, M., Catravas, J. D., and Marik, P. E. (2020). Quercetin and vitamin C: an experimental, synergistic therapy for the prevention and treatment of SARS-CoV-2 related disease (COVID-19). *Front. Immunol.* 11, 1451. doi:10.3389/fimmu.2020.01451

Dai, Z., Liu, W. C., Chen, X. Y., Wang, X., Li, J. L., and Zhang, X. (2023). Gasdermin D-mediated pyroptosis: mechanisms, diseases, and inhibitors. *Front. Immunol.* 14, 1178662. doi:10.3389/fimmu.2023.1178662

Deng, F., Cao, H. L., Liang, X. H., Li, Q. B., Yang, Y., Zhao, Z. H., et al. (2023). Analysis of cytokine levels, cytological findings, and MP-DNA level in bronchoalveolar lavage fluid of children with Mycoplasma pneumoniae pneumonia. *Immun. Inflamm. Dis.* 11 (5), e849. doi:10.1002/iid3.849

Dick, M. S., Sborgi, L., Rühl, S., Hiller, S., and Broz, P. (2016). ASC filament formation serves as a signal amplification mechanism for inflammasomes. *Nat. Commun.* 7, 11929. doi:10.1038/ncomms11929

Ding, X., Kambara, H., Guo, R., Kanneganti, A., Acosta-Zaldívar, M., Li, J., et al. (2021). Inflammasome-mediated GSDMD activation facilitates escape of Candida albicans from macrophages. *Nat. Commun.* 12 (1), 6699. doi:10.1038/s41467-021-27034-9

Dou, Y. Q., Ma, T., Li, Z. J., Ma, X. R., Zhang, C. J., Guo, Q. N., et al. (2024). Buyang Huanwu Decoction promotes arteriogenesis after hindlimb ischemia in mice by activating PDGF signaling pathway. *Zhongguo Zhong Yao Za Zhi* 49 (1), 216–223. doi:10.19540/j.cnki.cjcmm.20230919.402

Dunn, K. W., Kamocka, M. M., and McDonald, J. H. (2011). A practical guide to evaluating colocalization in biological microscopy. *Am. J. Physiol. Cell Physiol.* 300 (4), C723–C742. doi:10.1152/ajpcell.00462.2010

Elken, E. M., Tan, Z. N., Wang, Q., Jiang, X. Y., Wang, Y., Wang, Y. M., et al. (2022). Impact of sub-MIC Eugenol on *Klebsiella pneumoniae* biofilm formation via upregulation of rcsB. *Front. Vet. Sci.* 9, 945491. doi:10.3389/fvets.2022.945491

Fan, E. K. Y., and Fan, J. (2018). Regulation of alveolar macrophage death in acute lung inflammation. *Respir. Res.* 19 (1), 50. doi:10.1186/s12931-018-0756-5

Fu, J., and Wu, H. (2023). Structural mechanisms of NLRP3 inflammasome assembly and activation. *Annu. Rev. Immunol.* 41, 301–316. doi:10.1146/annurev-immunol-081022-021207

Hardy, R. D., Coalson, J. J., Peters, J., Chaparro, A., Techasaensiri, C., Cantwell, A. M., et al. (2009). Analysis of pulmonary inflammation and function in the mouse and baboon after exposure to Mycoplasma pneumoniae CARDS toxin. *PLoS One* 4 (10), e7562. doi:10.1371/journal.pone.0007562

Haute, G. V., Luft, C., Antunes, G. L., Silveira, J. S., de Souza Basso, B., da Costa, M. S., et al. (2020). Anti-inflammatory effect of octyl gallate in alveolar macrophages cells and mice with acute lung injury. *J. Cell Physiol.* 235 (9), 6073–6084. doi:10.1002/jcp.29536

He, J., Liu, M., Ye, Z., Tan, T., Liu, X., You, X., et al. (2016). Insights into the pathogenesis of mycoplasma pneumoniae (review). *Mol. Med. Rep.* 14 (5), 4030–4036. doi:10.3892/mmr.2016.5765

Hsiung, J. C. C., Ma, H. Y., Lu, C. Y., Yen, T. Y., Chi, H., Liau, Y. J., et al. (2022). Children with Mycoplasma pneumoniae infection in Taiwan: changes in molecular characteristics and clinical outcomes. *J. Formos. Med. Assoc.* 121 (11), 2273–2280. doi:10.1016/j.jfma.2022.05.001

Huo, J., Wang, T., Wei, B., Shi, X., Yang, A., Chen, D., et al. (2022). Integrated network pharmacology and intestinal flora analysis to determine the protective effect of Xuanbai-Chengqi decoction on lung and gut injuries in influenza virus-infected mice. *J. Ethnopharmacol.* 298, 115649. doi:10.1016/j.jep.2022.115649

Isazadeh, A., Heris, J. A., Shahabi, P., Mohammadinasab, R., Shomali, N., Nasiri, H., et al. (2023). Pattern-recognition receptors (PRRs) in SARS-CoV-2. *Life Sci.* 329, 121940. doi:10.1016/j.lfs.2023.121940

Jacobs, E., Ehrhardt, I., and Dumke, R. (2015). New insights in the outbreak pattern of Mycoplasma pneumoniae. *Int. J. Med. Microbiol.* 305 (7), 705–708. doi:10.1016/j.ijmm.2015.08.021

Ji, L., Song, T., Ge, C., Wu, Q., Ma, L., Chen, X., et al. (2023). Identification of bioactive compounds and potential mechanisms of scutellariae radix-coptidis rhizoma in the treatment of atherosclerosis by integrating network pharmacology and experimental validation. *Biomed. Pharmacother.* 165, 115210. doi:10.1016/j.biopha.2023.115210

Jiang, Z. L., Li, S. H., Zhu, C. M., Zhou, R. J., and Leung, P. H. M. (2021). Mycoplasma pneumoniae infections: pathogenesis and vaccine development. *Pathogens* 10 (2), 119. doi:10.3390/pathogens10020119

Jo, E. K., Kim, J. K., Shin, D. M., and Sasakawa, C. (2016). Molecular mechanisms regulating NLRP3 inflammasome activation. *Cell Mol. Immunol.* 13 (148), 159. doi:10.1038/cmi.2015.95

Kannan, T. R., Provenzano, D., Wright, J. R., and Baseman, J. B. (2005). Identification and characterization of human surfactant protein A binding protein of Mycoplasma pneumoniae. *Infect. Immun.* 73 (5), 2828–2834. doi:10.1128/iai.73.5.2828-2834.2005

Kaya, S., Albayrak Kaya, S., Polat, E., Fidanol Erboğa, Z., Duran, Y., Polat, F. R., et al. (2019). Protective effects of hesperetin on lipopolysaccharide-induced acute lung injury in a rat model. *Turk Gogus Kalp Damar Cerrahisi Derg.* 28 (2), 359–368. doi:10.5606/tgkdc.dergisi.2020.18816

Kayagaki, N., Wong, M. T., Stowe, I. B., Ramani, S. R., Gonzalez, L. C., Akashi-Takamura, S., et al. (2013). Noncanonical inflammasome activation by intracellular LPS independent of TLR4. *Science* 341 (6151), 1246–1249. doi:10.1126/science.1240248

Kennedy-Feitosa, E., Okuro, R. T., Pinho Ribeiro, V., Lanzetti, M., Barroso, M. V., Zin, W. A., et al. (2016). Eucalyptol attenuates cigarette smoke-induced acute lung inflammation and oxidative stress in the mouse. *Pulm. Pharmacol. Ther.* 41, 11–18. doi:10.1016/j.pupt.2016.09.004

Kim, K., Jung, S., Kim, M., Park, S., Yang, H. J., and Lee, E. (2022). Global trends in the proportion of macrolide-resistant mycoplasma pneumoniae infections: a systematic review and meta-analysis. *JAMA Netw. Open* 5 (7), e2220949. doi:10.1001/jamanetworkopen.2022.20949

Knoll, R., Schultze, J. L., and Schulte-Schrepping, J. (2021). Monocytes and macrophages in COVID-19. *Front. Immunol.* 12, 720109. doi:10.3389/fimmu.2021.720109

Krause, D. C. (1998). Mycoplasma pneumoniae cytadherence: organization and assembly of the attachment organelle. *Trends Microbiol.* 6 (1), 15–18. doi:10.1016/s0966-842x(97)01168-2

Kumar, S. (2018). Mycoplasma pneumoniae: a significant but underrated pathogen in paediatric community-acquired lower respiratory tract infections. *Indian J. Med. Res.* 147, 23–31. doi:10.4103/ijmr.IJMR_1582_16

Kumar, S., and Kumar, S. (2023). Mycoplasma pneumoniae: among the smallest bacterial pathogens with great clinical significance in children. *Indian J. Med. Microbiol.* 46, 100480. doi:10.1016/j.ijmmb.2023.100480

Kuo, M. Y., Liao, M. F., Chen, F. L., Li, Y. C., Yang, M. L., Lin, R. H., et al. (2011). Luteolin attenuates the pulmonary inflammatory response involves abilities of antioxidation and inhibition of MAPK and NFκB pathways in mice with endotoxin-induced acute lung injury. *Food Chem. Toxicol.* 49 (10), 2660–2666. doi:10.1016/j.fct.2011.07.012

Lee, K. L., Lee, C. M., Yang, T. L., Yen, T. Y., Chang, L. Y., Chen, J. M., et al. (2021). Severe Mycoplasma pneumoniae pneumonia requiring intensive care in children, 2010-2019. *J. Formos. Med. Assoc.* 120 (1 Pt 1), 281–291. doi:10.1016/j.jfma.2020.08.018

Leng, M., Yang, J., and Zhou, J. (2023). The molecular characteristics, diagnosis, and treatment of macrolide-resistant Mycoplasma pneumoniae in children. *Front. Pediatr.* 11, 1115009. doi:10.3389/fped.2023.1115009

Li, D. M., Tang, S. H., Liao, Q., Chen, W., and Zhang, H. C. (2017). Literature study on prevention and treatment of community acquired pneumonia by traditional Chinese medicine. *Zhongguo Zhong Yao Za Zhi* 42 (8), 1418–1422. doi:10.19540/j.cnki.cjcmm.2017.0037

Li, G., Fan, L., Wang, Y., Huang, L., Wang, M., Zhu, C., et al. (2019). High co-expression of TNF-α and CARDS toxin is a good predictor for refractory Mycoplasma pneumoniae pneumonia. *Mol. Med.* 25 (1), 38. doi:10.1186/s10020-019-0105-2

Li, Y., Huang, H., Liu, B., Zhang, Y., Pan, X., Yu, X. Y., et al. (2021). Inflammasomes as therapeutic targets in human diseases. *Signal Transduct. Target Ther* 6 (1), 247. doi:10.1038/s41392-021-00650-z

Li, Z., Li, D., Chen, R., Gao, S., Xu, Z., and Li, N. (2023). Cell death regulation: a new way for natural products to treat osteoporosis. *Pharmacol. Res.* 187, 106635. doi:10.1016/j.phrs.2022.106635

Lin, Y., Tan, D., Kan, Q., Xiao, Z., and Jiang, Z. (2018). The protective effect of Naringenin on airway remodeling after mycoplasma pneumoniae infection by inhibiting autophagy-mediated lung inflammation and fibrosis. *Mediat. Inflamm.* 2018, 8753894. doi:10.1155/2018/8753894

Liu, X., Xia, S., Zhang, Z., Wu, H., and Lieberman, J. (2021). Channelling inflammation: gasdermins in physiology and disease. *Nat. Rev. Drug. Discov.* 20 (5), 384–405. doi:10.1038/s41573-021-00154-z

Liu, X., Lin, Z., and Yin, X. (2022). Pellino2 accelerate inflammation and pyroptosis via the ubiquitination and activation of NLRP3 inflammation in model of pediatric pneumonia. *Int. Immunopharmacol.* 110, 108993. doi:10.1016/j.intimp.2022.108993

Lopez-Castejon, G., and Brough, D. (2011). Understanding the mechanism of IL-1β secretion. *Cytokine Growth Factor Rev.* 22 (4), 189–195. doi:10.1016/j.cytogfr.2011.10.001

Lou, Y., Ma, M., Jiang, Y., Xu, H., Gao, Z., Gao, L., et al. (2022). Ferroptosis: a new strategy for traditional Chinese medicine treatment of stroke. *Biomed. Pharmacother.* 156, 113806. doi:10.1016/j.biopha.2022.113806

Luo, H., He, J., Qin, L., Chen, Y., Chen, L., Li, R., et al. (2021). Mycoplasma pneumoniae lipids license TLR-4 for activation of NLRP3 inflammasome and autophagy to evoke a proinflammatory response. *Clin. Exp. Immunol.* 203 (1), 66–79. doi:10.1111/cei.13510

Man, S. M., and Kanneganti, T. D. (2015). Regulation of inflammasome activation. *Immunol. Rev.* 265 (1), 6–21. doi:10.1111/imr.12296

Malik, A., and Kanneganti, T. D. (2017). Inflammasome activation and assembly at a glance. *J. Cell Sci.* 130 (23), 3955–3963. doi:10.1242/jcs.207365

Narita, M. (2010). Pathogenesis of extrapulmonary manifestations of Mycoplasma pneumoniae infection with special reference to pneumonia. *J. Infect. Chemother.* 16 (3), 162–169. doi:10.1007/s10156-010-0044-x

Narita, M., Tanaka, H., Abe, S., Yamada, S., Kubota, M., and Togashi, T. (2000). Close association between pulmonary disease manifestation in Mycoplasma pneumoniae infection and enhanced local production of interleukin-18 in the lung, independent of gamma interferon. *Clin. Diagn. Lab. Immunol.* 7 (6), 909–914. doi:10.1128/CDLI.7.6.909-914.2000

Okubo, Y., Michihata, N., Morisaki, N., Uda, K., Miyairi, I., Ogawa, Y., et al. (2018). Recent trends in practice patterns and impact of corticosteroid use on pediatric Mycoplasma pneumoniae-related respiratory infections. *Respir. Investig.* 56 (2), 158–165. doi:10.1016/j.resinv.2017.11.005

Pan, P., Shen, M., Yu, Z., Ge, W., Chen, K., Tian, M., et al. (2021). SARS-CoV-2 N protein promotes NLRP3 inflammasome activation to induce hyperinflammation. *Nat. Commun.* 12 (1), 4664. doi:10.1038/s41467-021-25015-6

Razin, S., and Hayflick, L. (2010). Highlights of mycoplasma research--an historical perspective. *Biologicals* 38 (2), 183–190. doi:10.1016/j.biologicals.2009.11.008

Seoane, P. I., Lee, B., Hoyle, C., Yu, S., Lopez-Castejon, G., Lowe, M., et al. (2020). The NLRP3-inflammasome as a sensor of organelle dysfunction. *J. Cell Biol.* 219 (12), e202006194. doi:10.1083/jcb.202006194

Shi, J., Zhao, Y., Wang, K., Shi, X., Wang, Y., Huang, H., et al. (2015). Cleavage of GSDMD by inflammatory caspases determines pyroptotic cell death. *Nature* 526 (7575), 660–665. doi:10.1038/nature15514

Song, J., Zhang, L., Xu, Y., Yang, D., Zhang, L., Yang, S., et al. (2021). The comprehensive study on the therapeutic effects of baicalein for the treatment of COVID-19 *in vivo* and *in vitro*. *Biochem. Pharmacol.* 183, 114302. doi:10.1016/j.bcp.2020.114302

Song, Z., Jia, G., Luo, G., Han, C., Zhang, B., and Wang, X. (2023). Global research trends of Mycoplasma pneumoniae pneumonia in children: a bibliometric analysis. *Front. Pediatr.* 11, 1306234. doi:10.3389/fped.2023.1306234

Souza, T. N., Santos, F. M., Alves, P. R., Ferro, J. N., Correia, A. C. C., Melo, T. S., et al. (2021). Local administration of p-coumaric acid decreases lipopolysaccharide-induced acute lung injury in mice: *in vitro* and *in silico* studies. *Eur. J. Pharmacol.* 897, 173929. doi:10.1016/j.ejphar.2021.173929

Sun, J. H., Sun, F., Yan, B., Li, J. Y., and Xin, L. (2020). Data mining and systematic pharmacology to reveal the mechanisms of traditional Chinese medicine in Mycoplasma pneumoniae pneumonia treatment. *Biomed. Pharmacother.* 125, 109900. doi:10.1016/j.biopha.2020.109900

Sun, Y. L., Zhao, P. P., Zhu, C. B., Jiang, M. C., Li, X. M., Tao, J. L., et al. (2023). Integrating metabolomics and network pharmacology to assess the effects of quercetin on lung inflammatory injury induced by human respiratory syncytial virus. *Sci. Rep.* 13 (1), 8051. doi:10.1038/s41598-023-35272-8

Tanaka, T., Oishi, T., Miyata, I., Wakabayashi, S., Kono, M., Ono, S., et al. (2017). Macrolide-Resistant mycoplasma pneumoniae infection, Japan, 2008-2015. *Emerg. Infect. Dis.* 23 (10), 1703–1706. doi:10.3201/eid2310.170106

Techasaensiri, C., Tagliabue, C., Cagle, M., Iranpour, P., Katz, K., Kannan, T. R., et al. (2010). Variation in colonization, ADP-ribosylating and vacuolating cytotoxin, and pulmonary disease severity among mycoplasma pneumoniae strains. *Am. J. Respir. Crit. Care Med.* 182 (6), 797–804. doi:10.1164/rccm.201001-0080OC

Tong, L., Huang, S., Zheng, C., Zhang, Y., and Chen, Z. (2022). Refractory mycoplasma pneumoniae pneumonia in children: early recognition and management. *J. Clin. Med.* 11 (10), 2824. doi:10.3390/jcm11102824

Tsai, T. A., Tsai, C. K., Kuo, K. C., and Yu, H. R. (2021). Rational stepwise approach for Mycoplasma pneumoniae pneumonia in children. *J. Microbiol. Immunol. Infect.* 54 (4), 557–565. doi:10.1016/j.jmii.2020.10.002

Vázquez-Laslop, N., and Mankin, A. S. (2018). How macrolide antibiotics work. *Trends Biochem. Sci.* 43 (9), 668–684. doi:10.1016/j.tibs.2018.06.011

Vora, S. M., Lieberman, J., and Wu, H. (2021). Inflammasome activation at the crux of severe COVID-19. *Nat. Rev. Immunol.* 21 (11), 694–703. doi:10.1038/s41577-021-00588-x

Wang, N., Geng, C., Sun, H., Wang, X., Li, F., and Liu, X. (2019). Hesperetin ameliorates lipopolysaccharide-induced acute lung injury in mice through regulating the TLR4-MyD88-NF-κB signaling pathway. *Arch. Pharm. Res.* 42 (12), 1063–1070. doi:10.1007/s12272-019-01200-6

Wang, Y., Ye, Q., Yang, D., Ni, Z., and Chen, Z. (2016). Study of two separate types of macrolide-resistant mycoplasma pneumoniae outbreaks. *Antimicrob. Agents Chemother.* 60 (7), 4310–4314. doi:10.1128/aac.00198-16

Xiong, S., Hong, Z., Huang, L. S., Tsukasaki, Y., Nepal, S., Di, A., et al. (2020). IL-1β suppression of VE-cadherin transcription underlies sepsis-induced inflammatory lung injury. *J. Clin. Invest.* 130 (7), 3684–3698. doi:10.1172/JCI136908

Xu, L., Wang, H., Yu, Q. Q., Ge, J. R., Zhang, X. Z., Mei, D., et al. (2021). The monomer derivative of paeoniflorin inhibits macrophage pyroptosis via regulating TLR4/NLRP3/GSDMD signaling pathway in adjuvant arthritis rats. *Int. Immunopharmacol.* 101 (Pt A), 108169. doi:10.1016/j.intimp.2021.108169

Xu, X., Zhang, W., Huang, C., Li, Y., Yu, H., Wang, Y., et al. (2012). A novel chemometric method for the prediction of human oral bioavailability. *Int. J. Mol. Sci.* 13 (6), 6964–6982. doi:10.3390/ijms13066964

Yang, D., He, Y., Muñoz-Planillo, R., Liu, Q., and Núñez, G. (2015). Caspase-11 Requires the Pannexin-1 Channel and the Purinergic P2X7 Pore to Mediate Pyroptosis and Endotoxic Shock. *Immunity* 43 (5), 923–932. doi:10.1016/j.immuni.2015.10.009

Yin, M., Marrone, L., Peace, C. G., and O'Neill, L. A. J. (2023). NLRP3, the inflammasome and COVID-19 infection. *Qjm* 116 (7), 502–507. doi:10.1093/qjmed/hcad011

Yang, J., Hooper, W. C., Phillips, D. J., and Talkington, D. F. (2004). Cytokines in Mycoplasma pneumoniae infections. *Cytokine Growth Factor Rev.* 15 (2–3), 157–168. doi:10.1016/j.cytogfr.2004.01.001

You, J., Zhou, L., San, X., Li, H., Li, M., and Wang, B. (2023). NEDD4 regulated pyroptosis occurred from Co-infection between influenza A virus and Streptococcus pneumoniae. *J. Microbiol.* 61 (8), 777–789. doi:10.1007/s12275-023-00076-y

Zheng, C., Pei, T., Huang, C., Chen, Y., Bai, M., and Xue, J. (2016). A novel systems pharmacology platform to dissect action mechanisms of traditional Chinese medicines for bovine viral diarrhea disease. *Eur. J. Pharm. Sci.* 94, 33–45. doi:10.1016/j.ejps.2016.05.018

Zhang, C., Li, N., and Niu, F. (2019). Baicalein triazole prevents respiratory tract infection by RSV through suppression of oxidative damage. *Microb. Pathog.* 131, 227–233. doi:10.1016/j.micpath.2019.03.026

Zhang, H., Luan, Y., Jing, S., Wang, Y., Gao, Z., Yang, P., et al. (2020). Baicalein mediates protection against Staphylococcus aureus-induced pneumonia by inhibiting the coagulase activity of vWbp. *Biochem. Pharmacol.* 178, 114024. doi:10.1016/j.bcp.2020.114024

Zhang, X., Li, M., Wu, H., Fan, W., Zhang, J., Su, W., et al. (2022). Naringenin attenuates inflammation, apoptosis, and ferroptosis in silver nanoparticle-induced lung injury through a mechanism associated with Nrf2/HO-1 axis: *in vitro* and *in vivo* studies. *Life Sci.* 311 (Pt A), 121127. doi:10.1016/j.lfs.2022.121127

Zhang, Z. T., Zhang, D. Y., Xie, K., Wang, C. J., and Xu, F. (2021). Luteolin activates Tregs to promote IL-10 expression and alleviating caspase-11-dependent pyroptosis in sepsis-induced lung injury. *Int. Immunopharmacol.* 99, 107914. doi:10.1016/j.intimp.2021.107914

Zhao, C., Sun, J., Fang, C., and Tang, F. (2014). 1,8-cineol attenuates LPS-induced acute pulmonary inflammation in mice. *Inflammation* 37 (2), 566–572. doi:10.1007/s10753-013-9770-4

Zhao, C., and Zhao, W. (2020). NLRP3 inflammasome-a key player in antiviral responses. *Front. Immunol.* 11, 211. doi:10.3389/fimmu.2020.00211

Zheng, W., Wu, H., Wang, T., Zhan, S., and Liu, X. (2021). Quercetin for COVID-19 and DENGUE co-infection: a potential therapeutic strategy of targeting critical host signal pathways triggered by SARS-CoV-2 and DENV. *Brief. Bioinform* 22 (6), bbab199. doi:10.1093/bib/bbab199

Zou, Y., Wang, H., Fang, J., Sun, H., Deng, X., Wang, J., et al. (2023). Isorhamnetin as a novel inhibitor of pneumolysin against Streptococcus pneumoniae infection *in vivo*/*in vitro*. *Microb. Pathog.* 185, 106382. doi:10.1016/j.micpath.2023.106382

Glossary

ADPRT	ADP-ribosyltransferase
AIM2	absent in melanoma 2
ALRs	AIM2-like receptors
AZM	azithromycin
BSL-2	biosafety level-2
CAP	community-acquired pneumonia
CARDS TX	community-acquired respiratory distress syndrome toxin
CCU	color change units
DAMPs	damage-associated molecular patterns
FBS	fetal bovine serum
GSDMD	gasdermin D
GSDMD-NT	gasdermin D-N-terminal fragment
IFN-γ	interferon-γ
IL-1β	interleukin-1β
IL-18	interleukin-18
IL-1R	IL-1 receptor
LV	lentiviral
MP	Mycoplasma pneumoniae
MPP	Mycoplasma pneumoniae pneumonia
NLRs	NOD-like receptors
OB	oral bioavailability
OD	optical density
PAMPs	pathogen-associated molecular patterns
PCC	Pearson's correlation coefficient
PRRs	pattern recognition receptors
qPCR	quantitative real-time PCR
SEM	scanning electron microscope
TCM	traditional Chinese medicine
TIC	total ion chromatogram
TNF-α	tumor necrosis factor-α
TSA	tyramide signal amplification
WB	western blot
YQQFG	Yinqin Qingfei granules

frontiers | Frontiers in Pharmacology

TYPE Original Research
PUBLISHED 19 September 2024
DOI 10.3389/fphar.2024.1455126

Check for updates

OPEN ACCESS

EDITED BY
Marcello Iriti,
University of Milan, Italy

REVIEWED BY
Shafiq Ur Rahman,
Shenzhen Graduate School, Peking University, China
Songül KARAKAYA,
Atatürk University, Türkiye
Mustafa Karaköse,
Giresun University, Türkiye

*CORRESPONDENCE
Mirutse Giday,
mirutse.giday@aau.edu.et

RECEIVED 26 June 2024
ACCEPTED 28 August 2024
PUBLISHED 19 September 2024

CITATION
Nuro G, Tolossa K, Arage M and Giday M (2024) Medicinal plants diversity among the oromo community in heban-arsi district of Ethiopia used to manage human and livestock ailments. *Front. Pharmacol.* 15:1455126. doi: 10.3389/fphar.2024.1455126

COPYRIGHT
© 2024 Nuro, Tolossa, Arage and Giday. This is an open-access article distributed under the terms of the Creative Commons Attribution License (CC BY). The use, distribution or reproduction in other forums is permitted, provided the original author(s) and the copyright owner(s) are credited and that the original publication in this journal is cited, in accordance with accepted academic practice. No use, distribution or reproduction is permitted which does not comply with these terms.

Medicinal plants diversity among the oromo community in heban-arsi district of Ethiopia used to manage human and livestock ailments

Geritu Nuro, Ketema Tolossa, Mahlet Arage and Mirutse Giday*

Aklilu Lemma Institute of Pathobiology, Addis Ababa University, Addis Ababa, Ethiopia

Introduction: Medicinal plants are commonly employed mainly due their accessibility, affordability and potency. However, medicinal plants and the associated knowledge are disappearing at an alarming rate due to natural and anthropogenic causes and thus a need for their proper documentation conservation. This study was performed to document traditional knowledge related to use of medicinal plants in Heban-Arsi district, West-Arsi Zone, Oromia Regional State, Ethiopia.

Methods: Interviews were conducted with 185 informants to identify medicinal plants used in traditional therapies in the study area. Informant consensus factor (ICF), rank order priority (ROP) values were computed, and preference ranking exercises were performed to assess the relative importance of medicinal plants. Descriptive and inferential statistics were used to measure and compare medicinal plants knowledge between social groups.

Results: A total of 120 medicinal plants were identified for being used to treat different human and animal illnesses in the study area. Most of the medicinal plants (76.4%) were uncultivated ones obtained from different habitats. Leaf was the most frequently used plant part constituting 62.6% of preparations. Oral was the most commonly used route of remedy administration (46%) in treating diseases. Gastrointestinal ailments category had the highest ICF value (0.83). In the study area, the highest rank order priority (ROP) values were recorded for *Dombeya torrida* (J.F. Gmel.), *Artemisia absinthium* L., *Balanites aegyptiaca* (L.) Del., *Combretum pisoniiflorum* Klotzsch) Engl., *Celtis africana* Burm. f, *Ocimum gratissimum* L. and *Lagenaria* sp. for their uses against snake poison, tuberculosis, liver disorder, stomachache, tuberculosis, febrile illness and liver disorder, respectively, each scoring a value of 100. Significant differences in medicinal plant use knowledge were recorded between male and female informants of different educational level, age and experience. Anthropogenic factors were the primary threats to medicinal plants in the area.

Conclusion: The study area was found to be rich in medicinal plants that are useful in treating a wide range of human and animal illnesses. In future

Abbreviations: **AAU**, Addis Ababa University; **ALIPB**, Aklilu Lemma Institute of Pathobiology; **ALIPB-IRERC**, Aklilu Lemma Institute of Pathobiology Institutional Research Ethics Review Committee; **CSA**, Central Statistics Agency; **FL**, Fidelity level; **ICF**, Informant consensus factor; **ROP**, Rank order priority; **RPL**, relative popularity level; **WHO**, World Health Organization

pharmacological and phytochemical investigations, priority needs to be given to medicinal plants of the highest ROP values and those that were reported against ailment categories scoring the highest ICF values.

KEYWORDS

medicinal plants, traditional knowledge, traditional healers, general informants, Heban-Arsi district, Ethiopia

1 Introduction

Historically, humans have relied on nature to provide for their basic needs, including the use of plants as medicine to treat a variety of illnesses (Cragg and Newman, 2013). The World Health Organization estimates that 80% of people in developing countries receive their medical care from traditional medicines, most of which are made from plants (Rasul, 2018) due to the fact that the majority of individuals residing in developing nations inhabit rural regions with limited availability of modern healthcare facilities (World Health Organization, 2001). Furthermore, due to problems related to antimicrobial resistance to chemical drugs, affordability and accessibility, traditional medicines are still considered important and sustainable sources of treatment (Patwardhan, 2005). Researchers are thus compelled to explore compounds with potential antimicrobial properties derived from natural sources, specifically from traditionally utilized medicinal plants (Dhama et al., 2014; Dilbato et al., 2019). Medicinal plants are rich sources of pharmaceutical and therapeutic products because they can synthesize chemicals through secondary metabolism that have antibacterial properties (Reddy et al., 2022). Plant products consist of a variety of constituents that are chemically complex mixtures with various potential targets and modes of action (Mickymaray, 2019; Efferth and Koch, 2011). The distinct attributes possessed by plants, such as their abundant diversity of chemical compounds (Gurib-Fakim, 2006), established therapeutic effectiveness of their extracts in longstanding traditional medical practices worldwide (Yang et al., 2014), their widespread availability, and the potential for mutually synergetic effects between phytochemicals (Caesar and Cech, 2019), have positioned them as the preferred choice especially for addressing the issue of drug resistance.

Traditional medicine has been practiced in Ethiopia since antiquity and hence it has permeated all social groups, and continues to be important to both human and animal health (Giday et al., 2003; Kefalew et al., 2015). This could be because it is associated with spiritual, historical, or social values, or because the community believes that medicinal plants can heal (Bishaw, 1991). It is postulated that approximately 80% of the rural populace in Ethiopia and roughly 90% of their livestock depend on traditional medicine for the fulfillment of fundamental healthcare requirements (Abebe, 2001). Due to the heterogeneous nature of its ethnic communities, the extensive utilization of conventional therapeutic plant medicine throughout an extended duration, and diverse topography, Ethiopia harbors an extensive repository of traditional medicinal plants and indigenous wisdom. So far, 887 plant taxa have been reported to be used to treat various health problems in the country (Mesfin et al., 2009; Kidane et al., 2014).

Like other developing countries, Ethiopian plant resources, including medicinal plants (Asfaw and Tadesse, 2001) and related indigenous knowledge have been disappearing at an alarming rate (Regassa, 2013; Mesfin et al., 2014) mainly because of habitat loss, forest deforestation, excessive use of forest resources, population growth, poverty and illegal trade (Giday et al., 2003; Lulekal et al., 2008; Megersa et al., 2013; Tolossa et al., 2013). The predominantly oral culture of traditional knowledge transfer is also considered to have contributed to the deterioration of traditional medical knowledge in Ethiopia. (Getahun, 1976). Traditional healers in the country often share their knowledge only with their eldest sons and most of their traditional information is kept secret (Jansen, 1991). Over the past decade, ethnobotanical research in Ethiopia has been increasing, and several studies have documented the use of plants as medicines for various human and animal diseases. (Chekole, 2017; Kebebew and Mohamed, 2017; Agize et al., 2022; Tahir et al., 2023). In the Heban-Arsi district, the local communities are known for using medicinal plants to treat various human and animal diseases. However, there has been no comprehensive ethnobotanical study conducted so far that produced an exhaustive list of medicinal plants used in the district. A better medicinal plants diversity is expected in the district as there is a protected natural forest in the area known by the name Munesa Forest and wide practice of using medicinal plants to manage different human and livestock ailments. Thus, the aim of this study was to investigate and record the traditional use of medicinal plants by the residents of Heban-Arsi district and generate baseline data for ongoing studies aimed at developing plant-based products in the country for the treatment of human and animal ailments.

2 Materials and methods

2.1 Study area

The study was conducted in Heban-Arsi district, West-Arsi Zone of Oromia Regional State, southeastern Ethiopia (Figure 1). The district is located at 7° 9′–7° 42′N and 38° 25′–38° 54′E, with an elevation ranging from 1,500 to 3,000 m above sea level (m.a.s.l.) (Heban-Arsi district Agricultural Development Office, unpublished data). The annual average rainfall of the study area is 825 mm and the mean annual temperature is 19°C (Heban-Arsi district Agricultural development Office, unpublished data). The district has three major climatic zone: highland (2,000–3,000 m.a.s.l.) with annual temperature of 10°C–18°C), midland (1,800–2,000 m.a.s.l.) with annual temperature of 15°C–22°C), and lowland (1,500–1,600 m.a.s.l.) with annual temperature of 19°C–27°C (Heban-Arsi district Agricultural development Office,

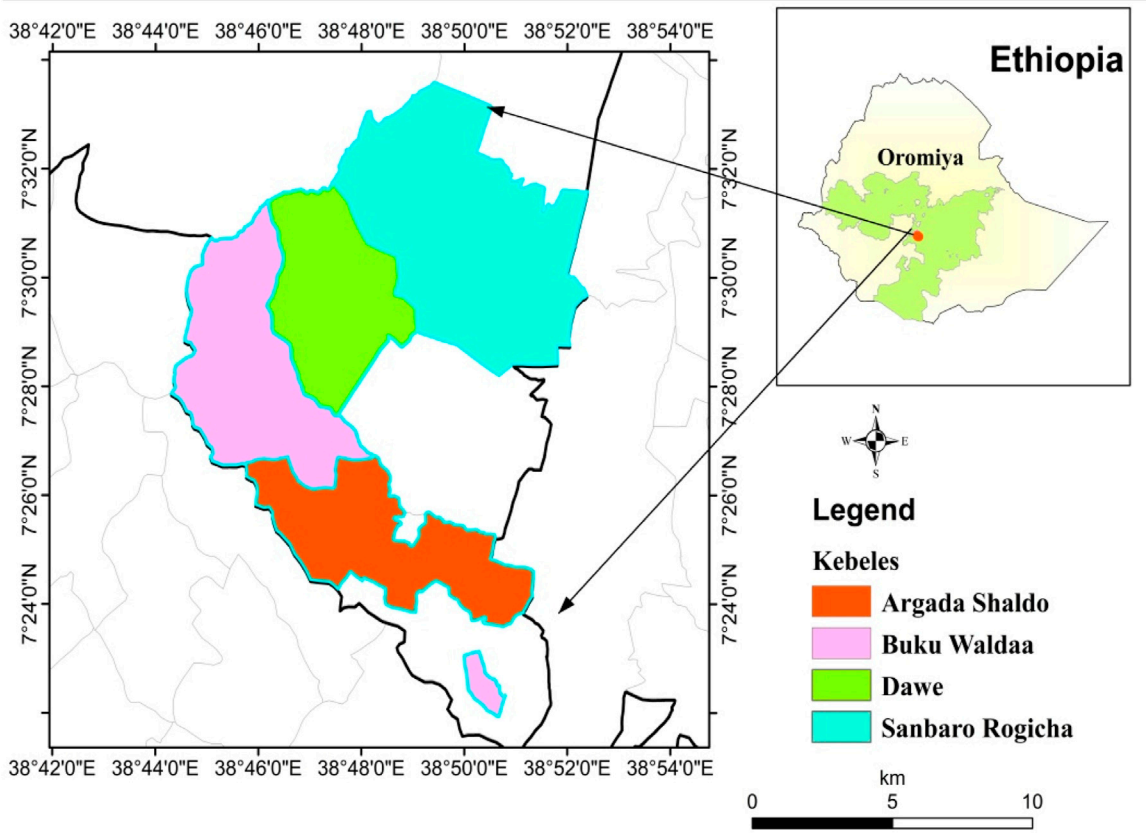


FIGURE 1
Map of Heban-Arsi district showing sampled kebeles.

TABLE 1 Study kebeles and sampled villages in the study district.

S.N.	Study kebele	Altitude (L)	Sampled villages	No. of sampled informants		
				GIs	THs	Total
1	Argada Shaldo	1701–2000 m.a.s	Koromi	21	3	24
			Argada	21	2	23
2	Sanbaro Rogicha	1600–1981 m.a.s	Rogicha	21	2	23
			Degaga	21	3	24
3	Buku Waldaa	1500–1550 m.a.s	Alembadaa	21	3	24
			Kimphe	21	2	23
4	Dawe	1501–1600 m.a.s	Langano	21	2	23
			Bishangaari	18	3	21
Grand total						185

Note: GIs, General informants; THs, Traditional Healers, m.a.s.l. = metre above sea level.

unpublished data). The district rainy period is from March to mid-September with peak in August. The district has nine kebeles (the smallest government administrative structure in Ethiopia) and three towns. According to the Central Statistics Agency (CSA) of Ethiopia, there are 75,831 people living in the district, of which 41,103 are men and 34,728 are women (CSA, 2007). Out of the total population, 94% are rural dwellers while 6% live in towns. In the district there is protected natural forest area known as Munesa Forest Enterprise. This forest is dwindling in terms of both vegetation coverage and species diversity because of land clearing for agricultural use, local

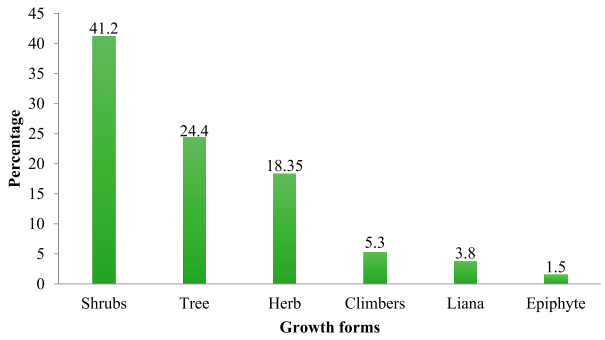


FIGURE 2
Growth forms of traditional medicinal plants.

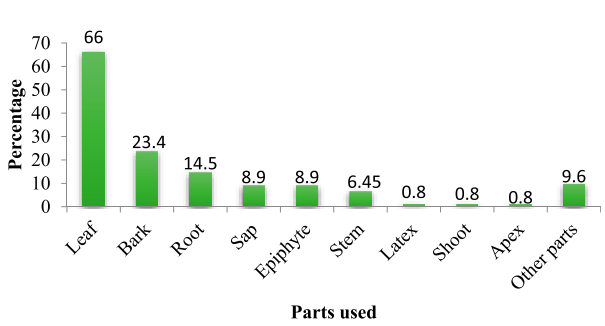


FIGURE 3
Proportions of medicinal plant parts used in remedy preparation.

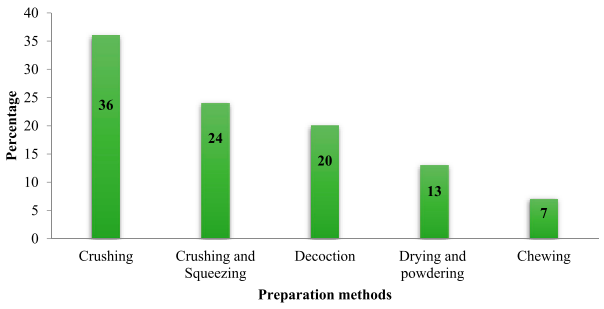


FIGURE 4
Proportions of plant remedies preparation methods.

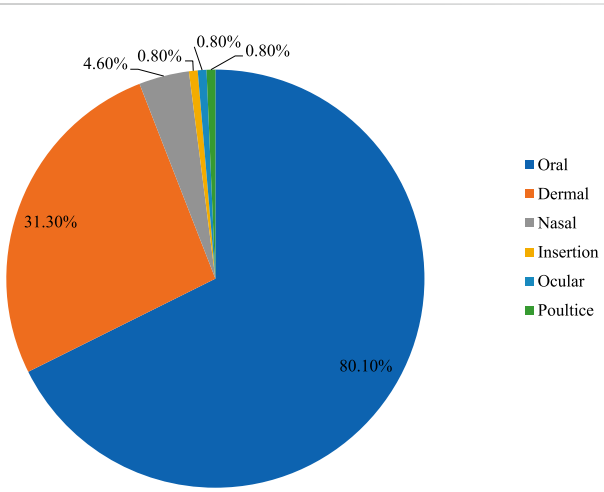


FIGURE 5
Routes of remedy administration.

timber production, collection of firewood and the production of charcoal by the local community. The district has nine health posts and three health centers. In terms of veterinary facilities, there are four veterinary clinics in the district. The district has a large population of livestock, including goats (60, 980), cattle (43,812), sheep (19,102), donkeys (19,468), horses (982), mules (919) and poultry (62,143) (Heban-Arsi district Agricultural development Office, unpublished data). The top-ten human diseases in the district are gastrointestinal disorders, skin infections, intestinal parasites, malaria, liver disorders, pneumonia, snakebite poisoning, tonsillitis, hemorrhoids and diabetes (Heban-Arsi district Healthcare Office unpublished data). Diseases that affect animals include bloat, mastitis, bovine TB, anthrax, pasterollisis, and dermatophilosis, external and internal parasites (Heban-Arsi district Agricultural development Office, unpublished data).

2.2 Study design, study sites and informants selection

A reconnaissance survey was conducted in Heban-Arsi district in September 2022 with the purpose of selecting study kebeles and informants. Accordingly, four kebeles distributed across two agro-ecological zones of the district, and known for rich plant-based traditional medical practice were purposively identified for the study with the help of elders and local authorities. Argada Shaldo and Sanbaro Rogicha kebeles were from midland agro-climatic zone and Buku Waldaa and Dawe kebeles were from lowland agro climatic zone. From each kebeles, two villages were selected for sampling (Table 1). For this study, a total of 185 informants were sampled using both random and purposive sampling methods. Of the total selected informants, 165 were general informants randomly sampled following procedures outlined in Kefalew et al. (2015) with minor modifications. The remaining twenty informants were traditional healers deliberately chosen based on suggestions provided by elders, local government officials, and health extension workers at every research site (Table 1).

2.3 Ethnobotanical data collection

Ethnobotanical data was gathered between November 2022 and September 2023. Prior to the initiation of interviews, every informant who took part in this investigation was provided with an explanation regarding the objectives of the study and assured of the utmost responsible and judicious handling of the information. The main methodologies employed for the collection of ethnobotanical data encompassed semi-structured interviews and field visits (Alexiades, 1996; Cotton, 1996; Martin, 1995). The data collection process was facilitated through the utilization of a

TABLE 2 Results of preference ranking of ten medicinal plants reported for treating human diarrhea in the study area.

Medicinal plants used for treatments of diarrhea	Informants designated A to J										Total	Rank
	A	B	C	D	E	F	G	H	I	J		
Withania somnifera (L.) Dunal	3	3	3	4	4	5	4	2	5	3	29	7
Allophylus abyssinicus Hochst. ex Benth	3	2	2	3	4	3	3	4	3	1	35	6
Vepris nobilis (Delile) Mziray	1	2	2	3	2	2	2	1	3	3	21	10
Ziziphus spina-christi (L.) Desf	2	1	2	2	3	3	2	2	3	3	23	9
Ximenia americana L	5	5	3	4	3	4	5	4	5	3	41	2
Bersama abyssinica Fresen	4	5	4	3	4	4	4	4	5	4	39	4
Syzygium guineense (willd.) DC.	4	5	3	5	5	3	4	5	5	4	43	1
Gymnanthemum amygdalinum (Del.) Sch.Bip. ex Walp	4	3	4	5	5	4	4	2	3	5	40	3
Combretum pisoniiflorum (Klotzsch) Engl	3	2	2	3	3	4	3	3	3	3	27	8
Prunus africana (Hook.f) Kalkman	4	3	4	5	5	4	4	3	2	4	38	5

TABLE 3 Results of preference ranking of ten medicinal plants reported for treating skin disease of livestock in the study area.

Medicinal plants used for the treatment of livestock skin diseases	Informants designated A to J										Total	Rank
	A	B	C	D	E	F	G	H	I	J		
Acokanthera schimperi (A.DC) Schweinf	1	2	3	2	2	3	2	4	2	4	25	9
Buddleja polystachya Fresen	3	4	3	4	5	2	3	3	3	2	32	6
Brucea antidysenterica JF. Mill	5	3	4	3	3	2	4	4	3	3	34	5
Dodonaea viscosa subsp. angustifolia (L.f.) J.G.West	5	4	4	5	4	5	5	5	5	4	46	1
Prunus africana (Hook.f) Kalkman	5	3	4	4	5	5	5	4	3	5	43	3
Maesa lanceolata Forssk	3	3	4	5	4	5	5	3	4	4	40	4
Calpurnia aurea (Aiton) Benth	4	4	4	5	5	4	5	5	3	5	44	2
Croton macrostachyus Hochst											30	7
Rhoicissus tridentata (L.f) Wild & Drummond	1	3	2	4	3	2	3	3	4	2	27	8

checklist containing predetermined interview questions. The interviews were conducted exclusively in the Afan Oromo language, the most widely spoken language in the area. During interviews, information on demographic characteristics of respondents, local names of medicinal plants used, specific parts of plants utilized, ailments against which reported medicinal plants were employed, methods of remedies preparations and administrations, prescribed doses, habits and habitats of the medicinal plants, utilization of other ingredients or additives, any notable adverse effects of remedies, use of antidotes, taboos and beliefs associated with the collection and use of plants, sources of knowledge, and methods of indigenous knowledge transferred was gathered. Information concerning current risks to medicinal plants and associated knowledge as well as any traditional preservation techniques was also obtained following known methodologies (Alexiades, 1996; Balick and Cox, 1996; Cotton, 1996). Field walks with informants were also made to note the morphology and habitats of the claimed medicinal plants (Alexiades, 1996; Cotton, 1996) in the study area. Plant specimens were collected, pressed, dried, and brought to Addis Ababa University, Aklilu Lemma Institute of Pathobiology (ALIPB). Voucher specimens were identified by botanists at ALIPB and the National Herbarium, Addis Ababa University (AAU), checked for their latest accepted names, on the website Plants of the World Online, and deposited for future reference.

2.4 Data analysis

Ethnobotanical data were compiled in Microsoft Excel spreadsheets and analyzed using SPSS version 20. The most useful information collected about medicinal plants was summarized using descriptive statistical methods, such as frequency and percentage. Preference ranking exercises were conducted on selected medicinal plants based on Martin (1995) to identify the most preferred ones. Selected key informants assigned

TABLE 4 ICF values of different human ailment categories in Heban-Arsi district.

Disease category	n_t	n_{ur}	ICF
Injury, poisoning (snake bite, insect bite/spider, animal bite/rabies) and certain other consequences of external cause	12	44	0.74
Diseases of the skin and subcutaneous tissue (hair loss, dandruff, eczema, boils, itching, ringworm, wound)	21	98	0.79
Diseases of the reproductive and genitourinary system (urination difficulty, delayed menstruation, erectile problem, syphilis and gonorrhea)	8	33	0.78
Gastrointestinal disorders (constipation, diarrhea, stomachache, toothache, indigestion, abdominal pain)	27	157	0.83
Musculoskeletal diseases and nervous disorders (arthritis, rheumatism, epilepsy)	8	22	0.66
Psychospritual diseases	6	21	0.75
Respiratory ailments (TB, pneumonia, asthma) and tonsillitis	14	43	0.69
Sensory organs diseases (eye/ear diseases)	3	6	0.60
Infectious and parasitic diseases (jaundice, hepatitis, ascariasis, tapeworm)	17	82	0.80
Malaria, discomfort, fever/body pain/headache and sudden sickness	16	71	0.78
Diseases of the circulatory system (Hemorrhoids and body swellings, Anemia, blood pressure)	7	18	0.64
Neoplasms (tumor, breast cancer, skin cancer)	6	66	0.76
Endocrine and metabolic diseases (diabetes,)	3	9	0.66

Key: n_{ur}: number of use citations in each disease category, n_t: number of species used in each category.

TABLE 5 ICF values different livestock ailment categories in Heban-Arsi District.

Disease category	n_t	n_{ur}	ICF
Bacterial infection (anthrax, pasterollosis, black leg and mastitis)	6	27	0.80
Viral diseases (rabies, African horse sickness)	4	21	0.85
Pain (eye pain)	2	9	0.87
Gastrointestinal disorders (bloat, diarrhea, stomachache)	10	80	0.88
Respiratory disease (pneumonia, Bovine TB)	3	9	0.75
Reproductive and urinary tract infection (retained placenta, urinating difficulty)	3	17	0.87
Parasitic and protozoa causes (ticks, lice, leech and babesiosis, epizootic lymphangitis)	5	18	0.76
Skin diseases (dermatological, external injuries, wound, abscess and lumpy skin disease, swelling and tumor, & fungal diseases)	14	130	0.89
Evil eye	3	11	0.80

Key: n_{ur}: number of use citations in each disease category, n_t: number of species used in each category.

values from 0 to 5 with 5 given for the most preferred and 0 for the least preferred plant species against certain diseases. The values were then summed, and ranks were assigned to each plant species. Informant consensus factor (ICF) was computed to determine the most culturally important human and livestock ailment categories in the study area and identify potentially effective medicinal plant species. Reported diseases were grouped into categories based on the International Classification of Diseases (ICD-10) by the World Health Organization (2011). Informant consensus factor was calculated using the formula, ICF = $(n_{ur} - n_t)/(n_{ur} - 1)$, where n_{ur} is the number of use reports for a particular use category and n_t is the number of taxa used for a particular use category by all informants (Heinrich et al., 1998). Informant Consensus index values range between 0 and 1. A high value (close to 1) indicates that relatively few species are used by a large proportion of healers. High ICF value is indicative of the plant's cultural importance and may show its high relevance for pharmacological studies. The relative healing potential of each reported medicinal plant used against human and livestock ailments were evaluated using an index known as rank order priority (ROP) computed based on fidelity level (FL) values, which were calculated for all reported medicinal plants using the formula: FL = Ip/Iu × 100 (Friedman et al., 1986), where Ip is the number of informants who reported the utilization of medicinal plants against a specific ailment and Iu is the total number of informants who mentioned the same plant against any ailment. Plants exhibiting comparable FL values known by varying numbers of informants could exhibit differences in their medicinal efficacy.

TABLE 6 Medicinal plants in the study area scoring an RPO value of above 90.

No.	Medicinal plants	Disease type	NP	N	FL	RPL	ROP
1	*Dombeya torrida* (J.F. Gmel.) Bamps	Snake poison	57	57	100	1	100
2	*Artemisia absinthium* L	Tuberculosis	47	47	100	1	100
3	*Balanites aegyptiaca* (L.) DelDC.	Liver disorder	46	46	100	1	100
4	Combretum pisoniiflorum (Klotzsch) Engl	Stomachache	40	40	100	1	100
5	*Celtis africana* Burm. f	Tuberculosis	38	38	100	1	100
6	*Ocimum gratissimum* L	Febrile illness	36	36	100	1	100
7	*Lagenaria* sp	Liver disorder	32	32	100	1	100
8	*Acokanthera schimperi* (A.DC). Schweinf	Malaria	61	63	96.8	1	96.8
9	*Phytolacca dodecandra* L 'Herit	Rabies	49	51	96	1	96
10	*Syzygium guineense* (willd.)DC	Stomach ache	52	56	92.8	1	92.8

Note: FL, fidelity level; RPL , relative popularity level; ROP , rank order priority; Np = number of informants who independently cited the importance of a species for treating a particular disease; N = total number of informants who reported the plant for any given disease.

TABLE 7 Comparison of medicinal plants knowledge between different social groups in the study area (n = 185).

Social group		Number of informants	Mean no of medicinal plants reported	*p*-value
Profession	Traditional healers	20	7.1	0.0001[a]
	General informants	165	3.2	
Gender	Male	145	5.9	0.0035[a]
	Female	40	3.1	
Ages	20–40	36	2.1	0.0001[a]
	41–89	149	5	
Educational level	Illiterate	112	3.12	0.007[a]
	Literate	73	1.5	

[a]shows significant difference between groups with *p*-value <0.05.

Therefore, correlation index called relative popularity level (RPL) was established to calculate rank order priority (ROP) value obtained by multiplying FL value by RPL to distinguish medicinal efficacy of plants with similar FL values. The plants were divided into "popular" (with RPL value of 1) and "unpopular" (with RPL value of less than1). "Popular" plants are cited by half or more of the highest number of informants who reported a given plant against any ailment, whereas "unpopular" plants are cited half by less than half of the maximum number of informants who cited a given plant against any ailment. Actual RP value for "unpopular" medicinal plant is calculated by dividing its number of informant citations by the maximum number of citation obtained for a given plant in the list.

2.5 Ethical consideration

The study proposal was reviewed and approved by the Addis Ababa University, Aklilu Lemma Institute of Pathobiology Institutional Research Ethics Review Committee (ALIPB-IRERC). Permissions were obtained from West-Arsi zone, and study district and Kebeles administrative offices to carry out the fieldwork. Verbal consent was obtained before interviewing each informant and traditional healer.

3 Results

3.1 Socio-demographic profile of informants

Out of the total 185 informants involved in this study, 78.4% (n = 145) were males and 21.6% (n = 40) were females. The age of the informants in the study ranged from 20 to 89. Most of the informants were aged 41–60 years (45.4%; 84), followed by those aged 61–89 years (35.1%; 65) and aged 20–30 years (19.5%; 36). Regarding educational status of the informants, the majority (60.5%; 112) were illiterate and the remaining (39.5%; 73) were literate.

3.2 Diversity of medicinal plants used

The study found that 120 traditional medicinal plants taxa, distributed across 98 genera and 55 families, were used by the community in Heban-Arsi district (Supplementary Table 1). Of the total medicinal plants, 43.4% belong to the families Fabaceae (7.6%), Asteraceae (5.3%), Solanaceae (5.3%), Euphorbiaceae (3.8%), Lamiaceae (3.8%), Olacaceae (3.05%), Tiliaceae (3.05%), Moraceae (2.3%), Vitaceae (2.3%), Cucurbitaceae (2.3%), Rosaceae (2.3%) and Myrtaceae (2.3%), and the rest families cover 56.6% of the taxa. The reported medicinal plants had different growth forms including shrubs (41.2%), tree (24.4%), herbs (18.35%), climbers (5.3%), lianas (3.8%) and epiphytes (1.5%) (Figure 2).

3.3 Habitat of medicinal plants

The majority of medicinal plants (76.4%) used in the study district were reported to be uncultivated that were harvested from forests, rivers banks, grasslands, farm fields, farm edges, hills sides, roadsides, life fences and school compounds. Some were cultivated in home gardens (15%), and few others were harvested from both the wild and homestead gardens (8.6%).

3.4 Part of medicinal plants used in remedy preparation

Leaf was the most commonly used plant part accounting for 62.6% of the remedy preparations, followed by bark (22.14%) (Figure 3).

3.5 Plant remedies preparation methods

Crushing and homogenizing in cold and clean water was the primary way of plant remedy preparation (36%), followed by crushing and squeezing (24%), decoction (20%), drying and powdering (13%) and chewing (7%), (Figure 4). Most remedies were prepared from freshly collected plant parts (89%) while some (11%) were prepared from dried plant parts.

3.6 Routes of remedy administration

Result revealed that oral application was the most common route of remedy administration (80.1%) followed by external/dermal (32.1%) and nasal (4.6%) application. Few remedies were reported to be administered by insertion into deep wound (0.8%) and ocular (0.8%) (Figure 5).

3.7 Dosage forms, side effects and use of antidotes

The majority of traditional healers (81%) in the study area understood the effects of overdose use of the medicinal plants on the health of patients. They determined the dosages based on patient's sex, age, presence and absence of pregnancy, body condition, nature of the ailment treated and the route of administration. Water glass, teacup, coffee cup, teaspoon, bottle cap, handful, and between two tips of fingers were used to determine dosages. Traditional healers advised their patients to drink fresh milk, coffee, yoghurt, roasted barley juice, butter and honey as antidotes during adverse effects. For example, leaves of *Discopodium penninervum* Hochest. were chewed and swallowed after orally taking *Gymnathemum auriculiferum* (Hiern) Isawumi decoction for the treatment of sexually transmitted diseases.

3.8 Frequently reported human and livestock ailments in the study district

In the district, 54 human and 25 livestock ailments were recorded during interviews. The highest cited human ailments in the district were gastrointestinal complaints (157; 84.9%), skin disorders (98; 52.9%), infectious and parasitic diseases (liver disorders and internal parasite) (82; 44.3%), and malaria (71; 38.3%), while gastrointestinal disorders (bloat, stomachache and diarrhea) (130; 70.2%) and bacterial infections (anthrax and pasterollosis) (27; 14.6%) were the highest cited diseases of livestock.

3.9 Preference ranking of selected medicinal plants

3.9.1 Preference ranking of medicinal plants used for treatment of human diarrhea

Result of preference ranking exercise conducted on medicinal plants that were used against diarrhea, the most commonly cited ailment in the study area, showed that Syzygium guineense (willd.) DC, Ximenia americana L., and Gymnathemum amygdalinum (Del.) Sch.Bip. ex Walp. were the most preferred plants (Table 2).

3.9.2 Preference ranking of medicinal plants used for treating livestock skin diseases

Preference ranking exercise conducted on nine medicinal plants that were reported to be used against skin diseases of the livestock in the study area was also conducted. The result showed that *Dodonaea viscosa* subsp. *angustifolia* (L.f.) J.G.West, *Calpurnia aurea* (Aiton) Benth and *Prunus africana* (Hook.f) Kalkman were the most preferred medicinal plants for the treatment of livestock skin diseases treatment in the area (Table 3).

3.10 Informants consensus factor

Of the disease categories affecting human, gastrointestinal disorder category scored the highest ICF value (0.83), followed by infectious and parasitic diseases with ICF value of 0.80 and diseases of the skin and subcutaneous tissue diseases category with ICF value of 0.79 (Table 4).

The twenty-five livestock diseases reported in the district were categorized into nine disease categories for the calculation of ICF values. Accordingly, skin disorders category was the commonly

reported livestock health problem with ICF of 0.89 (14 species, 130 use reports) followed by bloat and diarrhea, which is under the gastrointestinal disease category, was the second disease category with ICF of 0.88 (10 species, 80 use reports (Table 5).

3.11 Rank order priority values

Results show that the plants *Dombeya torrida* (J.F. Geal.) Bamps, Artemisia absinthium *L.*, *Balanites aegyptiaca* (L.) Del., Combretum pisoniiflorum (Klotzsch) Engl., *Celtis africana* Burm. f, *Ocimum gratissimum* L. and *Lagenaria* sp. scored the highest ROP values (100 for each plant) for their uses to treat snake poison, tuberculosis, liver disorder, stomachache, tuberculosis, febrile illness and liver disorder, respectively (Table 6).

3.12 Ways of traditional medical knowledge acquisition

Acquisition of traditional medicinal knowledge happens in multiple ways. Most of (167, 90.3%) informants said they acquired traditional healing knowledge through their family routes orally. The remaining (18, 9.7%) informants confirmed acquiring their healing knowledge from different sources through observation, friends and following the activities of traditional healers.

3.13 Comparison of medicinal plants knowledge between social groups

A significant difference ($p < 0.05$) was observed between the mean numbers of medicinal plants claimed by traditional healers and general respondents with traditional healers reporting higher number of medicinal plants than the general respondents. Further comparison of knowledge showed that there was significant difference between the mean numbers of medicinal plants reported by males and females ($p < 0.05$) with males reporting a higher than females. There was also a significant difference ($p < 0.05$) between the mean numbers of medicinal plants reported two age groups and two informants groups of different educational level. Older (above 40 years old) and illiterate informants reported more mean numbers of medicinal plants than their respective younger and literate informants (Table 7).

3.14 Threats against medicinal plants and traditional medical knowledge in the study area

The present study revealed a number of threats against medicinal plants in the study district. The most frequently cited threat was the expansion of agriculture into forest area and grasslands, which was reported by 55% of the respondents, followed by production of timber, unsustainable fuelwood collection and charcoal making, which accounted for 35% of the informants. Frequent drought was also reported by 10% of the informants as factor responsible for degradation and extinction of medicinal plants. Factors responsible for the depletion of traditional medical knowledge related to use of medicinal plants in the area include lack of interest by the younger generation to learn and practice it (14%), cultural changes and modernization (20%), the oral culture of medicinal plant knowledge transmission (14%), the secrecy surrounding the traditional medicine (25%), and the migration of youth from rural areas to cities in search of employment opportunities (27%).

4 Discussion

The fact that high diversity of medicinal plant are used in the study area indicates the high dependence of people on medicinal plants in the day-to-day management of a wide range of human and livestock diseases and this might be related to easy accessibility, cultural acceptability and affordability of medicinal plants, and the associated services. In the study area, Fabaceae contributed higher number of medicinal plants as compared to other families. Other studies conducted elsewhere in Ethiopia also reported the high contribution of Fabaceae to local medicinal flora (Fenetahun et al., 2017; Kidane et al., 2018; Gijan and Dalle, 2019). Shrubs contributed the majority of medicinal plants used in the study area, which could be related to their year round availability and ease of harvesting. The dominance of shrubs was also reported in other ethnobotanical studies conducted elsewhere in the country (Lulekal et al., 2008; Tolossa et al., 2013; Gijan and Dalle, 2019). All medicinal plants documented from the current study area were found to have same or similar medical application in elsewhere in Ethiopia and other parts of the world (Yineger et al., 2008; Bekalo et al., 2009; Giday et al., 2010; Eshete, 2011; Teklay et al., 2013; Enyew et al., 2014; Mesfin et al., 2014; Kassa et al., 2016; Chekole, 2017; Teklehaymanot, 2017; Gijan and Dalle, 2019; Karakaya et al., 2019; Tewelde and Mesfin, 2019; Tamene, 2020; Tewelde, 2020; Ali et al., 2021; Assefa et al., 2021; Hankiso et al., 2024; Nuro et al., 2024) that could be attributed to their pharmacological effect and/or wider distribution.

According to the results of the current study, oral administration of medicinal plants was the primary mode of administration. Traditional healers advised their patients to take the necessary precautions when administering medicinal plants, by oral route since there is possibility that the patient will experience short- and long-term health complications. When using herbal remedies externally through the skin as opposed to internally through the mouth, there was comparatively less chance of poisoning from improper use (Giday et al., 2007). Therefore, it is imperative to prioritize the development of standardized traditional treatment guidelines pertaining to the use of medicinal plants. Oral administration was also reported by other similar studies in Ethiopia (Tolossa et al., 2013; Chekole, 2017; Fenetahun et al., 2017; Eshete and Molla, 2021) and elsewhere in the world (Guler et al., 2021; Karakose, 2022).

In the study district, leaf was the most commonly used plant part in the preparation of traditional remedies. Other ethnobotanical studies conducted in other parts of Ethiopia (Tolossa et al., 2013; Kassa et al., 2020) and elsewhere in the world (Akbulut et al., 2019; Guler et al., 2021; Karakose, 2022; Şen et al., 2022) also reported the

frequent use of leaves in the preparation of remedies. The preference for leaves in remedy preparations could partly be related to their better availability. Harvesting leaves poses negative effect against survival of a plant compared to other parts (Seifu et al., 2004; Lulekal et al., 2008). The dominance of leaves could also be attributed to the production of higher concentrations of chemical compounds in the form of biologically active secondary metabolites to defend themselves from herbivores and different pathogens (Takele, 2018).

Crushing was the most commonly used method in the preparation of remedies in the study area, which is consistent with earlier reports of studies carried out elsewhere in the country (Chekole, 2017; Bekele et al., 2022). Freshly collected plant parts were predominantly used in the preparation of remedies in the area. The use of freshly harvested medicinal plant parts may be associated with the perception that such parts have a higher efficacy attributed to containing better amount of bioactive ingredients (Sofowora, 1982). Studies conducted in other parts of Ethiopia (Giday et al., 2010; Kidane et al., 2018; Kassa et al., 2020) also reported the common use of fresh plant parts in remedy preparation.

Inconsistency in dosage prescriptions of plant remedies used against same or similar ailments in the study area was frequently noted, which could be considered as one of the predicaments of traditional medicine. A study conducted elsewhere in the country also reported similar finding (Giday et al., 2009).

Among the human diseases categories reported, the high ICF value was scored for gastrointestinal problems (0.83). Similarly, of the livestock disease categories, the highest ICF value was scored for skin diseases (0.89), demonstrate the better agreement among informants in the selection of certain medicinal plants, which might be considered as indication of the potency of the plants used in treating such disorders.

In the study area, the highest ROP values (100 for each plant) were obtained for *D. torrida*, *Artemisia absinthium*, *B. aegyptiaca*, *Combretum pisoniiflorum*, *C. africana*, *O. gratissimum* and *Lagenaria* sp. for their uses against snake poison, tuberculosis, liver disorder, stomachache, tuberculosis, febrile illness and liver disorder, respectively. *Dombeya torrida* (Bekele et al., 2022), *A. absinthium* (Buffon et al., 2018), *B. aegyptiaca* (Chothani and Vaghasiya, 2011), *C. pisoniiflorum* (Danton et al., 2019) *C. africana*, (Getachew et al., 2022), *O. gratissimum* (Tedila and Dida, 2019) and *Lagenaria* sp. (Govind, 2011 were also reported to have same traditional medical application elsewhere in Ethiopia and other parts of the world. The anti snake poison activity of *D. torrida* may be attributed to the presence of friedelin (a triterpenoid compound), the anti-venom potency of which was revealed in a study lead by Mathias et. (2016). Extracts of the root and aerial parts of *A. absinthium* demonstrated good antibacterial effect against *Mycobacterium tuberculosis* H37Ra (Trifan et al., 2022), which may relate to the presence of bitter sesquiterpenoid lactones, flavonoids, other bitterness-imparting compounds, azulenes, phenolic acids, tannins and lignans (Szopa et al., 2020). A study conducted in Egypt on aqueous extract of the bark of *B. aegyptiaca* exhibited the high anti-hepatitis virus potential of the plant (Hafez et al., 2015). Furthermore, *in vivo* studies conducted on mice demonstrated significant hepatoprotective effect of the root bark (Traoré et al., 2020) and fruits *Balanites aegyptica* (Zein et al., 2024), which may be attributed to the presence of oil which contains mainly palmitic, stearic, oleic, and linoleic acids (Chothani and Vaghasiya, 2011). Evidence obtained from an *in vivo* study shows a significant analgesic activity of the leaf extract of *C. pisoniiflorum* (Ojewole, 2008). A related species (*Combretum micranthum*) was reported to have analgesic property due to the presence of alkaloids (Abdullahi et al., 2014) The phytochemicals kaempferol, myricetin, quercetin, and eugenol, isolated from *C. africana*, were reported to demonstrate promising antimicrobial activity. Another study demonstrated the antipyretic effect of the methanolic extracts of the leaves of *O. gratissimum* that were significant from 200 mg/kg to 300 mg/kg of body weight (Gege-Adebayo et al., 2013), the efficacy of which may be attributed to the presence of flavonoids that were previously reported to have antipyretic effect (Boakye-Gyasi et al., 2011; Achuta et al., 2011). The anti liver disorder property of *Lagenaria* sp. could be due the presence of phenolic compounds suggested to possess antioxidant activity (Thupakula and Rakesh, 2023).

In the Heban-Arsi district, it was discovered that men had better knowledge on the use of medicinal plants than women and that could be attributed to the choice of most traditional healers to transfer their knowledge on the use of medicinal plants along the male line, preferably through their first son. The traditional medical knowledge transfer through the male line is also a common occurrence elsewhere in the country (Gidey et al., 2015; Woldemariam et al., 2021).

The fact that traditional healers possess better knowledge on the use of medicinal plants shows the unevenly distribution of the knowledge among community members in the study area. Study conducted elsewhere also revealed the better knowledge on the use of medicinal plants by traditional healers compared to general informants (Woldemariam et al., 2021). Likewise, older informants mentioned higher number of medicinal plants than younger ones, which is in agreement with results of studies conducted elsewhere in the country (Giday et al., 2009; Kidane et al., 2018; Kassa et al., 2020). The better knowledge on the use of medicinal plants by older informants as compared to that of the younger ones might suggest that the latter are not interested in learning and practicing traditional medicine, the trend of which may contribute towards the deterioration of the knowledge. The study further revealed that illiterate informants reported more number of medicinal plants compared to literate informants, which is in agreement with that of Kassa et al. (2020) and that could be due to the fact that literate people are more exposed to Western modernization and as a result consider traditional medical as backward and harmful.

The majority of medicinal plants were reported to be harvested from the wild, which is consistent with results of studies conducted elsewhere in Ethiopian (Awas and Demissew, 2009; Kidane et al., 2018; Gijan and Dalle, 2019) which could be showing the poor culture of people in cultivating medicinal plant. This is very worrying in the face of the ongoing habitat destruction in the study area mainly due to clearing of forests for more agricultural lands.

5 Conclusion

Medicinal plants in Heban-Arsi district still play a vital role in fulfilling the primary healthcare needs of community members as

revealed by the high diversity of the reported medicinal plant species. Among the various ailments categories, human gastrointestinal disorders and skin disorders of animals scored the highest ICF values. Of all reported medicinal plants, *B. aegyptica* and *D. torrida* exhibited the highest fidelity level values in treating liver disease and snakebite poisoning, respectively. The factors that posed a higher threat to survival of medicinal plants and the associated knowledge in the area included population growth, poverty, forests clearing for more agricultural lands, the secrecy and oral transmission of knowledge. It is thus imperative to develop conservation strategy for the traditional medical practice to continue in the study area. It is recommended that attention for further bioactivity and phytochemical investigations should be given to medicinal plants reported to be used against diseases categories of high ICF values and those that scored the highest FL and preference ranking values.

Data availability statement

The original contributions presented in the study are included in the article/Supplementary Material, further inquiries can be directed to the corresponding author.

Author contributions

GN: Formal Analysis, Investigation, Writing–original draft, Writing–review and editing. KT: Conceptualization, Data curation, Funding acquisition, Supervision, Validation, Writing–review and editing. MA: Data curation, Writing–review and editing. MG: Conceptualization, Data curation, Funding acquisition, Methodology, Supervision, Validation, Writing–review and editing.

Funding

The author(s) declare that financial support was received for the research, authorship, and/or publication of this article. The fund for this research was obtained from the Office of the Vice President for Research and Technology Transfer of Addis Ababa University (grant number: TR/003/2021).

Acknowledgments

We would like to thank the staff of the Heban-Arsi district administration and Healthcare offices for their kind support during ethnobotanical data collection. We are also grateful to AAU for its financial support to conduct this study. We thank Melaku Wondafrash at the National Herbarium of AAU for his assistance in the identification of plant specimens. Last, but not least, we would like to thank informants in Heban-Arsi district who unreservedly shared their knowledge on medicinal plants, and field assistants and residents of the same district who facilitated the data collection work.

Conflict of interest

The authors declare that the research was conducted in the absence of any commercial or financial relationships that could be construed as a potential conflict of interest.

Publisher's note

All claims expressed in this article are solely those of the authors and do not necessarily represent those of their affiliated organizations, or those of the publisher, the editors and the reviewers. Any product that may be evaluated in this article, or claim that may be made by its manufacturer, is not guaranteed or endorsed by the publisher.

Supplementary material

The Supplementary Material for this article can be found online at: https://www.frontiersin.org/articles/10.3389/fphar.2024.1455126/full#supplementary-material

References

Abdullahi, M. H., Anuka, J. A., Yaro, A. H., and Musa, A. (2014). Analgesic and anti-inflammatory effects of aqueous leafextract of *Combretum micranthumg.* Don (*Combretaceae*). *Pure Appl. Sci.* 7, 78–82. doi:10.4314/bajopas.v7i2.15

Abebe, D. (2001). "The role of medicinal plants in healthcare coverage of Ethiopia, the possible benefits of integration," in *Conservation and sustainable use of medicinal plants in Ethiopia*. Editors M. Zewdu and A. Demissie (Addis Ababa: Institute of Biodiversity Conservation and Research), 6–21.

Achuta, V. N., Mannangati, V., Panda, S., Rani, E., and Prasanthi, P. (2011). Analgesics, antipyretic and anti-inflammatory studies on methanolic extract of Jasminum trichotonum leaves. *Int. J. Res. Ayurveda Pharm.* 2, 637–639.

Agize, M., Asfaw, Z., Nemomissa, S., and Gebre, T. (2022). Ethnobotany of traditional medicinal plants and associated indigenous knowledge in Dawuro Zone of Southwestern Ethiopia. *J. Ethnobiol. Ethnomed.* 18, 48. doi:10.1186/s13002-022-00546-4

Akbulut, S., Karakose, M., and Ozkan, Z. C. (2019). Traditional uses of some wild plants in kale and acıpayam provinces in denizli. *Kastamonu Univ. J. For. Fac.* 19, 72–81. doi:10.17475/kastorman.543529

Alexiades, M. N. (1996). Collecting ethnobotanical data: an introduction to basic concepts and techniques. *Adv. Econ. Bot.* 10, 53–94.

Ali, R., Rooman, M., Mussarat, S., Norin, S., Ali, S., Adnan, M., et al. (2021). A systematic review on comparative analysis, toxicology, and pharmacology of medicinal plants against *Haemonchus contortus*. *Front. Pharmacol. Front. Pharmacol.* 12, 644027. doi:10.3389/fphar.2021.644027

Asfaw, Z., and Tadesse, M. (2001). Prospects for sustainable use and development of wild food plants in Ethiopia. *Econ. Bot.* 55, 47–62. doi:10.1007/bf02864545

Assefa, B., Megersa, M., and Jima, T. T. (2021). Ethnobotanical study of medicinal plants used to treat human diseases in Gura Damole District, Bale Zone, Southeast Ethiopia. *Asian J. Ethnobiol.* 4, 42–52. doi:10.13057/asianjethnobiol/y040105

Awas, T., and Demissew, S. (2009). Ethnobotanical study of medicinal plants in Kafficho people, southwestern Ethiopia. *Proc. 16th Int. Conf. Ethiop. Stud.*

Balick, M. J., and Cox, A. (1996). "Plants that heal," in *Plants people and culture: scientific American library*, 25–62.

Bekalo, T. H., Demissew, S., and Asfaw, Z. (2009). An ethnobotanical study of medicinal plants used by local people in the lowlands of Konta Special Woreda, southern nations, nationalities and peoples regional state, Ethiopia. *J. Ethnobiol. Ethnomed.* 5, 26. doi:10.1186/1746-4269-5-26

Bekele, M., Woldeyes, F., Lulekal, E., Bekele, T., and Demissew, S. (2022). Ethnobotanical investigation of medicinal plants in Buska Mountain range, Hamar district, Southwestern Ethiopia. *J. Ethnobiol. Ethnomed.* 18, 60. doi:10.1186/s13002-022-00558-0

Bishaw, M. (1991). Promoting traditional medicine in Ethiopia: a brief historical review of government policy. *Soc. Sci. Med.* 33, 193–200. doi:10.1016/0277-9536(91)90180-k

Boakye-Gyasi, E., George, K. A., and Wonder, K. M. A. (2011). Anti-inflammatory, antipyretic and antioxidant properties of a hydroalcoholic Leaf Extract of Palisota hirsuta K. Schum. (Commelinaceae). *West Afr. J. Pharm.* 22, 10–18.

Buffon, M. C. M., Negrelle, R. R. B., Gonçalves, R. N., Branco, B. R., Yanaguizawa, J., Sasso, G. C., et al. (2018). Ethnobotanical study of medicinal plants used to treat oral diseases in an urban region of Southern Brazil. *Rev. Bras. Plantas Med.* 20, 222–229.

Caesar, L. K., and Cech, N. B. (2019). Synergy and antagonism in natural product extracts: when 1+1 does not equal 2. *Nat. Prod. Rep.* 36, 869–888. doi:10.1039/c9np00011a

Chekole, G. (2017). Ethnobotanical study of medicinal plants used against human ailments in Gubalafto District, Northern Ethiopia. *J. Ethnobiol. Ethnomed.* 13, 55. doi:10.1186/s13002-017-0182-7

Chothani, D. L., and Vaghasiya, H. U. (2011). A review on Balanites aegyptiaca Del (desert date): phytochemical constituents, traditional uses, and pharmacological activity. *Pharmacogn. Rev.* 5, 55–62. doi:10.4103/0973-7847.79100

Cotton, C. M. (1996). *Ethnobotany: principles and applications*. New York: John Wiley & Sons.

Cragg, G. M., and Newman, D. J. (2013). Natural products: a continuing source of novel drug leads. *Biochim. Biophys. Acta.* 1830, 3670–3695. doi:10.1016/j.bbagen.2013.02.008

CSA (2007). Annual statistics abstract. Addis Ababa: central statistical agency of Ethiopia (CSA).

Danton, O., Somboro, A., Fofana, B., Diallo, D., Sidibé, L., Rubat-Coudert, C., et al. (2019). Ethnopharmacological survey of plants used in the traditional treatment of pain conditions in Mali. *J. Herb. Med.* 17-18, 100271. doi:10.1016/j.hermed.2019.100271

Dhama, K., Karthik, K., Chakraborty, S., Tiwari, R., Kapoor, S., Kumar, A., et al. (2014). Loop-mediated isothermal amplification of DNA (LAMP): a new diagnostic tool lights the world of diagnosis of animal and human pathogens: a review. *Pak. J. Biol. Sci.* 17, 151–166. doi:10.3923/pjbs.2014.151.166

Dilbato, T., Begna, F., and Joshi, R. K. (2019). Reviews on challenges, opportunities and future prospects of antimicrobial activities of medicinal plants: alternative solutions to combat antimicrobial resistance. *Int. J. Herb. Med.* 7, 10–18.

Efferth, T., and Koch, E. (2011). Complex interactions between phytochemicals. The multi-target therapeutic concept of phytotherapy. *Curr. Drug Targets* 12, 122–132. doi:10.2174/138945011793591626

Enyew, A., Asfaw, Z., Kelbessa, E., and Nagappan, R. (2014). Ethnobotanical study of traditional medicinal plants in and around fiche district, Central Ethiopia. *Curr. Res. J. Biol.* 6, 154–167. doi:10.19026/crjbs.6.5515

Eshete, M. A. (2011). *Ethnobotanical study of medicinal plants in guji agro-pastorilists, blue hora district of borana zone, Oromia region, Ethiopia*. Addis Ababa, Ethiopia: Addis Ababa University. [Master's thesis]. [Addis Ababa].

Eshete, M. A., and Molla, E. L. (2021). Cultural significance of medicinal plants in healing human ailments among Guji semi-pastoralist people, Suro Barguda District, Ethiopia. *J. Ethnobiol. Ethnomed.* 17, 61. doi:10.1186/s13002-021-00487-4

Fenetahun, Y., Eshetu, G., Worku, A., and Abdella, T. (2017). A survey on medicinal plants used by traditional healers in Harari regional State, East Ethiopia. *J. Med. Plants Stud.* 5, 85–90.

Friedman, J., Yaniv, Z., Dafni, A., and Palewitch, D. (1986). A preliminary classification of the healing potential of medicinal plants, based on a rational analysis of an ethnopharmacological field survey among Bedouins in the Negev Desert, Israel. *J. Ethnopharmacol.* 6, 275–287. doi:10.1016/0378-8741(86)90094-2

Gege-Adebayo, G. I., Bassi, A. S., Igbokwe, V. U., and Shafe, M. O. (2013). Antipyretic effect of Ocimum gratissium on brewer's yeast induced fever in wistar rats. *J. Med. Med. Sci.* 4, 247–251.

Getachew, S., Medhin, G., Asres, A., Abebe, G., and Ameni, G. (2022). Traditional medicinal plants used in the treatment of tuberculosis in Ethiopia: a systematic review. *Heliyon* 8, e09478. doi:10.1016/j.heliyon.2022.e09478

Getahun, A. (1976). Some common medicinal and poisonous plants used in Ethiopian folk medicine. Available at: http://www.ethnopharmacologia.org/prelude2020/pdf/biblio-hg-07-getahun.pdf [Accessed June 24, 2024].

Giday, M., Asfaw, Z., Elmqvist, T., and Woldu, Z. (2003). An ethnobotanical study of medicinal plants used by the Zay people in Ethiopia. *J. Ethnopharmacol.* 85, 43–52. doi:10.1016/s0378-8741(02)00359-8

Giday, M., Asfaw, Z., and Woldu, Z. (2010). Ethnomedicinal study of plants used by Sheko ethnic group of Ethiopia. *J. Ethnopharmacol.* 132, 75–85. doi:10.1016/j.jep.2010.07.046

Giday, M., Asfaw, Z., Woldu, Z., and Teklehaymanot, T. (2009). Medicinal plant knowledge of the Bench ethnic group of Ethiopia: an ethnobotanical investigation. *J. Ethnobiol. Ethnomed.* 5, 34. doi:10.1186/1746-4269-5-34

Giday, M., Teklehaymanot, T., Animut, A., and Mekonnen, Y. (2007). Medicinal plants of the shinasha, agew-awi and amhara peoples in northwest Ethiopia. *J. Ethnopharmacol.* 110, 516–525. doi:10.1016/j.jep.2006.10.011

Gidey, M., Beyene, T., Signorini, M. A., Bruschi, P., and Yirga, G. (2015). Traditional medicinal plants used by Kunama ethnic group in Northern Ethiopia. *J. Med. Plant Res.* 9, 494–509. doi:10.5897/jmpr2014.5681

Gijan, M., and Dalle, G. (2019). Ethnobotanical study of medicinal plants in nagelle arsi district, west arsi zone of Oromia, Ethiopia. *J. Nat. Sci. Res.* 9, 13. doi:10.7176/JNSR

Govind, P. (2011). Medicinal plants against liver diseases. *Int. Res. J. Pharm.* 2, 115–121.

Guler, O., Polatb, R., Karakose, M., Cakılcıoglu, U., and Akbulu, S. (2021). An ethnoveterinary study on plants used for the treatment of livestock diseases in the province of Giresun (Turkey). *S. Afr. J. Bot.* 142, 53–62. doi:10.1016/j.sajb.2021.06.003

Gurib-Fakim, A. (2006). Medicinal plants: traditions of yesterday and drugs of tomorrow. *Mol. Asp. Med.* 27, 1–93. doi:10.1016/j.mam.2005.07.008

Hafez, E. E., El-Deeb, N., El Refaey, H., and Botrus, W. A. (2015). Balanites aegyptiaca extract as anti-HCV and the evidence of the non toxicity on human liver cell line. *AARJMD.* 2, 3.

Hankiso, M., Asfaw, Z., Warkineh, B., Abebe, A., Sisay, B., and Debella, A. (2024). Ethnoveterinary medicinal plants and their utilization by the people of Soro District, Hadiya Zone, southern Ethiopia. *J. Ethnobiol. Ethnomed* 20, 21. doi:10.1186/s13002-024-00651-6

Heinrich, M., Ankli, A., Frei, B., Weimann, C., and Sticher, O. (1998). Medicinal plants in Mexico: healers' consensus and cultural importance. *Soc. Sci. Med.* 47, 1859–1871. doi:10.1016/s0277-9536(98)00181-6

Jansen, P. C. M. (1991). Spices, condiments and medicinal plants in Ethiopia, their taxonomy and agricultural significance. *Wageningen Cent. Agric. Publ. Documentation*.

Karakaya, S., Polat, A., Aksakal, Ö., Sümbüllü, Y. Z., and İncekara, Ü. (2019). An ethnobotanical investigation on medicinal plants in South of Erzurum (Turkey). *Ethnobot. Res. Appl.* 18, 13. doi:10.32859/era.18.13.1-18

Karakose, M. (2022). An ethnobotanical study of medicinal plants in Güce district, north-eastern Turkey. *Plant divers.* 44, 577–597. doi:10.1016/j.pld.2022.03.005

Kassa, Z., Asfaw, Z., and Demissew, S. (2016). Ethnobotanical study of medicinal plants used by the local people in tulu korma and its surrounding areas of ejere district, western shewa zone of Oromia regional state, Ethiopia. *J. Med. Plants Stud.* 4, 24–47.

Kassa, Z., Asfaw, Z., and Demissew, S. (2020). An ethnobotanical study of medicinal plants in Sheka zone of southern Nations Nationalities and Peoples Regional State, Ethiopia. *J. Ethnobiol. Ethnomed.* 16, 7. doi:10.1186/s13002-020-0358-4

Kebebew, M., and Mohamed, E. (2017). Indigenous knowledge on use of medicinal plants by indigenous people of Lemo district, Haya zone, Southern Ethiopia. *Int. J. Herb. Med.* 5, 124–135.

Kefalew, A., Asfaw, Z., and Kelbessa, E. (2015). Ethnobotany of medicinal plants in ada'a district, east shewa zone of Oromia regional state, Ethiopia. *J. Ethnobiol. Ethnomed.* 11, 25. doi:10.1186/s13002-015-0014-6

Kidane, B., van Andel, T., van der Maesen, L. J., and Asfaw, Z. (2014). Use and management of traditional medicinal plants by Maale and Ari ethnic communities in southern Ethiopia. *J. Ethnobiol. Ethnomed.* 10, 46. doi:10.1186/1746-4269-10-46

Kidane, L., Gebremedhin, G., and Beyene, T. (2018). Ethnobotanical study of medicinal plants in Ganta Afeshum district, eastern zone of Tigray, northern Ethiopia. *J. Ethnobiol. Ethnomed.* 14, 64. doi:10.1186/s13002-018-0266-z

Lulekal, E., Kelbessa, E., Bekele, T., and Yineger, H. (2008). An ethnobotanical study of medicinal plants in Mana Angetu District, southeastern Ethiopia. *J. Ethnobiol. Ethnomed.* 4, 10. doi:10.1186/1746-4269-4-10

Martin, G. J. (1995). "Ethnobotany, A methods manual,". London: Chapman & Hall.

Mathias, S. N., Abubakar, K., October, N., Abubakar, M. S., and Mshelia, H. E. (2016). Anti-venom potentials of friedelin isolated from hexane extract fraction of Albizia chevalieri hams (Mimosaceae). *Ife J. Sci.* 18, 2.

Megersa, M., Asfaw, Z., Kelbessa, E., Beyene, A., and Woldeab, B. (2013). An ethnobotanical study of medicinal plants in Wayu Tuka district, east Welega zone of Oromia Regional State, West Ethiopia. *J. Ethnobiol. Ethnomed.* 9, 68. doi:10.1186/1746-4269-9-68

Mesfin, F., Demissew, S., and Teklehaymanot, T. (2009). An ethnobotanical study of medicinal plants in Wonago Woreda, SNNPR, Ethiopia. *J. Ethnobiol. Ethnomed.* 5, 28. doi:10.1186/1746-4269-5-28

Mesfin, F., Seta, T., and Assefa, A. (2014). An ethnobotanical study of medicinal plants in Amaro Woreda, Ethiopia. *Ethnobot. Res. Appl.* 12, 341–354. doi:10.17348/era.12.0.341-354

Mickymaray, S. (2019). Efficacy and mechanism of traditional medicinal plants and bioactive compounds against clinically important pathogens. *Antibiot* 8, 257. doi:10.3390/antibiotics8040257

Nuro, G. B., Tolessa, K., and Giday, M. (2024). Medicinal plants used by Oromo community in kofale district, West-Arsi zone, Oromia regional state, Ethiopia. *J. Exp. Pharmacol.* 16, 81–109. doi:10.2147/JEP.S449496

Ojewole, J. A. O. (2008). Analgesic and antiinflammatory effects of mollic acid glucoside, a 1 alpha-hydroxycycloartenoid saponin extractive from Combretum molle R. Br. ex G. Don (Combretaceae) leaf. *Phytother. Res.* 22, 30–35. doi:10.1002/ptr.2253

Patwardhan, B. (2005). Ethnopharmacology and drug discovery. *J. Ethnopharmacol.* 100, 50–52. doi:10.1016/j.jep.2005.06.006

Rasul, M. G. (2018). Extraction, isolation and characterization of natural products from medicinal plants. *Int. J. Basic Sci. Appl. Comput.* Available at: https://www.ijbsac.org/wp-content/uploads/papers/v2i6/F0076122618.pdf.

Reddy, K. R., DeLaune, R. D., and Inglett, P. W. (2022). *Biogeochemistry of wetlands: science and applications*. Boca Raton: CRC Press.

Regassa, R. (2013). Assessment of indigenous knowledge of medicinal plant practice and mode of service delivery in Hawassa city, southern Ethiopia. *J. Med. Plants Res.* 7, 517–535. doi:10.5897/JMPR012.1126

Seifu, T., Asres, K., and Gebre-Mariam, T. (2004). Ethnobotanical and ethnopharmaceutical studies on medicinal plants of Chifra district, Afar region, North Eastern Ethiopia. *Ethiop. Pharm. J.* 24, 41–58. doi:10.4314/epj.v24i1.35097

Şen, G., Akbulut, S., and Karaköse, M. (2022). Ethnopharmacological study of medicinal plants in Kastamonu province (Türkiye). *Open Chem.* 20, 873–911. doi:10.1515/chem-2022-0204

Sofowora, A. (1982). *Medicinal plants and traditional plants in Africa*. Hoboken: John Wiley and Sons Ltd.

Szopa, A., Pajor, J., Klin, P., Rzepiela, A., Elansary, H. O., Al-Mana, F. A., et al. (2020). Artemisia absinthium L.—importance in the history of medicine, the latest advances in phytochemistry and therapeutical, cosmetological and culinary uses. *Plants* 9, 1063. doi:10.3390/plants9091063

Tahir, M., Asnake, H., Beyene, T., van Damme, P., and Mohammed, A. (2023). Ethnobotanical study of medicinal plants in asagirt district, northeastern Ethiopia. *Trop. Med. Health* 51, 1. doi:10.1186/s41182-023-00493-0

Takele, W. (2018). *Evaluation of the antimicrobial activities and screening of the phytochemical composition of crude extracts from the leaf exudates of endemic Aloe species (A. pirottae Berger and A. mcloughlinii Christian) in eastern Ethiopia*. Haramaya: Haramaya University.

Tamene, S. (2020). Ethnobotanical study of indigenous knowledge on medicinal plant uses and threatening factors around the Malga District, Southern Ethiopia. *Int. J. Biodivers. Conserv.* 12, 215–226.

Tedila, H., and Dida, G. (2019). Ethno-medicinal study of plants used for treatment of human and livestock ailments by traditional healers in Goba Woreda, Bale Zone, Oromia, Ethiopia. *Adv. Life Sci. Technol.* 100. Available at: https://www.iiste.org/Journals/index.php/ALST/article/view/61942/63938. doi:10.7176/ALST

Teklay, A., Abera, B., and Giday, M. (2013). An ethnobotanical study of medicinal plants used in Kilte Awulaelo District, Tigray Region of Ethiopia. *J. Ethnobiol. Ethnomed.* 9, 65. doi:10.1186/1746-4269-9-65

Teklehaymanot, T. (2017). An ethnobotanical survey of medicinal and edible plants of Yalo Woreda in Afar regional state, Ethiopia. *J. Ethnobiol. Ethnomed.* 13, 40. doi:10.1186/s13002-017-0166-7

Tewelde, F. (2020). Threats and ethnobotanical use of plants in the weredas of Afar region, Ethiopia. *Int. J. Plant Biol. Res.* 8, 1122.

Tewelde, F., and Mesfin, M. (2019). An ethnobotanical study of plants in the adjoining area of kafta sheraro national park ethnic groups, Ethiopia. *Plant* 7, 76–87. doi:10.11648/j.plant.20190704.14

Thupakula, N., Prakash, and Rakesh, K. J. (2023). Hepatoprotective activity of Lagenaria sicerari extract against paracetamol induced hepatic damage in rats. *Int. J. Creat. Res. Thoughts* 11, 1.

Tolossa, K., Debela, E., Athanasiadou, S., Tolera, A., Ganga, G., and Houdijk, J. G. (2013). Ethno-medicinal study of plants used for treatment of human and livestock ailments by traditional healers in South Omo, Southern Ethiopia. *J. Ethnobiol. Ethnomed.* 9, 32. doi:10.1186/1746-4269-9-32

Traoré, K. T., Ouédraogo, N., Ouédraogo, G. G., Boly, G. A. L., Kabré, L. M. E. W., Sombié, E. N., et al. (2020). Hepatoprotective activity of aqueous extract of Balanites aegyptiaca L. Delile (Balanitaceae) roots bark. *Int. J. Phytomed.* 12, 054–059. doi:10.5138/09750185.2433

Trifan, A., Zengin, G., Sinan, K. I., Sinan, K. I., Sieniawska, E., Sawicki, E., et al. (2022). Unveiling the phytochemical profile and biological potential of five Artemisia species. *Antioxidants* 11, 1017. doi:10.3390/antiox11051017

Woldemariam, G., Demissew, S., and Asfaw, Z. (2021). An ethnobotanical study of traditional medicinal plants used for human ailments in Yem ethnic group, south Ethiopia. *Ethnobot. Res. Appl.* 22, 1–5. doi:10.32859/era.22.09.1-15

World Health Organization (2001). *Legal status of traditional medicine and complementary/alternative medicine: a worldwide review*. World Health Organization. Available at: https://iris.who.int/bitstream/handle/10665/42452/WHO_EDM_TRM_2001.2_eng.pdf (Accessed June 26, 2024).

World Health Organization (2011). International statistical classification of diseases and related health problems. , 1347, doi:10.1007/978-0-387-79948-3_3055Accessed June 25, 2024].

Yang, Y., Zhang, Z., Li, S., Ye, X., Li, X., and He, K. (2014). Synergy effects of herb extracts: pharmacokinetics and pharmacodynamic basis. *Fitoterapia* 92, 133–147. doi:10.1016/j.fitote.2013.10.010

Yineger, H., Kelbessa, E., Bekele, T., and Lulekal, E. (2008). Plants used in traditional management of human ailments at bale mountains national park, southeastern Ethiopia. *J. Med. Plant Res.* 2, 132–153.

Zein, N., Yassin, F., Ayoub, J. G., Elewa, Y. H. A., Mohamed, S. K. A., Mahmoud, M. H., et al. (2024). *In vivo* investigation of the anti-liver fibrosis impact of Balanites aegyptiaca chitosan nanoparticles. *Biomed. Pharmacother.* 172, 116193. doi:10.1016/j.biopha.2024.116193

frontiers | Frontiers in Pharmacology

TYPE Original Research
PUBLISHED 10 October 2024
DOI 10.3389/fphar.2024.1446749

Check for updates

OPEN ACCESS

EDITED BY
Qingquan Liu,
Capital Medical University, China

REVIEWED BY
Xiaolong Xu,
Capital Medical University, China
Huahao Fan,
Tianjin University, China
Jingxia Zhao,
Capital Medical University, China

*CORRESPONDENCE
Yuejuan Zheng,
13641776412@163.com,
zhengyj@shutcm.edu.cn
Wei Zhang,
zhangw1190@sina.com
Huazhang An,
anhzsmmu@126.com

†These authors have contributed equally to this work

RECEIVED 10 June 2024
ACCEPTED 26 September 2024
PUBLISHED 10 October 2024

CITATION
Dou B, Wu X, He Y, Xu G, Zhang H, Huang Q, Chen X, Duan N, Zhou L, Zhang W, An H and Zheng Y (2024) Fei-Yan-Qing-Hua decoction attenuates influenza virus infection by enhancing host antiviral response through microbiota-derived acetate.
Front. Pharmacol. 15:1446749.
doi: 10.3389/fphar.2024.1446749

COPYRIGHT
© 2024 Dou, Wu, He, Xu, Zhang, Huang, Chen, Duan, Zhou, Zhang, An and Zheng. This is an open-access article distributed under the terms of the Creative Commons Attribution License (CC BY). The use, distribution or reproduction in other forums is permitted, provided the original author(s) and the copyright owner(s) are credited and that the original publication in this journal is cited, in accordance with accepted academic practice. No use, distribution or reproduction is permitted which does not comply with these terms.

Fei-Yan-Qing-Hua decoction attenuates influenza virus infection by enhancing host antiviral response through microbiota-derived acetate

Biao Dou[1,2,3†], Xiao Wu[1,2†], Yurong He[1,2], Guihua Xu[4], Huan Zhang[1,2], Qilin Huang[1,2], Xuan Chen[4], Naifan Duan[4], Linqiong Zhou[4], Wei Zhang[4]*, Huazhang An[1,2]* and Yuejuan Zheng[1,2]*

[1]The Research Center for Traditional Chinese Medicine, Shanghai Institute of Infectious Diseases and Biosecurity, Shanghai University of Traditional Chinese Medicine, Shanghai, China, [2]Center for Traditional Chinese Medicine and Immunology Research, School of Integrative Medicine, Shanghai University of Traditional Chinese Medicine, Shanghai, China, [3]Department of Medical Laboratory, The First Affiliated Hospital of Henan University, Kaifeng, China, [4]Department of Pulmonary Diseases, ShuGuang Hospital Affiliated to Shanghai University of Traditional Chinese Medicine, Shanghai, China

Background: Fei-Yan-Qing-Hua decoction (FYQHD) is derived from the well-known Ma Xing Shi Gan decoction, which was documented in Zhang Zhong Jing's "Treatise on Exogenous Febrile Disease" during the Han Dynasty. Although FYQHD has been used in the treatment of pneumonia and has demonstrated clinical efficacy for decades, the underlying mechanism by which FYQHD protects against influenza virus infection through modulation of gut flora remains unclear. Here, we examined the regulatory impacts of FYQHD on an influenza virus-infected mouse model and explored the mechanisms involved.

Methods: An infectious mouse model was created by intranasal instillation of influenza A virus (IAV). The effectiveness of FYQHD was assessed through various measures, including weight loss, lung wet/dry ratio, oxidative stress levels, viral load in lung tissues, and intestinal injuries. Changes in gut microbiota and SCFA production were also examined.

Results: The results showed that FYQHD significantly reduced viral load, increased the production of type I interferon (IFN-I), and restored the integrity of the intestinal barrier following IAV challenge. Additionally, FYQHD significantly corrected the dysbiosis of gut microbiota induced by influenza virus infection, enhancing the abundance of SCFA-producing bacteria and acetate production. However, the depletion of gut microbiota significantly attenuated the protective effects of FYQHD against influenza virus infection. *In vitro*, the antiviral effect of acetate was demonstrated through the upregulation of concentrations of IFN-β.

Conclusion: FYQHD attenuates influenza virus-induced lung and intestinal injuries by boosting the host antiviral response through increasing the abundance of *Lachnospiraceae_NK4A136* and *Roseburia,* along with elevated

acetate levels. The study advances our understanding of the therapeutic mechanisms of FYQHD and provides a theoretical basis for the application of FYQHD in the treatment of influenza.

KEYWORDS

influenza virus, Fei-Yan-Qing-Hua decoction, interferon β, gut microbiota, short-chain fatty acids (SCFAs)

1 Introduction

The emergence of coronavirus disease (COVID-19) caused by severe acute respiratory syndrome coronavirus 2 (SARS-CoV-2) has garnered global attention since its initial report in December 2019 (Zhu et al., 2020). However, the global burden of influenza, especially that caused by influenza A virus (IAV), remains a critical public health concern. Influenza viruses are crucial respiratory pathogens that cause substantial seasonal outbreaks and pandemics, leading to high morbidity and mortality worldwide (Doherty et al., 2006; Herold et al., 2015). Particularly in recent years, seasonal influenza outbreaks and global pandemics happen frequently. Approximately 10%–30% of the global population is affected by influenza virus infection every year, resulting in about 3–5 million severe cases and up to 290,000–650,000 deaths from acute lung injury (ALI) or acute respiratory distress syndrome (ARDS) (Iuliano et al., 2018; Waehre et al., 2022). Vaccination is the main strategy for preventing influenza A. However, the high susceptibility of IAV to antigenic drift and shift and delays in vaccine production significantly challenge its effectiveness. Presently, a limited number of drugs can target the influenza M2 ion channel protein, whereas several inhibitors of influenza NA, RNA-dependent RNA polymerase, and protease, such as oseltamivir (OSV), baloxavir and favipiravir, etc., are either approved for clinical use or under investigation (Zhang et al., 2020). Oseltamivir is a well-known antiviral effective against influenza. However, due to its neuraminidase inhibition mechanism, its protective effect is temporary and requires administration within 48 h of infection to significantly limit viral replication and relieve symptoms. In summary, evolving mutations in IAV and resulting drug resistance challenge influenza treatment, underscoring the urgent need for new antiviral agents.

Traditional Chinese medicine (TCM) plays a significant role in treating viral pneumonia caused by SARS and SARS-CoV-2 due to its proven effectiveness and lower incidence of side effects (Huang et al., 2021). Chinese herbal formulas have unique medicinal effects resulting from the combination of various herbal medicines, exhibiting anti-infective effects through multiple mechanisms, such as antiviral, anti-inflammatory, and immunomodulatory effects (Xi et al., 2020). Fei-Yan-Qing-Hua decoction (FYQHD), derived from Ma-Xing-Shi-Gan decoction and consisting of five herbs known for dispersing phlegm and relieving fever or asthma. FYQHD had demonstrated efficacy against community-acquired pneumonia (CAP) in the clinic for 2 decades at Shuguang Hospital, affiliated with Shanghai University of Traditional Chinese Medicine. The multiple compounds in FYQHD can impact various aspects of the influenza virus, ensuring its effectiveness against influenza virus and its mutants.

The gut microbiome is crucial in the shift from homeostasis to disease. Studies have revealed a bi-directional link between the lungs and the gut, termed the lung-gut axis (He et al., 2017). Furthermore, according to TCM theory, "the lung and the large intestine are interior-exterior," suggesting a close relationship between lung diseases and the function of the large intestine. Literatures reported that IAV infection in mice is often linked to intestinal damage, including increased permeability and reduced levels of the zonula occludens-1 (ZO-1) protein (Zhu et al., 2018). Meanwhile, the gut microbiota also plays an important role in protecting the host from the infection of influenza virus (Stefan et al., 2020). According to TCM theory, dietary supplements with non-digestible carbohydrates, antioxidant phytochemicals, and natural compounds can pass through the stomach to the intestine, where gut microbiota can transform or ferment them into beneficial metabolites. Therefore, TCM components that regulate the gut-lung axis seem to be a promising strategy to alleviate IAV-induced lung and gut immune injury.

Gut bacteria partially break down non-digestible polysaccharides to produce short-chain fatty acids (SCFAs) (Rudiansyah et al., 2022). Among these SCFAs, acetate, propionate, and butyrate are well-documented for their crucial roles in regulating the host immune response (Kim, 2021). The activation of various interferon-stimulated genes (ISGs) by type I interferons is a key antiviral defense mechanism (Ivashkiv and Donlin, 2014). Notably, acetate has the capacity to modulate the host's immune response to viral infections. By activating G-protein coupled receptor 43 (GPR43), acetate induces an IFN-I response in lung epithelial cells, thereby suppressing the replication of respiratory syncytial virus (RSV) (Antunes et al., 2019). Furthermore, recent studies have demonstrated that the probiotic *Bifidobacterium pseudolongum NjM1* exhibits protective properties against IAV infection. This protective effect is associated with acetate production, which enhances MAVS clustering to activate IRF3, thus promoting the expression of IFN-I (Niu et al., 2023). In addition, IAV infection triggers the expression of superoxide dismutase (SOD) and xanthine oxidase, leading to a decrease in antioxidant levels and the onset of oxidative stress (OS) (Peterhans, 1997). Studies have shown that acetate and butyrate exhibit potent antioxidative effects at a concentration of 1 mM (Hu S. et al., 2020).

Although FYQHD has been used clinically for 2 decades, its precise mechanism of protecting against influenza, especially regarding its impact on gut function, remains unclear. FYQHD treatment was found to relieve lung damage and oxidative stress in flu mice, while altering the diversity and structure of gut microbiota to resemble that of normal mice. Additionally, it increased the abundance of SCFA-producing bacteria like *Roseburia, Clostridium, and Lachnospiraceae* (Sun et al., 2020; Zhao et al., 2021). The study also investigated the effect of FYQHD on mice

infected with IAV by depleting gut microbiota. Finally, the protective effect of FYQHD was linked to its ability to enhance the gut microbiota-derived acetate, which in turn boosted the induction of IFN-I during IAV infection. The current results provide evidence that FYQHD has therapeutic potential for the treatment of IAV infection. Furthermore, it offers insights into the mechanisms by which it influences the host and gut microbiota, laying the groundwork for understanding its clinical effectiveness.

2 Materials and methods

2.1 Reagents and chemicals

All traditional Chinese medicine materials were provided by the Department of Pulmonary Diseases, ShuGuang Hospital affiliated to Shanghai University of Traditional Chinese Medicine. Influenza virus A/Puerto Rico/8/1934 H1N1 (PR8) was used *in vitro* and *in vivo* experiments. Oseltamivir phosphate granules (OSV) was purchased from Yichang HEC Changjiang Pharmaceutical Co., Ltd. (Hubei, China). All the antibiotics used in this study were purchased from Sangon Biotech (Shanghai) Co.

2.2 Preparation and analysis of FYQHD for quality control

The FYQHD decoction was prepared following the methodology outlined in our previous report (Zhang et al., 2024). FYQHD consists of *Ephedra dahurica* Turcz. (Ephedraceae) (6 g), *Prunus mandshurica* (Maxim.) Koehne. (Rosaceae) (9 g), *Gypsum Fibrosum* (Sulfates) (30 g), *Glycyrrhiza uralensis* Fisch. ex DC. (Fabaceae) (9 g), *Bupleurum chinensis* DC. (Apiaceae) (9 g), *Scutellaria baicalensis* Georgi (Lamiaceae) (9 g), *Rheum officinale* Baill. (Polygonaceae) (6 g), *Fagopyrum acutatum* Mansf. ex K. Hammer (Polygonaceae) (30 g) and *Morus alba var. tatarica* (L.) Loudon (Moraceae) (9 g) in a ratio of 1:1.5:5:1.5:1.5:1.5:1:5:1.5. Detailed information on FYQHD is provided in Supplementary Table S1. While the family names, documented bioactivities, and identified compounds of these herbal remedies are elaborated in our prior investigation (Zhang et al., 2024).

A mixture of one mineral drug and 8 botanical drugs was soaked for 30 min with 5-fold of purified water (volume/weight), then decocted for 1 h. After completing the first decoction, the liquid was poured out and the remaining mixture was decocted for the second time by adding twice the volume of purified water. Once the second decoction was finished, the two decoctions were mixed and subjected to filter. Eventually, the filtered liquid was concentrated to 3.2 g crude drug/ml. FYQHD decoctions were freshly preserved at −20°C for no longer than 2 days prior to their application.

The chromatographic fingerprint of FYQHD was performed using UPLC-MS/MS. Then, 17 metabolites are confirmed by authentic standards, which are the major metabolites of corresponding botanical drugs in FYQHD (Committee, 2020), including ephedrine and pseudoephedrine from *Ephedra dahurica* Turcz., amygdalinare from *Prunus mandshurica* (Maxim.) Koehne., epicatechin and isorhamnetin from *Fagopyrum acutatum* Mansf. ex K. Hammer, baicalin, wogonin, luteolin and wogonoside from *Scutellaria baicalensis* Georgi, liquiritin and glycyrrhizic acid from *Glycyrrhiza uralensis* Fisch. ex DC., rhein and emodin from *Rheum officinale* Baill., morusin and kaempferol from *Morus alba var. tatarica* (L.) Loudon, saikosaponin D and saikosaponin A from *Bupleurum chinensis* DC. Typical base peak and ion flow chromatograms are shown in Supplementary Figure S1. And the standard curve of standards used in UPLC-MS/MS are shown in Supplementary Figure S2. Detailed characterizations for each metabolite are provided in Supplementary Table S2.

2.3 Lung index indicators

At specified time points following infection, mice were euthanized in accordance with approved protocols. The lungs were meticulously excised and rinsed with physiological saline solution. Subsequently, the total lung weight was recorded to calculate the lung index using the following formula: lung index = (lung wet weight/body weight) × 100%.

2.4 Animals

Female C57BL/6J mice (7 weeks old, 17–20 g) were obtained from Bikai Laboratory Animals Ltd. and then housed in a standard animal room (room temperature: 22°C ± 2°C; relative humidity: 30%–40%; light conditions: 12 h dark/light cycle).

Mice were randomly divided into 7 groups: control group, PR8 group, PR8 + OSV (30 mg/kg) group, PR8 + FYQHD (L) (low dosage, 24 g/kg) group, PR8 + FYQHD (M) (medium dosage, 48 g/kg) group, PR8 + FYQHD (H) (high dosage, 96 g/kg) group. In addition, the low dose administered to the mice corresponds to the dose used clinically in patients. Each mouse, weighing 20 g, received an administration of 150 μL FYQHD at a concentration of 3.2 g/mL. All groups of mice excepted control group were infected intranasally by influenza virus PR8 (2×10^4 PFU in 50 μl/mouse) intranasally and were then administered the indicated drugs within 2 h after infection. For the survival observation for 14 days, mice were monitored daily for body weight loss. If a mouse loses body weight over 25% of its original body weight, it would be humanely euthanized immediately.

Antibiotic Treatment: Mice were treated with a broad-spectrum cocktail of antibiotics to deplete the gut microbiota, as previously described (Ichinohe et al., 2011). The antibiotic cocktail (ABX) comprised 4 antibiotics: ampicillin (1 g/L), vancomycin (0.5 g/L), neomycin (1 g/L), and metronidazole (1 g/L). The feeding water containing antibiotics was changed every 2 days. After 28 days, mice were infected with the same volume of PR8 intranasally and were then administered the indicated drugs within 2 h after infection.

2.5 The detection of H1N1 viral titers

Mice were randomly divided into 2 groups (n = 6) and intranasally infected by PR8. Subsequently, the mice received a low dose of FYQHD (150 μL/day/mouse) for 2 or 3 days post-infection (dpi). Lung samples were homogenized and centrifuged at 13,000 rpm for 1 min at 4°C. The lung homogenate supernatant was transferred to a 96-well plate containing MDCK cells using a serial

10-fold dilution method. The cells were then incubated at 37°C in a 5% CO_2 environment to assess cytopathic effects (CPE). The $TCID_{50}$ was determined using the Reed-Muench method and reported as Log_{10} $TCID_{50}$/0.1 mL.

2.6 16S rRNA gene sequencing and analysis

Six cecum samples were collected and frozen at −80°C until 16S rRNA sequencing from each group on the 7th day after PR8 infection. Total genomic DNA was purified with a MagPure Soil DNA LQ Kit following the manufacturer's instructions. DNA concentration was determined with NanoDrop 2000 (Thermo Fisher Scientific, United States) and DNA integrity was evaluated by agarose gel electrophoresis. DNA samples were used as the template to PCR-amplify bacterial 16S rRNA genes with barcoded primers and a Taq polymerase (Takara, Dalian, China). For bacterial diversity analysis, V3-V4 variable regions of 16S rRNA genes were amplified with universal primers 343F (5′-TACGGRAGGCAGCAG-3′) and 798R (5′-AGGGTATCTAATCCT-3′) (Nossa et al., 2010). The PCR products were analyzed by agarose gel electrophoresis, purified, and quantified using Qubit dsDNA Assay Kit (Thermo Fisher Scientific, United States). The 16S rRNA gene sequencing was conducted by Shanghai OE Biotech. Co., Ltd. (Shanghai, China) following the established method (Ye et al., 2021).

2.7 SCFA concentration analysis

The levels of SCFAs in the sera of mice were measured with GC–MS analysis. Serum samples (400 μL) were supplemented with 100 μL 50% sulfuric acid. Then 500 μL of the supernatants was mixed with 500 μL of ethyl ether, vortexed (2 min) and centrifuged (12,000 × g, 10 min). The extracted samples underwent separation using an Agilent DB-WAX capillary column (30 m × 0.25 mm ID × 0.25 μm) gas chromatography system and detection was carried out using the 7000B GC-MS system by Agilent (United States). Mass Hunter Workstation software was used to quantitative analysis. The concentrations of SCFAs were determined based on standard curves.

2.8 Total RNA extraction and quantitative reverse-transcriptase PCR

Trizol reagent (Invitrogen, United States) was used for isolating total RNA from lung tissues of mice and RNA extraction kit (RNAfast200, Fastagen, Shanghai, China) was used for cells. $2^{-\triangle\triangle CT}$ method was performed to calculate the expression of relative mRNA in this study with β-Actin as a normalized reference. The primer sequences were listed in Supplementary Table S3.

2.9 Assessment of antioxidant indexes in the lungs and sera

Frozen lung tissues were homogenized with RIPA lysis buffer to extract total proteins. Following the centrifugation of 12,000 g for 15 min at 4°C, the protein content was measured using a bicinchoninic acid (BCA) protein assay kit as per the manufacturer's guidelines. Quantification of key redox enzymes such as MPO, T-SOD, CAT, T-AOC, GSH-Px, and MDA was performed using commercial kits obtained from Nanjing Jiancheng Bioengineering Institute, Nanjing, China, with adherence to the manufacturer's protocols.

2.10 *In vitro* sodium acetate treatment

A549 cells were pretreated with 260 μM sodium acetate (S5636, SIGMA) for 24 h in DMEM containing 10% FBS and the cells were infected with PR8 (MOI = 2) for 8 h and 24 h, as described previously (Niu et al., 2023). Viral loads were measured by Quantitative Real-time Polymerase Chain Reaction Analysis.

2.11 Histopathological examination

Freshly harvested lung tissues and proximal colon tissues of mice were fixed in 4% formaldehyde and paraffin-embedded, and then cut into 3 μm-thick sections for hematoxylin-eosin (HE) staining. These sections were further captured by light microscopy using an Axio Imager M2 microscope (Carl Zeiss Micro Imaging, Gottingen, Germany).

2.12 Immunohistochemistry

Immunohistochemical analysis was performed to assess the expression levels of zonula occludens 1 (ZO-1), Claudin-1, and Occludin, following established protocols (Schroeder et al., 2018). Briefly, colonic tissue slides embedded in paraffin were deparaffinized, treated with a citrate buffer solution (0.01 M, pH 6.0), and subjected to autoclave sterilization at 120°C for 5 min to aid in antigen retrieval. Following rinsing, incubation at room temperature for 60 min ensued after the addition of 5% bovine serum albumin (BSA). Without any preceding wash steps, rabbit anti-mouse primary antibodies against ZO-1, Claudin-1 and Occludin were added dropwise respectively, and the samples were then incubated overnight at 4°C. Tissue slides were washed in PBS and then exposed to a fluorophore-conjugated secondary antibody (diluted 1:200 in block solution) for 1 h. After the final wash, the sample was treated with 3,3′-diaminobenzidine tetrahydrochloride (DAB) at room temperature for 60 min.

2.13 Alcian blue staining

In the process of Alcian blue staining, the sections were dried in an oven and heated at 66°C for 20–30 min. Subsequently, 3 rounds of xylene and 3 rounds of ethanol were sequentially applied. Each slice was treated with 100 μL of Alcian blue staining solution, followed by incubation in a humid chamber for 1 h. The staining solution was aspirated, and 100 μL of nuclear solid red staining solution was introduced to each slice, with subsequent washing in water. The samples were then subjected to three sequential treatments of ethanol, phenol-xylene I, and xylene II.

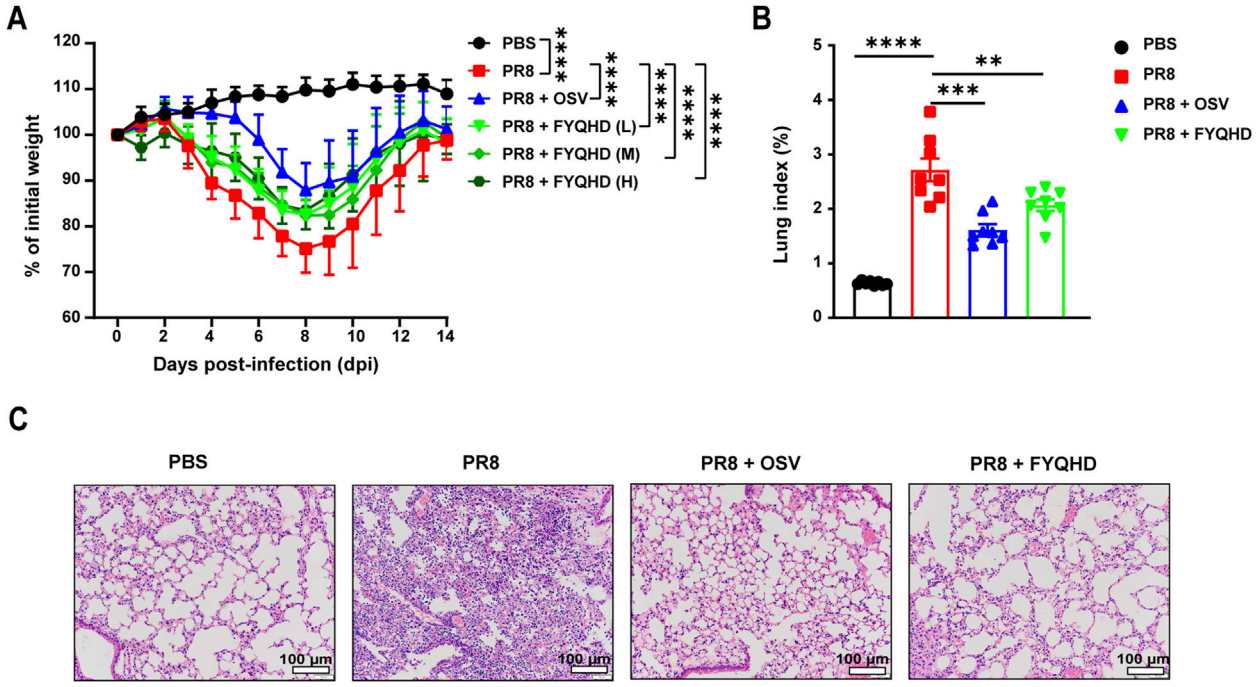


FIGURE 1
FYQHD attenuated the body weight loss and alleviated lung damage during IAV infection. Mice were infected with 50 μL PBS containing influenza A/PuertoRico/8/1934 H1N1 (PR8) virus, and were orally administered with FYQHD or Oseltamivir within 2 h after infection. **(A)** The percentage of weight loss post infection relative to initial body weight (day 0) (n = 14). PBS: Normal group, PR8: IAV group, PR8 + FYQHD (L): FYQHD-treated low-dose group, 24 g/kg, PR8 + FYQHD (M): FYQHD-treated medium-dose group, 48 g/kg, PR8 + FYQHD (H): FYQHD-treated high-dose group, 96 g/kg, PR8 + OSV: Oseltamivir-treated group, 30 mg/kg. **(B)** The change of lung indices of mice in each group (n = 8). **(C)** The pathological observation of mouse lung tissues. The dose of FYQHD used in **(B, C)** was 24 g/kg. Data were presented as mean ± SEM for each group. $^{*}P < 0.05$, $^{**}P < 0.01$, $^{***}P < 0.001$, $^{****}P < 0.0001$ vs. PR8 group. Scale bars represent 100 μm.

2.14 Statistical analysis

The data were analyzed with GraphPad Prism version 8.0, and the results were displayed as mean ± SD. Variations in mean values between groups were evaluated using an unpaired two-tailed Student's *t*-test. Statistical comparison of parameters across the 3 groups involved one-way analysis of variance (ANOVA) followed by Tukey's test. Correlation analysis was carried out using the Pearson statistical method. A P value < 0.05 was deemed to indicate statistical significance.

3 Results

3.1 Quantitative analysis of the major components in FYQHD

FYQHD is composed of 9 traditional Chinese medicines, and detailed information on FYQHD is provided in Supplementary Table S1. In addition, UPLC-MS/MS was utilized to establish the quality control of FYQHD and to quantify its representative metabolites. The total positive and negative ion chromatograms of the samples revealed the primary bioactive metabolites present in FYQHD-medicated serum (Supplementary Figure S1). Subsequently, 17 metabolites were verified using authentic standards, representing the primary metabolites of the respective botanical drugs in FYQHD (Committee, 2020) (Supplementary Figure S2). Comprehensive characterizations for each metabolite were presented in Supplementary Table S2.

3.2 FYQHD protected mice from lung injury induced by IAV infection

The therapeutic characteristic of FYQHD was assessed using the viral infection mouse model. Oseltamivir was used as an effective treatment. The mice's weights started to noticeably decrease on day 4 post-infection, reached their lowest points at day 8 post-infection, and then recovered by day 14. Administering low, medium, and high doses of FYQHD from day 4–10 post-infection helped alleviate the weight loss in PR8-infected mice. And OSV showed a protective effect on mice too (Figure 1A). Therefore, FYQHD demonstrated a significant protective effect on the body weight of PR8-infected mice, with the low dose proven to be effective ($P < 0.0001$). Subsequent experiments were conducted using the low dose of FYQHD (24 g/kg).

We then used mouse lung indices and H&E staining to evaluate the lung injury of flu mice. The mice of PR8 group showed significantly higher lung indices compared to those of PBS group. However, the administration of FYQHD or OSV notably reduced the lung indices caused by viral infection

10.3389/fphar.2024.1446749

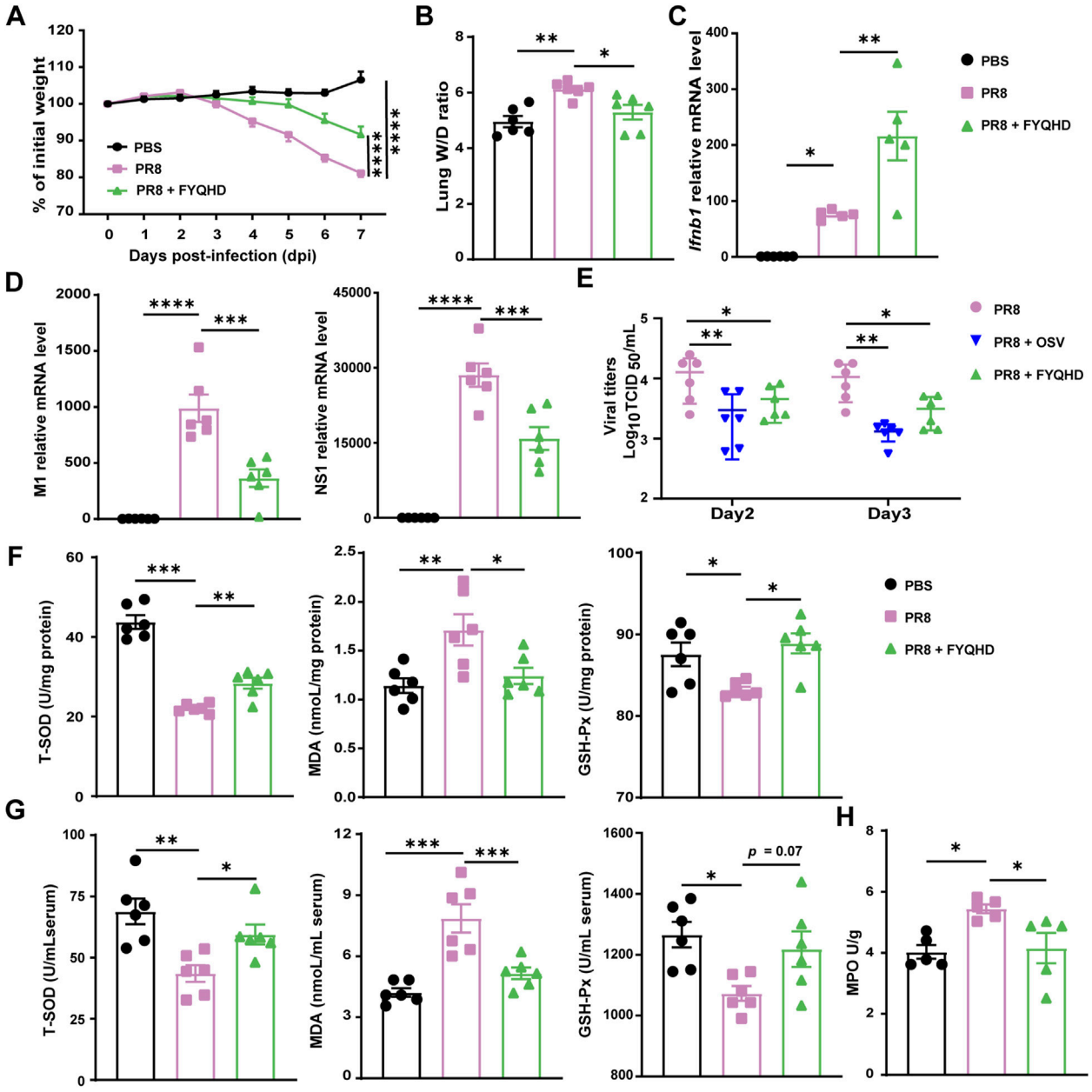


FIGURE 2
Oral FYQHD administration attenuated viral load and oxidative stress in the lungs upon IAV infection. **(A)** Percentage of weight loss post infection relative to initial body weight (day 0) (n = 6 - 7). **(B)** Lung W/D ratio of mice (n = 6). **(C)** The expression of *Ifnb1* detected in lung tissues by real-time PCR (n = 5). **(D)** Relative PR8 M1 and NS1 gene expression detected in lung tissues by real-time PCR (n = 6). **(E)** The virus titers in lung tissues of flu mice on 2 and 3 dpi were measured by $TCID_{50}$ using MDCK cells (n = 6). **(F)** Concentrations of T-SOD, MDA, and GSH-Px in lungs from each group (n = 6). **(G)** Concentrations of T-SOD, MDA, GSH-Px in the sera from each group (n = 6). **(H)** Concentrations of MPO in the lungs from each group (n = 6). Data were presented as means ± SEM. Statistical significance was determined using one-way ANOVA, followed by Tukey test. *$P < 0.05$, **$P < 0.01$, ***$P < 0.001$, ****$P < 0.0001$ vs. PR8 group.

(Figure 1B). The H&E staining results showed normal lung tissue morphology in the lungs of PBS group. On day 7 post-infection, the lung tissues of PR8 group displayed collapsed alveolar structures, thickened alveolar walls, extensive infiltration of inflammatory cells, and exudates in the airway lumen. Treatment with FYQHD or OSV resulted in reduced infiltration of inflammatory cells and exudates in the airway lumen, as well as preserved alveolar structure (Figure 1C).

3.3 FYQHD protects against influenza a virus infection by reducing viral load and oxidative stress

The results demonstrated that with the infection of influenza virus, the mice of PR8 group exhibited substantial weight loss compared to non-infective group. And the weight loss can be effectively reversed by FYQHD administration (Figure 2A). The

10.3389/fphar.2024.1446749

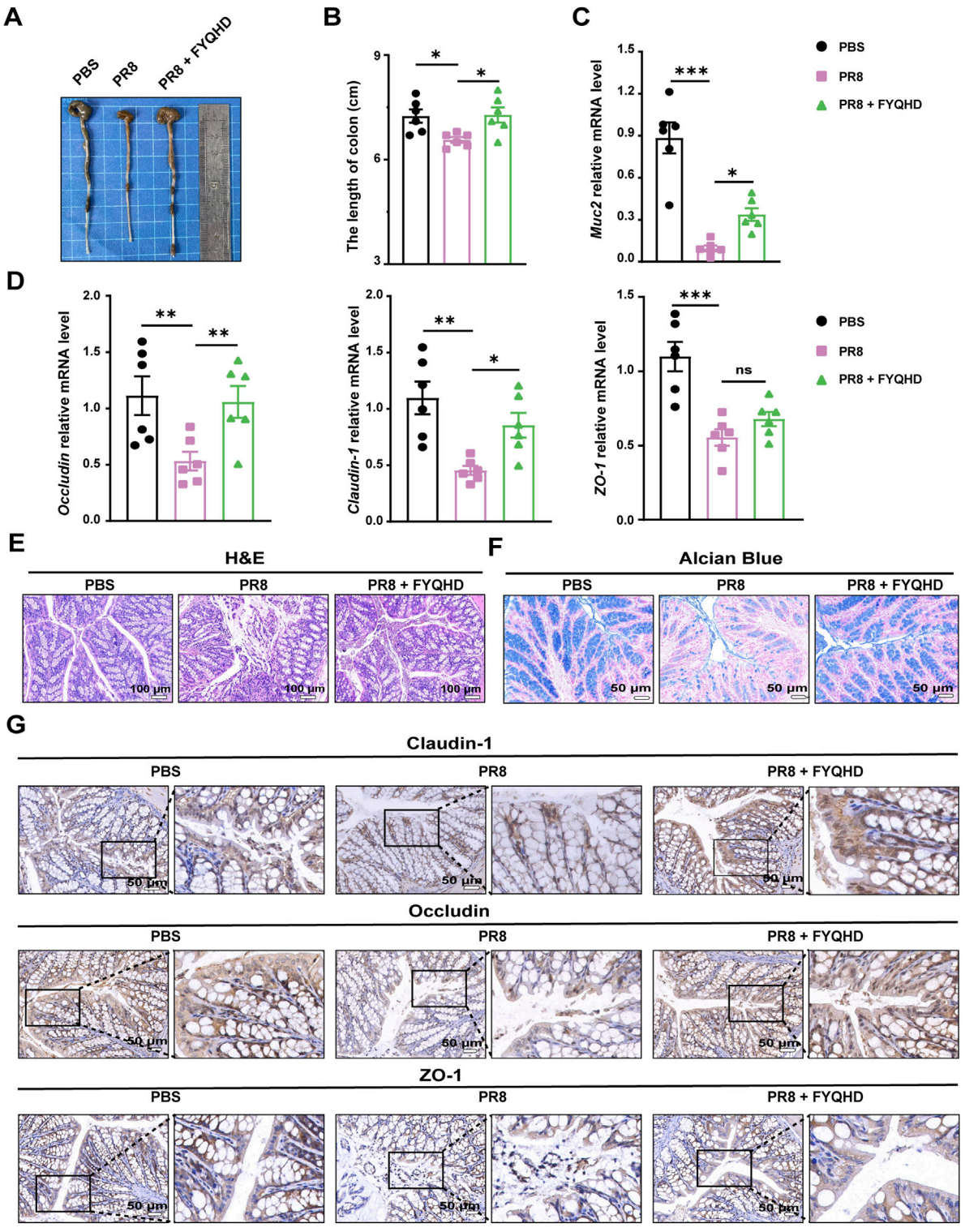


FIGURE 3
Protection of gut barrier damage in colons of flu mice by FYQHD. **(A, B)** Representative pictures of colons and colon lengths (n = 6). **(C, D)** Expressions of gut barrier-related molecules, *Muc2, Occludin, Claudin-1* and *ZO-1* in colon tissues detected by RT-qPCR. Data were presented as means ± SEM (n = 6 per group). Statistical significance was determined using one-way ANOVA, followed by Tukey test. *$P < 0.05$, **$P < 0.01$, ***$P < 0.001$, ****$P < 0.0001$ vs. PR8 group. **(E)** Representative microscopic pictures of H&E staining. (Scale bar: 100 μm). **(F)** Representative images of Alcian blue-stained inner mucus layer of colonic sections. (Scale bar: 50 μm). **(G)** Immunohistochemical staining of Occludin, Claudin-1 and ZO-1 in colons of different groups. (Scale bar: 50 μm).

10.3389/fphar.2024.1446749

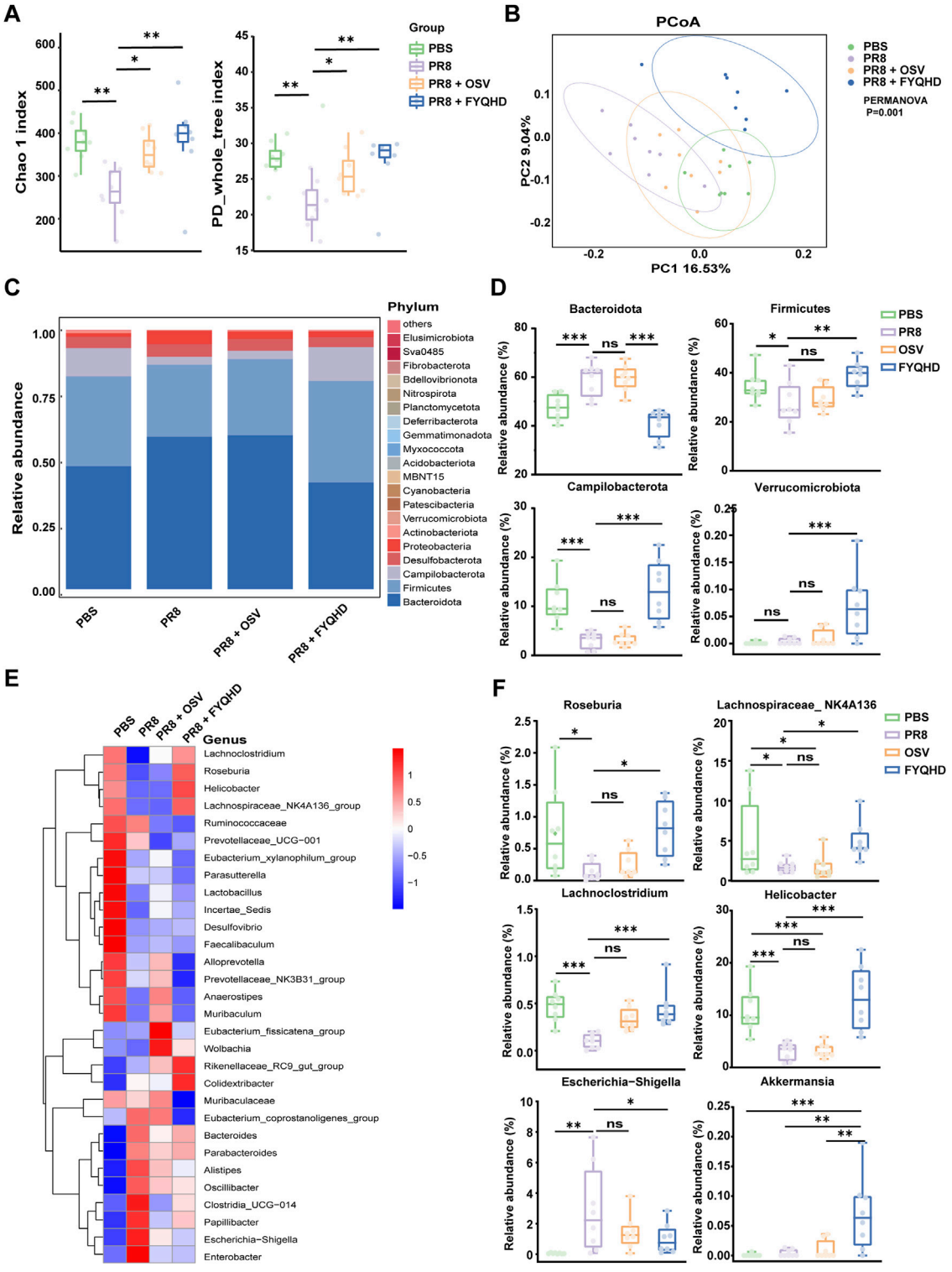


FIGURE 4
Influence of PR8 infection and FYQHD treatment on the homeostasis of intestinal microbiota in mice. **(A)** Alpha diversity upon oral therapy represented by the Chao1 and PD whole-tree indices. **(B)** Principal coordinate analysis (PCoA) plots upon different treatment assessed by PERMANOVA for β diversity. **(C)** Microbial community composition and the relative abundance for top 30 microbes at the phylum level. **(D)** Relative abundances of representative bacteria at phylum levels. **(E)** Relative abundance for top 30 microbes at the genus level. **(F)** Relative abundances of representative bacteria at genus levels. n = 8 for each group. Statistical analysis was performed using the one-way ANOVA. *$P < 0.05$, **$P < 0.01$, ***$P < 0.001$ vs. PR8 group.

10.3389/fphar.2024.1446749

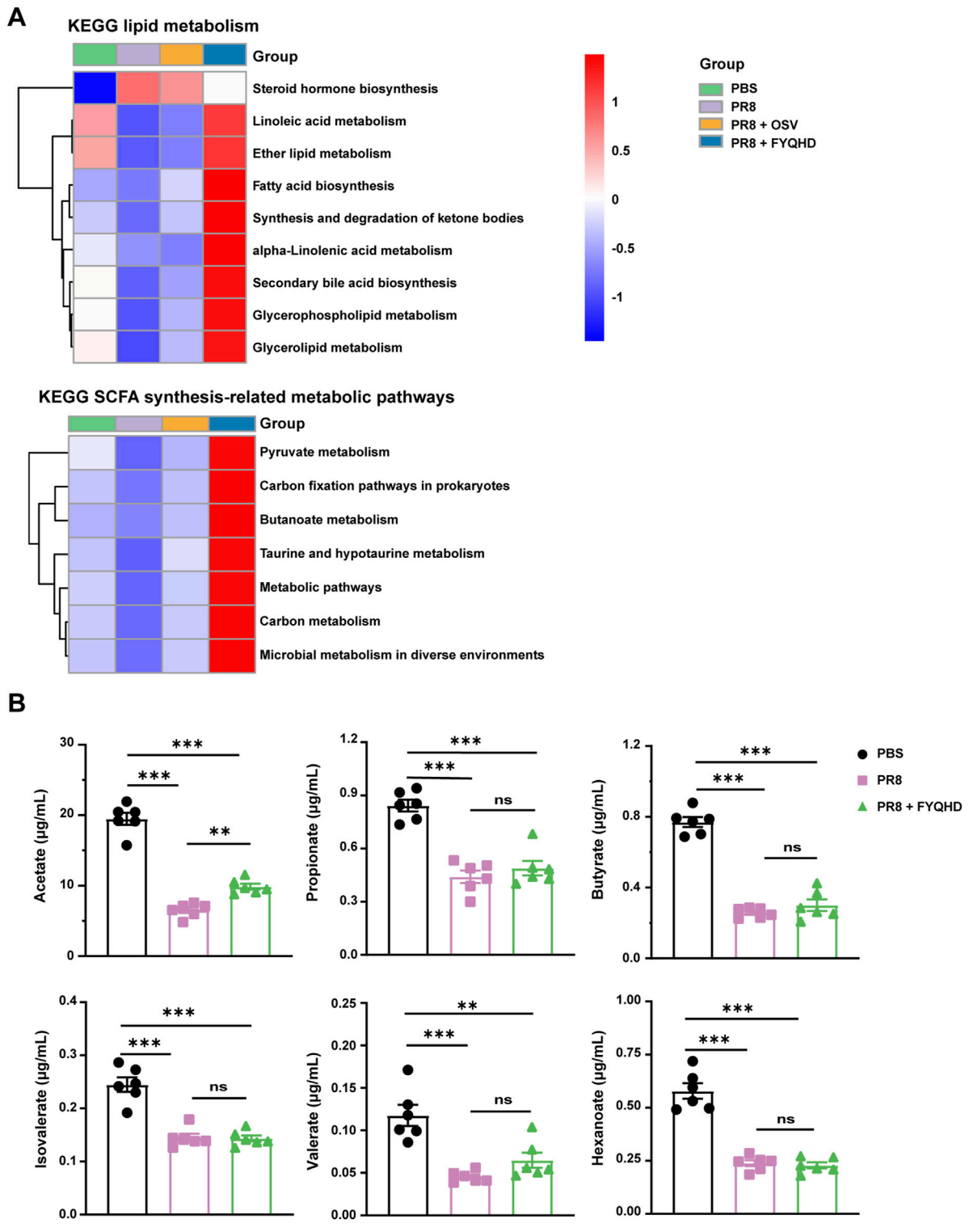


FIGURE 5
FYQHD regulated SCFA production of the gut microbiota in flu mice. **(A)** Analysis of differences in the Kyoto Encyclopedia of Genes and Genomes metabolic pathway. **(B)** Serum SCFA concentrations from mice of PBS, PR8 and PR8 + FYQHD groups (n = 6). Data were presented as means ± SD. *P* values were calculated by ANOVA followed by Tukey's test, $^{*}P < 0.05$, $^{**}P < 0.01$, $^{***}P < 0.001$, ns indicates $P > 0.05$ vs. PR8 group.

10.3389/fphar.2024.1446749

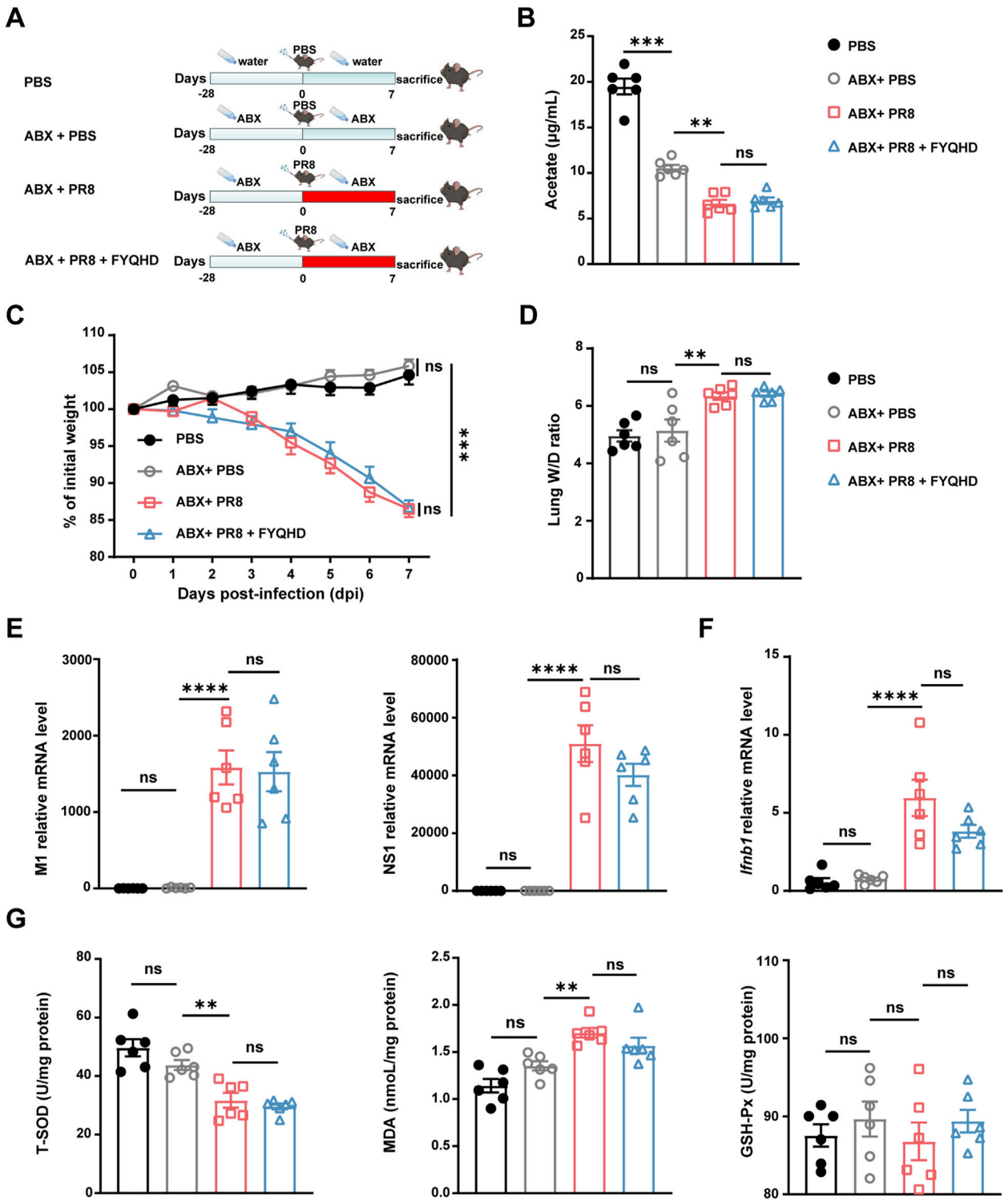


FIGURE 6
The protective effect of FYQHD on the lungs upon IAV infection was abrogated by antibiotic pretreatment. **(A)** Experimental schematic diagram. **(B)** Serum acetate concentrations from mice of PBS, ABX + PBS, ABX + PR8 and ABX + PR8+ FYQHD groups (n = 6). **(C)** Percentage of weight loss post infection relative to initial body weight (day 0) (n = 6 - 7). **(D)** Lung W/D ratio of mice (n = 6). **(E)** The relative gene expression of M1 and NS1 of PR8 detected in lung tissues by real-time PCR (n = 6). **(F)** *Ifnb1* gene expression detected in lung tissues by real-time PCR (n = 6). **(G)** Concentrations of T-SOD, MDA and GSH-Px in lungs from each group (n = 6). Data were presented as means ± SEM. Statistical significance was determined using one-way ANOVA, followed by Tukey test. $^{**}P < 0.01$, $^{****}P < 0.0001$, ns indicates $P > 0.05$ vs. ABX + PR8 group.

10.3389/fphar.2024.1446749

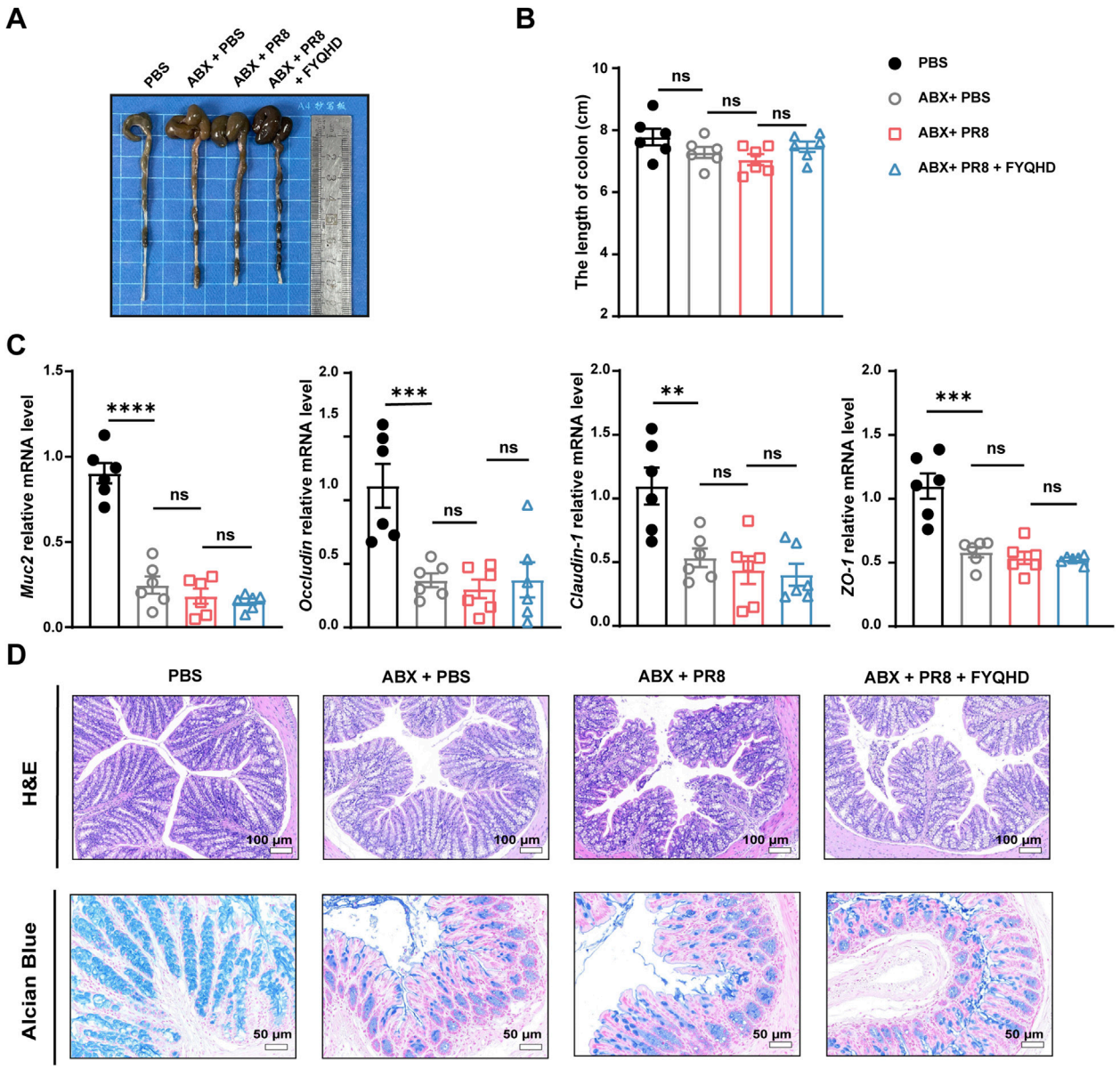


FIGURE 7
Protection of gut barrier damage in the colons of flu mice by FYQHD was abolished by antibiotic pretreatment. **(A, B)** Representative pictures of colons and colon lengths (n = 6). **(C)** The mRNA expressions of gut barrier-related molecules, *Muc2, Occludin, Claudin-1*, and *ZO-1* in colon tissues were detected by RT-qPCR. Data were presented as means ± SEM (n = 6 per group). Statistical significance was determined using one-way ANOVA, followed by Tukey test. $^{**}P < 0.01$, $^{***}P < 0.001$, $^{****}P < 0.0001$, ns indicates $P > 0.05$ vs. ABX + PR8 group. **(D)** Representative microscopic pictures of H&E staining (Scale bar: 100 μm) and representative images of Alcian blue-stained inner mucus layer of colonic sections. (Scale bar: 50 μm).

lung wet/dry ratios can assess the edema of lung tissues visually. The mice of PR8 group showed considerably higher lung wet/dry ratios than those of PBS group. Meanwhile, FYQHD treatment reduced the lung wet/dry ratio of mice significantly (Figure 2B).

Within 1 week post-infection, the lung tissues of mice with influenza experienced extensive viral replication. Our results also showed that FYQHD treatment reduced IAV replication in lungs, as indicated by the reduced expression of viral non-structural protein 1 (NS1) and viral M1 gene (Figure 2D). Consistently, the examination of viral titers on day 2 and day 3 post-infection showed that both OSV and FYQHD treatment successfully reduced the viral loads of the lungs from IAV mice (Figure 2E). Importantly, FYQHD administration increased the expression of *Ifnb1*and *Ifna1* in lungs compared to those of PR8 group on 7 dpi (Figure 2C; Supplementary Figure S7A). Therefore, we proposed that FYQHD regulated IAV replication probably by enhancing IFN-I expression in lung tissues.

To assess the influence of FYQHD on oxidative stress, total superoxide dismutase (T-SOD), glutathione peroxidase (GSH-Px), and malondialdehyde (MDA) in the sera and lungs were measured. Oral administration of FYQHD significantly improved the concentrations of T-SOD and GSH-Px while reducing MDA levels in the sera and lungs of mice compared to those of PBS controls (Figures 2F, G). Similarly, PR8 drastically elevated the

10.3389/fphar.2024.1446749

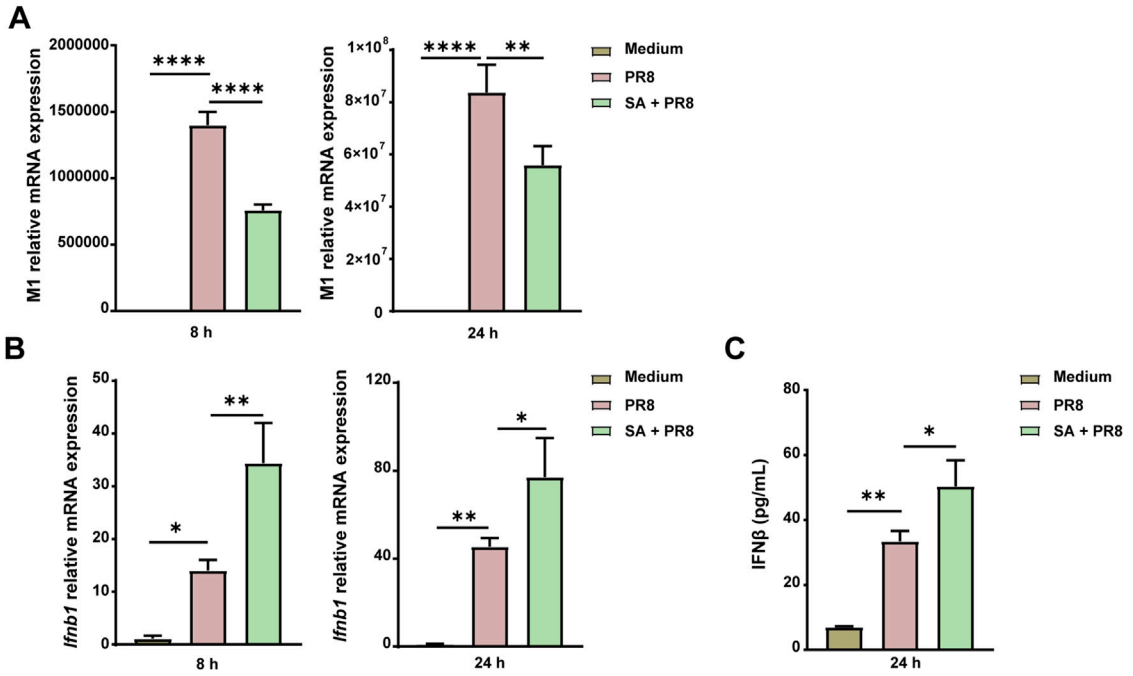


FIGURE 8
Acetate controls IAV replication by enhancing the expression of IFN-I in A549 cells. A549 cells were pretreated with 260 μM SA for 24 h and then infected with PR8 (MOI = 2) for 8 h or 24 h. **(A)** Relative PR8 M1 gene expression in A549. **(B)** Relative *Ifnb1* gene expression in A549. **(C)** Concentrations of IFN-β in the cell supernatant 24 h after infection were detected by ELISA. Data represented mean ± SD of 3 independent experiments. * $P < 0.05$, ** $P < 0.01$, **** $P < 0.0001$.

concentration of MPO in the lungs of mice, which was notably decreased by FYQHD treatment (Figure 2H). Hence, FYQHD showed strong antiviral and antioxidant effects during IAV infection.

3.4 FYQHD protected intestinal barrier against damage in flu mice

The colon length of PR8-infected mice was significantly shorter than those of PBS group on 7 dpi. FYQHD treatment restored the length of the colons (Figures 3A, B). Based on this observation, we examined the influence of FYQHD on the integrity of the intestinal barrier of flu mice. H&E staining served as a crucial indicator to evaluate the extent of colonic mucosa injury. As depicted in Figure 3E, compared to those of PBS group, the integrity of the intestinal mucosal structure was destroyed clearly in PR8 group. This was evidenced by incomplete crypt structures and disorganized villi with noticeable fractures and localized necrosis ranging from mild to severe. In contrast, FYQHD treatment rectified these pathological changes. Goblet cells in the colonic epithelium that secrete mucin were assessed utilizing Alcian blue staining. PR8 infection led to a substantial reduction in the thickness of the colonic epithelial mucosa and the amount of intestinal glycoprotein mucins. Remarkably, the administration of FYQHD exhibited significant restoration of these pathological changes (Figure 3F).

As we know, there are important protein components of the intestinal barrier related to intestinal integrity, including the tight junction proteins Claudin-1, ZO-1 and Occludin. The reduced expression of these proteins results in the destruction of the intestinal mucosa, arousing inflammatory response. As detected by qPCR, the expression of *Muc2, Occludin, Claudin-1*, and *ZO-1* displayed a noteworthy decrease in the colon tissues of PR8-infected mice. However, FYQHD intervention notably reversed their expression (Figures 3C, D). Consistently, immunohistochemical staining revealed the corresponding decrease of Claudin-1, ZO-1, and Occludin in the colons of PR8-infected mice. Encouragingly, FYQHD treatment effectively prevented the deteriorating loss of protein expression, and almost restored their expression to normal levels. The tight junctions between the intestinal epithelial cells were effectively maintained (Figure 3G).

These results implied that FYQHD may preserve the integrity of the intestinal barrier by restoring the expression of tight junction proteins. This allows for the maintenance of intestinal goblet cells in mice, highlighting the protective capacity of FYQHD on the intestinal barrier.

3.5 FYQHD treatment regulated the composition of gut microbiota

The influence of FYQHD on the gut microbial composition of PR8-treated mice was further investigated using 16S rRNA sequencing. The α diversity measure was employed to assess the richness and diversity of the gut microbiota. Several indices, including Chao1 and PD whole-tree index (Figure 4A), demonstrated comparable trends, suggesting that both OSV and

10.3389/fphar.2024.1446749

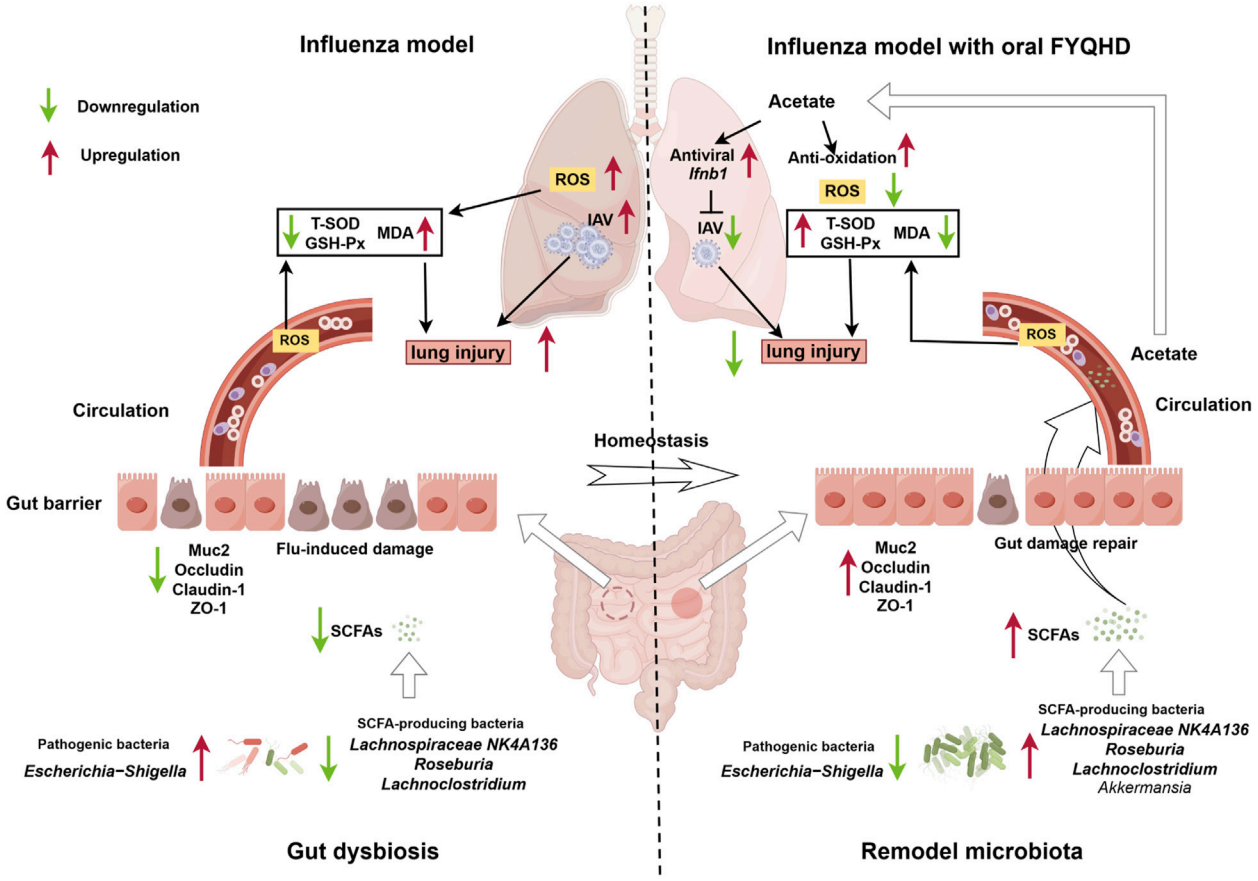


FIGURE 9
The administration of FYQHD remodeled the composition and diversity of gut microbiota, particularly up-regulated the abundance of SCFAs-producing bacteria such as *Lachnospiraceae_NK4A136, Lachnoclostridium, Roseburia and Akkermansia*. This led to increased production of acetate, which in turn promoted augmented IFN-I generation and antioxidative effects, resulting in the amelioration of lung injury (By Figdraw).

FYQHD treatment led to the maintenance of the diversity of gut microbiota, resulting in levels more closely resembling those of the PBS group. The dissimilarity of β-diversity was assessed using principal coordinate analysis (PCoA) (Figure 4B). PCoA using the unweighted UniFrac dissimilarity index revealed distinct clustering, PR8 group exhibited a noticeable separation from PBS group, whereas FYQHD and OSV treatment groups were demonstrated to be closer to PBS group (PERMANOVA P = 0.001). In general, the administration of FYQHD or OSV significantly changed the structural microbial diversity in the intestines of PR8-infected mice.

Subsequently, we evaluated the variances in populations and abundances among the 4 groups. The demonstrated top 30 microbes at the phylum (Figure 4C) and genus (Figure 4E) levels highlighted significant alterations within the composition of gut microbiota. At the phylum level (Figures 4C, D), *Bacteroidota*, *Firmicutes* and *Campilobacterota* were predominant phyla in the 4 groups. In PR8-infected mice, there was a notable increase in the relative abundance of *Bacteroidotas*, accompanied by a decrease in the levels of *Firmicutes* and *Campilobacterota*. However, the treatment of FYQHD effectively reversed these trends, restoring them to the levels comparable to those observed in PBS group. Furthermore, *Akkermansia* is well known to play a critical role in preserving intestinal mucosal function and is the sole enteric bacterium belonging to the *Verrucomicrobiota* phylum (Rajilic-Stojanovic and de Vos, 2014). As depicted in Figure 4D, there was a substantial increase in *Verrucomicrobiota* following FYQHD treatment, consistent with the initial findings of elevated intestinal glycoprotein mucins after FYQHD treatment as displayed in Figures 4C, E. At the genus level, there were remarkable changes in the levels of various gut microbiota in PR8-infected mice (Figure 4E). The infection of influenza virus decreased the relative abundance of the genera of *Roseburia*, *Lachnospiraceae_NK4A136*, *Lachnoclostridium*, and *Helicobacter*, while increased the level of genera of *Escherichia−Shigell*a. The treatment of FYQHD reinstated the composition of the gut microbiota to a level similar to that of the PBS group (Figure 4F). More notably, linear discriminant analysis effect size analysis (LEfSe) generated distribution histograms of LDA values, as illustrated in Supplementary Figure S3 (LDA >3, $p < 0.05$). Following FYQHD treatment, a number of bacterial genera such as *Helicobacter*, *Rikenellaceae_RC9*, *Roseburia*, and *Lachnospiraceae_NK4A136* exhibited enrichment, suggesting their potential as biomarkers for the FYQHD treatment group. Overall, FYQHD treatment significantly remodeled the composition and abundance of the gut microbiota and reversed the gut dysbiosis induced by PR8 infection.

3.6 FYQHD treatment altered microbiota-derived short-chain fatty acid (SCFA) profiles

Previous 16S rRNA sequencing analysis showed that gut microbiota in FYQHD-treated group displayed a predominance of the genera *Akkermansia, Lachnoclostridium, Roseburia*, and *Lachnospiraceae_NK4A136* group, which were generally associated with SCFA metabolism (Kasahara et al., 2018; Ma et al., 2020; Yang et al., 2021; Cani et al., 2022). SCFA represent the final products of anaerobic fermentation within the gastrointestinal tract and play a critical role in preserving immune homeostasis within the intestine (Lavelle and Sokol, 2020). The enrichment analysis of KEGG pathways was predicted from the results of 16S rRNA sequencing. Analysis of the KEGG metabolic pathways demonstrated that FYQHD predominantly enhanced lipid metabolic pathways, with the exception of steroid hormone biosynthesis. Furthermore, the analysis of KEGG metabolic pathways revealed that FYQHD notably enhanced metabolic pathways associated with the synthesis of SCFAs, such as pyruvate, carbon fixation pathways in prokaryotes, butanoate metabolism, taurine and hypotaurine metabolism, and carbon metabolism (Figure 5A). To further investigate the impact of FYQHD on the peripheral circulation of SCFAs, the amounts of acetate, propionate, butyrate, valerate, isobutyrate, and isovalerate in sera were measured. Interestingly, the acetate levels were found to be significantly elevated in sera from FYQHD-treated mice compared to PR8-infected mice, whereas concentrations of the other 5 SCFAs did not exhibit statistically significant differences (Figure 5B). Collectively, the administration of FYQHD resulted in changes in gut microbiota and increased synthesis of SCFAs in mice with influenza. These results indicated that acetate, a metabolite derived from gut microbiota, may play a crucial role in the therapeutic mechanism of FYQHD.

3.7 The protective effect of FYQHD on lung injury was abolished by antibiotic pretreatment

To investigate whether gut microbiota and the acetate participated in the protective effect of FYQHD against influenza-induced pulmonary damage, wild-type mice were given an antibiotic cocktail (ABX) in drinking water 28 days before PR8 inoculation (Figure 6A). After 4 weeks of antibiotic treatment, it was observed that FYQHD treatment did not increase acetate levels in the sera of mice (Figure 6B). Similarly, FYQHD did not change the levels of the remaining 5 SCFAs (Supplementary Figure S4). Strikingly, the ABX + PR8 + FYQHD group of mice exhibited similar severity of lung injury to those in ABX + PR8 group. This was supported by the indistinguishable body weight change (Figure 6C) and lung wet/dry ratios (Figure 6D). Furthermore, antiviral responses in ABX + PR8 + FYQHD group exhibited comparable trends to those in ABX + PR8 group, as evidenced by similar levels of lung viral load (Figure 6E) and *Ifnb1 and Ifna1* expression (Figure 6F; Supplementary Figure S7B). Meanwhile, the impact of FYQHD treatment on oxidative stress responses of gut microbiota-depleted mice was further investigated. The concentration of T-SOD, GSH-Px, and MDA in the lungs (Figure 6G) and sera (Supplementary Figure S5) displayed no significant difference between ABX + PR8 + FYQHD and ABX + PR8 groups. From the results mentioned above, it can be concluded that the presence of gut microbiota was indispensable for the protective effects of FYQHD on the lung injuries in PR8-infected mice.

3.8 FYQHD did not ameliorate the intestinal damage in flu mice with depleted gut microbiota

Whether microbiota and acetate were involved in the protection of FYQHD against intestinal damage in flu mice were investigated. As shown in Figures 7A, B, the 3 ABX-pretreated groups exhibited pronounced cecal oedema compared to those of PBS group, while no significant difference in colon lengths was observed. Strikingly, ABX + PR8 + FYQHD group mice displayed similar severity of intestinal barrier damage to ABX + PR8 group, as evidenced by indistinguishable expression of gut integrity markers *Muc2, Occludin, Claudin-1*, and *ZO-1* (Figure 7C). Meanwhile, the therapeutic effect of FYQHD was not observed in flu mice under the circumstances of gut microbiota depletion. Specifically, results of H&E staining, Alcian blue staining (Figure 7D), and immunohistochemical staining (Occludin, Claudin-1, and ZO-1) (Supplementary Figure S6) determinations revealed no obvious differences between the mice of ABX + PR8 + FYQHD group and ABX + PR8 group, suggesting that the absence of gut microbiota counteracted the beneficial effects of FYQHD. These experiments strongly suggested that the protection provided by FYQHD against intestinal barrier damage caused by PR8 infection relies on the homeostasis of gut microbiota.

3.9 Acetate suppresses IAV replication by enhancing IFN-I production in lung epithelial cells

Given the notable decline in viral load observed in the lungs and increased levels of acetate in the sera of PR8 + FYQHD group compared to PR8 mice, we hypothesized that acetate may exert a direct antiviral effect on pulmonary cells. Human lung epithelial cells (A549) were exposed to 260 μM sodium acetate (SA) 24 h before the infection of PR8. A549 cells treated with acetate showed a significant reduction in IAV replication at 8 h and 24 h post-infection, as evidenced by decreased expression of the viral M1 gene (Figure 8A). Remarkably, acetate treatment enhanced the expression of *Ifnb1* in A549 cells at 8 and 24 h post-IAV infection (Figure 8B) and increased IFN-β levels at 24 h post-IAV infection (Figure 8C). These findings suggest that the antiviral protective effect of FYQHD against IAV infection may be partially mediated by increased acetate levels and subsequent IFN-β production.

4 Discussion

FYQHD is a traditional Chinese medicine formula used clinically to treat influenza by experienced clinicians at Shuguang

Hospital, Shanghai University of Traditional Chinese Medicine. In the current study, the therapeutic effects of FYQHD on influenza were thoroughly demonstrated, including the inhibition of viral replication, alleviation of oxidative stress, amelioration of lung injury, and protection of survival in PR8-infected mice. The mechanisms are likely associated with restoring the balance of gut dysbiosis, increasing the enrichment of SCFA-producing bacteria, and upregulating the production of gut microbiota-derived acetate, which protected mice against IAV infection by enhancing IFN-I expression.

Our study showed that FYQHD improved the survival of mice with influenza. Mice in PBS group appeared lively with shiny fur, normal activity levels, consistent food and water intake, and gained body weight steadily. From 3 dpi on, the infected mice in PR8 group began to show flu symptoms, like messy and dull fur, decreased activity, lower food and water intake, experienced convulsions, hunchbacked, piloerection and shortness of breath, etc. In mice, infection with influenza virus resulted in body weight loss. The timely administration of FYQHD to treat flu has been demonstrated notably effective in attenuating viral replication and achieving therapeutic goals, including the recovery of body weights and decreased lung dry/wet weight ratios (D/W). Evidence has proven that ROS significantly increases in lung epithelial cell lines and primary murine cells upon IAV infection (Amatore et al., 2015). The nonstructural protein 1 (NS1) plays a significant role in the stimulation of ROS production by modulating the dynamics of mitochondria (Lee et al., 2021). Elevated levels of ROS facilitate IAV replication, thereby enhancing its pathogenesis (Peterhans, 1997). The influenza virus triggers an overproduction of ROS, ultimately exacerbating lung damage. FYQHD administration promoted the production of SOD and GSH-Px in mice with influenza while simultaneously reducing MDA levels, potentially alleviating the adverse effects of oxidative stress on lung injury.

FYQHD exhibited protective efficacy against influenza-associated intestinal damage in mice. While the H1N1 virus does not directly infect or replicate in human intestinal tissues, cytokines released by immune cells (e.g., Th17 cells) can lead to intestinal damage following IAV infection (Wang et al., 2014). Upon influenza virus infection, respiratory mucosa-derived lymphocytes migrate to the mesenteric lymph nodes via a chemokine-receptor (CCL25-CCR9) axis, disrupting the homeostasis of intestinal microbiome and ultimately causing intestinal immune damage (Ahmadi Badi et al., 2021). In our study, the colon lengths of PR8-infected mice were found to be much shorter than those of normal mice. However, FYQHD partially restored colon lengths to levels comparable to those of the PBS group. Consistent with our results, Wang *et al.* found that respiratory influenza virus infection resulted in intestinal immune damage and a decrease in colon length (Wang et al., 2014). Furthermore, other studies have shown that flu-infected mice experienced damage to both the lungs and intestines (Zhu et al., 2018). Our experiment indicated that the influenza virus significantly reduced the expression of the tight junction proteins Claudin-1, ZO-1, and Occludin, directly decreasing the integrity and causing damage to the intestinal epithelial barrier. Concurrently, the expression of *Muc2* was significantly reduced by influenza virus. Muc2 mucin is crucial for protecting the gut barrier and maintaining the balance of gut microbiota (Liu et al., 2020). Interestingly, FYQHD treatment ameliorated the aforementioned gut injury. Further research is needed to investigate the mechanism of FYQHD on PR8-induced intestinal injury.

Furthermore, evidence indicated that the gastrointestinal tract and respiratory system, along with their respective microbiomes, were interconnected and mutually influenced. This concept is known as the gut-lung axis (Dumas et al., 2018). The ancient theory in traditional Chinese medicine that describes the "the lung and the large intestine are interior-exterior" is consistent with the modern concept of the "gut-lung axis" as revealed by contemporary research. Thus, the gut microbiota has become a new therapeutic target for respiratory viral infection currently. Certain herbal medicines were reported to modulate the diversity and abundance of gut microbiota, which could have played a crucial role in inhibiting IAV replication and reducing inflammatory damage to lung tissues, such as GeGen QinLian decoction (Deng et al., 2021), Qingfeiyin decoction (Li et al., 2022), and Cangma Huadu granules (Liu et al., 2022). Hence, we proceeded to examine whether FYQHD regulated the composition of gut microbiota during IAV infection. The results demonstrated that IAV infection had a significant impact on the balance of the gut microbiota, as indicated by a decrease in the diversity and richness of the microbiota. In addition, IAV infection significantly increased the abundance of *Escherichia–Shigella*, while reduced the abundance of *Lachnospiraceae_NK4A136*, *Lachnoclostridium, Roseburia*, and *Helicobacter* in the mouse gut microbiota. Nevertheless, FYQHD treatment reversed these changes. Earlier studies had suggested that *Escherichia–Shigella*, a bacterium with conditional pathogenicity in the intestine, was a common trigger for vomiting and diarrhea (Wang et al., 2014). *Helicobacter* is thought to provide effective protection for mice against tissue inflammatory damage in asthma, easing the infiltration of inflammatory cells in the bronchioles and alveoli (Arnold et al., 2011). It is well-known that SCFAs are crucial for maintaining the homeostasis of the intestinal epithelial barrier (Parada Venegas et al., 2019). As demonstrated here, the abundance of *Lachnoclostridium, Roseburia*, and *Lachnospiraceae_NK4A136* were notably increased by FYQHD treatment, and they were all considered beneficial members *via* regulating SCFA metabolism (Kasahara et al., 2018; Ma et al., 2020; Yang et al., 2021). The abundance of *Lachnospiraceae* was significantly decreased in the intestines of COVID-19 patients, replaced by other potentially pathogenic bacteria, contributing to pulmonary hyperinflammation (Kaushal and Noor, 2022). In a recent study, mice that received *Lachnospiraceae* showed reduced airway RSV viral load, diminished lung injury, and increased overall lifespan (Antunes et al., 2019). *Akkermansia*, a well-established next-generation probiotic and producer of SCFAs, has been demonstrated to prominently feature in the connections between gut microbes and host responses (Bae et al., 2022). It contributed to an anti-H7N9 effect through its ability to regulate inflammation and the immune system (Hu X. et al., 2020). Interestingly, compared with the mice of PR8 group, the intestinal enrichment of *Akkermansia* was substantially promoted by FYQHD treatment in flu mice. Moreover, an important observation was that the modified microbiota diversity and composition after FYQHD administration appeared to align with those of PBS group. On the contrary, the change of gut microbiota in OSV-treated flu

mice was comparable to those of PR8-infected mice. This was mainly because the primary anti-viral mechanism of OSV was the inhibition of neuraminidase, so it did not have a critical impact on the gut microbiota. These results implied that the employment of FYQHD could be an effective treatment of influenza by restoring the unbalanced gut microbiota, enhancing microbial diversity, and promoting the proliferation of beneficial bacteria.

Previous research had indicated that SCFA produced in the gut could enter the systemic circulation and exert distant biological effects (Sencio et al., 2020). Evidence showed that TCM had the potential to improve lipid metabolism by increasing SCFA levels and modulating the biosynthesis of branched-chain amino acids (Li et al., 2021). Our results indicated that SCFA-producing bacteria in the gut may play a crucial role in the protective effect of FYQHD during IAV infection. To determine if FYQHD exerts protective effects on lung injuries by promoting the production of SCFAs in the gut, the concentration of SCFAs in sera was measured after FYQHD treatment. As expected, FYQHD-treated group exhibited increased levels of acetate in the sera compared to those of PR8 group. Our findings were in an agreement with previous reports (Hashemi et al., 2017), showing that an increased abundance of the *Lachnospiraceae* family was associated with elevated serum levels of acetate. To further substantiate the hypothesis that the gut-lung axis was a target of FYQHD, this study generated mice with depleted gut microbiota using a broad-spectrum antibiotic. The results demonstrated that the protective effects of FYQHD on IAV infection were significantly diminished following gut microbiota depletion. Measures of acetate, viral loads, *Ifnb1*, and oxidative stress factors were similar in both ABX + PR8 group and the ABX + PR8 + FYQHD group. Additionally, no significant differences were observed in intestinal histological injuries and the expression of tight junctions between these groups. We fully acknowledge that traditional Chinese medicine might operate through multiple targets via various ingredients entering the bloodstream or their metabolic products. Germ-free mouse models and additional experiments are necessary to further validate these results. It is possible that other protective effects, such as anti-inflammatory actions, may not be adequately demonstrated in this model.

Emerging evidence suggested that acetate, a microbiota-derived metabolite, influenced immune responses during viral infection in the lung. Recently, research demonstrated that acetate protected against RSV infection by boosting type 1 interferon responses in lung epithelial cells via GPR43 induction. Acetate administered orally enhanced IFN-β response by upregulating interferon-stimulated genes (ISGs) in the lung. The antiviral activity of acetate in pulmonary epithelial cell lines and its protective effect in RSV-infected mice relied on type 1 IFN signaling through the IFN-1 receptor (IFNAR) (Hashemi et al., 2017). It is well known that epithelial cells in the respiratory epithelium are the primary target cells for IAV replication (Ramos et al., 2019). Notably, our study showed that acetate treatment in A549 cells led to a significant enhancement of *Ifnb1* expression and a reduction in the replication of influenza A virus. Innate immune cells like macrophages and neutrophils play crucial roles in detecting IAV infection and suppressing the virus shortly after infection (Iwasaki and Pillai, 2014). A recent study highlighted the significance of acetate in macrophages in controlling IAV, as demonstrated by the decreased effectiveness of acetate after macrophage depletion (Niu et al., 2023). The study found that acetate from *Bifidobacterium pseudolongum NjM1* provided protection against influenza A virus infection by activating the GPR43-MAVS-IRF3 pathway and inducing the IFN-I signal. In summary, the data indicated a mechanism by which FYQHD boosted the presence of acetate-producing bacteria, resulting in heightened acetate concentrations in lungs. This facilitated the inhibition of IAV replication by augmenting IFN-I generation. Given the wide-ranging antiviral properties of IFN-I, FYQHD might also be effective against other viral infections, for example, SARS-CoV-2 or RSV.

There has been extensive research into TCM for the treatment of influenza, both as individual components and as TCM compound formulas. This study initially revealed the identification of 17 major compounds in sera following oral administration of FYQHD, including ephedrine, liquitin, baicalin, wogonoside, saikosaponin D, glycyrrhizic acid, wogonin, rhein, emodin, and so on. Increasing evidence has shown that baicalin can inhibit the replication of IAV *in vivo* and *in vitro*, as well as inhibit the inflammatory response (Ding et al., 2014; Jin et al., 2018; Pang et al., 2018). A prior investigation found that phillyrin could improve the survival of influenza mice, decrease the pulmonary viral titers and decreases lung indices (Qu et al., 2016). Glycyrrhizic acid is also demonstrated to enhance the survival rate of H1N1-infected mice, decreased the virus titers in lungs, and reduced the expression of inflammatory factors (Chen et al., 2015). Collectively, these studies indicated that multiple components of FYQHD might play a role in its anti-viral effects and protect against influenza through complicated mechanisms. However, further studies are still needed to verify which component of FYQHD is able to modulate the increase in the abundance of acetate-producing bacteria and consequently exhibiting an anti-viral effect.

FYQHD has demonstrated efficacy against community-acquired pneumonia (CAP) in clinical practice for nearly 2 decades. In our previous study, FYQHD showed efficacy in treating LPS challenge or carbapenem-resistant *Klebsiella pneumoniae* (CRKP) infection (Zhang et al., 2024). It displayed dual regulatory effects, dampening the inflammatory response by inhibiting the PI3K/AKT/mTOR/4E-BP1 and HMGB1/RAGE signaling pathways, while also boosting bacterial phagocytosis to manage bacterial burden in the liver and spleen. This research is the first to examine how the gut microbiome mediates the protective effects of FYQHD against influenza. However, this study has limitations, and additional research is necessary to determine how FYQHD specifically regulates microbiota function and intestinal barrier integrity. Our current findings demonstrate that FYQHD influences the composition and abundance of gut microbiota, enhancing populations of acetate-producing bacteria. Additional *in vivo* and *in vitro* studies are necessary to identify the precise compounds in FYQHD responsible for this biological activity. Our future work will focus on identifying the key active components of FYQHD and elucidating their roles in modulating gut microbiota and their metabolites. Another limitation is the lack of clinical data in this study. Fortunately, a randomized controlled trial (RCT) investigating the efficacy of FYQHD in influenza patients is currently underway. In future research, fecal and

blood samples from influenza patients will be analyzed between FYQHD-treated and control groups to elucidate its protective role and underlying mechanisms.

5 Conclusion

In conclusion, the present study demonstrated that the administration of FYQHD remodeled gut dysbiosis, particularly by increasing the abundance of acetate-producing bacteria such as *Lachnospiraceae_NK4A136*, *Lachnoclostridium*, and *Roseburia*, leading to higher acetate production. The acetate was transported to the lungs, where it stimulated IFN-β production, offering protection against IAV infection and enhancing the antioxidant stress response (Figure 9). These findings highlight the complex and critical relationship between the gut and lungs, providing an experimental basis for validating the concept of TCM based on the theory of 'simultaneous treatment of the lungs and intestines.' Our findings further support the clinical application of FYQHD and provide new insights into the mechanism of TCM for treating influenza.

Data availability statement

The raw 16S sequencing data is deposited at the NCBI repository, BioProject accession number PRJNA1120572. Available at: https://www.ncbi.nlm.nih.gov/bioproject/PRJNA1120572/.

Ethics statement

The animal study was approved by the Institute of Infection and Immunology, Chinese Academy of Sciences for the Care and Use of Laboratory Animals with the approval of the Institute Animal Welfare, and Care Committee with No. A2021-L027. The study was conducted in accordance with the local legislation and institutional requirements.

Author contributions

BD: Writing–review and editing, Writing–original draft, Project administration, Methodology, Investigation, Formal Analysis, Data curation. XW: Writing–review and editing, Methodology, Investigation, Formal Analysis, Data curation. YH: Writing–review and editing, Methodology, Investigation. GX: Writing–review and editing, Methodology, Investigation, Data curation. HZ: Writing–review and editing, Project administration, Formal Analysis, Data curation. QH: Writing–review and editing, Methodology, Investigation. XC: Writing–review and editing, Software, Formal Analysis. ND: Writing–review and editing, Software, Investigation, Data curation. LZ: Writing–review and editing, Investigation, Data curation. WZ: Writing–review and editing, Project administration, Supervision, Methodology. HA: Writing–review and editing, Validation, Supervision. YZ: Writing–original draft, Validation, Resources, Project administration, Funding acquisition.

Funding

The author(s) declare that financial support was received for the research, authorship, and/or publication of this article. This research was funded by the National Natural Science Foundation of China (82474159, 82073901, 32200955), National Key Research and Development Program of China (2021YFE0200900), Shanghai Municipal Science and Technology Major Project (ZD2021CY001) and Three-year Action Plan for Shanghai TCM Development and Inheritance Program [ZY (2021-2023)-0103].

Acknowledgments

The influenza viral strain (A/PR/8/34, PR8) was kindly provided by Prof. Robert G. Webster from St. Jude Children's Research Hospital (Memphis, United States).

Conflict of interest

The authors declare that the research was conducted in the absence of any commercial or financial relationships that could be construed as a potential conflict of interest.

Publisher's note

All claims expressed in this article are solely those of the authors and do not necessarily represent those of their affiliated organizations, or those of the publisher, the editors and the reviewers. Any product that may be evaluated in this article, or claim that may be made by its manufacturer, is not guaranteed or endorsed by the publisher.

Supplementary material

The Supplementary Material for this article can be found online at: https://www.frontiersin.org/articles/10.3389/fphar.2024.1446749/full#supplementary-material

References

Ahmadi Badi, S., Tarashi, S., Fateh, A., Rohani, P., Masotti, A., and Siadat, S. D. (2021). From the role of microbiota in gut-lung Axis to SARS-CoV-2 pathogenesis. *Mediat. Inflamm.* 2021, 6611222. doi:10.1155/2021/6611222

Amatore, D., Sgarbanti, R., Aquilano, K., Baldelli, S., Limongi, D., Civitelli, L., et al. (2015). Influenza virus replication in lung epithelial cells depends on redox-sensitive pathways activated by NOX4-derived ROS. *Cell. Microbiol.* 17 (1), 131–145. doi:10.1111/cmi.12343

Antunes, K. H., Fachi, J. L., de Paula, R., da Silva, E. F., Pral, L. P., Dos Santos, A. A., et al. (2019). Microbiota-derived acetate protects against respiratory syncytial virus infection through a GPR43-type 1 interferon response. *Nat. Commun.* 10 (1), 3273. doi:10.1038/s41467-019-11152-6

Arnold, I. C., Dehzad, N., Reuter, S., Martin, H., Becher, B., Taube, C., et al. (2011). *Helicobacter pylori* infection prevents allergic asthma in mouse models through the induction of regulatory T cells. *J. Clin. Investig.* 121 (8), 3088–3093. doi:10.1172/JCI45041

Bae, M., Cassilly, C. D., Liu, X., Park, S. M., Tusi, B. K., Chen, X., et al. (2022). Akkermansia muciniphila phospholipid induces homeostatic immune responses. *Nature* 608 (7921), 168–173. doi:10.1038/s41586-022-04985-7

Cani, P. D., Depommier, C., Derrien, M., Everard, A., and de Vos, W. M. (2022). Akkermansia muciniphila: paradigm for next-generation beneficial microorganisms. *Nat. Rev. Gastroenterol. Hepatol.* 19 (10), 625–637. doi:10.1038/s41575-022-00631-9

Chen, X. X., Zhou, H. X., Qi, W. B., Ning, Z. Y., Ma, Y. J., Li, Y. L., et al. (2015). Antiviral effects of the combination of glycyrrhizin and ribavirin against influenza A H1N1 virus infection *in vivo*. *Yao Xue Xue Bao* 50 (8), 966–972. doi:10.16438/j.0513-4870.2015.08.001

Deng, L., Shi, Y., Liu, P., Wu, S., Lv, Y., Xu, H., et al. (2021). GeGen QinLian decoction alleviate influenza virus infectious pneumonia through intestinal flora. *Biomed. Pharmacother.* 141, 111896. doi:10.1016/j.biopha.2021.111896

Ding, Y., Dou, J., Teng, Z., Yu, J., Wang, T., Lu, N., et al. (2014). Antiviral activity of baicalin against influenza A (H1N1/H3N2) virus in cell culture and in mice and its inhibition of neuraminidase. *Arch. Virol.* 159 (12), 3269–3278. doi:10.1007/s00705-014-2192-2

Doherty, P. C., Turner, S. J., Webby, R. G., and Thomas, P. G. (2006). Influenza and the challenge for immunology. *Nat. Immunol.* 7 (5), 449–455. doi:10.1038/ni1343

Dumas, A., Bernard, L., Poquet, Y., Lugo-Villarino, G., and Neyrolles, O. (2018). The role of the lung microbiota and the gut-lung axis in respiratory infectious diseases. *Cell. Microbiol.* 20 (12), e12966. doi:10.1111/cmi.12966

Hashemi, Z., Fouhse, J., Im, H. S., Chan, C. B., and Willing, B. P. (2017). Dietary pea fiber supplementation improves glycemia and induces changes in the composition of gut microbiota, serum short chain fatty acid profile and expression of mucins in glucose intolerant rats. *Nutrients* 9 (11), 1236. doi:10.3390/nu9111236

He, Y., Wen, Q., Yao, F., Xu, D., Huang, Y., and Wang, J. (2017). Gut-lung axis: the microbial contributions and clinical implications. *Crit. Rev. Microbiol.* 43 (1), 81–95. doi:10.1080/1040841X.2016.1176988

Herold, S., Becker, C., Ridge, K. M., and Budinger, G. R. (2015). Influenza virus-induced lung injury: pathogenesis and implications for treatment. *Eur. Respir. J.* 45 (5), 1463–1478. doi:10.1183/09031936.00186214

Hu, S., Kuwabara, R., de Haan, B. J., Smink, A. M., and de Vos, P. (2020a). Acetate and butyrate improve β-cell metabolism and mitochondrial respiration under oxidative stress. *Int. J. Mol. Sci.* 21 (4), 1542. doi:10.3390/ijms21041542

Hu, X., Zhao, Y., Yang, Y., Gong, W., Sun, X., Yang, L., et al. (2020b). Akkermansia muciniphila improves host defense against influenza virus infection. *Front. Microbiol.* 11, 586476. doi:10.3389/fmicb.2020.586476

Huang, K., Zhang, P., Zhang, Z., Youn, J. Y., Wang, C., Zhang, H., et al. (2021). Traditional Chinese Medicine (TCM) in the treatment of COVID-19 and other viral infections: efficacies and mechanisms. *Pharmacol. Ther.* 225, 107843. doi:10.1016/j.pharmthera.2021.107843

Ichinohe, T., Pang, I. K., Kumamoto, Y., Peaper, D. R., Ho, J. H., Murray, T. S., et al. (2011). Microbiota regulates immune defense against respiratory tract influenza A virus infection. *Proc. Natl. Acad. Sci. U. S. A.* 108 (13), 5354–5359. doi:10.1073/pnas.1019378108

Iuliano, A. D., Roguski, K. M., Chang, H. H., Muscatello, D. J., Palekar, R., Tempia, S., et al. (2018). Estimates of global seasonal influenza-associated respiratory mortality: a modelling study. *Lancet* 391 (10127), 1285–1300. doi:10.1016/S0140-6736(17)33293-2

Ivashkiv, L. B., and Donlin, L. T. (2014). Regulation of type I interferon responses. *Nat. Rev. Immunol.* 14 (1), 36–49. doi:10.1038/nri3581

Iwasaki, A., and Pillai, P. S. (2014). Innate immunity to influenza virus infection. *Nat. Rev. Immunol.* 14 (5), 315–328. doi:10.1038/nri3665

Jin, J., Chen, Y., Wang, D., Ma, L., Guo, M., Zhou, C., et al. (2018). The inhibitory effect of sodium baicalin on oseltamivir-resistant influenza A virus via reduction of neuraminidase activity. *Arch. Pharm. Res.* 41 (6), 664–676. doi:10.1007/s12272-018-1022-6

Kasahara, K., Krautkramer, K. A., Org, E., Romano, K. A., Kerby, R. L., Vivas, E. I., et al. (2018). Interactions between Roseburia intestinalis and diet modulate atherogenesis in a murine model. *Nat. Microbiol.* 3 (12), 1461–1471. doi:10.1038/s41564-018-0272-x

Kaushal, A., and Noor, R. (2022). Association of gut microbiota with inflammatory bowel disease and COVID-19 severity: a possible outcome of the altered immune response. *Curr. Microbiol.* 79 (6), 184. doi:10.1007/s00284-022-02877-7

Kim, C. H. (2021). Control of lymphocyte functions by gut microbiota-derived short-chain fatty acids. *Cell. Mol. Immunol.* 18 (5), 1161–1171. doi:10.1038/s41423-020-00625-0

Lavelle, A., and Sokol, H. (2020). Gut microbiota-derived metabolites as key actors in inflammatory bowel disease. *Nat. Rev. Gastroenterol. Hepatol.* 17 (4), 223–237. doi:10.1038/s41575-019-0258-z

Lee, J. H., Oh, S. J., Yun, J., and Shin, O. S. (2021). Nonstructural protein NS1 of influenza virus disrupts mitochondrial dynamics and enhances mitophagy via ULK1 and BNIP3. *Viruses* 13 (9), 1845. doi:10.3390/v13091845

Li, X., Wang, M., Liu, C., Xiao, Y., Li, M., Ban, C., et al. (2022). Qingfeiyin decoction inhibits H1N1 virus infection via modulation of gut microbiota and inflammatory pathways in a murine model. *Front. Pharmacol.* 13, 874068. doi:10.3389/fphar.2022.874068

Li, Y., Ji, X., Wu, H., Li, X., Zhang, H., and Tang, D. (2021). Mechanisms of traditional Chinese medicine in modulating gut microbiota metabolites-mediated lipid metabolism. *J. Ethnopharmacol.* 278, 114207. doi:10.1016/j.jep.2021.114207

Liu, M., Liu, T., Wang, X., Yu, C., Qin, T., Li, J., et al. (2022). Cangma Huadu granules attenuate H1N1 virus-induced severe lung injury correlated with repressed apoptosis and altered gut microbiome. *Front. Microbiol.* 13, 947112. doi:10.3389/fmicb.2022.947112

Liu, Y., Yu, X., Zhao, J., Zhang, H., Zhai, Q., and Chen, W. (2020). The role of MUC2 mucin in intestinal homeostasis and the impact of dietary components on MUC2 expression. *Int. J. Biol. Macromol.* 164, 884–891. doi:10.1016/j.ijbiomac.2020.07.191

Ma, L., Ni, Y., Wang, Z., Tu, W., Ni, L., Zhuge, F., et al. (2020). Spermidine improves gut barrier integrity and gut microbiota function in diet-induced obese mice. *Gut Microbes* 12 (1), 1–19. doi:10.1080/19490976.2020.1832857

Niu, J., Cui, M., Yang, X., Li, J., Yao, Y., Guo, Q., et al. (2023). Microbiota-derived acetate enhances host antiviral response via NLRP3. *Nat. Commun.* 14 (1), 642. doi:10.1038/s41467-023-36323-4

Nossa, C. W., Oberdorf, W. E., Yang, L., Aas, J. A., Paster, B. J., Desantis, T. Z., et al. (2010). Design of 16S rRNA gene primers for 454 pyrosequencing of the human foregut microbiome. *World J. Gastroenterol.* 16 (33), 4135–4144. doi:10.3748/wjg.v16.i33.4135

Pang, P., Zheng, K., Wu, S., Xu, H., Deng, L., Shi, Y., et al. (2018). Baicalin downregulates RLRs signaling pathway to control influenza A virus infection and improve the prognosis. *Evid. Based Complement. Altern. Med.* 2018, 4923062. doi:10.1155/2018/4923062

Parada Venegas, D., De la Fuente, M. K., Landskron, G., Gonzalez, M. J., Quera, R., Dijkstra, G., et al. (2019). Short chain fatty acids (SCFAs)-Mediated gut epithelial and immune regulation and its relevance for inflammatory bowel diseases. *Front. Immunol.* 10, 277. doi:10.3389/fimmu.2019.00277

Peterhans, E. (1997). Oxidants and antioxidants in viral diseases: disease mechanisms and metabolic regulation. *J. Nutr.* 127 (5 Suppl. l), 962S-965S–965S. doi:10.1093/jn/127.5.962S

Qu, X. Y., Li, Q. J., Zhang, H. M., Zhang, X. J., Shi, P. H., Zhang, X. J., et al. (2016). Protective effects of phillyrin against influenza A virus *in vivo*. *Arch. Pharm. Res.* 39 (7), 998–1005. doi:10.1007/s12272-016-0775-z

Rajilic-Stojanovic, M., and de Vos, W. M. (2014). The first 1000 cultured species of the human gastrointestinal microbiota. *FEMS Microbiol. Rev.* 38 (5), 996–1047. doi:10.1111/1574-6976.12075

Ramos, I., Smith, G., Ruf-Zamojski, F., Martinez-Romero, C., Fribourg, M., Carbajal, E. A., et al. (2019). Innate immune response to influenza virus at single-cell resolution in human epithelial cells revealed paracrine induction of interferon lambda 1. *J. Virol.* 93 (20), 00559–19. doi:10.1128/JVI.00559-19

Rudiansyah, M., Abdalkareem Jasim, S., B, S. A., Samusenkov, V., Kamal Abdelbasset, W., Yasin, G., et al. (2022). The emerging microbiome-based approaches to IBD therapy: from SCFAs to urolithin A. *J. Dig. Dis.* 23 (8-9), 412–434. doi:10.1111/1751-2980.13131

Schroeder, B. O., Birchenough, G. M. H., Stahlman, M., Arike, L., Johansson, M. E. V., Hansson, G. C., et al. (2018). Bifidobacteria or fiber protects against diet-induced microbiota-mediated colonic mucus deterioration. *Cell. Host Microbe* 23 (1), 27–40. doi:10.1016/j.chom.2017.11.004

Sencio, V., Barthelemy, A., Tavares, L. P., Machado, M. G., Soulard, D., Cuinat, C., et al. (2020). Gut dysbiosis during influenza contributes to pulmonary pneumococcal superinfection through altered short-chain fatty acid production. *Cell. Rep.* 30 (9), 2934–2947. doi:10.1016/j.celrep.2020.02.013

Stefan, K. L., Kim, M. V., Iwasaki, A., and Kasper, D. L. (2020). Commensal microbiota modulation of natural resistance to virus infection. *Cell.* 183 (5), 1312–1324. doi:10.1016/j.cell.2020.10.047

Sun, J., Ding, X., Liu, S., Duan, X., Liang, H., and Sun, T. (2020). Adipose-derived mesenchymal stem cells attenuate acute lung injury and improve the gut microbiota in septic rats. *Stem Cell. Res. Ther.* 11 (1), 384. doi:10.1186/s13287-020-01902-5

Waehre, T., Tunheim, G., Bodin, J. E., Laake, I., Kvale, D., Kran, A. B., et al. (2022). Clinical characteristics and outcomes in hospitalized adult influenza patients: an observational study from Norway 2014-2018. *Infect. Dis. (Lond)* 54 (5), 367–377. doi:10.1080/23744235.2021.2022196

Wang, J., Li, F., Wei, H., Lian, Z. X., Sun, R., and Tian, Z. (2014). Respiratory influenza virus infection induces intestinal immune injury via microbiota-

mediated Th17 cell-dependent inflammation. *J. Exp. Med.* 211 (12), 2397–2410. doi:10.1084/jem.20140625

Xi, S., Li, Y., Yue, L., Gong, Y., Qian, L., Liang, T., et al. (2020). Role of traditional Chinese medicine in the management of viral pneumonia. *Front. Pharmacol.* 11, 582322. doi:10.3389/fphar.2020.582322

Yang, J., Chen, W., Sun, Y., Liu, J., and Zhang, W. (2021). Effects of cadmium on organ function, gut microbiota and its metabolomics profile in adolescent rats. *Ecotoxicol. Environ. Saf.* 222, 112501. doi:10.1016/j.ecoenv.2021.112501

Ye, L., Zhang, Q., Xin, F., Cao, B., Qian, L., and Dong, Y. (2021). Neonatal milk fat globule membrane supplementation during breastfeeding ameliorates the deleterious effects of maternal high-fat diet on metabolism and modulates gut microbiota in adult mice offspring in a sex-specific way. *Front. Cell. Infect. Microbiol.* 11, 621957. doi:10.3389/fcimb.2021.621957

Zhang, H., Xu, G., Wu, X., Xu, Y., Xu, L., Zou, Y., et al. (2024). Fei-Yan-Qing-Hua decoction decreases hyperinflammation by inhibiting HMGB1/RAGE signaling and promotes bacterial phagocytosis in the treatment of sepsis. *J. Ethnopharmacol.* 321, 117553. doi:10.1016/j.jep.2023.117553

Zhang, Z. J., Morris-Natschke, S. L., Cheng, Y. Y., Lee, K. H., and Li, R. T. (2020). Development of anti-influenza agents from natural products. *Med. Res. Rev.* 40 (6), 2290–2338. doi:10.1002/med.21707

Zhao, L. N., Ma, S. W., Xiao, J., Yang, L. J., Xu, S. X., and Zhao, L. (2021). Bone marrow mesenchymal stem cell therapy regulates gut microbiota to improve post-stroke neurological function recovery in rats. *World J. Stem Cells* 13 (12), 1905–1917. doi:10.4252/wjsc.v13.i12.1905

Zhu, H., Lu, X., Ling, L., Li, H., Ou, Y., Shi, X., et al. (2018). Houttuynia cordata polysaccharides ameliorate pneumonia severity and intestinal injury in mice with influenza virus infection. *J. Ethnopharmacol.* 218, 90–99. doi:10.1016/j.jep.2018.02.016

Zhu, N., Zhang, D., Wang, W., Li, X., Yang, B., Song, J., et al. (2020). A novel coronavirus from patients with pneumonia in China, 2019. *N. Engl. J. Med.* 382 (8), 727–733. doi:10.1056/NEJMoa2001017

frontiers | Frontiers in Pharmacology

TYPE Systematic Review
PUBLISHED 25 October 2024
DOI 10.3389/fphar.2024.1453946

Check for updates

OPEN ACCESS

EDITED BY
Quansheng Feng,
Chengdu University of Traditional Chinese Medicine, China

REVIEWED BY
Junji Xing,
Houston Methodist Research Institute, United States
Yu-ling Ma,
University of Oxford, United Kingdom

*CORRESPONDENCE
Jie Qin,
qinjie7766@163.com

RECEIVED 24 June 2024
ACCEPTED 15 October 2024
PUBLISHED 25 October 2024

CITATION
Yang Q, Qin J, Li Z, He Y and Zhou Y (2024) Efficacy and safety of Shenmai injection in the treatment of viral myocarditis: a systematic review and meta-analysis.
Front. Pharmacol. 15:1453946.
doi: 10.3389/fphar.2024.1453946

COPYRIGHT
© 2024 Yang, Qin, Li, He and Zhou. This is an open-access article distributed under the terms of the Creative Commons Attribution License (CC BY). The use, distribution or reproduction in other forums is permitted, provided the original author(s) and the copyright owner(s) are credited and that the original publication in this journal is cited, in accordance with accepted academic practice. No use, distribution or reproduction is permitted which does not comply with these terms.

Efficacy and safety of Shenmai injection in the treatment of viral myocarditis: a systematic review and meta-analysis

Qianhe Yang[1], Jie Qin[1]*, Ziyue Li[2], Yue He[3] and Yabin Zhou[4]

[1]Graduate School, Heilongjiang University of Chinese Medicine, Harbin, Heilongjiang, China, [2]Endocrinology Department, The Fourth Affiliated Hospital of Harbin Medical University, Harbin, Heilongjiang, China, [3]Graduate School, Fujian University of Chinese Medicine, Fuzhou, Fujian, China, [4]Department of Cardiovascular Medicine, First Affiliated Hospital of Heilongjiang University of Chinese Medicine, Harbin, Heilongjiang, China

Purpose: To evaluate the efficacy and safety of Shenmai injection for the treatment of viral myocarditis (VMS) through systematic evaluation and meta-analysis.

Methods: Seven databases were searched to identify randomized controlled trials that examined the use of Shenmai injection for the treatment of VMS. The databases were searched from inception to 20 January 2024. The quality of the included studies was evaluated via the Cochrane risk of bias tool (RoB 2) version 2. Data analysis was performed using Review Manager 5.4 and Stata 16.

Results: In total, 18 randomized controlled trials were included. The trials were conducted in 2006–2024 and included 1,661 patients with VMS. The results reveal that Shenmai injection combined with conventional treatment was superior to conventional treatment alone in terms of the following outcomes: total effective rate [RR = 1.22, 95% CI (1.16, 1.28)], CKMB [SMD = −3.33, 95% CI (−4.85, −1.81)], electrocardiogram (ECG) efficacy [RR = 1.30, 95% CI (1.20, 1.40)], AST [SMD = -0.70, 95% CI (−1.28, −0.11)], LDH [SMD = −1.17, 95% CI (−1.37, −0.97], $p < 0.00001$], CK [SMD = −1.74, 95% CI (−2.34, −1.13)], TNF-α [SMD = −1.35, 95% CI (−1.85, −0.84)], and IL-6 [SMD = −1.40, 95% CI (−1.76, −1.05)]. There were no significant differences in the incidence of adverse reactions [RR = 1.56, 95% CI (0.73, 3.33), $p = 0.25$] or cTnI levels [SMD = −3.35, 95% CI (−6.81, 0.11)] between the groups.

Conclusion: Shenmai injection with conventional treatment can reduce the degree of myocardial injury in patients with VMS, weaken the inflammatory response and improve the clinical efficacy of the conventional treatment. This approach was found to be safe. However, additional high-quality studies are necessary to confirm the reliability of this treatment method.

Systematic Review Registration: https://www.crd.york.ac.uk/PROSPERO/logout.php, identifier PROSPERO (CRD42024518665).

KEYWORDS

Shenmai injection, viral myocarditis, safety, meta-analysis, systematic review

1 Introduction

Viral myocarditis (VMC) refers to a nonspecific disease caused by infection with various cardiomyotropic viruses, which damage the myocardial structure and function. Coxsackievirus, orphan (Echo) virus, and poliovirus are among the most common cardiomyotropic viruses, among which Coxsackievirus is the most common pathogen and accounts for approximately 30%–50% of VMC cases. In recent years, reports have indicated that parvovirus B19 and human herpesvirus are common causes of VMS (Tavares et al., 2010). In addition, human adenovirus, influenza, rubella, herpes simplex, encephalitis, and hepatitis (A, B, C type) viruses, EB virus, cytomegalovirus, and human immunodeficiency virus (HIV) can cause myocarditis (Pollack et al., 2015; Lasrado and Reddy, 2020). The incidence of VMS is relatively high at approximately 11–20 per 100,000 people (Olejniczak et al., 2020). VMC is an important cause of heart failure and sudden death in young people. The pathogenesis of VMC has not been fully elucidated, but the recognized pathogenesis mainly includes ① direct action of the virus and ② combined action of the virus and the body's immune response. The clinical manifestations of VMC are often related to the extent and location of the lesions. Patients with mild symptoms may experience only fatigue and shortness of breath, whereas those with severe symptoms may develop cardiogenic shock or even sudden death. Most patients may have prodromal symptoms of viral infection, such as fever, fatigue, sore throat, muscle aches and pains, or gastrointestinal symptoms, such as nausea and vomiting, 1–3 weeks before the onset of the disease. The main manifestations subsequently include cardiac pain, panic, dyspnea, edema, and even loss of consciousness and sudden death. Most patients with VMC complained of arrhythmia or had arrhythmia as the first symptom, and most of them had premature ventricular beats and conduction blocks. An increased heart rate may correspond to the degree of fever, and abnormal heart sounds or a gallop rhythm may be heard on auscultation. VMC is a self-limiting disease, and to date, it has no specific or effective treatment. Treatment often focuses on supportive therapy for left heart insufficiency. Appropriate rest, infection control, myocardial nourishment, antiviral treatment, free radical scavenging and other comprehensive therapeutic measures are recommended. Furthermore, symptomatic management of different clinical manifestations of VMC is performed.

The Shenmai injection is composed of the Chinese medicines *Panax ginseng* C. A. Mey [Araliaceae; *Ginseng radix et Rhizoma*] (Hong Shen) and *Ophiopogon japonicus* (Thunb.) Ker Gawl. [Asparagaceae; *O. japonicus radix*] (Mai Dong), which is included in the National Essential Drug List of China. Shenmai injection is derived from the TCM formula "Shen Mai Yin," which was described in the text "Zheng Yin Mai Zhi." This formula consists of the Chinese herbs Ren Shen and Mai Dong. In TCM, these herbs are believed to have the effects of "invigorating qi," "solid doff," and "nourishing yin." The formula can be used to treat symptoms such as "fatigue" and "thirst," which appear in the later stages of a fever (Dai et al., 2020). Shenmai injection is based on "Shen Mai Yin" but replaces Ren Shen with steamed Hong Shen. In TCM theory, the "invigorating qi" and "solid doff" effects of Hong Shen are stronger than those of regular ginseng, which is related to the unique ginsenosides produced during the hydrolysis and isomerization reactions that occur during the steaming process (Qu et al., 2023). Specifically, Hong Shen and Mai Dong were extracted by refluxing with ethanol; then, the filtrate was concentrated to obtain the red ginseng extract and maitake extract, which were subjected to crude filtration and ultrafiltration, respectively. The filtrate was further mixed, and polysorbate was added to dissolve it. After the solution had been rehydrated and the pH had been adjusted, Shenmai injection was performed, the main components of which were ginsenosides Rg1, Re, Rf, and Rb1. Previous studies have shown that the main active ingredient of Shenmai formula can reduce the inflammatory response in cardiovascular diseases by blocking the NF-κB pathway (Zhu et al., 2017). VMC commonly causes damage to cardiomyocytes, and studies have shown that Shenmai injection has various components that may improve myocardial injury through multiple targets and pathways (Zhang et al., 2021).

The Chinese medicine Hong Shen is the root of a perennial botanical drug of the family Wujiaceae. It is warm in nature, sweet in flavor and slightly bitter in taste and can tonify qi and blood, which can improve symptoms such as fatigue, insomnia and cough. In Chinese medicine, Mai Dong is the tuberous root on the collar root of leguminous plants (Liu and Wang, 2009). It is sweet, slightly bitter and slightly cold in nature. Traditional Chinese medicine (TCM) posits that sweetness can nourish yin, and coldness can clear heat, which nourishes yin, benefits the stomach, moistens the lung and generates fluids. Furthermore, Mai Dong can improve symptoms such as cough, dry throat and thirst. Pharmacological studies have shown that ginsenosides and a series of amino acids in Hong Shen can effectively improve the symptoms of myocardial ischemia and achieve cardiac strengthening. The results of high-performance liquid chromatography (HPLC) fingerprint peak identification reveal that the main active ingredients of Shenmai Injection include ginsenosides Rg1, Re, Rf, and Rb1 (Yang et al., 2023), of which ginsenosides Re and Rb3 can protect the myocardial cells of patients with VMC by reducing the level of peroxides in the body (Li et al., 2019). Mai Dong contains steroidal saponins and amino acids, which can actively improve the symptoms of cardiac arrhythmia. Shenmai injection can improve cardiac pumping, increase the cardiac output, reduce the peripheral vascular resistance, positively regulate the myocardial metabolism, and reduce symptoms of cardiac insufficiency. However, Shenmai injection can strengthen the function of mononuclear macrophages, increase the body's ability to resist infection and improve the immune function.

2 Materials and methods

This meta-analysis was conducted in accordance with the Preferred Reporting Items for Systematic Reviews and Meta-Analysis (PRISMA) guidelines (Supplementary Material 1). The study was successfully registered on PROSPERO (CRD42024518665).

2.1 Database and search strategies

The PubMed, Cochrane Library, Web of Science, Excerpta Medica Database (Embase), China National Knowledge Infrastructure Database (CNKI), Wanfang Database (WF) and China Science and Technology Journal Database (VIP) databases

were comprehensively searched from inception to 20 January 2024, with restricted languages of Chinese and English. In terms of search strategy, a combination of subject and free text terms was used, and different search strategies were applied to Chinese and foreign language databases. (Details of the search strategy are provided in Supplementary Table 1).

2.2 Inclusion criteria

The inclusion criteria for our study were constructed via the Population, Intervention, Control, and Outcome Study (PICOS) framework, which considers study design, participants, interventions, comparisons, and outcomes (Hutton et al., 2015). The specific inclusion criteria were as follows.

2.2.1 Study design

Randomized controlled trials (RCTs) were conducted in China or other countries and published in Chinese or English.

2.2.2 Participants

Patients were diagnosed with VMC regardless of age, sex, race, combined symptoms, or disease course.

2.2.3 Interventions

The intervention consisted of a single administration of Shenmai injection for intravenous drip treatment alone or in combination with conventional treatment for VMC.

2.2.4 Comparators

Control treatments were placebo or conventional treatment for VMC, which consisted of myocardial nourishment (e.g., coenzyme Q10, polarizing fluid, and inosine), antiviral agents, and immunomodulation agents.

2.2.5 Outcomes

The primary outcomes were the clinical effectiveness rate and creatine kinase isoenzyme (CKMB) concentration. The secondary outcomes were cardiac troponin I (cTnI), lactate dehydrogenase (LDH), creatine kinase (CK), tumor necrosis factor alpha (TNF-α), interleukin-6 (IL-6), aspartate transaminase (AST), adverse reactions, and the effective rate of the electrocardiogram (ECG).

2.3 Exclusion criteria

Studies that satisfied any of the following criteria were excluded:

1. Systematic reviews or meta-analyses, observational studies, theoretical explorations, case reports, and animal or cell experiments.
2. Duplicate publications (in cases of duplicate studies, studies with the most recent and comprehensive data were selected).
3. Lack of randomized controlled trials.
4. Studies for which the full text could not be accessed online or via email.
5. Inappropriate intervention: The experimental group used other traditional Chinese medical treatments in addition to Shenmai injection therapy.
6. Low-quality studies such as those with flawed study designs or improper statistical methods.
7. Incomplete studies such as those that were not validated for clinical efficacy assessments.

2.4 Literature screening and data extraction

The literature selection was independently conducted by two assessors, who excluded irrelevant studies by screening the titles and abstracts. The full-text versions of these studies were downloaded and reviewed, and data were extracted and cross-checked. If there was a disagreement between the two researchers, a third senior researcher conducted a comprehensive evaluation. If data were missing from the article or could not be directly obtained, we attempted to contact the corresponding authors of the article to obtain the relevant complete data. The following data were extracted: 1) basic information, including the study name, first author's name, publication year, and journal of publication; 2) baseline characteristics of the study subjects, including sample size, age, and sex; 3) intervention measures, including the dose of Shenmai injection, duration of intervention, and conventional treatment methods; 4) outcome indicators.

2.5 Risk of bias assessment

The methodological quality of each study was independently assessed by two reviewers via the Cochrane Risk of Bias 2 (RoB 2) tool (Higgins et al., 2023). Any discrepancies between the two reviewers were resolved via discussion with a third reviewer. The quality of the included RCTs was evaluated based on the following domains: 1) randomization process; 2) deviations from intended interventions; 3) missing outcome data; 4) measurement of the outcome; 5) selection of the reported result. The risk of bias of studies was classified into three levels: "high risk," "low risk" and "unclear risk."

2.6 Statistical analysis

This review used Review Manager 5.4 and Stata 16 for data analysis. Continuous variables were assessed by the standardized mean difference (SMD) and 95% confidence interval (95% CI), whereas categorical variables were measured by the risk ratio (RR) and 95% CI. $p < 0.05$ was considered to indicate statistical significance. An $I^2 \leq 50\%$ indicates low heterogeneity between studies, and a fixed effect model was selected for analysis. An $I^2 > 50\%$ indicates significant heterogeneity between studies, and a random effects model was selected for analysis. Furthermore, the potential sources of heterogeneity were analyzed via subgroup and sensitivity analyses.

2.7 Subgroup analysis

If the results were heterogeneous, subgroup analyses were performed according to the treatment duration (≤3 weeks

or >3 weeks) and dose (<50 mL/d or ≥50 mL/d) to explore sources of heterogeneity. Differences between subgroups were also analyzed.

2.8 Sensitivity analysis

When there was significant heterogeneity, sensitivity analyses were performed via the leave-one-out approach to assess the robustness of the findings and identify the sources of heterogeneity. These analyses were conducted via Review Manager 5.4.

2.9 Publication bias

When the number of included studies that examined a particular outcome exceeded 10, the publication bias was assessed by constructing a funnel plot with Review Manager 5.4 and performing Egger's test via Stata 16.0 (Sterne et al., 2011).

2.10 Evidence confidence

The GRADE framework (Schünemann et al., 2020) was used to assess the quality of evidence for the included studies. The quality of evidence for the outcomes was assessed across five domains: study limitations, inconsistency, indirectness, imprecision, and publication bias.

3 Results

3.1 Search results

In total, 946 studies were initially identified from the literature search, and 592 duplicates were manually excluded through EndNote. After screening the titles and abstracts of the remaining 354 studies, 96 studies were excluded, including pharmacological research, animal experiments, cell experiments, systematic reviews, meta-analyses, summaries of experience, summaries and case reports. After screening the full texts of the remaining 258 studies, 240 articles were excluded for the following reasons: the full text was not available, outcome indicators were not reported, combination treatment with other botanical drug injections was used, combination treatment with other TCM therapies was used, information was lacking, and low-quality research was performed.

Ultimately, 18 studies (Song, 2006; Weng, 2006; Zhu et al., 2006; Chan and Liu, 2007; Hu et al., 2007; Wang et al., 2007; Hou, 2009; Liu, 2009; Lei, 2010; Xu, 2010; Bai, 2014; Xing et al., 2014; Luo et al., 2017; Lu et al., 2018; Shi and Xiang, 2018; Wei and Sun, 2019; Wan et al., 2020; Liang et al., 2022) were considered eligible for this systematic review. The research selection process is shown in Figure 1.

3.2 Study characteristics

The 18 included studies were published between 2006 and 2024, were conducted in China, included 1,661 patients with VMC, and were RCTs. The duration of the interventions was 14–30 days. The control groups were treated with conventional therapy, mostly antiviral therapy plus myocardial nutrition, and antiarrhythmic therapy for patients with abnormal ECGs. Song's article stated the specific drugs and dosages, whereas the other studies listed only some of the drugs and did not state the dosages for the control treatments. The observation groups were treated with conventional therapy plus Shenmai injection or Shenmai injection combined with Western drugs. The dosages were 5–60 mL/d, and the frequency of use was once a day. The basic characteristics of the studies are shown in Table 1.

3.3 Quality assessment of the included studies

The quality of the 18 studies included was evaluated via RoB 2. The results of the ROB evaluation are shown in Figure 2. Seven randomized controlled trials described the use of the random number table method; thus, there was a low risk of bias regarding the randomization process. Eleven randomized controlled trials mentioned randomization without specifying the details of the generation of random sequences; therefore, there was an unclear risk of bias regarding the randomization process. Some of the randomized controlled trials in this article reported the use of blinding, but whether blinding was specifically used for patients, experimenters, and evaluators or only for patients was not described in detail; however, no patients were reassigned during the trial, and the researchers used appropriate statistical methods. Therefore, there was a low risk of bias regarding deviations from the intended intervention. The outcome data of all randomized controlled trials were complete with no reported missing outcome data; therefore, there was a low risk of bias regarding missing outcome data. There were no reports of blinding of the outcome assessors in randomized controlled trials, and it is unclear whether the intervention's outcome was affected; however, any such effect is likely small, and there was an unclear risk of bias regarding the outcome assessment process. Prespecified statistical plans were not available; therefore, it cannot be confirmed whether the statistical methods were consistent with the prespecified methods. However, there are no reports of different evaluation methods for the outcome, and there are no reports of the use of other analysis methods. Thus, the risk of bias regarding selective reporting bias is uncertain.

3.4 Meta-analysis results

3.4.1 Primary outcomes

3.4.1.1 Meta-analysis of the total effectiveness rate

Data on the total effectiveness rates were available in 16 studies, as shown in Figure 3. Due to the low level of heterogeneity (p = 0.85, I^2 = 0%), a fixed effect model was used. Compared with that of the control group, the overall clinical efficacy of the experimental group was significantly greater [RR = 1.22, 95% CI (1.16, 1.28), p < 0.00001]. Therefore, compared with conventional Western medicine treatment, the combined use of Shenmai injection and conventional Western medicine treatment showed better clinical efficacy. Due to the low

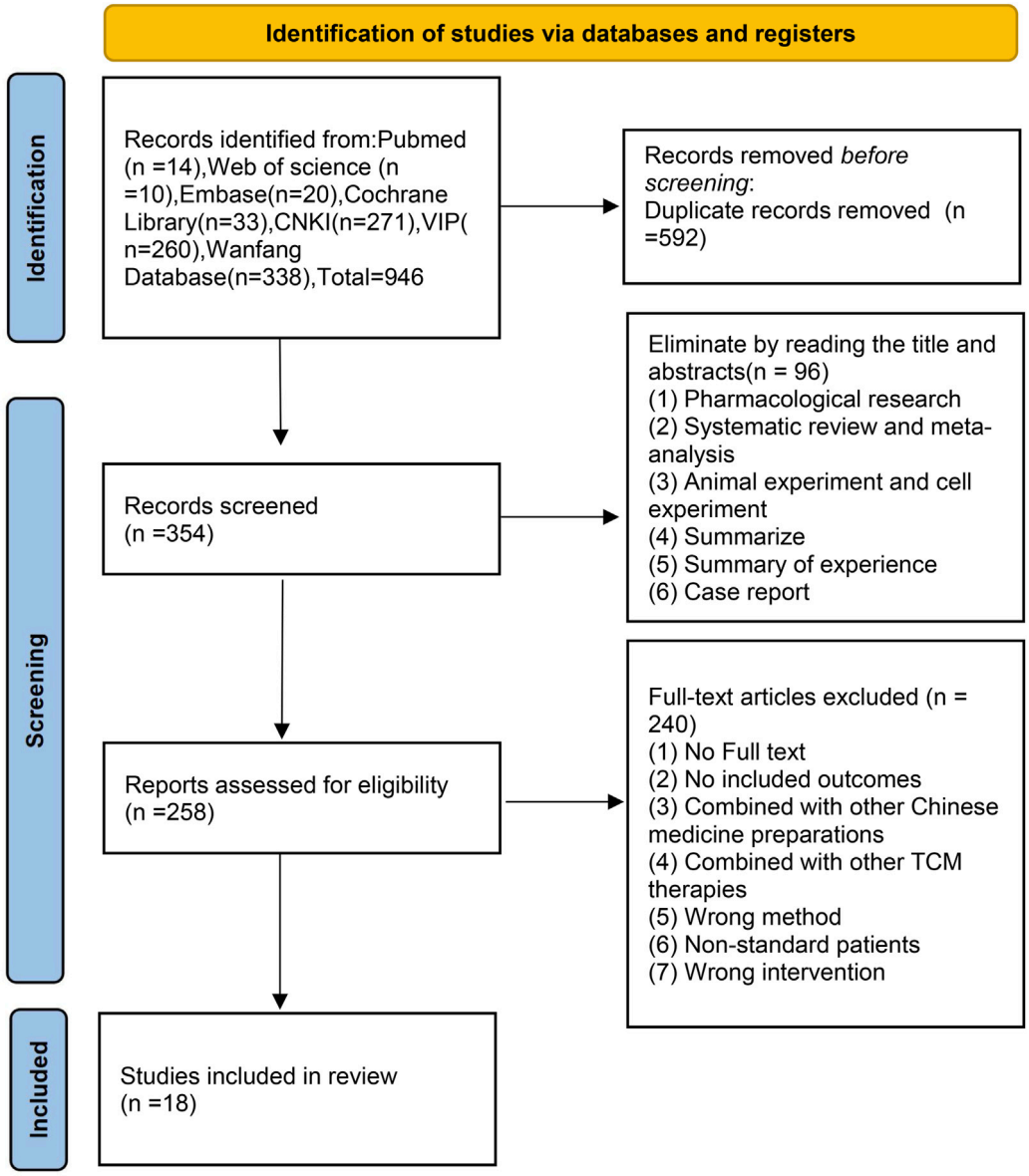


FIGURE 1
Literature screening process.

level of heterogeneity, subgroup and sensitivity analyses were not conducted.

3.4.1.2 Meta-analysis of CKMB

Eight studies reported data on CKMB, as shown in Figure 4. Due to the high level of heterogeneity ($p < 0.00001$, $I^2 = 98\%$), a random effect model was used. The results show that the combination of Shenmai injection with conventional Western medicine could better reduce CKMB in patients than the conventional Western medicine therapy alone [SMD = −3.33, 95% CI (−4.85, −1.81), $p < 0.0001$]. Subgroup analyses were performed based on differences in therapeutic dose and duration of treatment (Figure 5). Patients were further divided into two dosage subgroups: <50 mL/d ($p < 0.00001$, $I^2 = 95\%$) and ≥50 mL/d ($p < 0.00001$, $I^2 = 99\%$). The outcomes were significantly different between these dosage subgroups ($\chi^2 = 15.05$, df = 1, $p = 0.0001$), which indicates that there was a greater decrease in CKMB after treatment with high-dose Shenmai injection. Patients were also divided into two subgroups based on the duration of continuous treatment (Figure 6): ≤3 weeks ($p < 0.00001$, $I^2 = 99\%$) and >3 weeks ($p < 0.00001$, $I^2 = 96\%$). The outcomes were significantly different between these treatment duration subgroups ($\chi^2 = 11.01$, df = 1, $p = 0.0009$), which indicates that a treatment duration of 3 weeks or less was more beneficial for reducing CKMB. Sensitivity analyses were performed using the leave-one-out method; the pooled results were robust.

3.4.2 Secondary outcomes

3.4.2.1 Meta-analysis of the efficacy rate of ECG

Seven studies reported preliminary data on the ECG efficacy (Figure 7). Due to the low level of heterogeneity ($p = 0.99$,

TABLE 1 Feature list.

Studies	Sample sizes	Gender (M/F)		Age(y)		Intervention		Duration	CT drugs	Outcomes
	(T/C)	T	C	T	C	T	C			
Liang et al. (2022)	76/76	38/38	40/36	53.3 ± 9.7	54.1 ± 10.2	SI, 40 mL, qd + CT	CT	2 weeks	Antiviral, nourishing myocardium, polarizing liquid	⑧⑨⑩
Wan et al. (2020)	70/70	38/32	36/34	55.1 ± 10.1	54.3 ± 9.5	SI, 60 mL, qd + CT	CT	2 weeks	Antiviral, vitamin C tablets, polarizing liquid, Coenzyme Q10 capsules, anti-arrhythmia	①②④⑧⑩
Lu et al. (2018)	43/43	21/22	19/24	47.34 ± 2.01	46.03 ± 1.97	SI, 40 mL, qd + CT	CT	2 weeks	Antiviral, immunity, nutrition, myocardium, anti-arrhythmia, Trimetazidine	③⑨
Shi and Xiang (2018)	49/49	25/24	28/21	34.4 ± 4.3	34.8 ± 4.2	SI, 60 mL, qd + CT	CT	30 days	Nourishing myocardium (coenzyme Q10, polarizing liquid, inosine), antiviral, immune regulation, dexamethasone sodium phosphate	①②⑤⑥⑦⑧⑩
Luo et al. (2017)	68/68	35/33	37/31	52.8 ± 9.2	54.1 ± 8.8	SI,60 mL, qd + CT	CT	2 weeks	Trimetazidine, L-carnitine	①⑧⑨
Xing et al. (2014)	82/82	91/73		2–14		SI, 60 mL, qd+ +CT	CT	15 days	Antiviral, antibacterial agent, cytochrome C, nutritional cardiometabolic drug, creatine phosphate sodium injection	①②③
Hou (2009)	62/60	30/32	28/32	38.2	38.4	SI, 40 mL, qd + CT	CT	15 days	Myocardial nutrition drugs, etc	①
Wang et al. (2007)	32/30	18/14	17/13	7.6	7.8	SI, 0.5 mL/kg-1 ml/kg, qd + CT	CT	15 days	Riboside, vitamin C, energy mixture, coenzyme Q10, antiarrhythmic drug, fructose 1,6 diphosphate	①②③
Chan and Liu (2007)	30/30	34/26		8–40		SI, 60 mL, qd + CT	CT	30 days	Coenzyme A, adenosine diphosphate	①
Weng (2006)	24/24	10/14	8/16	25.12 ± 12.51	26.12 ± 10.52	SI, 40 mL, qd + CT	CT	20 days	Antiviral, infection prevention, energy mixture, polarizing liquid, potassium magnesium aspartate needle	①
Zhu et al. (2006)	40/30	38/32		7.5 (2–13)		SI, 60 mL, qd + CT	CT	21 days	Ribavirin, vitamin C, energy mixture	①②⑥
Wei and Sun (2019)	48/49	25/23	26/23	(7.87 ± 1.22)	(7.82 ± 1.25)	Fructose 1,6 diphosphate, .0.25 g/kg, qd + SI, 50 mL, qd + CT	CT + Fructose 1,6 diphosphate,.0.25 g/kg, qd	2 weeks	—	①②⑥⑦
Bai (2014)	40/40	23/17	22/18	(52.8 ± 6.7)	(53.2 ± 7.2)	SI, 60 mL, qd + CT	CT	4 weeks	Vitamin C, energy injection, cyclic adenosine phosphate, antiviral therapy	①②④⑤⑥⑩

(Continued on following page)

10.3389/fphar.2024.1453946

10.3389/fphar.2024.1453946

TABLE 1 (*Continued*) Feature list.

Studies	Sample sizes	Gender (M/F)		Age(y)		Intervention		Duration	CT drugs	Outcomes
	(T/C)	T	C	T	C	T	C			
Xu (2010)	22/18	—	—	—		SI, 30 mL, qd + CT	CT	21 days	Antiviral therapy, vitamin C, coenzyme A, α-interferon	①
Lei (2010)	36/33	43/26		8.1 (2–15)		SI, 5–20 mL, qd + CT	CT	30 days	Energy mixture, vitamin C, inosine, cytochrome C, antiviral therapy	①②③⑤⑥⑦
Liu (2009)	60/60	33/27	38/22	6–13		SI, 1–1.5 mL/kg, qd + CT	CT	28 days	Symptomatic treatment, nutritional support treatment, sodium fructose diphosphonate	①③
Hu et al. (2007)	25/24	31/18		7.5 (2–14)		SI, 5–20 mL, qd + CT	CT	30 days	Energy mixture, vitamin C, inosine, cytochrome C	①②⑤⑥⑦⑩
Song (2006)	52/52	29/23	26/26	31.4	30.2	SI, 20 mL, qd + CT	CT	3 weeks	Coenzyme A, 100 u, qd + ATP, 40 mg, qd + vitamin C,4 g, qd	①③

T, treatment group; C, control group; SI, shenmai injection; NM, not mentioned; w, week, d, day; tid, three times a day; qd, once a day; CT, conventional treatment. ① Total efficacy rate. ② CKMB. ③ Electrocardiogram efficacy rate. ④ cTnI, ⑤ AST, ⑥ LDH, ⑦ CK, ⑧ TNF-α, ⑨ IL-6, and ⑩ adverse reactions.

I^2 = 0%), a fixed effect model was used. The results of the analysis revealed that the ECG efficacy of the experimental group was significantly greater than that of the control group [RR = 1.30, 95% CI (1.20, 1.40), $p < 0.00001$]. Therefore, the combination of Shenmai injection samples with conventional Western drug therapy better improved the ECG results among VMC patients than conventional Western drug therapy. Subgroup and sensitivity analyses were not performed because the low level of heterogeneity was less than 50%.

3.4.2.2 Meta-analysis of cTnI

Two experiments reported data on cTnI, as shown in Figure 8. There was a high level of heterogeneity ($p < 0.00001$, I^2 = 98%); therefore, a random effect model was used. The results reveal no significant difference between conventional treatment with Western medicine and treatment with Shenmai injection in combination with Western medicine in terms of reducing the cTnI index of patients [SMD = −3.35, 95% CI (−6.81, 0.11), $p = 0.06$]. Due to the high heterogeneity, subgroup analyses were performed; however, because there was only one study in each subgroup, the I^2 value could not be calculated. The treatment dose was identical in both trials, so subgroup analysis was performed based on the treatment duration (Figure 9). There was a significant difference between the subgroups ($\chi^2 = 47.58$, df = 1, $p < 0.00001$), which indicates that a longer treatment duration of Shenmai injection may be more favorable for lowering cTnI in patients. However, too few randomized controlled trials were included in this analysis, which leads to a high degree of heterogeneity.

3.4.2.3 Meta-analysis of ASTs

Four studies reported AST data, as shown in Figure 10. There was a high level of heterogeneity ($p = 0.0006$, I^2 = 83%); thus, a random effects model was used. The results show that the combination of Shenmai injection with conventional Western medicine could better reduce the AST levels in patients than conventional Western medicine therapy alone [SMD = −0.70, 95% CI (−1.28, −0.11), $p = 0.02$]. At I^2>50%, the treatment duration was identical in all four experiments; therefore, we performed subgroup analysis only based on the treatment dosage. The studies were divided into a low-dosage group ($\chi^2 = 0.77$, I^2 = 0%) and a high-dosage group ($\chi^2 = 5.20$, I^2 = 81%). The results (Figure 11) reveal a significant difference between the subgroups ($\chi^2 = 4.51$, df = 1, $p = 0.03$), which indicates that Shenmai injection at a dosage of 50 mL/d or higher led to a more pronounced reduction in AST levels among VMC patients. Sensitivity analysis was performed using the leave-one-out approach, and the pooled results were shown to be robust.

3.4.2.4 Meta-analysis of LDH

Six studies reported data on LDH (Figure 12). There was a low level of heterogeneity ($p = 0.27$, I^2 = 22%); thus, a fixed effect model was used. The meta-analysis reveals that Shenmai injection in combination with conventional treatment could better reduce LDH in patients than the conventional treatment alone [SMD = −1.17, 95% CI (−1.37, 0.97), $p < 0.00001$]. Subgroup and sensitivity analyses were not performed because of the low level of heterogeneity.

3.4.2.5 Meta-analysis of CK

Four studies reported data on CK (Figure 13). There was a high level of heterogeneity ($p = 0.002$, I^2 = 80%); thus, a random effect

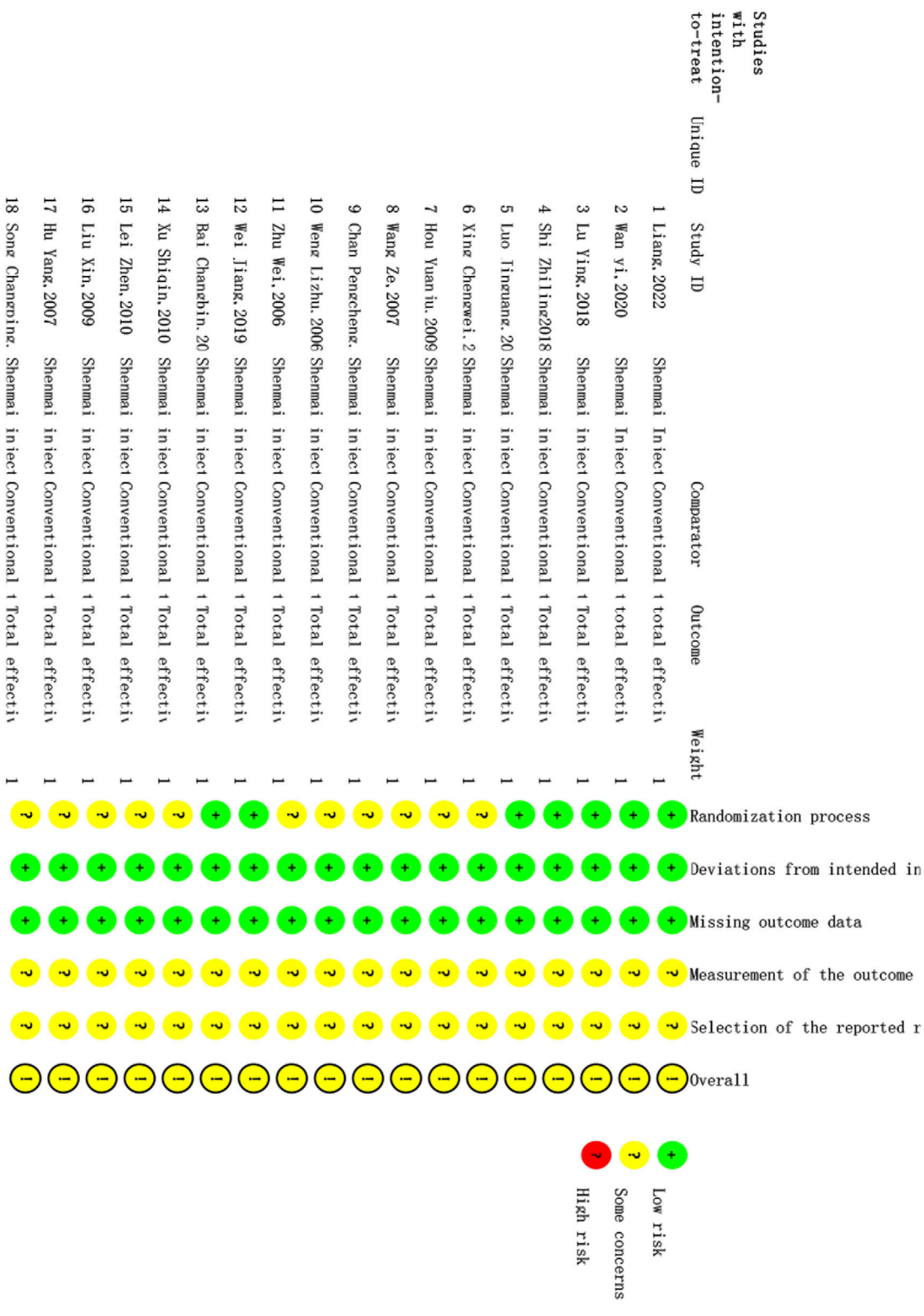


FIGURE 2
Quality assessment.

model was used. The meta-analysis reveals that the CK index more significantly decreased in patients treated with the combination of Shenmai injection and conventional Western medicine than in those treated with conventional therapy [SMD = −1.74, 95% CI (−2.34, −1.13), $p < 0.00001$]. Due to I^2>50%, subgroup analysis was conducted based on the treatment dosage (Figure 14) and treatment duration (Figure 15). There were no significant differences between the low-dosage subgroup (χ^2 = 4.08, I^2 =

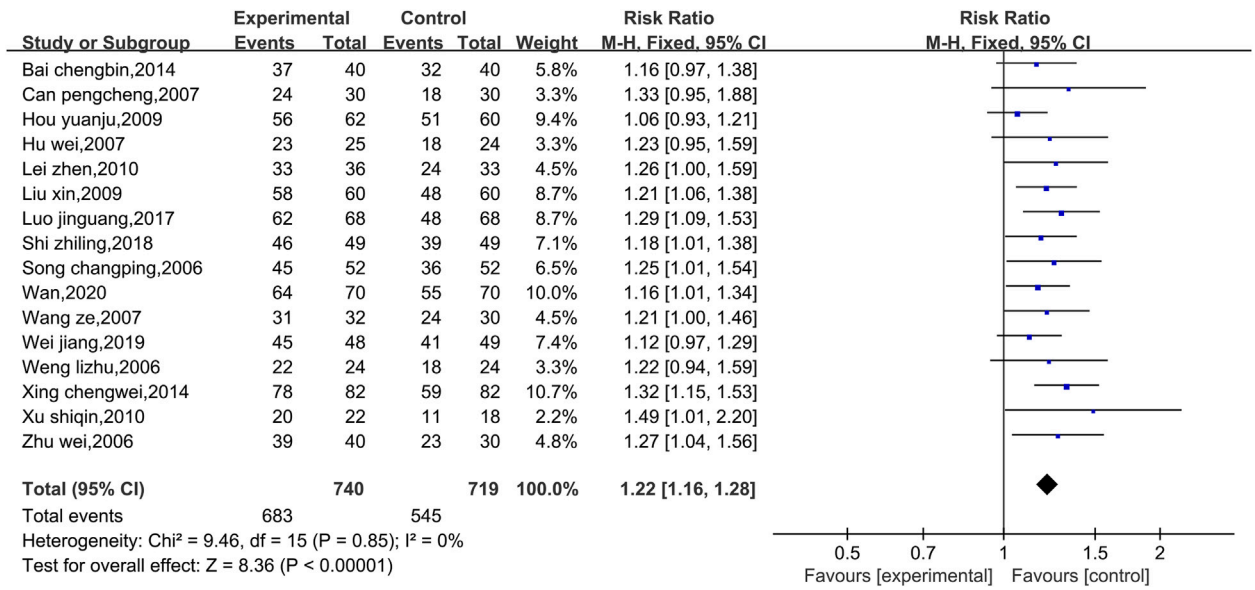


FIGURE 3
Comparative forest plots of the total efficacy rates.

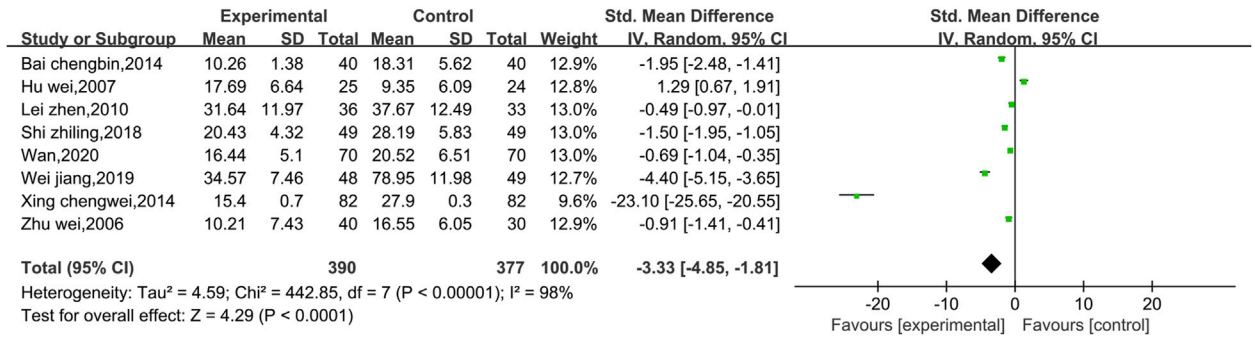


FIGURE 4
Comparative forest plots of the CKMB levels.

75%) and the high-dosage subgroup (χ^2 = 10.00, I^2 = 90%) (χ^2 = 0.33, df = 1. p = 0.56). With respect to treatment duration, there was only one study in the <3-week subgroup; therefore, no I^2 value could be calculated. There were 3 studies in the >3-week subgroup (χ^2 = 4.33, I^2 = 54%). Subgroup analysis reveals significant differences between the treatment duration subgroups (χ^2 = 8.26, df = 1, p = 0.004), which indicates that the treatment with Shenmai injection for 3 weeks or fewer led to a more pronounced reduction in CK among VMC patients. Sensitivity analysis was performed using the leave-one-out approach, and the pooled results were shown to be robust.

3.4.2.6 Meta-analysis of TNF-α

Four studies reported data on TNF-α, as shown in Supplementary Figure 1. There was a high level of heterogeneity (p = 0.0001, I^2 = 85%); thus, a random effect model was used. The results of the meta-analysis revealed that the combination of Shenmai injection with conventional treatment was more beneficial to the recovery of TNF-thin patients, since the TNF-y of TNF was lower after Shenmai injection treatment than after the conventional treatment alone [SMD = −1.35, 95% CI (−1.85, −0.84), p < 0.00001]. I^2 > 50%, and subgroup analyses were performed based on the therapeutic dosage (Supplementary Figure 2). There was only one study in the low-dosage group, which prevented the calculation of an I^2 value. There were three studies in the high-dosage subgroup (χ^2 = 20.41, I^2 = 90%). There was no significant difference between the treatment dosage subgroups (χ^2 = 0.00, df = 1, p = 0.99). With respect to the treatment duration (Supplementary Figure 3), there was only one study in the >3-week subgroup, which prevented the calculation of an I^2 value. There was no significant difference between the > 3-week subgroup and the < 3-week subgroup (χ^2 = 15.71, I^2 = 87%) (χ^2 = 2.04, df = 1, p = 0.15). Sensitivity analysis was performed using the leave-one-out method and revealed that the level of heterogeneity was significantly reduced (I^2 = 12%) when the study by Wan et al. (2020) was removed. The heterogeneity may have been due to differences in interventions, as no

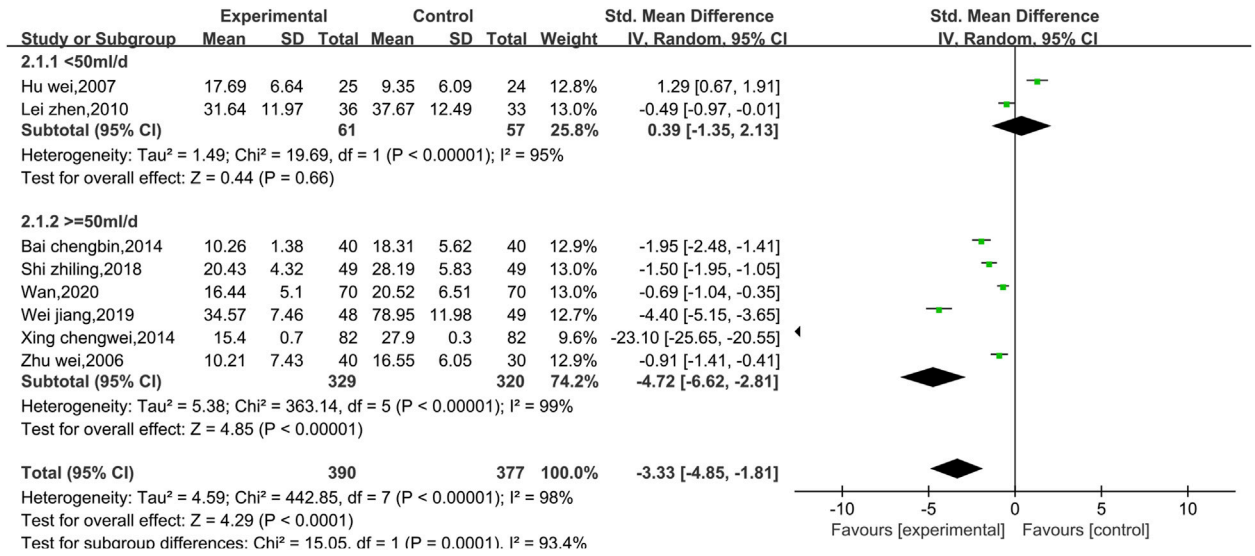


FIGURE 5
Forest plots of the subgroup analysis at different doses (CKMB level).

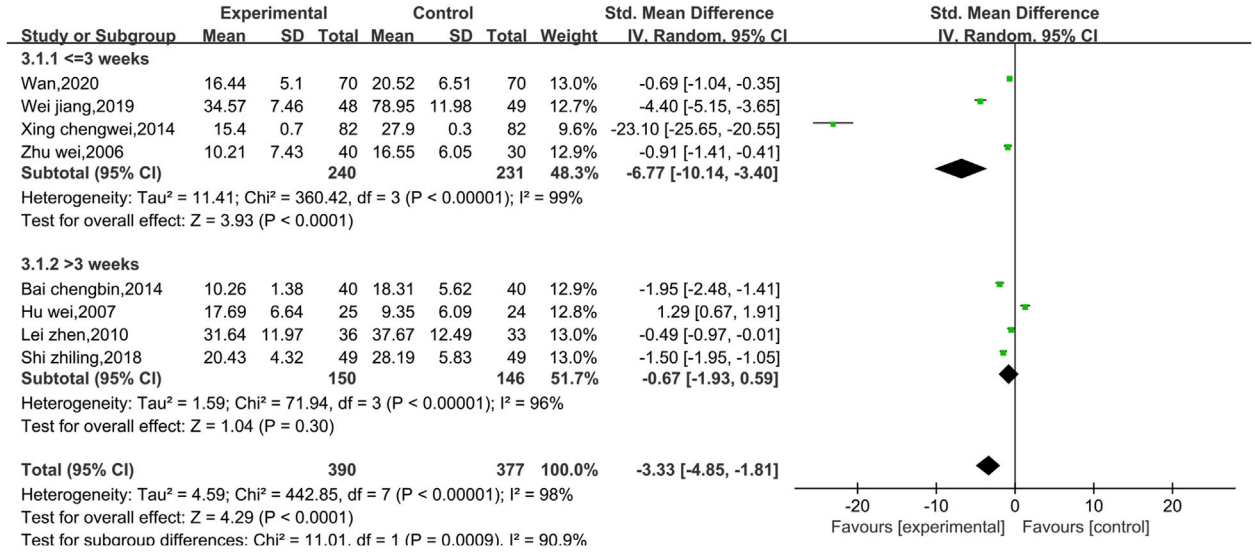


FIGURE 6
Forest plots of the subgroup analysis at different durations of treatment (CKMB level).

included trials specified the use of specific conventional treatments. No other sources of clinical heterogeneity were identified. After excluding this RCT, the meta-analysis was performed again via a fixed effects model (Supplementary Figure 4). The results reveal that the addition of Shenmai injection to conventional treatment was more favorable for reducing TNF-α levels in patients [SMD = −1.56, 95% CI (−1.78, −1.33), $p < 0.00001$].

3.4.2.7 Meta-analysis of IL-6

Three studies reported data on IL-6, as shown in Supplementary Figure 5. There was a high level of heterogeneity ($p = 0.09$, $I^2 = 58\%$); thus, a random effects model was used. The meta-analysis reveals that the combination of Shenmai injection with conventional treatment more significantly reduced the IL-6 index of patients than the conventional treatment [SMD = −1.40, 95% CI (−1.76, −1.05), $p < 0.00001$]. With $I^2 > 50\%$, subgroup analysis was performed based on the treatment dosage but not the treatment duration (the same treatment duration was used in all three articles) (Supplementary Figure 6). There was only one in the high-dosage subgroup, which prevented the calculation of an I^2 value. There was also a low-dosage subgroup ($\chi^2 = 4.17$, $I^2 = 76\%$). The subgroup analysis reveals no significant differences between the treatment dosage

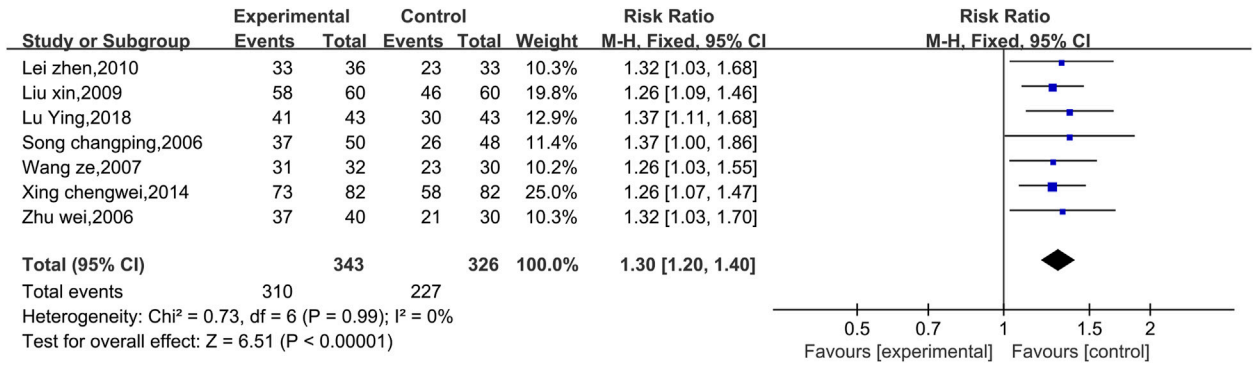


FIGURE 7
Comparative forest plots of the efficacy rates of electrocardiography.

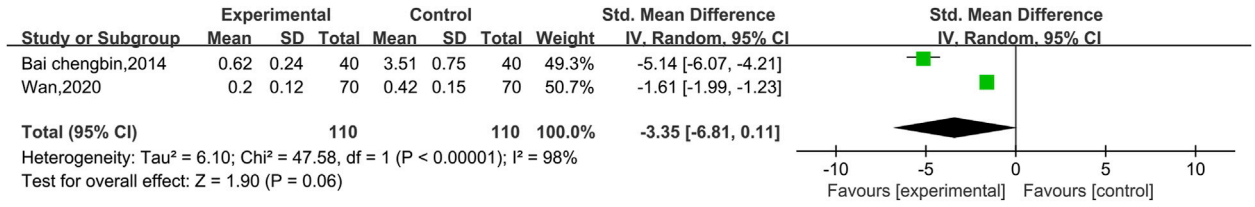


FIGURE 8
Comparative forest plots of the cTnI levels.

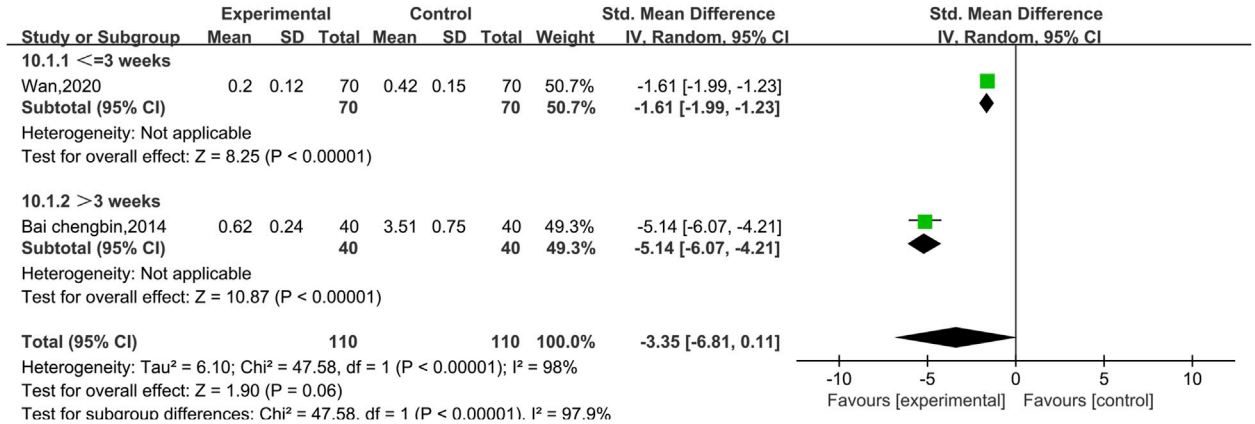


FIGURE 9
Forest plots of the subgroup analysis at different durations of treatment (cTnI level).

subgroups (χ^2 = 0.54, df = 1, p = 0.46). The sensitivity analysis reveals a significant reduction in heterogeneity (I^2 = 0%) when the study of Lu et al. (2018) was excluded. The heterogeneity may have been due to the sample size of this study, which was significantly smaller than that in the other two studies. After excluding this RCT, the meta-analysis was performed again via a fixed effect model (Supplementary Figure 7). The results reveal that the addition of Shenmai injection to the conventional treatment better decreased the patients' IL-6 levels [SMD = −1.24, 95% CI (−1.49, −0.98), p < 0.00001].

3.4.2.8 Meta-analysis of adverse reactions

Nine of the included studies mentioned information about adverse reactions, four of which reported no adverse reactions during the treatment phase, and the remaining five studies reported the presence of adverse events during the treatment phase. Among them, 16 patients in the Shenmai injection treatment group experienced adverse reactions during treatment, including 4 cases of nausea and vomiting, 3 cases of headache, 2 cases of dizziness, 1 case of rash, 1 case of abdominal discomfort, 1 case of delirium, and 1 case of

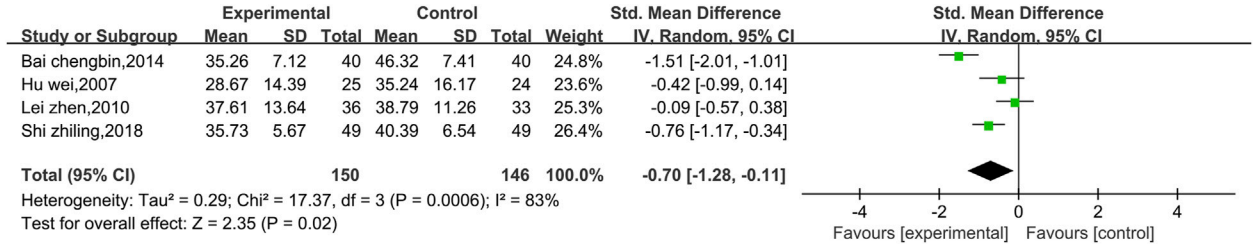


FIGURE 10
Comparative forest plots of the AST levels.

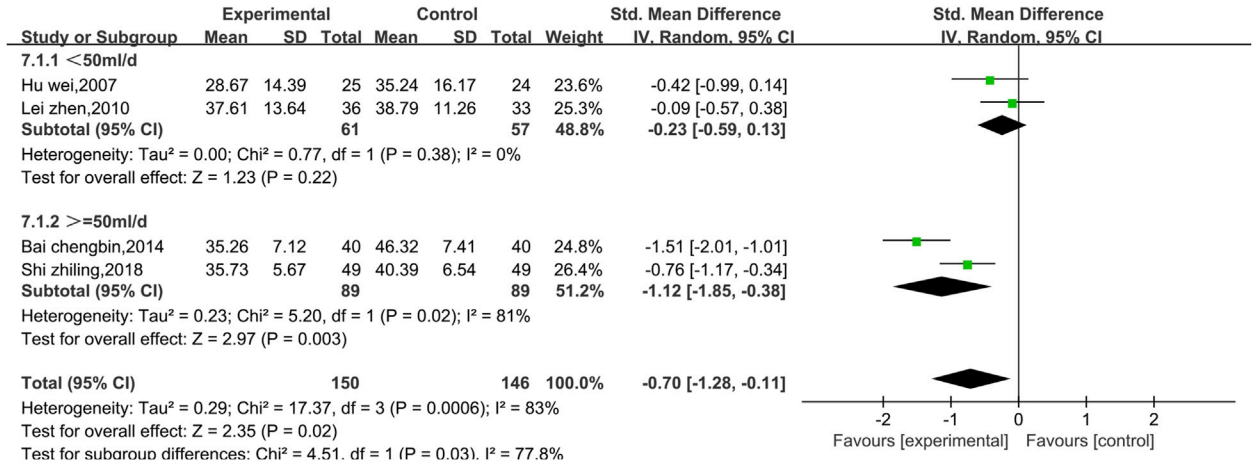


FIGURE 11
Forest plots of the subgroup analysis at different doses (AST level).

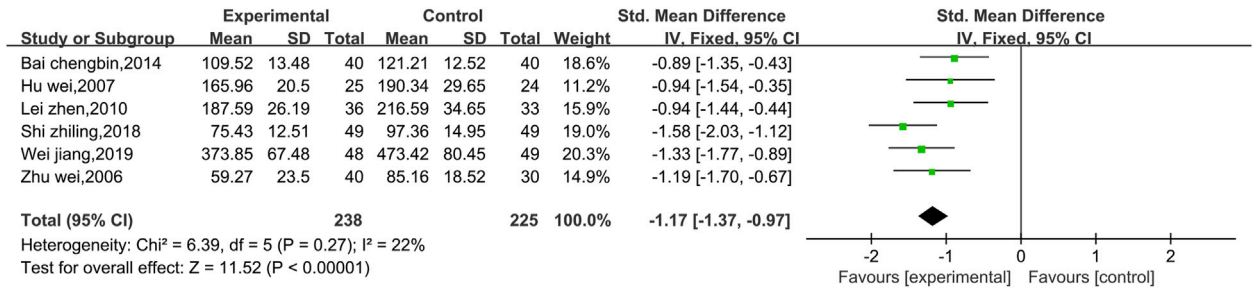


FIGURE 12
Comparative forest plots of the LDH levels.

insomnia. In total, 10 patients in the conventional treatment group experienced adverse reactions during treatment, including 6 patients with headache, 3 patients with nausea and vomiting, and 1 patient with delirium. No significant heterogeneity was observed (I^2 = 0.%, p = 0.87). Meta-analysis was performed via the fixed effects model (Supplementary Figure 8), and the results reveal that there was no significant difference between Shenmai injection group and conventional treatment group [RR = 1.56, 95% CI (0.73, 3.33), p = 0.25]. Subgroup and sensitivity analyses were not performed because of the low level of heterogeneity.

3.5 Sensitivity analysis

When there was significant heterogeneity, we used sensitivity analyses, including CKMB, AST, CK, TNF-α, and IL-6. Sensitivity analyses were performed by deleting articles

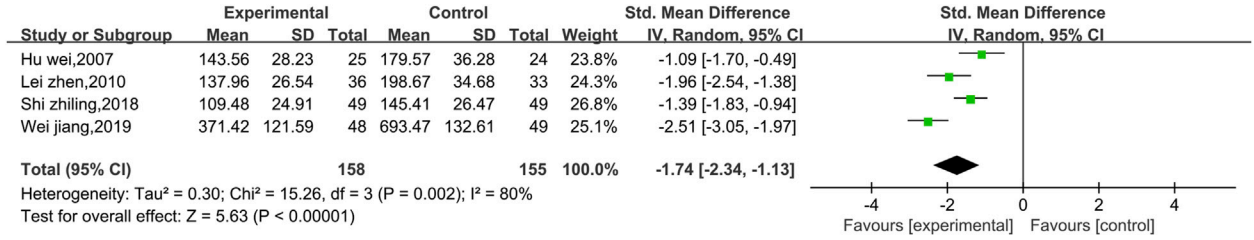


FIGURE 13
Comparative forest plots of the CK levels.

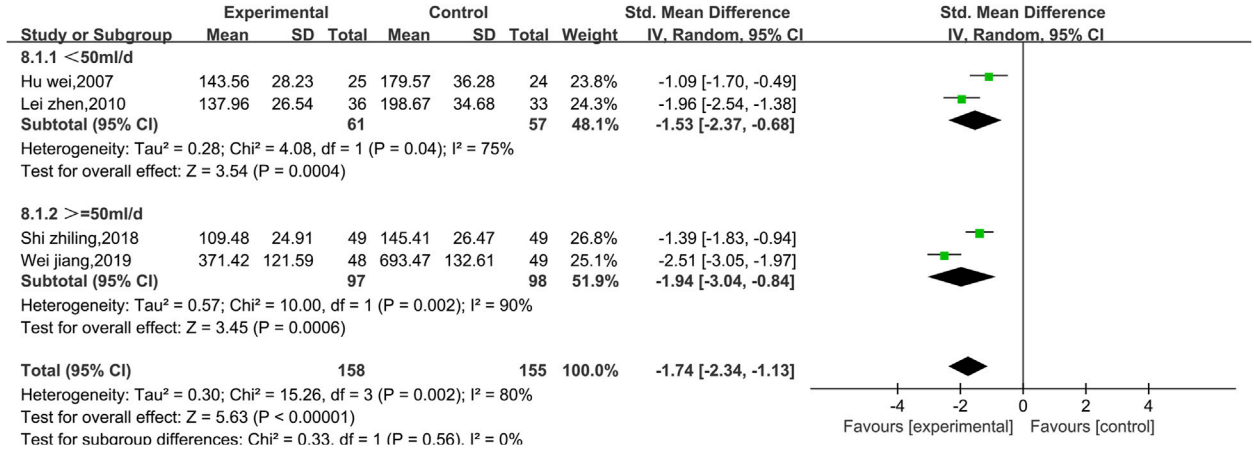


FIGURE 14
Forest plots of the subgroup analysis at different doses (CK level).

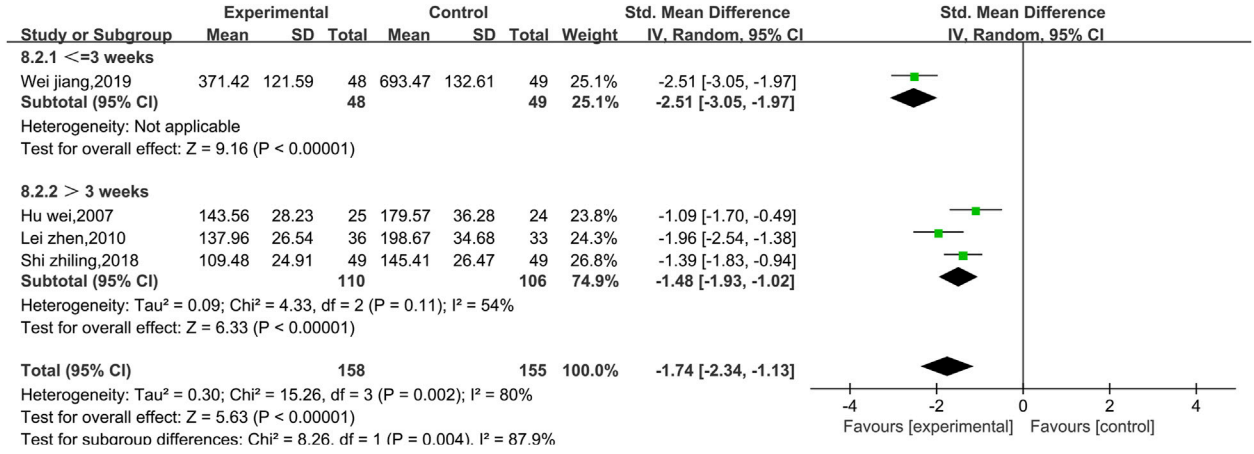


FIGURE 15
Forest plots of the subgroup analysis at different durations of treatment (CK level).

one at a time. The level of heterogeneity appeared to change after the articles by Wan et al. (2020) or Lu et al. (2018) were excluded. The sensitivity analysis results are shown in Table 2.

3.6 Publication bias

We detected publication bias in the total efficacy rate, since ≥10 studies reported this outcome. The results are shown

TABLE 2 Sensitivity analysis.

Outcome	Study removed [first author (year)]	*p*-value, I^2 value(%)	*p*-value	RR/SMD [95% CI]
TNF-α	Liang et al. (2022)	$p < 0.0001$, $I^2 = 90$	$p = 0.003$	−1.35 [−2.08, −0.62]
	Luo et al. (2017)	$p = 0.0004$, $I^2 = 87$	$p < 0.0001$	−1.24 [−1.87, −0.62]
	Shi and Xiang (2018)	$p = 0.0004$, $I^2 = 87$	$p < 0.0001$	−1.22 [−1.80, −0.63]
	Wan et al. (2020)	$p = 0.32$, $I^2 = 12$	$p < 0.00001$	−1.56 [−1.80, −1.32]
IL-6	Liang et al. (2022)	$p = 0.05$, $I^2 = 73$	$p < 0.00001$	−1.53 [−2.14, −0.92]
	Luo et al. (2017)	$p = 0.04$, $I^2 = 76$	$p < 0.00001$	−1.52 [−2.15, −0.89]
	Lu et al. (2018)	$p = 0.94$, $I^2 = 0$	$p < 0.00001$	−1.24 [−1.49, −0.98]

in Supplementary Figure 9. The effect points of each trial were symmetrically distributed in an inverted funnel shape, which indicates that there was a low risk of publication bias. However, this analysis was not sufficiently precise. Therefore, we used Stata 16.0 to perform Egger's test; the results show that $p = 0.1081$, which is >0.05 and suggests that there was no significant publication bias.

3.7 Quality of evidence

The included studies did not provide detailed descriptions of allocation concealment or blinding specifics; therefore, all evidence was downgraded by one level due to limitations in the studies. There was significant heterogeneity for the following outcomes: CKMB, AST, CK, TNF-α, IL-6, and cTnI. Therefore, the evidence for these outcomes was downgraded by two grades in the inconsistency aspects. All endpoints could be used as direct evidence, so indirectness was not downgraded. AST, CK, IL-6, and cTnI were downgraded by one grade because the sample size was <400. Regarding adverse reactions, although they satisfied the OIS criteria, the evidence was downgraded by one grade for imprecision because the corresponding forest plots showed that the confidence intervals contained null values, and the credible intervals did not exclude significant benefit or harm. There was no risk of publication bias in terms of the effective rates; therefore, this evidence was not downgraded. Overall efficiency, ECG efficiency, and LDH were rated as "moderate"-quality evidence; adverse effects were rated as "low"-quality evidence; CKMB, AST, CK, TNF-α, IL-6, and cTnI were rated as "very low"-quality evidence; CKMB, AST, CK, TNF-α, IL-6, and cTnI were rated as "very low"-quality evidence. Supplementary Figure 10 shows the evidence quality analysis of the continuous variables. Supplementary Figure 11 shows the evidence quality analysis of the bicategorical variables.

4 Discussion

In total, 18 randomized controlled trials were included in this meta-analysis. The results indicate that compared to conventional treatment, the combination of Shenmai injection with conventional treatment more effectively improved the clinical efficacy of VMC treatment by improving the ECG findings of the patients and decreasing the physicochemical indices of the patients, including CKMB, AST, LDH, CK, TNF-α, and IL-6.

In cases of high heterogeneity, sensitivity analyses were performed by excluding individual studies one at a time and reconducting the meta-analyses. The results indicate that differences in the control group interventions and sample sizes of the studies can be sources of heterogeneity. This heterogeneity was reduced by excluding two experiments that were potential sources of heterogeneity. To assess the clinical heterogeneity, we performed subgroup analyses based on the treatment dosage and duration; we found that neither factor was a source of heterogeneity.

The clinical features of acute VMC include chest pain, fever, flu-like symptoms, gastrointestinal or respiratory symptoms and dyspnea. Some patients also experience syncope. Most patients with acute VMC experience ECG changes, the most common of which include similar ST-segment elevation to that in acute myocardial infarction, QRS width >120 ms, and arrhythmias. The gold standard for the diagnosis of myocarditis is endocardial myocardial biopsy and cardiac magnetic resonance imaging (Sayegh et al., 2023). However, laboratory tests are recommended when endocardial myocardial biopsy and cardiac magnetic resonance imaging are not feasible or when the patient's status is unstable. Recommended laboratory tests include biomarkers of myocardial necrosis (e.g., CKMB, CK, cTnI), inflammatory markers (e.g., C-reactive protein, TNF-α, and IL-6) (Ammirati et al., 2020), and the myocardial enzymes serum LDH and aspartate transferase (AST), which may also be used as secondary evidence to diagnose VMS. Therefore, these endpoints were selected to assess the therapeutic effect in this study and provide a reference basis for the efficacy of Shenmai injection in combination with conventional modalities in the treatment of VMS.

Shenmai injection is made from the extracts of Hong Shen and Mai Dong. Hong Shen is composed of fresh Ren Shen; during the concoction process, ginsenosides undergo decarboxylation, hydrolysis and isomerization and result in new metabolites with stronger activity, such as ginsenosides Rg3, Rg5 and Rg6, which are unique to Hong Shen (Chu et al., 2013). These metabolites have been shown to have antiviral effects (Li et al., 2019), enhance body immunity (Zhao et al., 2014) and exhibit other effects. Their related preparations are mostly used to treat VMS. The main bioactive metabolites of maitake are steroidal saponins and flavonoids. Studies have shown that its metabolites have immunomodulatory, antiviral, and anti-inflammatory effects and protect the cardiovascular system (Lei et al., 2021)

The E3 ubiquitin ligase family members TRIM18 and TRIM29 may be involved in the development of viral myocarditis and can be therapeutic targets for viral myocarditis. TRIM18 recruits PPM1A, interacts with TANK-binding kinase 1

(TBK1), dephosphorylates and inactivates TBK1, blocks the interaction between TBK1 and its upstream mitochondrial antiviral signaling protein (MAVS) and STING, and inhibits type-I IFN-mediated antiviral signaling during viral infection. The knockdown of TRIM18 effectively protects the model mice from viral myocarditis, which further illustrates its potential as a therapeutic target. TRIM29 promotes cardiomyocyte apoptosis through the activation of the ER kinase (PKR)-like ER kinase (PERK)/activating transcription factor 4 (ATF4)/CHOP pathway, exacerbates myocardial damage caused by cardiomyopathic viruses and promotes the cardiomyopathic virus replication (Fang et al., 2022; Wang et al., 2024). However, the specific molecular mechanism of Shenmai injection in the treatment of viral myocarditis remains unclear. Shenmai injection may inhibit the expression of the autophagy-related genes Beclin-1 and LC3-II and apoptosis-related genes in viral myocarditis, inhibit excessive autophagy and apoptosis of cardiomyocytes in viral myocarditis, and subsequently inhibit the replication and release of viruses (Liang et al., 2022). Whether Shenmai injection can reduce the apoptosis of cardiomyocytes in viral myocarditis by inhibiting TRIM29 requires further research. Studies have also revealed that Shenmai injection may alleviate myocardial injury in viral myocarditis by lowering the expression levels of the NLRP3 inflammasome in peripheral blood mononuclear cells, which inhibits the cascading amplification of downstream inflammatory pathways (Wan et al., 2020). Currently, no reports indicate that Shenmai injection can improve viral myocarditis by inhibiting TRIM18 and TRIM29. TRIM18 and TRIM29 may be potential research directions for the treatment of viral myocarditis with Shenmai injection and herbal formulations.

According to the spontaneous reporting system (SRS) safety data analysis of Shenmai injection, among all adverse drug reaction (ADR) reports in 2005–2012, the adverse reactions associated with Shenmai injection mainly involved the dermatological system, gastrointestinal system, respiratory system, and systemic damage. The top 10 ADR manifestations were breathlessness, rash, anaphylaxis, pruritus, chills, palpitations, flushing, dizziness, nausea, and dyspnea. Breathlessness, anaphylaxis and flushing are safety warning signs for Shenmai injection. Further prospective, multi-center, large-sample safety hospital-based monitoring of Shenmai injection was conducted in 32,358 cases. ADRs occurred in 30 patients with an incidence of 0.093% and were characterized by chest tightness, chills, itchy skin, palpitations, fever, nausea, dizziness, vomiting, flushing, paresthesia, anaphylactic reactions, cyanosis, rash and back pain. Patients with chronic pulmonary heart disease, thyroid disease, combined cerebrovascular disease, and continuous use of prostaglandin and cyclophosphopyridine before Shenmai injection combined with quinolones, penicillins, and TCM expectorants are prone to adverse reactions (Wang et al., 2015).

Xiang et al. (2017) reported the occurrence of the abovementioned adverse reactions. They noted that the adverse reactions caused by Shenmai injection mostly concentrated in the first 30 min of the medication process, and most of them were rapid-onset metamorphic reactions. Therefore, when Shenmai injection is used clinically, it is necessary to pay close attention to changes in patients' signs in the first 30 min (Xiang et al., 2017).

Another study involving the use of Shenmai injection in 26 hospitals throughout China revealed that of 30,012 patients, 356 had adverse drug events (ADEs), and 45 had ADRs with an ADR incidence rate of 0.15%. Additionally, the adverse reactions disappeared after slowing the drip rate, discontinuing the drug, and treating the symptoms, which suggests that the safety of Shenmai injection is high (Wang et al., 2021).

With respect to the use of Shenmai injection, studies do not recommend the use of Shenmai injection with potassium chloride or vitamin C injection. The concomitant infusion of Shenmai injection with Xiangdan injection and LMWI should be avoided. Shenmai injection is contraindicated with pantoprazole sodium for injection (Deng and Xu, 2004; Zhang et al., 2008; Li and Xu, 2010).

In summary, compared with other therapeutic drugs, Shenmai injection has notable advantages in terms of safety, multi-target action, and efficacy in the treatment of VMC. In addition to its conventional antiviral, immune-regulating, and antioxidant properties, specifically in accelerating the clearance of oxygen free radicals, Shenmai injection improves microcirculation in VMC, enhances the myocardial contractility, and optimizes the myocardial metabolism. Therefore, Shenmai injection helps to prevent damage to myocardial cells in VMC and contributes to the repair of damaged myocardial cells. Furthermore, compared with traditional treatment methods for VMC, Shenmai injection combined with standard therapy has greater clinical efficacy. The findings of this study support the effectiveness of Shenmai injection in VMC (Shen, J. 2007; Liu, M. 2007; Shi et al., 2021).

4.1 Limitations

The limitations of this paper are as follows. First, too few randomized controlled trials were included in this study, and some of the articles were of low quality. More high-quality RCTs on this topic must be conducted to substantiate the efficacy of this treatment. Some of the randomized controlled trials in this article reported the use of blinding but did not specify whether blinding was used for patients, experimenters and evaluators or only for patients, which may have led to exaggerated results of the intervention group, biased results of the meta-analysis, and imperfect conclusion of this study. Although the studies in this paper mentioned the approximate medication for conventional treatment, the exact dosage and frequency of medication were not described in detail, which may have led to clinical heterogeneity. Clinical heterogeneity may increase due to different levels of care at different times and in different hospitals, but such limitations are difficult to avoid. The randomized controlled trials in this study are limited to China only, and the reference significance of this treatment regimen for populations in other countries or regions must be verified in larger clinical trials.

4.2 Prospects

This study highlights the inadequacy of the current clinical trials of Shenmai injection for the treatment of VMC. Future clinical studies should strengthen the application of blinding and ensure strict randomization in the trials. The type, dosage, and frequency of administration of conventional therapeutic drugs in the control group should also be clarified in clinical studies. Further in-depth studies on the target of action, clinical minimum starting concentration, and optimal treatment period of Shenmai injection to treat VMC are also necessary. Moreover, there are

few reports on the side effects of Shenmai injection, which must be examined.

5 Conclusion

The combination of Shenmai injection with conventional therapy can improve the degree of myocardial damage, weaken the inflammatory response and improve the clinical efficacy of treatment for patients with VMC, which has a degree of safety. However, the quality of the current evidence is relatively low, and more high-quality studies are necessary to confirm the effectiveness of this treatment and provide more reliable evidence for its clinical application.

Data availability statement

The datasets presented in this study can be found in online repositories. The names of the repository/repositories and accession number(s) can be found in the article/Supplementary Material.

Author contributions

QY: Writing–original draft, Writing–review and editing. JQ: Writing–original draft, Writing–review and editing. ZL: Writing–original draft, Writing–review and editing. YH: Funding acquisition, Supervision, Validation, Writing–review and editing. YZ: Funding acquisition, Supervision, Validation, Writing–review and editing.

Funding

The author(s) declare that no financial support was received for the research, authorship, and/or publication of this article.

Conflict of interest

The authors declare that the research was conducted in the absence of any commercial or financial relationships that could be construed as a potential conflict of interest.

Publisher's note

All claims expressed in this article are solely those of the authors and do not necessarily represent those of their affiliated organizations, or those of the publisher, the editors and the reviewers. Any product that may be evaluated in this article, or claim that may be made by its manufacturer, is not guaranteed or endorsed by the publisher.

Supplementary material

The Supplementary Material for this article can be found online at: https://www.frontiersin.org/articles/10.3389/fphar.2024.1453946/full#supplementary-material

SUPPLEMENTARY FIGURE S1
Comparative forest plots of the TNF-α levels.

SUPPLEMENTARY FIGURE S2
Forest plots of the subgroup analysis at different doses (TNF-α level).

SUPPLEMENTARY FIGURE S3
Forest plots of the subgroup analysis at different durations of treatment (TNF-α level).

SUPPLEMENTARY FIGURE S4
Comparative forest plots of the TNF-α levels (removing sources of heterogeneity).

SUPPLEMENTARY FIGURE S5
Comparative forest plots of the IL-6 level.

SUPPLEMENTARY FIGURE S6
Forest plots of the subgroup analysis at different doses (IL-6 level).

SUPPLEMENTARY FIGURE S7
Comparative forest plots of the IL-6 level (removing sources of heterogeneity).

SUPPLEMENTARY FIGURE S8
Comparative forest plots of the adverse reactions.

SUPPLEMENTARY FIGURE S9
Funnel plot of the publication bias.

SUPPLEMENTARY FIGURE S10
Evidence quality analysis of the continuous variables.

SUPPLEMENTARY FIGURE S11
Evidence quality analysis of the bicategorical variables.

References

Ammirati, E., Frigerio, M., Adler, E. D., Basso, C., Birnie, D. H., Brambatti, M., et al. (2020). Management of acute myocarditis and chronic inflammatory cardiomyopathy: an expert consensus document. *Circ. Heart Fail.* 13, e007405. doi:10.1161/circheartfailure.120.007405

Bai, C. (2014). Effect of integrated Chinese and Western medicine on acute viral myocarditis. *J. Mod. Integr. Tradit. Chin. West. Med.* 23, 1784–1785. doi:10.3969/j.issn.1008-8849.2014.16.031

Chan, P., and Liu, S. (2007). Effect of shenmai injection on 30 cases of viral myocarditis. *Shandong Med.* 38.

Chu, C., Xu, S., Li, X., Yan, J., and Liu, L. (2013). Profiling the ginsenosides of three ginseng products by LC-Q-TOF/MS. *J. Food Sci.* 78, C653–C659. doi:10.1111/1750-3841.12102

Dai, L., Guan, W., Zhang, D., Zhang, Y., Liu, J., Zhou, K., et al. (2020). Network pharmacology research and experimental verification of shenmai decoction in improving diabetic nephropathy. *Traditional Chin. Med. Pharmacol. Clin.* 36 (04), 81–87. doi:10.13412/j.cnki.zyyl.20200826.00

Deng, N., and Xu, R. (2004). Microparticle changes of Shenmai, Danshen and Huangqi injection mixed with potassium chloride or vitamin C injection. *Chin. J. Mod. Appl. Pharm.* 21 (7), 76–77. doi:10.13748/j.cnki.issn1007-7693.2004.s1.100

Fang, M., Zhang, A., Du, Y., Lu, W., Wang, J., Minze, L. J., et al. (2022). TRIM18 is a critical regulator of viral myocarditis and organ inflammation. *J. Biomed. Sci.* 29 (1), 55. doi:10.1186/s12929-022-00840-z

Higgins, J., Thomas, J., Chandler, J., Cumpston, M., Li, T., Page, M., et al. (2023). *Cochrane handbook for systematic reviews of interventions*. Canada, UK: Cochrane.

Hou, Y. J. (2009). Curative effect of shenmai injection on viral myocarditis. *J. Integr. Chin. West. Med.* 18, 533.

Hu, W., Hu, J., Wu, Q., and Zhang, J. (2007). Shenmai injection George infantile viral myocarditis clinical observation. *J. Pediatr. Pharm.*, 53–54. doi:10.13407/j.cnki.jpp.1672-108x.2007.03.010

Hutton, B., Salanti, G., Caldwell, D. M., Chaimani, A., Schmid, C. H., Cameron, C., et al. (2015). The PRISMA extension statement for reporting of systematic reviews

incorporating network meta-analyses of health care interventions: checklist and explanations. *Ann. Intern. Med.* 162, 777–784. doi:10.7326/m14-2385

Lasrado, N., and Reddy, J. (2020). An overview of the immune mechanisms of viral myocarditis. *Rev. Med. Virol.* 30 (6), 1–14. doi:10.1002/rmv.2131

Lei, F., Weckerle, C. S., and Heinrich, M. (2021). Liriopogons (genera *Ophiopogon* and *Liriope*, Asparagaceae): a critical review of the phytochemical and pharmacological research. *Front. Pharmacol.* 12, 769929. doi:10.3389/fphar.2021.769929

Lei, Z. (2010). Observation on the curative effect of shenmai injection on viral myocarditis in children. *Chin. J. Prim. Med.*, 1339–1340. doi:10.3760/cma.j.issn.1008-6706.2010.10.024

Li, X., Shi, S., and Zhao, Y. (2019). Research progress of ginseng and its saponins and ginseng prescriptions for prevention and treatment of viral diseases. *Chin. Herb. Med.* 51, 2379–2389. doi:10.7501/j.issn.0253-2670.2020.09.012

Li, X., and Xu, Li. (2010). There is incompatibility between Shenmai injection and Weidi. *Shandong Pharm.* 50 (25), 46.

Liang, B., Peng, X., and Chen, L. (2022). Effect of shenmai injection on expression of autophagy and apoptosis-related proteins in peripheral blood of patients with viral myocarditis. *J. Cardio-Cerebrovasc. Dis. Integr. Chin. West. Med.* 20, 2791–2795. doi:10.12102/j.issn.1672-1349.2022.15.019

Liu, G., and Wang, W. (2009). Clinical observation of astragalus and shengmai injection in the treatment of angina pectoris of coronary heart disease. *Chin. Mod. Dr.*, 82–83.

Liu, M. (2007). Clinical observation of shenmai injection in the treatment of viral myocarditis. *China Natl. Health Med.*, (09) : 405 + 350.

Liu, X. (2009). Sodium fructose diphosphate combined with shenmai Injection in treatment of 60 cases of viral myocarditis in children: clinical nursing care. *J. Qilu Nurs.* 15, 55–56.

Lu, Y., Ruan, X., Lu, J., Ma, C., and Jiang, C. (2018). Effects of shenmai Injection combined with trimetazidine on serum sIL-2R, miR, Th, electrocardiogram and stress response in patients with viral myocarditis. *Chin. J. Gerontol.* 38, 4370–4374. doi:10.3969/j.issn.1005-9202.2018.18.008

Luo, J., Zhang, J., Wang, Z., Liu, M., Wang, Y., and Jin, P. (2017). Clinical efficacy of shenmai Injection combined with trimetazidine and levocarnitine in the treatment of acute viral myocarditis and its effect on serum TNF-α and IL-6 levels. *Chin. J. Nosocom. Infect.* 27, 576–579. doi:10.11816/cn.ni.2016-162887

Olejniczak, M., Schwartz, M., Webber, E., Shaffer, A., and Perry, T. E. (2020). Viral myocarditis-incidence, diagnosis and management. *J. Cardiothorac. Vasc. Anesth.* 34, 1591–1601. doi:10.1053/j.jvca.2019.12.052

Pollack, A., Kontorovich, A. R., Fuster, V., and Dec, G. W. (2015). Viral myocarditis--diagnosis, treatment options, and current controversies. *Nat. Rev. Cardiol.* 12 (11), 670–680. doi:10.1038/nrcardio.2015.108

Qu, W., Xu, W., Li, C., Yang, L., Zhang, S., Wen, J., et al. (2023). HPLC method was used to simultaneously determine the content of six rare ginsenosides in red ginseng. *Chin. J. Traditional Chin. Med.* 38 (06), 2874–2877.

Sayegh, M. N., Goins, A. E., Hall, M. A. K., and Shin, Y. M. (2023). Presentations, diagnosis, and treatment of post-COVID viral myocarditis in the inpatient setting: a narrative review. *Cureus* 15, e39338. doi:10.7759/cureus.39338

Schünemann, H. J., Mustafa, R. A., Brozek, J., Steingart, K. R., Leeflang, M., Murad, M. H., et al. (2020). GRADE guidelines: 21 part 1. Study design, risk of bias, and indirectness in rating the certainty across a body of evidence for test accuracy. *J. Clin. Epidemiol.* 122, 129–141. doi:10.1016/j.jclinepi.2019.12.020

Shen, J. (2007). Efficacy of Shenmai injection in the treatment of viral myocarditis. *Chin. Community Physicians* (06), 46.

Shi, S., Liu, M., Gao, Y., Xu, J. G., Kang, Y. Y., Xing, L. N., et al. (2021). Systematic review and re-evaluation of Shenmai injection in the prevention and treatment of diseases. *Chin. J. Traditional Chin. Med.* 46 (15), 3998–4007. doi:10.19540/j.cnki.cjcmm.20210113.501

Shi, Z., and Xiang, M. (2018). Clinical study on shenmai injection combined with dexamethasone in treatment of viral myocarditis. *Drugs Clin.* 33, 1366–1370. doi:10.7501/j.issn.1674-5515.2018.06.016

Song, C. (2006). Shenmai injection in treatment of acute viral myocarditis 52 cases. *J. Henan Tradit. Chin. Med.* 73. doi:10.16367/j.issn.1003-5028.2006.03.058

Sterne, J. A., Sutton, A. J., Ioannidis, J. P., Terrin, N., Jones, D. R., Lau, J., et al. (2011). Recommendations for examining and interpreting funnel plot asymmetry in meta-analyses of randomised controlled trials. *BMJ* 343, d4002. doi:10.1136/bmj.d4002

Tavares, P. S., Rocon-Albuquerque, R. J., and Leite-Moreira, A. F. (2010). Innate immune receptor activation in viral myocarditis: pathophysiologic implications. *Rev. Port. Cardiol.* 29, 57–78. doi:10.1038/ki.2010.111

Wan, Y., Gao, Y., and Zhang, W. (2020). Effect of shenmai Injection on patients with viral myocarditis and influence of NLRP3 inflammasome in peripheral blood. *J. Hunan Univ. Tradit. Chin. Med.* 40, 100–104. doi:10.3969/j.issn.1674-070X.2020.01.022

Wang, J., Lu, W., Zhang, J., Du, Y., Fang, M., Zhang, A., et al. (2024). Loss of TRIM29 mitigates viral myocarditis by attenuating PERK-driven ER stress response in male mice. *Nat. Commun.* 15 (1), 3481. doi:10.1038/s41467-024-44745-x

Wang, L., Xie, Y., Ai, Q., and Song, N. b. (2015). Post-marketing clinical safety assessment of Shenmai injection based on active monitoring and passive monitoring in large data background. *Chin. J. Traditional Chin. Med.* 40 (24), 4752–4756. doi:10.4268/cjcmm20152406

Wang, M., Wang, S., Liu, M., Gao, Y., and Tian, J. (2021). Usage and safety evaluation of 30 012 cases of Shenmai injection in the real world. *Chin. J. Evidence-based Med.* 21 (02), 133–138. doi:10.7507/1672-2531.202010001

Wang, Z., Yang, J., and Zhang, L. (2007). Effect of shenmai injection combined with fructose 1,6 diphosphate on viral myocarditis in children. *J. Cardio-Cerebrovasc. Dis. Integr. Chin. West. Med.*, 440–441.

Wei, J., and Sun, H. (2019). Effects of Shenmai Injection combined with fructose 1, 6-diphosphate on electrocardiogram and myocardial enzymes in children with viral myocarditis. *Guizhou Med.* 43, 1562–1563.

Weng, L. Z. (2006). Curative effect of shenmai Injection combined with potassium magnesium aspartate needle in the treatment of acute viral myocarditis. *J. Mod. Chin. West. Integr. Med.* 2485.

Xiang, D., Huang, Y., Deng, L., Liu, J., Zhang, C., and He, G. (2017). Analysis of 1533 cases of clinical adverse reactions/events of Shenmai injection. *Chin. J. Hosp. Pharm.* 37 (04), 393–396. doi:10.13286/j.cnki.chinhosppharmacyj.2017.04.21

Xing, C., Cao, S., Hu, S., Tang, X., Zhang, Y., and Han, L. (2014). Effect of sodium creatine phosphate combined with shenmai injection on viral myocarditis in children. *Hebei Med.* 36, 2799–2801. doi:10.3969/j.issn.1002-7386.2014.18.034

Xu, S. (2010). Therapeutic effect of shenmai injection combined with α-interferon on viral myocarditis in children. *Chin. J. Misdiagnosis* 10, 7354.

Yang, G., Li, S., Sun, X., Lv, Y., and Huang, H. (2023). Quality monitoring of shenmai injection by HPLC pharmacodynamic fingerprinting. *BMC Chem.* 17, 28. doi:10.1186/s13065-023-00920-7

Zhang, H., Fan, B., and Li, H. (2008). Compatible application of low molecular dextran with Shenmai and Xiangdan injection. *Chin. Pat. Med.* 30 (12), 1879–1880.

Zhang, X., Lv, S., Zhang, W., Jia, Q., Wang, L., Ding, Y., et al. (2021). Shenmai injection improves doxorubicin cardiotoxicity via miR-30a/Beclin 1. *Biomed. Pharmacother.* 139, 111582. doi:10.1016/j.biopha.2021.111582

Zhao, Y., Dai, J., Lv, J., and Jia, T. (2014). Ginseng and its processed products. Study of effects of hypoxia in mice anti-fatigue. *J. Liaoning Tradit. Chin. Med. J.* 9, 1040–1042. doi:10.13192/j.issn.1000-1719.2014.05.090

Zhu, J., Liang, Y., Yue, S., Fan, G., Zhang, H., and Zhang, M. (2017). Combination of panaxadiol and panaxatriol type saponins and ophioponins from shenmai formula attenuates lipopolysaccharide-induced inflammatory injury in cardiac microvascular endothelial cells by blocking NF-kappa B pathway. *J. Cardiovasc. Pharmacol.* 69, 140–146. doi:10.1097/fjc.0000000000000450

Zhu, W., Lu, G., and Wang, G. (2006). Clinical effect of shenmai injection on 40 cases of viral myocarditis in children. *Pharm. Ind. Inf.* 228.

frontiers | Frontiers in Pharmacology

TYPE Systematic Review
PUBLISHED 27 November 2024
DOI 10.3389/fphar.2024.1497072

Check for updates

OPEN ACCESS

EDITED BY
Qingquan Liu,
Capital Medical University, China

REVIEWED BY
Wentai Pang,
Tianjin University of Traditional Chinese Medicine, China
Bo Li,
Capital Medical University, China

*CORRESPONDENCE
Jian-ping Liu,
liujp@bucm.edu.cn

†These authors have contributed equally to this work

RECEIVED 16 September 2024
ACCEPTED 05 November 2024
PUBLISHED 27 November 2024

CITATION
Liu X-x, Ma Y-q, Kong L-y, Su Y-z, Robinson N and Liu J-p (2024) Unveiling the therapeutic role of Dachaihu decoction in acute cholecystitis: a comprehensive systematic review and meta-analysis of its efficacy and safety.
Front. Pharmacol. 15:1497072.
doi: 10.3389/fphar.2024.1497072

COPYRIGHT
© 2024 Liu, Ma, Kong, Su, Robinson and Liu. This is an open-access article distributed under the terms of the Creative Commons Attribution License (CC BY). The use, distribution or reproduction in other forums is permitted, provided the original author(s) and the copyright owner(s) are credited and that the original publication in this journal is cited, in accordance with accepted academic practice. No use, distribution or reproduction is permitted which does not comply with these terms.

Unveiling the therapeutic role of Dachaihu decoction in acute cholecystitis: a comprehensive systematic review and meta-analysis of its efficacy and safety

Xin-xin Liu[1†], Ying-qi Ma[2†], Ling-yao Kong[1], You-zhu Su[1], Nicola Robinson[1,3] and Jian-ping Liu[1,4*]

[1]Centre for Evidence-Based Chinese Medicine, Beijing University of Chinese Medicine, Beijing, China, [2]The First Clinical Medical College, Shandong University of Traditional Chinese Medicine, Jinan, Shandong, China, [3]School of Health and Social Care, London South Bank University, London, United Kingdom, [4]Department of Community Medicine, The National Research Center in Complementary and Alternative Medicine (NAFKAM), Faculty of Health Science, UiT The Arctic University of Norway, Tromsø, Norway

Background: Dachaihu decoction (Dachaihu tang) plays a crucial role in treating acute illnesses. Recently, a significant number of clinical studies on Dachaihu decoction for acute cholecystitis (AC) have been published. This study was conducted to assess the efficacy and safety of Dachaihu decoction in patients with this condition.

Methods: To identify relevant randomized controlled trials (RCTs), eight databases and three clinical trial registries were searched from inception to 30 June 2024. Two researchers independently screened and extracted data from eligible studies using EndNote X9 and Microsoft Office Excel 2019. RoB 2.0 was used to assess the risk of bias in the included studies. Stata 17.0 was used for data analysis. Publication bias and its impact on result stability were evaluated using a funnel plot and the "trim-and-fill" method. The quality of evidence was graded using the GRADE assessment system.

Results: Thirty-three RCTs involving 2,851 participants were included. The treatment group demonstrated improved clinical efficacy (RR = 1.18; 95% CI = 1.13 to 1.24), significantly reduced length of hospital stay (MD = −1.78 days; 95% CI = −2.02 to −1.53), and the incidence of adverse events (RR = 0.31; 95% CI = 0.20 to 0.48). Additionally, there appeared to be reductions in the time for abdominal pain to resolve (MD = −1.92 days; 95% CI = −2.33 to −1.51), fever to disappear (MD = −1.52 days; 95% CI = −1.90 to −1.14), white blood cell count to return to normal (MD = −2.89 days; 95% CI = −3.32 to −2.46), alanine aminotransferase (ALT) levels (MD = −11.88 U/L; 95% CI = −15.29 to −8.47), aspartate aminotransferase (AST) levels (MD = −8.74 U/L; 95% CI = −9.76 to −7.72), neutrophil percentage (MD = −9.68; 95% CI = −11.33 to −8.03), TNF-α levels (SMD = −2.10 pg/L; 95% CI = −2.43 to −2.78), and certainty of evidence (moderate-to-low certainty).

Conclusion: Dachaihu decoction may be an effective botanical formula for managing AC and a lower incidence of adverse events. However, due to the

substantial risk of bias and heterogeneity across the included studies, these findings should be interpreted with caution and require further validation through well-designed, high-quality trials.

Systematic Review registration: https://www.crd.york.ac.uk/PROSPERO/display_record.php?RecordID=573332.

KEYWORDS

Dachaihu decoction, acute cholecystitis, clinical efficacy, systematic review, meta-analysis

1 Introduction

Acute cholecystitis (AC) is an acute infectious gallbladder disease caused by cystic duct obstruction, chemical stimulation, and bacterial infection. It represents 10% of all acute abdominal cases in clinical practice (Abdulrahman et al., 2022; Kimura et al., 2007; China Association Of Integrative Medicine Emergency Medicine Committee et al., 2019). The clinical manifestations include paroxysmal colic in the right upper abdomen, often accompanied by nausea, vomiting, fever, and jaundice. The incidence of AC increases among individuals aged 50 and above, with an overall mortality rate of approximately 3%, increasing significantly in patients with comorbidities. In cases without gallstones, mortality can escalate to 15%–40% (Bedirli et al., 2001; González-Castillo et al., 2021). This higher risk is not only due to AC being secondary to critical illnesses—such as trauma, surgery, shock, burns, sepsis, total parenteral nutrition, and mechanical ventilation—but also because it is more likely to lead to gangrene, perforation, and pyothorax, or empyema compared to calculous cholecystitis (Kimura et al., 2007; Gluhovschi et al., 2023).

AC arises from a confluence of factors, including systemic inflammatory responses, multiorgan dysfunction, and gallbladder damage caused by gallstones and infection (Markaki et al., 2021; Nitzan et al., 2017; Regimbeau et al., 2014; Halpin, 2014). Treatment typically involves medication (such as anti-infection agents, antispasmodics, and analgesics) and surgical interventions. However, in elderly patients with comorbidities, a conservative approach is favored as it effectively relieves symptoms and controls infection during the acute phase (Mencarini et al., 2024). Despite targeting the initial pathological event, there are no specific agents for AC treatment. The risk of postoperative infectious complications in grade 1 and 2 AC is approximately 17% (Regimbeau et al., 2014). The role of antibiotics and surgical interventions, whether administered early in the disease or during the perioperative period, remains a topic of debate (Singh et al., 2023; Dietrich et al., 2024). Therefore, on the basis of modern medical treatments, exploring alternative treatments for AC is crucial.

A large number of traditional Chinese medicine (TCM) formulas are utilized in Chinese clinical practice to treat diseases with complex mechanisms. Recently, the focus has shifted toward combination therapies involving multi-target and multi-component drugs, which has become fundamental in exploring the molecular mechanisms of TCM prescription components for disease treatment (Li et al., 2023). TCM formulas have demonstrated significant efficacy and safety over thousands of years of clinical practice (Sheehan et al., 1992; Deng and Xu, 2017). Dachaihu decoction (Dachaihu Tang), a classic TCM formula, was documented in the Treatise on Febrile Diseases by Zhang Zhongjing, a prominent traditional Chinese physician from 150 to 219 AD. Comprising eight botanical drugs, namely, *Bupleurum chinense* DC. [Apiaceae; *Bupleuri radix*], *Scutellaria baicalensis* Georgi [Lamiaceae; *Scutellariae radix*], *Citrus aurantium* L. [Rutaceae; *Citri aurantii fructus immaturus*], *Pinellia ternata* (Thunb.) *Makino* [Araceae; *Pinelliae rhizoma*], *Rheum officinale* Baill. [Polygonaceae; *Rhei radix et rhizoma*], *Paeonia lactiflora* Pall. [Paeoniaceae; *Paeoniae radix alba*], *Zingiber officinale* Roscoe [Zingiberaceae; *Zingiberis rhizoma*], and *Ziziphus jujuba* Mill. [Rhamnaceae; *Ziziphi jujubae fructus*], it is noted for its ability to relieve abdominal pain, reduce fever, alleviate gastrointestinal symptoms, and lower inflammation (Bi et al., 2023).

In 1994, Japanese Kampo medicine scholars first demonstrated its capability to ameliorate liver injury in a mechanistic study of Dachaihu decoction (Ji et al., 2024). The main bioactive components include saikosaponin B2, baicalin, baicalein, epiberberine, naringin, hesperidin, neohesperidin, and nobiletin. These efficacy markers may influence various signaling pathways such as MAPK, NF-κB, and Toll-like receptors by targeting molecules like JUN, TNF, EGFR, MAPK3, RELA, TNF, HIF1A, AKT1, IGF1R, CREB1, and SIRT1, HIF-1, PI3K-AKT, and AMPK, thus regulating the ERK1/ERK2 cascade, NF-κB transcription factor activity, inflammatory responses, glucose metabolism, angiogenesis, and adipocyte differentiation (Mao et al., 2017; Ohta et al., 1995). Dachaihu decoction protects the liver, promotes bile flow, and exerts anti-inflammatory effects, making it a commonly prescribed botanical drug treatment for AC among clinicians (Bi et al., 2023; Zhou, 2020). It can reduce inflammatory responses and alleviate gastrointestinal symptoms in patients with AC by regulating CRP levels and inflammatory factors (TNF-α, IL-6, and IL-8), without apparent side effects (Liu et al., 2021). Given the global prevalence of AC, the high rate of perioperative infections, and the limitations of Western medications such as anti-infective drugs and analgesics in managing this condition, along with extensive clinical study data from clinical studies, there is a pressing need for a comprehensive review of existing research. This study aims to review the relevant literature to summarize previous findings on the efficacy of Dachaihu decoction alone or in combination with conventional treatment for managing AC, thereby providing a deeper understanding of its overall efficacy and safety in AC treatment.

2 Methods

This study has been registered on the PROSPERO platform (Registration No.: CRD42024573332; https://www.crd.york.ac.uk/PROSPERO/display_record.php?RecordID=573332).

TABLE 1 Basic information on botanical drugs in Dachaihu decoction.

Common English name	Botanical Latin name	Authorities	Family	Parts and form used	Processing of botanical drugs	Dosage (grams)	Main bioactive compounds	Medicinal source (Pharmacopoeia)
Bupleuri radix	*Bupleurum chinense* DC.	Augustin Pyramus de Candolle	Apiaceae	Root and dried root	Remove impurities and remaining stems, wash thoroughly, moisten until fully softened, slice thickly, and dry	15	Saikosaponins, flavonoids, essential oils, and phytosterols	China Pharmacopoeia (2015)
Chinese skullcap root	*Scutellaria baicalensis* Georgi	Johann Gottlieb Georgi	Lamiaceae	Root and dried root	Remove impurities and boil in water for 10 min. Take out and let it fully soften, then slice thinly, and dry. Alternatively, steam for 30 min, then slice thinly, and dry (avoiding direct sunlight)	9	Baicalin, baicalein, wogonin, and wogonoside	U.S. Pharmacopoeia USP 43 (2020)
Citron fruit	*Citrus aurantium* L.	Carl Linnaeus	Rutaceae	Fruit and dried ripe fruit	Remove impurities, wash thoroughly, moisten until fully softened, slice thinly, and dry	9	Synephrine, naringin, hesperidin, and limonin	China Pharmacopoeia (2010)
Banxia	*Pinellia ternata* (Thunb.) Makino.	Carl Peter Thunberg	Araceae	Tuber and dried tuber	Separate *Pinellia ternata* by size and soak in water until fully softened. Remove and set aside. Boil *Glycyrrhiza uralensis* twice, combine the decoctions, and mix with lime solution. Add the soaked *Pinellia*, stir 1–2 times daily, keeping pH above 12. Soak until the cross section is uniformly yellow and slightly tingling to taste. Remove, wash, and dry	9	Pinellia alkaloids, pinellin, polysaccharides, and volatile oils	China Pharmacopoeia (2015)
Rhubarb	*Rheum officinale* Baill	Henri Ernest Baillon	Polygonaceae	Rhizome, root, and dried root and rhizome	Remove impurities, wash thoroughly, moisten until softened, cut into thick slices or chunks, and air-dry	6	Anthraquinones, rhein, chrysophanol, emodin-8-glucoside, and aloe emodin	European Pharmacopoeia, 7th edn. (2012)
Chinese peony	*Paeonia lactiflora* Pall	Peter Simon Pallas	Paeoniaceae	Root and dried root	Wash thoroughly, moisten until softened, slice thinly, and dry	9	Paeoniflorin, albiflorin, and catechins	U.S. Pharmacopoeia USP 39 (2016)

(Continued on following page)

TABLE 1 (*Continued*) Basic information on botanical drugs in Dachaihu decoction.

Common English name	Botanical Latin name	Authorities	Family	Parts and form used	Processing of botanical drugs	Dosage (grams)	Main bioactive compounds	Medicinal source (Pharmacopoeia)
Ginger	*Zingiber officinale* Roscoe	William Roscoe	Zingiberaceae	Rhizome and dried rhizome	Remove impurities and wash thoroughly. Slice thickly before use	15	Gingerols, shogaols, zingerone, volatile oils, and flavonoids	U.S. Pharmacopoeia USP 43 (2020)
Ba	*Ziziphus jujuba* Mill	Philip Miller	Rhamnaceae	Fruit and dried ripe fruits	Remove impurities, wash thoroughly, and sun-dry. Break open or remove the seeds before use	9	Polysaccharides, saponins, and vitamin C	U.S. Pharmacopoeia USP 39 (2016)

Note: According to the Chinese Pharmacopoeia, the decoction preparation method for traditional Chinese medicine (TCM) is as follows: weigh *Bupleurum chinense* DC. [Apiaceae; *Bupleuri radix],* Scutellaria baicalensis *Georgi* [Lamiaceae; *Scutellariae radix], Citrus aurantium* L. [Rutaceae; *Citri aurantii fructus immaturus], Pinellia ternata (Thunb.)* Makino [Araceae; *Pinelliae rhizoma], Rheum officinale* Baill. [Polygonaceae; *Rhei radix et rhizoma], Paeonia lactiflora* Pall. [Paeoniaceae; *Paeoniae radix alba], Zingiber officinale* Roscoe [Zingiberaceae; *Zingiberis rhizoma], and Ziziphus jujuba* Mill. [Rhamnaceae; *Ziziphi jujubae fructus]*, according to the specified dosages (grams). Remove any impurities and wash thoroughly. Place the botanical drugs in a clean container, add sufficient water, and soak for approximately 30 min until softened. Transfer both the botanical drugs and soaking liquid to a clay or stainless-steel pot, add 6–10 times the herb weight in water, bring to a boil, and then simmer for 30 min. After the initial decoction, strain the liquid, add more water to the residue, and decoct again for 20–25 min. Combine and mix the two decoctions and then filter through a fine sieve or cloth for clarity. Pour the decoction into a clean container while hot, seal tightly, and consume within 24 h. For longer storage, reboil to sterilize and refrigerate. It should be taken warm, in divided doses, with dosage and frequency adjusted based on medical advice.

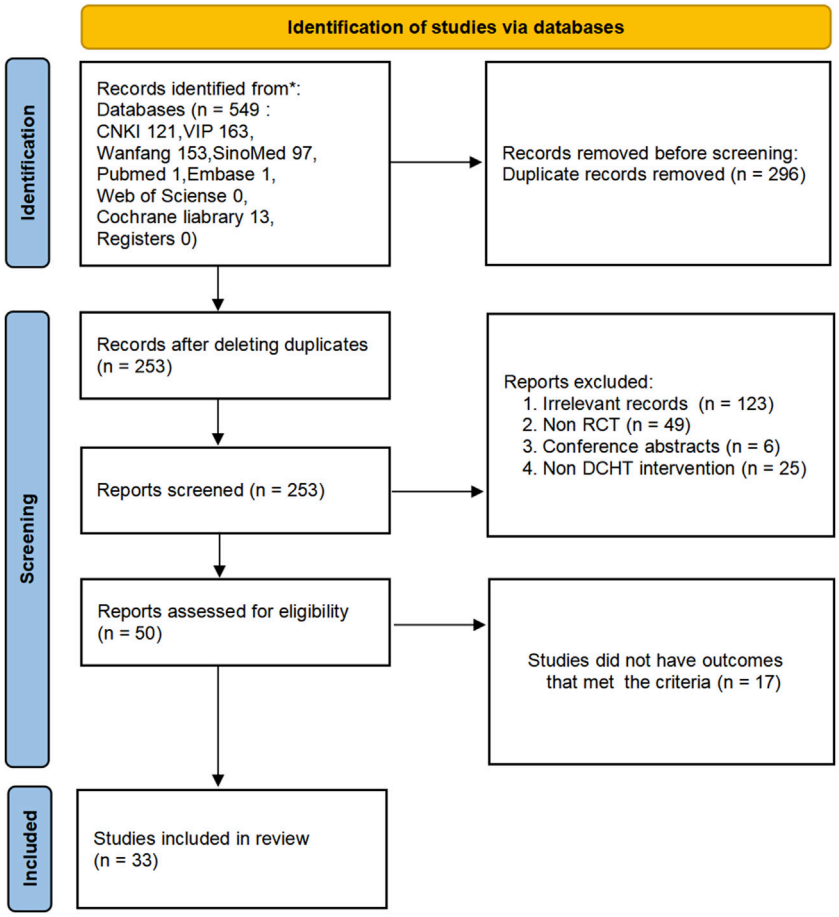


FIGURE 1
Flow diagram of the literature screening process.

TABLE 2 Study characteristics.

No.	Study ID	Sample size		Gender (male/female)		Age [mean (SD)]		Onset time (days)		Intervention		Duration (days)	Outcomes
		T	C	T	C	T	C	T	C	T	C		
1	Cai MK2022	103	103	48/55	47/56	51.24 ± 5.65	51.16 ± 5.72	8.14 ± 1.03	8.08 ± 1.10	DCHT + CT	CT	14	②, ③, ④, and ⑩
2	Chen JT2023	40	40	21/19	22/18	42.42 ± 4.74	42.37 ± 4.65	NR	NR	DCHT + LC	LC	5	①, ②, ③, ④, ⑤, ⑥, ⑦, and ⑩
3	Deng H2018	32	32	NR	NR	79.2 ± 6.8	80.4 ± 5.8	NR	NR	DCHT + CT	CT	14	② and ③
4	Deng YH2018	43	43	23/20	24/19	53.40 ± 13.50	53.60 ± 14.20	NR	NR	DCHT + CT	CT	28	①, ②, ③, and ⑧
5	Gu KK2021	30	30	17/13	16/14	62.71 ± 1.05	62.69 ± 1.06	0.29 ± 0.06	0.29 ± 0.05	DCHT + LC	LC	15	②, ③, ⑤, and ⑥
6	Guo AL2012	35	35	16/19	17/18	41.63 ± 10.21	40.23 ± 11.51	2.86 ± 1.35	3.0 ± 1.15	DCHT + CT	CT	7	⑤ and ⑩
7	Guo HL2023	40	40	17/23	16/24	56.34 ± 4.24	56.83 ± 4.57	NR	NR	DCHT + CT	CT	14	②, ③, ④, and ⑨
8	Hong JX2018	41	41	18/23	20/21	56.16 ± 10.23	54.02 ± 11.87	2.31 ± 0.86	2.46 ± 1.08	DCHT + CT	CT	7	⑦, ⑧, and ⑩
9	Li J2016	63	63	40/23	38/25	42.37 ± 5.63	43.68 ± 5.36	NR	NR	DCHT + CT	CT	10	①
10	Liang JB2013	50	50	32/18	30/20	47.00 ± 7.90	48.00 ± 8.30	1~5	1~6	DCHT	CT	10	①, ②, and ③
11	Liang JY2006	30	30	12/18	10/20	42.00 ± 11.20	43.52 ± 11.18	NR	NR	DCHT + CT	CT	7	② and ③
12	Liao XM2014	30	30	16/14	12/18	39.00 ± 3.70	38.00 ± 4.50	NR	NR	DCHT + CT	CT	30	②, ③, and ⑩
13	Liu H2021	35	35	19/16	18/17	52.34 ± 4.25	52.73 ± 4.59	3.02 ± 0.28	3.04 ± 0.26	DCHT + CT	CT	14	⑩
14	Liu WG2021	30	30	11/19	13/17	48.24 ± 8.13	48.71 ± 8.04	0.26 ± 0.05	0.28 ± 0.05	DCHT + LC	LC	14	①, ②, ③, ⑨, and ⑩
15	Liu YQ2015	52	52	22/30	21/31	53.63 ± 7.47	53.41 ± 7.62	3.01 ± 1.84	3.17 ± 1.96	DCHT + CT	CT	7	①, ②, ③, and ④
16	Su YB2016	41	41	20/21	17/24	39.65 ± 3.05	58.21 ± 4.35	NR	NR	DCHT + LC	LC	5	⑩
17	Sun JF2015	80	40	46/34	22/18	36~65	38~63	1~5	1~6	DCHT + CT	CT	10	①
18	Wang EC2020	40	40	26/14	22/18	NR	NR	2.00 ± 0.80	1.80 ± 0.60	DCHT + CT	CT	7	① and ⑥
19	Wang HR2014	59	59	25/34	27/32	39.58 ± 12.35	40.42 ± 11.92	NR	NR	DCHT + CT	CT	10	①, ②, ③, and ⑩
20	Wang SS2010	40	40	20/20	18/22	46.00 ± 10.80	40.60 ± 10.60	NR	NR	DCHT + CT	CT	7	② and ③
21	Wei YS2016	34	34	20/14	18/16	49.47 ± 8.13	50.34 ± 9.28	2.52 ± 0.96	2.47 ± 0.87	DCHT	CT	7	①, ②, ③, and ⑩
22	Xia CG2020	47	47	15/32	18/29	49.84 ± 16.92	48.05 ± 17.24	1.08 ± 0.47	1.00 ± 0.48	DCHT + LC	LC	10	②, ③, ④, ⑤, ⑥, and ⑦
23	Xiong Y2021	50	50	31/19	29/21	47.41 ± 9.81	48.28 ± 9.65	3.71 ± 1.37	3.45 ± 1.32	DCHT + CT	CT	5	②, ③, ⑧, and ⑩
24	Xu T2017	34	33	18/16	19/14	44.63 ± 7.81	45.37 ± 8.24	NR	NR	DCHT + LC	LC	5	③, ⑤, and ⑩

(Continued on following page)

10.3389/fphar.2024.1497072

10.3389/fphar.2024.1497072

TABLE 2 (*Continued*) Study characteristics.

No.	Study ID	Sample size		Gender (male/female)		Age [mean (SD)]		Onset time (days)		Intervention		Duration (days)	Outcomes
		T	C	T	C	T	C	T	C	T	C		
25	Yang DD2016	41	41	26/15	27/14	53.18 ± 5.32	52.34 ± 5.36	NR	NR	DCHT + CT	CT	14	②, ③, ④, and ⑩
26	Yu XJ2009	36	36	39/33		NR	NR	NR	NR	DCHT + CT	CT	20	①, ②, ③, and ④
27	Zhang JY2003	30	20	11/19	8/12	21~65	19~67	NR	NR	DCHT + CT	CT	5	⑥
28	Zhang N2018	45	45	21/24	22/23	71.32 ± 11.20	74.70 ± 13.90	NR	NR	DCHT + CT	CT	14	①, ⑥, and ⑨
29	Zhou H2019	20	20	10/10	11/9	54.17 ± 13.02	53.45 ± 13.19	NR	NR	DCHT + CT	CT	14	① and ⑥
30	Zhou MJ2020	38	38	23/15	22/16	41.60 ± 5.00	39.70 ± 5.10	NR	NR	DCHT + CT	CT	30	①, ②, ③, and ⑧
31	Zhu WB2017	50	50	27/23	26/24	76.50 ± 1.50	75.50 ± 2.50	NR	NR	DCHT	CT	14	⑩
32	Zhuang LL2021	40	40	18/22	15/25	43.57 ± 10.89	41.50 ± 8.65	NR	NR	DCHT + CT	CT	14	⑧ and ⑩
33	Zuo YZ2021	72	72	35/37	36/36	60.83 ± 60.83	59.83 ± 17.17	0.26 ± 0.12	0.28 ± 0.09	DCHT + CT	CT	7	⑥

Note: T, treatment group; C, control group; NR, not reported; CT, conventional treatment; DCHT, Dachaihu tang; LC, laparoscopic cholecystectomy; ① clinical efficacy; ② time for resolution of abdominal pain; ③ time for resolution of fever; ④ time for white blood cell counts to normalize; ⑤ length of hospital stay; ⑥ levels of alanine aminotransferase (ALT); ⑦ levels of aspartate aminotransferase (AST); ⑧ neutrophil percentage (NEUT%); ⑨ levels of tumor necrosis factor-α (TNF-α); ⑩ incidence of adverse events.[2]

2.1 Eligibility criteria

(1) Participants: Individuals aged 18 years or older who met the diagnostic criteria for AC, as outlined in the Tokyo Guidelines (2018) (Kimura et al., 2007), including ① obvious right upper-abdominal pain with tenderness or a positive Murphy sign; ② fever, elevated C-reactive protein, or elevated white blood cell count; and ③ imaging examination suggested acute cholecystitis. The diagnosis of acute cholecystitis could be confirmed if any one of the criteria in ①, ②, and ③ was met. Exclusion criteria encompassed patients with severe cardiovascular, hepatic, or renal insufficiency; malignant tumors or significant organic lesions; a history of severe neurological dysfunction or mental illness; and pregnant or lactating women, or those allergic to Dachaihu decoction.

(2) Interventions: The treatment group received Dachaihu decoction alone/or in combination with the conventional treatment (CT)/laparoscopic cholecystectomy (LC). The composition of Dachaihu decoction includes *B. chinense* DC. [Apiaceae; *B. radix]*, *S. baicalensis* Georgi [Lamiaceae; *S. radix*], *C. aurantium* L. [Rutaceae; *C. aurantii fructus immaturus*], *P. ternata* (Thunb.) Makino [Araceae; *P. rhizoma*], *R. officinale* Baill. [Polygonaceae; *R. radix et rhizoma*], *P. lactiflora* Pall. [Paeoniaceae; *P. radix alba*], *Z. officinale* Roscoe [Zingiberaceae; *Z. rhizoma*], and *Z. jujuba* Mill. [Rhamnaceae; *Z. jujubae fructus]*. All botanical drugs were selected and reported according to the guidelines of the "Consortium for Phytochemical Characterization of Medicinal Plants (ConPhyMP)" (Heinrich et al., 2022; Heinrich et al., 2020). Moreover, in accordance with the modification principles of TCM, there were no restrictions on the dosage (grams), slight adjustments, formulation, or the route of administration for this decoction. Information on the botanical drugs, standard dosage (grams), and decoction preparation method of Dachaihu decoction is given in Table 1 and Supplementary Material S1.

(3) Comparisons: The control group was treated with CT, including antibiotics (β-lactams, 4-quinolones, and nitroimidazoles), along with antispasmodic, hepatoprotective, and choleretic drugs. Surgical intervention (LC), specifically laparoscopic cholecystectomy, was carried out when indicated.

(4) Outcomes: ① Clinical efficacy was assessed using criteria adapted from the Guiding Principles for Clinical Research of New Chinese Medicines (Ministry of Health of the PRC, 2002): cured—significant improvement in symptoms and signs, evidence point reduction ≥95%; obvious efficacy—notable improvement in symptoms and signs, evidence point reduction ≥70% but <95%; efficacy—some improvement in symptoms and signs, evidence point reduction ≥30% but <70%; inefficacy—no significant improvement in symptoms and signs, evidence point reduction <30%; calculated using the nimodipine method—efficacy index (%) = [(pre-treatment points - post-treatment points)/pre-treatment points × 100%]. ② Time for resolution of abdominal pain. ③ Time for resolution of fever. ④ Time for white blood cell counts to

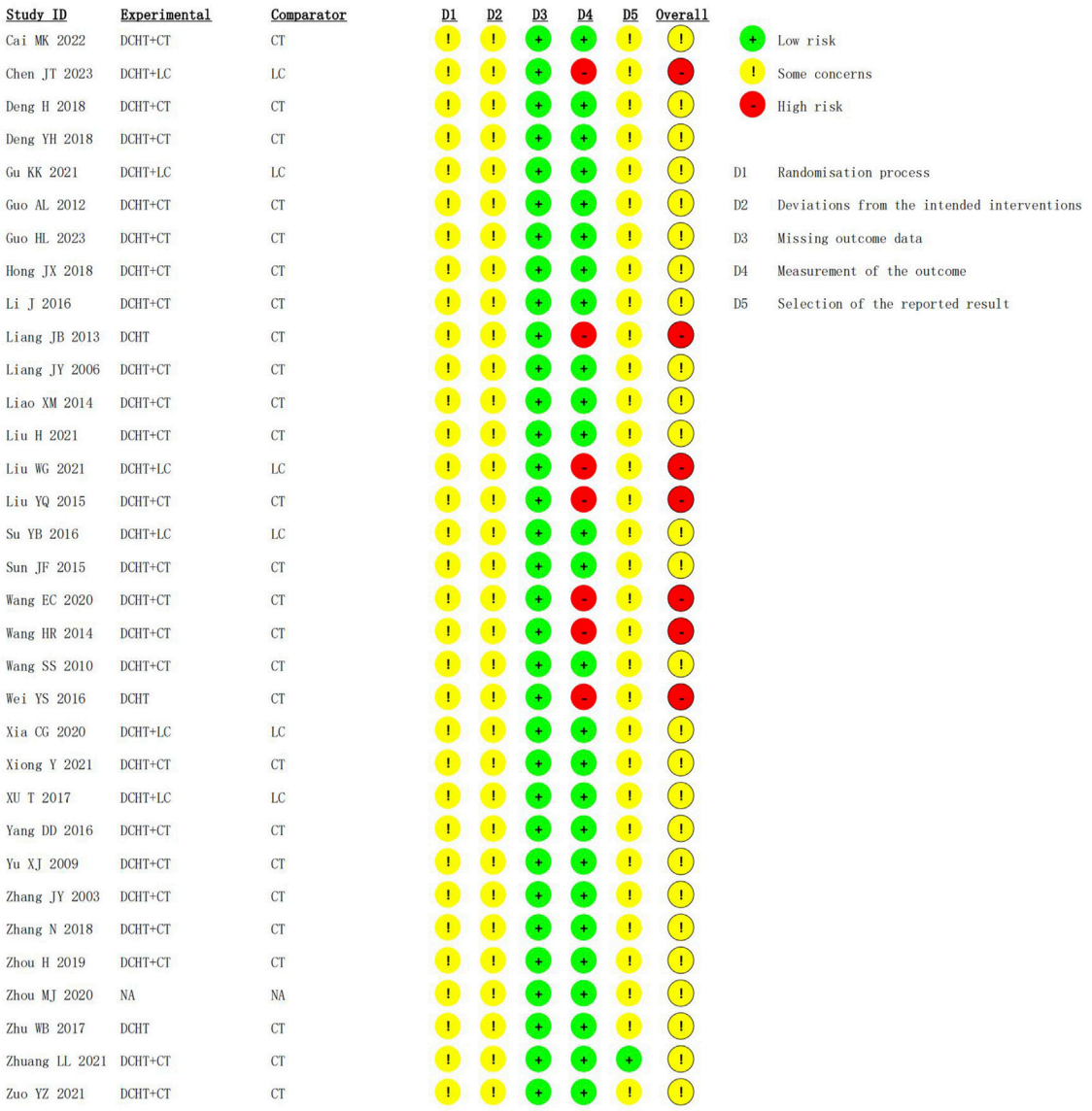


FIGURE 2
Risk of bias plot of included studies.

normalize. ⑤ Length of hospital stay. ⑥ Levels of alanine aminotransferase (ALT). ⑦ Levels of aspartate aminotransferase (AST). ⑧ Neutrophil percentage (NEUT %). ⑨ Levels of tumor necrosis factor-α (TNF-α). ⑩ Incidence of adverse events. Primary outcomes included ⑤and⑩, and secondary outcomes included ①, ②, ③, ④, ⑥, ⑦, ⑧, and ⑨.

(5) Study design: All randomized controlled trials (RCTs).

2.2 Literature search

Two researchers (Xin-xin Liu and You-zhu Su) systematically searched eight databases, i.e., four English databases (Web of Science, Cochrane Database of Systematic Reviews, PubMed, and EMBASE) and four Chinese databases (CNKI, Wanfang, VIP, and SinoMed). Additionally, three clinical trial registration platforms (International Clinical Trials Registry Platform, ClinicalTrials.gov, and Chinese Clinical Trial Registry) were searched from their inception to 30 June 2024. The search terms included "acute cholecystitis" and "Dachaihu decoction." There were no language restrictions. The complete search strategy is given in Supplementary Material S2.

2.3 Research selection and data extraction

Two researchers (Xin-xin Liu and Ying-qi Ma) independently reviewed the literature, extracted data, and cross-checked the findings. Any disagreements were resolved by consulting a third reviewer (Jian-ping Liu). The initial

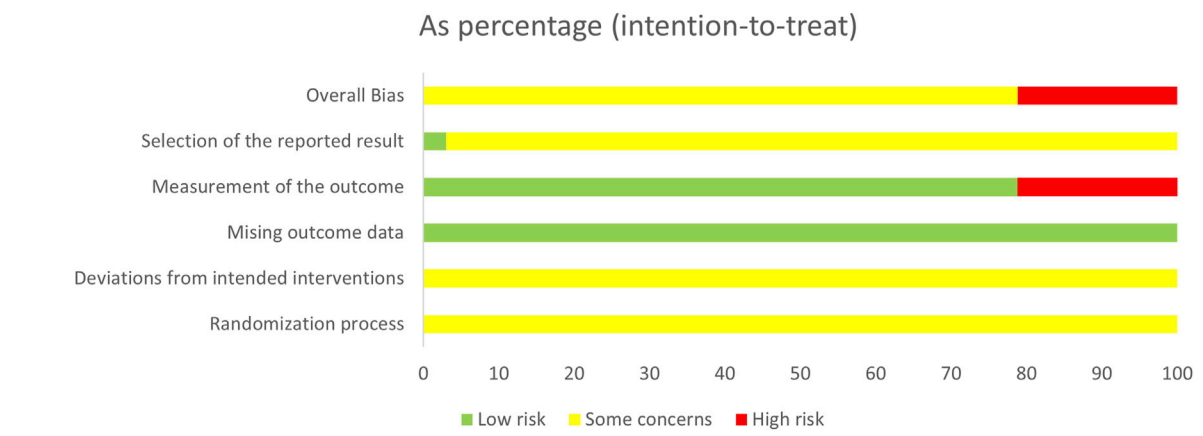


FIGURE 3
Summary of risk of bias in the included studies.

screening involved reviewing titles and abstracts to filter out irrelevant studies, followed by a full-text review to decide on final inclusion. The extracted data covered the first author, year of publication, sample size, gender and age of participants, symptom onset, intervention types, treatment duration, and outcomes. In this study, species classification and validation of the phytomedicines in Dachaihu decoction were performed using the ConPhyMP tool to meet drug classification standards.

2.4 Assessment of the risk of bias

Two researchers (Xin-xin Liu and Ling-yao Kong) independently evaluated the risk of bias in the included studies using the Cochrane's Risk of Bias 2.0 tools, and the results were cross-checked. Any disagreements were resolved through consultation with a third reviewer (Jian-ping Liu). The assessment criteria included random sequence generation, allocation concealment, blinding (of implementers, participants, and outcome evaluators), incomplete outcome data, selective reporting, and other potential bias sources. Risks were categorized as "low risk," "high risk," or "some concerns" based on this assessment.

2.5 Statistical analysis

A meta-analysis was conducted using Stata 17.0 software, with the results reported as 95% confidence intervals (95% CIs) and statistical significance defined as $p < 0.05$. (1) Heterogeneity across studies was assessed using the I^2 test. A fixed-effect model was used when heterogeneity was low ($p > 0.1$; $I^2 < 50\%$), while a random-effects model was applied for high heterogeneity ($p < 0.1$; $I^2 > 50\%$). (2) For a dichotomous variable, the effect size was calculated using relative risk (RR), and for continuous variables, mean difference (MD) was used. When studies used different units of measurement, standardized mean difference (SMD) was applied.

2.6 Subgroup and sensitivity analyses

Subgroup analyses were carried out according to the type of intervention to evaluate the consistency and reliability of the results. Sensitivity analyses were used to assess whether the results and heterogeneity changed when a single study was excluded.

2.7 Publication bias

Publication bias was assessed if the funnel plot showed asymmetry or if the Egger test indicated bias ($p < 0.05$). In such cases, the "trim-and-fill" method was used to estimate the adjusted combined effect size.

2.8 Assessment of certainty of evidence

The certainty of evidence for an outcome measure was evaluated using the Grading of Recommendations Assessment, Development, and Evaluation (GRADE) assessment system. Two researchers (Xin-xin Liu and Ling-yao Kong) independently evaluated GRADE. Any disagreements were resolved by consulting a third reviewer (Jian-ping Liu). This evaluation considers five factors: risk of bias, consistency of results, indirectness of evidence, imprecision, and potential publication bias. Based on these criteria, the evidence was classified as "high," "moderate," "low," or "very low" (Grade Working Group, 2017).

3 Results

3.1 Results of the literature search

A comprehensive computerized search retrieved 549 studies (121 studies in CNKI, 163 in VIP, 153 in Wanfang, 97 in SinoMed, 1 in PubMed, 1 in Embase, 0 in Web of Science, 13 in Cochrane Library, 0 in International Clinical Trials Registry Platform, 0 in ClinicalTrials.gov, and 0 in Chinese Clinical Trial

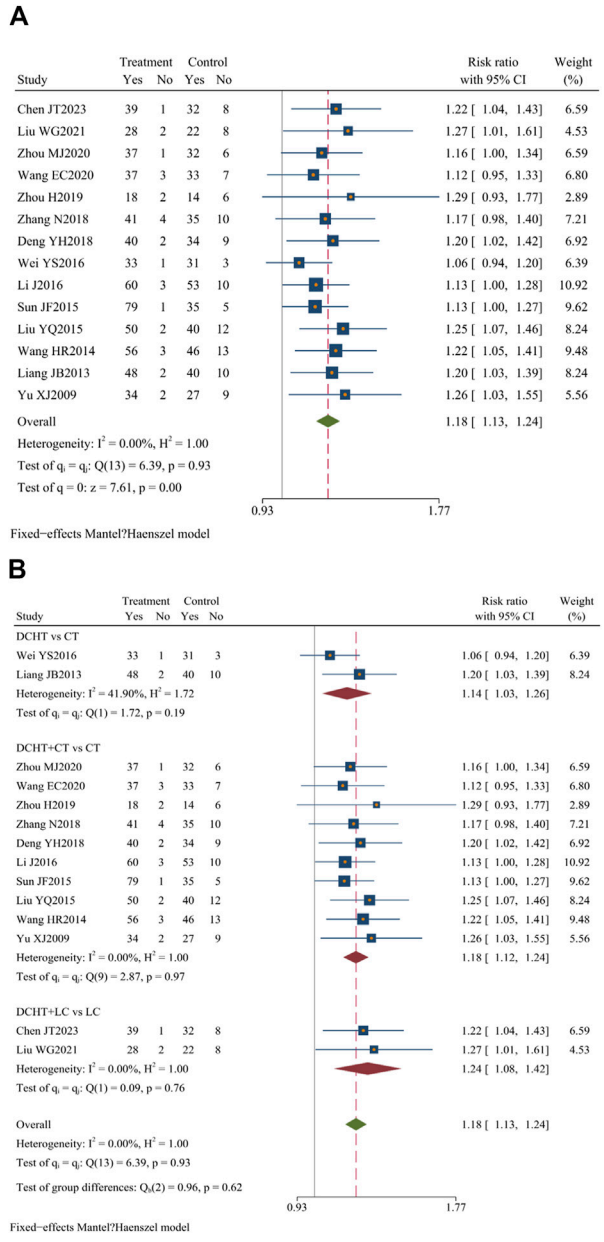


FIGURE 4
(A) Clinical efficacy, **(B)** Subgroup analysis of clinical efficacy. DCHT, Dachaihu tang; CT, Conventional treatment; LC, Laparoscopic cholecystectomy.

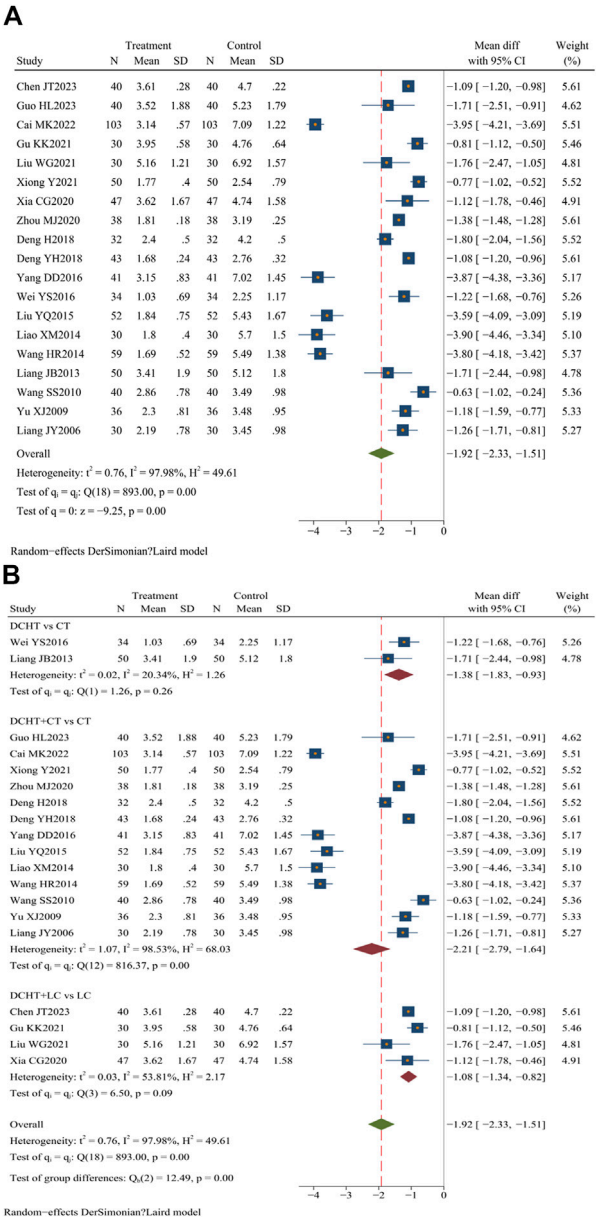


FIGURE 5
(A) Time for resolution of abdominal pain, **(B)** Subgroup analysis of time for resolution of abdominal pain. DCHT, Dachaihu tang; CT, Conventional treatment; LC, Laparoscopic cholecystectomy.

Registry). A total of 296 duplicate records were removed, and full texts of the remaining 253 studies were reviewed. Studies that did not meet the inclusion criteria were excluded. Ultimately, 33 RCTs (Zhou, 2020; Liu et al., 2021; Cai, 2022; Chen et al., 2023; Deng, 2018; Deng et al., 2018; Gu, 2021; Guo, 2012; Guo, 2023; Hong and Gao, 2018; Li, 2016; Liang and Deng, 2013; Liang et al., 2013; Liao, 2014; Liu, 2021; Liu, 2015; Su, 2016; Sun, 2005; Wang et al., 2020; Wang and Li, 2014; Wang, 2010; Wei, 2016; Xia, 2020; Xiong and Yi, 2021; Xu, 2017; Yang, 2016; Yu, 2009; Zhang et al., 2003; Zhang, 2018; Zhou, 2019; Zhu, 2017; Zhuang, 2021; Zuo, 2021) were included. The flow diagram of the selection process is shown in Figure 1.

3.2 Study characteristics

The selected studies, published between 2003 and 2023, accounted for 81.81% (27/33) of the studies conducted in the past decade. The 33 RCTs included 2,851 Chinese patients diagnosed with AC, comprising 1,404 male and 1,447 female individuals. Sample sizes ranged from 40 to 206 cases. Nineteen studies did not specify the duration of the onset of illness, and the intervention was Dachaihu decoction or a combination of conventional treatment/LC, with the treatment duration ranging from 5 to 30 days. Outcomes included time to the disappearance of clinical symptoms, inflammation levels, reports of adverse events,

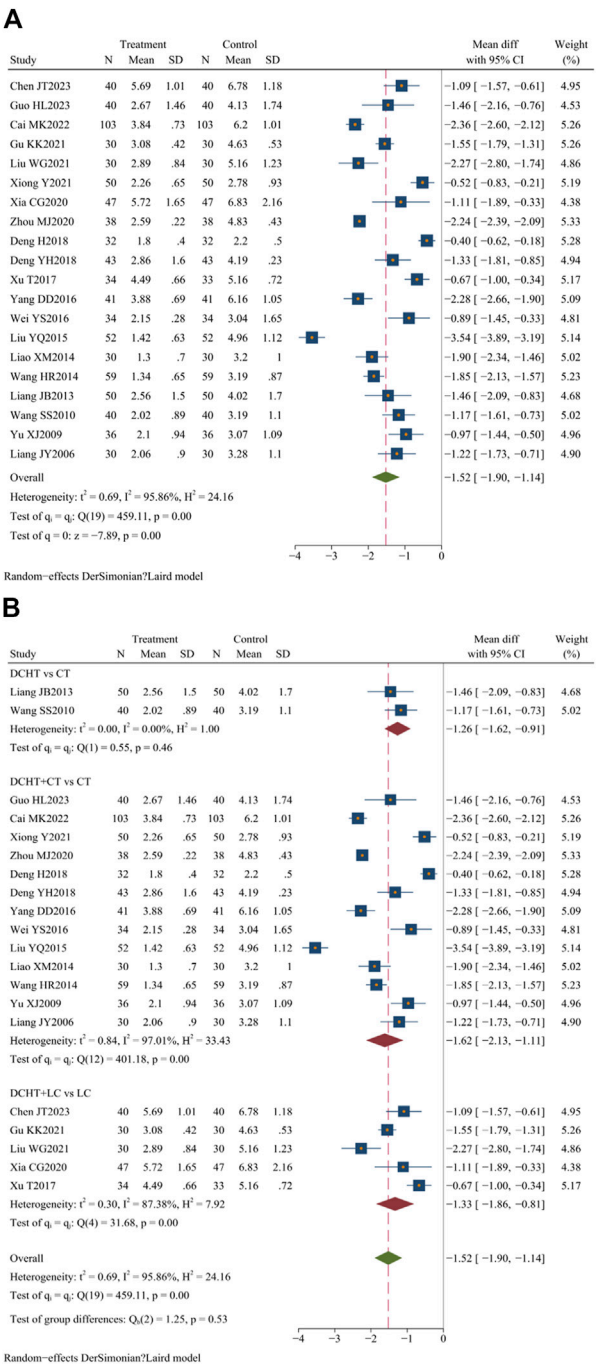


FIGURE 6
(A) Time for resolution of fever, **(B)** Subgroup analysis of time for resolution of fever. DCHT, Dachaihu tang; CT, Conventional treatment; LC, Laparoscopic cholecystectomy.

clinical efficacy, length of hospital stay, and liver function. Study characteristics are given in Table 2.

3.3 Risk of bias assessments

Among the 33 RCTs, 16 (Liu et al., 2021; Deng et al., 2018; Gu, 2021; Hong and Gao, 2018; Liao, 2014; Liu, 2021; Liu, 2015; Wang et al., 2020; Wang and Li, 2014; Xia, 2020; Xiong and Yi, 2021; Xu, 2017; Yang, 2016; Zhang, 2018; Zhu, 2017; Zhuang, 2021) used random number tables, 1 (Chen et al., 2023) utilized lotteries, and 1 (Zhou, 2020) adopted two-color ballots, while the remaining 15 merely mentioned "random." All studies were comparable at baseline; however, none provided details on the implementation of allocation concealment, making it unclear whether it was properly executed. As such, this aspect was rated as having "some concerns" regarding randomization. Furthermore, none of the studies reported blinding of participants or outcome assessors, leading to a rating of "some concerns" for potential deviation from the intended intervention. Despite these limitations, all included studies presented complete data, thus receiving a "low-risk" rating for data completeness. In terms of outcome assessment, 26 studies were rated as "low risk," whereas 7 (Liu et al., 2021; Li, 2016; Liang and Deng, 2013; Liu, 2015; Wang et al., 2020; Wang and Li, 2014; Wei, 2016) were considered "high risk" due to inappropriate measurement methods. Regarding selective reporting, only one study was rated as "low risk," while the others lacked registration program documentation, resulting in a "some concerns" rating due to potential selective reporting bias (Figures 2, 3).

3.4 Meta-analysis of the results

3.4.1 Clinical efficacy

Among the 33 included studies, 14 (Zhou, 2020; Liu et al., 2021; Chen et al., 2023; Deng et al., 2018; Li, 2016; Liang and Deng, 2013; Liu, 2015; Sun, 2005; Wang et al., 2020; Wang and Li, 2014; Wei, 2016; Yu, 2009; Zhang, 2018; Zhou, 2019) (n = 1,219) assessed clinical efficacy, revealing a statistically significant difference between the groups (RR = 1.18; 95% CI = 1.13 to 1.24; I^2 = 0.00%; Q (13) = 6.39; p = 0.00) (Figure 4A).

3.4.1.1 Subgroup analysis of clinical efficacy

Subgroup analysis revealed that, compared with the CT group, the Dachaihu decoction group showed an improvement in clinical efficacy (RR = 1.14; 95% CI = 1.03 to 1.26; I^2 = 41.90%). The combination of Dachaihu decoction and CT also showed notable improvements (RR = 1.18; 95% CI = 1.12 to 1.24; I^2 = 0.00%). Similarly, combining Dachaihu decoction with LC significantly enhanced clinical efficacy (RR = 1.24; 95% CI = 1.08 to 1.42; I^2 = 0.00%) Figure 4B.

3.4.2 Time for resolution of abdominal pain

Nineteen studies (Zhou, 2020; Liu et al., 2021; Cai, 2022; Chen et al., 2023; Deng, 2018; Deng et al., 2018; Gu, 2021; Guo, 2023; Liang and Deng, 2013; Liang et al., 2013; Liao, 2014; Liu, 2015; Wang and Li, 2014; Wang, 2010; Wei, 2016; Xia, 2020; Xiong and Yi, 2021; Yang, 2016; Yu, 2009) (n = 1,648) evaluated the time required for abdominal pain to disappear. The results showed that the treatment group significantly shortened the time for abdominal pain to subside compared to the control group (MD = −1.92 days; 95% CI = −2.33 to −1.51; I^2 = 97.98%; Q (18) = 893.00; p = 0.00) (Figure 5A).

3.4.2.1 Subgroup analysis

Subgroup analysis demonstrated that the Dachaihu decoction group significantly reduced the time for abdominal pain relief

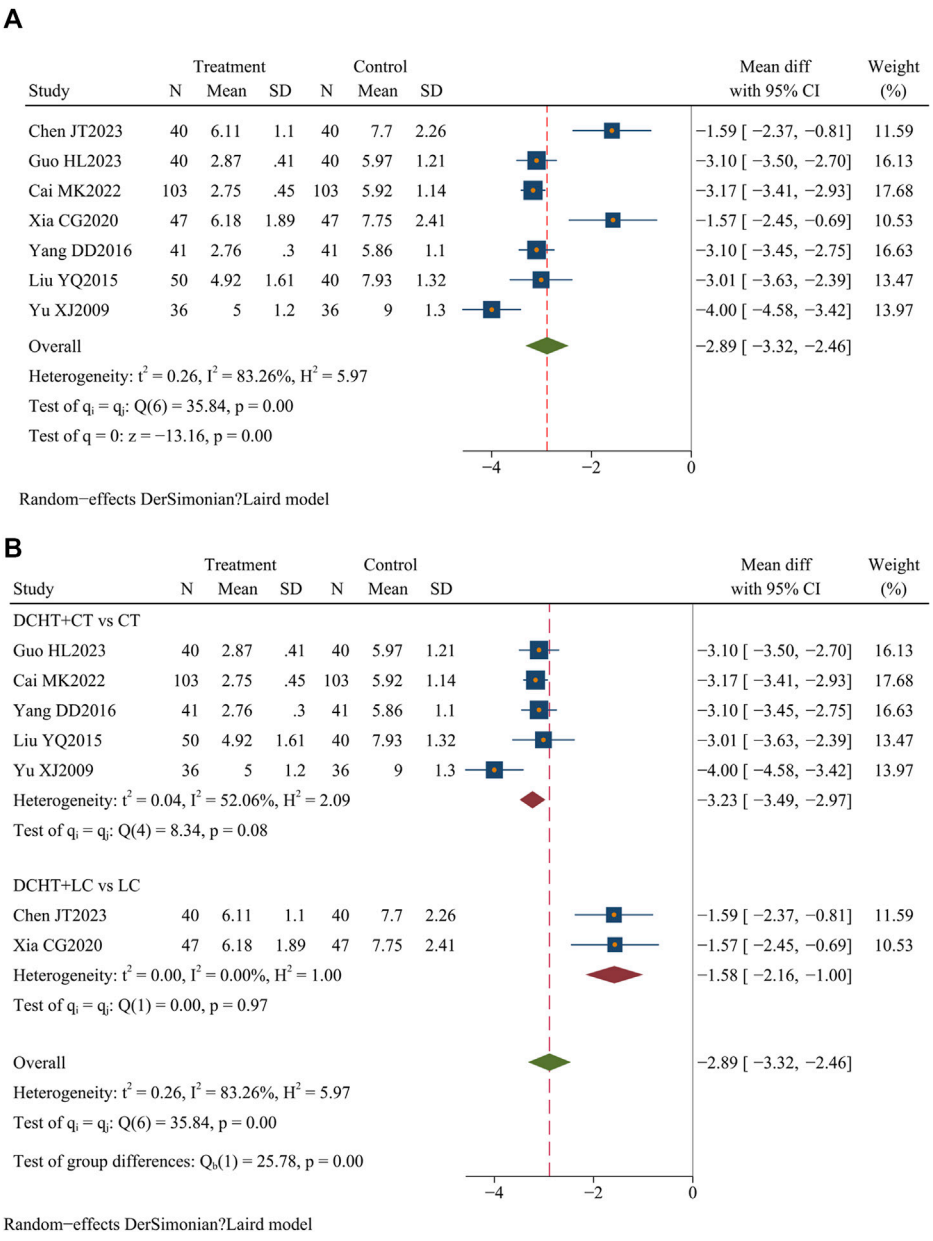


FIGURE 7
(A) Time for white blood cell counts to normalize, **(B)** Subgroup analysis of time for white blood cell counts to normalize. DCHT, Dachaihu tang; CT, Conventional treatment; LC, Laparoscopic cholecystectomy.

compared to the CT group (MD = −1.38 days; 95% CI = −1.83 to −0.93; I^2 = 20.34%). The Dachaihu decoction combined with CT also significantly reduced abdominal pain duration (MD = −2.21 days; 95% CI −2.79 to −1.64; I^2 = 98.53%). When combined with LC, the decoction further reduced the time for abdominal pain to disappear (MD = −1.08 days; 95% CI = −1.34 to −0.82; I^2 = 53.81%) (Figure 5B).

3.4.2.2 Sensitivity analysis

In the Dachaihu decoction combined with CT compared to the CT group, we further analyzed the reason for heterogeneity. Two studies (Zhou, 2020; Liao, 2014) were excluded because the time of treatment was >28 days, one (Deng, 2018) was excluded as a result of patients being ≥80 years old, two (Cai, 2022; Liu, 2015) were excluded because the onset time was >3 days, and two studies (Liu et al., 2021; Xu, 2017) were excluded because they did not mention the type and dosage of anti-infective drugs. The heterogeneity was reduced when the above studies were excluded (I^2 = 62%). There were still statistical differences ($p < 0.05$) (Supplementary Material S3).

3.4.3 Time for resolution of fever

Twenty studies (Zhou, 2020; Liu et al., 2021; Cai, 2022; Chen et al., 2023; Deng, 2018; Deng et al., 2018; Gu, 2021; Guo, 2023; Liang and Deng, 2013; Liang et al., 2013; Liao, 2014; Liu, 2015; Wang and Li, 2014; Wang, 2010; Wei, 2016; Xia, 2020; Xiong and Yi, 2021;

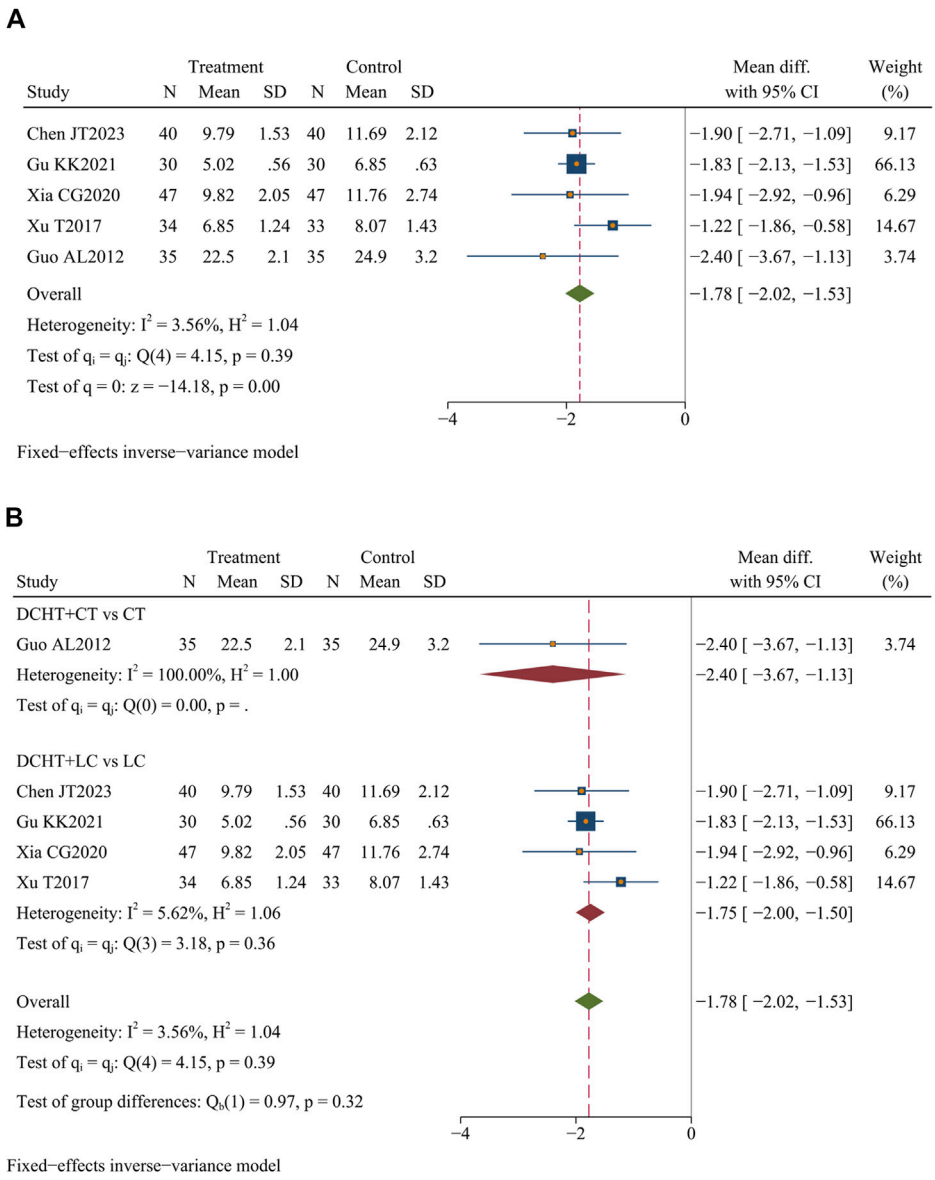


FIGURE 8
(A) Length of hospital stay, **(B)** Subgroup analysis of length of hospital stay. DCHT, Dachaihu tang; CT, Conventional treatment; LC, Laparoscopic cholecystectomy.

Xu, 2017; Yang, 2016; Yu, 2009) (n = 1717) assessed the time for fever resolution. Compared with the control group, the Dachaihu decoction group appeared to significantly shorten the duration of fever in patients (MD = −1.52 days; 95% CI = −1.90 to −1.14; I^2 = 95.86%; Q (19) = 459.11; p = 0.00) (Figure 6A).

3.4.3.1 Subgroup analysis

The subgroup analysis showed that compared with the CT group, the Dachaihu decoction group significantly reduced fever duration (MD = −1.26 days; 95% CI = −1.62 to −0.91; I^2 = 0.00%). The combination of Dachaihu decoction and CT also significantly reduced fever duration (MD = −1.62 days; 95% CI = −2.13 to −1.11; I^2 = 97.01%). When combined with LC, the duration of fever was significantly reduced (MD = −1.33 days; 95% CI = −1.86 to −0.81; I^2 = 87.38%) (Figure 6B).

3.4.3.2 Sensitivity analysis

Further analysis of heterogeneity was conducted. In the Dachaihu decoction combined with the CT group versus the CT group, two studies (Zhou, 2020; Guo, 2012) were excluded due to treatment durations exceeding 28 days, one study (Deng, 2018) was excluded due to the inclusion of patients aged ≥80 years, and three studies (Cai, 2022; Liu, 2015; Xiong and Yi, 2021) were excluded because the onset time exceeded 3 days, resulting in reduced heterogeneity (I^2 = 79.00%). In the Dachaihu decoction combined with the LC group versus the LC group, two studies (Liu et al., 2021; Xu, 2017) were excluded because they did not mention the type and dosage of anti-infective drugs, significantly reducing heterogeneity (I^2 = 40%). Statistical differences remained (p < 0.05) (Supplementary Material S3).

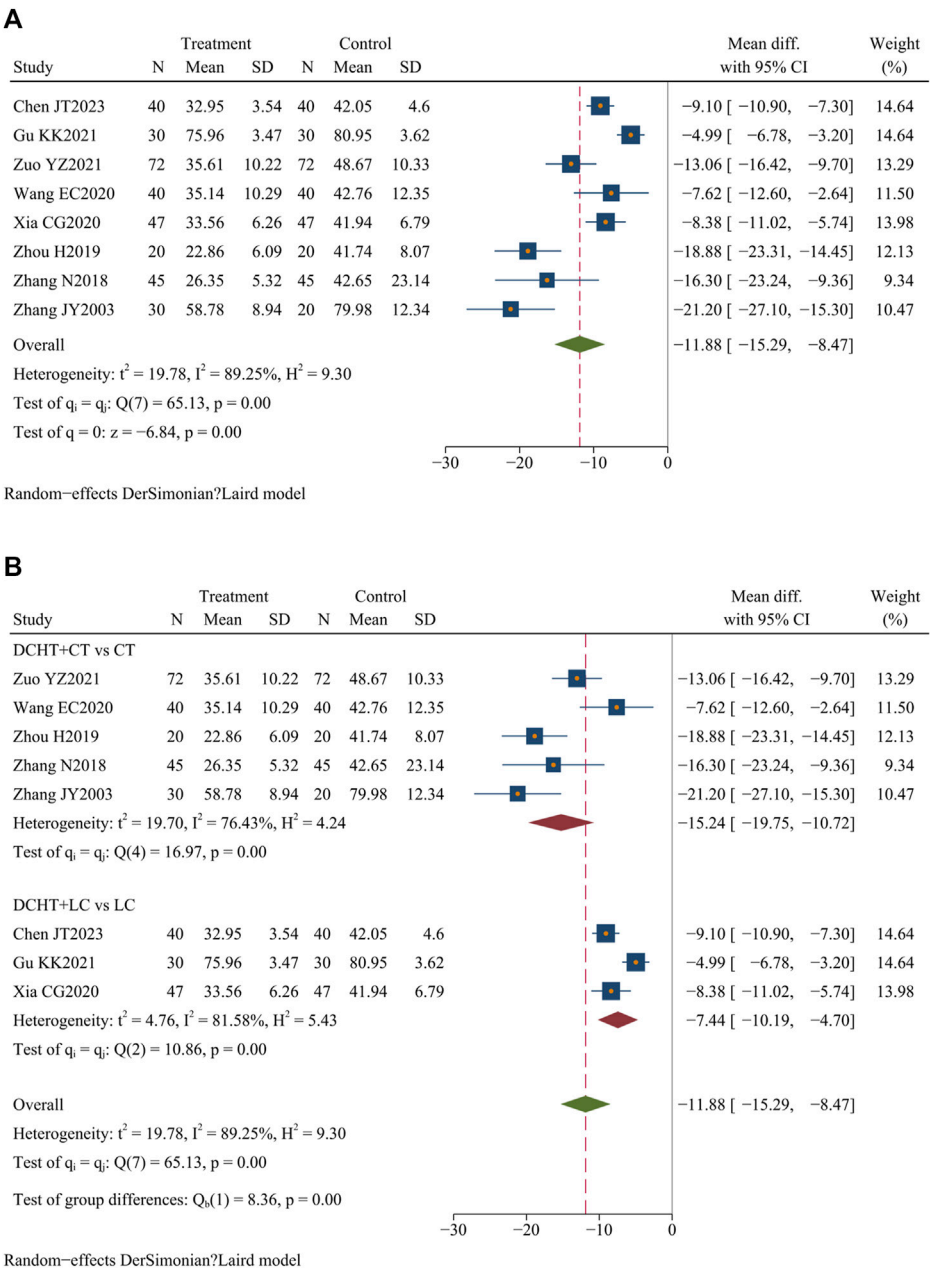


FIGURE 9
(A) ALT levels, **(B)** Subgroup analysis of ALT levels. DCHT, Dachaihu tang; CT, Conventional treatment; LC, Laparoscopic cholecystectomy.

3.4.4 Time for white blood cell counts to normalize

Of the 33 included studies, 7 (Cai, 2022; Chen et al., 2023; Guo, 2023; Liu, 2015; Xia, 2020; Yang, 2016; Yu, 2009) (n = 704) assessed the time required for white blood cell counts to normalize. The results showed that the treatment group significantly reduced the time compared to the control group (MD = −2.89 days; 95% CI = −3.32 to −2.46; I^2 = 83.26%; Q (6) = 35.84; p = 0.00) (Figure 7A).

3.4.4.1 Subgroup analysis

The subgroup analysis revealed that compared with the CT group, the Dachaihu decoction combined with CT significantly reduced the time required for white blood cell counts to normalize (MD = −3.23 days; 95% CI = −3.49 to −2.97; I^2 = 52.06%). Compared with the LC group, the combination of Dachaihu decoction and LC also significantly shortened this time (MD = −1.58 days; 95% CI = −2.16 to −1.00; I^2 = 0.00%) (Figure 7B).

3.4.4.2 Sensitivity analysis

In the Dachaihu decoction combined with the CT group versus the CT group, one study (Yu, 2009) was excluded due to the treatment duration exceeding 14 days and publication before 2010, significantly reducing heterogeneity (I^2 = 0.00%). The results remained statistically significant (p < 0.05) (Supplementary Material S3).

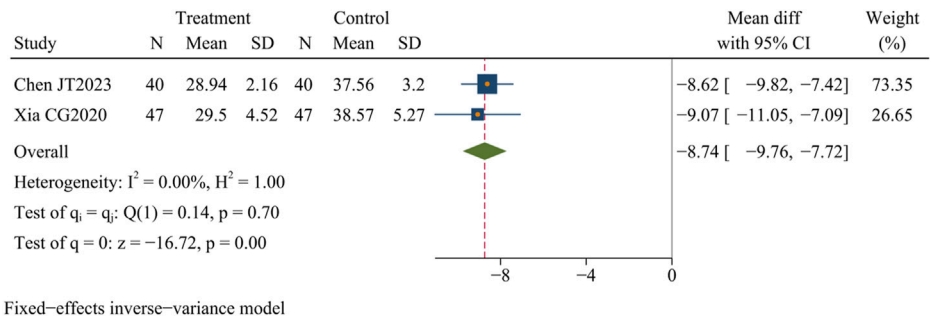


FIGURE 10
AST levels.

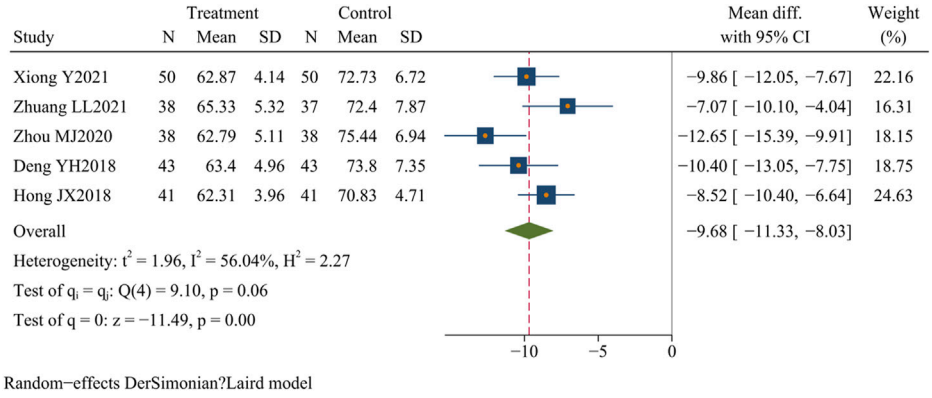


FIGURE 11
Neutrophil percentage.

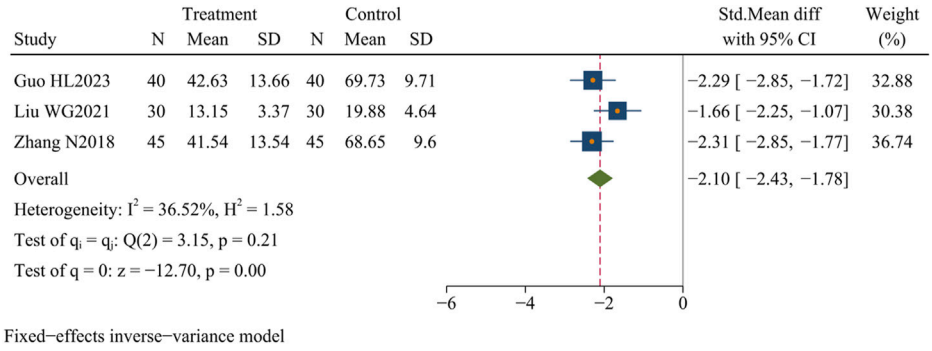


FIGURE 12
TNF-α levels.

3.4.5 Length of hospital stay

Five studies (Chen et al., 2023; Gu, 2021; Guo, 2012; Xia, 2020; Xu, 2017) (n = 371) assessed the length of stay. The results demonstrated that the Dachaihu decoction significantly shortened the length of hospital stay compared to the control group (MD = −1.78 days; 95% CI = −2.02 to −1.53; I^2 = 3.56%; Q (4) = 4.15; p = 0.00) (Figure 8A).

3.4.5.1 Subgroup analysis

Subgroup analysis revealed that compared with the LC, the combination of Dachaihu decoction and LC significantly shortened

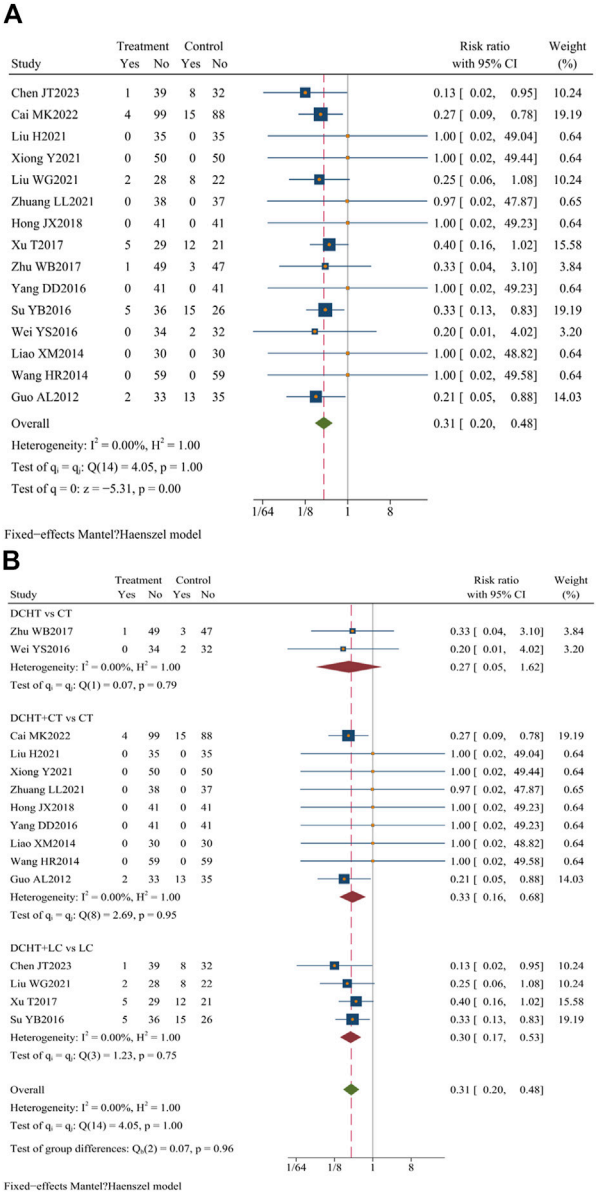


FIGURE 13
(A) Incidence of adverse events, **(B)** Subgroup analysis of incidence of adverse events. DCHT, Dachaihu tang; CT, Conventional treatment; LC, Laparoscopic cholecystectomy.

the length of hospital stay (MD = −1.75 days; 95% CI = −2.00 to −1.50; I^2 = 5.62%) (Figure 8B).

3.4.6 ALT levels

Eight studies (Chen et al., 2023; Gu, 2021; Wang et al., 2020; Xia, 2020; Zhang et al., 2003; Zhang, 2018; Zhou, 2019; Zuo, 2021) (n = 638) assessed ALT levels. The results indicated that Dachaihu decoction significantly lowered ALT levels compared to the control group (MD = −11.88 U/L; 95% CI = −15.29 to −8.47; I^2 = 89.25%; Q (7) = 65.13; p = 0.00) (Figure 9A).

3.4.6.1 Subgroup analysis

The subgroup analysis indicated that the Dachaihu decoction combined with the CT group significantly reduced ALT levels compared with the CT group alone (MD = −15.24 U/L; 95% CI = −19.75 to −10.72; I^2 = 76.43%). Dachaihu decoction combined with LC also significantly lowered ALT levels (MD = −7.44 U/L; 95% CI = −10.19 to −4.70; I^2 = 81.58%) (Figure 9B).

3.4.6.2 Sensitivity analysis

In the Dachaihu decoction combined with the CT group versus the CT group, heterogeneity was significantly reduced after excluding studies for specific reasons: one study (Wang et al., 2020) due to the mean age of included patients being <40 years, one (Zuo, 2021) for differing onset times, and one (Gu, 2021) because the included patients were elderly. Heterogeneity was significantly reduced (I^2 = 0.00%), and the results remained statistically significant (p < 0.05) (Supplementary Material S3).

3.4.7 AST levels

Two studies (Chen et al., 2023; Xia, 2020) (n = 174) evaluated the AST levels in patients with AC, and the findings showed that Dachaihu decoction significantly decreased AST levels compared to the control group (MD = −8.74 U/L; 95% CI = −9.76 to −7.72; I^2 = 0.00%; Q (1) = 0.14; p = 0.00) (Figure 10).

3.4.8 Neutrophil percentage

Five studies (Deng et al., 2018; Hong and Gao, 2018; Xiong and Yi, 2021; Zhou, 2020; Zhuang, 2021) (n = 419) assessed neutrophil levels. The results demonstrated that Dachaihu decoction significantly reduced neutrophil levels compared with the control group (MD = −9.68; 95% CI = −11.33 to −8.03; I^2 = 56.04%; Q (4) = 9.10; p = 0.00) (Figure 11).

3.4.9 TNF-α levels

Three studies (Liu et al., 2021; Guo, 2023; Zhang, 2018) (n = 230) assessed the TNF-α levels. The results showed that Dachaihu decoction significantly lowered TNF-α levels compared to the control group (SMD = −2.10 pg/L; 95% CI = −2.43 to −1.78; I^2 = 36.52%; Q (2) = 3.15; p = 0.00) (Figure 12).

3.4.10 Incidence of adverse events

Fifteen studies (Liu et al., 2021; Cai, 2022; Chen et al., 2023; Guo, 2012; Hong and Gao, 2018; Liao, 2014; Liu, 2021; Su, 2016; Wang and Li, 2014; Wei, 2016; Xiong and Yi, 2021; Xu, 2017; Yang, 2016; Zhu, 2017; Zhuang, 2021) (n = 1,333) evaluated the incidence of adverse events. Cai (2022) and Guo (2012) indicated that the combination of Dachaihu decoction with CT was more effective in minimizing mild adverse reactions, such as diarrhea, nausea, insomnia, and palpitations, compared to using conventional treatment alone. Additionally, four studies (Liu et al., 2021; Chen et al., 2023; Su, 2016; Xu, 2017) observed that Dachaihu decoction combined with LC significantly reduced the occurrence of incision infection, biliary fistula, and bile duct injury. Furthermore, two studies (Wei, 2016; Zhu, 2017) found a lower incidence of mild adverse events, such as gastrointestinal discomfort, dizziness, and

TABLE 3 Incidence of adverse events.

Comparison	Study ID	Adverse event category	Experimental group	Control group
DCHT + CT VS CT	Cai MK2022	Diarrhea	0 (0%)	2 (2%)
		Nausea	2 (2%)	6 (6%)
		Insomnia	1 (1%)	4 (4%)
		Palpitations	1 (1%)	3 (3%)
	Liu H2021	None	0 (0%)	0 (0%)
	Xiong Y2021	None	0 (0%)	0 (0%)
	Zhuang LL2021	None	0 (0%)	0 (0%)
	Hong JX2018	None	0 (0%)	0 (0%)
	Yang DD2016	None	0 (0%)	0 (0%)
	Liao XM2014	None	0 (0%)	0 (0%)
	Wang HR2014	None	0 (0%)	0 (0%)
	Guo AL2012	Gastrointestinal symptom	2 (2%)	13 (14%)
DCHT + LC VS LC	Chen JT2023	Incision/abdominal infection	1 (3%)	4 (10%)
		Biliary fistula	0 (0%)	2 (5%)
		Bile duct injury	0 (0%)	2 (5%)
	Liu WG2021	Liver abscess	1 (3%)	2 (6%)
		Incision infection	1 (3%)	4 (12%)
		Peritoneal abscess	0 (0%)	2 (6%)
	Xu T2017	Incision bleeding/infection and biliary fistula	5 (14%)	12 (36%)
	Su YB2016	Incision bleeding/infection and biliary fistula	5 (12%)	15 (36%)
DCHT VS CT	Zhu WB2017	Nausea	1 (2%)	3 (6%)
	Wei YS2016	Dizziness and gastrointestinal symptom	0 (0%)	1 (3%)
		Skin itching and redness	0 (0%)	1 (3%)

skin itching, in the Dachaihu decoction group than in routine treatment. In summary, Dachaihu decoction demonstrated better safety and tolerability in the treatment of acute cholecystitis, with potential benefits in reducing postoperative complications and alleviating gastrointestinal discomfort (RR = 0.31; 95% CI = 0.20 to 0.48; I^2 = 0.00%; Q (14) = 4.05; p = 0.00) (Figure 13A; Table 3).

3.4.10.1 Subgroup analysis

The subgroup analysis revealed that the Dachaihu decoction group significantly lowered the incidence of adverse events (RR = 0.27; 95% CI = 0.05 to 1.62; I^2 = 0.00%). Compared with the CT group, the Dachaihu decoction combined with CT markedly decreased the incidence of adverse events (RR = 0.33; 95% CI = 0.16 to 0.68; I^2 = 0.00%), including gastrointestinal symptoms, insomnia, and palpitations. Compared with the LC group, the Dachaihu decoction combined with LC significantly reduced the incidence of adverse events (surgical incision bleeding/infection, biliary fistula, bile duct injury, abdominal abscess, and fall) (RR = 0.30; 95% CI = 0.17 to 0.53; I^2 = 0.00%). Seven studies (Hong and Gao, 2018; Liao, 2014; Liu, 2021; Wang and Li, 2014; Xiong and Yi, 2021; Yang, 2016; Zhuang, 2021) reported no adverse events (Figure 13B).

3.5 Assessment of publication bias

As funnel plot analysis requires at least 10 original studies, this method was used to evaluate clinical efficacy, time required for the resolution of abdominal pain and fever, and the incidence of adverse events. Subsequent Egger's test results indicated a significant difference in clinical efficacy ($p < 0.05$), suggesting publication bias. To address this, the "trim-and-fill" method was used to estimate combined effect sizes adjusted for publication bias. The adjusted pooled effect size remained significant ($p < 0.01$), suggesting that publication bias did not influence the assessment of clinical efficacy (Figures 14A–E).

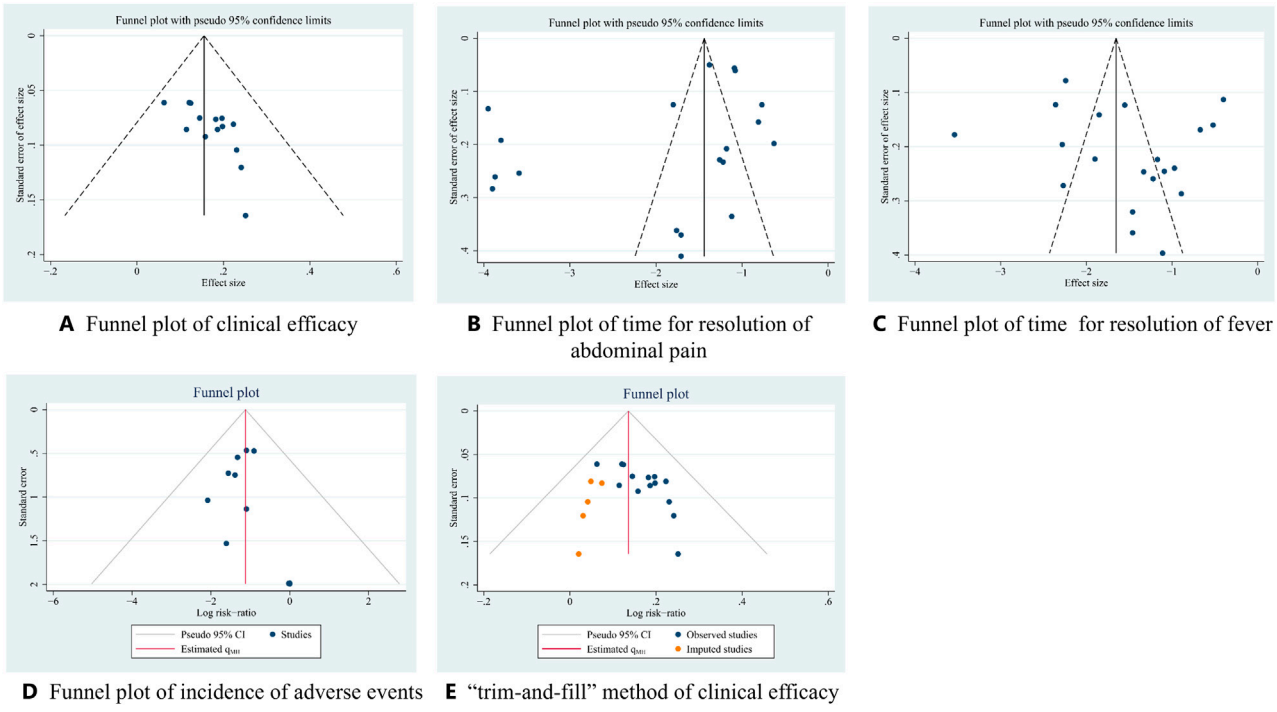


FIGURE 14
Funnel plot and "trim-and-fill" method.

3.6 Certainty of evidence

Certainty of evidence and the reasons for the upgrade and downgrade are presented in Table 4. The evidence for all outcomes was assessed as moderate to low certainty due to the risk of bias, imprecision, inconsistency, or indirectness.

4 Discussion

4.1 Main findings

A total of 33 eligible RCTs involving 2,851 participants evaluated the use of Dachaihu decoction alone or in combination with conventional treatment/LC for treating AC. Dachaihu decoction demonstrated potential benefits in improving clinical symptoms, shortening hospital stays, protecting liver function, reducing inflammatory responses, and decreasing adverse events (adverse drug reactions and postoperative complications). Subgroup analyses revealed that Dachaihu decoction alone may alleviate abdominal pain and fever, with no significant adverse events reported. When combined with CT or LC, it may further improve liver function, reduce inflammation, and enhance the symptoms of fever and abdominal pain in AC. Additionally, it may shorten the length of hospital stay, increase clinical efficacy, and decrease adverse event rates, indicating potential for clinical use. The sensitivity analysis showed that excluding different studies did not significantly alter the primary outcome's direction or significance, suggesting consistent findings. Despite variations in study quality, the results remained applicable and interpretable. Due to an insufficient description of the randomization process and blinding design, these studies demonstrated a high risk of bias. No publication bias was observed, except in clinical efficacy. The evidence was assessed as having moderate-to-low certainty.

Classical TCM formulas (Dachaihu decoction) have distinct components and therapeutic properties. According to evidence-based TCM principles, clinicians can slightly adjust the grammage and composition of botanical drugs of Dachaihu decoction to meet individual patient needs. Multiple studies have shown that modifying Dachaihu decoction can improve symptom management through synergistic and complementary effects (Cheang et al., 2024; Dai et al., 2016; Li et al., 2014). The inclusion of multiple RCTs showed significant improvements in efficacy by customizing Dachaihu decoction's grammage of certain botanical drugs to target the primary symptoms of diverse patients, underscoring its potential as an extension of the therapeutic system.

In the United States, approximately 20 million people experience AC annually, leading to healthcare costs exceeding $6.3 billion and imposing a substantial economic burden (Anderloni and Fugazza, 2022). A study reported that perioperative AC requires prolonged antibacterial treatment, which significantly increases hospitalization medical expenses and contributes to antibiotic resistance (Murata et al., 2013). The association of surgical infection is put forward for the quiet line in low-risk patients with laparoscopic cholecystectomy, not recommended for the routine use of perioperative antibiotics (Colling et al., 2022). Another study found that the complication rate associated with antibiotic therapy in elderly patients with AC was approximately 33% (Kivivuori et al., 2023). Our study found that the treatment of this disease with Dachaihu decoction might shorten the average

TABLE 4 Certainty of evidence.

Quality assessment							No of patients		Effect		Quality	Importance
No. of studies	Design	Risk of bias	Inconsistency	Indirectness	Imprecision	Other considerations	Dachaihu decoction	Control	Relative (95% CI)	Absolute		
Clinical efficacy												
14	Randomized trials	Serious[a]	No serious inconsistency	No serious indirectness	No serious imprecision	Reporting bias[b]	600/629 (95.4%)	474/590 (80.3%) 0%	RR 1.18 (1.13–1.24)	145 more per 1,000 (from 104 more to 193 more)	⊕⊕◯◯ LOW	CRITICAL
Time for resolution of abdominal pain (better indicated by lower values)												
19	Randomized trials	Serious[a]	Serious[c]	No serious indirectness	No serious imprecision	None	825	823	-	MD 1.92 lower (2.33–1.51 lower)	⊕⊕◯◯ LOW	IMPORTANT
Time for resolution of fever (better indicated by lower values)												
20	Randomized trials	Serious[a]	Serious[c]	No serious indirectness	No serious imprecision	None	859	858	-	MD 1.52 lower (1.90–1.14 lower)	⊕⊕◯◯ LOW	IMPORTANT
Time for white blood cell counts to normalize (better indicated by lower values)												
7	Randomized trials	Serious[a]	Serious[c]	No serious indirectness	No serious imprecision	None	357	347	-	MD 2.89 lower (3.32–2.46 lower)	⊕⊕◯◯ LOW	IMPORTANT
Length of hospital stay (better indicated by lower values)												
5	Randomized trials	Serious[a]	No serious inconsistency	No serious indirectness	Serious[d]	None	186	185	-	MD 1.78 lower (2.02–1.53 lower)	⊕⊕◯◯ LOW	CRITICAL
ALT levels (better indicated by lower values)												
8	Randomized trials	Serious[a]	Serious[c]	No serious indirectness	No serious imprecision	None	324	314	-	MD 11.88 lower (15.29–8.47 lower)	⊕⊕◯◯ LOW	IMPORTANT
AST levels (better indicated by lower values)												
2	Randomized trials	Serious[a]	No serious inconsistency	No serious indirectness	Serious[d]	None	87	87	-	MD 8.74 lower (9.76–7.72 lower)	⊕⊕◯◯ LOW	IMPORTANT
NEUT% (better indicated by lower values)												
5	Randomized trials	Serious[a]	Serious[c]	No serious indirectness	No serious imprecision	None	210	209	-	MD 9.68 lower (11.33–8.03 lower)	⊕⊕◯◯ LOW	IMPORTANT

(Continued on following page)

10.3389/fphar.2024.1497072

TABLE 4 (*Continued*) Certainty of evidence.

Quality assessment							No of patients		Effect		Quality	Importance
No. of studies	Design	Risk of bias	Inconsistency	Indirectness	Imprecision	Other considerations	Dachaihu decoction	Control	Relative (95% CI)	Absolute		
TNF-α levels (better indicated by lower values)												
3	Randomized trials	Serious[a]	No serious inconsistency	No serious indirectness	Serious[d]	None	115	115	-	SMD 2.10 lower (2.43–1.78 lower)	⊕⊕◯◯ LOW	IMPORTANT
Incidence of adverse events												
15	Randomized trials	Serious[a]	No serious inconsistency	No serious indirectness	No serious imprecision	None	20/661 (3%)	76/672 (11.3%)	RR 0.31 (0.20–0.48)	78 fewer per 1,000 (from 59 fewer to 90 fewer)	⊕⊕⊕◯ MODERATE	CRITICAL
								0%		-		

Note:
[a]Have not implemented allocation concealment and blinding methods.
[b]There is publication bias in this outcome.
[c]High heterogeneity and little overlapping confidence intervals.
[d]Sample size < 400.

length of hospital stay by nearly 2 days. This potential shortened the duration of symptoms but also reduced the nation's health expenditure and the patients' individual economic burden.

AC, a common inflammatory condition of the gallbladder, is characterized by inflammation and dyskinesia. Research has demonstrated that neutrophils contribute to both inflammation and gallbladder dysmotility in AC, potentially leading to gallbladder injury through the inhibition of SCF and c-kit expression (Zhou, 2020; Huang et al., 2016; Lin et al., 2019). TNF-α, a polymorphic hormone, is essential for regulating the body's inflammatory and immune responses while promoting monocyte activity. It is involved in various local and systemic inflammatory reactions (Kalliolias and Ivashkiv, 2016). During AC episodes, a significant release of TNF-α occurs, resulting in the local inflammation of the gallbladder, fever, increased exudation, and right upper quadrant abdominal pain (Chen and Chen, 2023; Psaltis et al., 2024). This study suggested a potential reduction in the duration of abdominal pain and fever, neutrophil percentages, TNF-α levels, and white blood cell recovery times, following Dachaihu decoction treatment. These effects may be attributed to various active ingredients such as saikosaponin a, paeoniflorin, and aloe emodin, which inhibit IL-6, TNF-α, and CCK, thus modulating inflammation, enhancing immunity, repairing gallbladder damage, and promoting bile excretion and stone expulsion (Lin et al., 2019).

Dachaihu decoction reduces liver injury and enhances liver function through multiple mechanisms such as scavenging oxygen free radicals, reducing lipid peroxidation, promoting liver cell regeneration, and enhancing liver blood flow (Yang et al., 2019). AST, ALT, and serum total bilirubin (TBIL) are recognized as sensitive markers of hepatocyte injury. Extensive clinical and experimental research has demonstrated that Dachaihu decoction may significantly reduce serum AST and ALT levels, potentially aiding in liver function recovery and minimizing liver cell damage (Law et al., 2014; Han et al., 2016; Mou et al., 2024), which was consistent with our findings. This effect is likely mediated by the activation of the PI3K/AKT/STAT3 and PPARα signaling pathways, which regulate the expression of E-cadherin, N-cadherin, p53, Bax, Bcl-2, PI3K, p-AKT, AKT, STAT3, CYP7a1, and Cyp8b1, thereby reducing liver cell damage (Xu et al., 2022; Duan et al., 2024).

Antibiotics and non-steroidal anti-inflammatory drugs (NSAIDs) are frequently used to treat infections and relieve biliary colic. However, their use may increase the risk of severe and potentially life-threatening side effects, including gastrointestinal bleeding, kidney damage, and cardiovascular complications (Fraquelli et al., 2016). The risk of adverse events in perioperative patients ranges from 16% to 25% (Ishii et al., 2023), and significant controversy persists regarding the risk associated with different surgical protocols (Do et al., 2023; Gurusamy and Samraj, 2006; Cucchetti et al., 2022). Dachaihu decoction has been well-

documented in the TCM literature, indicating a long-standing history of safe use. Several studies have shown that the eight botanicals in its formula usually have a better safety profile under conventional dosage (grams) (Yang et al., 2017; Song et al., 2020; Ali et al., 2008; Bai et al., 2022). Clinical reports showed that adverse reactions were typically mild gastrointestinal symptoms, which usually resolved on their own without the need for special intervention. Furthermore, Dachaihu decoction exhibits hepatoprotective effects in alpha-naphthyl isothiocyanate (ANIT)-induced liver injury models (Chen et al., 2016). Recent studies further demonstrate that Dachaihu decoction has protective effects on liver and kidney function, indicating a relatively safe profile (Huang et al., 2023; Qiao et al., 2022). However, while most clinical trials on drug interactions have highlighted its effects in reducing toxicity and enhancing efficacy, experimental research remains relatively limited, underscoring the need for careful monitoring during clinical use. Although some studies suggested that Dachaihu decoction did not increase adverse reactions and might have reduced complications when used preoperatively, a comprehensive assessment is still necessary. Current toxicity data are mostly derived from small-scale studies, lacking large-scale randomized controlled trials. More research is needed to further evaluate its safety and inform clinical applications.

5 Strengths and limitations

This study performed a systematic search across eight databases and three clinical trial registries to ensure broad literature coverage. A language-unrestricted search strategy was used to minimize selection bias. A total of 33 RCTs involving 2,851 patients were included, providing sufficient evidence to evaluate the efficacy and safety of Dachaihu decoction in treating acute cholecystitis. In terms of outcome measures, this study assessed a variety of indicators, such as clinical efficacy, time to resolution of abdominal pain and fever, time to white blood cell normalization, length of hospital stay, liver function, and inflammatory markers. These diverse measures allowed for a comprehensive evaluation of Dachaihu decoction's effects, showcasing its potential multi-target and multi-mechanism benefits in managing acute cholecystitis. In addition, Dachaihu decoction is widely used in clinical practice and generally has a higher safety profile. Subgroup and sensitivity analyses were also conducted to identify the sources of heterogeneity and verify the stability of the results, thereby enhancing the findings' reliability. The GRADE assessment system was utilized to evaluate the quality of evidence, offering a structured framework for interpreting results and guiding clinical decision-making and future research.

Nonetheless, our study has several limitations. First, the included studies were all conducted in China and involved only Chinese patients, which may introduce regional publication bias; therefore, additional international clinical trials are recommended. Second, the risk-of-bias assessment showed that most studies reported random sequence generation, but most lacked proper blinding or did not report it. It is essential to recognize that this methodological issue presents a frequent obstacle in many investigations of botanical drug tonics. Given that these tonics are mainly used in practical clinical environments, achieving full implementation of double-blind methods and allocation concealment is often difficult. Furthermore, the complex nature of botanical drug formulations, combined with the distinctive smells or colors of certain botanical drugs, adds to the challenge of blinding. To determine the potential influence of bias on study outcomes, a sensitivity analysis was performed, showing that the results maintained a reasonable degree of credibility. To improve the validity and consistency of future research on botanical drugs of tonic effectiveness, researchers are encouraged to apply stricter randomization and blinding techniques. Additionally, the control groups in these studies were limited to traditional modern medicine, with no placebo controls, and most studies did not include a follow-up period. Moreover, the GRADE assessment system found that most studies were of low quality, indicating a need for better quality and improved methods in current randomized controlled trials. The small sample size in this study may limit the generalizability and reliability of the results. Therefore, larger-scale studies are needed to confirm these findings. We also suggest that future researchers focus on implementing blinding and registering clinical trials to enhance study quality and credibility.

6 Conclusion

Dachaihu decoction may provide benefits in treating acute cholecystitis, such as reducing the length of hospital stay and improving symptoms, with a lower incidence of adverse events. However, due to the varying quality of the included studies and potential bias and heterogeneity, the accuracy of these findings may be limited. Caution is needed when interpreting the results. Future high-quality, large-scale, multi-center studies are necessary to further confirm the efficacy and safety of Dachaihu decoction for acute cholecystitis.

Data availability statement

The original contributions presented in the study are included in the article/Supplementary Material; further inquiries can be directed to the corresponding author.

Author contributions

X-xL: conceptualization, data curation, formal analysis, methodology, software, writing–original draft, and writing–review and editing. Y-qM: data curation, validation, and writing–original draft. L-yK: formal analysis, methodology, software, and writing–review and editing. Y-zS: data curation, software, and writing–review and editing. NR: funding acquisition, supervision, and writing–review and editing. J-pL: conceptualization, funding acquisition, supervision, and writing–review and editing.

Funding

The author(s) declare that financial support was received for the research, authorship, and/or publication of this article. This work was funded by the High-Level Talent Research Start-up Fund (90011451310039) and project "Research and Development of Evidence-Based Chinese Medicine" (B23041). Funders did not play any role in the study design, data collection and analysis, decision to publish, or preparation of the manuscript.

Conflict of interest

The authors declare that the research was conducted in the absence of any commercial or financial relationships that could be construed as a potential conflict of interest.

Publisher's note

All claims expressed in this article are solely those of the authors and do not necessarily represent those of their affiliated organizations, or those of the publisher, the editors, and the reviewers. Any product that may be evaluated in this article, or claim that may be made by its manufacturer, is not guaranteed or endorsed by the publisher.

Supplementary material

The Supplementary Material for this article can be found online at: https://www.frontiersin.org/articles/10.3389/fphar.2024.1497072/full#supplementary-material

References

Abdulrahman, R., Hashem, J., and Walsh, T. N. (2022). A review of acute cholecystitis. *JAMA* 328 (1), 76–77. doi:10.1001/jama.2022.7768

Ali, B. H., Blunden, G., Tanira, M. O., and Nemmar, A. (2008). Some phytochemical, pharmacological and toxicological properties of ginger (Zingiber officinale Roscoe): a review of recent research. *Food Chem. Toxicol.* 46 (2), 409–420. doi:10.1016/j.fct.2007.09.085

Anderloni, A., and Fugazza, A. (2022). Acute cholecystitis: which is the best therapeutic option? *Gastrointest. Endosc.* 95 (3), 407–409. doi:10.1016/j.gie.2021.11.010

Bai, J., Qi, J., Yang, L., Wang, Z., Wang, R., and Shi, Y. (2022). A comprehensive review on ethnopharmacological, phytochemical, pharmacological and toxicological evaluation, and quality control of Pinellia ternata (Thunb.) Breit. *J. Ethnopharmacol.* 298, 115650. doi:10.1016/j.jep.2022.115650

Bedirli, A., Sakrak, O., Sözüer, E. M., Kerek, M., and Güler, I. (2001). Factors effecting the complications in the natural history of acute cholecystitis. *Hepatogastroenterology* 48 (41), 1275–1278.

Bi, S., Liu, Y., Lv, T., Ren, Y., Liu, K., Liu, C., et al. (2023). Preliminary exploration of method for screening efficacy markers compatibility in TCM prescriptions based on Q-markers: anti-inflammatory activity of Dachaihu decoction as an example. *J. Ethnopharmacol.* 312, 116539. doi:10.1016/j.jep.2023.116539

Cai, M. K. (2022). The therapeutic effect of Dachaihu decoction on acute cholecystitis and cholelithiasis and its impact on psychological indicators. *Med. HEALTH* (09), 150–153.

Cheang, I., Yao, W., Zhou, Y., Zhu, X., Ni, G., Lu, X., et al. (2024). The traditional Chinese medicine Qiliqiangxin in heart failure with reduced ejection fraction: a randomized, double-blind, placebo-controlled trial. *Nat. Med.* 30 (8), 2295–2302. doi:10.1038/s41591-024-03169-2

Chen, J. T., Li, X., Liu, L., Hou, X. X., and Wang, J. (2023). Clinical study on the promotion of postoperative rehabilitation of acute cholecystitis and cholecystectomy with modified Dachaihu decoction. *Med. Health* (11), 170–173.

Chen, L., and Chen, X. (2023). Th1/Th2 cytokine profile in patients with acute and chronic calculus cholecystitis. *Eur. Cytokine Netw.* 34 (3), 22–28. doi:10.1684/ecn.2023.0488

Chen, Z., Zhu, Y., Zhao, Y., Ma, X., Niu, M., Wang, J., et al. (2016). Serum metabolomic profiling in a rat model reveals protective function of paeoniflorin against ANIT induced cholestasis. *Phytother. Res.* 30 (4), 654–662. doi:10.1002/ptr.5575

China Association Of Integrative Medicine Emergency Medicine Committee, Editorial Committee Of Chinese Journal Of Integrated Traditional And Western MedicineLi, Z., Wang, D., and Li, Y. (2019). Expert consensus on diagnosis and treatment of septic shock with integrated traditional Chinese and Western medicine. *Zhonghua Wei Zhong Bing Ji Jiu Yi Xue* 31 (11), 1317–1323. doi:10.3760/cma.j.issn.2095-4352.2019.11.002

Colling, K. P., Besshoff, K. E., Forrester, J. D., Kendrick, D., Mercier, P., and Huston, J. M. (2022). Surgical infection society guidelines for antibiotic use in patients undergoing cholecystectomy for gallbladder disease. *Surg. Infect. (Larchmt)* 23 (4), 339–350. doi:10.1089/sur.2021.207

Cucchetti, A., Binda, C., Dajti, E., Sbrancia, M., Ercolani, G., and Fabbri, C. (2022). Trial sequential analysis of EUS-guided gallbladder drainage versus percutaneous cholecystostomy in patients with acute cholecystitis. *Gastrointest. Endosc.* 95 (3), 399–406. doi:10.1016/j.gie.2021.09.028

Dai, M., Yang, Y. W., Guo, W. H., Wang, F. L., Xiao, G. M., Li, Y. M., et al. (2016). Addition and subtraction theory of TCM using xiao-chaihu-decoction and naturopathy in predicting survival outcomes of primary liver cancer patients: a prospective cohort study. *Evid. Based Complement. Altern. Med.* 2016, 4723530. doi:10.1155/2016/4723530

Deng, H., Chen, J. F., She, L., and Li, Z. X. (2018). Randomized controlled study on the treatment of elderly acute cholecystitis with modified Dachaihu decoction. *Diet Sci.* (6X), 47.

Deng, H., and Xu, J. (2017). Wendan decoction (Traditional Chinese medicine) for schizophrenia. *Cochrane Database Syst. Rev.* 6 (6), CD012217. doi:10.1002/14651858.CD012217.pub2

Deng, Y. H., Chen, J. F., She, L., et al. (2018). Clinical study on the treatment of acute cholecystitis (gallbladder heat syndrome) with modified Dachaihu decoction. *J. Emerg. Traditional Chin. Med.* 27 (03), 462–464. doi:10.3969/j.issn.1004-745X.2018.03.025

Dietrich, C. F., Arcidiacono, P. G., Bhutani, M. S., Braden, B., Burmester, E., Fusaroli, P., et al. (2024). Controversies in endoscopic ultrasound-guided biliary drainage. *Cancers (Basel)* 16 (9), 1616. doi:10.3390/cancers16091616

Do, Y. A., Yoon, C. J., Lee, J. H., Choi, W. S., and Lee, C. H. (2023). Percutaneous cholecystostomy as a definitive treatment for acute acalculous cholecystitis: clinical outcomes and risk factors for recurrent cholecystitis. *Br. J. Radiol.* 96 (1147), 20220943. doi:10.1259/bjr.20220943

Duan, Z. W., Liu, Y., Zhang, P. P., Hu, J. Y., Mo, Z. X., Liu, W. Q., et al. (2024). Da-Chai-Hu-Tang Formula inhibits the progression and metastasis in HepG2 cells through modulation of the PI3K/AKT/STAT3-induced cell cycle arrest and apoptosis. *J. Ethnopharmacol.* 331, 118293. doi:10.1016/j.jep.2024.118293

Fraquelli, M., Casazza, G., Conte, D., and Colli, A. (2016). Non-steroid anti-inflammatory drugs for biliary colic. *Cochrane Database Syst. Rev.* 9 (9), CD006390. doi:10.1002/14651858.CD006390.pub2

Gluhovschi, C., Gadalean, F., Velciov, S., Petrica, L., Duta, C., Botoca, M., et al. (2023). Acute acalculous cholecystitis associated with abscesses-an unknown dual pathology. *Biomedicines* 11 (2), 632. doi:10.3390/biomedicines11020632

González-Castillo, A. M., Sancho-Insenser, J., De Miguel-Palacio, M., Morera-Casaponsa, J. R., Membrilla-Fernández, E., Pons-Fragero, M. J., et al. (2021). Mortality risk estimation in acute calculous cholecystitis: beyond the Tokyo Guidelines. World journal of emergency surgery. *WJES* 16 (1), 24. doi:10.1186/s13017-021-00368-x

Grade Working Group (2017). The grading of Recommendations assessment, development and evaluation.

Gu, K. K. (2021). Effect of laparoscopic cholecystectomy combined with da chaihu decoction on calculous cholecystitis. *Reflexology Rehabilitation Med.* 2 (10), 70–72.

Guo, A. L. (2012). Clinical analysis of integrated traditional Chinese and Western medicine in the treatment of acute cholecystitis. *China Med. Pharm.* 2 (01), 118+147.

Guo, H. L. (2023). Exploration of the clinical efficacy of modified Dachaihu decoction in the treatment of acute cholecystitis and gallstones. *Med.* (12), 181–184.

Gurusamy, K. S., and Samraj, K. (2006). Early versus delayed laparoscopic cholecystectomy for acute cholecystitis. *Cochrane Database Syst. Rev.* (4), CD005440. doi:10.1002/14651858.CD005440.pub2

Halpin, V. (2014). Acute cholecystitis. *BMJ Clin. Evid.* 2014, 0411.

Han, L., Wang, X. W., Shan, H. Y., and Zhang, X. (2016). World Chinese Medicine. 11 (06), 1063–1065+1069. doi:10.3969/j.issn.1673.7202.2016.06.034

Heinrich, M., Appendino, G., Efferth, T., Fürst, R., Izzo, A. A., Kayser, O., et al. (2020). Best practice in research–Overcoming common challenges in phytopharmacological research. *J. Ethnopharmacol.* 246, 112230. doi:10.1016/j.jep.2019.112230

Heinrich, M., Jalil, B., Abdel-Tawab, M., Echeverria, J., Kulić, Ž., McGaw, L. J., et al. (2022). Best practice in the chemical characterisation of extracts used in pharmacological and toxicological research—the ConPhyMP—guidelines. *Front. Pharmacol.* 13, 953205. doi:10.3389/fphar.2022.953205

Hong, J. X., and Gao, Y. H. (2018). Modified Dachaihu decoction combined with drug therapy treatment of acute cholecystitis (stagnation of gallbladder heat) randomized parallel control study. *J. Pract. Traditional Chin. Intern. Med.* 32 (06), 40–43. doi:10.13729/j.issn.1671-7813.z20170547

Huang, N., Wei, Y., Liu, M., Yang, Z., Yuan, K., Chen, J., et al. (2023). Dachaihu decoction ameliorates septic intestinal injury via modulating the gut microbiota and glutathione metabolism as revealed by multi-omics. *J. Ethnopharmacol.* 312, 116505. doi:10.1016/j.jep.2023.116505

Huang, Z. P., Qiu, H., Yang, Y., and Yu, B. P. (2016). Effect of neutrophils on gallbladder interstitial Cajal like cells in Guinea pig model of acute cholecystitis. *Cell. Physiology Biochem.* 39, 2033–2043. doi:10.1159/000447899

Ishii, K., Fujita, Y., Suzuki, E., Koyama, Y., Tsujino, S., Nagao, A., et al. (2023). The efficacy and safety of EUS-guided gallbladder drainage as a bridge to surgery for patients with acute cholecystitis. *J. Clin. Med.* 12 (8), 2778. doi:10.3390/jcm12082778

Ji, X. L., Zhou, Y., Li, Z. H., Qiang, F. J., Bing, Y. F., Zhao, J. Y., et al. (2024). Progress on historical evolution, clinical application, and pharmacological effects of Dachaihu decoction and predictive analysis of its quality markers. *Zhongguo Zhong Yao Za Zhi* 49 (8), 2064–2075. doi:10.19540/j.cnki.cjcmm.20231209.201

Kalliolias, G. D., and Ivashkiv, L. B. (2016). TNF biology, pathogenic mechanisms and emerging therapeutic strategies. *Nat. Rev. Rheumatol.* 12 (1), 49–62. doi:10.1038/nrrheum.2015.169

Kimura, Y., Takada, T., Kawarada, Y., Nimura, Y., Hirata, K., Sekimoto, M., et al. (2007). Definitions, pathophysiology, and epidemiology of acute cholangitis and cholecystitis: Tokyo Guidelines. *J. Hepato-Biliary-Pancreat.Surg.* 14, 15–26. doi:10.1007/s00534-006-1152-y

Kivivuori, A., Salminen, P., Ukkonen, M., Ilves, I., Vihervaara, H., Zalevskaja, K., et al. (2023). Laparoscopic cholecystectomy versus antibiotic therapy for acute cholecystitis in patients over 75 years: randomized clinical trial and retrospective cohort study. *Scand. J. Surg.* 112 (4), 219–226. doi:10.1177/14574969231178650

Law, B. Y., Mo, J. F., and Wong, V. K. (2014). Autophagic effects of chaihu (dried roots of Bupleurum chinense DC or Bupleurum scorzoneraefolium WILD). *Chin. Med.* 9, 21. doi:10.1186/1749-8546-9-21

Li, B., Tao, W., Zheng, C., Shar, P. A., Huang, C., Fu, Y., et al. (2014). Systems pharmacology-based approach for dissecting the addition and subtraction theory of traditional Chinese medicine: an example using Xiao-Chaihu-Decoction and Da-Chaihu-Decoction. *Comput. Biol. Med.* 53, 19–29. doi:10.1016/j.compbiomed.2014.05.007

Li, J. (2016). Clinical observation of Dachaihu decoction in the treatment of acute cholecystitis. *China Snaturopathy*. 24 (07), 61–62. doi:10.19621/j.cnki.11-3555/r.2016.07.053

Li, X., Liu, Z., Liao, J., Chen, Q., Lu, X., and Fan, X. (2023). Network pharmacology approaches for research of Traditional Chinese Medicines. *Chin. J. Nat. Med.* 21 (5), 323–332. doi:10.1016/S1875-5364(23)60429-7

Liang, J. B., and Deng, H. J. (2013). The clinical efficacy decoction Dachaihu for acute cholecystitis in 50 patients. *Int. Med. Health Guid. News*. 19 (15), 2304–2307. doi:10.3760/cma.j.issn.1007-1245.2013.15.018

Liang, J. Y., Liu, X. Y., and Zhing, F. P. (2013). 30 cases of acute cholecystitis treated with integrated traditional Chinese and Western medicine. 19 (15), 2304–2307. doi:10.13457/j.cnki.jncm.2006.04.048

Liao, X. M. (2014). Clinical efficacy of integrated traditional and western in the treatment of acute cholecystitis. *Mod. Diagnosis Treat.* 25 (12), 2684–2686.

Lin, M. J., Chen, L., Huang, Z. P., Qiu, H., and Yu, B. P. (2019). Neutrophils injure gallbladder interstitial Cajal-like cells in a Guinea pig model of acute cholecystitis. *J. Cell Physiol.* 234 (4), 4291–4301. doi:10.1002/jcp.27197

Liu, H. (2021). Effects of Dachaihu decoction combined with western medicine non-surgical conventional treatment of acute cholecystitis. *Med. J. Chin. People's Health* 33 (15), 68–70. doi:10.3969/j.issn.1672-0369.2021.15.027

Liu, W. G., Ding, X. J., and Yu, C. (2021). Clinical observation on the therapeutic effect of modified Dachaihu decoction as an adjuvant therapy for acute cholecystitis with gallstones (damp heat syndrome of liver and gallbladder). *J. Emerg. Traditional Chin. Med.* 30 (12), 2192–2194. doi:10.3969/j.issn.1004-745X.2021.12.033

Liu, Y. Q. (2015). Clinical observation of integrated traditional Chinese and western medicine in the treatment of acute cholecystitis. *J. Emerg. Traditional Chin. Med.* 24 (10), 1834–1835. doi:10.3969/j.issn.1004-745X.2015.10.051

Mao, C., Zhou, Y., Ji, D., Tan, X., Tao, Y., Zang, W., et al. (2017). Chemical fingerprint of Dachaihu granule and its chemical correlation between raw herbs. *J. Chromatogr. Sci.* 55 (4), 405–410. doi:10.1093/chromsci/bmw194

Markaki, I., Konsoula, A., Markaki, L., Spernovasilis, N., and Papadakis, M. (2021). Acute acalculous cholecystitis due to infectious causes. *World J. Clin. Cases* 9 (23), 6674–6685. doi:10.12998/wjcc.v9.i23.6674

Mencarini, L., Vestito, A., Zagari, R. M., and Montagnani, M. (2024). The diagnosis and treatment of acute cholecystitis: a comprehensive narrative review for a practical approach. *J. Clin. Med.* 13 (9), 2695. doi:10.3390/jcm13092695

Ministry of Health of the PRC (2002). *Reference to the guiding principles for clinical research of New Chinese medicines*. Beijing: China Medical Science and Technology Press.

Mou, Z., Gong, T., Wu, Y., Liu, J., Yu, J., and Mao, L. (2024). The efficacy and safety of Dachaihu decoction in the treatment of nonalcoholic fatty liver disease: a systematic review and meta-analysis. *Front. Med. (Lausanne)* 11, 1397900. doi:10.3389/fmed.2024.1397900

Murata, A., Okamoto, K., Matsuda, S., Kuwabara, K., Ichimiya, Y., Matsuda, Y., et al. (2013). Multivariate analysis of factors influencing length of hospitalization and medical costs of cholecystectomy for acute cholecystitis in Japan: a national database analysis. *Keio J. Med.* 62 (3), 83–94. doi:10.2302/kjm.2012-0015-oa

Nitzan, O., Brodsky, Y., Edelstein, H., Hershko, D., Saliba, W., Keness, Y., et al. (2017). Microbiologic data in acute cholecystitis: ten years' experience from bile cultures obtained during percutaneous cholecystostomy. *Surg. Infect. (Larchmt)* 18 (3), 345–349. doi:10.1089/sur.2016.232

Ohta, Y., Sasaki, E., Nishida, K., Kobayashi, T., Nagata, M., and Ishiguro, I. (1995). Preventive effect of dai-saiko-to (da-chai-hu-tang) extract on disrupted hepatic active oxygen metabolism in rats with carbon tetrachloride-induced liver injury. *Am. J. Chin. Med.* 23 (1), 53–64. doi:10.1142/S0192415X95000080

Psaltis, E., Zaitoun, A. M., Neal, K. R., and Lobo, D. N. (2024). Immunohistochemical inflammation in histologically normal gallbladders containing gallstones. *World J. Surg.* 48 (7), 1662–1673. doi:10.1002/wjs.12219

Qiao, X., Xu, S. H., Wang, Y. W., Peng Pk, and Shen, K. K. (2022). Da chaihutang inhibits hepatocellular carcinoma by regulating p38 MAPK/IL-6/STAT3 signaling pathway. *Chin. J. Exp. Tradit. Med. Form.* 28 (16), 19–31. doi:10.13422/j.cnki.syfjx.20221026

Regimbeau, J. M., Fuks, D., Pautrat, K., Mauvais, F., Haccart, V., Msika, S., et al. (2014). Effect of postoperative antibiotic administration on postoperative infection following cholecystectomy for acute calculous cholecystitis: a randomized clinical trial. *JAMA* 312 (2), 145–154. doi:10.1001/jama.2014.7586

Sheehan, M. P., Rustin, M. H., Atherton, D. J., Buckley, C., Harris, D. W., Brostoff, J., et al. (1992). Efficacy of traditional Chinese herbal therapy in adult atopic dermatitis. *Lancet* 340 (8810), 13–17. doi:10.1016/0140-6736(92)92424-e

Singh, A., Kaur, M., Swaminathan, C., Subramanian, A., Singh, K. K., and Sajid, M. S. (2023). Preoperative antibiotic prophylaxis in acute cholecystectomy: a systematic review and meta-analysis of randomised controlled trials. *Transl. Gastroenterol. Hepatol.* 8, 37. doi:10.21037/tgh-23-48

Song, J., Kim, Y. S., Lee, D., and Kim, H. (2020). Safety evaluation of root extract of Pueraria lobata and Scutellaria baicalensis in rats. *BMC Complement. Med. Ther.* 20 (1), 226. doi:10.1186/s12906-020-02998-1

Su, Y. B. (2016). Clinical observation of the effect of laparoscopic cholecystectomy and Dachaihu decoction in the treatment of acute calculous cholecystitis. *Contemp. Med. Symp.* 14 (21), 64–65.

Sun, J. F. (2005). Clinical observation on the therapeutic effect of modified Dachaihu decoction on acute cholecystitis. *J. Sichuan Traditional Chin. Med.* (11), 55–56.

Wang, E. C., Yao, W., Li, J., Wang, X. D., Li, B., and Mi, S. P. (2020). Clinical observation on oral administration of Dachaihu decoction combined with external application of shaoyao gancao in the treatment of acute cholecystitis. *Chin. Med. Mod. Distance Educ. China*. 18 (03), 69–70. doi:10.3969/j.issn.1672-2779.2020.03.028

Wang, H. R., and Li, L. (2014). Clinical observation of Dachaihu decoction combined with western medicine in the treatment of acute cholecystitis. *J. Emerg. Traditional Chin. Med.* 23 (11), 2070–2071. doi:10.3969/j.issn.1004-745X.2014.11.043

Wang, S. S. (2010). Clinical observation on the diagnosis and treatment of 80 cases of acute cholecystitis with modified Dachaihu decoction. *Chin. Med. Mod. Distance Educ. Chin*, 8 (20), 21. doi:10.3969/j.issn.1672-2779.2010.20.017

Wei, Y. S. (2016). Clinical analysis of traditional Chinese medicine treatment for acute cholecystitis. *Asia-Pacific Tradit. Med.* 12 (16), 136–137. doi:10.11954/ytctyy.201616059

Xia, C. G. (2020). Clinical study on Dachaihu tang combined with routine therapy in promoting postoperative rehabilitation for acute cholecystitis after cholecystectomy. *J. New Chin. Med.* 52 (5), 26–29. doi:10.13457/j.cnki.jncm.2020.05.007

Xiong, Y., and Yi, X. L. (2021). Clinical research of Macro-bupleuri Decoction on acute cholecystitis of syndrome of stagnation of heat in gallbladder. *China Med. Pharm.* 11 (7), 106–109. doi:10.3969/j.issn.2095-0616.2021.07.028

Xu, S., Qiao, X., Peng, P., Zhu, Z., Li, Y., Yu, M., et al. (2022). Da-Chai-Hu-tang protects from acute intrahepatic cholestasis by inhibiting hepatic inflammation and bile accumulation *via* activation of PPARα. *Front. Pharmacol.* 13, 847483. doi:10.3389/fphar.2022.847483

Xu, T. (2017). Clinical observation of the therapeutic effect of Da Chai Hu Tang combined with surgery on 34 cases of acute cholecystitis caused by Gallstones. *Yunnan J. Traditional Chin. Med. Materia Medica*, 38 (6), 58–59. doi:10.16254/j.cnki.53-1120/r.2017.06.029

Yang, D. D. (2016). Clinical observation on the clinical efficacy of modified Dachaihu decoction in the treatment of acute cholecystitis and gallstones. *For All Health*. 10 (5), 77–78.

Yang, F., Dong, X., Yin, X., Wang, W., You, L., and Ni, J. (2017). Radix bupleuri: a review of traditional uses, botany, phytochemistry, pharmacology, and toxicology. *Biomed. Res. Int.* 2017, 7597596. doi:10.1155/2017/7597596

Yang, J. M., Sun, Y., Wang, M., Zhang, X. L., Zhang, S. J., Gao, Y. S., et al. (2019). Regulatory effect of a Chinese herbal medicine formula on non-alcoholic fatty liver disease. *World J. Gastroenterol.* 25 (34), 5105–5119. doi:10.3748/wjg.v25.i34.5105

Yu, X. J. (2009). 36 cases of acute cholecystitis treated with integrated traditional Chinese and Western medicine. *Chin. J. Ethnomedicine Ethnopharmacy*. 18 (20), 100–101. doi:10.3969/j.issn.1007-8517.2009.20.083

Zhang, J. Y., Guo, Y. Z., and Yu, A. S. (2003). Treating 30 cases of acute cholecystitis and cholecystolithiasis with Dachaihu decoction. *Chin. J. Ethnomedicine Ethnopharmacy*, (2), 96–97. doi:10.3969/j.issn.1007-8517.2003.02.015

Zhang, N. (2018). The therapeutic effect of modified Dachaihu decoction on elderly patients with acute cholecystitis of liver gallbladder damp heat type and its impact on inflammatory factors and liver function indicators. *Yunnan J. Traditional Chin. Med. Materia Medica*, 39 (11), 42–43. doi:10.3969/j.issn.1007-2349.2018.11.018

Zhou, H. (2019). Clinical observation on Dachaihu decoction in the treatment of senile acute cholecystitis with liver gallbladder dampness-heat. *Guangming J. Chin. Med.* 34 (9), 1349–1351. doi:10.3969/j.issn.1003-8914.2019.09.018

Zhou, M. J. (2020). Clinical efficacy of jiawei Dachaihu decoction in the treatment of acute cholecystitis (syndrome of stagnation and heat of gallbladder and viscera). *World J. Complex Med.* 6 (02), 144–146. doi:10.11966/j.issn.2095-994X.2020.06.02.47

Zhu, W. B. (2017). Observation of effect of modified Dachaihu decoction on elderly acute cholecystitis. *Shanxi J. Traditional Chin. Med.* 33 (07), 7–8.

Zhuang, L. L. (2021). "Study on the clinical effect of modified Dachaihu decoctionon acute cholecystitis complicated with gallstone (Syndrome of heat stagnation in biliary organs),". Sichuan, China: Chengdu University of Traditional Chinese Medicine. [Master Dissertation]. doi:10.26988/d.cnki.gcdzu.2021.000180

Zuo, Y. Z. (2021). Clinical study on the treatment of acute cholecystitis with internal administration of Dachaihu decoction combined with external application of peony and licorice. *Self-Care*, (12), 13.

frontiers | Frontiers in Pharmacology

TYPE Original Research
PUBLISHED 04 December 2024
DOI 10.3389/fphar.2024.1476152

Check for updates

OPEN ACCESS

EDITED BY
Qingquan Liu,
Capital Medical University, China

REVIEWED BY
Zhixing Wu,
Texas A and M University, United States
Ibrahim Ahmed Shaikh,
Najran University, Saudi Arabia

*CORRESPONDENCE
Hossein Bannazadeh Baghi,
hbannazadeh@tbzmed.ac.ir,
hb.zadeh@gmail.com

RECEIVED 05 August 2024
ACCEPTED 18 November 2024
PUBLISHED 04 December 2024

CITATION
Shiri Aghbash P, Sadri Nahand J, Rahbar Farzam O, Hosseini SMR, Bayat M, Entezari Maleki T and Bannazadeh Baghi H (2024) Combination of *Vitex pseudo-negundo* methanolic-extract with cisplatin can induce antioxidant activity and apoptosis in HeLa and Caski cells.
Front. Pharmacol. 15:1476152.
doi: 10.3389/fphar.2024.1476152

COPYRIGHT
© 2024 Shiri Aghbash, Sadri Nahand, Rahbar Farzam, Hosseini, Bayat, Entezari Maleki and Bannazadeh Baghi. This is an open-access article distributed under the terms of the Creative Commons Attribution License (CC BY). The use, distribution or reproduction in other forums is permitted, provided the original author(s) and the copyright owner(s) are credited and that the original publication in this journal is cited, in accordance with accepted academic practice. No use, distribution or reproduction is permitted which does not comply with these terms.

Combination of *Vitex pseudo-negundo* methanolic-extract with cisplatin can induce antioxidant activity and apoptosis in HeLa and Caski cells

Parisa Shiri Aghbash[1,2,3], Javid Sadri Nahand[1,2], Omid Rahbar Farzam[3], Seyed Mohammad Reza Hosseini[4], Mobina Bayat[1], Taher Entezari Maleki[5,6] and Hossein Bannazadeh Baghi [1,2,3]*

[1]Infectious and Tropical Diseases Research Center, Tabriz University of Medical Sciences, Tabriz, Iran, [2]Department of Virology, Faculty of Medicine, Tabriz University of Medical Sciences, Tabriz, Iran, [3]Immunology Research Center, Tabriz University of Medical Sciences, Tabriz, Iran, [4]School of Medicine, Zanjan University of Medical Sciences, Zanjan, Iran, [5]Faculty of Pharmacy, Tabriz University of Medical Sciences, Tabriz, Iran, [6]Cardiovascular Research Center, Tabriz University of Medical Sciences, Tabriz, Iran

Background: Cisplatin-based chemotherapy as a common therapeutic regimen for cervical cancer patients, is becoming more and more ineffective due to high resistance. This urges the need for introducing novel metabolics such as botanical drugs with the capacity to increase the cisplatin effectiveness. In that regard, here we investigated the anticancer effects of the Cisplatin-*Vitex pseudo-Negundo* combination in cervical cancer cell lines.

Method and Material: *V. pseudo-Negundo* fruits were dried and extracted methanolic fraction. The MTT assay was performed to evaluate cytotoxicity of both drugs in CaSki and HeLa cells. Then, apoptosis, ROS production, and cell cycling were assessed by flow cytometry assay in cells treated with *V. pseudo-Negundo* and Cisplatin and their combination. Also, the rate of cell migration and colony formation were measured, using wound healing and colony formation assay, respectively. Also, the expression level of related genes (*CD133*, *BAX*, *BCL2*, *Casp-3/8/9*, *MMP-3)* was evaluated using the RT-PCR method.

Results: The obtained results established that the *V. pseudo-Negundo* plant has medicinal properties to induce apoptotic and antioxidant signals. The combination treatment of methanol extraction and Cisplatin had a cytotoxic effect on cervical cancer cell lines (HeLa and CaSki) compared to monotherapy. Also, combination therapy resulted in an increased apoptosis rate and diminished ROS production in both CaSki and HeLa cell lines. Furthermore, *V. pseudo-Negundo* and Cisplatin combination therapy leads to cell cycle arrest in the G2-M and G0-G1 phase in HeLa and CaSki cell lines, respectively. Moreover, combination therapy decreased the colony formation and cell motility in both cell lines and upregulated caspases gene expression.

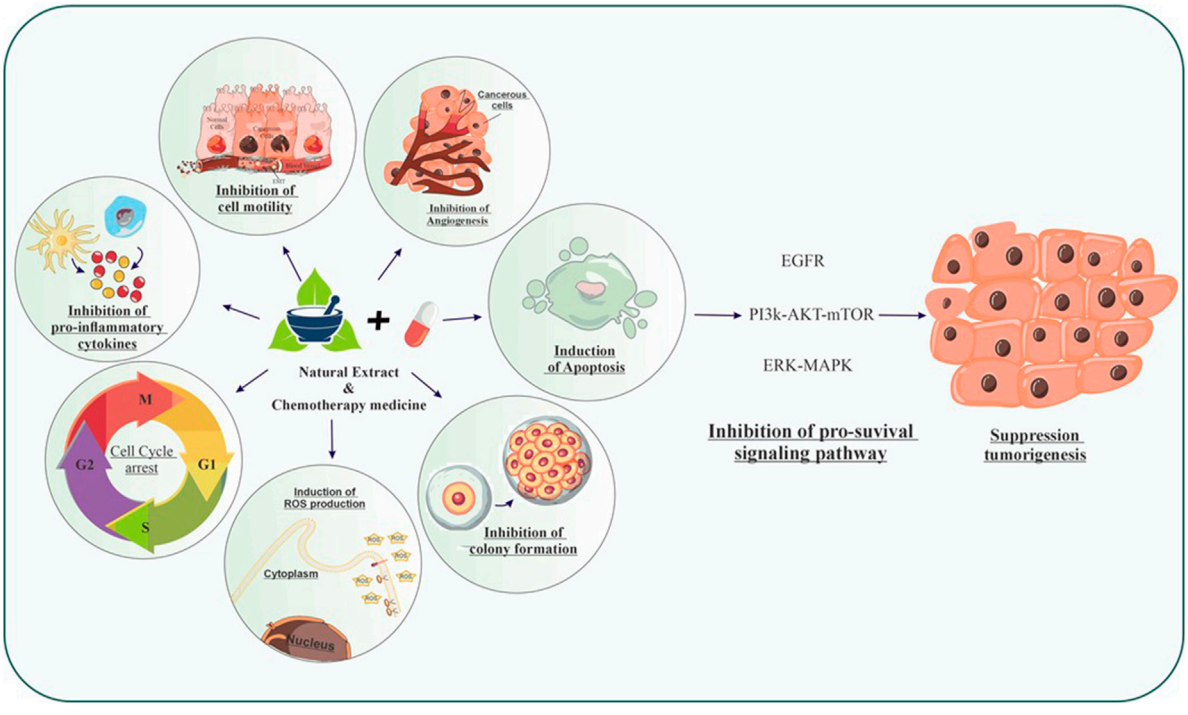
Conclusion: The combination of *V. pseudo-Negundo* with Cisplatin therapy results in a significant anti-cancer and antioxidant effect compared to cisplatin, representing a promising candidate for future clinical investigations.

KEYWORDS

Vitex pseudo-negundo, cisplatin, combination therapy, human papillomavirus, cervical cancer, botanical drug

1 Introduction

Accounting for more than a quarter of a million annual fatalities, cervical cancer (CC) is a vital health concern worldwide (Small et al., 2017). The financial and medical burden of CC requires global efforts to achieve advancements in treatment methods. The International Federation of Gynecology and Obstetrics staging system provides the foundation for cervical cancer treatment (Tsikouras et al., 2016). Patients can get standard therapies such as surgery, chemotherapy, and radiation depending on the stage of their malignancy; however, women with metastatic cervical cancer are not yet eligible for any mainstream therapies (Li et al., 2016). Chemotherapy and preventative immunization are now the main treatment interventions for cervical cancer (Shiri Aghbash et al., 2023). Similar to other treatments, chemotherapy is faced with several limitations, including the requirement for high dosages, toxicity, and activation of pro-survival pathways after prolonged exposure, all of which result in diminished effectiveness and chemo-resistance (Florea and Büsselberg, 2011; Rastogi et al., 2015; Liu et al., 2019a). Moreover, one of the side effects of chemotherapy medicines such as Cisplatin is nephrotoxicity the related mechanism of which is not known during the use of Cisplatin. Also, currently, there is no effective methods or strategies to protect the kidneys during chemotherapy (Ahmad et al., 2019). In this regard, research indicates that the side effects caused by the use of Cisplatin, such as oxidative damage, are reduced or improved following the use of antioxidants (Almutairi et al., 2017; Darwish et al., 2018; Hazman et al., 2018). In other words, human cancer antitumor therapy frequently involves the administration of antioxidant and apoptosis-inducing medicines that prevent growth, invasion, and metastasis (Talib et al., 2022). Advances in the field of cancer treatment have become a high-profile and multi-billion-dollar industry; hence, targeted therapy has led to the reduction of limitations associated with chemotherapy (Dasari et al., 2022). Human cancer antitumor therapy frequently involves the administration of antioxidant and apoptosis-inducing medicines that prevent growth, invasion, and metastasis. Also, for decades herbal medicines have been utilized to treat various disorders and malignancies (Graham et al., 2000). Some species of *Vitex*, such as *Vitex agnus-castus*, *Vitex trifolia*, *Vitex rotundifolia,* and *Vitex negundo* can be used as herbal medicines (Jing et al., 2019). In this way, in the study conducted by Puglia et al., in 2023, it was shown that *Vitex-agnus-castus* can lead to the regulation of prolactin in individuals with mild prolactinemia (Puglia et al., 2023). Therefore, developing novel and potent anticancer substances derived from natural sources are useful for cancer treatment.



GRAPHICAL ABSTRACT

This encourages further investigations to develop promising cancer treatments. In this regard, with the ultimate objective of identifying and creating new anti-CC drugs, medicinal plants have been thoroughly considered. It is also suggested that botanical drugs and natural medicines be considered in order to investigate the effectiveness of chemotherapy and reduce drug resistance (Nimlamool et al., 2022). *Vitex Pseudo-Negundo* (Hausskn.) is a plant from the Lamiaceae family and grows naturally near the seasonal rivers of Iran (Salehpour et al., 2018). This botanical drug is a traditional medicine that is used for the treatment of various diseases and disorders that affect women, including amenorrhea, dysmenorrhea, corpus luteum failure, hyperprolactinemia, infertility, acne, and menopause (Tandon and Gupta, 2005). Preclinical investigations have confirmed pharmacological roles for several of these substances. The existence of estrogenic, dopaminergic, opioids, antineoplastic, immunomodulatory, and antioxidant activities has therefore been established by several researchers (Adamov et al., 2022). Moreover, studies on phytochemistry have revealed that this genus's members include substances such as flavonoids, terpenoids, ecdysteroids, and iridoid glycosides (Kirtikar and Basu, 1918). The *V. pseudo-Negundo* fruit extraction includes 20 flavonoids, 11 phenolic acids, 10 iridoids, 12 terpenes, and 3 diterpene alkaloids. Therefore, it can be used as an anti-cancer and antioxidant medicine in malignancies. Moreover, while many novel medicines are currently being developed in cancer treatment, combination therapies are highly anticipated. Most regions of the world have historically used natural botanical drugs for cancer treatment (Liu et al., 2019b). Natural botanical drugs have showed the capacity to elevate the efficiency of conventional chemo- and radio-therapy and promote cell death in cancer cells, prevent metastasis, as well as trigger the anticancer immunity (Liu et al., 2019b). In this regard, in 2022, Dasari et al., reported that the combined treatment of cisplatin and natural products as new strategic approaches to cancer treatment, are effective (Dasari et al., 2022). In addition, due to the existence of some bioactive metabolites in medicinal plants, they can be considered as promising sources for the treatment of various human malignancies (Dasari et al., 2022). During clinical studies, it has been established that the metabolites in medicinal plants can increase the therapeutic activity of Cisplatin as well as reduce the toxicity caused by chemotherapy. Also, metabolites found in medicinal plants modulate multiple gene transcription factors and induce cell death via apoptosis or necrosis, as a result lead to protection against organ toxicity caused by Cisplatin (Dasari et al., 2022).

Considering the need for overcoming the cisplatin-based chemo-resistance and the effectiveness of botanical drug's metabolites for increasing the efficacy of this therapeutic regimens, here we investigated the combined effect of *Vitex* botanical medicine and cisplatin chemotherapy drug on synergistic toxicity, improving the effectiveness of chemotherapy drugs and inhibiting the drug resistance of CC cells.

2 Methods

2.1 Methanolic extraction of *Vitex pseudo-Negundo* fruit

This plant with the local name Five Fingers belongs to the Lamiaceae family. The *Vitex pseudo-Negundo* is a shrub with a height of about 3 m and is used as a medicinal species and grows naturally around the seasonal rivers and streams of Iran. After collection of the *V. pseudo-Negundo* in winter, the *V. pseudo-Negundo* fruits were dried and ground into a powder before being subjected to a soaking extraction method. In this process, an alcoholic solvent was utilized, with 100 mL employed for each extraction to yield the methanolic extract. To purify the final extract, 1 gr of the plant material underwent freeze-drying. The final *V. pseudo-Negunda* extract (3 mg of 1 gr) was dissolved in 30 µL of dimethyl sulfoxide (DMSO) (Sigma-Aldrich, United States) as a stock. Using a sensitive scale, 3 mg of the desired extract was weighed and placed in a microtube. Then about 30 µL of DMSO and 1,000 µL of distilled water were added to the extract to reduce the cytotoxicity of DMSO. The final volume of our stock reached 3 mg/mL. To reduce the toxicity effect of DMSO on the cells in the per wells, the concentration of this substance in each well was less than 1% (Aldaghi et al., 2016; Garbi et al., 2015).The obtained solution was stored on covered glass plates at −20°C, at dark, for cell culture experiments (Aldaghi et al., 2016; Gong et al., 2021). Also, according to the Heinrich et al., we speculated that our botanical drug is in the type C group (Heinrich et al., 2022).

2.2 Cell culture and treatment

Human cervical cancer cell lines, CaSki and HeLa, were sourced from the Iranian Biological Resource Centre (IBRC). They were cultured in a monolayer form using Roswell Park Memorial Institute medium (RPMI 1640; Gibco, United States), supplemented with 10% fetal bovine serum (FBS; Gibco, United States), along with 100 units/mL of penicillin and streptomycin in T25 flasks. The cells were maintained at 37°C in a humidified atmosphere with 5% CO2 until they reached logarithmic growth. When the cells achieved about 70% confluency, they were detached using a 0.25% Trypsin-EDTA solution (Gibco, United States) for subsequent experiments.

2.3 MTT assay

The 3-(4,5-dimethylthiazol-2-yl)-2,5-diphenyltetrazolium bromide (MTT) assay was performed to evaluate the viability and proliferation of CaSki and HeLa cells, determining the IC_{50} values for Cisplatin in both monotherapy and conjunction with varying concentrations of *V. pseudo-Negundo* extract (1, 10, 20, 30, 40, 50, 60, 70, 80, 90, 100, 110, 120, 130, 140, 150, 160, 170, 180, 190, 200 µg/mL). Among other treatments. Normal human foreskin fibroblast (HFF2) cells were included for comparison. Approximately 1.5×10^4 CaSki and 1×10^4 HeLa and HFF_2 cells were seeded in a 96-well plate. The cell lines were divided into four treatment groups: control, Cisplatin only, *V. pseudo-Negundo* extract only, and a combination of both. After a 24-h incubation, various concentrations of the agents replaced the medium. Subsequent incubation for another 24 h was followed by adding 150 µL of MTT solution (2 mg/mL) and incubating for another 4 h at 37°C with 5% CO2. The solution was then removed,

TABLE 1 The primer pairs sequences used for qRT-PCR.

Gene name	Forward	Reverse
CD133	5′-GACCGACTGAGACCCAACATC-3′	5′-GGCTAGTTTTCACGCTGGTCA-3′
BAX	5′-TTTGCTTCAGGGTTTCATCCA-3′	5′-TCTGCAGCTCCATGTTACTGTC-3′
BCL2	5′-CTGTGGATGACTGAGTACCTG-3′	5′-GAGACAGCCAGGAGAAATCA-3′
Casp-3	5′-CAAACCTCAGGGAAACATTCAG-3′	5′-CACACAAACAAAACTGCTCC-3′
Casp-8	5′-CGGACTCTCCAAGAGAACAGG-3′	5′-TCAAAGGTCGTGGTCAAAGCC-3′
Casp-9	5′-CTGTCTACGGCACAGATGGAT-3′	5′-GGGACTCGTCTTCAGGGGAA-3′
MMP3	5′-CACTCACAGACCTGACTCGGTT-3′	5′-AAGCAGGATCACAGTTGGCTGG-3′

and to dissolve the resultant formazan crystals, 150 µL of DMSO was added. Absorbance at 570 nm (reference at 620 nm) was measured using a microplate reader (Tecan, Switzerland). Each assay was conducted in triplicate. Also, we examined 50% cell viability at different concentrations of both agents in both cell lines, using a [0.5:10] ratio of cisplatin to *V. pseudo-Negundo*, respectively.

2.4 Wound healing assay

To evaluate cell migration, an assay was performed using CaSki (3×10^5 cells) and HeLa (2×10^5 cells) lines after treatment with Cisplatin and *V. pseudo-Negundo* extract. Cells were plated as a singular layer in 24-well plates and incubated for 24 h at 37°C with 5% CO_2. A linear wound was created with a 100 µL pipette, and the respective IC_{50} concentrations of the treatments were administered. Migration was tracked at three-time intervals—0, 24, and 48 hours—utilizing an inverted microscope (Optika, XDS-3, Italy).

2.5 Real-time PCR (RT-PCR)

For this experiment, 3×10^5 CaSki cells and 2×10^5 HeLa cells were cultured in 6-well plates, and divided into four treatment groups as specified earlier. Following a 24-h incubation at 37°C in a 5% CO_2 atmosphere, cells were treated for an additional 24 h with their respective IC50 doses of Cisplatin and *V. pseudo-Negundo*. RNA extraction was executed using TRIzol reagent (RiboEX, South Korea), and RNA concentrations were quantified with a Nano-Drop spectrophotometer (Thermo Scientific, United States) at various wavelengths (230, 260, and 280 nm). Complementary DNA (cDNA) synthesis followed using the 2X RT-PCR Pre-Mix (BioFACT™, South Korea) to assess relative gene expression levels. Genes of interest included CD133, BAX, BCL2, Casp-3, Casp-8, Casp-9, and MMP-3, evaluated using the 2X Real-Time PCR Master Mix (BioFACT™, South Korea) on a StepOnePlus Real-Time PCR system (Applied Biosystems, Foster City, United States). GAPDH served as a normalization control, and analysis was performed with the $2^{-\Delta\Delta CT}$ method (Shiri Aghbash et al., 2023). All primer sequences were confirmed with NCBI's Primer-BLAST before the experiment; their sequences are presented in Table 1.

2.6 Apoptosis assay

In the apoptosis evaluation, 3×10^5 CaSki cells and 2×10^5 HeLa cells were cultured in separate 6-well plates (Shiri Aghbash et al., 2023). After 24 h, the groups were treated with their respective IC_{50} concentrations of Cisplatin and *V. pseudo-Negundo*. The Annexin V/PI staining kit (Exbio-Czech) was employed to prepare samples for flow cytometry. Cells were washed with 1X PBS and labeled with FITC-conjugated Annexin V and propidium iodide (PI) per the manufacturer's protocol. Apoptotic cells were then quantified via flow cytometry.

2.7 Cell cycle assay

Following the seeding of 3×10^5 CaSki cells and 2×10^5 HeLa cells in 6-well plates, the cells were treated with their respective IC_{50} concentrations. After washing with PBS, cells were fixed in 70% ethanol and stored at −20°C overnight. They were then re-suspended in PBS with RNase A (200 µg/mL) and incubated at 37°C for 30 min before being stained with DAPI (50 µg/mL) for analysis. Flow cytometry (Miltenyi Biotec MACSQuant 10) was used to assess cell cycle distributions, and data were analyzed using FlowJo FACS software.

2.8 Assessment of cellular ROS generation

Intracellular ROS levels were evaluated using the dichloro-dihydro-fluorescein diacetate (DCFH-DA; Meilunbio, China) assay. CaSki and HeLa cells (3×10^5 and 2×10^5 respectively) were grown in 6-well plates. Following treatment with their respective IC_{50} concentrations, cells were washed twice with PBS in a dark setting and stained with 20 µM DCFH-DA for 30 min at 37°C.

2.9 Colony formation assay

For the colony formation assessment, 10^4 CaSki cells and 5×10^3 HeLa cells were placed in 6-well plates. After an incubation period of 24 h at 37°C with 5% CO_2, cells were treated with their designated drug doses. The medium was refreshed every 2–3 days, with colony counts performed after 10–12 days. Colonies were stained with crystal violet for 30 min, and the number of colonies was quantified using ImageJ software.

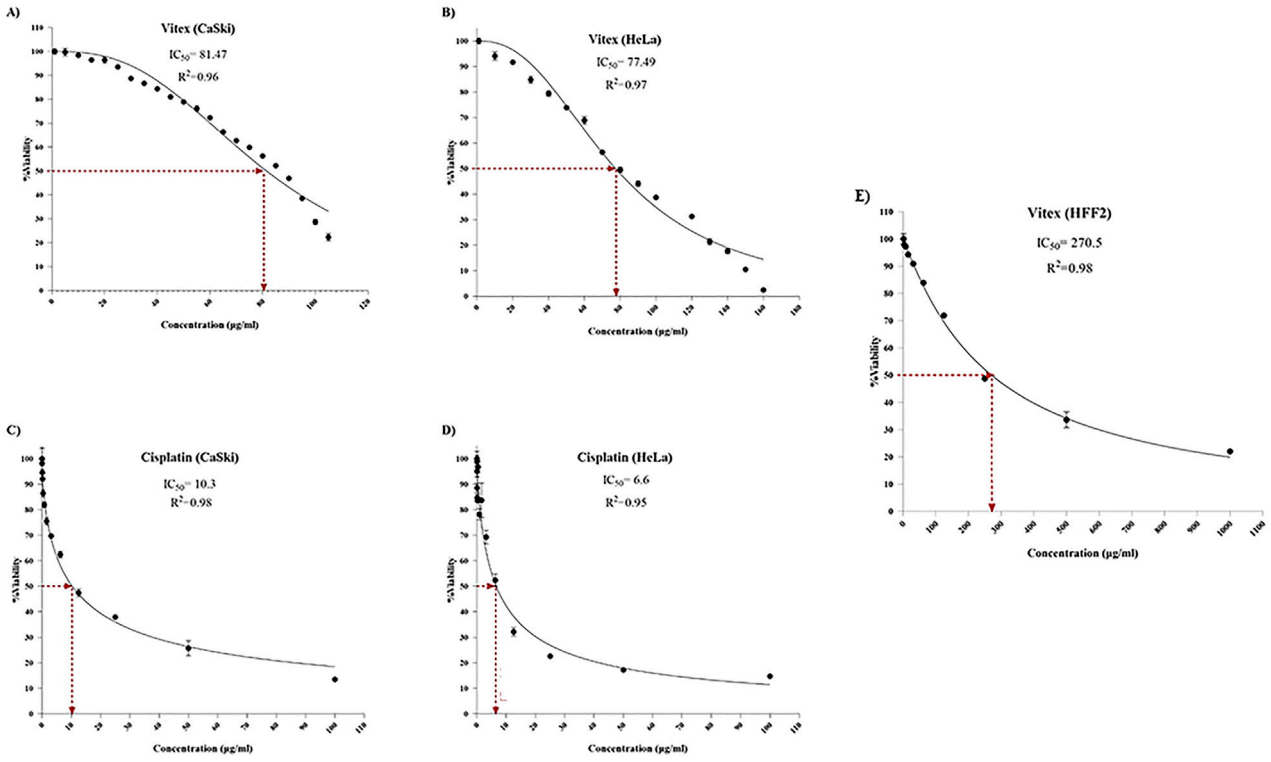


FIGURE 1
The impact of *Vitex* extraction and Cisplatin monotherapy on the viability of **(A)** *Vitex* (CaSki); **(B)** *Vitex* (HeLa); **(C)** Cisplatin (CaSki); **(D)** Cisplatin (HeLa); **(E)** *Vitex* (HFF_2).

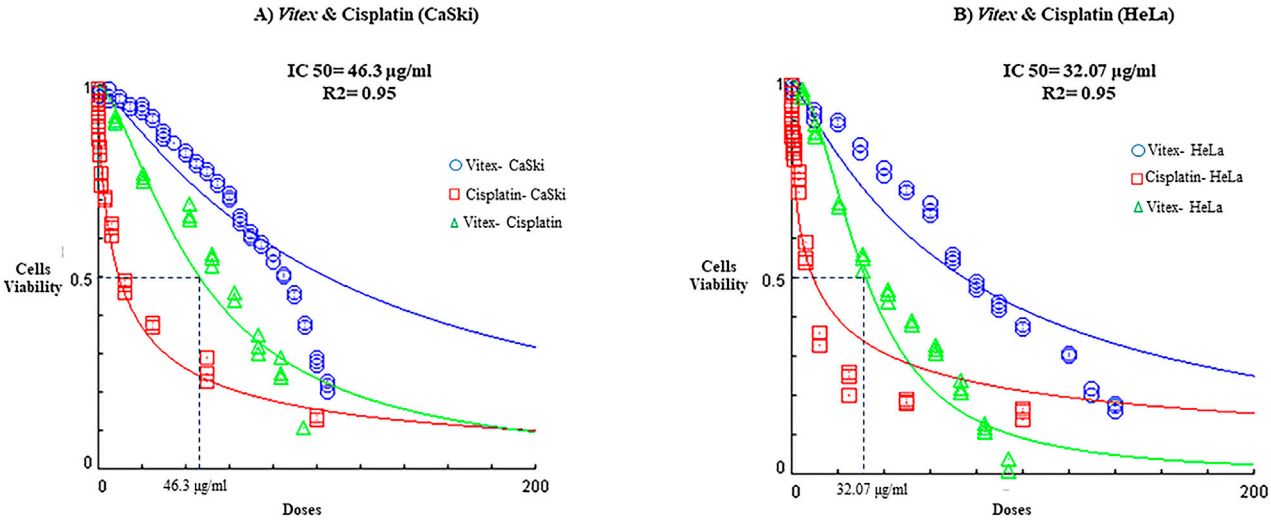


FIGURE 2
The impact of *Vitex* extraction and cisplatin combination on the viability of **(A)** CaSki cell line; **(B)** HeLa cell line.

2.10 Statistical analysis

Statistical analyses were carried out using SPSS version 26 (SPSS Inc., Chicago, IL, United States), Prism 8.0 (GraphPad, San Diego, CA, United States), and CompuSyn software. The distribution of quantitative variables was assessed through the Kolmogorov-Smirnov test. Data were presented as mean ± standard deviation (SD), with a significance level established at $p < 0.05$. The Wilcoxon signed-rank test or paired t-test tested paired measurements, while one-way ANOVA compared group differences.

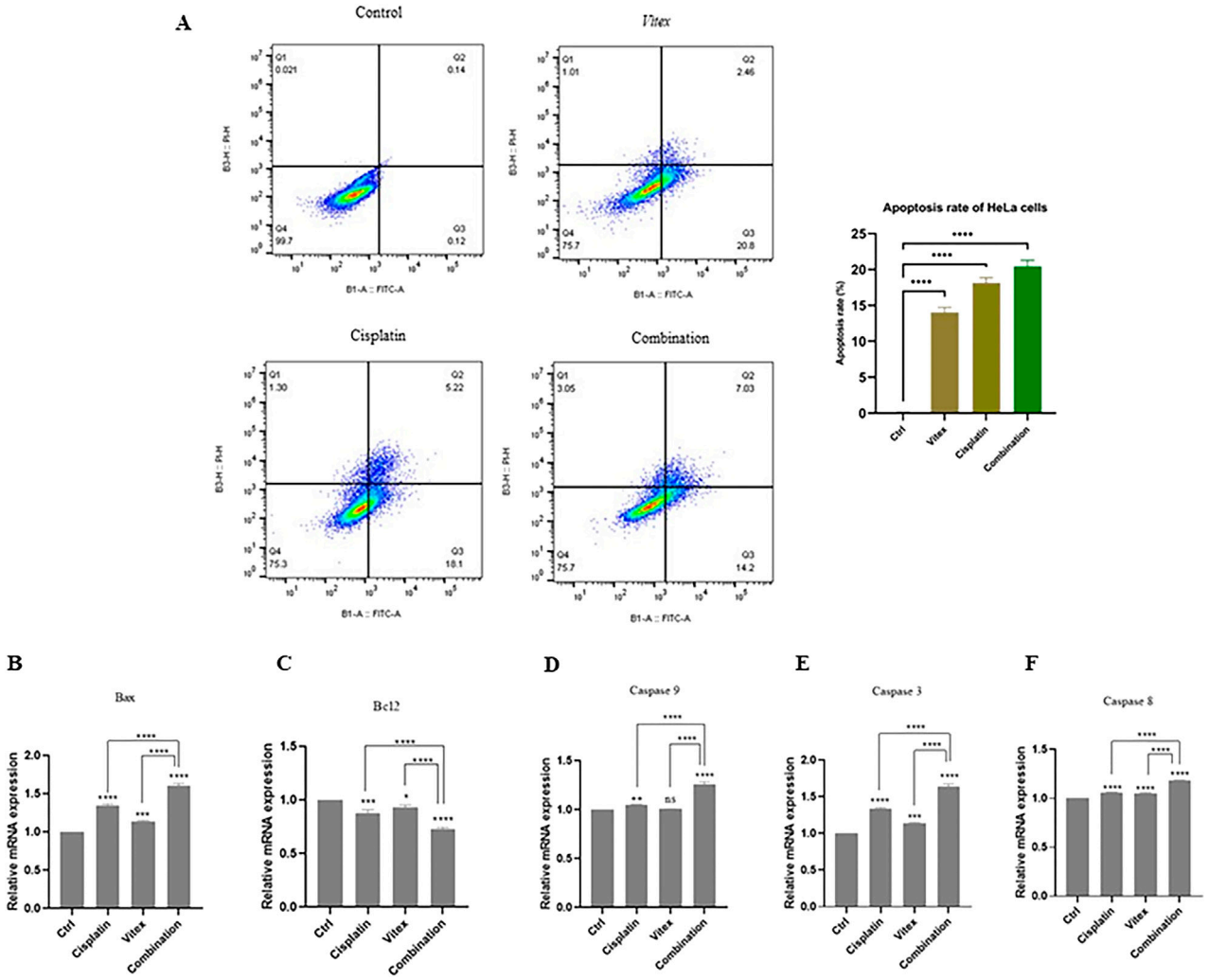


FIGURE 3
The effect of the *Vitex* extract combined with Cisplatin on apoptosis in HeLa cells. **(A)** The combination notably enhances HeLa cell apoptosis; **(B, C)** Bax levels increasing and Bcl_2 levels decreasing compared to controls. **(D, E, F)** Caspase gene expression significantly rose following combination therapy versus monotherapy with either *Vitex* or Cisplatin (*p < 0.05, **p < 0.01, ***p < 0.001, ****p < 0.0001).

3 Results

3.1 Combination of cisplatin and *Vitex pseudo-negundo* suppresses cervical cancer cells viability

The treatment with Cisplatin alone resulted in approximately 50% inhibition of cell viability and proliferation in CaSki and HeLa cells at concentrations of 10.3 μg/mL and 6.6 μg/mL, respectively, compared to controls. In contrast, the extraction of *V. pseudo-Negundo* displayed a notable growth-inhibiting effect on cervical cancer cells, particularly at 81.47 μg/mL for CaSki and 77.49 μg/mL for HeLa. The application of various *V. pseudo-Negundo* extract concentrations demonstrated a significant reduction in cell viability for both cancer cell lines. Specifically, the concentrations at which cell viability in CaSki cells dropped were between 125 μg/mL and 150 μg/mL, while for HeLa cells, it ranged from 150 μg/mL to 200 μg/mL. For comparison, HFF2 cells showed an IC_{50} value of 270.5 μg/mL for *V. pseudo-Negundo* (Figure 1).

Importantly, *V. pseudo-Negundo* extraction was found to lower the IC_{50} threshold for Cisplatin, effectively reducing the required concentration of Cisplatin to achieve less than 50% viability. The synergy between *V. pseudo-Negundo* and Cisplatin was evident, with a 10:0.5 ratio leading to IC_{50} values of 32.07 μg/mL and 42.3 μg/mL for HeLa and CaSki cells, respectively (Figure 2).

3.2 *Vitex pseudo-negundo* can sensitize cervical cancer cells to cisplatin-induced apoptosis

Data suggest that the combination therapy led to an increased rate of apoptosis in cervical cancer cells when compared to control and monotherapy conditions. In HeLa cells, the rates of apoptosis following individual treatments of *V. pseudo-Negundo* and Cisplatin were recorded at 14.2% and 18.1%, respectively, while the combination treatment achieved a rate of 20.8%. There were no significant

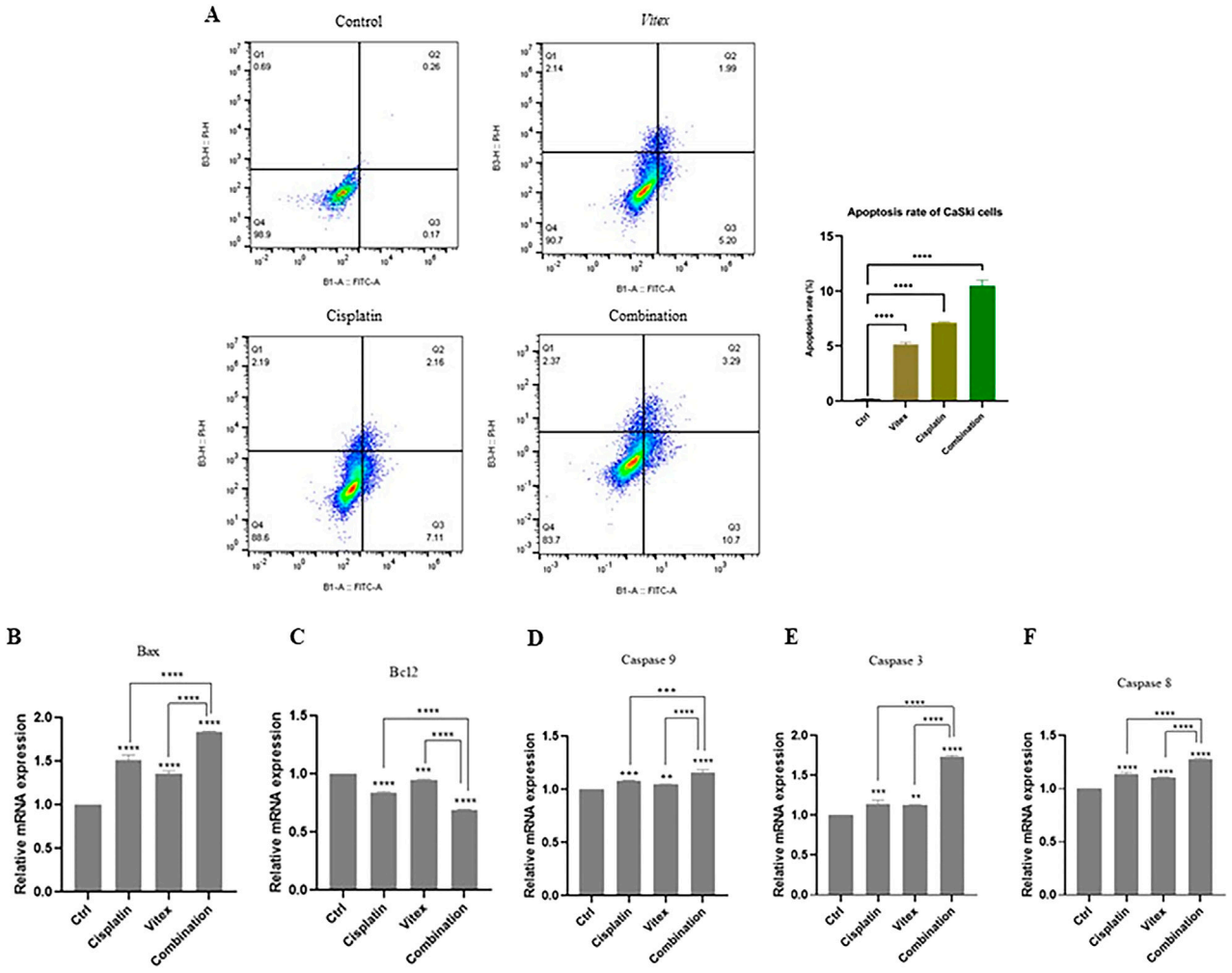


FIGURE 4
The impact of the *Vitex* extract and Cisplatin combination on apoptosis in CaSki cells. **(A)** the combination promotes increased apoptosis in CaSki cells, **(B, C)** expression level of Bax and Bcl_2 changed, **(D, E, F)** significant rise in Caspase gene expression compared to monotherapy (*p < 0.05, **p < 0.01, ***p < 0.001, ****p < 0.0001).

differences between the monotherapy and combination groups; however, each was significantly different from the controls (p< 0.0001) (Figures 3C–F). In CaSki cells, the monotherapy groups showed marked differences (*V. pseudo-Negundo:* 5.20%, Cisplatin: 7.11%) compared to the combination group (10.7%), with all treatments yielding significant differences from the control (p < 0.0001). Additionally, a remarkable increase in the expression of apoptosis-related genes such as Casp-3, -8, -9, and Bax was observed after combination therapy, contrasting with a notable decrease in the expression of the anti-apoptotic gene Bcl_2 (Figures 4C–F).

3.3 *Vitex pseudo-negundo* extraction in combination with cisplatin arrested CaSki and HeLa cells on G0-G1 and G2-M stage

To better understand the impact of the combined treatment on cell division, the distribution of cell cycles in both cell lines was examined. The findings revealed that CaSki cells underwent an arrest in the G0-G1 phase, while HeLa cells showed arrest predominantly in the G2-M phase after treatment (Figures 5, 6). Following combined treatment with *V. pseudo-Negundo* and Cisplatin (p < 0.0001), a significant increase in cell populations was noted within the G2-M phase, moving from 3.60% to 14.7% for CaSki cells and from 11.1% to 20.1% for HeLa cells, relative to controls. This indicates that the combination therapy enhanced the presence of HeLa cells in the G2-M phase, thereby effectively promoting cell cycle arrest at this juncture (Figure 5). In addition, CaSki cells were also observed to be arrested in the G0-G1 or sub-G1 phase (Figure 6).

3.4 ROS production was inhibited by *Vitex pseudo-negundo* in combination with cisplatin

To investigate whether the combined treatment with *V. pseudo-Negundo* and Cisplatin affected intracellular ROS levels in cervical

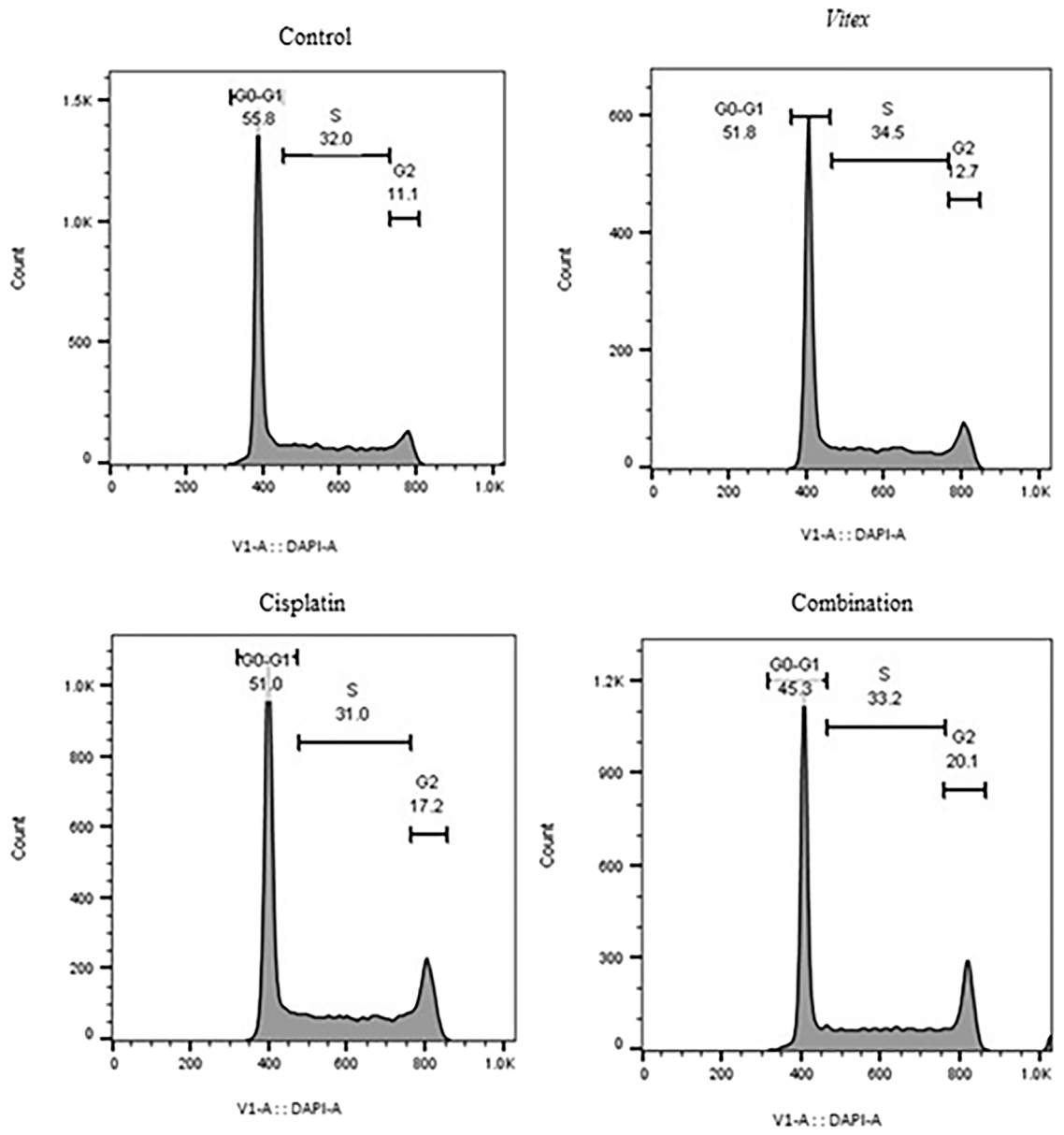


FIGURE 5
The effect of the *Vitex* extract combined with Cisplatin on the cell cycle in HeLa cells, resulting in cell cycle arrest at the G2-M phase.

cancer cells, measurements were taken after 24 h of either combination therapy or monotherapy. The results demonstrated a significant increase in intracellular ROS levels (DCF) in the combination therapy group compared to controls ($p < 0.0001$). Notably, in the HeLa cells, ROS levels were found to rise from 0.74% in controls to 89.9% following combination treatment, whereas in CaSki cells, levels increased from 0.68% to 62.6% (Figures 7, 8). Overall, there were no statistically meaningful differences in ROS production among the monotherapy groups (Cisplatin: 89.7%, *V. pseudo-Negundo*: 83.7%) compared to the combination group (89.9%); however, each exhibited significant variations when contrasted with the control ($p< 0.0001$) (Figure 7). Additionally, the highest ROS production was seen in the CaSki cells treated with both agents, peaking at 62.6%, followed by monotherapy with Cisplatin (35.4%) and *V. pseudo-Negundo* (33%) (Figure 8).

3.5 Stemness features in cervical cancer cells were decreased by *Vitex pseudo-negundo* fraction in combination with cisplatin

To assess the influence of *V. pseudo-Negundo* extract combined with Cisplatin on the stemness traits of cervical cancer cells, a colony formation assay was conducted. Treatments involving both CaSki and HeLa cell lines with the dual agents resulted in a marked reduction in colony formation, particularly notable in the combination group when compared to controls (Figures 9A, B). Treatments with either *V. pseudo-Negundo* or Cisplatin alone also exhibited declines in colony numbers compared to controls, but the combination showed a more substantial impact. To support these findings, RT-PCR analysis was utilized to investigate the expression

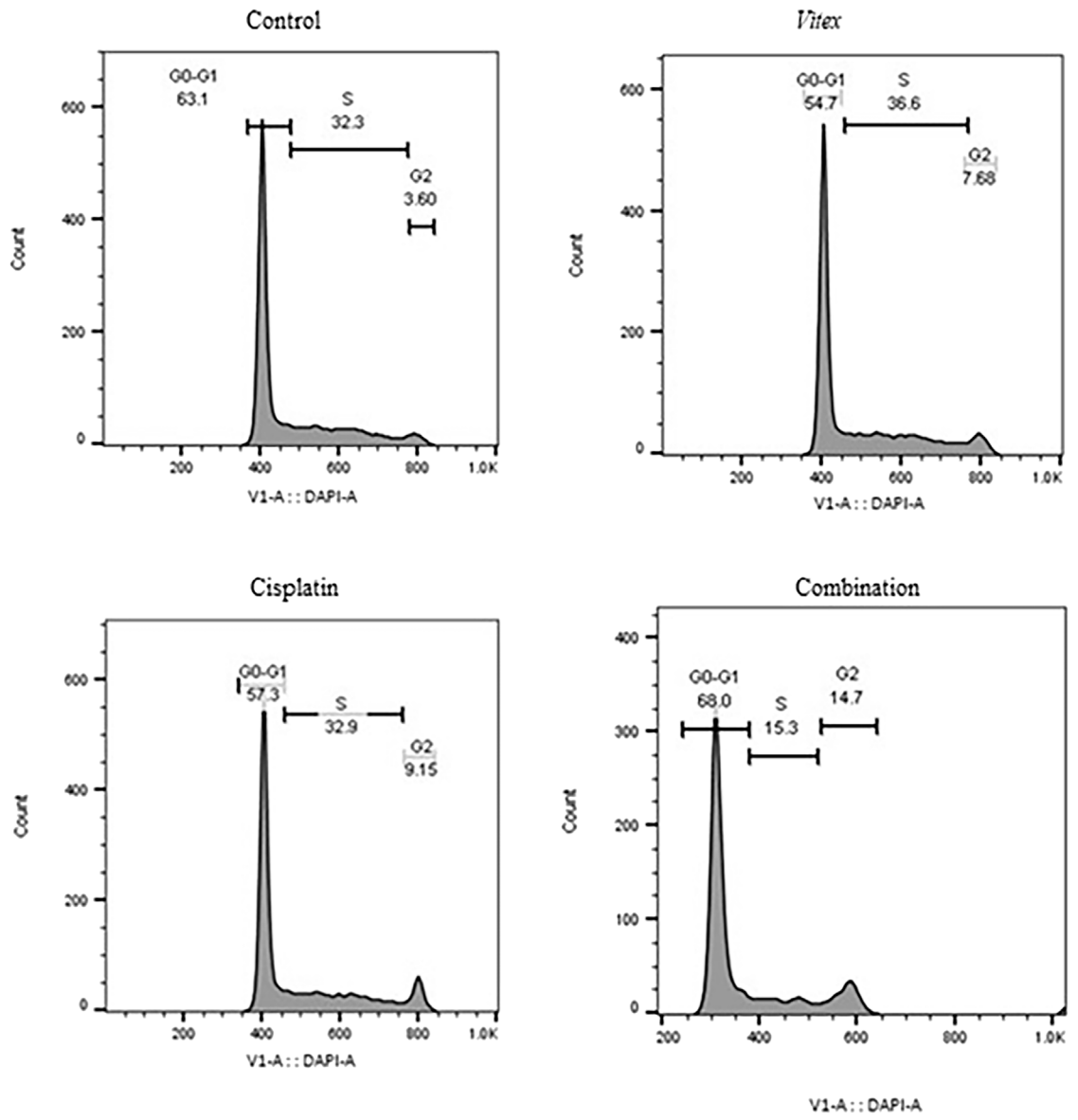


FIGURE 6
The effect of the Vitex extract combined with Cisplatin on the cell cycle in CaSki cells, leading to cell cycle arrest in the sub-G1 phase.

of stemness-related genes like CD133. Results revealed a significant disparity in CD133 expression levels between the combination treatment group and controls ($p < 0.0001$) for both cell lines. While reductions in CD133 were noted across all treatment groups, no significant differences were observed among those groups.

3.6 Cervical cancerous cells' motility and related genes have been inhibited by *Vitex pseudo-negundo* -cisplatin combination

The wound healing assay results indicated that individual treatments with Cisplatin or *V. pseudo-Negundo* had minimal effects on cervical cancer cell migration. In contrast, the synergistic application of both agents resulted in a significant reduction in the migration of CaSki and HeLa cells following 48 h of treatment compared to controls (Figures 10, 11). Further analysis into the effects of combination treatment on cellular motility employed RT-PCR techniques to evaluate MMP-3 gene expression. This analysis confirmed that the combination of *V. pseudo-Negundo* and Cisplatin effectively reduced MMP-3 levels in both cell lines ($p < 0.0001$) (Figures 10B, 11B). Although each monotherapy presented reductions in migration and MMP-3 expression, the combination treatment yielded far greater reductions than Cisplatin alone ($p < 0.0001$), demonstrating significant efficacy even at lower Cisplatin doses.

4 Discussion

In this study, we explored the effects of combining *V. pseudo-Negundo* extraction with Cisplatin for cervical cancer (CC) therapy.

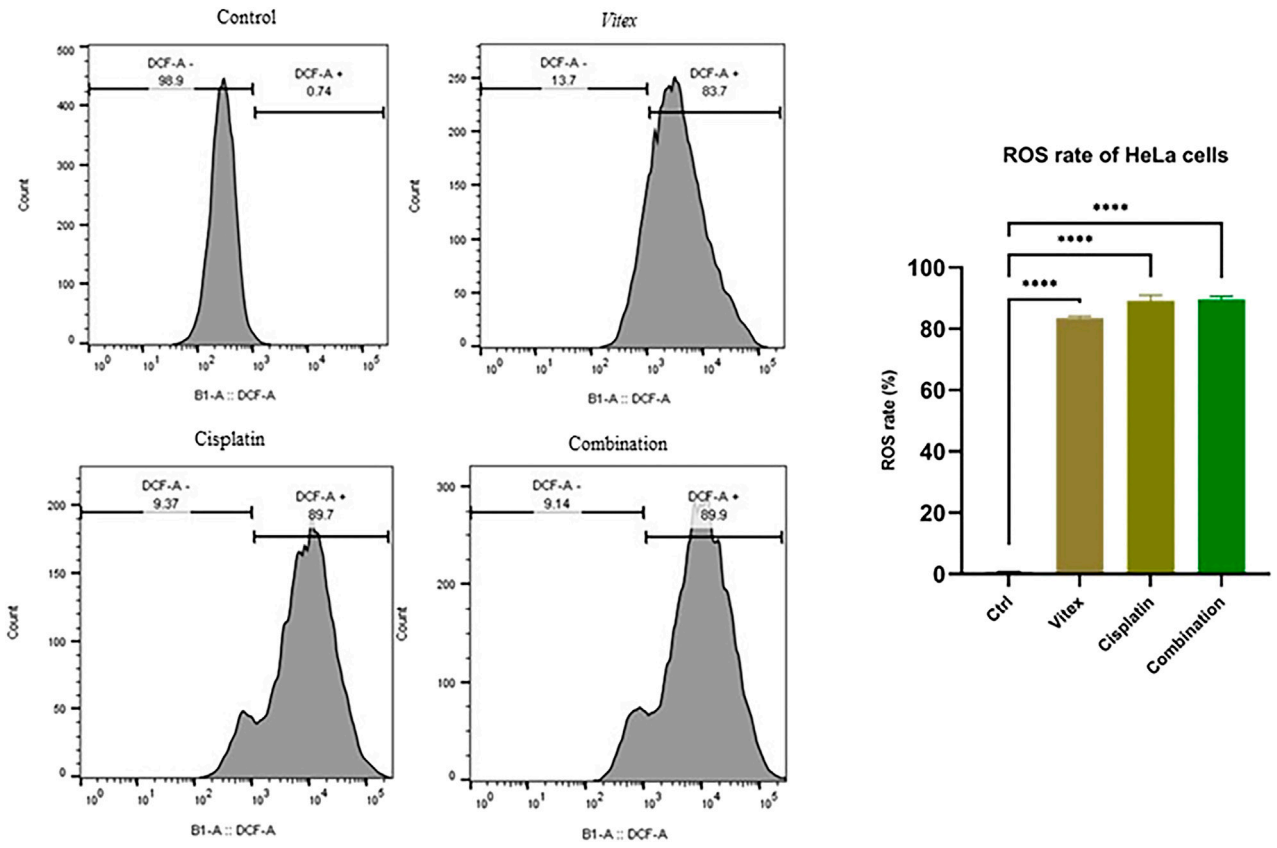


FIGURE 7
The influence of the Vitex and Cisplatin combination on ROS levels in HeLa cells. Cells in exponential growth were treated with the specified concentrations, and ROS levels were measured via flow cytometry, showing ROS (DCF) levels (%) in relation to the control (*p < 0.05, **p < 0.01, ***p < 0.001, ****p < 0.0001).

Our findings indicate that *V. pseudo-Negundo* extract significantly inhibits the growth and proliferation of tumor cells through its growth-inhibitory properties. Specifically, the methanolic extract of *V. pseudo-Negundo* demonstrated a growth inhibitory impact on HeLa and CaSki cell lines at concentrations of 150 μg/mL and 200 μg/mL, with IC_{50} values of 77.49 μg/mL and 81.47 μg/mL, respectively. Notably, the IC_{50} values were higher for CaSki cells than HeLa cells, likely due to the former's resistance to treatment. Additionally, we observed that the Cisplatin combination with botanical drug remedies enhances the sensitivity of HeLa cells to lower doses of Cisplatin (Madhulika Singh et al., 2013). This suggests that certain plant extracts can improve the response of cancer cells that are resistant to Cisplatin, thereby enhancing the overall efficacy of the treatment (Dasari et al., 2022; Liu et al., 2020). For instance, Erdogan et al. demonstrated that flavonoids could increase the sensitivity of $CD44^+$ prostate cancer cells to Cisplatin (Erdogan et al., 2017). In contrast, Li et al. noted similar effects in ovarian cancer cells treated with platinum-based therapies (Li et al., 2014).

Cisplatin is a widely utilized chemotherapeutic agent for various cancers, functioning by disrupting DNA repair mechanisms, causing DNA damage, and promoting apoptosis in cancer cells. However, its effectiveness is often hampered by drug resistance, as well as a range of side effects. Consequently, combination therapies involving Cisplatin and other agents have emerged as a strategy to overcome resistance and mitigate toxicity (Dasari and Bernard Tchounwou, 2014). Herbal medicines in combination therapies have resulted in long-lasting and more potent therapeutic results. Furthermore, they might shield the healthy tissues and trigger sensitivity to chemotherapy and radiotherapy, as well as suppress tumor metastasis and recurrence. Considering the unique characteristics, low side effects, availability, and ease of access, botanical drugs from different regions around the world have been explored, in particular for cancer research (Zulfiker et al., 2017). For instance, the consumption of flavonoids as a part of the *V. pseudo-Negundo* plant leads to cancer prevention and increased sensitivity in Cisplatin-resistant cases, and as a result, promotes Cisplatin treatment. In combined treatments with Cisplatin and flavonoid-rich plants, flavonoids have been associated with increased effectiveness in disrupting the cellular oxidative system, inducing mitochondrial dysfunction, and ultimately leading to apoptosis (Kachadourian et al., 2007). Consistent with our findings, we observed that combining *V. pseudo-Negundo* with Cisplatin resulted in higher levels of reactive oxygen species (ROS) and more pronounced apoptotic responses via a mitochondrial-dependent pathway. Moreover, since Cisplatin is known to induce nephrotoxicity, flavonoids have shown protective effects against this side effect (Casanova et al., 2021). Specifically, they can prevent kidney cell damage by inhibiting

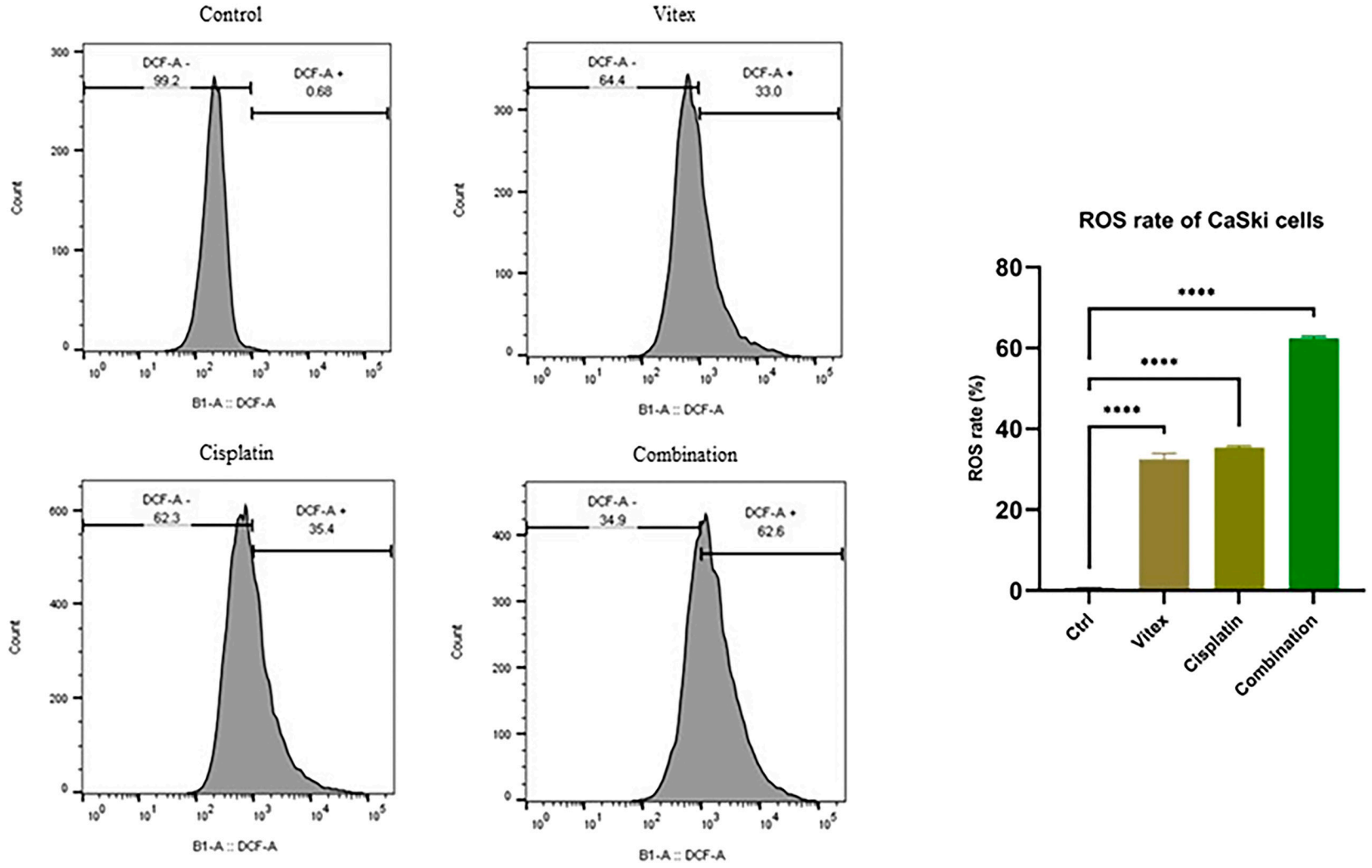


FIGURE 8
The influence of the Vitex and Cisplatin combination on ROS levels in CaSki cells. Cells in exponential growth were treated with the specified concentrations, and ROS levels were measured via flow cytometry, showing ROS (DCF) levels (%) in relation to the control (*p < 0.05, **p < 0.01, ***p < 0.001, ****p < 0.0001).

10.3389/fphar.2024.1476152

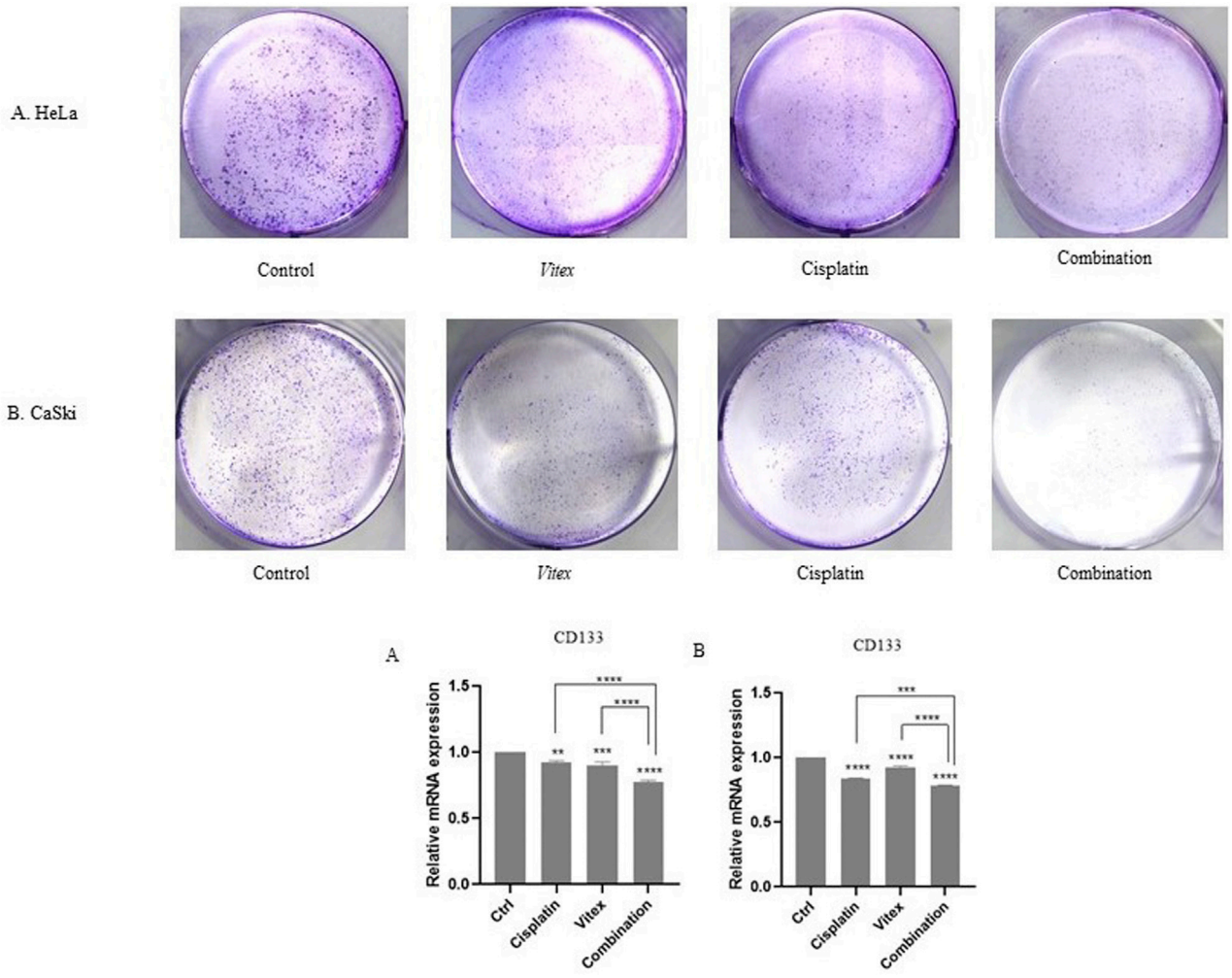


FIGURE 9
The effect of the *Vitex* and Cisplatin combination on stemness characteristics. **(A)** In HeLa cells, the number of colonies greatly decreases in the combination group when compared to the control. **(B)** A similar decrease in colony numbers is observed in the CaSki cell line with combination treatment. Changes in the stem cell marker CD_{133} are noted in the combination group (*p < 0.05, **p < 0.01, ***p < 0.001, ****p < 0.0001).

apoptosis through the inactivation of p53, mitogen-activated protein kinase (MAPK), and protein kinase B (AKT) signaling pathways (Ju et al., 2015; Wang et al., 2018).

A study conducted by Lui, N et al., in 2018, on *V. negundo L* found that its metabolic, VB1 (vitexin metabolic 1), can induce apoptosis by increasing the expression of pro-apoptotic Bax and decreasing the anti-apoptotic Bcl-2, thereby leading to cell cycle arrest at the G2/M phase in melanoma cells (Liu et al., 2018).

Our data also confirmed that the *V. pseudo-Negundo* can promote cell cycle arrest at the G2-M phase in HeLa cell lines, whereas Cisplatin causes the cell cycle arrest in the G0-G1 phase. Additionally, following treatment with Cisplatin and *V. pseudo-Negundo* fraction, cell cycle arrest in CaSki cell line is comparable to that in the HeLa cell line; however, the rate of cell cycle arrest in the G0-G1 phase remains greater than that in the G2-M phase in the CaSki cell lines. These suggest a synergistic effect for the *V. pseudo-Negundo* and Cisplatin combination. In this regard, Meng et al. reported that Cyclin B1 and CDK1 proteins are significantly reduced after treatment of prostate cancer cells, which results in cell cycle arrest in the G2/M phase (Meng et al., 2012).

Moreover, we observed that monotherapy with *V. pseudo-Negundo* extraction significantly induced apoptosis at high concentrations while inhibiting apoptosis at low concentrations in both cell lines. With that context, we observed that combination therapy enables more effectiveness at lower dosages of *V. pseudo-Negundo* than monotherapy in both cell lines.

Furthermore, our results indicated that the methanolic extraction of *V. pseudo-Negundo* promotes apoptosis through downregulating Bcl-2-related genes and upregulating Bax. Furthermore, the high apoptotic levels were associated with a significant upregulation in the expression level of caspase-3/8/9 in both cell lines, suggesting that apoptosis induction occurs through the caspase-dependent mitochondrial pathway following the combination therapy of *V. pseudo-Negundo* extraction and Cisplatin. Lui et al. also highlighted that changes in gene expression of p53 significantly alter apoptosis and cell cycle

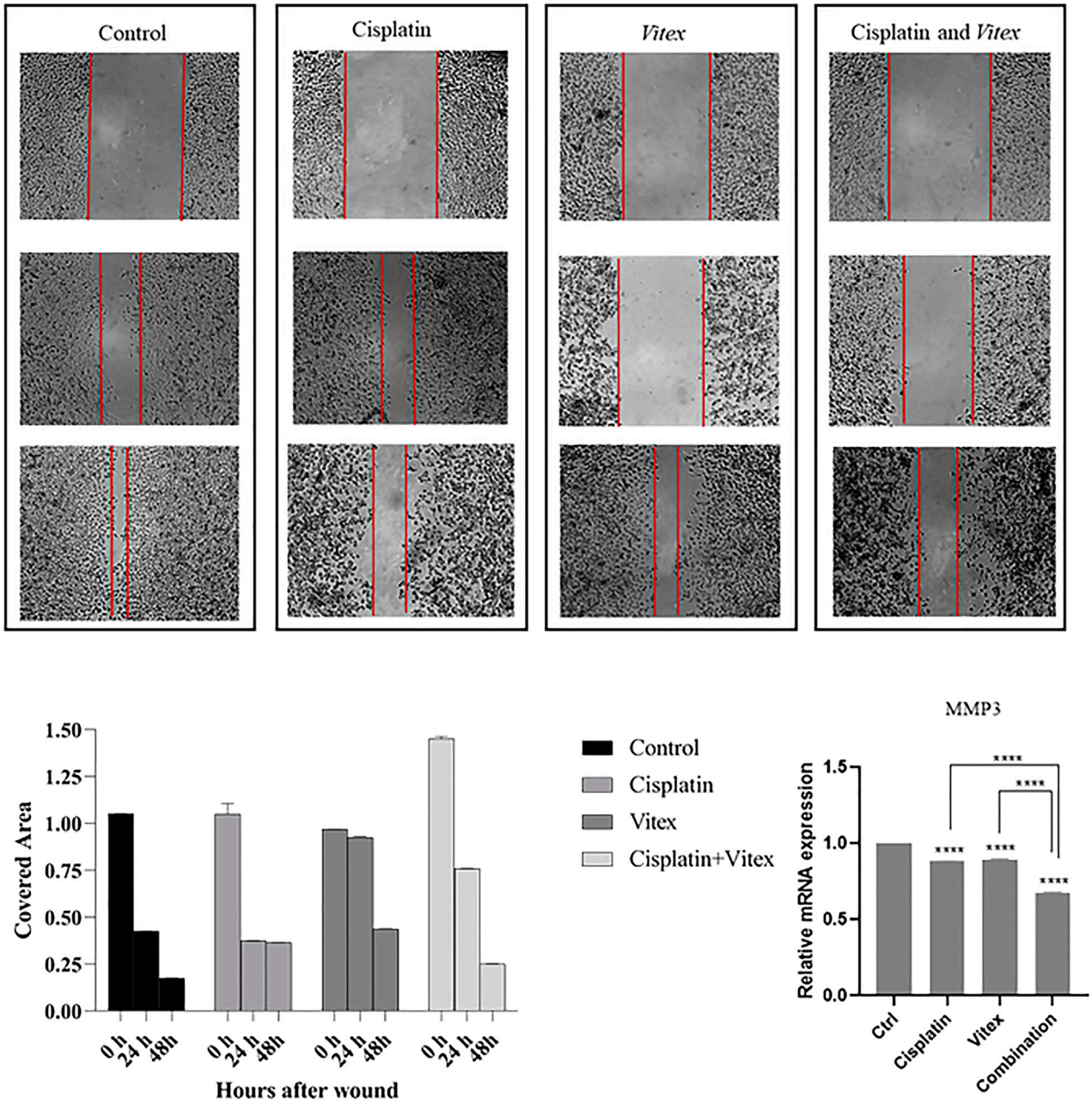


FIGURE 10
The effect of the *Vitex* and Cisplatin combination on migration and motility in HeLa Cell. After 48 h, this combination results in a significant reduction of motility characteristics compared to control groups. **(A)** Shows covered area by cells after 48 h treatment in which groups. **(B)** Shows alteration of MMP3 expression and compression of it in treatment groups and control group (*p < 0.05, **p < 0.01, ***p < 0.001, ****p < 0.0001).

pathways (Liu et al., 2018). Thus, we hypothesize that the observed apoptosis rates in our study may hinge on p53 induction, subsequently promoting caspase gene expression and apoptosis through the mitochondrial pathway. Moreover, Khan et al., noted that increased levels of ROS could lead to oxidative damage and DNA damage, ultimately modulating Bcl-2 and reducing mitochondrial membrane integrity, which triggers mitochondrial-dependent apoptosis (Khan et al., 2012).

Furthermore, ROS generation following the use of specific chemotherapeutic agents, can effectively destroy tumor cells through promoting apoptosis. Consequently, it is useful to consider effective ways to achieve significant synergy by combining agents with similar ability to alter redox conditions. Cisplatin is capable of producing ROS that leads to oxidative stress (Poveda et al., 2007; Serkies and Jassem, 2004). While increased ROS can facilitate cancer progression, excessive accumulation leads to apoptosis induction (Gorrini et al., 2013). As a result, to promote the induction of cell death as an anticancer strategy, it is suggested to increase the level of ROS (Raj et al., 2011; Wang et al., 2015; Hang et al., 2018). It has been reported that medicinal metabolites

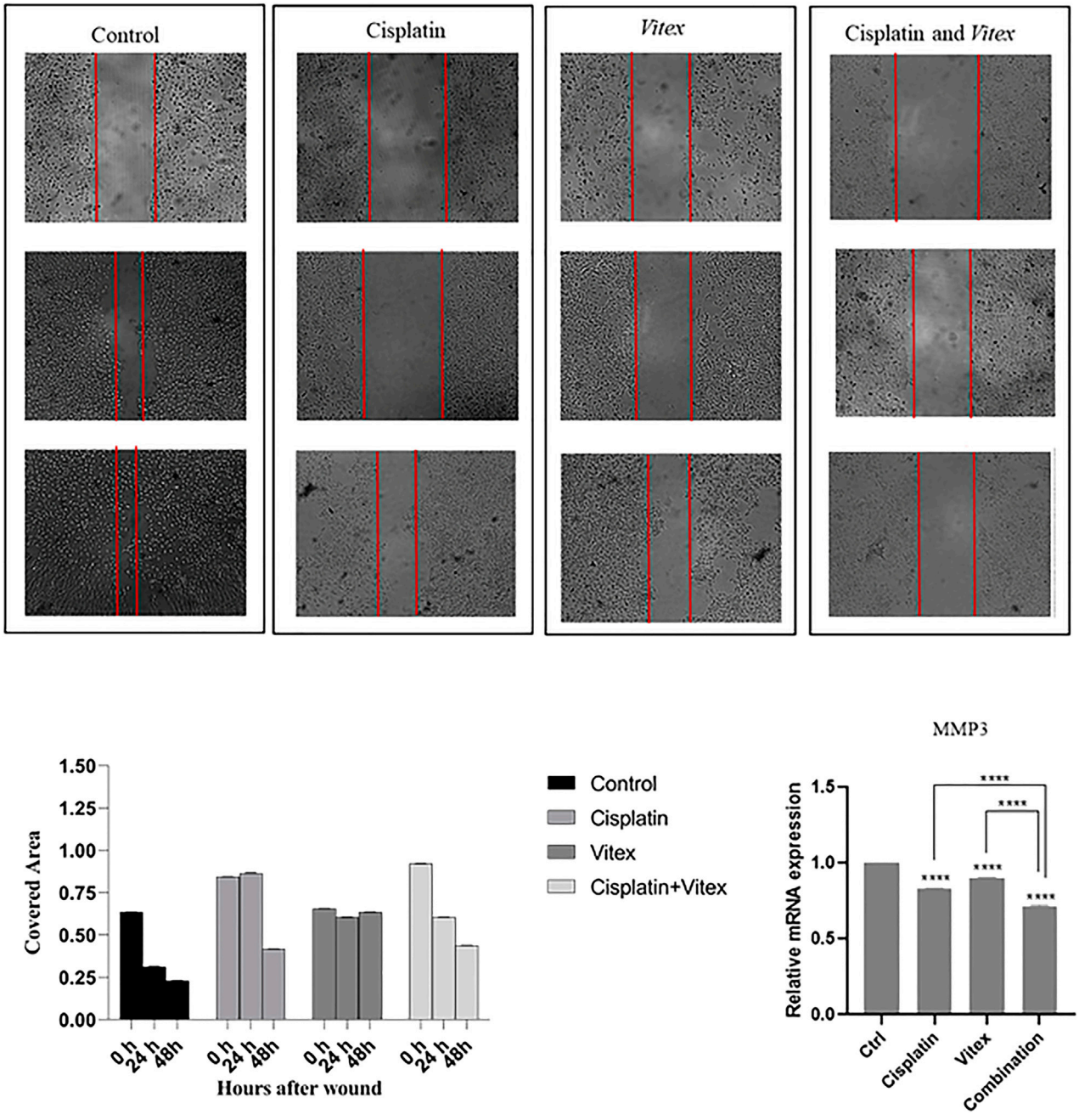


FIGURE 11
The effect of the *Vitex* and Cisplatin combination on migration and motility in CaSki Cell. After 48 h, this combination results in a significant reduction of motility characteristics compared to control groups. **(A)** Shows covered area by cells after 48 h treatment in which groups. **(B)** Shows alteration of MMP3 expression and compression of it in treatment groups and control group (*p < 0.05, **p < 0.01, ***p < 0.001, ****p < 0.0001).

extracted from plants can lead to the induction of intracellular ROS and subsequently DNA damage and increased apoptosis (Hang et al., 2018; Yang et al., 2017).

Here, we demonstrated that *V. pseudo-Negundo* can increase the toxic effect of cisplatin through promoting ROS generation, thereby promoting apoptosis in CC cells. It has been shown that *V. pseudo-Negundo* can enhance the cytotoxic effects of Cisplatin by promoting ROS generation, resulting in increased apoptosis in cervical cancer cells. ROS facilitates the migration of immune cells to damaged tissues and plays a role in infection control during the inflammatory response (Gulumian et al., 2018). Furthermore, ROS promotes the proliferation of keratinocytes, endothelial cells, and fibroblasts, potentially leading to apoptosis and tissue damage (Dunnill et al., 2017). As suggested in this study, elevated ROS levels post-combination treatment was associated with enhanced apoptosis through a mitochondria-dependent pathway in Cisplatin-resistant cells. Liu et al. similarly found that VB1 enhances intracellular ROS accumulation, resulting in DNA damage and increased apoptosis

alongside G2/M phase cell cycle arrest in vemurafenib-resistant melanoma cells (Liu et al., 2018).

In addition to apoptosis, which is a critical aspect of cancer progression, we assessed other hallmarks of cancer progression through this experiment. Metastasis is one the most pivotal processes in cancer progression, and MMPs appear to a play critical role in both metastasis and apoptosis processes (Mannello et al., 2005). It has been demonstrated that Cisplatin can suppress cell migration through targeting MMPs (Urso et al., 2010; Montiel et al., 2009). With that context, we established that the Cisplatin- *V. pseudo-Negundo* combination therapy might decrease the expression level of MMPs such as MMP-3 in CC cells.

In addition, significant morphological changes have appeared in CaSki and HeLa cells following *V. pseudo-Negundo* treatment. The combination treatment persuaded a notable number of CC cells to adopt a floating and round-shaped morphology. In this regard, it is speculated that *V. pseudo-Negundo* extract leads to interference in the normal physiological conditions of HeLa and CaSki cells. Moreover, the effect of Cisplatin on morphological alterations has been previously demonstrated in different cells (Gonçalves et al., 2006). Also, the results of the colony formation test indicated that the number of colonies decreased significantly after 14 days compared to the initial days following combination therapy in both cell lines. In other words, the number of colonies in combination groups compared to monotherapy and control groups decreased dramatically, while the colony numbers are not significant between treatment groups ($p < 0.0001$).

In addition to the prominent anticancer activity of Cisplatin through induction of mitochondrial apoptosis, the high side effects and frequent chemoresistance results in therapeutic failure (Galluzzi et al., 2012). Here, we introduced the ethanolic extraction of the *V. pseudo-Negundo* plant as a promising candidate for combination therapy with Cisplatin in CC treatment. We demonstrated that *V. pseudo-Negundo* has a lethal and antioxidant effect on CaSki and HeLa cancerous cells. Our data also suggested that this natural metabolic exhibited synergistic effects with Cisplatin and can increase cervical cancerous cell features such as apoptosis, ROS production, colony formation, and cell motility suggesting a novel approach for CC treatment.

5 Conclusion

In recent decades, preclinical studies have indicated the interaction between chemotherapy drugs and medicinal plant extracts as a therapeutic strategy for many malignancies. Improving the effectiveness of treatment while reducing side effects is one of the aims of combination therapy. Despite the advantages of combined treatments, they may also have disadvantages (Déciga-Campos et al., 2022). So far, the combination therapy of Cisplatin and Paclitaxel is considered a standard chemotherapeutic regimen for the treatment of recurrent or metastatic CC. However, the overall response rate and the median overall survival of patients receiving this regimen are unsatisfactory. In addition, either intrinsic or acquired resistance to Cisplatin can seriously compromise the efficacy of this widely used drug. This underscores the urgent need to introduce novel metabolites that can overcome this resistance, and increase efficacy while exerting minimal cytotoxicity. In this regard, natural metabolites appear to be promising for the treatment of malignancies including CC. Here, we established that the ethanolic extraction of *V. pseudo-Negundo* in combination with Cisplatin can increase its efficacy for the treatment of cervical cancer, suggesting a novel potential for further investigations and offering promise for future clinical therapeutic methods. According to the conducted studies, it has been reported that natural products can prevent the toxicity caused by Cisplatin in different parts of the body, such as the liver, kidney, and nervous system. As a result, the combination therapy of Cisplatin with natural products leads to a reduction in the side effects caused by Cisplatin. Therefore, it is suggested that formulations based on the natural metabolites of Cisplatin be considered and developed as a novel treatment method to prevent the progression of malignancy.

6 Limitations

Unfortunately, the number of studies and reports published in our area of study is very limited. Reported studies varied significantly according to the type of cell line, which may have affected the results. In this study, we focused on the main extract; however, it would be preferable to examine the individual active metabolites in the methanolic extract of the *V. pseudo-Negundo* plant in future clinical studies. Also, the lack of access to latest techniques and technologies such as HPLC, NMR, and lack of time for researchers had been influenced. Furthermore, future studies should investigate other genes involved in cellular mechanisms.

Data availability statement

The original contributions presented in the study are included in the article/supplementary material, further inquiries can be directed to the corresponding author.

Ethics statement

Ethical approval was not required for the studies on humans in accordance with the local legislation and institutional requirements because only commercially available established cell lines were used.

Author contributions

PSA: Writing–review and editing, Writing–original draft, Methodology, Investigation, Formal Analysis. JSN: Writing–review and editing, Project administration, Formal Analysis. ORF: Writing–review and editing, Formal Analysis. SMRH: Writing–review and editing, Formal Analysis. MB: Writing–review and editing. TEM: Writing–review and editing. HBB: Writing–review and editing, Supervision, Project administration.

Funding

The author(s) declare that financial support was received for the research, authorship, and/or publication of this article. This study was financially supported by a grant from Tabriz University of Medical Sciences, (Grant No: IR.TBZMED.VCR.REC.1400.162).

Acknowledgments

This project was supported by the Infectious and Tropical Diseases Research Center, Tabriz University of Medical Sciences, Tabriz, Iran.

Conflict of interest

The authors declare that the research was conducted in the absence of any commercial or financial relationships that could be construed as a potential conflict of interest.

Publisher's note

All claims expressed in this article are solely those of the authors and do not necessarily represent those of their affiliated organizations, or those of the publisher, the editors and the reviewers. Any product that may be evaluated in this article, or claim that may be made by its manufacturer, is not guaranteed or endorsed by the publisher.

References

Adamov, G. V., Rendyuk, T. D., Saybel, O. L., Dargaeva, T. D., Tsitsilin, A. N., and Bokov, D. O. (2022). Vitex agnus-castus: botanical features and area, chemical composition of fruit, pharmacological properties, and medicinal uses. *J. Appl. Pharm. Sci.* 12 (3), 034–044. doi:10.7324/JAPS.2022.120304

Ahmad, S. N. S., Rashtchizadeh, N., Argani, H., Roshangar, L., Ghorbanihaghjo, A., Sanajou, D., et al. (2019). Tangeretin protects renal tubular epithelial cells against experimental cisplatin toxicity. *Iran. J. basic Med. Sci.* 22 (2), 179–186. doi:10.22038/ijbms.2018.32010.7691

Aldaghi, L. S., Rezaee Seresht, H., and Cheshomi, H. (2016). The cytotoxic effect of Vitex pseudo negundo fruit in breast cancer (MCF7) cell line. *J. Sabzevar Univ. Med. Sci.* 23 (2), 353–359.

Almutairi, M. M., Alanazi, W. A., Alshammari, M. A., Alotaibi, M. R., Alhoshani, A. R., Al-Rejaie, S. S., et al. (2017). Neuro-protective effect of rutin against Cisplatin-induced neurotoxic rat model. *BMC complementary Altern. Med.* 17, 472–479. doi:10.1186/s12906-017-1976-9

Casanova, A. G., Prieto, M., Colino, C. I., Gutiérrez-Millán, C., Ruszkowska-Ciastek, B., de Paz, E., et al. (2021). A micellar formulation of quercetin prevents cisplatin nephrotoxicity. *Int. J. Mol. Sci.* 22 (2), 729. doi:10.3390/ijms22020729

Darwish, M. A., Abo-Youssef, A. M., Khalaf, M. M., Abo-Saif, A. A., Saleh, I. G., and Abdelghany, T. M. (2018). Resveratrol influences platinum pharmacokinetics: a novel mechanism in protection against cisplatin-induced nephrotoxicity. *Toxicol. Lett.* 290, 73–82. doi:10.1016/j.toxlet.2018.03.023

Dasari, S., and Bernard Tchounwou, P. (2014). Cisplatin in cancer therapy: molecular mechanisms of action. *Eur. J. Pharmacol.* 740, 364–378. doi:10.1016/j.ejphar.2014.07.025

Dasari, S., Njiki, S., Mbemi, A., Yedjou, C. G., and Tchounwou, P. B. (2022). Pharmacological effects of cisplatin combination with natural products in cancer chemotherapy. *Int. J. Mol. Sci.* 23 (3), 1532. doi:10.3390/ijms23031532

Déciga-Campos, M., Ventura-Martínez, R., González-Trujano, M. E., and Silveira, D. (2022). Editorial: Pharmacological interaction between drugs and medicinal plants. *Front. Pharmacol.* 13, 1081090. doi:10.3389/fphar.2022.1081090

Dunnill, C., Patton, T., Brennan, J., Barrett, J., Dryden, M., Cooke, J., et al. (2017). Reactive oxygen species (ROS) and wound healing: the functional role of ROS and emerging ROS-modulating technologies for augmentation of the healing process. *Int. wound J.* 14 (1), 89–96. doi:10.1111/iwj.12557

Erdogan, S., Turkekul, K., Serttas, R., and Erdogan, Z. (2017). The natural flavonoid apigenin sensitizes human CD44+ prostate cancer stem cells to cisplatin therapy. *Biomed. and Pharmacother.* 88, 210–217. doi:10.1016/j.biopha.2017.01.056

Florea, A.-M., and Büsselberg, D. (2011). Cisplatin as an anti-tumor drug: cellular mechanisms of activity, drug resistance and induced side effects. *Cancers* 3 (1), 1351–1371. doi:10.3390/cancers3011351

Galluzzi, L., Senovilla, L., Vitale, I., Michels, J., Martins, I., Kepp, O., et al. (2012). Molecular mechanisms of cisplatin resistance. *Oncogene* 31 (15), 1869–1883. doi:10.1038/onc.2011.384

Garbi, M. I., Osman, E. E., Kabbashi, A. S., Saleh, M. S., Yuosof, Y. S., Mahmoud, S. A., et al. (2015). Cytotoxicity of Vitex trifolia leaf extracts on MCF-7 and Vero cell lines. *J. Sci. Innov. Res.* 4 (2), 89–93. doi:10.31254/jsir.2015.4208

Gonçalves, E. M., Ventura, C. Â., Yano, T., Rodrigues Macedo, M. L., and Genari, S. C. (2006). Morphological and growth alterations in Vero cells transformed by cisplatin. *Cell Biol. Int.* 30 (6), 485–494. doi:10.1016/j.cellbi.2005.12.007

Gong, G., Shen, Y.-L., Lan, H.-Y., Jin, J.-M., An, P., Zhang, L.-J., et al. (2021). The Cyr61 is a potential target for rotundifuran, a natural labdane-type diterpene from Vitex trifolia L., to trigger apoptosis of cervical cancer cells. *Oxidative Med. Cell. Longev.* 2021 (1), 6677687. doi:10.1155/2021/6677687

Gorrini, C., Harris, I. S., and Mak, T. W. (2013). Modulation of oxidative stress as an anticancer strategy. *Nat. Rev. Drug Discov.* 12 (12), 931–947. doi:10.1038/nrd4002

Graham, J. G., Quinn, M. L., Fabricant, D. S., and Farnsworth, N. R. (2000). Plants used against cancer–an extension of the work of Jonathan Hartwell. *J. Ethnopharmacol.* 73 (3), 347–377. doi:10.1016/s0378-8741(00)00341-x

Gulumian, M., Yahaya, E. S., and Steenkamp, V. (2018). African herbal remedies with antioxidant activity: a potential resource base for wound treatment. *Evidence-Based Complementary Altern. Med.* 2018 (1), 4089541. doi:10.1155/2018/4089541

Hang, W., Yin, Z.-X., Liu, G., Zeng, Q., Shen, X.-F., Sun, Q.-H., et al. (2018). Piperlongumine and p53-reactivator APR-246 selectively induce cell death in HNSCC by targeting GSTP1. *Oncogene* 37 (25), 3384–3398. doi:10.1038/s41388-017-0110-2

Hazman, Ö., Bozkurt, M. F., Fidan, A. F., Uysal, F. E., and Çelik, S. (2018). The effect of boric acid and borax on oxidative stress, inflammation, ER stress and apoptosis in cisplatin toxication and nephrotoxicity developing as a result of toxication. *Inflammation* 41, 1032–1048. doi:10.1007/s10753-018-0756-0

Heinrich, M., Jalil, B., Abdel-Tawab, M., Echeverria, J., Kulić, Ž., McGaw, L. J., et al. (2022). Best practice in the chemical characterisation of extracts used in pharmacological and toxicological research—the ConPhyMP—guidelines. *Front. Pharmacol.* 13, 953205. doi:10.3389/fphar.2022.953205

Jing, R., Ban, Y., Xu, W., Nian, H., Guo, Y., Geng, Y., et al. (2019). Therapeutic effects of the total lignans from Vitex negundo seeds on collagen-induced arthritis in rats. *Phytomedicine* 58, 152825. doi:10.1016/j.phymed.2019.152825

Ju, S. M., Kang, J. G., Bae, J. S., Pae, H. O., Lyu, Y. S., and Jeon, B. H. (2015). The flavonoid apigenin ameliorates cisplatin-induced nephrotoxicity through reduction of p53 activation and promotion of PI3K/akt pathway in human renal proximal tubular epithelial cells. *Evidence-Based Complementary Altern. Med.* 2015 (1), 186436. doi:10.1155/2015/186436

Kachadourian, R., Leitner, H. M., and Day, B. J. (2007). Selected flavonoids potentiate the toxicity of cisplatin in human lung adenocarcinoma cells: a role for glutathione depletion. *Int. J. Oncol.* 31 (1), 161–168. doi:10.3892/ijo.31.1.161

Khan, M., Zheng, B., Yi, F., Rasul, A., Gu, Z., Li, T., et al. (2012). Pseudolaric Acid B induces caspase-dependent and caspase-independent apoptosis in u87 glioblastoma cells. *Evidence-based Complementary Altern. Med.* 2012 (1), 957568. doi:10.1155/2012/957568

Kirtikar, K. R., and Basu, B. D. (1918). *Indian medicinal plants: publisher not identified Basu*. Bhuwaneśwari Âśrama.

Li, H., Wu, X., and Cheng, X. (2016). Advances in diagnosis and treatment of metastatic cervical cancer. *J. Gynecol. Oncol.* 27 (4), e43. doi:10.3802/jgo.2016.27.e43

Li, J., Wang, Y., Lei, J.-C., Hao, Y., Yang, Y., Yang, C.-X., et al. (2014). Sensitisation of ovarian cancer cells to cisplatin by flavonoids from Scutellaria barbata. *Nat. Prod. Res.* 28 (10), 683–689. doi:10.1080/14786419.2013.871547

Liu, N., Wang, K. S., Qi, M., Zhou, Y. J., Zeng, G. Y., Tao, J., et al. (2018). Vitexin compound 1, a novel extraction from a Chinese herb, suppresses melanoma cell growth through DNA damage by increasing ROS levels. *J. Exp. and Clin. Cancer Res.* 37, 269–316. doi:10.1186/s13046-018-0897-x

Liu, W., Yang, B., Yang, L., Kaur, J., Jessop, C., Fadhil, R., et al. (2019a). Therapeutic effects of ten commonly used Chinese herbs and their bioactive compounds on cancers. *Evidence-Based Complementary Altern. Med.* 2019 (1), 6057837. doi:10.1155/2019/6057837

Liu, W., Yang, B., Yang, L., Kaur, J., Jessop, C., Fadhil, R., et al. (2019b). Therapeutic effects of ten commonly used Chinese herbs and their bioactive compounds on cancers. *Evidence-Based Complementary Altern. Med.* 2019, 6057837. doi:10.1155/2019/6057837

Liu, Y., Wang, X., Li, W., Xu, Y., Zhuo, Y., Li, M., et al. (2020). Oroxylin A reverses hypoxia-induced cisplatin resistance through inhibiting HIF-1α mediated XPC transcription. *Oncogene* 39 (45), 6893–6905. doi:10.1038/s41388-020-01474-x

Madhulika Singh, M. S., Kulpreet Bhui, K. B., Richa Singh, R. S., and Yogeshwer Shukla, Y. S. Tea polyphenols enhance cisplatin chemosensitivity in cervical cancer cells via induction of apoptosis. 2013.

Mannello, F., Luchetti, F., Falcieri, E., and Papa, S. (2005). Multiple roles of matrix metalloproteinases during apoptosis. *Apoptosis* 10 (1), 19–24. doi:10.1007/s10495-005-6058-7

Meng, F.-M., Yang, J.-B., Yang, C.-H., Jiang, Y., Zhou, Y.-F., Yu, B., et al. (2012). Vitexicarpin induces apoptosis in human prostate carcinoma PC-3 cells through G2/M phase arrest. *Asian Pac. J. Cancer Prev.* 13 (12), 6369–6374. doi:10.7314/apjcp.2012.13.12.6369

Montiel, M., Urso, L., de la Blanca, E. P., Marsigliante, S., and Jiménez, E. (2009). Cisplatin reduces endothelial cell migration via regulation of type 2-matrix metalloproteinase activity. *Cell. Physiology Biochem.* 23 (4-6), 441–448. doi:10.1159/000218191

Nimlamool, W., Chansakaow, S., Potikanond, S., Wikan, N., Hankittichai, P., Ruttanapattanakul, J., et al. (2022). The leaf extract of *Mitrephora chulabhorniana* suppresses migration and invasion and induces human cervical cancer cell apoptosis through caspase-dependent pathway. *BioMed Res. Int.* 2022, 2028082. doi:10.1155/2022/2028082

Poveda, A., Salazar, R., Del Campo, J. M., Mendiola, C., Cassinello, J., Ojeda, B., et al. (2007). Update in the management of ovarian and cervical carcinoma. *Clin. Transl. Oncol.* 9, 443–451. doi:10.1007/s12094-007-0083-7

Puglia, L. T., Lowry, J., and Tamagno, G. (2023). Vitex agnus castus effects on hyperprolactinaemia. *Front. Endocrinol.* 14, 1269781. doi:10.3389/fendo.2023.1269781

Raj, L., Ide, T., Gurkar, A. U., Foley, M., Schenone, M., Li, X., et al. (2011). Selective killing of cancer cells by a small molecule targeting the stress response to ROS. *Nature* 475 (7355), 231–234. doi:10.1038/nature10167

Rastogi, N., Duggal, S., Singh, S. K., Porwal, K., Srivastava, V. K., Maurya, R., et al. (2015). Proteasome inhibition mediates p53 reactivation and anti-cancer activity of 6-gingerol in cervical cancer cells. *Oncotarget* 6 (41), 43310–43325. doi:10.18632/oncotarget.6383

Salehpour, Z., Jahantab, E., Morshedloo, M. R., Iraji, A., and Mohamadi, J. (2018). Essential oil composition of aerial parts of Vitex pseudo-negundo populations collected from Southwest of Iran. *J. Essent. Oil Bear. Plants* 21 (2), 570–576. doi:10.1080/0972060x.2018.1438928

Serkies, K., and Jassem, J. (2004). Concurrent weekly cisplatin and radiotherapy in routine management of cervical cancer: a report on patient compliance and acute toxicity. *Int. J. Radiat. Oncology* Biology* Phys.* 60 (3), 814–821. doi:10.1016/j.ijrobp.2004.04.042

Shiri Aghbash, P., Hemmat, N., Baradaran, B., and Bannazadeh Baghi, H. (2023). siRNA-E6 sensitizes HPV-16-related cervical cancer through Oxaliplatin: an *in vitro* study on anti-cancer combination therapy. *Eur. J. Med. Res.* 28 (1), 42. doi:10.1186/s40001-023-01014-9

Small, Jr W., Bacon, M. A., Bajaj, A., Chuang, L. T., Fisher, B. J., Harkenrider, M. M., et al. (2017). Cervical cancer: a global health crisis. *Cancer* 123 (13), 2404–2412. doi:10.1002/cncr.30667

Talib, W. H., Awajan, D., Hamed, R. A., Azzam, A. O., Mahmod, A. I., and Al-Yasari, I. H. (2022). Combination anticancer therapies using selected phytochemicals. *Mol. Basel, Switz.* 27 (17), 5452. doi:10.3390/molecules27175452

Tandon, V. R., and Gupta, R. K. (2005). An experimental evaluation of anticonvulsant activity of Vitex-negundo. *Indian J. physiology Pharmacol.* 49 (2), 199–205.

Tsikouras, P., Zervoudis, S., Manav, B., Tomara, E., Iatrakis, G., Romanidis, C., et al. (2016). Cervical cancer: screening, diagnosis and staging. *J. buon* 21 (2), 320–325.

Urso, L., Muscella, A., Calabriso, N., Vetrugno, C., Jiménez, E., Montiel, M., et al. (2010). Effects of cisplatin on matrix metalloproteinase-2 in transformed thyroid cells. *Biochem. Pharmacol.* 79 (6), 810–816. doi:10.1016/j.bcp.2009.10.013

Wang, L., Yu, Y., Chow, D.-C., Yan, F., Hsu, C.-C., Stossi, F., et al. (2015). Characterization of a steroid receptor coactivator small molecule stimulator that overstimulates cancer cells and leads to cell stress and death. *Cancer cell* 28 (2), 240–252. doi:10.1016/j.ccell.2015.07.005

Wang, S.-w., Xu, Y. I., Weng, Y.-y., Fan, X.-y., Bai, Y.-f., Zheng, X.-y., et al. (2018). Astilbin ameliorates cisplatin-induced nephrotoxicity through reducing oxidative stress and inflammation. *Food Chem. Toxicol.* 114, 227–236. doi:10.1016/j.fct.2018.02.041

Yang, Y., Zhang, Y., Wang, L., and Lee, S. (2017). Levistolide A induces apoptosis via ROS-mediated ER stress pathway in colon cancer cells. *Cell. Physiology Biochem.* 42 (3), 929–938. doi:10.1159/000478647

Zulfiker, A. H. M., Hashimi, S. M., Good, D. A., Grice, I. D., and Wei, M. Q. (2017). Cane toad skin extract—induced upregulation and increased interaction of serotonin 2A and D2 receptors via gq/11 signaling pathway in CLU213 cells. *J. Cell. Biochem.* 118 (5), 979–993. doi:10.1002/jcb.25627

frontiers | Frontiers in Pharmacology

TYPE Original Research
PUBLISHED 14 January 2025
DOI 10.3389/fphar.2024.1501744

Check for updates

OPEN ACCESS

EDITED BY
Qingquan Liu,
Capital Medical University, China

REVIEWED BY
Gabriela Cristina Fernandez,
National Scientific and Technical Research Council (CONICET), Argentina
Jose Vitor Lima-Filho,
Federal Rural University of Pernambuco, Brazil

*CORRESPONDENCE
Linsen Li,
2008027@muc.edu.cn
Dan Zhu,
zhudanred@aliyun.com

RECEIVED 25 September 2024
ACCEPTED 16 December 2024
PUBLISHED 14 January 2025

CITATION
Dong S, Bai X, Chen B, Fan M, Liu Q, Zhao Y, Li L and Zhu D (2025) *Panzerina lanata* accelerates methicillin-resistant *Staphylococcus aureus* eradication by promoting migration and activation of neutrophils.
Front. Pharmacol. 15:1501744.
doi: 10.3389/fphar.2024.1501744

COPYRIGHT
© 2025 Dong, Bai, Chen, Fan, Liu, Zhao, Li and Zhu. This is an open-access article distributed under the terms of the Creative Commons Attribution License (CC BY). The use, distribution or reproduction in other forums is permitted, provided the original author(s) and the copyright owner(s) are credited and that the original publication in this journal is cited, in accordance with accepted academic practice. No use, distribution or reproduction is permitted which does not comply with these terms.

Panzerina lanata accelerates methicillin-resistant *Staphylococcus aureus* eradication by promoting migration and activation of neutrophils

Shuai Dong, Xingyuan Bai, Bin Chen, Minzhe Fan, Qi Liu, Yubo Zhao, Linsen Li* and Dan Zhu*

Laboratory of Pharmacology, Key Laboratory of Ethnomedicine of Ministry of Education, School of Pharmacy, Minzu University of China, Beijing, China

Background: *Panzerina lanata* (Lanata) is generally used to treat pustule infection in Inner Mongolia folk medicine and is called "the holy medicine for pustule." However, the pharmacological mechanism of Lanata in treating pustule infection is still unclear.

Aims: This study aimed to investigate the therapeutic effects of Lanata on skin infection and explore the underlying mechanisms.

Methods: A skin wound methicillin-resistant *Staphylococcus aureus* (MRSA) infection mouse model was established to evaluate the healing effect of Lanata on infected wounds. *In vitro* assays were also conducted to determine the antibacterial activity of Lanata. Flow cytometry and immunohistochemistry were used to dynamically detect the number of neutrophils in the bone marrow, peripheral blood, and MRSA-infected wound. Protein expression in the infected wound skin was detected by a protein chip. Using an air pouch MRSA infection mouse model, the number of neutrophils, reactive oxygen species (ROS) level in neutrophils, and neutrophil extracellular trap (NET) formation were dynamically detected by flow cytometry and immunofluorescence. RNA-seq, RT-qPCR, flow cytometry, ELISA, and CXC chemokine receptor 2 (CXCR2) and P-selectin glycoprotein ligand-1 (PSGL-1) inhibitors were used to explore the mechanism of Lanata in regulating neutrophils.

Results: *In vitro* assays showed that Lanata had no direct antibacterial activity. In skin wound MRSA-infected mouse, Lanata promoted the rapid migration of neutrophils from the bone marrow via peripheral blood to the wound site to eradicate MRSA in the acute stage of infection and accelerate wound healing. Skin

Abbreviations: ABAH, 4-aminobenzoic hydrazide; CXCR2, CXC chemokine receptor 2; DEGs, differentially expressed genes; DEPs, differentially expressed proteins; H&E, hematoxylin and eosin; MFI, mean fluorescence intensity; MPO, myeloperoxidase; MRSA, methicillin-resistant *Staphylococcus aureus*; NE, neutrophil elastase; NETs, neutrophil extracellular traps; NOX, nicotinamide adenine dinucleotide phosphate oxidase; PAD4, peptidyl arginine deiminase 4; PSGL-1, P-selectin glycoprotein ligand-1; RBC, red blood cell; ROS, reactive oxygen species; TTC, 2,3,5-triphenyltetrazolium chloride.

protein chip analysis showed that Lanata upregulated CXCR2 and PSGL-1 protein levels in skin wounds. Furthermore, analysis using the air pouch MRSA infection mouse model found that Lanata not only promoted the rapid migration of neutrophils from peripheral blood to the air pouch but also enhanced the activation of neutrophils, including the increase of ROS and the release of NETs, and upregulated the expression of CXCR2, PSGL-1, and myeloperoxidase (MPO) in neutrophils. Inhibition of CXCR2 and MPO significantly attenuated the effect of Lanata on promoting migration and activation of neutrophils.

Conclusion: *Panzerina lanata* resists MRSA infection by promoting migration and activation of neutrophils to rapidly eradicate MRSA.

KEYWORDS

***Panzerina lanata*, methicillin-resistant *Staphylococcus aureus*, migration, activation, neutrophil**

1 Introduction

Bacterial infectious diseases are highly prevalent and are an important cause of death worldwide. An estimated 7.7 million infection-related deaths were reported to be linked to 33 bacterial pathogens worldwide in 2019 (Collaborators, 2022). Skin and soft tissue infection is one of the most common bacterial infections, and the rapid spread of methicillin-resistant *Staphylococcus aureus* (MRSA) strains contributes to its increasing incidence (Watkins and David, 2021). With the widespread use of antibiotics, multi-drug resistant bacteria continue to emerge, and the treatment of bacterial infectious diseases is facing major challenges. This forces medical workers to open up new ideas and ways to find anti-infective drugs.

Panzerina lanata (Lanata) is a plant of the Lamiaceae family and genus *Panzerina*, and its aboveground part is the characteristic Mongolian medicinal herb called Baiyimucao in China. Lanata is generally used to treat pustule infection in Inner Mongolia folk medicine and is called "the holy medicine of pustule" (Wu and Fu, 1988; Xing, 2006; Meng, 2009). We have been studying the efficacy, toxicity, and chemical composition of Lanata since 2009 (Li, 2011; Zhou, 2022). Our previous research identified a total of 20 natural products in Lanata, including alkaloids, flavonoids, organic acids, and lignans (Mi et al., 2021). However, the pharmacological mechanism of Lanata in treating pustule infection is still unclear. In this study, we used MRSA as the source of infection to first evaluate the effect of Lanata on skin MRSA infection in mice. We found that Lanata clearly promoted healing of infected wounds, accompanied by a significant change in the number of neutrophils in peripheral blood. However, we also observed that Lanata had no direct antibacterial activity *in vitro*. Therefore, our study mainly focused on investigating neutrophils' dynamics and activity in the context of infection.

Neutrophils are the key effector cells of the innate immune system, and being the professional phagocytes, they are the first one migrating to the site of infection, thus constituting the first line of defense (Rawat et al., 2023). Upon arrival at the site of infection, neutrophils eradicate bacteria through phagocytosis and the release of reactive oxygen species (ROS), degranulation, and neutrophil extracellular traps (NETs) (Cristinziano et al., 2022), which are crucial for the body's ability to eradicate bacteria. Neutrophils are becoming a new target for the treatment of multi-inflammatory diseases (Cross et al., 2020).

In this study, we investigated the therapeutic effect of Lanata on skin infection and its underlying mechanisms, including migration and activation of neutrophils during MRSA infection.

2 Materials and methods

2.1 Materials and reagents

The following materials and reagents were purchased: MRSA strain ATCC43300 (General Microbiological Culture Collection Center, Beijing, China); 2,3,5-triphenyltetrazolium chloride (TTC) (Beijing Wanjing Lizhi I Biotechnology Ltd., Beijing, China); linezolid (Aladdin Industrial Corporation, Los Angeles, United States); SB225002 and 4-aminobenzoic hydrazide (ABAH) (TargetMol Chemicals Inc., Boston, United States); APC anti-mouse CD45 antibody (Clone: 30-F11), PE anti-mouse/human CD11b antibody (Clone: M1/70), PerCP/Cyanine5.5 anti-mouse Ly-6G antibody (Clone: 1A8), FITC anti-mouse CXCR2 antibody (Clone: SA044G4), and RBC lysis buffer (BioLegend Inc., San Diego, United States); Alexa Fluor 488 anti-mouse PSGL-1 antibody (Clone: 4RA10) (Thermo Fisher Scientific, Inc., New York, United States); rabbit monoclonal MPO antibody (Abcam Ltd., Cambridge, United Kingdom); rabbit neutrophil elastase antibody (Novus Biologicals Inc., Littleton, United States); Alexa Fluor 488 goat anti-rabbit IgG secondary antibody and DAPI (Wuhan Servicebio Technology Ltd., Wuhan, China); DCFH-DA (Beyotime Biotechnology Ltd., Shanghai, China); Mouse PSGL-1 and CXCR2 ELISA kits (Jingmei Biotechnology Ltd., Yancheng, China); MPO ELISA kit (Jiubang Science & Technology Ltd., Quanzhou, China); RIPA lysis buffer (Lablead Biotechnology Ltd., Beijing, China); and Mouse StarScript III RT Mix with gDNA Remover and 2 × RealStar Fast SYBR qPCR Mix (GenStar Biotech Ltd., Beijing, China).

2.2 Preparation of Lanata

The Lanata herb was collected from the Dalad Banner of Inner Mongolia Province, China, and identified by Professor Chun-Lin

Long (College of Life and Environmental Sciences, Minzu University of China). The herb (10 kg) was reflux-extracted with 80 L 75% ethanol (1:8, w/v) for 2 h. The extracting liquid was transferred to the concentration tank; then, the herb remnant was reflux-extracted for 1 h. The two extraction solutions were concentrated under reduced pressure, and 1.25 kg extract was obtained. The extract rate was 12.5%. The extract was stored at −20°C and dissolved in distilled water to the indicated concentrations before use.

2.3 Experimental animals

Male ICR mice (23–25 g, 5 weeks old) were purchased from SPF (Beijing) Biotechnology Co., Ltd. (SCXK 2019-0010) and housed in a room with stable temperature (22°C ± 2°C), humidity (50% ± 10%), and 12 h/12 h light/dark cycle. All mice had access to free water and food and underwent one-week accommodation before experiments. All procedures were approved by the Biological and Medical Ethics Committee, Minzu University of China (approval no. ECMU2023001AO).

2.4 Skin wound MRSA infection

After the mice were anesthetized with 1% pentobarbital sodium (50 mg/kg), hair was removed from a 3 cm × 3 cm area on the back of anesthetized mice and a skin area of 5-mm-diameter area was cut. Then, 5 μL of the 2×10^8 CFU/mL MRSA bacterial solution (0.9% saline) was added to the wound. Mice in the sham group were subjected to the same surgical procedures without MRSA.

The skin wound MRSA infection mice were divided into the following five groups: MRSA (model, vehicle), MRSA + Lanata-L (Lanata low-dose, 2 g/kg herb), MRSA + Lanata-M (Lanata medium-dose, 4 g/kg herb), MRSA + Lanata-H (Lanata high-dose, 8 g/kg herb), and MRSA + Linezolid (linezolid, 0.12 g/kg). All drugs with distilled water as the vehicle were administered by oral gavage immediately after infecting with MRSA. Mice in the sham and the control groups were given an equal volume of vehicle. Mice in all groups were administered five times (0 day, 1 day, 2 days, 3 days, and 4 days).

2.5 Air pouch MRSA infection

After the mice were anesthetized, 3 mL air sterilized through a 0.22-μM filter was injected subcutaneously on the dorsal region of anesthetized mice to generate an air pouch, which was then injected with 1 mL 1×10^6 CFU/mL MRSA bacterial solution (0.9% saline) or 1 mL of 0.9% saline (control group).

The air pouch MRSA infection mice were divided into two groups: MRSA (model, vehicle) and MRSA + Lanata (Lanata, 4 g/kg herb). Lanata and distilled water as the vehicle were administered by oral gavage immediately after infecting with MRSA. Mice in the control group were given an equal volume of vehicle. Mice in all groups were administered once.

2.6 Healing rate of infected wounds

A metal foil with an inner diameter of 9 mm was placed over the wound as a reference for area measurement, and ImageJ software was used to calculate the area of photographed wounds. The healing rate of infected wounds was calculated according to the following formula: healing rate of infected wound = (wound area 0 day post-operation − wound area n days post-operation)/wound area 0 day post-operation × 100%.

2.7 Antibacterial activity of Lanata

The zone of growth inhibition test was performed according to previous reports (Moussa et al., 2013). The concentrated extract of Lanata was dissolved in the tryptic soy broth (TSB) liquid medium to a concentration of 200 mg/mL, and serial dilutions of Lanata (100, 50, 25, 12.5, and 6.25 mg/mL) were prepared in a 96-well plate in a maximum volume of 100 μL of TSB. The 100 μL 1×10^6 CFU/mL MRSA bacterial solution was added to each well. Here, 200 μL TSB was used as negative control, while 100 μL of the TSB +100 μL 1×10^6 CFU/mL MRSA bacterial solution was used as positive control. After incubation at 37°C for 24 h, 20 μL of the 0.5% TTC solution was added to each well, followed by incubation at 37°C for 24 h and OD measurement at 485 nm.

2.8 Detection of neutrophils in peripheral blood

Blood was collected from the orbital sinus of anesthetized mice at 2 h, 6 h, 12 h, 24 h, 48 h, and 72 h (skin wound) or at 4 h, 6 h, 12 h, and 24 h (air pouch) post-MRSA infection. A volume of 20 μL blood was added to 1 mL of 1 × red blood cell (RBC) lysis buffer and incubated at 37°C protected from light for 5 min, followed by centrifugation at 350 g/min for 5 min. The supernatant was discarded, and the cell pellet was washed with PBS and incubated with the APC anti-mouse CD45 antibody, PE anti-mouse CD11b antibody, and PerCP/Cyanine5.5 anti-mouse Ly-6G antibody. After washing with PBS, the cells were analyzed on a FACSCelesta (BD, America), and data were analyzed with FlowJo v10.

2.9 Detection of neutrophils in the bone marrow

Mice were sacrificed following blood collection, and hind limbs were separated. The bone marrow cavity was rinsed with 1 mL PBS for three times to obtain the bone marrow cells, which were analyzed by flow cytometry, as described above.

2.10 Detection of neutrophils in air pouch

At 4 h, 6 h, 12 h, and 24 h post-infection, 1 mL solution (PBS containing 5.4 mM EDTA-Na_2) was injected into the air pouch for lavage, and the lavage fluid was collected and centrifuged at 500 g/min for 10 min. The supernatant was discarded, and the cells in the

air pouch were collected and analyzed by flow cytometry, as described above.

2.11 Hematoxylin and eosin staining and immunohistochemistry

At 2 h, 6 h, 12 h, 24 h, 48 h, and 72 h post-infection, the mice were sacrificed and a 2-cm × 2-cm wound skin was obtained to perform H&E staining and immunohistochemistry, according to previous reports (Yuan et al., 2014).

2.12 Detection of bacterial load

At 6 h, 12 h, 24 h, and 48 h post-MRSA infection, skin samples of 2 cm × 2 cm around the wound were obtained and added to 1 mL of 0.9% saline and immediately homogenized. At 4 h, 6 h, 12 h, and 24 h post-infection, the lavage fluid in the air pouch was collected and serially diluted in saline.

Serially diluted solutions of skin homogenates and air pouch lavage fluids were spread on a TSA plate and incubated at 37°C for 24 h to conduct colony count.

2.13 Protein chip analysis of the wound skin

At 6 h post-infection, skin samples of 2 cm × 2 cm around the wound were obtained, and RIPA lysis buffer was added and homogenized immediately. Lysates were centrifuged at 12,000 g/min for 10 min and sent to RayBiotech Guangzhou Co., Ltd. to detect the concentration of 200 proteins. A p-value < 0.05 and fold change >2 or <0.5 were set as thresholds for significantly differentially expressed proteins (DEPs). Enrichment analysis of DEPs was conducted using the GO (http://www.geneontology.org/) and KEGG (http://www.kegg.jp/) databases.

2.14 Detection of ROS in neutrophils

At 4 h, 6 h, 12 h, and 24 h post-MRSA infection, cells in the air pouch were washed with PBS and incubated with the APC anti-mouse CD45 antibody, PE anti-mouse CD11b antibody, PerCP/Cyanine5.5 anti-mouse Ly-6G antibody, and DCFH-DA. After washing with PBS, the cells were analyzed by flow cytometry, as described above.

2.15 Immunofluorescence staining of NETs

At 4 h, 6 h, 12 h, and 24 h post-infection, 5 μL cell suspension was evenly distributed on a slide in an area of 1 cm^2, blocked with 5% BSA overnight at 4°C and incubated with the rabbit anti-neutrophil elastase (NE) antibody for 4 h at room temperature, washed with PBS, and incubated with Alexa Fluor 488 goat anti-rabbit IgG secondary antibody for 1 h and DAPI for 15 min at room temperature. Images were captured with the FV3000 confocal system (Olympus, Japan).

2.16 RNA-seq analysis of neutrophils

At 6 h post-infection, neutrophils in the air pouch were collected in both the MRSA and MRSA + Lanata groups. Cells were washed with PBS, and total RNA was extracted and quantified. The sequencing library was sequenced on a NovaSeq 6000 platform by Beijing Qinglian Biotech Co., Ltd. Differential expression analysis was performed using the Love et al. (2024) R package. A p-value < 0.05 and fold change >2 or <0.5 were set as thresholds for significantly differentially expressed genes (DEGs). Enrichment analysis of DEGs was conducted using GO and KEGG databases.

2.17 RT-qPCR determination

Neutrophils in the air pouch and blood were collected at 4 h, 6 h, 12 h, and 24 h post-infection. According to the RNA extraction method, total mRNA was extracted with TRIzol, chloroform, isopropanol, ethanol, and other reagents. The total RNA concentration was measured using NanoDrop 2000 (Thermo Fisher Scientific, United States), and reverse transcription was performed with StarScript III RT Mix with gDNA Remover. Results were analyzed using 2 × RealStar Fast SYBR qPCR Mix on LightCycler® 96. Primers used are presented in Supplementary Table S1.

2.18 ELISA determination

Skin samples of 2 cm × 2 cm around the wound were obtained at 6 h post-infection. At 4 h, 6 h, 12 h, and 24 h post-infection, neutrophils in the air pouch and blood were collected. P-selectin glycoprotein ligand-1 (PSGL-1) and CXC chemokine receptor 2 (CXCR2) in the skin and myeloperoxidase (MPO) in neutrophils were determined, following the manufacturer's instructions.

2.19 Detection of CXCR2 and PSGL-1 in neutrophils

At 4 h, 6 h, 12 h, and 24 h post-infection, cells in peripheral blood and air pouch were washed with PBS and incubated with the APC anti-mouse CD45 antibody, PE anti-mouse CD11b antibody, PerCP/Cyanine5.5 anti-mouse Ly-6G antibody, and FITC anti-mouse CXCR2 antibody or Alexa Flour 488 (AF488) anti-mouse PSGL-1 antibody. After washing with PBS, the cells were analyzed on a FACSCelesta instrument, and data were analyzed with FlowJo v10.

2.20 Inhibition of MPO and CXCR2 in neutrophils

At 0.5 h before MRSA was injected into the air pouch, the CXCR2 inhibitor SB225002 (10 mg/kg) or MPO inhibitor ABAH (40 mg/kg) was intraperitoneally injected into mice. The air pouch MRSA infection mice were divided into the following six groups: the model group (MRSA, vehicle), MRSA + Lanata group (MRSA +

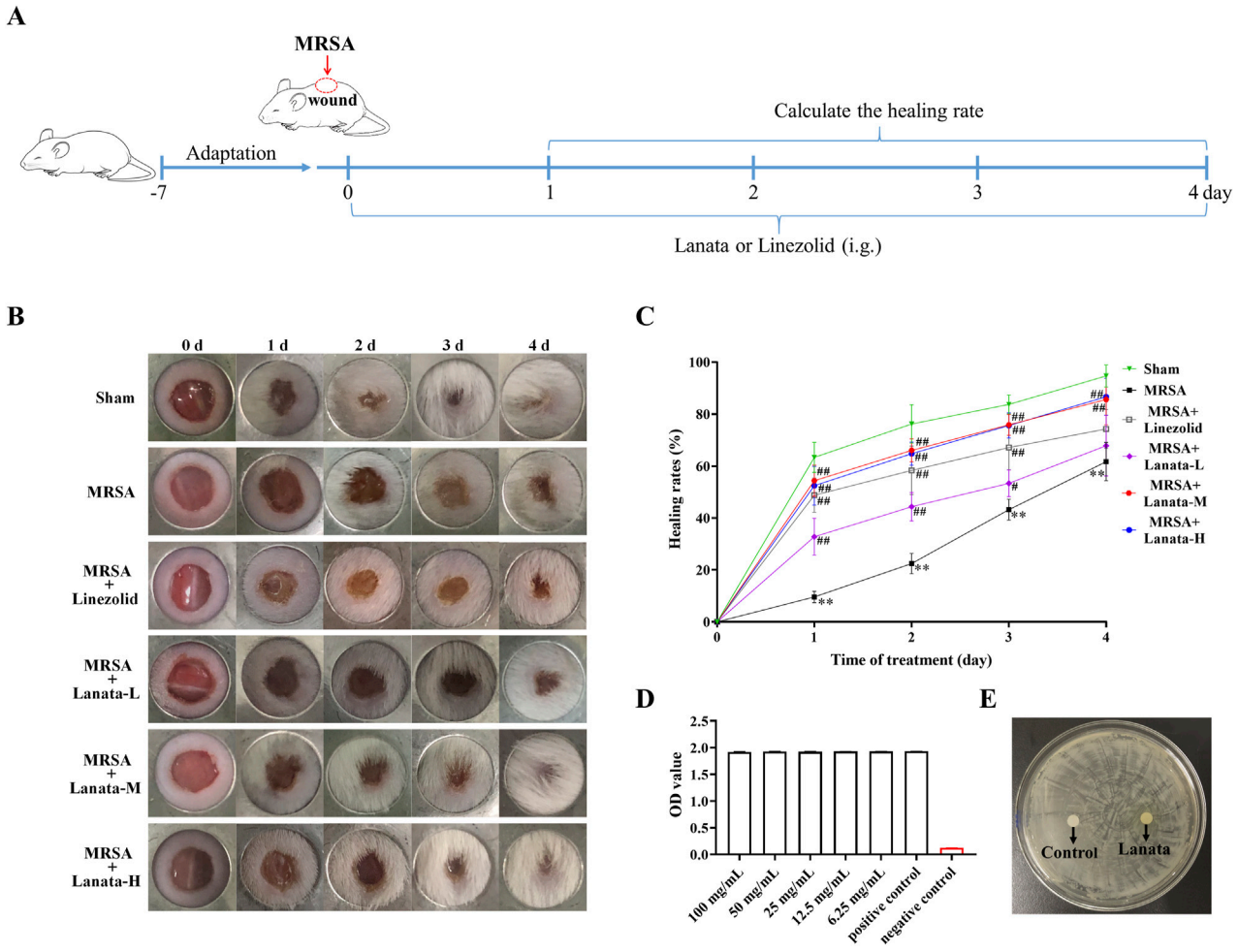


FIGURE 1
Lanata promoted healing of MRSA-infected wounds without direct antibacterial activity. **(A)** Experimental design. **(B, C)** Healing rates of MRSA infected wounds in each group of mice. **(D)** TCC assay and **(E)** zone of growth inhibition test were used to evaluate the antibacterial activity of Lanata. Data were presented as the mean ± SD, $n = 6$. $^{**}p < 0.01$ vs. Sham group; $^{\#}p < 0.05$, $^{\#\#}p < 0.01$ vs. MRSA group.

Lanata, 4 g/kg herb), MRSA + SB225002 group (MRSA + SB225002, vehicle), MRSA + ABAH group (MRSA + ABAH, vehicle), MRSA + Lanata + SB225002 group (MRSA + Lanata + SB225002, 4 g/kg herb), and MRSA + Lanata + ABAH group (MRSA + Lanata + ABAH, 4 g/kg herb). At 4 h post-infection, immunofluorescence of NETs in the air pouch was performed. At 6 h post-infection, the number of neutrophils and ROS levels in neutrophils from the air pouch were determined.

2.21 Statistical analysis

Statistical analysis was conducted with SPSS 26.0. Comparisons between two groups were assessed using Student's t-test. Comparisons for three or more groups were analyzed using one-way analysis of variance (ANOVA), followed by a least significant difference (LSD) *post hoc* test. All data were expressed as mean ± standard deviation (SD). $p < 0.05$ was considered to be statistically significant.

3 Results

3.1 Lanata promoted healing of MRSA-infected wounds without exerting direct antibacterial activity

Considering the therapeutic effect of Lanata on abscess infection, we established a skin wound MRSA infection mouse model to investigate the healing effect of Lanata on infected wounds (Figure 1A). Wound healing of mice in the Sham group was the fastest, being almost completely healed at 72 h post-infection (Figures 1B, C), while healing in the MRSA group was significantly slower due to bacterial infection. Compared with the MRSA group, the healing rate in MRSA + Linezolid and MRSA + Lanata groups increased in different degrees. The healing effect in the MRSA + Lanata-M and MRSA + Lanata-H groups was most prominent, with the largest difference observed at 24 h. However, Lanata had no direct antibacterial activity against MRSA *in vitro* (Figures 1D, E).

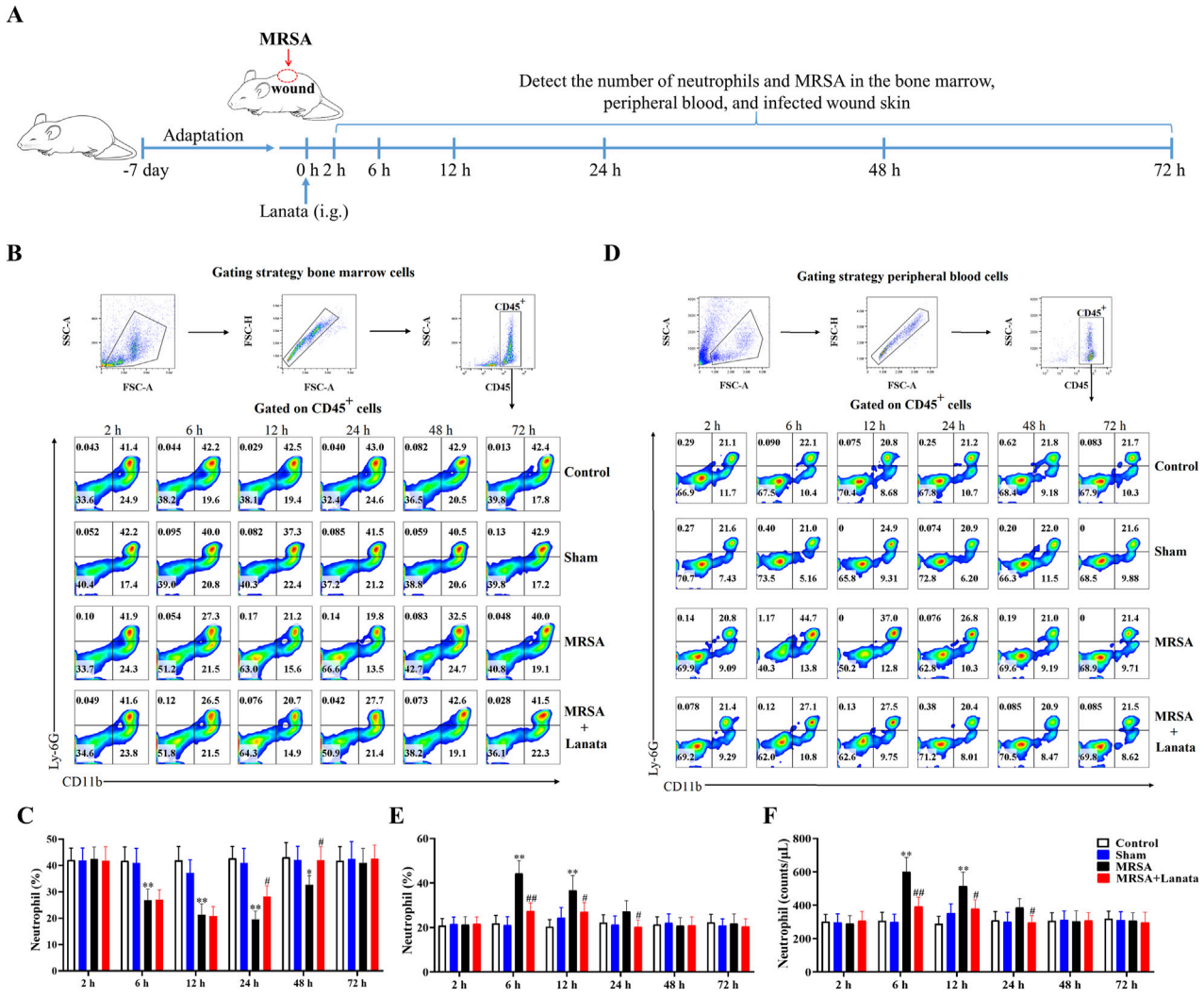


FIGURE 2
Lanata promoted migration of neutrophils to infected wound. **(A)** Experimental design. **(B)** Flow cytometry analysis of neutrophils in the bone marrow. **(C)** Percentage of neutrophils in bone marrow leukocytes. **(D)** Flow cytometry analysis of neutrophils in peripheral blood leukocytes. **(E)** Percentage and **(F)** number of neutrophils in peripheral blood leukocytes. The data are presented as the mean ± SD, $n = 3$. $^{*}p < 0.05$, $^{**}p < 0.01$ vs. Control group; $^{\#}p < 0.05$, $^{\#\#}p < 0.01$ vs. MRSA group.

3.2 Lanata promoted migration of neutrophils to the infected wound and eradication of MRSA

We observed the spatiotemporal dynamics of neutrophil migration during MRSA infection to investigate whether mice treated with Lanata could resist MRSA infection by regulating neutrophils (Figure 2A). At 2 h post-infection, there was no neutrophil infiltration in the infected wound of mice in the MRSA and MRSA + Lanata groups (Figure 3A), and the proportion and number of neutrophils in the bone marrow and the peripheral blood remained homeostatic (Figures 2B–F).

At 6 h, a considerable number of neutrophils began to migrate into the infected wound in the MRSA group (Figures 3A–C) and the proportion of neutrophils in the bone marrow significantly decreased, while the number of neutrophils in the peripheral blood significantly increased (Figures 2B–F), indicating that neutrophils in the bone marrow had been rapidly mobilized into the peripheral blood. Compared with the MRSA group, the number of neutrophils in the infected wound in the MRSA + Lanata group significantly increased, while simultaneously, MRSA and the number of neutrophils in the peripheral blood significantly decreased (Figures 2F, 3A–D).

At 12 h, the number of neutrophils in the infected wound in the MRSA group significantly increased compared with 6 h (Figure 3A), while the proportion and number of neutrophils in the bone marrow and peripheral blood were significantly reduced (Figures 2B–F). Interestingly, the peak in the number of neutrophils in the infected wound in the MRSA + Lanata group was observed in the acute stage of infection, and MRSA and the number of neutrophils in the peripheral blood were significantly lower than those in the MRSA group (Figures 2F, 3A–D).

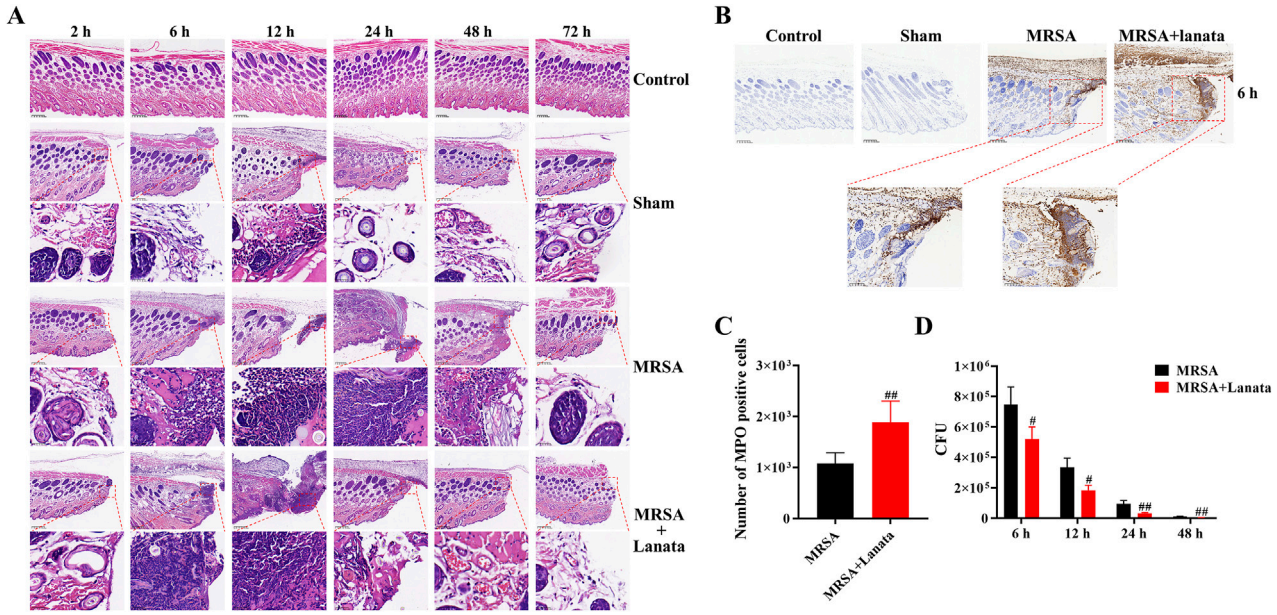


FIGURE 3
Neutrophil infiltration in the infected wound skin of mice. **(A)** H&E was used to observe neutrophil infiltration in the infected wound skin. **(B)** Immunohistochemistry of MPO expression was used to observe the number of neutrophils in the infected wound skin at 6 h post-infection. **(C)** The number of MPO-expressing positive cells in each group of mice was counted based on the location and area of the frame-selected skin-infected wounds in this figure **(B)**. **(D)** Number of MRSA in the infected wound skin. Data were presented as the mean ± SD, $n = 3$. $^{\#}p < 0.05$, $^{\#\#}p < 0.01$ vs. MRSA group.

At 24 h, the number of neutrophils in the infected wound in the MRSA group reached the peak (Figure 3A), while the number of neutrophils in the bone marrow and peripheral blood further decreased (Figures 2B–F). Meanwhile, the number of neutrophils in the infected wound in the MRSA + Lanata group was significantly reduced compared with 12 h and that in the MRSA group, and MRSA was almost completely eradicated, and the number of neutrophils in the bone marrow and peripheral blood began to return to a steady state.

At 48 h, MRSA was almost completely eradicated in the MRSA group, the number of neutrophils was significantly reduced compared with 24 h (Figure 3A), and the number of neutrophils in the peripheral blood and the bone marrow began to return to the steady state (Figures 2B–F). In the MRSA + Lanata group, there was no obvious neutrophil infiltration in the infected wound, and the number of neutrophils in the bone marrow and peripheral blood had returned to a homeostatic state.

Together, the above results suggest that Lanata promoted the rapid migration of neutrophils from the peripheral blood to the infected wound to eradicate MRSA quickly in the acute stage of infection, thus promoting healing of the infected wound.

3.3 Lanata upregulated the protein levels of CXCR2 and PSGL-1 in the infected wound

To explore the mechanism by which Lanata resists MRSA infection, protein expression in the infected wound skin at 6 h post-infection was analyzed by protein chip technology (Figure 4A). Compared with the Sham group, 145 and 55 proteins were upregulated and downregulated in the MRSA group, respectively (Figure 4B). Compared with the MRSA group, 133 and 67 proteins were upregulated and downregulated in the MRSA + Lanata group, respectively (Figure 4C). As shown in Figure 4D, 17 DEPs were identified to be upregulated in the MRSA group compared with the Sham group, and GO enrichment analysis indicated that these proteins were mainly involved in neutrophil migration and leukocyte adhesion to vascular endothelial cells (Figure 4E). Meanwhile, 10 DEPs were identified to be upregulated in the MRSA + Lanata group compared with the MRSA group (Figure 4F), which were mainly involved in leukocyte and neutrophil migration (Figure 4G).

Some DEPs identified in the comparison MRSA vs. Sham overlapped with those identified in the MRSA vs. MRSA + Lanata group, with four main upregulated DEPs (PSGL-1, CXCR2, CXCL2, and CXCL1) identified as the action target of Lanata (Figure 4H). Upregulation of PSGL-1 and CXCR2 in the infected skin was confirmed by ELISA (Figures 4I, J).

3.4 Lanata promoted migration of neutrophils to the air pouch

In order to obtain the accurate number of neutrophils in the MRSA-infected site and directly study neutrophils, we established an air pouch MRSA infection mouse model. At 4 h, 6 h, 12 h, and 24 h post-infection (Figure 5A), there were almost no neutrophils migrating into the air pouch of mice in the control group (Supplementary Table S2). Compared with the MRSA group, Lanata promoted the migration of neutrophils from the

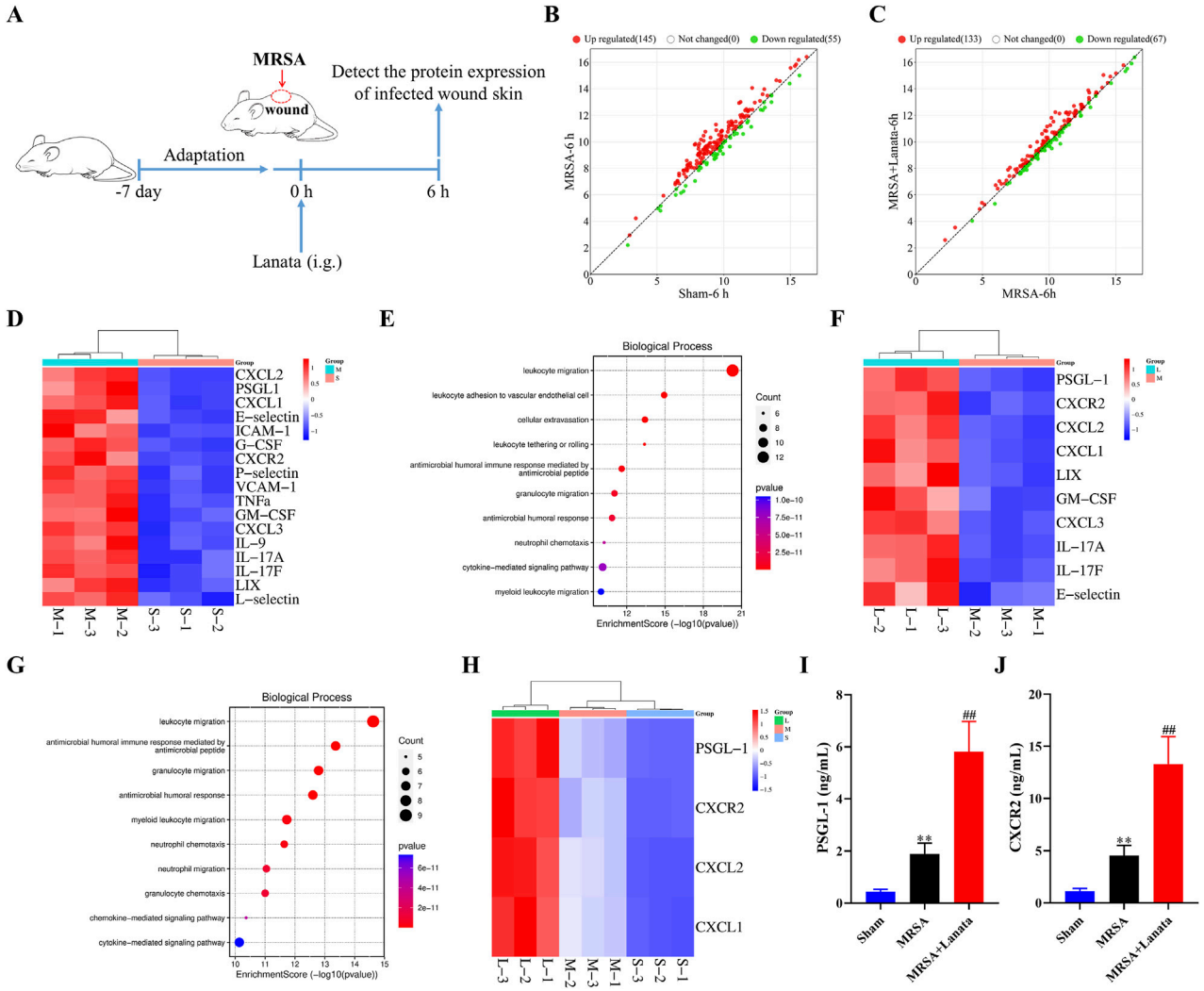


FIGURE 4
Lanata upregulated the protein levels of CXCR2 and PSGL-1 in the infected wound. **(A)** Experimental design. **(B, C)** Scatter plot of protein expression between groups. **(D)** Cluster heatmaps and **(E)** GO enrichment analysis of DEGs between the MRSA and Sham groups. **(F)** Cluster heatmaps and **(G)** GO enrichment analysis of DEGs between the MRSA and Lanata groups. **(H)** Cluster heatmaps of the major DEGs among three groups. **(I)** Protein levels of PSGL-1 and **(J)** CXCR2 in the skin were detected by ELISA. Data were presented as the mean ± SD, $n = 3$ **(A–H)**, $n = 6$ **(I, J)**. $^{**}p < 0.01$ vs. Control group; $^{\#\#}p < 0.01$ vs. MRSA group.

peripheral blood to the air pouch (Figures 5B–G) to quickly eradicate MRSA (Figure 5H).

3.5 Lanata promoted activation of neutrophils in the infected air pouch

Next, we measured the ROS levels in neutrophils and NET formation in the air pouch at 4 h, 6 h, 12 h, and 24 h post-infection to explore the effect of Lanata on activation of neutrophils (Figure 6A). As shown in Figures 6B, C, ROS levels in neutrophils in both MRSA + Lanata and MRSA groups showed the same trend of an initial increase, followed by a decrease (of note, levels in the MRSA + Lanata group were higher at 6 h and lower at 12 h post-infection than those in the MRSA group), which was related to the continuous elimination of MRSA. As shown in Figures 6D–F, Lanata promoted NET formation in the air pouch at 4 h and 6 h post-infection. At 24 h, there were almost no NETs left, which was related to the eradication of MRSA (Figure 5H).

3.6 Lanata regulated mRNA expression in neutrophils

We conducted RNA-seq analysis on neutrophils in the air pouch at 6 h post-infection to understand the mechanism by which Lanata regulates neutrophils (Figure 7A). Compared with the MRSA group, 501 and 97 genes were significantly upregulated and downregulated in the MRSA + Lanata group, respectively (Figure 7B). The top 10 upregulated genes with Lanata included *CXCR2*, *PSGL-1*, *MPO*, *CXCL2*, *CXCL1*, *CXCL5*, *CXCL3*, *LFA-1*, *PAD4*, and *IL-17A* (Figure 7C). GO and pathway enrichment analysis indicated that

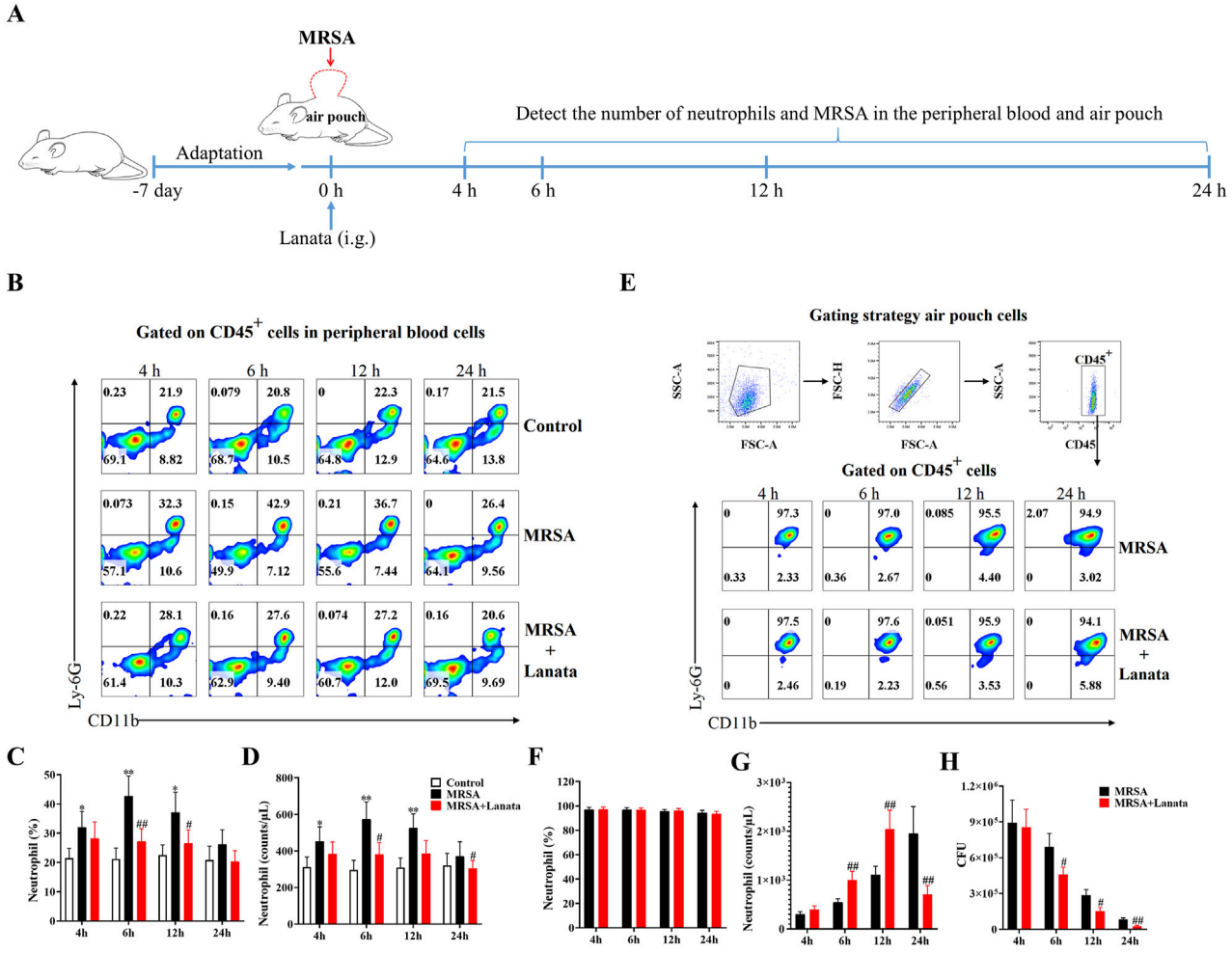


FIGURE 5
Lanata promoted migration of neutrophils to air pouch. **(A)** Experimental design. **(B, C)** Percentage and **(D)** number of neutrophils in peripheral blood leukocytes and flow cytometric analysis of CD45$^+$ cells in peripheral blood leukocytes are shown in Figure 2B. **(E)** Flow cytometric analysis of neutrophils in air pouch leukocytes. **(F)** Percentage and **(G)** number of neutrophils in air pouch leukocytes. **(H)** Number of MRSA in the air pouch. Data were presented as the mean ± SD, $n = 3$. $^*p < 0.05$, $^{**}p < 0.01$ vs. Control group; $^{\#}p < 0.05$, $^{\#\#}p < 0.01$ vs. MRSA group.

the DEGs were mainly involved in neutrophil chemotaxis and migration (Figures 7D, E).

3.7 Lanata upregulated mRNA and protein expressions of CXCR2, PSGL-1, and MPO in neutrophils in the peripheral blood and the air pouch

To validate the RNA-seq findings, we measured the mRNA and protein expressions of CXCR2, PSGL-1, and MPO in neutrophils regulated by Lanata (Figure 8A). As shown in Figures 8B–H, mRNA and protein expression of CXCR2, PSGL-1, and MPO in neutrophils in the peripheral blood in both MRSA + Lanata and MRSA groups first increased post-infection, followed by a decrease. Of note, mRNA and protein expression of the three genes increased significantly at 6 h post-infection and were lower at 12 h in the MRSA + Lanata group compared with the MRSA group.

Similarly, the expression of CXCR2, PSGL-1, and MPO in neutrophils in the air pouch in the MRSA + Lanata group increased significantly at 6 h post-infection and were lower than those in the MRSA group at 12 h (Figures 9A–G).

3.8 Inhibition of CXCR2 and MPO significantly attenuated the effect of Lanata on promoting migration and activation of neutrophils

To further investigate the role of CXCR2 and MPO in Lanata-promoted migration and activation of neutrophils, we used ABAH and SB225002 to inhibit MPO and CXCR2, respectively (Figure 10A). As shown in Figure 10B, in the absence of treatment, there was no NET formation in the air pouch in the MRSA group at 4 h post-infection, while NETs had already begun to be released in the MRSA + Lanata group. However, after administration of ABAH, there was almost no NET formation in

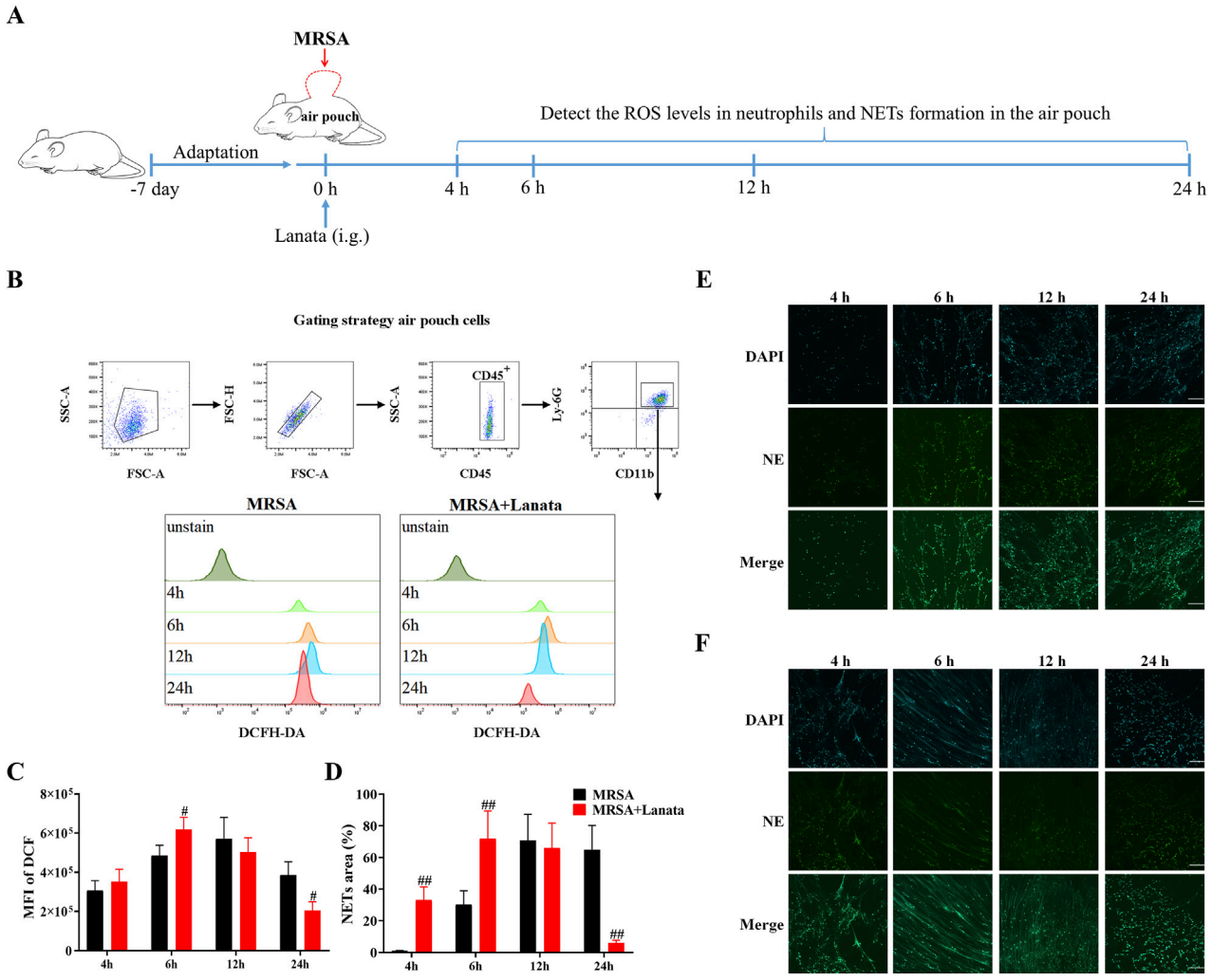


FIGURE 6
Lanata promoted activation of neutrophils in the infected air pouch. **(A)** Experimental design. **(B)** Flow cytometric analysis of the ROS level in neutrophils. The mean fluorescence intensity of DCF was used to evaluate ROS levels in neutrophils. **(C)** Mean fluorescence intensity of DCF in neutrophils. **(D)** NET area in this figure **(E, F)**. NET formation in the air pouch in **(E)** Model and **(F)** Lanata groups was observed by immunofluorescence staining. Scale bar: 100 μm. Data were presented as the mean ± SD, $n = 3$. $^{\#}p < 0.05$ vs. MRSA group.

the MRSA + Lanata group. Similarly, in the absence of treatment, ROS levels in neutrophils in the air pouch in the MRSA + Lanata group were significantly higher than that in the MRSA group at 6 h post-infection (Figures 10C, D). However, after ABAH treatment, ROS levels in neutrophils in the two groups were significantly reduced without significant differences between groups.

As shown in Figures 10E, F, the number of neutrophils in the air pouch in the MRSA + Lanata group was significantly higher than that in the MRSA group at 6 h post-infection. However, after administration of SB225002, the number of neutrophils in the two groups was significantly reduced, and no significant differences were observed between groups.

4 Discussion

When tissue is infected by bacteria, a large number of neutrophils from the bone marrow are released into the peripheral blood (Heim et al., 2015) and migrate across the vascular barrier to the infected site to eradicate the bacteria. In this study, we found that after the wound was infected with MRSA and in the absence of treatment, neutrophils from the bone marrow were released into the peripheral blood and migrated to the infected wound to rapidly eradicate the bacteria, with the number of neutrophils in the wound skin reaching its peak at 24 h post-infection. Treatment with Lanata accelerated this migration and eradicated MRSA earlier, specifically in the acute stage (6 h and 12 h) of infection. Moreover, we found that the expression of PSGL-1 and CXCR2 was significantly increased at 6 h post-infection in the wound skin of Lanata-treated mice. PSGL-1 and CXCR2 are highly expressed on the surface of neutrophils and play an important role in recruiting neutrophils to migrate to inflammatory sites (Stadtmann et al., 2013; Wang et al., 2022). Therefore, our findings suggested that Lanata may have a direct effect on neutrophils by upregulating the expression of PSGL-1 and CXCR2, thereby accelerating the migration of neutrophils to the

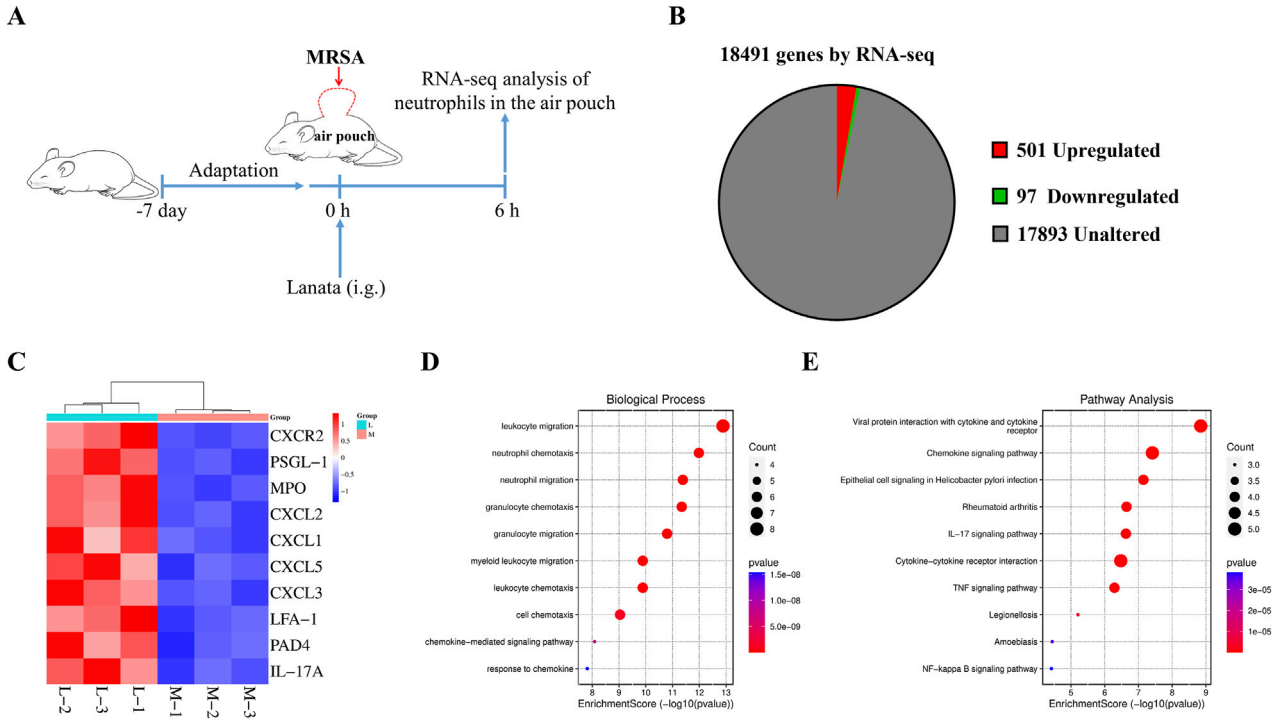


FIGURE 7
Lanata regulated mRNA expression in neutrophils. **(A)** Experimental design. **(B)** Pie chart of differentially expressed genes between the Lanata and MRSA groups. **(C)** Cluster heat map, **(D)** GO, and **(E)** KEGG enrichment analysis of DEGs between the Lanata and MRSA groups.

infected wounds to rapidly eradicate MRSA and promote the healing of infected wounds.

Given that the skin infection model is not suitable for the direct study of neutrophils (it is difficult to obtain neutrophils from the skin), we used the subcutaneous air pouch model–an *in vivo* model in which sterile air is injected into the back of mice to form an air pouch, where irritants can be injected to cause an inflammatory response (Fehrenbacher and McCarson, 2021). The characteristics and changes in the inflammatory response derived from MRSA infection were observed by collecting immune cells in the air pouch. Using this model, we found that Lanata promoted the migration of neutrophils from the peripheral blood to the air pouch to quickly eradicate MRSA in the acute stage of infection.

When neutrophils reach the infected site, specific receptors on their surfaces bind to the bacteria and induce the neutrophils to phagocytose the bacteria and form phagosomes within the neutrophils (Rungelrath and DeLeo, 2021). Neutrophils then eradicate bacteria by releasing ROS and NETs, which are signs of neutrophil activation (Winterbourn et al., 2016). Our results showed that ROS levels in the neutrophils in the air pouch of mice in the MRSA + Lanata group were higher than those in the MRSA group at 4 h and 6 h post-infection, reaching the peak at 6 h, suggesting that Lanata promoted the activation of neutrophils in the acute stage of infection and enhanced the bactericidal ability of neutrophils. At 12 h, ROS levels in the neutrophils of the Lanata-treated mice began to decrease, indicating a gradual decrease in neutrophil activity with the gradual eradication of MRSA, until almost complete eradication at 24 h. Overall, changes in ROS levels occurred earlier in the MRSA + Lanata group, as compared with the MRSA group (i.e., accelerated by 6 h approximately).

In addition to producing ROS, a large number of studies have shown that neutrophils can capture and eradicate bacteria by releasing NETs (Brinkmann et al., 2004). NETs are a network structure composed of nuclear chromatin; histone; granular proteins such as NE, MPO, or cathepsin G; and cytoplasmic proteins such as glycolytic enzymes and catalase (Urban et al., 2009; Schultz et al., 2022). When neutrophils are activated, they undergo through a series of processes to produce NETs (Cristinziano et al., 2022). NETs are released to the extracellular space, greatly increasing the contact area with the bacteria, and as a consequence, the bacteria are dissociated by the granular proteins and histones of the NETs. We found that NET formation and release to the air pouch was accelerated in the MRSA + Lanata group during the acute stage of the infection (at 4 h and 6 h), while there were almost no NETs left in the air pouch of Lanata-treated mice at 24 h compared with the MRSA group. Our results suggest that Lanata increased the speed and intensity of NET release in the acute stage of infection to quickly eradicate MRSA.

Next, we conducted RNA-seq analysis on the neutrophils in the air pouch at 6 h post-infection to understand the mechanism by which Lanata regulates neutrophils. We found that Lanata significantly upregulated the expressions of CXCR2, PSGL-1, and MPO mRNA in neutrophils. Using RT-qPCR, flow cytometry, and

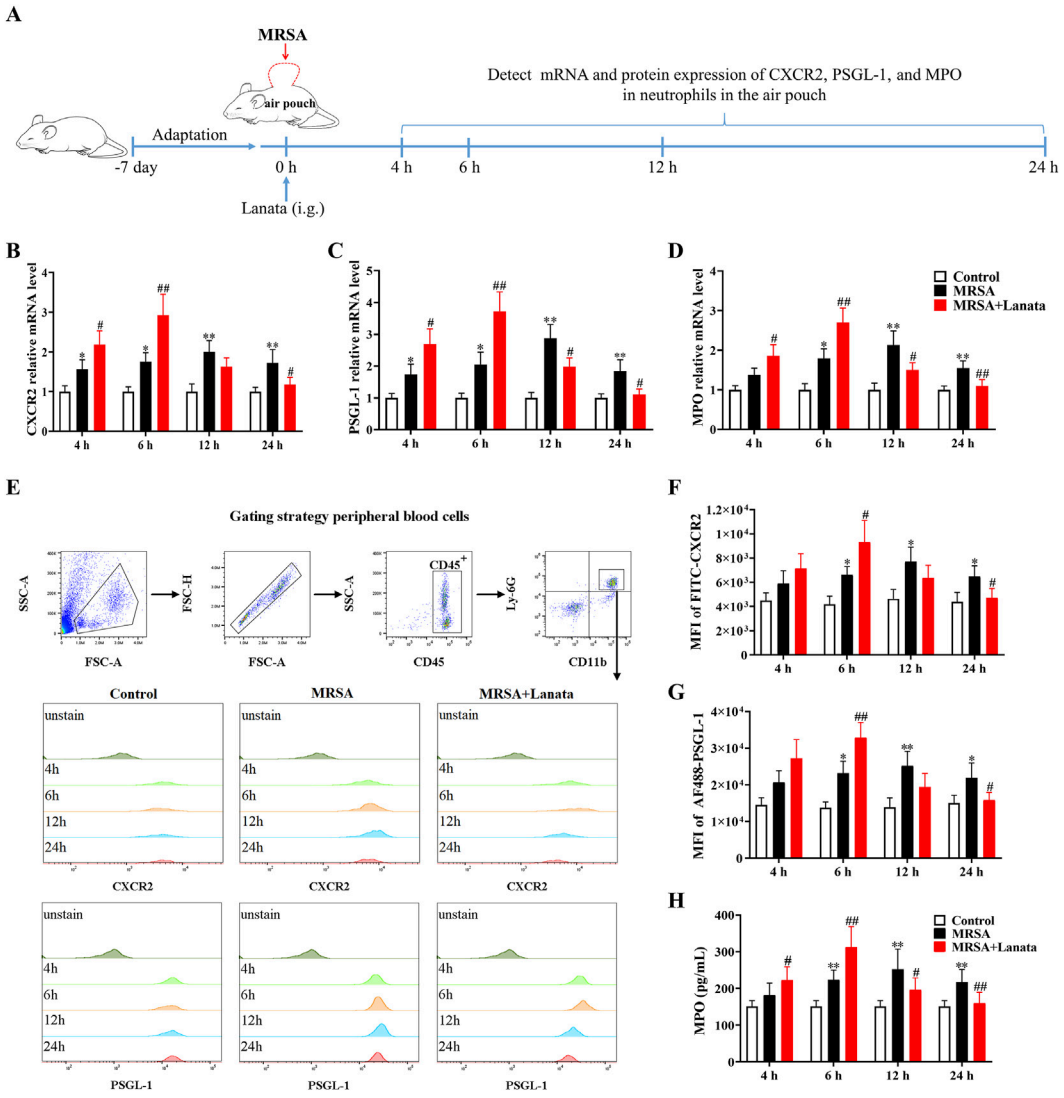


FIGURE 8
Lanata upregulated mRNA and protein expressions of CXCR2, PSGL-1, and MPO in neutrophils in peripheral blood. **(A)** Experimental design. **(B–D)** The mRNA expression levels of CXCR2, PSGL-1, and MPO in neutrophils were detected by RT-qPCR. **(E)** The protein expression of CXCR2 and MPO in neutrophils was detected by flow cytometry. Median fluorescence intensity of **(F)** CXCR2 and **(G)** PSGL-1 in neutrophils. **(H)** The concentration of MPO in neutrophils was detected by ELISA. Data were presented as the mean ± SD, $n = 3$. $^{*}p < 0.05$, $^{**}p < 0.01$ vs. Control group; $^{\#}p < 0.05$, $^{\#\#}p < 0.01$ vs. MRSA group.

ELISA, we found that the mRNA and protein levels of CXCR2, PSGL-1, and MPO in the neutrophils of the MRSA + Lanata group increased significantly at 6 h post-infection and were lower than those in the MRSA group after 12 h.

It has been described that upon infection, neutrophils in the peripheral blood need to go through a series of processes to migrate to the local tissue. In the first step of this process, neutrophils must contact with the vascular endothelial cells at the site of infection for neutrophils to leave the blood stream (Eriksson et al., 2001; Sperandio et al., 2003). Endothelial cells are activated by inflammatory cytokines released by sentinel cells in the infected tissues, which induce the rapid expression of P-selectin and E-selectin on their surfaces (Sais et al., 1997; Liu et al., 2010). PSGL-1 is the most effective selectin ligand expressed on the surface of neutrophils (Xia et al., 2002). When PSGL-1 of the neutrophils present in the blood stream binds to P-selectin and E-selectin of endothelial cells, the neutrophils are captured on the surface of the vascular endothelium. A previous study has shown that after PSGL-1 was knocked out, the number of neutrophils in inflamed sites of mice decreased significantly (Zhang et al., 2020), suggesting that this interaction driven by PSGL-1 is essential for neutrophil migration to inflamed sites. In our study, we found that PSGL-1 expression in the neutrophils in the peripheral blood of Lanata-treated mice was increased in the acute stage of infection, improving the efficiency of neutrophils being captured by endothelial cells and allowing that neutrophils in the blood stream to be quickly captured by the vascular

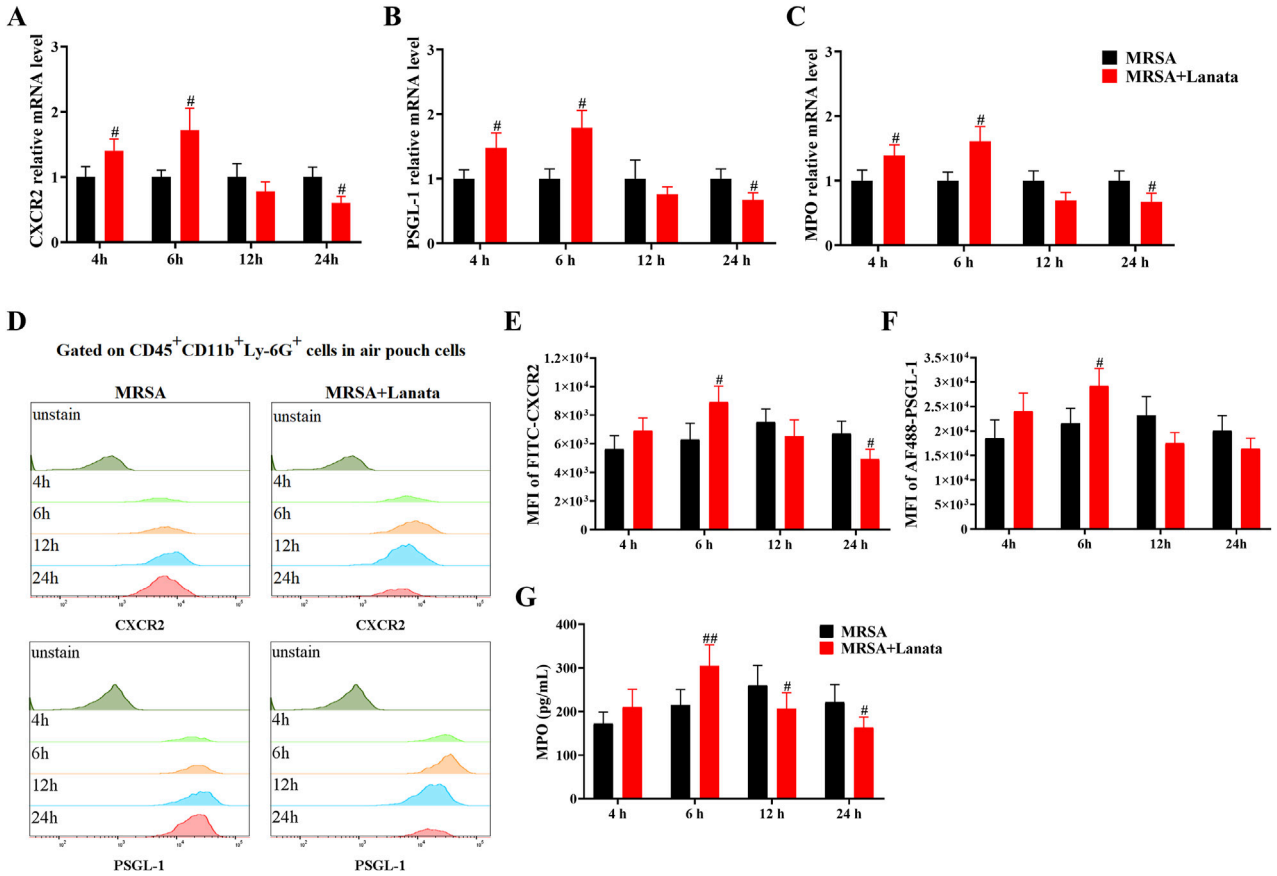


FIGURE 9
Lanata upregulated mRNA and protein expressions of CXCR2, PSGL-1, and MPO in neutrophils in the air pouch. **(A–C)** The mRNA expressions of CXCR2, PSGL-1, and MPO in neutrophils were detected by RT-qPCR. **(D)** The protein expression of CXCR2 and MPO in neutrophils was detected by flow cytometry. The median fluorescence intensity of **(E)** CXCR2 and **(F)** PSGL-1 in neutrophils. **(G)** The concentration of MPO in neutrophils was detected by ELISA. Data were presented as the mean ± SD, $n = 3$. $^{\#}p < 0.05$, $^{\#\#}p < 0.01$ vs. MRSA group.

endothelium for subsequent migration. This may explain the significant increase in the number of neutrophils in the air pouch in the MRSA + Lanata group when compared with the MRSA group.

When neutrophils in the peripheral blood are captured by the vascular endothelium, they migrate to the inflamed site influenced by the concentration of chemokines such as CXCL1 and CXCL2 through CXCR2 (Michael and Vermeren, 2019). A previous study showed that inhibition of CXCR2 significantly attenuated the migration of neutrophils to inflammatory sites (Wu et al., 2020). In our study, we found that CXCR2 expression in neutrophils in peripheral blood in the Lanata group followed the same trend as PSGL-1 (i.e., increase in the acute stage of infection as compared with the MRSA group). This greatly improved the chemotaxis and migration ability of the neutrophils and promoted the rapid migration of neutrophils in peripheral blood to the infected site. After treatment with the CXCR2 inhibitor SB225002, the number of neutrophils in both MRSA + Lanata and MRSA groups was significantly reduced, and no significant differences were observed between both groups, suggesting that inhibition of CXCR2 significantly attenuated the effect of Lanata on promoting migration of neutrophils.

MPO is a heme protein that is abundantly stored in the neutrophils' azurophilic granules (Klebanoff et al., 2013). In phagosomes, MPO catalyzes the reaction of hydrogen peroxide and chloride to produce ROS-hypochlorous acid, which has a potent bactericidal ability (Rigby and DeLeo, 2012). Previous studies have shown that MPO plays an important role not only in the production of ROS in neutrophils but also in the release of NETs (Papayannopoulos et al., 2010). We found that, similar to that observed with expression of PSGL-1 and CXCR2, MPO expression in the neutrophils of Lanata-treated mice increased at 4 h and 6 h post-infection, reaching the peak at 6 h. As a consequence, this not only increased ROS levels in the neutrophils but also promoted the release of NETs. Upon treatment with the MPO inhibitor ABAH, ROS levels in the neutrophils in both the MRSA + Lanata and MRSA groups were significantly reduced with no significant differences between the two groups, and the release of NETs was delayed. Together, our results suggest that inhibition of MPO significantly attenuated the effect of Lanata on promoting activation of neutrophils.

Our study demonstrated that mice treated with Lanata, which is called the "the holy medicine of pustule," resists MRSA infection by promoting migration and activation of neutrophils. This finding

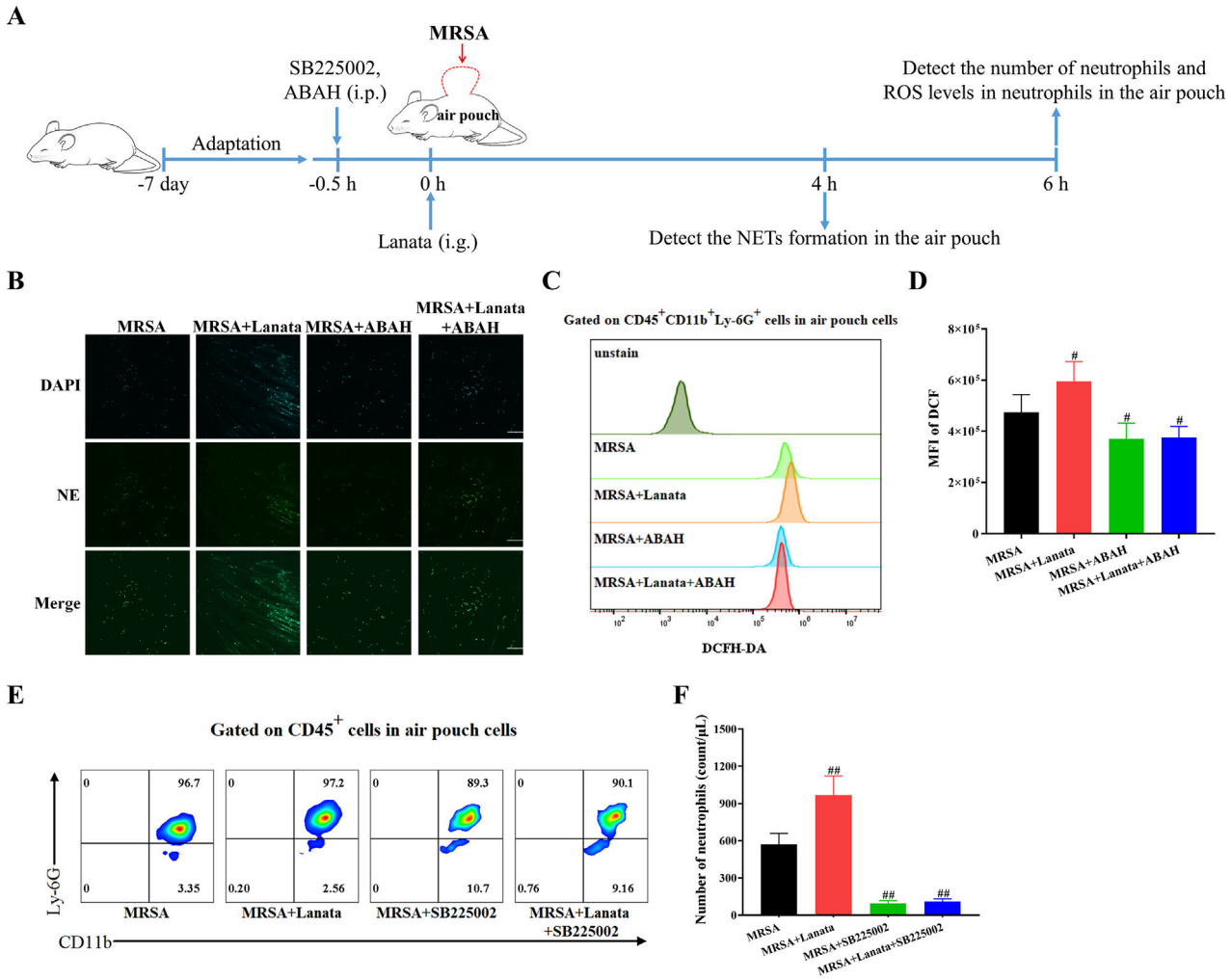


FIGURE 10
Inhibition of CXCR2 and MPO significantly attenuated the effect of Lanata on promoting migration and activation of neutrophils. **(A)** Experimental design. **(B)** Immunofluorescence staining was used to observe the NET formation in the air pouch of mice. Scale bar: 100 μm. **(C, D)** Mean fluorescence intensity of DCF in neutrophils in the air pouch of mice was detected by flow cytometry at 6 h post-infection. **(E, F)** The number of neutrophils in the air pouch was detected by flow cytometry at 6 h post-infection. Data were presented as the mean ± SD, $n = 4$. $^{\#}p < 0.05$, $^{\#\#}p < 0.01$ vs. MRSA group.

provides a scientific basis for the use of Lanata for the treatment of skin infections, as well as a new option for the treatment of infectious diseases. Future research including *in vitro* mechanistic assays aimed to uncover the direct effect of Lanata on neutrophils is warranted.

5 Conclusion

Our study reveals the mechanism by which mice treated with *Panzerina lanata* resists MRSA infection by promoting migration and activation of neutrophils. Under the action of *Panzerina lanata*, the captured speed of neutrophils with high expression of PSGL-1 in peripheral blood by vascular endothelial cells was greatly improved, and the neutrophils with high expression of CXCR2 acquired stronger chemotaxis and migration ability; consequently, a larger number of neutrophils arrived to the infected site; upon reaching the infected site, the neutrophils with high expression of MPO were activated after recognizing MRSA, further strengthening production of ROS and rapid release of NETs to eradicate MRSA, thus exerting an anti-infection effect.

Data availability statement

The transcriptome sequencing data presented in the study are deposited in the NCBI SRA BioProject repository, accession number PRJNA1163875.

Ethics statement

The animal study was approved by the Biological and Medical Ethics Committee of Minzu University of China. The study was conducted in accordance with the local legislation and institutional requirements.

Author contributions

SD: data curation, formal analysis, investigation, methodology, writing–original draft, and writing–review and editing. XB: data curation, formal analysis, and writing–review and editing. BC: data curation, methodology, and writing–review and editing. MF: data curation and writing–review and editing. QL: investigation and writing–review and editing. YZ: investigation and writing–review and editing. LL: supervision and writing–review and editing. DZ: funding acquisition, investigation, methodology, supervision, and writing–review and editing.

Funding

The author(s) declare that financial support was received for the research, authorship, and/or publication of this article. This study was supported by the National Natural Science Foundation of China (No. 81673694) and the Graduate Research and Practice Projects of Minzu University of China (No. SZKY2024067).

Conflict of interest

The authors declare that the research was conducted in the absence of any commercial or financial relationships that could be construed as a potential conflict of interest.

Publisher's note

All claims expressed in this article are solely those of the authors and do not necessarily represent those of their affiliated organizations, or those of the publisher, the editors and the reviewers. Any product that may be evaluated in this article, or claim that may be made by its manufacturer, is not guaranteed or endorsed by the publisher.

Supplementary material

The Supplementary Material for this article can be found online at: https://www.frontiersin.org/articles/10.3389/fphar.2024.1501744/full#supplementary-material

References

Brinkmann, V., Reichard, U., Goosmann, C., Fauler, B., Uhlemann, Y., Weiss, D. S., et al. (2004). Neutrophil extracellular traps kill bacteria. *Science* 303 (5663), 1532–1535. doi:10.1126/science.1092385

Collaborators, G. A. R. (2022). Global mortality associated with 33 bacterial pathogens in 2019: a systematic analysis for the Global Burden of Disease Study 2019. *Lancet* 400 (10369), 2221–2248. doi:10.1016/s0140-6736(22)02185-7

Cristinziano, L., Modestino, L., Antonelli, A., Marone, G., Simon, H. U., Varricchi, G., et al. (2022). Neutrophil extracellular traps in cancer. *Semin. Cancer Biol.* 79, 91–104. doi:10.1016/j.semcancer.2021.07.011

Cross, A. L., Hawkes, J., Wright, H. L., Moots, R. J., and Edwards, S. W. (2020). APPA (apocynin and paeonol) modulates pathological aspects of human neutrophil function, without supressing antimicrobial ability, and inhibits TNFα expression and signalling. *Inflammopharmacology* 28 (5), 1223–1235. doi:10.1007/s10787-020-00715-5

Eriksson, E. E., Xie, X., Werr, J., Thoren, P., and Lindbom, L. (2001). Importance of primary capture and L-selectin-dependent secondary capture in leukocyte accumulation in inflammation and atherosclerosis *in vivo*. *J. Exp. Med.* 194 (2), 205–218. doi:10.1084/jem.194.2.205

Fehrenbacher, J. C., and McCarson, K. E. (2021). Models of inflammation: carrageenan air pouch. *Curr. Protoc.* 1 (8), e183. doi:10.1002/cpz1.183

Heim, C. E., Vidlak, D., Scherr, T. D., Hartman, C. W., Garvin, K. L., and Kielian, T. (2015). IL-12 promotes myeloid-derived suppressor cell recruitment and bacterial persistence during *Staphylococcus aureus* orthopedic implant infection. *J. Immunol.* 194 (8), 3861–3872. doi:10.4049/jimmunol.1402689

Klebanoff, S. J., Kettle, A. J., Rosen, H., Winterbourn, C. C., and Nauseef, W. M. (2013). Myeloperoxidase: a front-line defender against phagocytosed microorganisms. *J. Leukoc. Biol.* 93 (2), 185–198. doi:10.1189/jlb.0712349

Li, X. L. (2011). "Research on quality standards and components activity evaluation of Mongolian medicine Baiyimucao,". Beijing, China: Minzu University of China. Master's thesis.

Liu, Z., Miner, J. J., Yago, T., Yao, L., Lupu, F., Xia, L., et al. (2010). Differential regulation of human and murine P-selectin expression and function *in vivo*. *J. Exp. Med.* 207 (13), 2975–2987. doi:10.1084/jem.20101545

Love, M. I., Huber, W., and Anders, S. (2014). Moderated estimation of fold change and dispersion for RNA-seq data with DESeq2. *Genome Biol.* 15 (12). doi:10.1186/s13059-014-0550-8

Meng, K. (2009). Oral Mongolian medicine combined with rectal drip treatment for 137 cases of ulcerative colitis. *J. Med. & Pharm. Chin. Minorities* (5), 9.

Mi, Y., Zheng, W., Zhao, X., Zhang, X., Yang, K., Shen, G., et al. (2021). Chemical profiling and multicomponents quantitative analysis of *Panzerina lanata* by ultra-fast liquid chromatography with tandem mass spectrometry. *J. Sep. Sci.* 44 (13), 2524–2535. doi:10.1002/jssc.202000944

Michael, M., and Vermeren, S. (2019). A neutrophil-centric view of chemotaxis. *Essays Biochem.* 63 (5), 607–618. doi:10.1042/ebc20190011

Moussa, S. H., Tayel, A. A., Al-Hassan, A. A., and Farouk, A. (2013). Tetrazolium/formazan test as an efficient method to determine fungal chitosan antimicrobial activity. *J. Mycol.* 2013, 1–7. doi:10.1155/2013/753692

Papayannopoulos, V., Metzler, K. D., Hakkim, A., and Zychlinsky, A. (2010). Neutrophil elastase and myeloperoxidase regulate the formation of neutrophil extracellular traps. *J. Cell Biol.* 191 (3), 677–691. doi:10.1083/jcb.201006052

Rawat, K., Syeda, S., and Shrivastava, A. (2023). A novel role of Tinospora cordifolia in amelioration of cancer-induced systemic deterioration by taming neutrophil infiltration and hyperactivation. *Phytomedicine* 108, 154488. doi:10.1016/j.phymed.2022.154488

Rigby, K. M., and DeLeo, F. R. (2012). Neutrophils in innate host defense against *Staphylococcus aureus* infections. *Semin. Immunopathol.* 34 (2), 237–259. doi:10.1007/s00281-011-0295-3

Rungelrath, V., and DeLeo, F. R. (2021). *Staphylococcus aureus*, antibiotic resistance, and the interaction with human neutrophils. *Antioxid. Redox Signal* 34 (6), 452–470. doi:10.1089/ars.2020.8127

Sais, G., Vidaller, A., Jucglá, A., Condom, E., and Peyrí, J. (1997). Adhesion molecule expression and endothelial cell activation in cutaneous leukocytoclastic vasculitis. An immunohistologic and clinical study in 42 patients. *Arch. Dermatol* 133 (4), 443–450. doi:10.1001/archderm.133.4.443

Schultz, B. M., Acevedo, O. A., Kalergis, A. M., and Bueno, S. M. (2022). Role of extracellular trap release during bacterial and viral infection. *Front. Microbiol.* 13, 798853. doi:10.3389/fmicb.2022.798853

Sperandio, M., Smith, M. L., Forlow, S. B., Olson, T. S., Xia, L., McEver, R. P., et al. (2003). P-selectin glycoprotein ligand-1 mediates L-selectin-dependent leukocyte rolling in venules. *J. Exp. Med.* 197 (10), 1355–1363. doi:10.1084/jem.20021854

Stadtmann, A., Germena, G., Block, H., Boras, M., Rossaint, J., Sundd, P., et al. (2013). The PSGL-1-L-selectin signaling complex regulates neutrophil adhesion under flow. *J. Exp. Med.* 210 (11), 2171–2180. doi:10.1084/jem.20130664

Urban, C. F., Ermert, D., Schmid, M., Abu-Abed, U., Goosmann, C., Nacken, W., et al. (2009). Neutrophil extracellular traps contain calprotectin, a cytosolic protein complex involved in host defense against Candida albicans. *PLoS Pathog.* 5 (10), e1000639. doi:10.1371/journal.ppat.1000639

Wang, Y., Dikeman, D., Zhang, J., Ackerman, N., Kim, S., Alphonse, M. P., et al. (2022). CCR2 contributes to host defense against *Staphylococcus aureus* orthopedic implant-associated infections in mice. *J. Orthop. Res.* 40 (2), 409–419. doi:10.1002/jor.25027

Watkins, R. R., and David, M. Z. (2021). Approach to the patient with a skin and soft tissue infection. *Infect. Dis. Clin. North Am.* 35 (1), 1–48. doi:10.1016/j.idc.2020.10.011

Winterbourn, C. C., Kettle, A. J., and Hampton, M. B. (2016). Reactive oxygen species and neutrophil function. *Annu. Rev. Biochem.* 85, 765–792. doi:10.1146/annurev-biochem-060815-014442

Wu, F., Chen, X., Zhai, L., Wang, H., Sun, M., Song, C., et al. (2020). CXCR2 antagonist attenuates neutrophil transmigration into brain in a murine model of LPS induced neuroinflammation. *Biochem. Biophys. Res. Commun.* 529 (3), 839–845. doi:10.1016/j.bbrc.2020.05.124

Wu, Z. H., and Fu, Q. (1988). Second batch precious rare and endangered plants of China from shaan xi. *Shaanxi For. Sci. Technol.* (2), 19–22.

Xia, L., Sperandio, M., Yago, T., McDaniel, J. M., Cummings, R. D., Pearson-White, S., et al. (2002). P-selectin glycoprotein ligand-1-deficient mice have impaired leukocyte tethering to E-selectin under flow. *J. Clin. Invest* 109 (7), 939–950. doi:10.1172/jci14151

Xing, S. R. (2006). *Ningxia traditional Chinese medicine chronicles*. Yin Chuan, China: Ningxia People's Publishing Press.

Yuan, Q., Jiang, Y. W., and Fang, Q. H. (2014). Improving effect of Sivelestat on lipopolysaccharide-induced lung injury in rats. *Apmis* 122 (9), 810–817. doi:10.1111/apm.12222

Zhang, X., Zhu, M., Jiang, X. L., Liu, X., Liu, X., Liu, P., et al. (2020). P-selectin glycoprotein ligand 1 deficiency prevents development of acute pancreatitis by attenuating leukocyte infiltration. *World J. Gastroenterol.* 26 (41), 6361–6377. doi:10.3748/wjg.v26.i41.6361

Zhou, X. (2022). *Study on the mechanism of Mongolian medicine Baiyimucao on vascular remodeling in spontaneously hypertensive rats*. Beijing, China: Minzu University of China. Master's thesis.

frontiers | Frontiers in Pharmacology

TYPE Original Research
PUBLISHED 11 February 2025
DOI 10.3389/fphar.2025.1528398

Check for updates

OPEN ACCESS

EDITED BY
Quansheng Feng,
Chengdu University of Traditional Chinese Medicine, China

REVIEWED BY
Adnan Amin,
Gomal University, Pakistan
Pavel Klouček,
Czech University of Life Sciences Prague, Czechia

*CORRESPONDENCE
Congli Xu,
bshxucongli@163.com
Chunlin Long,
long.chunlin@muc.edu.cn,
long@mail.kib.ac.cn

RECEIVED 14 November 2024
ACCEPTED 21 January 2025
PUBLISHED 11 February 2025

CITATION
Wang M, Hu X, Liu L, Zhong Y, Li W, Zhang Q, Xu C and Long C (2025) Hexane extract from *Lindera communis* roots: wound healing properties and membrane-disruptive activities against methicillin-resistant *Staphylococcus aureus*.
Front. Pharmacol. 16:1528398.
doi: 10.3389/fphar.2025.1528398

COPYRIGHT
© 2025 Wang, Hu, Liu, Zhong, Li, Zhang, Xu and Long. This is an open-access article distributed under the terms of the Creative Commons Attribution License (CC BY). The use, distribution or reproduction in other forums is permitted, provided the original author(s) and the copyright owner(s) are credited and that the original publication in this journal is cited, in accordance with accepted academic practice. No use, distribution or reproduction is permitted which does not comply with these terms.

Hexane extract from *Lindera communis* roots: wound healing properties and membrane-disruptive activities against methicillin-resistant *Staphylococcus aureus*

Miaomiao Wang[1,2,3], Xian Hu[1,3,4], Liya Liu[1,2,3,5], Yi Zhong[1,2,3], Wanlin Li[1,2,3], Qing Zhang[1,2,3], Congli Xu[6]* and Chunlin Long[1,2,3,5,7]*

[1]Key Laboratory of Ecology and Environment in Minority Areas (Minzu University of China), National Ethnic Affairs Commission, Beijing, China, [2]College of Life and Environmental Sciences, Minzu University of China, Beijing, China, [3]Key Laboratory of Ethnomedicine (Minzu University of China), Ministry of Education, Beijing, China, [4]College of Ethnology and Sociology, Minzu University of China, Beijing, China, [5]Mass Spectrometry Imaging and Metabolomics (Minzu University of China), National Ethnic Affairs Commission, Beijing, China, [6]Baoshan Administration of Gaoligongshan National Nature Reserve, Baoshan, Yunnan, China, [7]Institute of National Security Studies, Minzu University of China, Beijing, China

Introduction: The extensively used *Lindera communis* Hemsl. (Lauraceae) in traditional Chinese medicine has been specifically employed for wound healing and treating skin diseases in cattle and horses, suggesting its potential antibacterial properties. To explore the antibacterial activities of *L. communis* plants, we investigated the chemicals, antibacterial activities and wound healing and of the n-hexane fraction of *L. communis* roots (LCH).

Methods: Our study included detecting phytochemical constituents, determining minimum inhibitory concentration (MIC) for different extract fractions, analyzing growth curves, assessing membrane integrity, monitoring potential changes in the membrane using scanning electron microscopy, and evaluating wound healing in rat excisional wounds.

Results: Based on our findings, humulene-type sesquiterpenes, guaiane-type sesquiterpenes, and lauric acid were identified from the LCH, responsible for antibacterial and wound healing activities. The results are that LCH affected the growth of methicillin-resistant *Staphylococcus aureus* (MIC: 0.1 mg/mL) through morphological alterations and disrupting cell surface structures, causing membrane hyperpolarization and altering membrane integrity. This result was subsequently validated through SEM analysis and cytotoxicity against HaCaT cells (IC_{50} 1.83 ± 0.21 mg/mL). LCH also has exhibited remarkable effectiveness in healing rat excisional wounds, reinforcing its traditional use as a wound-healing agent.

Discussion: The findings substantiate the scientific essence of traditional applications, while also exhibiting significant potential as a promising candidate for the development of innovative and readily accessible wound healing agents.

KEYWORDS

***Lindera communis*, antibacterial activity, methicillin-resistant *Staphylococcus aureus*, hexane extract, wound healing**

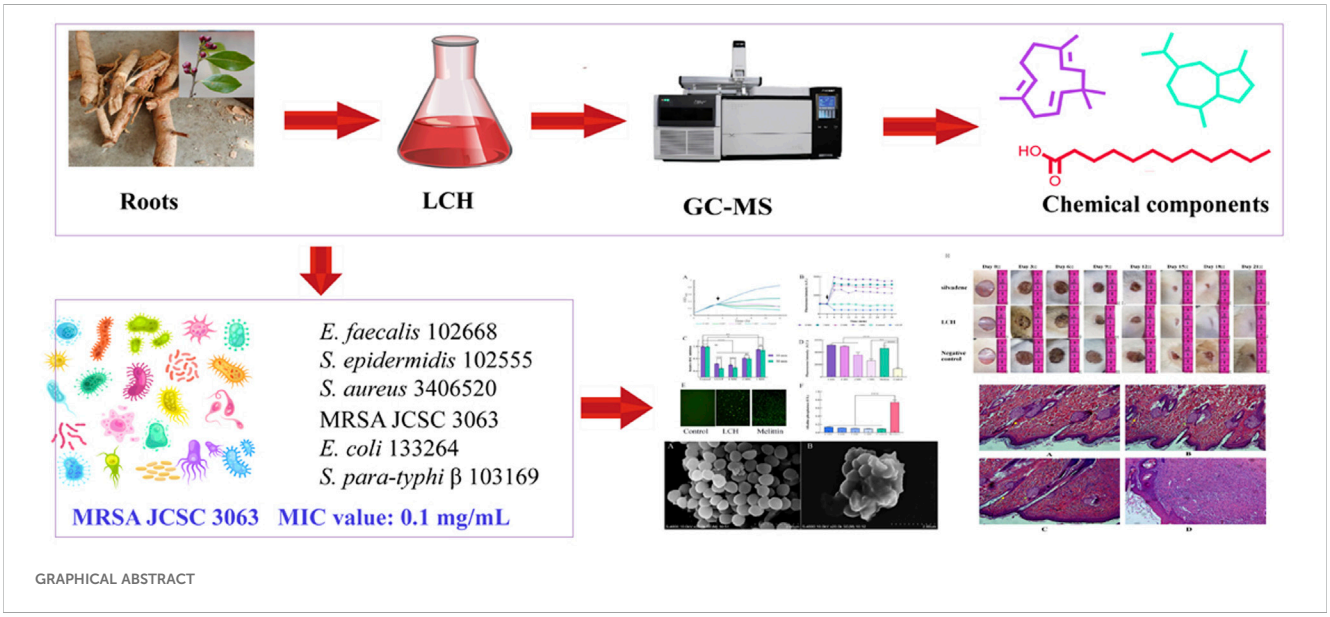
1 Introduction

The genus *Lindera* Thunb., encompassing approximately ninety-nine species within the Lauraceae family, is renowned for its aromatic leaves. It is primarily distributed across the warm regions of Asia and North America, where it dominates the dominant evergreen broad-leaved forests (Plants of the World Online: https://powo.science.kew.org/, accessed on March 20, 2024). *Lindera* species have multifaceted economic applications, including timber production, edible fruits, spices, and essential oils for perfumes and soaps (Editorial Committee of Flora Republicae Popularis Sinicae, 1982). These species also have a long history in traditional medicine for various ailments, including rheumatism, headaches, indigestion, and gastroenteritis. Numerous species are rich in natural compounds, particularly the roots of *L. aggregata* (Sims) Kosterm, which is a renowned TCM referred to as "wuyao" (Cao et al., 2015). Most *Lindera* plants produce complex secondary constituents, such as flavonoids, terpenoids, and steroids, and exhibits notable antibacterial activities (Cao et al., 2015).

L. communis Hemsl., the target species of this study is an evergreen plant native to central and southern China, Vietnam, Myanmar, India and southern Japan (Liao, 1996). The usage of this substance in Chinese traditional medicine dates back to ancient times due to its well-documented hemostatic, analgesic, and antipyretic properties. Additionally, its fruit can be used to extract aromatic oil for fragrance. The roots, branches and leaves have been traditionally employed as a remedy for wound healing and skin diseases in cattle and horses (Hu, 1996). This traditional knowledge suggests that the *L. communis* may possess antibacterial properties, which aligns with findings in the existing literature (Yang et al., 1999). Based on this, we hypothesize that *L. communis* possesses potential therapeutic properties for bacterial infections. The hexane extract from *Lindera* roots, known for its high activity within the *Lindera* genus, is being investigated for antimicrobial activity due to the different constituents such as sesquiterpenes.

The emergence of drug-resistant (MDR) microorganism has presented a serious threat to healthcare in recent decades and is responsible for various bacterial infections (Kupferschmidt, 2016). These strains, including MRSA, vancomycin-resistant *Enterococci*, carbapenem-resistant bacteria, and colistin-resistant Enterobacteriaceae, presents a significant menace to the wellbeing of the general public (Chambers and Deleo, 2009; Tacconelli and Cataldo, 2008; Walsh et al., 2011). As a result, the discovery of new antibacterial agents has become a priority. The utilization of natural constituents, particularly plant extracts and their components, has been extensively employed in bacterial infections (Sohn et al., 2004; More et al., 2017).

Therefore, we selected MRSA to investigate the antibacterial activity of LCH. Our study included the detection of phytochemical constituents, determination of the MIC of various fractions of *L. communis* extracts, investigation of the growth pattern of bacteria, examination of the integrity of cell membranes, observation of alterations in membrane potential, and assessment of the effectiveness against MRSA using scanning electron microscopy (SEM). Moreover, wound healing models were employed to



GRAPHICAL ABSTRACT

evaluate the possibility and scientifically substantiate its uneventful application as a wound healing agent.

2 Materials and methods

2.1 Sample collection and preparation

The roots of *L. communis* were collected from Tengchong in Yunnan Province, China, in June 2022. A voucher specimen was expertly identified by Dr. Chunlin Long and has been archived in the Herbarium at MUC.

Briefly, the air-dried and powdered roots of *L. communis* (1.2 kg) were extracted with 95% EtOH (30 L × 3) at room temperature. The solvent was evaporated under reduced pressure, resulting in a brown residue (LCR, 276.2 g), which was then suspended in ddH_2O (3 L) and subjected to sequential extractions with n-hexane (3 L × 3) and EtOAc (3 L × 3), ultimately yielding hexane-soluble fractions: the *n*-hexane-soluble (LCH) fraction (101.2 g), EtOAc-soluble (LCE) fraction (87.1 g) and H_2O -soluble (LCW) fraction (67.3 g).

2.2 Chemical analysis

Sample (100 ± 2 mg) was put into the 20 mL headspace bottle, and 10 μL of 2-Octanol (10 mg/L stock in dH_2O) was added as internal standard. All samples were analyzed by gas chromatograph system coupled with a spectrometer (GC-MS) and GC-MS analysis of each biological replicate was replicated three times. In SPME cycle of PAL rail system, the incubate temperature was controlled at 60°C. Preheat time is 15 min; Incubate time is 30 min; Desorption time is 4 min. GC-MS analysis was performed using an Agilent 7,890 gas chromatograph system coupled with a 5977B mass spectrometer. The system utilized a DB-Wax. Injected in Splitless Mode. Helium was used as the carrier gas, the front inlet purge flow was 3 mL min^{-1}, and the gas flow rate through the column was 1 mL min^{-1}. The initial temperature was kept at 40°C for 4 min, then raised to 245°C at a rate of 5°C min^{-1}, kept for 5 min. The injection, transfer line, ion source, and quad temperatures were 250, 250, 230, and 150°C, respectively. The energy was −70 eV in electron impact mode. The mass spectrometry data were acquired in scan mode with the m/z range of 20–400, a solvent delay of 2.37 min. Chroma TOF 4.3X software of LECO Corporation and Nist database were used for raw peaks exacting, the data baselines filtering and calibration of the baseline, peak alignment, deconvolution analysis, peak identification, integration, and spectrum match of the peak area.

2.3 MIC and time-killing assay

The LCH was diluted in MHB medium at 37°C and incubated in a 96-well microtiter plate format for the MIC of LCH against *E. faecalis* (*Enterococcus faecalis* 102668), *S. epidermidis* (*Staphylococcus epidermidis* 102555), *S. aureus* (*Staphylococcus aureus* 3406520), *E. coli* (*Escherichia coli* 133264), *S. para-typhi β* (*Salmonella para-typhi β* 103169), and, Methicillin-resistant *Staphylococcus aureus* MRSA JCSC 3063 were cultured under aerobic condition. Through previous experimental validation, it was confirmed that dimethyl sulfoxide (DMSO), used as the solvent, exhibited no significant toxic effects on methicillin-resistant *Staphylococcus aureus* (MRSA) at a concentration of 2.5%. Different concentrations of LCH groups were solubilized using 2.5% DMSO, while the control group received an equivalent volume of 2.5% DMSO without LCH. MRSA was cultured in MHB at 37°C until at an OD_{600} of 0.3 and then treated with LCH at 0.1, 0.2, 0.4, and 0.8 mg/mL (1, 2, 4, and 8 MIC) (Epoch full-wavelength microplate reader, BioTek Company, United States). To ensure the consistency of experimental conditions, in addition to maintaining uniform drug administration protocols, we rigorously controlled other factors that could influence bacterial growth, such as temperature, humidity, shaker speed, and incubation time.

2.4 Membrane potential measured with DiOC2(3)

MRSA (logarithmic growth phase) was subjected to three washes with 5 mM HEPES. Following this, the bacterial were adjusted to achieve an OD_{600} of 0.5, thoroughly mixed, and subsequently incubated with DIOC2(3) (30 μM) (Thermo Fisher Scientific 66, Massachusetts, United States) for 20 min at 37°C. Following an incubation period, the bacterial cells were exposed to various concentrations of LCH (0.1, 0.2, 0.4, and 0.8 mg/mL) as well as CCCP at a concentration of 100 μM. Measurements were conducted in fluorimeter equipped with 530 nm excitation and 630 nm emission filters (Multifunctional enzyme marker, Espire, PerkinElmer, United States).

2.5 Resazurin assay

MRSA was cultured at 37°C until reaching an OD_{600} of 0.3 and subjected to treatment with LCH at 0.1, 0.2, 0.4, and 0.8 mg/mL, or 100 μM CCCP. Samples were collected at 10, and 30 min, diluted to an OD_{600} of 0.15, and then incubate with resazurin at 30°C. Fluorescence intensities were measured at 540 and 630 nm (Multifunctional enzyme marker, Enspire, PerkinElmer, United States).

2.6 Membrane integrity measured with PI

The MRSA (OD_{600} = 0.4) was treated with the LCH for 4 h, then incubated with 10 μg/mL PI until the fluorescence reading stabilized. The fluorescence intensity was measured at 535 nm (excitation) and 617 nm (emission) of (Multifunctional enzyme marker, Enspire, PerkinElmer, United States).

2.7 SYTOX green assay

The MRSA suspension (logarithmic growth phase, OD_{600} = 0.4) was washed three times with 0.85% NaCl, then treated with 4 MIC of LCH and melittin for 3 hours, and incubated with 3 μM of SYTOX

green. Finally, the suspension was fixed on a 6-well plate and then observed using a fluorescence microscope (IX81 electric inverted microscope, Olympus, Japan) with an excitation wavelength of 485 nm.

2.8 Morphological observation of MRSA

Scanning electron microscopy (SEM) was used to observe the morphological changes in MRSA. MRSA were treated with 0.2 mg/mL LCH for 4 h, collected by centrifuge at 5,000 g for 10 min, and then fixed with 2%–5% glutaraldehyde overnight at 4°C. A gradient dehydration protocol was employed, sequentially immersing the samples in ethanol solutions with concentrations of 30%, 50%, 70%, 85%, 90%, 95% and finally, absolute ethanol (100%). The sample underwent drying, followed by deposition of a 10 nm-thick coating using an ion sputtering device. Subsequently, it was stored in a desiccator until examination under a scanning electron microscope operating at 20–0 kV (Hitachi S-4800, Tokyo, Japan).

2.9 AKP activity

The MRSA was washed three times with centrifuge, and the cell was adjusted to 10^6 CFU/mL. Then, the bacterial was supplemented with LCH at 0.1, 0.2, 0.4, and 0.8 mg/mL and subjected to incubation at 37°C for a duration of 10 h. Following bacterial collected by centrifuge at 8,000 g for 10 min, and alkaline phosphatase was tested by AKP assay kit (Beyotime, Shanghai, China).

2.10 Mammalian cytotoxicity

The cell viability of LCH on HaCaT were assessed using the Cell Counting Kit-8 (CCK-8). Briefly, HaCaT cells were seeded in 96-well plates with 100 μL (2×10^5 cells/well). Following incubation with varying concentrations of the tested substance, then tested with CCK-8 assay kit. Finally, we measured the OD value at 450 nm using a Microplate Reader (Beyotime, Shanghai, China).

2.11 Wound healing on the epithelialization

A total of 32 SD rats were procured from the Department of Experimental Animal Science, Peking University Health Science Center (SCXK(JING)2021-0013) and acclimated for 1 week prior to the experiment. The animals were housed in 22° ± 2° with natural light/dark cycles and provided clean water and chow. The rats with excision wounds were divided into four groups, each consisting of eight rats: the model M group (wounds + no treatment), the control (C) group (no wounds), the positive group (wounds + treated with 1% SSD (Silver sulfadiazine)), and the LCH group (excision wounds + treated with 10 mg LCH (red oil)). After 24 h of wound creation, LCH (red oil) 10 mg, 1% silver sulfadiazine (SSD) 0.1 g were topically applied to gently cover the wounded area once daily until complete wound healing. Wound area and wound contraction were monitored every 48 h until complete wound healing was achieved for all groups. All the wounds received daily standard wound cleansing with 0.9% normal saline prior to the topical application of treatments (0.1 g/unit wounded area [4 cm^2]/day). The experimental procedure was carried out in compliance with the ethics requirements (ECMUC2021012AO).

2.12 Histology of healed tissue

Upon full wound healing, rats were euthanized approved by the ethical review of MUC. The sections of tissue were prepared using an established method (George et al., 1995). In brief, the healed tissues were initially fixed in 10% formalin, followed by progressive dehydration by graded ethanol, clearing in xylene, and subsequent embedding in paraffin wax for histological assessment. The tissue samples were sectioned into four-mm slices using a microtome, followed by staining with Harris hematoxylin and eosin (HE). The stained sections were then mounted onto microscopic slides, covered with coverslips, and subsequently examined using a light microscope. Images were acquired using Ultra View ERS confocal laser scanning microscopy (Nikon/OLYMPUS, E100/CX23, Japan).

2.13 Statistical analysis

All the data were subjected to ANOVA for multiple groups using GraphPad Prism 10.0 software (Prism GraphPad) ($P < 0.05$).

3 Results

3.1 GC-MS analysis

The phytochemical components present with their name, molecular formula, compound types, retention time (RT), as well as their relative abundance (Aera), which was quantified as the percentage of peak area detected by GC-MS. The results revealed that 49 compounds, based on comparisons with the NIST library. These compounds belong to different classes, including fatty acids, terpenes and other compounds. The chemical composition of the LCH is shown in Table 1, accounting for 85.68% of the total content. The volatile oils in the root hexane Extract of *L. communis* included characteristic detected components such as humulene-type sesquiterpenes, elemane-type sesquiterpenes, guaiane-type sesquiterpenes and Decanoic acid, ethyl ester (lauric acid), which is consistent with the phytoconstituents reported the review of *Lindera* species (Cao et al., 2015).

3.2 MIC and time-killing assay

The roots of *L. communis* were extracted using 95% ethanol, and the resulting crude ethanol extracts was fractionated to obtain n-hexane, EtOAc, and water fractions. As shown in Table 2, all of the extracts presented bactericidal activity against bacteria. The antimicrobial activity of LCH against MRSA JCSC 3063 (MIC: 0.1 mg/mL). The fractions exhibited limited efficacy against Gram-negative bacteria.

TABLE 1 Analysis of volatile components of LCH.

No.	Compounds	Molecular formula	Class	RT (minutes)	Aera
1	Humulene	$C_{15}H_{24}$	H-S	23.1	10.29%
2	Aciphyllene	$C_{15}H_{24}$	G-S	24.1	9.79%
3	Decanoic acid, ethyl ester	$C_{12}H_{24}O_2$	fatty acid	22.4	6.22%
4	(1*R*,1a*R*,2a*S*,6*R*,6a*S*,7a*S*)-1,6,6a-Trimethyldecahydro-1,2a-methanocyclopropa[b]naphthalene	$C_{15}H_{24}$	sesquiterpene	22.6	5.84%
5	(-)-α Panasinsen	$C_{15}H_{24}$	sesquiterpene	25.2	4.33%
6	2,4-Di-tert-butylphenol	$C_{14}H_{22}O$	phenols	35.9	3.36%
7	Hexanoic acid, ethyl ester	$C_8H_{16}O_2$	fatty acid	11.6	2.18%
8	Guaiol	$C_{15}H_{26}O$	G-S	31.9	2.14%
9	Nonanoic acid, ethyl ester	$C_{11}H_{22}O_2$	fatty acid	19.9	2.11%
10	(2*R*,8*R*,8a*S*)-8,8a-Dimethyl-2-(prop-1-en-2-yl)-1,2,3,7,8,8a-hexahydronaphthalene	$C_{15}H_{22}$	E-S	26.4	2.11%
11	Calamenene	$C_{15}H_{22}$	sesquiterpene-Calamenene	26.7	2.06%
12	5,7-dimethyl-undecane	$C_{13}H_{28}$	fatty acid	13.5	1.85%
13	6,7-Dimethyl-1,2,3,5,8,8a-hexahydronaphthalene	$C_{12}H_{18}$	E-S	17.6	1.63%
14	Dihydro-3-methylene-5-methyl-2-furanone	$C_6H_8O_2$	ester	26.6	1.60%
15	Calamenene	$C_{15}H_{24}O$	E-S	25.6	1.50%
16	4a,8-Dimethyl-2-(prop-1-en-2-yl)-1,2,3,4,4a,5,6,7-octahydronaphthalene	$C_{15}H_{24}$	E-S	23.2	1.40%
17	Propanoic acid	$C_3H_6O_2$	fatty acid	20.1	1.33%
18	4a,5-Dimethyl-3-(prop-1-en-2-yl)-1,2,3,4,4a,5,6,7-octahydronaphthalen-1-ol	$C_{15}H_{24}O$	E-S	28.24	1.31%
19	1,4-Dimethyl-7-(prop-1-en-2-yl)decahydroazulen-4-ol	$C_{15}H_{24}$	G-S	34.1	1.30%
20	2-pentyl-Furan	$C_9H_{14}O$		11.5	1.18%
21	2-((2*R*,4a*R*,8a*S*)-4a-Methyl-8-methylenedecahydronaphthalen-2-yl) acrylaldehyde	$C_{15}H_{22}O$	E-S	37.5	1.10%
22	Pentanoic acid	$C_5H_{10}O_2$	fatty acid	25.1	1.06%
23	(-)-Nootkatene	$C_{15}H_{22}$	E-S	25.6	1.04%
24	Heptanoic acid, ethyl ester	$C_9H_{18}O_2$	fatty acid	14.5	1.01%
25	Epicubenol	$C_{15}H_{26}O$	E-S	32.1	0.99%
26	Myrtenol	$C_{10}H_{16}O$	monoterpene	25.9	0.98%
27	6,7-Dimethyl-1,2,3,5,8,8a-hexahydronaphthalene	$C_{12}H_{18}$		20.5	0.98%
28	(*E*)- Calacorene	$C_{15}H_{20}$	E-S	28.4	0.95%
29	delta-Amorphene	$C_{15}H_{24}$	E-S	25.1	0.90%
30	delta-Guaiene	$C_{15}H_{24}$	G-S	24.9	0.90%
31	2-methylene-5-(1-methylvinyl)-8-methyl-Bicyclo[5.3.0]decane	$C_{15}H_{24}$	G-S	21.6	0.90%
32	1-Naphthalenol	$C_{15}H_{24}O$	E-S	26.8	0.84%
33	1-Hexanol	$C_6H_{14}O$	fatty acid	15.9	0.76%
34	Hexadecane	$C_{16}H_{34}$	fatty acid	12.0	0.75%
35	Decane	$C_{10}H_{22}$	fatty acid	5.0	0.71%

(Continued on following page)

TABLE 1 (*Continued*) Analysis of volatile components of LCH.

No.	Compounds	Molecular formula	Class	RT (minutes)	Aera
36	Glaucyl alcohol	$C_{15}H_{24}O$	G-S	37.7	0.67%
38	(1*R*,3*E*,7*E*,11*R*)-1,5,5,8-Tetramethyl-12-oxabicyclo[9.1.0]dodeca-3,7-diene	$C_{15}H_{24}O$	H-S	30.9	0.64%
39	Dodecane	$C_{12}H_{26}$	alkane	10.5	0.62%
40	2-Ethylhexan-1-ol	$C_8H_{18}O$	fatty acid	18.8	0.61%
41	Terpineol	$C_{10}H_{18}O$	alcohol	23.8	0.60%
42	(*E*)-2-Undecene, 3-methyl	$C_{12}H_{24}O_2$	alcohol	11.9	0.59%
43	Diethyl butanedioate	$C_8H_{14}O_4$	ester	23.3	0.58%
44	Benzaldehyde	C_7H_6O	aldehyde	19.4	0.58%
45	(1*R*,4*S*,5*R*)-Verbenyl, ethyl ether	$C_{12}H_{20}O$	fatty acid	15.6	0.56%
46	3-methyl-Butanoic acid	$C_5H_{10}O_2$	fatty acid	23.4	0.55%
47	5-Hexen-2-one	$C_6H_{10}O$	ester	8.6	0.54%
48	Pinocarveol	$C_{10}H_{16}O$	monoterpene	22.8	0.54%
49	10-epi-gamma-Eudesmol	$C_{15}H_{26}O$	phenolic acids	34.0	0.54%

Note: RT: retention time, E-S, elemane-type sesquiterpene: G-S, guaiane-type sesquiterpene: H-S, humulene-type sesquiterpene.

TABLE 2 The screening of antibacterial activity.

Bacteria	MIC (mg/mL)					
	E. faecalis 102668	*S. epidermidis* 102555	*S. aureus* 3406520	MRSA JCSC 3063	*E. coli* 133264	*S. para-typhi β* 103169
G^+/G^-	G^+	G^+	G^+	G^+	G^-	G^-
LCR	2.875	0.65	0.65	0.65	>100	>100
LCW	3.56	0.79	1.56	1.56	>100	>100
LCE	6.25	6.25	12.5	12.5	>100	>100
LCH	0.2	0.1	0.1	0.1	>100	>100
Vancomycin	ND	ND	0.62×10^{-3}	0.62×10^{-3}	ND	ND
Kanamycin	ND	ND	ND	ND	12.5	12.5

ND: not detected.

As shown in Figure 1A, the impact of LCH on the growth of MRSA is detected. Arrow marks are the time point of LCH addition. The bactericidal activity of LCH was equivocal after 1 h exposure at concentrations of 1× MIC and 2× MIC, while a pronounced bactericidal effect was observed with a marked reduction in CFU following 1 h exposures to doses of different multiples of MIC values.

3.3 Membrane potential measured with DiOC2(3)

DIOC2(3) is a potentiometric probe known for its affinity to visualized the change of membrane permeability. Disruption of membrane permeability results in the release of the probe into the surrounding medium, thereby inducing a substantial enhancement in fluorescence. DIOC2(3) is a widely acknowledged membrane potential probe that specifically localizes within the bacterial membrane to detect alterations in membrane potential (Minderman et al., 1996; Aqawi et al., 2021). We investigated whether LCH disrupts the membrane potential using the probe DiOC2(3) (Figure 1B). Indeed, our results revealed hyperpolarization of cells, in contrast to the depolarization induced by the proton ionophore CCCP (Figure 1B), showing that LCH may give an ion channel, a membrane pore, or even potentially influence the respiratory chain. And further studies will be conducted to confirm this hypothesis (Saeloh et al., 2018).

3.4 Resazurin assay

To ascertain the impact of LCH on respiratory chain, we evaluated the decrease of resazurin, a widely used indicator for quantifying cellular reductive capacity (Abu-Amero and Bosley, 2005; Müller et al., 2016).

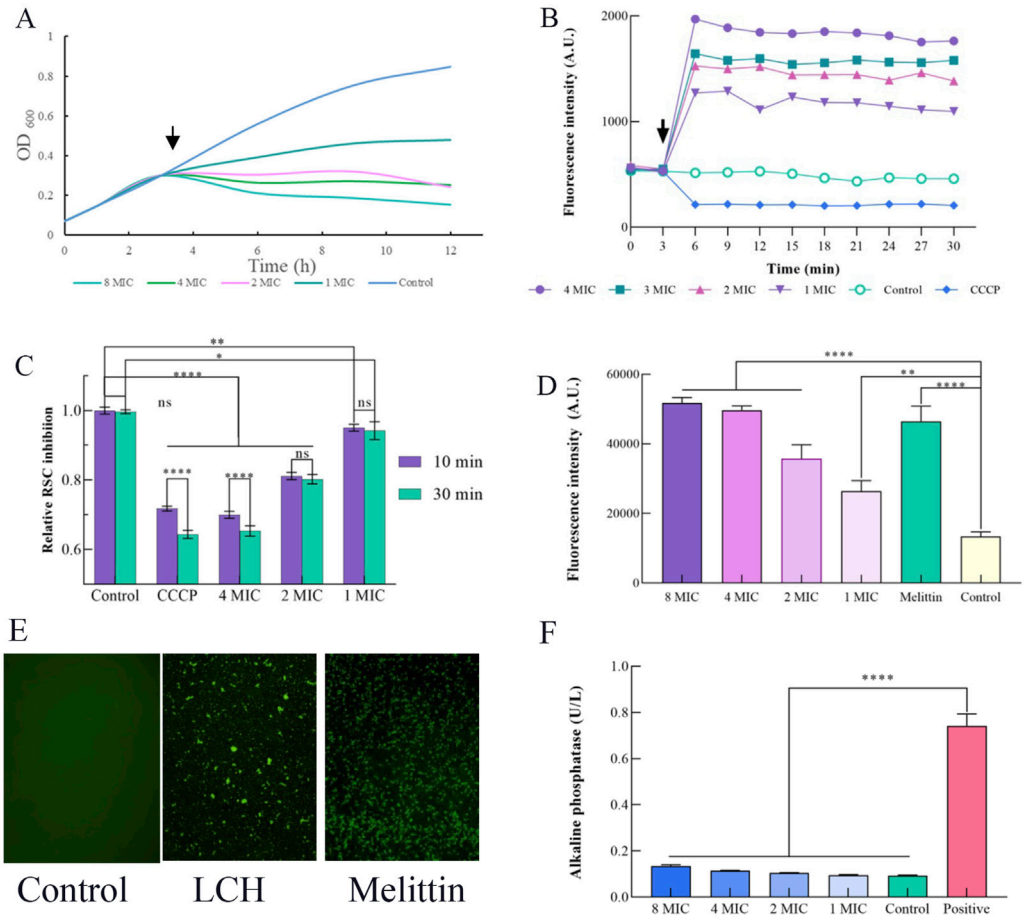


FIGURE 1
Effects of LCH on the cell envelope of MRSA (0.1, 0.2, 0.4, and 0.8 mg/mL that is 1× MIC, 2× MIC, 4× MIC and 8× MIC). **(A)** Growth curve. Impact of LCH on MRSA growth. Arrow indicates the time point of LCH addition. **(B)** Measurement of membrane potential using the fluorescent dye DiOC(3)5 with 0.1, 0.2, 0.4, and 0.8 mg/mL LCH. The arrow denotes the time point of LCH addition, and CCCP was used as a positive control. **(C)** Resazurin assay. Assessment of respiratory chain activity through resazurin reduction to resorufin with the treatment of 0.1, 0.2, 0.4, and 0.8 mg/mL LCH. CCCP served as a positive control. **(D)** Staining with PI. The fluorescent dye serves as an indicator for the presence of substantial membrane pores or significant membrane disruption in MRSA with the treatment of 0.1, 0.2, 0.4, and 0.8 mg/mL LCH, while melittin was employed as a positive control. **(E)** The fluorescence emission of MRSA with the LCH was detected through SYTOX Green binding to nucleic acid. The use of SYTOX Green showed that LCH at 1 mg/mL for 4 h significantly inhibited membrane rupture in MRSA, while no fluorescence increase was seen in the control group. Melittin was used as a positive control. **(F)** Influence of LCH on the cell wall. AKP activity of MRSA treated by LCH. *$P < 0.05$, **$P < 0.01$***, $P < 0.001$****, $P < 0.0001$. Data are expressed as mean ± SD, n = 3. LCH: Hexane Extract from *Lindera communis* Roots.

Certainly, after incubation with LCH, there was only a slight reduction in the reductive capacity of MRSA, suggesting a relatively modest impact on the electron transport chain (Figure 1C). The observed effect exhibited a comparable magnitude to that elicited by CCCP, known for its role in decoupling the electron transport chain, and was closer to the control group (Figure 1C). Consequently, the influence of LCH on the maintenance and generation of the proton motive force can be deduced.

3.5 Membrane integrity measured with PI

PI was employed to further investigate and probe the membrane-disrupting effects of LCH, which was utilized to assess the integrity of the cell membrane through binding to exposed nucleic acids in a fluorescent fashion (Lin et al., 2017). Melittin, used as a positive control, resulted in substantial increases in fluorescence intensity, signifying the disruption of cell membranes. This effect was further validated through the use of the fluorescent indicator PI is capable of cellular entry through pores or in cases of severe membrane breaches (Wenzel et al., 2013). After treatment with LCH, a notable PI influx was observed at concentrations of 1×, 2×, 4× and 8× MIC, closely resembling the results obtained with Melittin (Figure 1D). This indicated that LCH may either disrupt bacterial cell membranes or create small breaches in them. Thus, the PI assay corroborates the findings from the membrane potential study, where significant fluorescence intensity was observed across different concentrations. It is speculated that LCH exerts its antibacterial effects by affecting the membrane.

3.6 SYTOX green assay

Most satisfyingly, the SYTOX Green assay yielded consistent results with the fluorescence intensity, which was observed in the PI

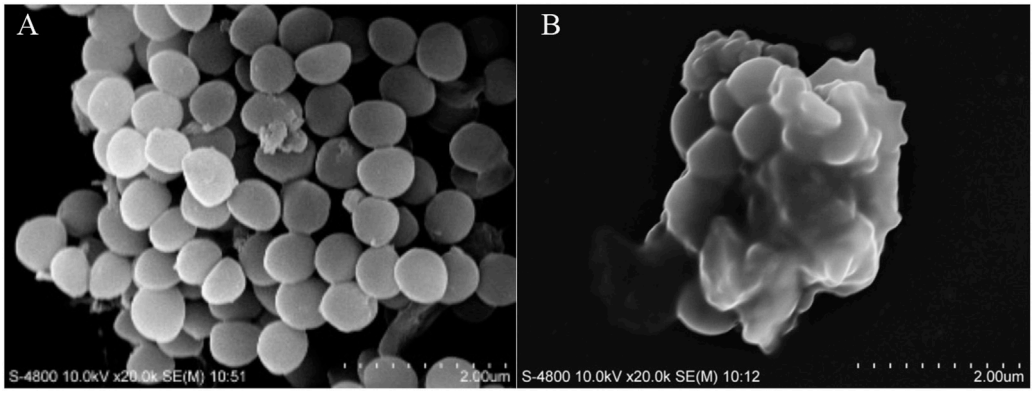


FIGURE 2
Morphological observation of MRSA by SEM. **(A)** Control. **(B)** 2× MIC (0.2 mg/mL).

assay (Figure 1E). When LCH was treated with 1 mg/mL LCH for 4 h, the fluorescence was clearly observed in the SYTOX Green assay. The control group, in contrast, exhibited no change in fluorescence, whereas the melittin group induced a sharp increase in fluorescence intensity under identical conditions. This result aligns with the findings of the PI assay, further confirming that LCH disrupts the cell membrane (Lebaron et al., 1998).

3.7 AKP activity

Alkaline phosphatase (AKP), located within the space between the cellular membrane and wall, is released into the extracellular milieu upon compromise or damage to the cell wall (Diao et al., 2018). Therefore, the AKP activity serves as an indicative measure of the cell wall's integrity. As depicted in Figure 1F, AKP activity in the C group and the LCH-treated groups at 1×, 2×, 4×, and 8× MIC remained relatively stable even after a 10 h incubation period, whereas the standard group exhibited a significant 5.39-fold increase in AKP activity, which indicates that the permeability of the MRSA cell wall remained largely unchanged following treatment with LCH.

3.8 Morphological observation of MRSA

The morphological alterations in MRSA induced by LCH were observed using SEM. As illustrated in Figure 2, the cell surface of the control group appeared smooth and round, with well-defined edges, intact structure, and uniform short rods. After a 4 h incubation with 0.2 mg/mL of LCH, significant morphological alterations were observed, characterized by distinct ruptured membranes and the collapse of cell surface structures. The observed alterations in cell morphology strongly indicate that the potent biological activities of LCH primarily result from its ability to disrupt membrane integrity.

3.9 Mammalian cytotoxicity

An assessment of the toxicities of LCH was conducted on the HaCaT cell lines (Human immortal keratinocyte lines). The IC_{50} value against HaCaT cells was 1.83 ± 0.21 mg/mL, Which is far higher than the MIC agaisnst MRSA and safety with an appropriate dosage.

3.10 Wound healing on the epithelialization

After establishing wounds model in rats, receiving daily treatments subsequently, it was observed that the untreated excisional-wounded rats had a longer period of epithelialization compared to 1% SSD group. Additionally, LCH treatment shortened the period of epithelialization compared to the M group (Figure 3). The wound contraction rate was observed to be slower in the Mrats compared to the 1% SSD group. However, treatment with LCH group significantly improved the wound contraction rate compared to the model group (Figure 3). Meanwhile, the control group exhibited noticeable pus formation from day 6–12, while the LCH-treated group did not. Previous studies have demonstrated the potential of *Lindera* extracts as analgesic agents due to their remarkable anti-inflammatory effects and pain-relieving properties in traditional medicine (Cao et al., 2015). It showed that antibacterial, noninflammatory and antinociceptive effects have resulted in the wounding healing.

3.11 Histology of healed tissue

The control group showed variable-sized hair follicles, large sebaceous glands, and loose granulation tissue with limited inflammatory cell infiltration (Figure 4A). The positive control group showed a thin epidermis and loose granulation dermis with widespread eosinophilic collagen fibers, moderate inflammatory cell infiltration, coagulation within the hair follicle, fewer hair follicles, and sebaceous glands (Figure 4B). The model group exhibited a thickened epidermis and compact fibrotic granulation dermis with mild eosinophilia of collagen fibers, accompanied by significant infiltration of inflammatory cells and minimal presence of sebaceous glands (Figure 4D). The LCH group exhibited a thickened epidermis and a loosely arranged granulation dermis with moderate inflammation and sparse sebaceous glands

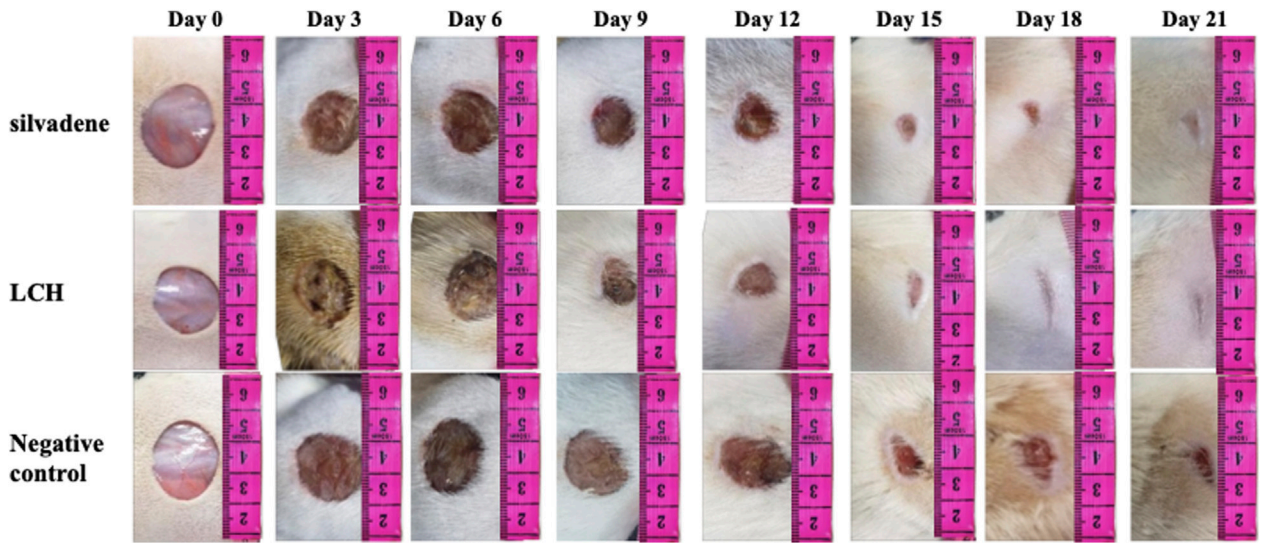


FIGURE 3
The effect of LCH on wound contraction was monitored every 72 h during treatment.

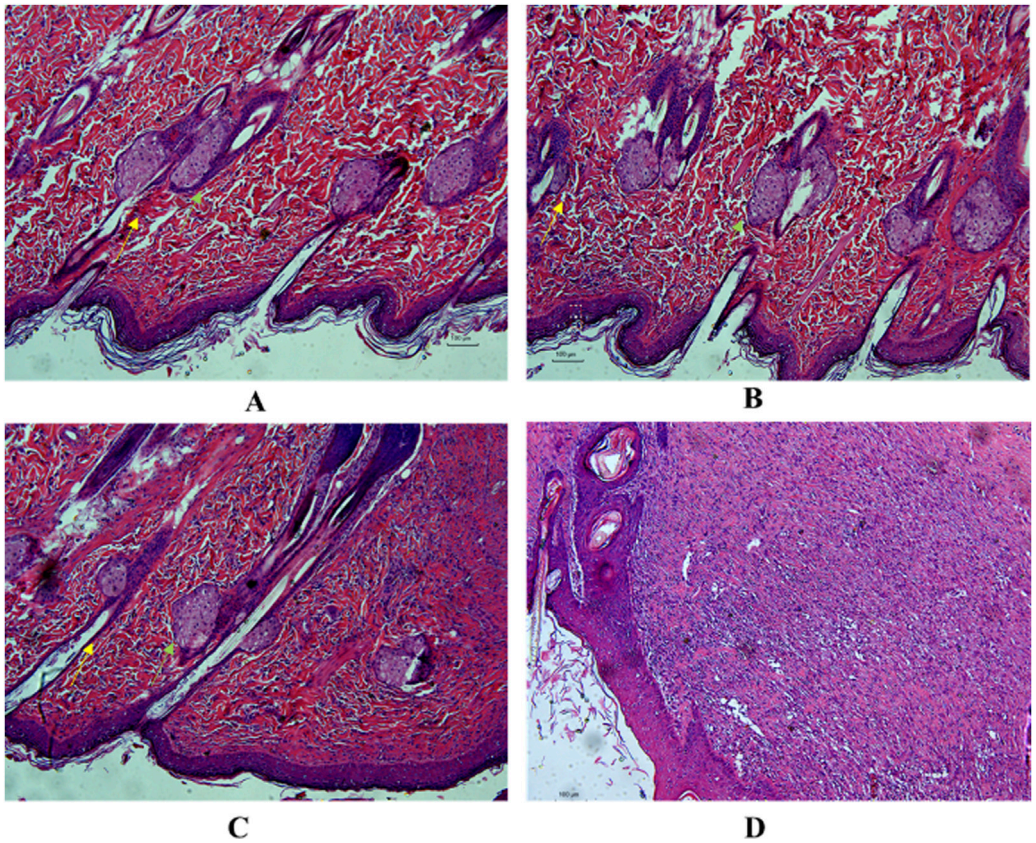


FIGURE 4
Histological section displays the regenerated epidermis and dermis in the healed wound tissue. **(A)** Control, **(B)** 1% SSD (0.1 g), **(C)** LCH (10 mg), **(D)** Model.

(Figure 4C). The histomicrographs indicate that LCH demonstrates a significant decrease in the infiltration of inflammatory cells compared to the model, suggesting its potential as an effective anti-inflammatory and antibacterial agent.

4 Discussion

The mixture and the isolated compounds from *Lindera* hexane extract exhibit potential therapeutic activity against various diseases. The extract of *Lindera* has demonstrated significant antifungal and antibacterial properties and these antibacterial activities can be attributed to low polar compounds, such as sesquiterpenes, monoterpenes and fatty acids (Cao et al., 2015; Lv et al., 2023; Tao et al., 2024). Before the antibacterial experiment, we compared the antibacterial activities of various plant parts (roots, stems, leaves, and fruits) and found the roots to have the highest activity. Further tests on root fractions revealed the n-hexane fraction as the most active. Literature review (Yan et al., 2009) indicated that antibacterial components in *Lindera* root extracts are likely present in essential oils. Thus, we used SPME GC-MS for analysis. This aligns with reported effective antibacterial components in Lauraceae plants or Lindera (Wang et al., 1999; Kim et al., 2009; Yan et al., 2009; Joshi et al., 2010). Based on prior studies and fraction activity screening, we speculate that the antibacterial components are low-polarity compounds.

The major compounds detected in root LCH of *L. communis* includes the following groups: humulene-type sesquiterpenes, elemane-type sesquiterpenes, guaiane-type sesquiterpenes and lauric acids and others. Characterizations of GC-MS revealed the presence of humulane-type sesquiterpenoids, widely distributed in plants and microbes, which possessed antibacterial for *B. fragilis* (MIC 2 μg/mL) (Al-Taweel et al., 2004; Djabou et al., 2013; Jiao et al., 2018; Jang et al., 2020). The guaiane-type sesquiterpenes were also detected by GC-MS and the active constituents derived from medicinal plants are believed to yield enhanced and targeted pharmaceuticals. Guaiane-type sesquiterpenoids were identified based on their molecular weight and are known for their antibacterial, anti-inflammatory, and anticancer effects (Guo et al., 2023). In addition, fatty acids and their monoglyceride derivatives, such as lauric acid, show strong antimicrobial activities (Borrelli et al., 2021). After detection, the humulene-type sesquiterpenes, guaiane-type sesquiterpenes and lauric acid may be responsible for the antibacterial activities. Then we conducted assessments of antibacterial activity against MRSA and other common bacteria. In our present study, LCH exhibited antibacterial activities solely against MRSA (MIC = 0.1 mg/mL). It is anticipated that our future research will elucidate the primary active ingredients in greater detail, rather than solely relying on literature reviews and SPME GC-MS analysis.

To enhance comprehension LCH's antibacterial mechanism, we assessed its time-kill kinetics, which demonstrated that LCH efficiently achieved reductions with different dose drugs within 15 h, displaying a concentration-dependent and time-dependent antibacterial activity pattern. Notably, many antibiotics target the cell membrane, membrane potential, and cell wall (Sani and Separovic, 2016; Epand et al., 2016). It is suggested that LCH may primarily target cytoplasmic membranes, as membrane composition is likely a key factor in the varying sensitivities of different bacterial species to LCH.

With the assistance of the DiOC2(3) probe, significant alterations in fluorescence intensity were observed upon treatment of MRSA with LCH. The resazurin assay further confirmed that LCH disrupted the membrane potential through affecting the respiratory chain of MRSA cells. Fluorescence probe PI and SYTOX Green, which bind to nucleic acids, along with fluorescence imaging technology, were to investigate the impact of LCH on the enhancement of membrane permeability (Strahl and Hamoen, 2010). As a result, they consistently showed detectable fluorescence intensity after bacterial treatment with 0.1–0.2 mg/mL LCH. However, LCH did not significantly increase AKP activity, even at 8 x MIC of LCH. SEM analysis of LCH-treated MRSA revealed changes in cell morphology, including noticeable perforations in the cell membrane. These consistent findings indicate that LCH inhibits MRSA by disrupting the cell membrane. The findings of the time-killing assay could be explained, where the bactericidal activity of LCH became evident after 1 h of exposure at all concentrations, and maintained persistent bactericidal efficacy throughout the entire 15-h duration. Therefore, these informative findings collectively substantiate the conclusion that the bactericidal activity of LCH is attributed to aberrations occurring at the cellular membrane.

A key characteristic of an ideal antibiotic is its harmlessness to the host. To evaluate this, cytotoxicity assays were conducted using HaCaT cells, determining an to be 1.83 ± 0.21 mg/mL with a therapeutic index of 0.1 μg/mL. Additionally, we assessed the impact of the LCH wound healing formula on the epithelialization period, which demonstrated significant effects. Histological analysis of the healed tissue also confirmed these findings. These results validate the scientific basis of the traditional knowledge regarding LCH.

5 Conclusion

Based on our findings, humulene-type sesquiterpenes, guaiane-type sesquiterpenes and lauric acid were identified as the main chemical constituents of LCH. At the same time, the LCH possessed excellent antibacterial activity against G^+ bacteria especially the MRSA (MIC value: 0.1 mg/mL). The time-killing curve and SEM were employed to assess the efficacy of LCH against MRSA and effectively suppress its growth. We further investigated the impact of LCH on the membrane of MRSA and hypothesized that it exerted a profound influence on MRSA growth by inducing significant morphological alterations, leading to the disruption of cell surface structures, hyperpolarization of the membrane, and perturbations in membrane integrity. That is, the mode of action of the substance involves membrane perturbation as one of its mechanisms. LCH exhibited antibacterial efficacy against G^+ bacteria with low minimal cytotoxicity. Meanwhile, LCH has exhibited wound-healing efficacy and bacteriostatic effects in excisional wounds in rats, confirming the potential use of *L. communis* root as a wound-healing agent. All the findings presented in this study collectively demonstrate that LCH exhibits significant inhibitory effects on the growth of MRSA by disrupting its membrane. These results suggest that LCH holds great

promise as a candidate for the advancement of innovative and readily available wound healing agents, and it proves the scientific essence of traditional uses.

Data availability statement

The original contributions presented in the study are included in the article material, further inquiries can be directed to the corresponding authors.

Ethics statement

The animal studies were approved by Care and Use of Laboratory Animals and received ethical approval from MUC. The studies were conducted in accordance with the local legislation and institutional requirements. Written informed consent was obtained from the owners for the participation of their animals in this study.

Author contributions

CL: Conceptualization, Funding acquisition, Resources, Supervision, Visualization, Writing–review and editing. MW: Data curation, Methodology, Writing–original draft, Writing–review and editing. XH: Data curation, Writing–review and editing. LL: Methodology, Writing–review and editing. YZ: Data curation, Writing–review and editing. WL: Data curation, Investigation, Writing–review and editing. QZ: Data curation, Methodology, Writing–review and editing. CX: Data curation, Methodology, Supervision, Writing–review and editing.

Funding

The author(s) declare that financial support was received for the research, authorship, and/or publication of this article. The research in this paper was financially supported by the Yunnan Provincial Sci & Tech Talent and Platform Program (202305AF150121), the Baoshan Administration of Gaoligongshan National Nature Reserve (GBP-2022-01), the National Natural Science Foundation of China (32370407, 31761143001 & 31870316). We are grateful to all members in the Ethnobotanical Laboratory at Minzu University of China for their valuable insights.

Conflict of interest

The authors declare that the research was conducted in the absence of any commercial or financial relationships that could be construed as a potential conflict of interest.

Generative AI statement

The authors declare that no Generative AI was used in the creation of this manuscript.

Publisher's note

All claims expressed in this article are solely those of the authors and do not necessarily represent those of their affiliated organizations, or those of the publisher, the editors and the reviewers. Any product that may be evaluated in this article, or claim that may be made by its manufacturer, is not guaranteed or endorsed by the publisher.

References

Abu-Amero, K. K., and Bosley, T. M. (2005). Detection of mitochondrial respiratory dysfunction in circulating lymphocytes using resazurin. *Arch. Pathol. Lab. Med. U. S. A.* 129, 1295–1298. doi:10.5858/2005-129-1295-domrdi

Alafnan, A., Dogan, R., Bender, O., Celik, I., Mollica, A., Malik, J. A., et al. (2023). Beta Elemene induces cytotoxic effects in FLT3 ITD-mutated acute myeloid leukemia by modulating apoptosis. *Eur. Rev. Med. Pharmacol. Sci.* 27, 3270–3287. doi:10.26355/eurrev_202304_32098

Al-Taweel, A., El-Deeb, K., and Al-Muhtadi, F. (2004). Chemical composition and antimicrobial activity of the essential oil of *Kleinia odora*. *Saudi Pharm. J.* 12, 47. doi:10.1080/14786419.2012.715291

Aqawi, M., Sionov, R. V., Gallily, R., Friedman, M., and Steinberg, D. (2021). Anti-bacterial properties of cannabigerol toward streptococcus mutans. *Front. Microbiol.* 12, 656471. doi:10.3389/fmicb.2021.656471

Borrelli, L., Varriale, L., Dipineto, L., Pace, A., Menna, L. F., and Fioretti, A. (2021). Insect derived lauric acid as promising alternative strategy to antibiotics in the antimicrobial resistance scenario. *Front. Microbiol.* 12, 620798. doi:10.3389/fmicb.2021.620798

Cao, Y., Xuan, B., Peng, B. F., Li, C., Chai, X. Y., and Tu, P. F. (2015). The genus *Lindera*: a source of structurally diverse molecules having pharmacological significance. *Phytochem. Rev.* 15, 869–906. doi:10.1007/s11101-015-9432-2

Chambers, H. F., and Deleo, F. R. (2009). Waves of resistance: *Staphylococcus aureus* in the antibiotic era. *Nat. Rev. Microbiol.* 7, 629–641. doi:10.1038/nrmicro2200

Deng, Z., Zhong, H., Cui, S., Wang, F., Xie, Y., and Yao, Q. (2011). Cytotoxic sesquiterpenoids from the fruits of *Lindera communis*. *Fitoterapia* 82, 1044–1046. doi:10.1016/j.fitote.2011.06.012

Diao, M., Qi, D., Xu, M., Lu, Z., Lv, F., Bie, X., et al. (2018). Antibacterial activity and mechanism ofmonolauroyl-galactosylglycerol against *Bacillus cereus*. *Food Control* 85, 339–344. doi:10.1016/j.foodcont.2017.10.019

Djabou, N., Lorenzi, V., Guinoiseau, E., Andreani, S., Giuliani, M., Desjobert, J. M., et al. (2013). Phytochemical composition of Corsican teucrium essential oils and antibacterial activity against foodborne or toxi-infectious pathogens. *Food Control* 30, 354–363. doi:10.1016/j.foodcont.2012.06.025

Epand, R. M., Walker, C., Epand, R. F., and Magarvey, N. A. (2016). Molecular mechanisms of membrane targeting antibiotics. *BBA-Biomembranes* 1858 (5), 980–987. doi:10.1016/j.bbamem.2015.10.018

George, M. H., Morgan, J. B., Glock, R. D., Tatum, J. D., Schmidt, G. R., Sofos, J. N., et al. (1995). Injection-site lesions: incidence, tissue histology, collagen concentration, and muscle tenderness in beef rounds. *J. Anim. Sci.* 73, 3510–3518. doi:10.2527/1995.73123510x

Guo, J., Wang, J. P., Peng, B., Liu, X. Q., Yang, C. X., Yan, L. H., et al. (2023). Research progress on natural guaiane-type sesquiterpenoids and their biological activities. *China J. Chin. Meter Med.* 48, 5727–5749. doi:10.19540/j.cnki.cjcmm.20230731.301

Hu, S. M. (1996). *Zhonghua bencao, volume III*. Shanghai: Shanghai Science and Technology Press, 61–62.

Jang, H. I., Rhee, K. J., and Eom, Y. B. (2020). Antibacterial and antibiofilm effects of α-humulene against *Bacteroides fragilis*. *Can. J. Microbiol.* 66, 389–399. doi:10.1139/cjm-2020-0004

Jiao, S. G., Zhang, R. F., Li, J. J., Wuken, S. N., Zhang, H. X., Tu, P. F., et al. (2018). Phytochemical and pharmacological progress on humulane-type sesquiterpenoids. *China J. Chin. Mater Med.* 43, 4380–4390. doi:10.19540/j.cnki.cjcmm.20180725.001

Joshi, S. C., Verma, A. R., and Mathela, C. S. (2010). Antioxidant and antibacterial activities of the leaf essential oils of Himalayan Lauraceae species. *Food Chem. Toxicol.* 48 (1), 37–40. doi:10.1016/j.fct.2009.09.011

Kim, S. S., Song, G., Oh, T. H., Kim, K. N., Yang, E. J., Kim, J. Y., et al. (2009). Antimicrobial effect of *Lindera erythrocarpa* essential oil against antibiotic-resistant skin pathogens. *J. Pure Appl. Microbiol.* 3 (2), 429–434.

Kupferschmidt, K. (2016). Resistance fighters. *Science* 352, 758–761. doi:10.1126/science.352.6287.758

Lebaron, P., Catala, P., and Parthuisot, N. (1998). Effectiveness of SYTOX Green stain for bacterial viability assessment. *Appl. Environ. Microbiol.* 64, 2697–2700. doi:10.1128/AEM.64.7.2697-2700.1998

Liao, J. C. (1996). *Lauraceae in Flora of taiwan, editorial committee of the Flora of taiwan, volume II*. Taipei: Tah Jinn Printing Company Ltd, 458–460.

Lin, S., Koh, J. J., Aung, T. T., Sin, W. L. W., Lim, F., Wang, L., et al. (2017). Semisynthetic flavone-derived antimicrobials with therapeutic potential against methicillin-resistant *Staphylococcus aureus* (MRSA). *J. Med. Chem.* 60, 6152–6165. doi:10.1021/acs.jmedchem.7b00380

Lv, Y., Zou, Y., Zhang, X., Liu, B., Peng, X., and Chu, C. (2023). A review on the chemical constituents and pharmacological efficacies of *Lindera aggregata* (Sims) Kosterm. *Front. Nutr.* 9, 1071276. doi:10.3389/fnut.2022.1071276

Minderman, H., Vanhoefer, U., Toth, K., Yin, M. B., Minderman, M. D., Wrzosek, C., et al. (1996). DiOC2(3) is not a substrate for multidrug resistance protein (MRP)-mediated drug efflux. *Cytometry* 25, 14–20. doi:10.1002/(SICI)1097-0320(19960901)25:1<14::AID-CYTO2>3.0.CO;2-E

More, N. V., Kharat, K. R., and Kharat, A. S. (2017). Berberine from *Argemone mexicana* L. exhibits a broadspectrum antibacterial activity. *Acta Biochim. Pol.* 64, 653–660. doi:10.18388/abp.2017_1621

Müller, A., Wenzel, M., Strahl, H., Grein, F., Saaki, T. N. V., Kohl, B., et al. (2016). Daptomycin inhibits cell envelope synthesis by interfering with fluid membrane microdomains. *Proc. Natl. Acad. Sci. U. S. A.* 113, E7077–E7086. doi:10.1073/pnas.1611173113

Saeloh, D., Tipmanee, V., Jim, K. K., Dekker, M. P., Bitter, W., Voravuthikunchai, S. P., et al. (2018). The novel antibiotic rhodomyrtone traps membrane proteins in vesicles with increased fluidity. *PLoS Pathog.* 14, e1006876. doi:10.1371/journal.ppat.1006876

Sani, M. A., and Separovic, F. (2016). How membrane-active peptides get into lipid membranes. *Acc. Chem. Res.* 49, 1130–1138. doi:10.1021/acs.accounts.6b00074

Sohn, H. Y., Son, K. H., Kwon, C. S., Kwon, G. S., and Kang, S. S. (2004). Antimicrobial and cytotoxic activity of 18 prenylated flavonoids isolated from medicinal plants: *Morus alba* L., *Morus mongolica* Schneider, *Broussnetia papyrifera* (L.) Vent, *Sophora flavescens* Ait and *Echinosophora koreensis* Nakai. *Phytomedicine* 11, 666–672. doi:10.1016/j.phymed.2003.09.005

Strahl, H., and Hamoen, L. W. (2010). Membrane potential is important for bacterial cell division. *Proc. Natl. Acad. Sci. U. S. A.* 107, 12281–12286. doi:10.1073/pnas.1005485107

Tacconelli, E., and Cataldo, M. A. (2008). Vancomycin-resistant enterococci (VRE): transmission and control. *Int. J. Antimicrob. Agents* 31, 99–106. doi:10.1016/j.ijantimicag.2007.08.026

Tao, Y., Deng, Y., and Wang, P. (2024). Traditional uses, phytochemistry, pharmacology, processing methods and quality control of *Lindera aggregata* (Sims) Kosterm: a critical review. *J. Ethnopharmacol.* 318, 116954. doi:10.1016/j.jep.2023.116954

Walsh, T. R., Weeks, J., Livermore, D. M., and Toleman, M. A. (2011). Dissemination of NDM-1 positive bacteria in the new delhienvironment and its implications for human health: an environmental point prevalence study. *Lancet Infect. Dis.* 11, 355–362. doi:10.1016/S1473-3099(11)70059-7

Wang, F. S., Yang, D. P., Ren, S. X., and Peng, J. F. (1999). Chemical constituents of volatile oil from fruits of *Lindera communis* and its antifungal and antibacteria activities. *Nat. Prod. Res. Devel* 11 (6), 1–5.

Wenzel, M., Patra, M., Senges, C. H., Ott, I., Stepanek, J. J., Pinto, A., et al. (2013). Analysis of the mechanism of action of potent antibacterial hetero-tri-organometallic compounds: a structurally new class of antibiotics. *ACS Chem. Biol.* 8, 1442–1450. doi:10.1021/cb4000844

Yan, R., Yang, Y., Zeng, Y., and Zou, G. (2009). Cytotoxicity and antibacterial activity of *Lindera strychnifolia* essential oils and extracts. *J. Ethnopharmacol.* 121, 451–455. doi:10.1016/j.jep.2008.06.010

Yang, D., Wang, F., Peng, J., and Ren, S. (1999). GC-MS analysis and inhibitory activity of the essential oil extracted from the leaves of *Lindera communis*. *Chin. Trad. Herb. Drugs* 22, 128–131.

frontiers | Frontiers in Pharmacology

TYPE Original Research
PUBLISHED 18 February 2025
DOI 10.3389/fphar.2025.1542425

Check for updates

OPEN ACCESS

EDITED BY
Marcello Iriti,
University of Milan, Italy

REVIEWED BY
Verónica Mayela Rivas-Galindo,
Autonomous University of Nuevo León, Mexico
Eman El-Wakil,
Theodor Bilharz Research Institute, Egypt

*CORRESPONDENCE
Hossein Mahmoudvand,
dmahmodvand@gmail.com

RECEIVED 09 December 2024
ACCEPTED 24 January 2025
PUBLISHED 18 February 2025

CITATION
Salimikia I, Yaghoubi SE, Khalaf AK, Masoori L, Ghasemian Yadegari J and Mahmoudvand H (2025) Potential activity of *Ferula macrecolea* essential oil for treating *Giardia lamblia* infection through modulating electrolytes and suppressing NF-κB p65 pathway. *Front. Pharmacol.* 16:1542425. doi: 10.3389/fphar.2025.1542425

COPYRIGHT
© 2025 Salimikia, Yaghoubi, Khalaf, Masoori, Ghasemian Yadegari and Mahmoudvand. This is an open-access article distributed under the terms of the Creative Commons Attribution License (CC BY). The use, distribution or reproduction in other forums is permitted, provided the original author(s) and the copyright owner(s) are credited and that the original publication in this journal is cited, in accordance with accepted academic practice. No use, distribution or reproduction is permitted which does not comply with these terms.

Potential activity of *Ferula macrecolea* essential oil for treating *Giardia lamblia* infection through modulating electrolytes and suppressing NF-κB p65 pathway

Iraj Salimikia[1], Seyed Ehsan Yaghoubi[1], Amal Khudair Khalaf[2], Leila Masoori[3], Javad Ghasemian Yadegari[1] and Hossein Mahmoudvand[3,4]*

[1]Department of Pharmacognosy, Lorestan University of Medical Sciences, Khorramabad, Iran, [2]Department of Microbiology, College of Medicine, University of Thi-qar, Thi-qar, Iraq, [3]Razi Herbal Medicines Research Center, Lorestan University of Medical Sciences, Khorramabad, Iran, [4]Hepatitis Research Center, Lorestan University of Medical Sciences, Khorramabad, Iran

Background: The pharmacological treatment of *Giardia lamblia* infection involves the use of chemical agents, such as metronidazole (MNZ). However, these medications are associated with a range of adverse effects, and their effectiveness is not definitively established. In light of the previously discussed information and the recognized antimicrobial properties of *Ferula macrecolea*, this study aims to investigate both the *in vitro* and *in vivo* anti-giardial effects of *F. macrecolea* essential oil (FME) on *G. lamblia* infection.

Methods: Gas chromatography-mass spectrometry (GC-MS) was utilized to analyze the chemical composition of the prepared FME. The MTT colorimetric assay was employed to assess FME's *in vitro* anti-giardial and cytotoxic activities. FME's *in vivo* effects were evaluated compared to MNZ in mice infected with *G. lamblia*. Additionally, the effects of FME therapy on serum electrolyte levels and the expression levels of inflammatory cytokines were assessed.

Results: The primary components of FME were identified as terpinolene (78.72%), n-nonanal (4.47%), and linalool (4.35%). FME significantly reduced the viability and growth rate of *G. lamblia* trophozoites (IC_{50} = 21.6 μg/mL) and cysts (IC_{50} = 27.6 μg/mL) in a dose-dependent manner compared to the control group ($p < 0.001$). The CC_{50} value for FME against normal intestinal cells was determined to be 207.4 μg/mL. *In vivo*, assays demonstrated that the administration of various doses of FME, particularly in combination with MNZ over 7 days, resulted in a statistically significant reduction in the mean number and viability of *Giardia* cysts, serum level electrolytes (sodium and potassium), and the expression levels of interleukin-1 (*IL-1*), tumor necrosis factor-alpha (*TNF-α*), nuclear factor κB p65 (*NF-κB p65*), and Toll-like receptor 4 (*TLR-4*) in mice with giardiasis ($p < 0.001$).

Conclusion: This study's results demonstrate the extract's efficacy *in vitro* against *G. lamblia*, exhibiting minimal cytotoxicity towards normal cells. Furthermore, the extract was shown to manage giardiasis in murine models by modulating electrolyte levels and inflammatory responses via suppressing the NF-κB p65/

TLR pathways. However, further research is necessary to clarify the specific efficacy and mechanisms of action of the extract in combating *G. lamblia* infection.

KEYWORDS

herbal medicines, natural products, giardiasis, inflammation, diarrhea

1 Introduction

Giardia lamblia is a flagellated protozoan that resides in the human small intestine and has been reported worldwide (Adam, 2001). The primary mode of human infection is through the ingestion of contaminated food and water, as well as through direct fecal-oral transmission. The durability of the parasite's cysts against chlorination processes in water increases its potential for transmission via aquatic sources. Although infection can occur at any age, it is notably more common among children (Laishram et al., 2012). Current estimates suggest that there are approximately 280 million cases of human infection each year. *G. lamblia*, the causative agent of giardiasis, is widespread in both temperate and tropical regions and is linked to clinical symptoms such as diarrhea (steatorrhea), particularly in pediatric populations, as well as malabsorption, abdominal cramps, and weight loss (Hooshyar et al., 2019).

The pharmacological treatment of this disease entails the use of chemical agents, including metronidazole (MNZ) and furazolidone (Watkins and Eckmann, 2014). However, these medications are linked to a variety of adverse effects, and their effectiveness is not definitively established. Moreover, certain agents have been reported to exhibit carcinogenic and mutagenic characteristics, particularly in vulnerable populations such as women and children, and are contraindicated during pregnancy (Watkins and Eckmann, 2014; Vivancos et al., 2018). Additionally, there are documented cases of parasitic resistance to these pharmacological agents (Watkins and Eckmann, 2014; Vivancos et al., 2018). As a result, there is an increasing interest in research focused on identifying alternative compounds that demonstrate fewer or no adverse effects. Recent research work has underscored the therapeutic potential of certain herbs and their derivatives, including *Zataria* spp., *Eucalyptus* spp., and *Allium* spp., in the management of *Giardia* infections (Alnomasy et al., 2021). However, the wider utilization of herbal remedies for giardiasis is currently hindered by inconclusive research findings that frequently lack adequate empirical validation.

The *Ferula* genus, comprising over 150 distinct species, is recognized as one of the most extensively utilized groups of plants in traditional medicine globally (Yaqoob and Nawchoo, 2016). Among these, *Ferula macrecolea* Boiss stands out due to its diverse therapeutic properties, which include analgesic, anti-inflammatory, antihypertensive, antibacterial, anti-parasitic, antiviral, antifungal, and insecticidal effects (Yaqoob and Nawchoo, 2016; Salehi et al., 2019). This plant plays a significant role in the treatment of cardiovascular and gastrointestinal disorders within both traditional and contemporary medical practices (Yaqoob and Nawchoo, 2016; Salehi et al., 2019). Recent studies have identified terpenoid compounds, such as terpinolene, α-pinene, and myrcene, as the primary constituents of the essential oils derived from various *Ferula* species (Boghrati and Iranshahi, 2019). The chemical composition of essential oils is influenced by several factors, including the specific plant part utilized, the timing of the harvest, the geographical location of the harvest, and the method of extraction employed (Sahebkar and Iranshahi, 2011; Asili et al., 2009). In light of the previously discussed information and the recognized antimicrobial properties of the *F. macrecolea*, this study seeks to investigate both the *in vitro* and *in vivo* anti-giardial effects of the *F. macrecolea* essential oil (FME) on *G. lamblia* infection.

2 Material and methods

2.1 Plant collection

In the present study, the aerial portions of the plant were collected from the western regions of Islamabad, located in Kermanshah province, during April 2021. Following confirmation and identification by a botanist, an herbarium specimen (No. 1400.2276) was prepared and subsequently deposited at the herbarium of the Razi Herbal Medicines Research Center at Lorestan University of Medical Sciences in Khorramabad, Iran. The plant materials were then dried, ground into a powder, and stored in opaque containers to ensure preservation.

2.2 Preparing of the essential oil

The essential oil was isolated utilizing the hydro-distillation method employing a Clevenger apparatus. The extraction process lasted for a duration of 4 h. Following the extraction, the essential oil was separated from the aqueous phase and subsequently dried using sodium sulfate. The extracted essential oil was stored at refrigeration temperatures in clean containers wrapped in aluminum foil until the chemical and antigiardial assays were conducted (Mahmoudvand et al., 2017).

2.3 Gas chromatography-mass spectrometry (GC-MS)

GC-MS was employed to analyze the chemical composition of the prepared essential oil. The analysis utilized an HP6890-Packard-Hewlett gas chromatograph, which was fitted with a 30-meter-long column with a diameter of 25 mm and a stationary phase thickness of 0.25 μm, specifically of the 5MS-HP type. The temperature program for the column commenced at an initial temperature of 50°C, maintained for 5 min, followed by a temperature ramp to 250°C at a rate of 5°C per minute, with a final hold at 250°C for 20 min. Helium was used as the carrier gas at a flow rate of 1 mL/min. The mass spectrometer employed was an Agilent Model 5,975, operating with an ionization voltage of 70 eV, utilizing electron impact ionization, and an ionization source temperature set at

220°C. The identification of the essential oil compounds was conducted by comparing their retention indices and mass spectra against the WILEY 09 and NIST 11 mass spectral databases (Adams, 2004; NIST, 2014).

2.4 Cells culture

Normal human intestinal epithelial cells (NCM460) were procured from the Pasteur Institute located in Tehran, Iran. These cells were cultured in Dulbecco's Modified Eagle's Medium (DMEM, Sigma-Aldrich, Germany), which was supplemented with 10% fetal bovine serum, and were maintained at a temperature of 37°C in an atmosphere containing 5% CO_2.

2.5 Parasite

To isolate *G. lamblia* cysts, stool samples were obtained from patients diagnosed with giardiasis who were referred to healthcare facilities in Khorramabad, Iran. Positive samples were confirmed through direct examination and the formalin-ether concentration technique. Subsequently, the sucrose gradient method (0.85 M) was utilized to concentrate the *Giardia* cysts. The cysts were then diluted with distilled water (DW) in a 12:1 ratio, and the resulting solution was filtered. An additional 5 mL of DW was added to the sediment, and the upper phase was carefully combined with 3 mL of sucrose solution. This mixture was centrifuged at 700 g for 10 min at 4°C. The cysts were subsequently extracted from the middle layer using a Pasteur pipette, washed with normal saline, and stored at 4°C until further analysis. The concentration of the cysts was adjusted to 1×10^5 cysts/mL using a hemocytometer (Ghasemian Yadegari et al., 2022).

2.6 *G. lamblia* trophozoites collection

The excystation of *Giardia* cysts to yield trophozoite forms was conducted in accordance with established protocols (Bingham and Meyer, 1979). In brief, an induction solution comprising aqueous hydrochloric acid was introduced to the cyst suspension at a ratio of 1:9 and incubated at 37°C for 120 min. Following this incubation, the suspension underwent centrifugation at 600 rpm for 10 min, after which the supernatant was removed, and the sediment was resuspended in a medium consisting of filter-sterilized TYI-S-33 culture, supplemented with bovine bile, 20% heat-inactivated fetal calf serum, streptomycin (500 μg/mL), and penicillin (500 IU/mL). The resulting mixture was subsequently incubated at 37°C in a slant culture.

2.7 *In vitro* antigiardial effects of FME

An initial volume of 100 μL containing trophozoite and cysts at a concentration of 1×10^5 cells/mL was separately dispensed into each well of a 96-well plate. Subsequently, various concentrations of the FME and MNZ were separately added to the wells containing the cells, followed by incubation at 24°C for a duration of 48 h. After the supernatant was removed from the wells, 20 μL of MTT solution (0.5 mg/mL in PBS) was introduced into each well and incubated for 4 h in a 5% CO_2 atmosphere at 37°C. Following the addition of 100 μL of dimethyl sulfoxide, the absorbance of each well was measured at 570 nm using an ELISA plate reader. The 50% inhibitory concentrations (IC_{50}) was calculated using Probit analysis in SPSS software (Version 26.0) (Masoori et al., 2024).

2.8 Cytotoxic effects of FME

At first, 100 μL containing normal NCM460 cells at a concentration of 1×10^5 cells/mL was separately dispensed into each well of a 96-well plate. Subsequently, various concentrations of the FME were separately added to the wells containing the cells, followed by incubation at 24°C for a duration of 48 h. After the supernatant was removed from the wells, 20 μL of MTT solution was introduced into each well and incubated for 4 h in a 5% CO_2 atmosphere at 37°C. Following the addition of 100 μL of dimethyl sulfoxide, the absorbance of each well was measured at 590 nm using an ELISA plate reader. The 50% cytotoxic concentration (CC_{50}) was calculated using Probit analysis in SPSS software (Version 26.0) (Mahmoudvand et al., 2016).

2.9 *In vivo* effects on giardiasis in mice

2.9.1 Ethics

The study obtained ethical approval from the ethics committee of Lorestan University of Medical Sciences in Khorramabad, Iran, with the ethics identification number IR.LUMS.REC.1400.200.

2.9.2 Animals

A cohort of sixty male BALB/C mice, aged 8–10 weeks and weighing between 25 and 30 g, was housed under optimal conditions, with continuous access to food and water.

2.9.3 Study design

The mice were infected via oral administration of 0.2 mL of a cyst solution (2000 cysts). Subsequently, the animals were monitored through stool examination (SE), employing methods such as direct smear and the formalin-ether concentration technique, until the presence of *Giardia* cysts was confirmed in their feces (Masoori et al., 2024). After a period of 6 days, the mice were divided into six groups, each receiving one of the following treatments orally for 1 week including:

(i) Normal saline
(ii) MNZ at 15 mg/kg/day
(iii) FME at dose of 5 mg/kg/day
(iv) FME at dose of 10 mg/kg/day.
(v) FME at dose of 5 mg/kg/day + MNZ at 7.5 mg/kg/day
(vi) FME at dose of 10 mg/kg/day + MNZ at 7.5 mg/kg/day

2.9.4 Antiparasitic effects on giardiasis in mice

On the eighth day post-treatment, stool examinations were conducted to assess the presence of *Giardia* cysts and to determine the reduction rate of these cysts. Additionally, the viability of the collected cysts was evaluated using the eosin exclusion assay, where pink cysts were classified as dead and colorless cysts as viable (Masoori et al., 2024).

TABLE 1 The sequence of primer used in this study.

Primer	Sequence (5′–3′)
TNF-α	F: TGAACTTCGGGGTGATCGGT R: GGTGGTTTGTGAGTGTGAGGG
IL-1β	F: AACCTGCTGGTGTGTGACGTTC R: CAGCACGAGGCTTTTTTGTTGT
NF-κB p65	F: AGGCAAGGAATAATGCTGTCCTG R: ATCATTCTCTAGTGTCTGGTTGG
TLR4	F: AGCTTTGGTCAGTTGGCTCT R: CAGGATGACACCATTGAAGC
β-actin	F: GTGACGTTGACATCCGTAAAGA R: GCCGGACTCATCGTACTCC

2.10 Blood collection

In accordance with the established protocol, the experimental mice were subjected to deep euthanasia via intraperitoneal injection of a ketamine (100 mg/kg) + xylazine (10 mg/kg). Following the administration of deep anesthesia, an incision was made to access the abdominal cavity, from which blood samples were obtained directly from the cardiac region and were centrifuged, whereas the resultant serum was analyzed for biochemical analysis.

2.11 Evaluating the serum level electrolytes

The objective of this analysis was to quantify the serum level electrolytes of sodium (Na+) and potassium (K+) using diagnostic biochemical kits produced by Parsazmon, Iran.

2.12 Evaluating the expression level of proinflammatory cytokines

Total RNA was extracted utilizing Total RNA Extraction Kit, Favaorgen, Iran from the duodenal tissue of the tested mice. Subsequently, complementary DNA (cDNA) was generated employing the cDNA synthesis Kit, Yekta Tajhiz Azma, Iran. Quantitative real-time polymerase chain reaction (qRT-PCR) was performed using SYBR Green PCR master mix sourced from Yekta Tajhiz Azma, Iran. Table 1 presents the primers designed to target genes associated with inflammatory cytokines (Masoori et al., 2024). The protocol commenced with an initial denaturation step at 96°C for a duration of 8 min, followed by 40 cycles of amplification, and concluded with a final extension at 76°C for 4 min. Subsequently, the $2^{-\Delta\Delta CT}$ method was employed for analysis, which was performed utilizing the Bio-Rad iQ5 Optical System Software, United States.

2.13 Statistical analysis

After collecting the data and entering it into the SPSS 24 statistical software, appropriate measures of central tendency and dispersion were calculated. A one-way analysis of variance (ANOVA) were employed to analyze the data. If the results were significant, Tukey's *post hoc* tests were conducted for paired comparisons. In cases where the data do not follow a normal distribution, alternative non-parametric tests were utilized. The significance level was set at $p < 0.05$.

TABLE 2 Gas chromatography-mass spectrometry analysis of essential oil of *Ferula macrocolea*.

Constituent	RI	Percent (%)
α–pinene	936	0/11
p–cymene	1,010	0/23
β–phellandrene	1,028	1/31
Benzeneacetaldehyde	1,032	1/35
α–Thujene	1,035	3/92
Limonene	1,036	0/25
Methyl carvacrol	1,076	1/94
Terpinolene	1,094	78/72
Geijerene	1,098	0/58
n-Nonanal	1,102	4/47
α–campholenal	1,125	0/32
Linalool	1,139	4/35
Camphor	1,148	0/24
Thuj-3-en-lo-al	1,186	0/29
Myrtenal	1,196	1/22
Allo-ocimene	1,198	0/42
di-sec-butyl disulfide	1,212	0/17
Piperiton	1,252	0/1
Total		99/99

3 Results

3.1 GC/MS analysis

The findings presented in Table 2 indicate that the GC/MS analysis identified a total of 18 compounds, accounting for 99.99% of the composition. The predominant components of the FME were identified as terpinolene (78.72%), n-nonanal (4.47%), and linalool (4.35%), respectively.

3.2 *In vitro* antigiardial effects against trophozoite and cyst of *G. lamblia*

The data illustrated in Figure 1 demonstrate that FME and MNZ, significantly ($p < 0.001$) diminished the viability and growth rate of *G. lamblia* trophozoites and cysts in a dose-dependent manner when compared to the control group. The IC_{50} values for FME and MNZ against *G. lamblia* trophozoites were determined to be 21.6 ± 2.43 and 28.7 ± 2.15 μg/mL, respectively. Furthermore, the IC_{50} values for FME and MNZ

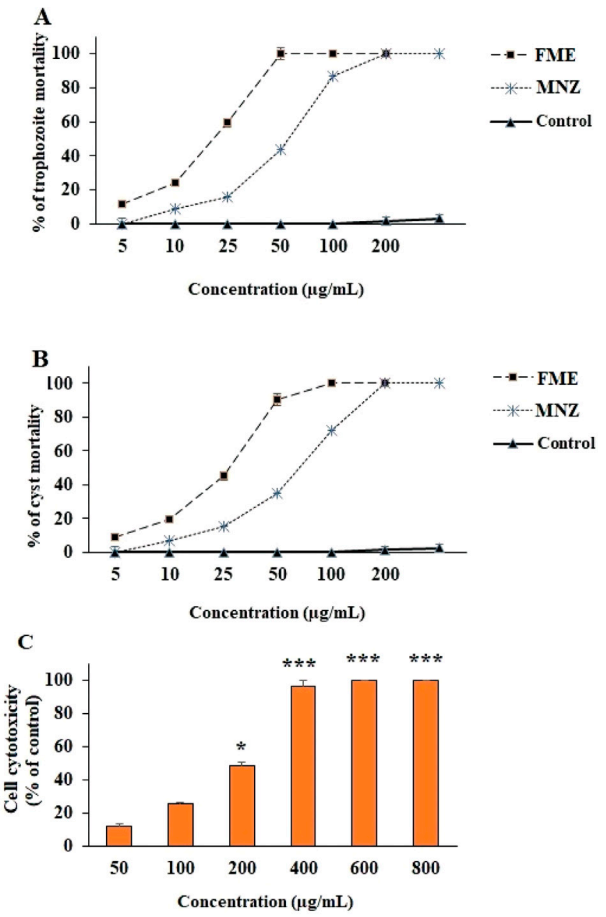


FIGURE 1
The effect of different concentrations of *Ferula macrecolea* essential oil (FME) on the trophozoites **(A)** and cysts **(B)** of *Giardia lamblia* in comparison to metronidazole (MNZ). The cytotoxicity of FME on normal human intestinal epithelial cells **(C)**. The results are presented as mean ± standard deviation (SD) with a sample size of n = 3.

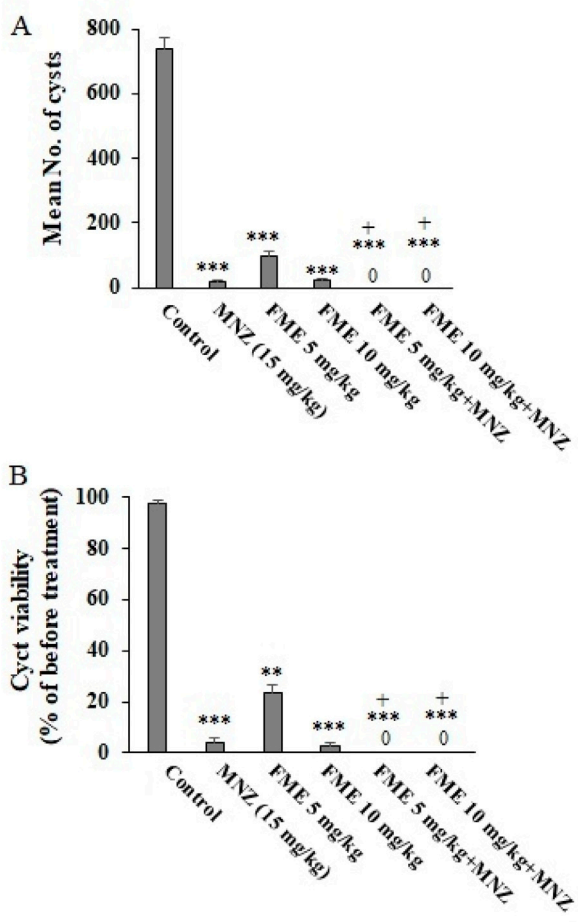


FIGURE 2
The *in vivo* effect of different doses of *Ferula macrecolea* essential oil (FME) on the number **(A)** and viability **(B)** of *Giardia lamblia* cysts in mice with giardiasis in comparison to metronidazole (MNZ). The results are presented as mean ± standard deviation (SD) with a sample size of n = 10. **P < 0.01; ***P < 0.001 compared to normal saline; + P < 0.05 compared to MNZ.

against *G. lamblia* cysts were determined to be 27.6 ± 1.51 and 35.6 ± 3.22 µg/mL, respectively.

3.3 Cytotoxicity effects of FME against normal intestinal cells

Figure 1C illustrates the cytotoxic effects of FME on both intestinal normal and cancerous cells, as assessed by the MTT assay. The findings indicate that the FME significantly decreased cell viability in a dose-dependent manner. The calculated CC_{50} values for FME against normal NCM460 cells were determined to be 207.4 µg/mL.

3.4 *In vivo* effects on giardiasis in mice

Following a 7-day administration of FME, the feces of infected mice were analyzed for the presence of *G. lamblia* cysts using the formalin-ether method. The percentage viability of cysts was assessed through eosin staining. As illustrated in Figure 2A, the application of various doses of FME, particularly in combination with MNZ (7.5 mg/kg/day) over the 7-day period, resulted in a statistically significant reduction ($P < 0.001$) in the average number of cysts. The observed reductions were 97.7%, 86.9%, 96.6%, 100%, and 100% in the groups treated with MNZ (15 mg/kg), FME 5 mg/kg, FME 10 mg/kg, FME 5 mg/kg + MNZ, FME 10 mg/kg + MNZ, respectively. Furthermore, Figure 2B demonstrates a significant decline ($P < 0.001$) in the viability of *Giardia* cysts following treatment with various doses of FME, particularly when combined with MNZ over the same 7-day period. The reductions in viability were recorded at 96.1%, 76.2%, 97.3%, 100% and 100% for the groups treated with MNZ (15 mg/kg), FME 5 mg/kg, FME 10 mg/kg, FME 5 mg/kg + MNZ, FME 10 mg/kg + MNZ, respectively.

3.5 Evaluating the serum level electrolytes

The biochemical analysis indicated a significant reduction in serum levels of Na and K in the infected mice ($p < 0.05$). Conversely,

TABLE 3 *In vivo* effects of *Ferula macrecolea* essential oil (FME) on giardiasis in mice. Mean ± standard deviation (SD).

Drug	Sodium level (nmol/L)	Potassium level (nmol/L)
Normal saline	63.4 ± 5.6	3.4 ± 0.41
MNZ (15 mg/kg)	132.6 ± 7.6	7.3 ± 0.52
FME 5 mg/kg	102.3 ± 7.5	5.8 ± 0.36
FME 10 mg/kg	141.6 ± 6.9	6.8 ± 0.62
FME 5 mg/kg + MNZ	153.2 ± 8.3	7.4 ± 0.46
FME 10 mg/kg + MNZ	159.6 ± 7.9	7.9 ± 0.56

**P < 0.01; ***P < 0.001 compared to normal saline; + P < 0.05 compared to metronidazole (MNZ).

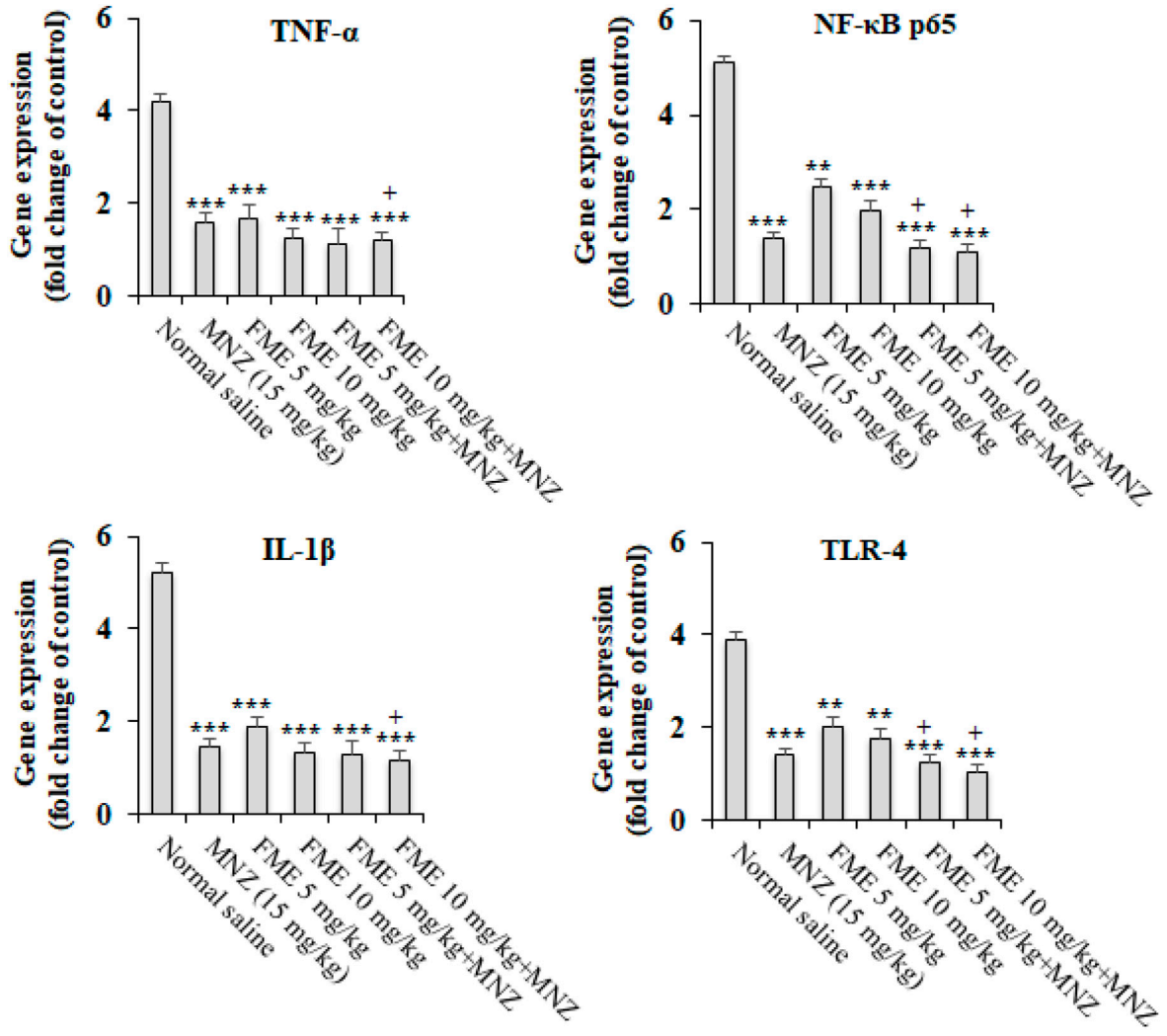


FIGURE 3
The *in vivo* effect of different doses of *Ferula macrecolea* essential oil (FME) on the expression level of interleukin-1 (IL-1), tumor necrosis factor-alpha (TNF-α), nuclear factor κB p65 (NF-κB p65), and Toll-like receptor 4 (TLR-4) in mice with giardiasis in comparison to metronidazole (MNZ). The results are presented as mean ± standard deviation (SD) with a sample size of n = 10. **P < 0.01; ***P < 0.001 compared to normal saline; + P < 0.05 compared to MNZ.

the oral administration of FME, particularly in combination with MNZ, resulted in a substantial modulation of serum Na and K levels in the infected mice ($p < 0.001$) when compared to the control group treated with normal saline (Table 3).

3.6 Evaluating the expression level of proinflammatory cytokines

The findings from the real-time PCR analysis indicated that in the infected animal subjects, there was a notable elevation in the expression levels of the genes *IL-1β, TNF-α, NF-κB p65, and TLR-4* ($p < 0.05$). On the other hand, the administration of FME at dosages of 5 and 10 mg/kg, especially in combination with MNZ, resulted in a statistically significant decrease ($P < 0.001$) in the expression of the *IL-1β, TNF-α, NF-κB p65, and TLR-4* (Figure 3) in comparison to the infected mice that were treated with normal saline ($P < 0.05$).

4 Discussion

Today, the pharmacological management of giardiasis involves the administration of chemical agents, notably MNZ. Nonetheless, these agents are associated with a range of adverse effects, and their efficacy remains inconclusive such as carcinogenic and mutagenic properties, particularly affecting susceptible groups such as women and children, and are contraindicated for use during pregnancy (Watkins and Eckmann, 2014; Vivancos et al., 2018). The utilization of herbal medicines for addressing a range of health issues is experiencing significant growth globally. In particular, herbal medicinal products serve as the primary source of healthcare for a substantial portion of the population residing in developing nations (Alnomasy et al., 2021).

Our *in vitro* results showed that FME significantly diminished the viability and growth rate of *G. lamblia* trophozoites and cysts in a dose-dependent manner when compared to the control group. In addition, *in vivo* assay showed that the application of various doses of FME, particularly in combination with MNZ over the 7-day period, resulted in a statistically significant reduction in the mean number and viability of *Giardia* cysts. Numerous studies have demonstrated the antimicrobial properties of *Ferula* species against a diverse array of pathogenic bacteria (e.g., *Staphylococcus*., *Salmonella*) as well as fungi such as *Candida* and *Trichophyton* species (Boghrati and Iranshahi, 2019; Asili et al., 2009). In the term of antiparasitic activities, in a study by Mahmoudvand et al. (2022), the findings exhibited that FME had potent antileishmanial effects against promastigote and amastigotes of *Leishmania tropica* with IC_{50} of 27.6 and 42.3 μg/mL, respectively (Mahmoudvand et al., 2022). Another study conducted by Iranshahi et al. (2007) exhibited that *F. szowitsiana* acetone extract demonstrated considerable antileishmanial activity against *L. major* promastigotes, with an IC_{50} value of 11.8 μg/mL (Iranshahi et al., 2007). Another study conducted by Alyousif et al. (2021) revealed that FME demonstrated effective *in vitro* and *ex vivo* anthelminthic effects against *Echinococcus granulosus* protoscoleces, whereas entirely eliminating the parasites at concentrations of 150 and 300 μL/mL (Alyousif et al., 2021). In addition, Esmaeili et al. (2009) showed the strong antiparasitic properties of the *F. oopoda* extract against *Plasmodium falciparum* strains K1 and 3D7, exhibiting IC_{50} values of 26.6 μg/mL and 24.9 μg/mL, respectively (Esmaeili et al., 2009). Furthermore, Khanmohammadi et al. (2014) found that *F. szowitsiana* extract exhibited effective antiparasitic effects against *Trichomonas vaginalis* trophozoites, with an IC_{50} value of 0.360 mg/mL (Khanmohammadi et al., 2014). The discrepancies noted in the results can be ascribed to a variety of factors, including the specific type of parasite involved, the particular species of *Ferula* utilized, the characteristics of the extract employed, the concentration levels applied, and the methodologies implemented in the research studies.

The results of our GC/MS analysis indicate that the predominant compounds identified were terpinolene, n-nonanal, and linalool, respectively. Prior researches have established that the primary constituents of the essential oil derived from *Ferula* spp. are terpenoid compounds, including terpinolene, α-terpineol, α-pinene, β-pinene, myrcene, among others (Sahebkar and Iranshahi, 2011). Furthermore, existing literature suggests that the chemical composition of essential oils is influenced by various factors, including the geographical location and timing of plant collection, as well as the techniques employed in the extraction of the oils (Delfani et al., 2017). Terpenes and terpenoids are classified as hydrocarbon compounds that exhibit a range of pharmacological and therapeutic properties, particularly demonstrating antimicrobial activity against a diverse array of bacterial, fungal, viral, and parasitic strains (Guimarães et al., 2019; Mahizan et al., 2019). According to existing researches, terpene and terpenoid compounds demonstrate antimicrobial properties through various mechanisms of action, including the disruption of the cell wall, interference with oxygen consumption, and inhibition of virulence factors, among others (Guimarães et al., 2019; Mahizan et al., 2019; Srivastava and Singh, 2019).

Previous researches revealed that *Giardia* infection leads to malabsorption of glucose, sodium, and water, as well as a decrease in disaccharidase activity, which may be associated with a reduction in the absorptive surface area of epithelial cells (Buret, 2007). Our biochemical analyses indicated that the oral administration of FME, particularly in combination with MNZ, resulted in a substantial modulation of serum Na and K levels in the infected mice ($p < 0.001$) when compared to the control group treated with normal saline. These findings suggest that FME may have the potential to alleviate symptoms of giardiasis by regulating serum electrolyte levels in infected mice.

Researches have shown that *G. lamblia* elicits an inflammatory response marked by the secretion of IL-1β and TNF-α via various signaling pathways, including NF-κB p65, p38, and extracellular signal-regulated kinase (ERK) pathways (Pu et al., 2021). Prior investigations have established that the equilibrium and variations in cytokine concentrations can significantly affect or reflect clinical outcomes (Masoori et al., 2024). It has been proven that essential oils and their primary constituents modulate inflammatory responses through some pathways such as TLR pathways, as well as associated mitogen-activated protein kinase (MAPK) and ERK signaling pathways, and peroxisome proliferator-activated receptor gamma (PPAR-γ) signaling

(Stojanović et al., 2024). We found that the administration of FME at dosages of 5 and 10 mg/kg, especially in combination with MNZ, resulted in a statistically significant decrease ($P < 0.001$) in the expression of the *L-1β, TNF-α, NF-κB p65, and TLR-4*. These findings suggest that these agents can effectively manage giardiasis in mice through their anti-inflammatory properties and suppressing specific inflammatory cytokines and NF-κB p65/TLR pathways.

In the context of cytotoxicity, the findings indicate that the FME significantly decreased cell viability in a dose-dependent manner for both cell types. While, the calculated CC_{50} values for FME against normal intestinal cells was determined to be 207.4 μg/mL. Similarly, a prior investigation revealed that the CC_{50} values for FME was 471.3 μg/mL against J774-A1 macrophage cells. They also reported that SI exceeding 10 for FME indicates a preferential efficacy against *L. tropica* amastigotes, while demonstrating limited cytotoxicity towards macrophage cells (Mahmoudvand et al., 2022).

5 Conclusion

This study's results demonstrate the extract's efficacy *in vitro* against *G. lamblia*, exhibiting minimal cytotoxicity towards normal cells. Furthermore, the extract was shown to manage giardiasis in murine models by modulating electrolyte levels and inflammatory responses via suppressing the NF-κB p65/TLR pathways. However, further research is necessary to clarify the specific efficacy and mechanisms of action of the extract in combating *G. lamblia* infection.

Data availability statement

The original contributions presented in the study are included in the article/supplementary material, further inquiries can be directed to the corresponding author.

Ethics statement

The study was conducted in accordance with the local legislation and institutional requirements and was approved by the ethics committee of Lorestan University of Medical Sciences in Khorramabad, Iran, with the ethics identification number IR.LUMS.REC.1400.200.

Author contributions

IS: Investigation, Writing–review and editing, Methodology, Validation. SY: Investigation, Methodology, Validation, Writing–review and editing. AK: Investigation, Resources, Writing–original draft, Writing–review and editing. LM: Investigation, Writing–review and editing, Data curation, Methodology. JG: Methodology, Conceptualization, Validation, Writing–review and editing. HM: Writing–review and editing, Investigation, Supervision, Writing–original draft.

Funding

The author(s) declare that no financial support was received for the research, authorship, and/or publication of this article.

Acknowledgments

The authors thank the staff of the Department of Pharmacognosy, Lorestan University of Medical Sciences, Khorramabad, Iran for their help in performing the work.

Conflict of interest

The authors declare that the research was conducted in the absence of any commercial or financial relationships that could be construed as a potential conflict of interest.

Generative AI statement

The author(s) declare that no Generative AI was used in the creation of this manuscript.

Publisher's note

All claims expressed in this article are solely those of the authors and do not necessarily represent those of their affiliated organizations, or those of the publisher, the editors and the reviewers. Any product that may be evaluated in this article, or claim that may be made by its manufacturer, is not guaranteed or endorsed by the publisher.

References

Adam, R. D. (2001). Biology of *Giardia lamblia*. *Clin. Microbiol. Rev.* 14 (3), 447–475. doi:10.1128/CMR.14.3.447-475.2001

Adams, R. P. (2004). *Identification of essential oil components by gas chromatography/mass spectroscopy*. Illinois, IL, USA: Allured Publishing Corporation.

Alnomasy, S., Al-Awsi, G. R., Raziani, Y., Albalawi, A. E., Alanazi, A. D., Niazi, M., et al. (2021). Systematic review on medicinal plants used for the treatment of Giardia infection. *Saudi J. Biol. Sci.* 28 (9), 5391–5402. doi:10.1016/j.sjbs.2021.05.069

Alyousif, M. S., Al-Abodi, H. R., Almohammed, H., Alanazi, A. D., Mahmoudvand, H., Shalamzari, M. H., et al. (2021). Chemical composition, apoptotic activity, and antiparasitic effects of Ferula macrecolea essential oil against Echinococcus granulosus protoscoleces. *Molecules* 26 (4), 888. doi:10.3390/molecules26040888

Asili, J., Sahebkar, A., Bazzaz, B. S. F., Sharifi, S., and Iranshahi, M. (2009). Identification of essential oil components ofFerula badrakemaFruits by GC-MS and13C-NMR methods and evaluation of its antimicrobial activity. *J. Essent. Oil Bear. Plants* 12, 7–15. doi:10.1080/0972060x.2009.10643685

Bingham, A. K., and Meyer, E. A. (1979). Giardia excystation can be induced *in vitro* in acidic solutions. *Nature* 277 (5694), 301–302. doi:10.1038/277301a0

Boghrati, Z., and Iranshahi, M. (2019). Ferula species: a rich source of antimicrobial compounds. *J. Herb. Med.* 16, 100244. doi:10.1016/j.hermed.2018.10.009

Buret, A. G. (2007). Mechanisms of epithelial dysfunction in giardiasis. *Gut* 56 (3), 316–317. doi:10.1136/gut.2006.107771

Delfani, S., Mohammadrezaei-Khorramabadi, R., Abbaszadeh, S., Naghdi, N., and Shahsavari, S. (2017). Phytotherapy for Streptococcus pyogenes. *J. Pharm. Sci. Res.* 9, 513.

Esmaeili, S., Naghibi, F., Mosaddegh, M., Sahranavard, S., Ghafari, S., and Abdullah, N. R. (2009). Screening of antiplasmodial properties among some traditionally used Iranian plants. *J. Ethnopharmacol.* 121, 400–404. doi:10.1016/j.jep.2008.10.041

Ghasemian Yadegari, J., Khudair Khalaf, A., and Darabi, R. (2022). Antiparasitic effects and cellular mechanism of Astragalus maximus chloroform extract against clinical isolates of Giardia lamblia. *Res. J. Pharmacogn.* 9 (3), 5–15. doi:10.22127/RJP.2022.330464.1849

Guimarães, A. C., Meireles, L. M., Lemos, M. F., Guimarães, M. C. C., Endringer, D. C., Fronza, M., et al. (2019). Antibacterial activity of terpenes and terpenoids present in essential oils. *Molecules* 24, 2471. doi:10.3390/molecules24132471

Hooshyar, H., Rostamkhani, P., Arbabi, M., and Delavari, M. (2019). *Giardia lamblia* infection: review of current diagnostic strategies. *Gastroenterology hepatology bed bench* 12 (1), 3–12.

Iranshahi, M., Arfa, P., Ramezani, M., Jaafari, M. R., Sadeghian, H., Bassarello, C., et al. (2007). Sesquiterpene coumarins from Ferula szowitsiana and *in vitro* antileishmanial activity of 7-prenyloxycoumarins against promastigotes. *Phytochemistry* 68, 554–561. doi:10.1016/j.phytochem.2006.11.002

Khanmohammadi, M., Ganji, S., and Rad, S. R. (2014). Anti-protozoan effects of methanol extracts of the ferula szowitsiana on the trichomonas vaginalis trophozoites *in vitro*. *Int. J. Women Health Rep. Sci.* 2, 301–306. doi:10.15296/ijwhr.2014.49

Laishram, S., Kang, G., and Ajjampur, S. S. (2012). Giardiasis: a review on assemblage distribution and epidemiology in India. *Indian J. Gastroenterology* 31 (1), 3–12. doi:10.1007/s12664-012-0161-9

Mahizan, N. A., Yang, S.-K., Moo, C.-L., Song, A.A.-L., Chong, C.-M., Chong, C. W., et al. (2019). Terpene derivatives as a potential agent against antimicrobial resistance (AMR) pathogens. *Molecules* 24, 2631. doi:10.3390/molecules24142631

Mahmoudvand, H., Ghasemian Yadegari, J., Khalaf, A. K., Hashemi, M. J., Dastyarhaghighi, S., and Salimikia, I. (2022). Chemical composition, antileishmanial, and cytotoxic effects Ferula macrecolea essential oil against Leishmania tropica. *Parasite Epidemiol. Control* 19, e00270. PMID: 36118048; PMCID: PMC9475300. doi:10.1016/j.parepi.2022.e00270

Mahmoudvand, H., Mirbadie, S. R., Sadooghian, S., Harandi, M. F., Jahanbakhsh, S., and Saedi Dezaki, E. (2017). Chemical composition and scolicidal activity of Zataria multiflora Boiss essential oil. *J. Essent. Oil Res.* 29 (1), 42–47. doi:10.1080/10412905.2016.1201546

Mahmoudvand, H., Sepahvand, P., Jahanbakhsh, S., and Azadpour, M. (2016). Evaluation of the antileishmanial and cytotoxic effects of various extracts of garlic (Allium sativum) on Leishmania tropica. *J. Parasit. Dis.* 40, 423–426. doi:10.1007/s12639-014-0520-9

Masoori, L., Khalaf, A. K., Ezzatkhah, F., Balaña-Fouce, R., and Mahmoudvand, H. (2024). Promising effects of 1, 8 Cineole to control Giardia lamblia infection: targeting the inflammation, oxidative stress, and infectivity. *Acta trop.* 255, 107201. doi:10.1016/j.actatropica.2024.107201

Nist, N. (2014). Gaithersburg: National Institute of Standards and Technology. EPA/NIH Mass Spectral Library.

Pu, X., Li, X., Cao, L., Yue, K., Zhao, P., Wang, X., et al. (2021). Giardia duodenalis induces proinflammatory cytokine production in mouse macrophages via TLR9-mediated p38 and ERK signaling pathways. *Front. Cell Dev. Biol.* 9, 694675. doi:10.3389/fcell.2021.694675

Sahebkar, A., and Iranshahi, M. (2011). Volatile constituents of the genus *Ferula* (apiaceae): a review. *Plants* 14, 504–531. doi:10.1080/0972060x.2011.10643969

Salehi, M., Naghavi, M. R., and Bahmankar, M. (2019). A review of Ferula species: biochemical characteristics, pharmaceutical and industrial applications, and suggestions for biotechnologists. *Ind. Crop. Prod.* 139, 111511. doi:10.1016/j.indcrop.2019.111511

Srivastava, A. K., and Singh, V. K. (2019). Biological action of essential oils (terpenes). *Int. J. Biol. Med. Res.* 10, 6854–6859.

Stojanović, N. M., Randđelović, P. J., Simonović, M., Radić, M., Todorović, S., Corrigan, M., et al. (2024). Essential oil constituents as anti-inflammatory and neuroprotective agents: an insight through microglia modulation. *Int. J. Mol. Sci.* 25 (10), 5168. doi:10.3390/ijms25105168

Vivancos, V., González-Alvarez, I., Bermejo, M., and Gonzalez-Alvarez, M. (2018). Giardiasis: characteristics, pathogenesis and new insights about treatment. *Curr. Top. Med. Chem.* 18 (15), 1287–1303. doi:10.2174/1568026618666181002095314

Watkins, R. R., and Eckmann, L. (2014). Treatment of giardiasis: current status and future directions. *Curr. Infect. Dis. Rep.* 16, 396–398. doi:10.1007/s11908-014-0396-y

Yaqoob, U., and Nawchoo, I. A. (2016). Distribution and taxonomy of Ferula L.: a review. *Res. Rev. J. Bot.* 5 (3), 15–23.

frontiers | Frontiers in Pharmacology

TYPE Review
PUBLISHED 19 March 2025
DOI 10.3389/fphar.2025.1538311

Check for updates

OPEN ACCESS

EDITED BY
Yong Guo,
University of South China, China

REVIEWED BY
Najwan Jubair,
Al-Ameen University, Iraq
Hailian Yuan,
Yangzhou University, China

*CORRESPONDENCE
Dong Wang,
wangdong@cdutcm.edu.cn

RECEIVED 02 December 2024
ACCEPTED 27 February 2025
PUBLISHED 19 March 2025

CITATION
Liang Y, Liu T, Wang D and Liu Q (2025) Exploring the antimicrobial, anti-inflammatory, antioxidant, and immunomodulatory properties of *Chrysanthemum morifolium* and *Chrysanthemum indicum*: a narrow review. *Front. Pharmacol.* 16:1538311. doi: 10.3389/fphar.2025.1538311

COPYRIGHT
© 2025 Liang, Liu, Wang and Liu. This is an open-access article distributed under the terms of the Creative Commons Attribution License (CC BY). The use, distribution or reproduction in other forums is permitted, provided the original author(s) and the copyright owner(s) are credited and that the original publication in this journal is cited, in accordance with accepted academic practice. No use, distribution or reproduction is permitted which does not comply with these terms.

Exploring the antimicrobial, anti-inflammatory, antioxidant, and immunomodulatory properties of *Chrysanthemum morifolium* and *Chrysanthemum indicum*: a narrow review

Yuqing Liang[1], Tengwen Liu[1], Dong Wang[1]* and Qingquan Liu[2,3,4]

[1]School of Basic Medical Sciences, Chengdu University of Traditional Chinese Medicine, Chengdu, China, [2]Beijing Hospital of Traditional Chinese Medicine, Capital Medical University, Beijing, China, [3]Beijing Institute of Chinese Medicine, Beijing, China, [4]Beijing Key Laboratory of Basic Research with Traditional Chinese Medicine on Infectious Diseases, Beijing, China

Infectious diseases continue to be a major global public health concern, which is exacerbated by the increasing prevalence of antimicrobial resistance. This review investigates the potential of herbal medicine, particularly *Chrysanthemum morifolium* (CM) and *Chrysanthemum indicum* (CI), in addressing these challenges. Both herbs, documented in traditional Chinese medicine (TCM) and the Pharmacopoeia of the People's Republic of China (2020 edition), are renowned for their heat-clearing and detoxifying properties. Phytochemical studies reveal that these botanicals contain diverse bioactive compounds, including flavonoids, terpenoids, and phenylpropanoids, which exhibit antimicrobial, anti-inflammatory, and antioxidant properties, among other effects. Comparative analysis reveals that distinct compound profiles and differential concentrations of core phytochemicals between CM and CI may lead to differentiated therapeutic advantages in anti-infective applications. By systematically examining their ethnopharmacological origins, phytochemical fingerprints, and pharmacological mechanisms, this review highlights their synergistic potential with conventional antimicrobial therapies through multi-target mechanisms, proposing novel integrative approaches for global health challenges.

KEYWORDS

***Chrysanthemum morifolium*, *Chrysanthemum indicum*, anti-infection, major compounds, pharmacological effects**

1 Introduction

Infectious diseases continue to pose a persistent and significant threat to global public health, contributing substantially to morbidity and mortality worldwide. The rise of antimicrobial resistance has further complicated the management of these diseases, highlighting the urgent need for alternative therapeutic strategies (Sangeetha Vijayan et al., 2024). Botanical drug, with its extensive historical and cultural heritage, presents a promising avenue for addressing both infectious diseases and the challenges posed by antimicrobial resistance.

Chrysanthemum morifolium (CM, known as "Juhua" in China) refers to the flower head of *C. morifolium* Ramat. Originating from China, CM has been utilized for over 3,000 years,

predominantly as a dietary flower tea for health maintenance and as an integral component of traditional Chinese medicine (TCM) (Yuan et al., 2020). CM is listed in the Pharmacopoeia of the people's Republic of China (ChP) as a significant botanical drug with properties that include dispersing wind-heat, clearing liver fire, brightening the eyes, and detoxifying (Commission CP, 2020). *Chrysanthemum indicum* (CI, known as "Yeju" in China) is the flower head of *C. indicum* Linné. According to the 2020 edition of ChP, CI is recognized for its properties in clearing heat, detoxifying, purging fire, and pacifying the live (Commission CP, 2020). The similar names and appearances of the two botanical drugs frequently cause confusion and misidentification. Although both CM and CI belong to the Compositae family, their plant morphology and phytochemical compositions differ significantly. In TCM, CI is considered more effective for heat-clearing and detoxifying, while CM exhibits a broader range of therapeutic functions. Nonetheless, both botanical drugs show potential in the treatment of infectious diseases.

The pharmacological potential of CM and CI in infectious disease management is underscored by their rich phytochemical composition. These plants contain a plethora of compounds, including flavonoids (Miyazawa and Hisama, 2003; Wang et al., 2010; Wu et al., 2015; Yang et al., 2019a), terpenoids (Commission CP, 2020; Liu et al., 2017), phenolic acids (Yang et al., 2019b; Gao et al., 2008), and others (Guo et al., 2010). Notably, these compounds demonstrate antibacterial (Park and Kang, 2021; Zhang et al., 2024; Wang et al., 2020), antiviral (Shen et al., 2018; Boudou et al., 2024), anti-inflammatory (Boudou et al., 2024; Hamad et al., 2023), antioxidant effects (Boudou et al., 2024; Han et al., 2018), among others (Chen et al., 2024; Yang et al., 2017; Xie et al., 2009; Sun et al., 2012). Due to the differences in the types of compounds and the concentrations of the main compounds between the two, they may have different characteristics and advantages in anti-infection treatment. However, there has been no comprehensive summary or comparison of the effects of CM and CI in the treatment of infectious diseases.

This article aims to explore the main compounds and potential mechanisms by which CM and CI play a role in the treatment of infectious diseases. By delving into the ethnopharmacological origins, major phytochemical compounds, and associated pharmacological activities of these botanicals, we aim to elucidate their potential in complementing conventional anti-infection therapies and addressing the challenges of antimicrobial resistance. Finally, the paper summarizes the current research status and discusses future prospects of CM and CI in the context of infectious diseases.

2 Ethnopharmacology

2.1 Botany, description and distribution

Both CM and CI belong to the Compositae family and are utilized both medicinally and for environmental applications. The dried flower heads of CM are commonly utilized as medicinal parts for treatment, while both the dried flower heads and whole plants of CI serve as primary medicinal components for treating various diseases. To better differentiate between CM and CI, we conducted a macroscopic identification, as detailed in Table 1.

CM (Juhua) has been utilized in China for over 3,000 years, with historical records dating back to the Qin and Han dynasties (Liang et al., 2014). It was introduced to Japan during the Tang Dynasty (AD 710–784) as a highly regarded spice and subsequently spread Europe and the United States in the 17th century (Li, 1993). The genus CM comprises 41 species, which are widely distributed across Asia, including Mongolia, Russia, China, Japan, and Korea, as well as eastern Europe (Chen et al., 2020; Committee FoCE, 1983). In China, excluding Tibet and the Northwest regions, approximately 21 species are predominantly found in humid areas at middle and low altitudes (Chen et al., 2020). The botanical morphological characteristics of CM are described as follows: 1) Life form: Perennial herb. 2) Stem: Erect, either branched or unbranched, covered with pubescent. 3) Leaves: Ovate to lanceolate in shape, measuring 5–15 cm in length, pinnately lobed or semi-lobed, short-petioled, and white pubescent on the underside. 4) Flowers: The capitulum ranges from 2.5 to 20 cm in diameter. The involucrum consists of multiple layers, with the outer layer being pilose. The ray florets exhibit a variety of colors, whereas the disk florets are yellow. 5) Fruits: Achenes measure approximately 1.3 mm in length, slightly pointed at the apex, flat-wedge shaped, longitudinally ribbed on the surface, and brown in color (Committee FoCE, 1983).

The application of CI (Yeju) in TCM can be traced back to the Qin and Han dynasties (Chen Caiying et al., 2015). The native range of CI includes China, the Eastern Himalayas, Inner Mongolia, Japan, South Korea, Nepal, *etc.* Additionally, it has a broad distribution across various Asian countries, as well as in several European and South American nations (Committee FoCE, 2011). This plant thrives in wide range of habitats, from grasslands on mountain slopes and thickets to wet areas near rivers, fields, roadsides, saline zones by seashores, and under scrub, typically at altitudes ranging from 100 to 2,900 m (Committee FoCE, 2011). The botanical morphological characteristics of CI are as follows: 1) Life form: Perennial herb. 2) Stem: Long or short procumbent rhizomes, with erect or diffuse stems that branch and are sparsely pilose; lower leaves senesce by anthesis. 3) Leaves: Middle stem leaves have petioles measuring 1–2 cm, with leaf blades ovate to long-ovate or elliptic-ovate, ranging from 3–7 (-10) × 2–4 (-7) cm. Both surfaces are pale green or olive-green, with the adaxial surface being sparsely pubescent and the abaxial surface less densely. The leaves are pinnatifid, pinnatilobed, or inconspicuously divided, with a truncate, somewhat cordate, or broadly cuneate base. 4) Flowers: The synflorescence is a lax terminal flat-topped cyme, bearing numerous or few capitula. Phyllaries are arranged in 5 rows, featuring broad scarious margins that are white or brown, with obtuse or rounded apices. Outer phyllaries are ovate or ovate-triangular, measuring 2.5–3 mm, while middle phyllaries are ovate at 6–8 mm, and inner phyllaries are narrowly elliptic, approximately 1.1 cm. Ray floret laminae are yellow, measuring 1–1.3 cm, with entire or 3-denticulate apices. 5) Fruits: Achenes measure 1.5–1.8 mm (Committee FoCE, 2011). (Figure 1).

2.2 Traditional uses

CM has a long history as a TCM. The earliest record of CM can be traced back to the *Shennong's Herbal Classic*, which described its taste as bitter and neutral, and indicated its primary use for dizziness

TABLE 1 The macroscopic identification of CM and CI.

Macroscopic	CM	CI
Appearance	Conical, inverted conical, flat spherical, irregular spheroidal, disc-shaped	Spheroid
Size	2.5–20 cm in diameter	0.25–1.3 cm in diameter
Surface feature	Involucrum composed of 3–4 layers, ovate to oval in shape, herbaceous in texture, colored yellow-green to brown-green. The outer surface is pilose, while the margin is membranous. The receptacle is hemispherical. Ligulate flowers are arranged in several layers, female, located peripherally, off-white in color, stiff and straight with longitudinal folds, and scattered with golden glands. Numerous tubular flowers, which are bisexual and centrally located, are hidden by the ligulate flowers, appearing yellow with apically 5-dentate corollas. Achenes are undeveloped and glabrous	Involucrum composed of 4–5 bracts. The outer bracts are ovate or striate, colored grayish-green to pale brown, often bearing white hairs, with membranous margins. The inner bracts are elongated and oval-shaped, membranous, and have a glabrous outer surface. Residual pedicels are present at the base of the involucre. Ligulate flowers range from yellow to brownish, exhibiting wrinkled and curled morphology. Numerous tubular flowers are present, characterized by a dark yellow color
Texture	Lightweight, with a soft texture and crispness when dry	Lightweight
Smell	Fresh	Fragrant
Taste	Sweet with a subtle bitterness	Bitter



FIGURE 1
Chrysanthemum morifolium Ramat. and *Chrysanthemum indicum* Linné. **(A)** *Chrysanthemum morifolium* (CM) is the flower head of *Chrysanthemum morifolium* Ramat. **(B)** *Chrysanthemum indicum* (CI) is the flower head of *Chrysanthemum indicum* Linné. Two images are from Guangmin Li and Xinxin Zhu, respectively. Both images are from Plant Data Center of Chinese Academy of Sciences (https://www.plantplus.cn).

and pain caused by wind, and other conditions. The *Mingyi Bielu* noted CM tastes sweet and is non-toxic. According to *The Compendium of Materia Medica*, Juhua is widely believed to dispel wind-heat, benefit the liver, and tonify Yin". A Qing Dynasty doctor, Xu Dachun, recorded that prolonged consumption of Juhua can tonify blood and Qi, enhance physical wellbeing, and promote longevity. Since Juhua can survive for a long time, there is a belief that consuming it can extend human life. ChP recorded that CM disperses wind and clears heat, pacifies the liver and brightens the eyes, and detoxifies. Clinically, it is used to treat wind-heat colds, headaches and dizziness, red and swollen eyes, diminished eyesight, sores, and abscess swelling (Commission CP, 2020). CM is extensively utilized in TCM, particularly as a primary ingredient in TCM prescription formulations such as Sangju Ganmao Wan, Huanglian Shangqing Wan, and Jinsang Kaiyin Wan. The 2020 edition of the ChP lists 1605 TCM formula and single-botanical drug preparations, among which 55 containing CM, accounting for approximately 3.4% of the total (Commission CP, 2020).

There are limited records of CI in ancient medical literature. The earliest record of CI can be traced back to the *Sheng Nong's herbal classic* and it was recorded as "Jiehua" (Chen Caiying et al., 2015). In the *Bencao Qiuzhen*, CI is described as having the properties of "entering the lung and liver meridians". The *Bencao Huiyan* noted: "CI has a bitter taste, is cold in nature, and slightly toxic. It functions to break up blood stasis, soothe the liver, and detoxify whitlow. Additionally, it can be used as a douche for scabies to dispel wind and kill parasites". The 2020 edition of ChP recorded that CI has the functions of clearing heat, detoxifying, purging fire, and pacifying the liver, and clinically, it is used to treat conditions such as whitlow, sores, abscesses, and swelling, as well as symptoms like redness of the eyes, headache, and dizziness (Commission CP, 2020). The 2020 edition of ChP includes 16 TCM formula preparations containing CI (Commission CP, 2020). Table 2 provides details on the utilization of CM and CI as monarch medications.

3 Pharmacology

We conducted a comprehensive literature search in PubMed from 2000 to 2024 using the terms "Chrysanthemum morifolium", "Chrysanthemum morifolium Ramat.", "Chrysanthemum

TABLE 2 The preparations of CM and CI as monarch medicine were listed in ChP 2020 edition.

Name		Function
CM	Xiaoer Ganmao Keli (Cha, Koufuye)	Disperse wind and release the exterior, clear heat and detoxify
	Qiju Dihuang Wan (Koufuye, Pian)	Enrich the kidney and nourish the liver
	Xiongju Shangqing Wan (Pian, Shuiwan)	Clear heat and release the exterior, relieve pain
	Sangju Ganmao Wan (Pian, Heji)	Disperse wind and clear heat, diffuse the lung to suppress cough
	Qingre Yinhua Tangjiang	Clear heat and detoxify, diuresis
	Tianju Naoan Jiaonang	Pacify the liver to extinguish wind, activate blood and resolve stasis
	Mingmu Shangqing Pian	Clear heat and disperse wind, improve vision and relieve pain
	Shanju Jiangya Pian	Pacify the liver to subdue Yang
	Fuming Pian	Enrich the kidney and nourish the liver, tonify Yin and engender fluid, clear the liver to improve vision
	Xiaoer Tuirening Koufuye	Release the exterior and clear heat, resolve phlegm to suppress cough, detoxify to soothe the throat
CI	Yejuhua Shuan	Antibacterial and anti-inflammatory
	Xiasangju Keli	Clear the liver to improve vision, disperse wind and clear heat, relieve the dampness fixed impediment, detoxify the sore
	Biyan Qingdu Keli	Clear heat and detoxify, resolve phlegm and dissipate binds

indicum", "Chrysanthemum indicum Linné.", as well as related keywords such as "Juhua", "Yeju", and "Yejuhua". This search yielded a total of 785 articles (CM: n = 582, CI: n = 203.). After removing duplicates (n = 47) and review articles (n = 23), we carefully screened the titles and abstracts of the remaining articles and excluded those (n = 469) not relevant to the pharmacological effects of CM and CI. Ultimately, we included twenty-nine studies that explicitly examined the antimicrobial (n = 10), anti-inflammatory (n = 8), antioxidant (n = 7), and immunomodulatory (n = 4) effects of CM and CI, with a focus on their potential applications in infectious diseases.

With the exploration of the potential applications of CM and CI in food, health products, and cosmetics, research into their chemical components has significantly expanded. They contain a rich array of compounds, including flavonoids, phenylpropanoids, terpenoids, triterpenoids, and others, which may endow them with anti-infective pharmacological effects such as antimicrobial, anti-inflammatory, and antioxidant properties. Our review of studies investigating the potential roles of CM and CI in combating infectious diseases revealed that they possess distinct advantages, which can be attributed to their different content and composition of specific compounds, particularly terpenoids and flavonoids. Consequently, we have summarized the major compounds analyzed in the included studies of CM and CI in Table 3 and illustrated these compounds in Figure 2.

3.1 Antimicrobial effects

CM and CI extracts exhibit potent antimicrobial effects, demonstrating potential to inhibit a wide range of microorganisms including bacteria, fungi, viruses, mycobacteria, and parasite and others (Kuang et al., 2018; Liu et al., 2022; Youssef et al., 2020; Shunying et al., 2005; Gu et al., 2013; Zhang et al., 2020; Akihisa et al., 2005; Lee et al., 2003). The differences in the types of inhibited microorganisms between CM and CI may be attributed to variations in their primary compounds, such as terpenoids and flavonoids.

3.1.1 Antibacterial effect

Terpenoids have been reported to exhibit significant antibacterial activity by destroying the integrity of bacterial cell membranes or impairing essential bacteria functions (Yamaguchi, 2022; Meenu et al., 2023; Zacchino et al., 2017). Essential oils from CM and CI are rich in terpenoids (Liu et al., 2017; Peng et al., 2020; Shao et al., 2020; Wang Xl et al., 2006; Xue et al., 2018), which suggest that they possess potent antibacterial properties. For instance, the study conducted by Kuang et al. (Kuang et al., 2018) demonstrated that CM essential oil exhibits significant inhibitory effects against five bacterial strains: *Pseudomonas aeruginosa* (*P. aeruginosa*), *Salmonella enteritids* (*S. enteritidis*), *B. subtilis* (*Bacillus subtilis*), *Staphylococcus aureus* (*S. aureus*), and *Escherichia coli* (*E. coli*). The minimum inhibitory concentrations (MICs) were determined as follows: 0.33% for *P. aeruginosa*, 0.67% for both *S. enteritidis* and *B. subtilis*, and 1.30% for both *E. coli* and *S. aureus*. The main compounds isolated from CM essential oil are monoterpenes and sesquiterpenes, including α-curcumene (No.1), α-farnesene (No.2), β-bisabolene (No.3), bisabolol (No.4), n-heptadecane (No.5), nonadecane (No.6) and n-pentacosane (No.7) (Table 3). Notably, α-curcumene (No.1) is the most abundant compound among these compounds, accounting for 12.55% of the total composition (Kuang et al., 2018). These compounds are potentially associated with the antibacterial properties of CM essential oils. Furthermore, in a separate study, the content of α-curcumene (No.1) extracted from CI *via* hydro-distillation (1.23%) was significantly lower at 1.23% compared to 10.50% obtained from CM (Youssef et al., 2020). This suggests that CI may exhibit a weaker inhibitory effect on the aforementioned five bacteria.

TABLE 3 The primary compounds in CM and CI that are likely to exert anti-infection-related pharmacological effects.

No.	Compound	CM	CI	CM			CI		
				Plant part	Extraction	Ref.	Plant part	Extraction	Ref.
	Alkenes and terpenoids								
1	α-Curcumene	✓	✓	Flowers	HDE	Kuang et al. (2018), Liu et al. (2022), Youssef et al. (2020)	Flowers	HDE	Youssef et al. (2020)
2	α-Farnesene	✓		Flowers	HDE	Kuang et al. (2018)			
3	β-Bisabolene	✓		Flowers	HDE	Kuang et al. (2018)			
4	Bisabolol	✓		Flowers	HDE	Kuang et al. (2018)			
5	N-heptadecane	✓		Flowers	HDE	Kuang et al. (2018)			
6	Nonadecane	✓		Flowers	HDE	Kuang et al. (2018)			
7	N-pentacosane	✓	✓	Flowers	HDE	Kuang et al. (2018)	Flowers	HDE	Youssef et al. (2020)
8	Camphor	✓	✓	Flowers	HDE	Youssef et al. (2020)	Flowers	HDE	Youssef et al. (2020)
9	Isoborneol		✓				Flowers	HDE	Youssef et al. (2020)
10	α-Terpinene		✓				Flowers	HDE	Youssef et al. (2020)
11	Caryophyllene oxide	✓	✓	Flowers	HDE	Youssef et al. (2020)	Flowers	HDE	Youssef et al. (2020)
12	α-Terpineol	✓	✓	Flowers	HDE	Youssef et al. (2020)	Flowers	HDE	Youssef et al. (2020), Shunying et al. (2005)
13	Cedren-13-ol, 8-	✓	✓	Flowers	HDE	Youssef et al. (2020)	Flowers	HDE	Youssef et al. (2020)
14	τ-Eudesmol	✓		Flowers	HDE	Youssef et al. (2020)			
15	Borneol	✓		Flowers	HDE	Youssef et al. (2020)			
16	Chrysanolide A		✓				Flowers	EE	Gu et al. (2013)
17	Chrysanolide B		✓				Flowers	EE	Gu et al. (2013)
18	Chrysanolide C		✓				Flowers	EE	Gu et al. (2013)
19	α-Cadinol	✓		Flowers	HDE	Liu et al. (2022), Youssef et al. (2020)			
20	β-Sesquiphellandrene	✓		Flowers	HDE	Liu et al. (2022)			
21	Caryophyllene	✓		Leaves and stems	HDE	Liu et al. (2022)			
22	Spathulenol	✓		Flowers	HDE	Liu et al. (2022)			
23	Caryophyllen-5-ol	✓		Flowers	HDE	Liu et al. (2022)			
24	Junenol	✓		Flowers	HDE	Liu et al. (2022)			
25	β-Cadinol	✓		Flowers	HDE	Liu et al. (2022)			
26	Iso-caryophyllene	✓		Flowers	HDE	Liu et al. (2022)			
27	(*E*)-β-Farnesene	✓		Flowers	HDE	Liu et al. (2022)			
28	α-Longipinene	✓		Roots	EAE	Zhang et al. (2020)			
29	α-Pinene	✓		Roots	EAE	Zhang et al. (2020)			

(Continued on following page)

TABLE 3 (*Continued*) The primary compounds in CM and CI that are likely to exert anti-infection-related pharmacological effects.

No.	Compound	CM	CI	CM			CI		
				Plant part	Extraction	Ref.	Plant part	Extraction	Ref.
30	*β*-Pinene	✓		Roots	EAE	Zhang et al. (2020)			
31	(*E*)-*β*-caryophyllene	✓		Roots	EAE	Zhang et al. (2020)			
32	Silphinene	✓		Roots	EAE	Zhang et al. (2020)			
33	Modephene	✓		Roots	EAE	Zhang et al. (2020)			
34	*α*-Isocomene	✓		Roots	EAE	Zhang et al. (2020)			
35	*β*-Isocomene	✓		Roots	EAE	Zhang et al. (2020)			
36	*β*-Copaene	✓		Roots	EAE	Zhang et al. (2020)			
37	*α*-Fenchene	✓		Roots	EAE	Zhang et al. (2020)			
38	Lupeol	✓	✓	Flowers	NSL of ME	Akihisa et al. (2005)	Flowers	70% EE	Kang et al. (2013)
39	Faradiol	✓		Flowers	NSL of ME	Akihisa et al. (2005)			
40	22*α*-Methoxyfaradiol	✓		Flowers	NSL of ME	Akihisa et al. (2005)			
41	Faradiol *α*-epoxide	✓		Flowers	NSL of ME	Akihisa et al. (2005)			
42	Taraxasterol	✓		Flowers	NSL of ME	Akihisa et al. (2005)			
43	Arnidiol	✓		Flowers	NSL of ME	Akihisa et al. (2005)			
44	Maniladiol	✓		Flowers	NSL of ME	Akihisa et al. (2005)			
45	Longispinogenin	✓		Flowers	NSL of ME	Akihisa et al. (2005)			
46	*α*-Amyrin	✓		Flowers	NSL of ME	Akihisa et al. (2005)			
47	Uvaol	✓		Flowers	NSL of ME	Akihisa et al. (2005)			
48	3-Epilupeol[a]	✓		Flowers	NSL of ME	Akihisa et al. (2005)			
49	Calenduladiol	✓		Flowers	NSL of ME	Akihisa et al. (2005)			
50	24-Methylenecycloartanol	✓		Flowers	NSL of ME	Akihisa et al. (2005)			
51	(24*S*)-Cycloartane-3*β*,24,25-triol	✓		Flowers	NSL of ME	Akihisa et al. (2005)			
52	4,5*α*-Epoxyhelianol	✓		Flowers	NSL of ME	Akihisa et al. (2005)			
53	Dammaradienol	✓		Flowers	NSL of ME	Akihisa et al. (2005)			
	Flavonoids								
54	Apigenin 7-*O*-*β*-D-(4″-caffeoyl)glucuronide	✓		Flowers	ME	Lee et al. (2003)			
55	Linarin	✓		Flowers	95% EE	Liu et al. (2020)			
56	Luteolin-7-*O*-glucoside	✓	✓	Flowers	95% EE; AE	Liu et al. (2020), Lee et al. (2021), Zhou et al. (2023)	Flowers	95% EBE	Cheng et al. (2005)
57	Luteolin	✓	✓	Flowers	95% EE; AE	Liu et al. (2020), Lii et al. (2010)	Flowers, leaves, and stems	ME; 95% EBE	Cheng et al. (2005), Yu et al. (2019)
58	Apigenin	✓		Flowers	95% EE; AE	Liu et al. (2020), Lii et al. (2010)			
59	Acacetin	✓		Flowers	EE	Liu et al. (2020)			
60	Luteolin-7-*O*-glucuronide	✓		Flowers	AE	Lee et al. (2021)			

(Continued on following page)

TABLE 3 (*Continued*) The primary compounds in CM and CI that are likely to exert anti-infection-related pharmacological effects.

No.	Compound	CM	CI	CM			CI		
				Plant part	Extraction	Ref.	Plant part	Extraction	Ref.
61	Apigenin-7-*O*-glucoside	✓		Flowers	AE	Lee et al. (2021), Zhou et al. (2023)			
62	Eriodictyol-7-*O*-glucoside	✓		Flowers	AE	Zhou et al. (2023)			
63	Diosmetin-7-*O*-glucoside	✓		Flowers	AE	Zhou et al. (2023)			
64	Acacetin-7-rhamnoglucoside		✓				Flowers	95% EBE	Cheng et al. (2005)
	Phenylpropanoids								
65	Neochlorogenic acid	✓		Flowers	95% EE	Liu et al. (2020)			
66	Chlorogenic acid	✓	✓	Flowers	95% EE; AE	Liu et al. (2020), Lee et al. (2021)	Flowers, leaves, and stems	ME	Yu et al. (2019)
67	Caffeic acid	✓		Flowers	95% EE	Liu et al. (2020)			
68	Isochlorogenic acid C; 3,4-Dicaffeoylquinic acid	✓		Flowers	95% EE	Liu et al. (2020)			
69	Isochlorogenic acid A; 3,5-Dicaffeoylquinic acid	✓		Flowers	95% EE; AE	Liu et al. (2020), Lee et al. (2021)			
70	Isochlorogenic acid B 4,5-Dicaffeoylquinic acid	✓		Flowers	95% EE	Liu et al. (2020)			
71	1,3-Dicaffeoylquinic acid; 1,5-Dicaffeoylquinic acid	✓	✓	Flowers	95% EE; AE	Liu et al. (2020), Lee et al. (2021)	Flowers, leaves, and stems	ME	Yu et al. (2019)
	Others								
72	Capric acid	✓		Flowers	HDE	Kuang et al. (2018)			
73	Linoleic acid	✓		Flowers	HDE	Kuang et al. (2018)			
74	A New bisepoxylignan dendranlignan A	✓		Flowers	50% ACE	Zeng et al. (2020)			
75	Polysaccharide CMJA0S2	✓		Flowers	AE	Zheng et al. (2015)			
76	Polysaccharides	✓		Flowers	95% EE	Tao et al. (2018)			
77	Polysaccharides	✓		Flowers	95% EE	Tao et al. (2017)			
78	Polysaccharides	✓		Flowers	EE	Wang et al. (2022)			

HDE, Hydro distillation extraction; EE, ethanol extract; EAE, ethyl acetate extract; NSL of ME, NSL fraction of the methanol extract; ME, methanol extract; AE, aqueous extract; EBE, ethanol and butanol extract; ACE, acetone extract. a) Semisynthesized from compound lupeol (No.38).

Additionally, camphor (No.8), an oxygenated monoterpene, is the predominant compound in both CM (14.56%) and CI (36.69%) oils (Youssef et al., 2020). Notably, the essential oil of CI demonstrated superior antimicrobial activity against Gram-positive bacteria, including *B. subtilis*, *Streptococcus agalactiae*, and *Streptococcus pyogenes*, compared to the CM essential oil (Youssef et al., 2020). This enhanced activity may be attributed to the higher concentrations of camphor (No.8) and isoborneol (No.9) (7.64%) in CI (Youssef et al., 2020), which have been associated with antibacterial and antiviral properties (Chen et al., 2013; Astani et al., 2011; Costa et al., 2021). Therefore, in this study, essential oils rich in terpenoids demonstrated greater efficacy against Gram-positive bacteria than compared to Gram-negative bacteria (Youssef et al., 2020; Shunying et al., 2005). Moreover, the processed and air-dried flower oils of CI were evaluated against 15 microorganisms (Shunying et al., 2005). The processed flower oil exhibited the strongest antimicrobial activity against *Staphylococcus saprophyticus* (*S. saprophyticus*) (MIC: 0.78 mg/mL, minimum bactericidal concentration (MBC): 0.78 mg/mL), and the air-dried flower oil showed the most effective bactericidal activity against *E. coli* (MIC: 0.39 mg/mL, MBC: 0.39 mg/mL). The two oils possessed good inhibitory effects on *S. saprophyticus* (MIC: 1.56 mg/mL, MBC: 1.56 mg/mL) (Shunying et al., 2005). Furthermore, the air-dried essential oil showed superior bactericidal activity against *E. coli* (102 strains) at concentrations ranging from 3 to 56 μg/mL, likely due to its higher content of α-terpineol (No.12) at 3.32%, compared to 2.94% in the processed flower essential oil (Shunying et al., 2005). CM also contains α-terpineol (No.12), but at a lower concentration of only 0.65% (Youssef et al., 2020).

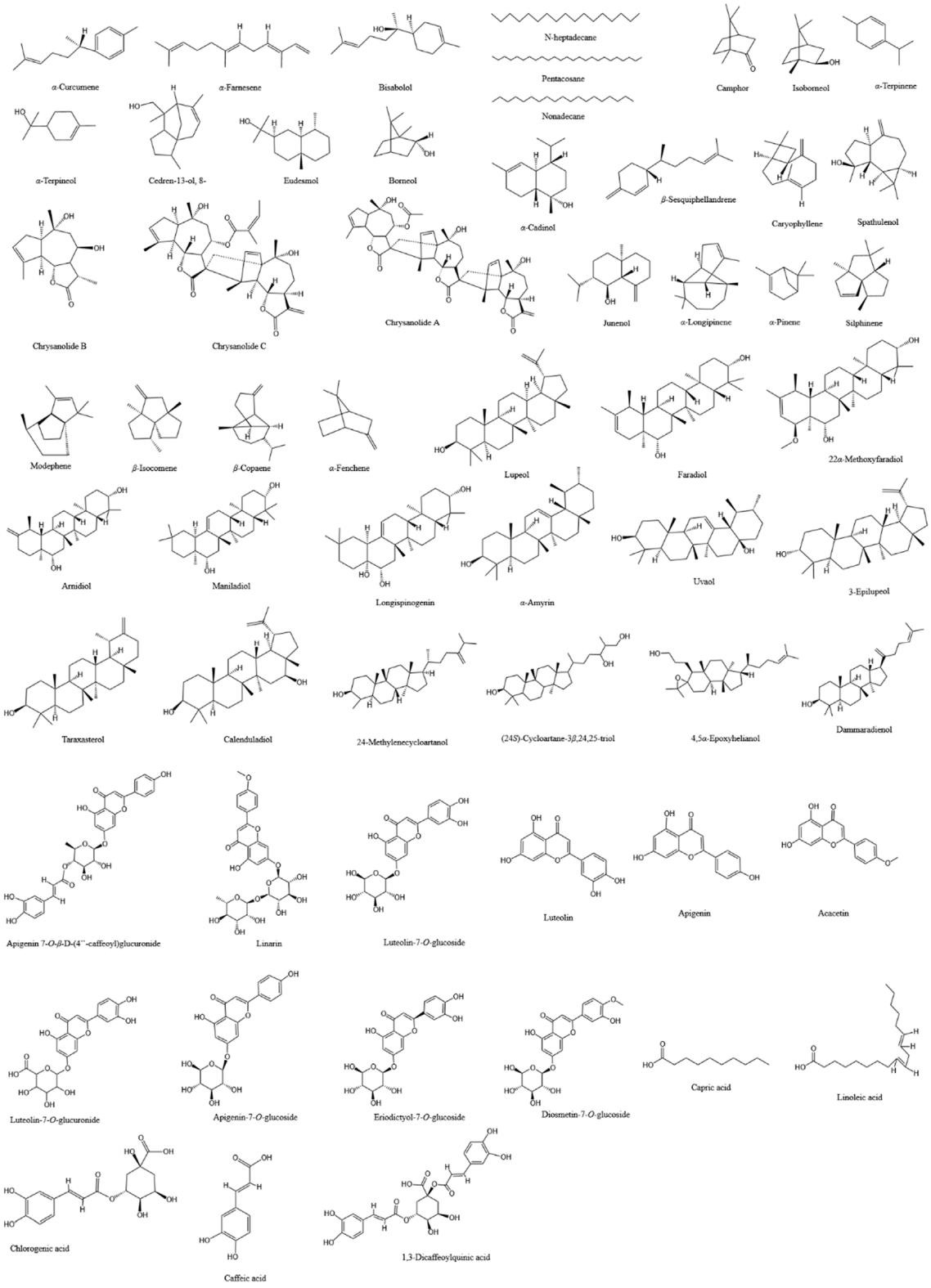


FIGURE 2
The chemical structures of the main compounds that may exert anti-infection-related pharmacological effects in CM and CI.

Furthermore, essential oils derived from different nonmedicinal parts of CM exhibit varying degrees of antibacterial activity. Specifically, Juhua demonstrates the most potent antibacterial effect against *S. aureus* (MIC: 10 mg/mL) compared to the stem and leaf extracts as well as root extracts of CM (Liu et al., 2022). The antibacterial efficacy of Juhua and stem and leaf extracts against

TABLE 4 Detailed information of antimicrobial effects of CM and CI.

Extracts/compounds	Control	Mode	Detail	MIC/IC_{50}/EC_{50}/ Active concentration	Ref.
CM					
Essential oil (Hydro distillation extraction)	Negative control: ethanol solution (95%)	-	Inhibits *P. aeruginosa*, *S. enteritidis*, *B. subtilis*, *S. aureus*, and *E. coli*	MIC = 0.33%, 0.67%, 0.67%, 1.30%, and 1.30%	Kuang et al. (2018)
Jumi, Tianju, Juhua, roots, and the stem and leaf essential oil (Hydro distillation extraction)	Positive control: Penicillin (*S. aureus*); erythromycin lactobionate (*P. acnes*)	*P. acnes*/*S. aureus*-induced THP-1 cells	Anti-bacterial: Inhibits *P. acnes* and *S. aureus*	Jumi: MIC = 25 and 10 mg/mL; Tianju: MIC = 25 and 10 mg/mL; Juhua: MIC = 25 and 10 mg/mL; stem and leaf: MIC = 25 and 20 mg/mL; roots: MIC = 50 and 50 mg/mL Control: penicillin: *S. aureus*: MIC = 0.0035 mg/mL; erythromycin lactobionate: *P. acnes*: MIC = 0.061 mg/mL. The MIC of the remaining bacteria was not detected Juhua and stem and leaf: IL-1β in *P. acnes*-induced THP-1 cells↓	Liu et al. (2022)
Twenty-nine 3-hydroxytriterpenoids (NSL fraction of the methanol extract)	Positive control: Rifampin	Vero cells	Anti-tuberculosis activity agaist *M. tuberculosis* strain H37Rv	1)3-epilupeol: MIC = 4 μg/mL, IC_{50} > 62.5 μg/mL 2)Compounds 39–47, 49–53: MIC = 4–64 μg/mL 3)Others: MIC >64 μg/mL	Akihisa et al. (2005)
Apigenin 7-*O*-*β*-D-(4″-caffeoyl) Glucuronide (Methanol extract)	Positive control: Apigenin 7-*O*-*β*-D-glucuronide and L-chicoric acid	$HIV\text{-}1_{IIIB}$ infected MT-4 cells	Antiviral: Inhibits HIV and HIV-1 integrase activity	IC_{50} = 7.2 ± 3.4 μg/mL, EC_{50} = 41.86 ± 1.43 μg/mL	Lee et al. (2003)
12 cultivars of CM roots extracts (Ethyl acetate extract)	Negative control: Organic solvent ethyl acetate	-	Antifungal: "Xiao Huang Ju" was the only cultivar that exhibited significant inhibitory effects on all three species of *Magnaporthe oryzae*, *Verticillium dahliae*, and *Fusarium oxysporum* ($p < 0.05$)	-	Zhang et al. (2020)
CI					
Essential oils of air-dried and processed flowers (Hydro distillation extraction)	Positive control: Levofloxacin	-	Antimicrobial activity against 15 microorganisms *Bacillus subtilis*, *Staphylococcus aureus*, *Staphylococcus aureus*, *Proteus vulgaris*, *Salmonella typhi*, *Saccharomyces cerevisiae*, *Hansenula anomala*, *Candida* sp., *Klcbsiella pneumoniae*, *Citrobacter freundill*, *Enterobacter cloacae*, *Escherichia coli*, *Staphylococcus saprophyticus*, *Enterococcus faecalis*, and *Proteus mirabilis*	A concentration of 3.00 mg/disc Air-dried: MIC = 3.13, 3.13, 3.13, 12.50, 6.25, 12.50, 6.25, 3.13, 6.25, 25.00, 6.25, 0.39, 1.56, 25.00, and 50.00 mg/mL Processed: MIC = 3.13, 6.25, 3.13, 50.00, 12.50, 12.50, 1.56, 0.39, 6.25, 25.00, 6.25, 6.25, 0.78, 3.13, and 25.00 mg/mL Control: MIC = 0.61, 0.61, 0.61, 0.61, 1.22, nt, nt, nt, 0.31, 39.06, 4.88, 2.44, 9.77, 9.77, and 39.06 mg/mL	Shunying et al. (2005)
Chrysanolide B, Chrysanolide C, Chrysanolide A (ethanol extract)	Positive control: Lamivudine	HepG 2.2.15 cell line	Antiviral: Inhibits the secretion of HBsAg and HBeAg	HBsAg: IC_{50} = 131.28, 33.91, and 6.67 μM; HBeAg: IC_{50} = 144.48, 30.09, and 6.23 μM	Gu et al. (2013)

(Continued on following page)

TABLE 4 (*Continued*) Detailed information of antimicrobial effects of CM and CI.

Extracts/compounds	Control	Mode	Detail	MIC/IC_{50}/EC_{50}/ Active concentration	Ref.
70% ethanol extract	Blank control: DMSO	Parental BL41 cells, their LMP1 expressing counterparts, and LCL	Antiviral:1)Inhibits LMP1 CTAR 1 and 2-induced NF-κB activation possibly by interfering with IKKα and IKKβ activation 2)Reduces the viability of EBV-transformed LCL viability by inducing apoptosis	Concentration: 1, 2, 3, and 4 μg/mL (in a dose- and time-dependent manner)	Kim et al. (2012)
1)CH_2Cl_2 fraction of CI 2)lupeol (80% ethanol extract)	1)DMSO 2)HEK293 cells were co-transfected with Renilla luciferase plasmids	1)LCLs, HFF, HeLa and BL41 cells 2)HEK293 cells were co-transfected with pSG5 or pSG5-FLAG-LMP1 plus NF-κB dependent firefly luciferase	Antiviral: Attenuates LMP1-induced NF-κB activation and LCL viability	1)CH_2Cl_2 fraction: LCLs: Active concentration: 100 μg/mL; IC_{50} at 24, 48 and 72 h were 97.3, 55.8 and 45.2 mM, respectively. HFF: IC_{50} at 72 h was 145.5 mM. HeLa: IC_{50} at 48 and 72 h were 84.3 and 109.7 mM BL41: IC_{50} at 24, 48 and 72 h were 150.9, 93.7 and 91.4 mM. Other data were not determined 2)Lupeol: Active concentration: 50 μg/mL; IC_{50} at 24, 48 and 72 h were 109.9, 57.6 and 51.8 mM, respectively	Kang et al. (2013)
CM &CI					
Essential oils (Hydro distillation extraction)	Positive control: acyclovir	Vero cells	Antiviral: Inhibits VSV, HAV, and HSV-1	CI: IC_{50} = 3.14, 3.38, and 3.51 μg/mL. CM: IC_{50} = 3.69, 3.80, and 3.73 μg/mL (Control: IC_{50} = 2.21, 1.84, and 1.49 μg/mL) ($p < 0.05$)	Youssef et al. (2020)
	Positive control: Ampicillin (Gram-positive bacteria); gentamycin (Gram-negative bacteria); clotrimazole (fungi)	-	Antimicrobial: Gram-positive bacteria *Bacillus subtilis, Streptococcus agalactiae and Streptococcus pyogenes*	CI was more effective than CM. CI: MIC = 62.5 μg/mL. CM and CI exerted weak activity *versus* the examined Gram-negative bacteria and fungal strains with MICs >500 μg/mL	Youssef et al. (2020)
	Positive control: Isoniazid	-	Anti-mycobacterial activity against *M. tuberculosis*	CM and CI: IC_{50} = 7.36 and 6.73 μg/mL (Control: IC_{50} = 0.038 μg/mL) ($p < 0.05$)	Youssef et al. (2020)
	Positive control: Clarithromycin	-	Anti-Helicobacter pylori	CM and CI: IC_{50} = 3.78 and 3.63 μg/mL (Control: IC_{50} = 0.76 μg/mL) ($p < 0.05$)	Youssef et al. (2020)
	Positive control: Diminazene	-	Antiparasitic: Anti-trypanosomal activity	CM and CI: IC_{50} = 49.02 and 45.89 μg/mL (Control: IC_{50} = 0.075 μg/mL) ($p < 0.05$)	Youssef et al. (2020)

"-": Not mentioned. "nt": Not tested. Concentration for 50% of maximal effect (EC50), C-terminal activation regions (CTAR).

Propionibacterium acnes (*P. acnes*) is comparable (MIC: 25 mg/mL), both of which are significantly higher than that of the root extract (Liu et al., 2022). This may be related to the high content of terpenoids in Juhua oil compared with the other two parts of essential oils. In this study, Juhua essential oil exhibited the highest terpenoid content among processed flowers at different stages (Jumi, Tianju, Juhua) and different parts of CM (Juhua, Stem and Leaf, Root), which likely contributes to its superior antibacterial efficacy. The composition of Juhua essential oil was predominantly oxygenated sesquiterpenes, with α-cadinol being the major constituent (28.62%, No.19). Notably, the content of heterospiroolefins, such as (*E*)-tibetin spiroether, decreased significantly from 44.81% in Jumi essential oil to 7.27% in Juhua essential oil. Despite this reduction, heterospiroolefins appear to have minimal impact on the antibacterial activity of CM (Liu et al., 2022). It is worth noting that heterospiroolefins were first isolated from CM, yet their specific antibacterial effects remain unclear.

3.1.2 Antimycobacterial effect

Triterpenoids and essential oils extracted from CM and CI showed significant anti-mycobacterial activity against *Mycobacterium tuberculosis* (*M. tuberculosis*) (Youssef et al.,

2020; Akihisa et al., 2005). For instance, Akihisa et al. (Akihisa et al., 2005) utilized the microplate Alamar Blue Assay (MABA) to identify twenty-nine 3-hydroxytriterpenoids from unsaponified lipid extracts of CM. Among these compounds, fourteen exhibited MIC values ranging from 4 to 64 μg/mL against *M. tuberculosis* (as detailed in Tables 3, 4). 3-Epilupeol (MIC: 4 μg/mL, No.48), derived from lupeol (No.38), and maniladiol (MIC: 4 μg/mL, No.44) showed the most potent anti-mycobacterial activity among the tested compounds (Akihisa et al., 2005). Notably, the half maximal inhibitory concentration (IC_{50}) value of three-epilupeol exceeded 62.5 μg/mL, suggesting a selective toxicity towards *M. tuberculosis* (Akihisa et al., 2005). Although the antitubercular effect of CM and the extract was much lower compared to first-line antitubercular drugs, such as rifampin and isoniazid, these compounds still exhibited substantial activity against *M. tuberculosis* (Youssef et al., 2020; Akihisa et al., 2005).

3.1.3 Antifungal effect

A study evaluating the antifungal activities of extracts from 12 cultivars of CM roots against *Magnaporthe oryzae*, *Verticillium dahliae*, and *Fusarium oxysporum* revealed that only "Xiao Huang Ju" exhibited significant inhibitory effects on all tested fungi (Zhang et al., 2020). Table 3 summarizes the key compounds identified in the 12 cultivars through principal component analysis. However, a separate study reported that both CM and CI oils demonstrated weak antifungal activity against *Aspergillus fumigatus*, *Candida albicans*, *Geotrichum candidum*, and *Syncephalastrum racemosum*, with MIC values exceeding 500 μg/mL (Youssef et al., 2020).

3.1.4 Antiviral effect

Both CM and CI possess antiviral properties (Youssef et al., 2020; Gu et al., 2013; Kang et al., 2013; Lee et al., 2003; Kim et al., 2012). For instance, the flavonoid compound apigenin 7-*O*-*β*-D-(4″-caffeoyl)glucuronide (No.54), isolated from CM, exhibited potent HIV-1 integrase inhibitory activity and anti-HIV effects in HIV-1_{IIIB}-infected MT-4 cells (Lee et al., 2003). Moreover, a unique sesquiterpenoid trimer (Chrysanolide A, No.16), along with its biogenetically related monomer (Chrysanolide B, No.17) and dimer (Chrysanolide C, No.18), isolated from CI, exhibited strong inhibitory activity against the secretion of HBsAg and HBeAg (Gu et al., 2013). Additionally, both CM and CI essential oils showed antiviral activity against vesicular stomatitis virus (VSV), hepatitis A (HAV) and herpes simplex type-1 (HSV-1) (Youssef et al., 2020). Notably, the antiviral activity of CI was dose-dependent, with VSV being the most sensitive to CI's antiviral effects (Youssef et al., 2020).

Epstein-Barr virus (EBV) latent infection membrane protein 1 (LMP1) plays a critical role in EBV-mediated B lymphocyte transformation, with LMP1-induced nuclear factor kappa-B (NF-κB) activation being crucial for the survival of lymphoblastoid cell lines (LCLs). CI exhibited a potent inhibitory effect on EBV LMP1-induced NF-κB activation and significantly reduced the viability of EBV-transformed LCLs in a dose- and time-dependent manner (Kim et al., 2012). This inhibition likely involves blocking LMP1-induced IKK*α* and IKK*β* activation, without affecting the viability of human foreskin fibroblasts, EBV-negative Burkitt lymphoma cells, or HeLa cells (Kim et al., 2012). Furthermore, both the CH2Cl2 fraction of CI and lupeol (No.38) significantly attenuated LMP1-induced NF-κB activation and reduced the viability of LCLs. Notably, the CH_2Cl_2 fraction of CI exhibited superior antiviral properties compared to lupeol. Additionally, lupeol may synergistically interact with unidentified compounds in the CH_2Cl_2 fraction of CI to further diminish LMP1-induced NF-κB activation and LCL viability (Kang et al., 2013).

3.1.5 Other effects

CM and CI have also exhibited potential antimicrobial effects against various microorganisms, including *Helicobacter pylori* and trypanosomes (Youssef et al., 2020). For example, the essential oils of CM and CI showed an anti-*H. pylori* activity with IC_{50} values of 3.63 μg/mL and 3.78 μg/mL, respectively, which are comparable to those of clarithromycin (Youssef et al., 2020).

The antimicrobial activity of CM and CI is strongly correlated with their terpenoid and triterpenoid content. Terpenes enhance lipophilicity and membrane permeability, leading to significant disruption of oxidative phosphorylation and electron transport chains, thereby severely impairing energy production and inducing autooxidation and peroxidation, ultimately resulting in bacterial lysis (Gamal El-Din et al., 2018). The potency of their antimicrobial effects is also influenced by the concentration of key compounds such as *α*-curcumene (No.1), camphor (No.8), and *α*-terpineol (No.12). Studies have demonstrated that while CI and CM exhibit weak antifungal activity, CM shows superior antifungal efficacy when different parts of the extract are used. Furthermore, CI demonstrates a stronger inhibitory effect on specific viruses. Additionally, some studies report antimicrobial activity using only IC_{50} or MIC values, but not both, which may introduce bias in their results. More details are provided in Table 4. Although the antimicrobial activity of CM and CI has been extensively studied, the detailed mechanism of their antimicrobial action has not been reported.

3.2 Anti-inflammatory effects

When an infection occurs, the immune system initiates an inflammatory response to combat invading pathogens (Zhang and Wang, 2014). However, excessive or prolonged inflammation can cause tissue damage and exacerbate disease severity. In severe cases, uncontrolled inflammation may lead to sepsis, widespread tissue injury, and organ failure (Esposito et al., 2017). Reducing inflammation can mitigate pathogen-induced tissue damage and bodily discomfort. Studies have shown that both CM and CI extracts exhibit significant anti-inflammatory effects by modulating inflammation-related pathways (Liu et al., 2020; Lee et al., 2021; Zhou et al., 2023; Yu et al., 2019; Zeng et al., 2020; Wu et al., 2014; Lee et al., 2009; Cheon et al., 2009).

CM and CI extracts demonstrated potential efficacy in treating acute lung injury (ALI). In a mouse model of lipopolysaccharide (LPS)-induced, both extracts significantly alleviated lung histopathological damage, reduced the wet-to-dry lung weight ratio and lung injury score, and were associated with decreased levels of pro-inflammatory cytokines, including IL-6 and tumor necrosis factor (TNF)-*α* (Liu et al., 2020; Wu et al., 2014). CM extract can attenuate the production of pro-inflammatory cytokines

(such as IL-6 and TNF-α), enhance the secretion of anti-inflammatory cytokines (including transforming growth factor-β1 (TGF-β1) and IL-10), and mitigate the oxidative stress by increasing total antioxidant capacity (TAC) and reducing malondialdehyde (MDA) levels in mice with ALI. However, the precise mechanisms underlying these effects remain to be elucidated (Liu et al., 2020). The therapeutic efficacy of CI may be attributed to its ability to downregulate both the Toll-like receptor 4 (TLR4) and MyD88-dependent NF-κB signaling pathways (Wu et al., 2014).

The other TLR4 signaling pathway is MyD88-independent and TRIF-dependent, leading to the phosphorylation and nuclear translocation of IRF3. A newly discovered compound, bisepoxylignan dendranlignan A (BDA), isolated from CM, has been shown to reduce the production of inflammatory cytokines TNF-α, IL-2, and interferon (IFN)-γ in LPS-stimulated H9c2 cells (Zeng et al., 2020). BDA significantly decreased the nuclear translocation and phosphorylation levels of IRF3, the NF-κB heterodimer component p65, and one of the AP-1 components, c-Jun. However, it did not significantly affect the protein expression of TLR4, MyD88, or TRIF, suggesting that BDA inhibits TLR4 signaling downstream of these proteins (Zeng et al., 2020). Additionally, molecular docking studies revealed that BDA can occupy the ligand-binding site of the TLR4-MD2 complex, indicating that it may inhibit inflammation by blocking the TLR4 signaling pathway (Zeng et al., 2020).

Hyaluronidase (HAase) is an endoglycosidase important for the metabolism of hyaluronic acid (HA), a linear acidic mucopolysaccharide. HAase plays a significant role in inflammation by enhancing the production of cytokines IL-1β and TNF-α by macrophages, as well as their allostimulatory capacity (Sudha and Rose, 2014; Jiang et al., 2011; Termeer et al., 2000). Studies have found that inhibiting HAase can prevent HA degradation, thereby mitigating inflammatory responses (Shibata et al., 2002). For example, in an *in vitro* inflammatory model, Zhou et al. (2023) reported that CM extract dose-dependently inhibited HAase activity. Further screening identified four compounds 56, 61, 62 and 63 as the key inhibitors, and these compounds significantly reduced the production of inflammatory mediators nitric oxide (NO) and IL-6, and suppressed the mRNA expression of inducible NO synthase (iNOS) and IL-1β in both mouse and human macrophages.

In addition, the anti-inflammatory mechanism of CI may be associated with the regulation of apoptosis-associated speck-like protein (ASC) phosphorylation and the MAPKs and NF-κB-dependent signaling pathways (Yu et al., 2019; Cheon et al., 2009). For instance, *in vivo* studies have demonstrated that CI can inhibit the recruitment of total cells and $Ly6G^{+}/F4/80^{-}$ neutrophils as well as reduce the secretion of inflammatory cytokines in peritonitis mice. *In vitro,* CI has been shown to inhibit the activation of the nucleotide-binding oligomerization domain (NOD)-like receptor (NLR)3 and the HIN-200 family member absent in melanoma 2 (AIM2) inflammasomes, leading to decreased production of IL-1β and caspase-1 (Yu et al., 2019). The phosphorylation of ASC regulates the activity of inflammasomes such as NLR3 and AIM2 inflammasomes through the formation of ASC specks (Hara et al., 2013). In studies, treatment with CI resulted in reduced translocation formation and inhibited phosphorylation, while JNK phosphorylation was not implicated in this pathway (Yu et al., 2019). Given that JNK phosphorylation is recognized as an upstream regulator of ASC phosphorylation (Hara et al., 2013), the observed effects may be associated with the modulation of ASC phosphorylation. However, the specific pathway through which this occurs remains to be elucidated.

LPS can activate a signaling pathway involving mitogen-activated protein kinases (MAPKs), including ERK1/2, JNK1/2 and p38MAPK (Moens et al., 2013). MAPKs inhibitors have been shown to suppress the regulation of iNOS and cyclooxygenase (COX)-2 genes (Kim and Kim, 2005). Overexpression of iNOS and COX-2 leads to NF-κB activation, resulting in increased production of nitric oxide (NO) and prostaglandin E_2 (PGE_2), which exacerbates inflammatory responses (D'Acquisto et al., 1997). CI extract significantly inhibited the LPS-induced production of inflammatory mediators NO and PGE_2, as well as inflammatory cytokines TNF-α and IL-1β, in RAW 264.7 macrophages in a dose-dependent manner (Cheon et al., 2009). Additionally, CI extract suppressed the mRNA and protein expression of iNOS and COX-2. Further studies revealed that CI can inhibit the nuclear translocation of NF-κB p65 subunits by preventing IκBα phosphorylation and also inhibit the phosphorylation of ERK and JNK, suggesting that the anti-inflammatory effects of CI are mediated through both MAPK and NF-κB pathways (Cheon et al., 2009). More details are provided in Table 5.

3.3 Antioxidant effects

Treating oxidative imbalance is crucial in the management of infectious diseases (Ashique et al., 2025). Reactive oxygen species (ROS), which are by-products of cellular metabolism, exhibit a dual nature: they are beneficial to cells at low concentrations but become detrimental at high levels (Sander et al., 2022). For instance, ROS contribute to pathogen destruction; however, their excessive accumulation can induce damage to cellular components such as lipids, proteins, and DNA (Sander et al., 2022). Moreover, overproduction of ROS leads to oxidative stress, resulting in bodily damage, various disease states, impaired immune function, and exacerbated inflammatory responses. This creates a vicious cycle that hinders recovery (Ashique et al., 2025). In contrast, inflammation can result in the recruitment of intravascular neutrophils to the alveolar space and lung parenchyma (Looney et al., 2006), leading to the subsequent release of proteases and generation of ROS. Moreover, ROS are closely associated with lipid peroxidation products such as myeloperoxidase (MPO) and MDA, as well as the modulation of antioxidant enzyme activities, including SOD, CAT, and GPX (Looney et al., 2006). Antioxidants can neutralize ROS, thereby protecting cells from oxidative damage and enhancing the immune system's ability to combat infections effectively. Essential oils derived from CM and CI exhibit potential as natural preservatives due to their antioxidant properties (Lii et al., 2010; Zheng et al., 2015; Zhan et al., 2022; Hao et al., 2021; Lin et al., 2010; Tian et al., 2019; Zhang et al., 2019; Kim et al., 2017).

CM extract and its flavonoids, apigenin and luteolin, exhibit potent antioxidant properties by resisting oxidative stress (Lii et al., 2010; Zhan et al., 2022; Hao et al., 2021). They enhance the levels of antioxidant enzymes such as SOD, CAT, and GPX, upregulate the expression of the antioxidant gene heme oxygenase-1 (HO-1), and decrease the production of reactive oxygen species (ROS), MDA, MPO, and 2,2-diphenyl-1-picrylhydrazyl (DPPH) radicals (Lii et al.,

TABLE 5 Detailed information of anti-inflammatory effects of CM and CI.

Extracts/ compounds	Active concentration/ dose	Vitro/ vivo	Mode	Detail	Mechanism	Ref.
CM						
95% ethanol extract	50, 100, and 200 mg/kg for 7 days	Vivo	LPS-induced ALI in mice	1)Lung histopathological injury and the ratio of wet/dry lung weight and lung index↓; the number of white blood cells, lymphocytes and neutrophils↓ 2)TNF-α and IL-6 production↓; TGF-β1 and IL-10 production↑ 3)TAC activity↑; MDA contents↓	-	Liu et al. (2020)
Hot water extract	2 and 4 g/kg for 13 weeks	Vivo	45% HF rats	1)In serum: TC, TG, and HDL-C↓ 2)In epididymal adipose tissue: Gene expression involved in adipogenesis↓, pro-inflammation (TNF-α, IL-6, and MCP1 mRNA levels of in eWAT)↓; the M1 macrophage phenotype↓; GPDH and NF-κB activities↓ 3)In the liver: AMPK activity↑: Hepatic fat accumulation↓, gene expression related to fat synthesis↓ and oxidation↓ 4)Muscle mitochondrial size↑; mtDNA content↑; SIRT1, PGC-1α, and PGC-1α-target genes expression↑	AMPK-SIRT1 pathway	Lee et al. (2021)
1)Aqueous extract 2)Compound 89, 71, 65 and 67	1)1.00, 2.00, and 4.00 mg/mL 2)1,000 μM	Vitro	1)LPS-induced RAW 264.7 and THP1 cells 2)Murine and human macrophages	1)Showed 8.31, 24.25, and 66.51% inhibition of HAase, respectively 2)Showed 40.15, 44.85, 18.04, and 24.15% inhibition of HAase, respectively; iNOS and IL-1β mRNA expression↓, and NO and IL-6 production↓	-	Zhou et al. (2023)
Bisepoxylignan dendranlignan A (50% acetone extract)	1.97 μM	Vitro	LPS-stimulated H9c2 cells	1) TNF-α, IL-2 and IFN-γ production↓ 2)The nuclear localization and the levels of phosphorylated of c-JUN, p-P65 and p-IRF3↓	TLR4 signaling pathway	Zeng et al. (2020)
CI						
Supercritical carbon dioxide fluid extract	40, 80 and 120 mg/kg for 7 days	Vivo	LPS-induced ALI mice	1)Lung histopathological injury↓ 2)TNF-α, IL-1β, and IL-6 production↓ 3)MPO and MDA levels↓; SOD, CAT, amd GPX activities↑ 4)The NF-κB activation and TLR4/MyD88 expression↓	TLR4/MyD88-dependent NF-κB signaling pathway	Wu et al. (2014)
70% ethanol extract	200 mg/kg for 10 days	Vivo	TPA-induced dermatitis mice	1)Local ear edema, skin thickness and tissue weight↓ 2)TNF-α and IL-β production↓ 3)Neutrophil-mediated MPO activity↓	-	Lee et al. (2009)

(Continued on following page)

TABLE 5 (*Continued*) Detailed information of anti-inflammatory effects of CM and CI.

Extracts/ compounds	Active concentration/ dose	Vitro/ vivo	Mode	Detail	Mechanism	Ref.
Methanol extract	1)100 μg/mL 2)intraperitoneal: 50 and 100 mg/kg; oral: 200 g/kg	1)Vitro 2)Vivo	1)LPS-primed BMDMs 2)MSU-induced murine peritonitis model	1)*In vitro*: NLRP3 and AIM2 inflammasomes activation↓ ASC speck formation and translocation↓, caspase-1 and IL-1β production↓; ASC phosphorylation↓ and no changes of JNK phosphorylation 2)*In vivo*: The recruitment of MSU-induced total cells and $Ly6G^{+}/F4/80^{-}$neutrophils in peritonium↓; IL-1β production↓	ASC phosphorylation independently of JNK phosphorylation	Yu et al. (2019)
70% ethanol extract	25, 50, 100 and 200 μg/mL	Vitro	LPS-induced RAW 264.7 macrophages	1)NO, PGE_2, TNF-α, and IL-1β production↓ 2)mRNA and protein expression of iNOS and COX-2↓ 3)Nuclear translocation of NF-κB p65 subunits↓ and IκBα phosphorylation↓ 4)Phosphorylation of ERK, JNK, and p38. (only at 200 μg/mL)↓	MAPKs and NF-κB-dependent pathways	Cheon et al. (2009)

"↓": Reduce or downregulate. "↑": Increase or upregulate. "-": not mentioned.
HF, high-fat; TC, total cholesterol; TG, triglyceride; HDL-C, high-density lipoprotein cholesterol; GPDH, glycerol-3-phosphate dehydrogenase; mtDNA, mitochondrial DNA; TPA, 12-O-tetradecanoyl-phorbol-13-acetate; SOD, superoxide dismutase; CAT, catalase; GPX, glutathione peroxidase; MSU, monosodium urate; BMDMs, bone marrow-derived macrophages.

2010; Zheng et al., 2015; Zhan et al., 2022; Hao et al., 2021; Lin et al., 2010; Tian et al., 2019). Moreover, CM can inhibit cell apoptosis, modulate cell cycle progression, and reduce the expression of pro-apoptotic proteins including Bax, cleaved caspase-3, and cleaved poly (ADP-ribose) polymerase (PARP) (Zheng et al., 2015; Hao et al., 2021; Tian et al., 2019). Further studies suggest that these effects may be mediated through several signaling pathways, such as arginine and purine metabolism, phosphatidylinositol 3-kinase (PI3K)/Akt, PI3K/Akt-mediated nuclear factor erythroid 2-related factor 2 (Nrf2)/HO-1, and Nrf2 signaling pathways (Lii et al., 2010; Zhan et al., 2022; Hao et al., 2021; Tian et al., 2019).

CI also exhibits comparable antioxidant effects to CM, such as significantly enhancing the activities of antioxidant enzymes (Zhang et al., 2019; Kim et al., 2017). In addition, CI could not only inhibit the increased Bax/Bcl-2 ratio and activation of cleaved caspase-3 in the liver and brain but also reduce the levels of inflammatory cytokines, including IL-1β, IL-6, and TNF-α (Zhang et al., 2019). Furthermore, studies have found that both CM and CI exhibit peak antioxidant capacity when heated at 100°C for 45 min (Yu et al., 2023). Detailed information is provided in Table 6. Moreover, the anti-inflammatory effects of CM and CI are discussed in Section 3.2, while their antioxidant properties are summarized in Table 5 (Liu et al., 2020; Lee et al., 2021; Wu et al., 2014; Lee et al., 2009).

3.4 Immunomodulatory effects

The immune system responds to exogenous factors encountered by the body and employs defense mechanisms to counteract these challenges. For instance, LPS, a major component of the outer membrane of Gram-negative bacteria, can bind to TLR4 and activate the MyD88-mediated NF-κB signaling pathway, ultimately leading to inflammatory responses (Hamad et al., 2023). Consequently, LPS is frequently utilized to induce inflammatory models in experimental settings. Moreover, abnormal immune responses are prevalent in infectious diseases such as influenza and COVID-19 (Han et al., 2018; Chen et al., 2024). Furthermore, with the increasing prevalence of antibiotic resistance, immunomodulatory agents have emerged as promising alternatives for treating infectious diseases (Yang et al., 2017). Studies have shown that CM polysaccharides and the butanol-soluble fraction of CI exhibit immunomodulatory effects and hold potential as therapeutic agents for infectious diseases (Xie et al., 2009; Sun et al., 2012; Liang et al., 2014; Li, 1993).

Inflammatory bowel disease (IBD) is an autoimmune disorder characterized by dysregulation of multiple immune-related pathways and cells, including the NF-κB signaling pathway, helper T (Th) cells, and regulatory T (Treg) cells (Chen et al., 2020; Committee FoCE, 1983; Chen Caiying et al., 2015; Committee FoCE, 2011). Numerous studies have demonstrated that inflammatory cytokine genes involved in IBD pathogenesis, such as IL-1β, IL-2, TNF-α, and IL-6, contain NF-κB binding sites and are transcriptionally regulated by NF-κB (Chen et al., 2020; Committee FoCE, 1983). Recent research has shown that CM polysaccharides can mitigate intestinal pathological changes in colitis rats, reduce levels of inflammatory cytokines (*e.g.*, TNF-α, IL-6, and IL-1β), and alleviate oxidative stress responses (*e.g.*, SOD and MPO). Furthermore, these effects are associated with decreased mRNA

TABLE 6 Detailed information of antioxidative effects of CM and CI.

Extracts/ compounds	Active concentration/ dose	Vitro/ vivo	Mode	Detail	Mechanism	Ref.
CM						
Aqueous extract	800, 1,600 and 2,400 μg/mL	Vitro	H_2O_2-treated L-O_2 cells	1)H_2O_2-induced cell death↓ 2)SOD, CAT and GPX activities↑; MDA↓, ROS content↓ and mitochondrial membrane potential↑ 3)L-arginosuccinate, citrulline and inositol monophosphate↑. ($p < 0.05$)	Arginine biosynthesis and IMP synthesis	Zhan et al. (2022)
Aqueous extract	20, 60, and 100 μg/mL	Vitro	Human retinal pigment epithelial cell line (ARPE-19 cells)	1)ROS production↓. (in dose-dependent) 2)Proapoptotic related protein expression: cleaved caspase-3, cleaved PARP, and Bax/Bcl-2 ratio↓. (in dose-dependent) 3)Catalase, GCLc, SOD2, and NQO-1 expression↑. (100 μg/mL) 4)Akt phosphorylation↑(100 μg/mL); Nrf2 nuclear translocation and its downstream HO-1↑. (in a dose-dependent manner) (These protective effects can be reversed by a PI3K inhibitor. (LY294002)) ($p < 0.05$)	PI3K/Akt-mediated Nrf2/HO-1 signaling pathway	Hao et al. (2021)
1)Aqueous extract 2)95% ethanol extract 3) Flavonoids: apigenin (No.58) and luteolin (No.57)	1)100, 250 and 1,000 μg/mL 2)25, 100 and 250 μg/mL 3)Flavonoids: 20 and 50 μM	Vitro	oxLDL-induced HUVEC and HL-60 cells	1)ROS production in dose-dependent↓. (250 and 1,000 μg/mL; 100 and 250 μg/mL; 50 μM; 20 and 50 μM) 2)Dephosphorylation of Akt and CREB in a dose-dependent manner↓; the expression of ICAM-1 and E-selectin and adhesion of HL-60↓. (250 μg/mL; 250 μg/mL; 50 μM; 50 μM) (These protective effects can be reversed by a PI3K/Akt signaling pathway inhibitor (Wortmannin)). ($p < 0.05$)	PI3K/Akt signaling pathway	Lii et al. (2010)
A water-soluble polysaccharide (CMJA0S2) (Boiling-water extraction)	Active concentration: 0.1 mg/mL	Vitro	H_2O_2-induced PC12 cells	1)Scavenging rate with DPPH in concentration-dependent↑. (0.1–0.8 mg/mL) 2)cell viability↑	-	Zheng et al. (2015)
70% ethanol extract	1)Vivo: 110, 220 and 440 mg/kg for 8 days 2)Vitro: 50, 100 and 200 μg/mL	Vivo and vitro	1)Alcohol-, CCl_4-induced liver injury rats 2)APAP-treated HL-7702 cells	*In vivo*: 1)Liver index↓ and serum ALT and AST↓. 2)In serum: MDA content↓ and SOD activity↑ *In vitro*:1)ALT and AST↓. 2)Cell viability↑ and cell morphological deterioration↓(in a dose-dependent manner). 3)ROS production↓, SOD activity↓ and GSH content↓ (in a dose-dependent manner). 4)Bcl-2, Bax and Caspase-3 expression↓. 5) Nuclear translocation and the expression of Nrf2 as well as its downstream gene HO-1↑. (These antioxidant effects can be reversed by Nrf2 siRNA) ($p < 0.05$)	Nrf2 signaling pathway	Tian et al. (2019)

(Continued on following page)

TABLE 6 (*Continued*) Detailed information of antioxidative effects of CM and CI.

Extracts/ compounds	Active concentration/ dose	Vitro/ vivo	Mode	Detail	Mechanism	Ref.
CI						
Supercritical carbon dioxide fluid extract	100, 150 and 300 mg/kg	Vivo	D-galactose-induced hepatic and cerebral injury mice	1)Body weight↑, the decline of thymus and spleen indexes↑, and ALT and AST levels↓ 2)In the liver and brain: SOD, CAT, and GPX activities↑; MDA↓. IL-1β, IL-6, and TNF-α production↓. The increase of Bax/Bcl-2 ratio↓ and cleaved caspase-3 activation↓. ($p < 0.05$)	-	Zhang et al. (2019)
70% ethanol extract	200 mg/kg	Vivo	Male Mongolian gerbils underwent ischemia surgery	In CA1 pyramidal cells: SOD1, CAT and GPX immunoreactivities↑. ($p < 0.05$)	-	Kim et al. (2017)

"↓": Reduce or downregulate. "↑": Increase or upregulate. "-": not mentioned.
H_2O_2, Hydrogen peroxide; GCLc, glutamate-cysteine ligase catalytic subunit; NQO1, NAD(P)H:quinone xidoreductase 1; ALT, alanine transaminase; AST, aspartate aminotransferase; siRNA, small interfering RNA; ox, oxidized; HUVEC, human umbilical vein endothelial cells.

expression levels of TLR4, Janus kinase (JAK)2, and signal transducer and activator of transcription (STAT)3, as well as reduced protein levels of p65, TLR4, p-STAT3, and p-JAK2. Additionally, improvements were observed in the metabolic profiles of plasma and urine (Xie et al., 2009). All these findings indicate that the NF-κB/TLR4 and IL-6/JAK2/STAT3 signaling pathways play a role in the mechanism by which CM exerts its effects on IBD. Further studies have demonstrated that CM polysaccharides can reduce the production of pro-inflammatory cytokines and promote the production of anti-inflammatory cytokines by regulating the imbalance between Th1/Th2 and Th17/Treg (Sun et al., 2012). Additionally, improvements in gut microbiota have also been observed (Sun et al., 2012). However, while the effects of CM polysaccharides on IBD have been extensively studied, the depth of investigation is limited. Consequently, the specific mechanisms remain unclear, particularly regarding the rigorous validation of the signaling pathways involved.

Moreover, the immunomodulatory abilities of polysaccharides from different varieties of CM vary. Wang et al. (2022) investigated the immunomodulatory effects of polysaccharides from five cultivars: Qiju, Gongju, Boju, Hangbaiju, and Huaiju. The study found that all these polysaccharides could enhance the phagocytosis and proliferation of RAW264.7 cells without significant cytotoxicity, and upregulate the release of TNF-α, IFN-γ, and NO. Notably, polysaccharides from Boju and Hangbaiju exhibited superior immune-enhancing activities, making them more suitable for developing functional foods aimed at boosting immunity. These findings provide a reference for selecting appropriate varieties based on specific immune requirements, which are related to their relative molecular mass, glucuronic acid and arabinose content, and microstructure (Wang et al., 2022). Additionally, the potential role of these polysaccharides as vaccine adjuvants is currently under investigation (Han et al., 2021).

Additionally, the butanol soluble fraction of CI exhibited a significant inhibitory effect on dimethylbenzene-induced ear edema in mice and markedly enhanced the 2, 4-dinitro-fluorobenzene (DNFB)-induced delayed-type hypersensitivity (DTH) response (Cheng et al., 2005). Furthermore, CI was found to elevate the levels of sheep red blood cell (SRBC) antibodies, serum IgG, and IgM, while significantly enhancing the phagocytic function of monocytes in cyclophosphamide (CP)-induced immunosuppressed mice (Cheng et al., 2005). These findings indicate that CI possesses anti-inflammatory properties, as well as humoral and cellular immunomodulatory activities, including enhancement of mononuclear phagocytic function. The presence of flavonoids (53%) may contribute to these effects (Cheng et al., 2005).

Although the diseases examined in the aforementioned studies are not infectious in nature, the findings indicate that CM and CI possess certain immunomodulatory effects, which hold significant reference value for the subsequent management of infectious diseases. Further details are provided in Table 7.

3.5 Toxicology and safety profile

In the acute toxicity study, a single oral dose of 15 g/kg body weight (bw) CM extract was administered to rats, then the rats were observed for 14 days. No treatment-related death was observed, and the maximal tolerance dose estimated was greater than 15 g/kg bw in rats. For long-term toxicity studies, rats were given daily intragastric doses of 320, 640, and 1,280 mg/kg bw/day for 26 weeks, followed by a 4-week recovery period (Li et al., 2010). The results showed that there were no toxicological changes in body weight, food intake, water intake, blood biochemistry, organ weight and histopathological examination in each treatment group. Thus, CM extract is generally safe for rats at limited dose levels. Dosage of annotation in the ChP for 5–10 g (Commission CP, 2020).

Different doses of CI extract prepared in saline were given orally to groups of 10 mice. For 30 days subsequent to treatment, the animals were observed daily, and dead animals were subjected to

TABLE 7 Detailed information of immunomodulatory effects of CM and CI.

Extracts/ compounds	Dose	Vitro/ vivo	Mode	Detail	Mechanism	Ref.
CM						
Polysaccharides (Aqueous extract)	50, 100 and 200 mg/kg	Vivo	TNBS/ethanol-induced colitis rats	In the colon tissue 1)TNF-α, IFN-γ, IL-6, and IL-1β production↓; NF-κB and IL-6 relative mRNA levels↓ 2)SOD↑, MPO↓, and MDA↓ activities 3)TLR4 (100 mg/kg), JAK2 (50 mg/kg), and STAT3 (50 and 100 mg/kg) mRNA expression levels↓; pp65, TLR4, p-STAT3, and p-JAK2 levels↓ 4)The metabolic profiles of plasma and urine were improved. ($p < 0.05$)	NF-κB/TLR4 and IL-6/ JAK2/STAT3 and metabolic profiling signaling pathways	Tao et al. (2018)
Polysaccharides (95% ethanol extract)	50, 100 and 200 mg/kg	Vivo	TNBS/ethanol-induced colitis rats	1)The imbalance of Th1/ Th2 and Th17/Treg↓: Th1: IFN-γ, IL-1β and TNF-α production↓; Th17: IL-6, IL-17 and IL-23 production↓; Th2: IL-13, IL-10 and IL-4 production↑ 2)Opportunistic pathogens *Escherichia, Enterococcus* and *Prevotella* abundance↓; protective bacteria such as *Butyricicoccus* and *Clostridium* (butyrate-producing bacteria), *Lactobacillus* and *Bifidobacterium* (probiotics), Lachnospiraceae and Rikenellaceae levels↑. ($p < 0.05$)	-	Tao et al. (2017)
Polysaccharides from five cultivars (ethanol extract)	12.5, 50 and 200 μg/mL	Vitro	RAW264.7 cells	1)The phagocytosis and proliferation of RAW264.7 cells↑ 2)TNF-α, IFN-γ, and NO production↑. ($p < 0.001$)	-	Wang et al. (2022)
CI						
A butanol soluble fraction (95% ethanol and butanol extract)	p.o.: 75, 150 and 300 mg/kg for 5 days i.p.: 50 mg/kg on day 3 and continued for 2 days	Vivo	1)Dimethylbenzene-induced mice 2)DNFB-induced mice 3)CP-induced mice	In dimethylbenzene-induced mice: Auricle tumidity↓. (150 mg/kg, p.o.) In DNFB-induced mice: DTH reactivity↑. (150 and 300 mg/kg, p.o.). In CP-induced mice: 1) Antibody generation by the splenic cells↑. 2)Serum IgG and IgM levels↑ in response to SRBC. 3)Macrophage phagocytic activity: the rate of carbon clearance↑ and phagocytic index↑. (150 and 300 mg/kg, p.o.) ($p < 0.01$)	-	Cheng et al. (2005)

Note: "↓": Reduce or downregulate. "↑": Increase or upregulate. "-": not mentioned.
Oral administration (p.o.), intraperitoneal injection (i.p.).

postmortem examination for determination of the cause of death. No animals died during the acute toxicity test, nor were any adverse effects detected in animals treated with different doses of CI extract. This indicates that CI extract was nearly nontoxic in mice up to an oral dose of 2.0 g/kg body weight (Lee et al., 2009). No studies have investigated the long-term toxicity of CI. Dosage of annotation in the ChP for 9–15 g (Commission CP, 2020). In addition to oral administration, it can also be used for

external use, decoction for washing or paste for external application.

4 Conclusion and future perspectives

CM and CI, two major traditional Chinese herbs recognized in the theory of food and medicine homology, have a long history of medicinal use and demonstrated significant clinical efficacy. By systematically reviewing literature from the perspectives of ethnopharmacology, phytochemistry, and pharmacology, this study aims to provide an updated understanding of the anti-infective effects of CM and CI, thereby facilitating a more comprehensive grasp of their potential clinical applications and current research status in the context of infectious diseases.

A 2020 review reported that over 176 compounds, including 60 flavonoids, 28 phenylpropanoids, 68 triterpenoids, three steroids, and 17 others, were isolated and identified in CM. Notably, the "other" category included a small number of terpenoids (only 20 compounds) (Yuan et al., 2020). Subsequently, Peng et al. (Peng et al., 2020) detected a significant number of terpenoids, primarily monoterpenes, from CM, thereby supplementing the earlier review. Overall, a total of 109 terpenoids, including monoterpenoids, sesquiterpenoids, and unidentified diterpenes, have been identified in CM. Additionally, it has been reported that 191 natural compounds were isolated and identified from CI, comprising 42 flavonoids, 96 terpenoids, 21 phenylpropanoids and phenolic acids, 12 spiro ketones, and 20 other compounds (Shao et al., 2020). In this study, we summarize the main compounds reported in studies on the anti-infection-related antimicrobial, anti-inflammatory, antioxidant, and immunomodulatory effects of CM or CI, including 53 alkenes and terpenoids, 11 flavonoids, 7 phenylpropanoids, and other compounds. These compounds play a crucial role in inhibiting microbial growth, reducing inflammation, combating oxidative stress, and modulating immune responses.

Although CM has been reported to contain a higher number of compounds compared to CI, CI has shown superior antimicrobial effects in certain studies (Youssef et al., 2020). This may be attributed to the high concentration of key compounds in CI. For instance, camphor (No.8), a bicyclic monoterpene, exhibits a wide range of biological activities, including insecticidal, analgesic, antimicrobial, antiviral, anticoccidial, antinociceptive, anticancer, and antitussive properties (Sokolova et al., 2015; Zielińska-Błajet and Feder-Kubis, 2020). Studies have shown that symmetrical compounds containing camphor fragments, two imino groups, and/or a charged quaternary nitrogen atom exhibit potent antiviral activity (Sokolova et al., 2014; Sokolova et al., 2013). Additionally, research evaluating the antiviral activity of camphor-based imine derivatives against the H1N1 influenza virus pdm09 and their inhibitory effects on H5N1 pseudovirus infection revealed that the critical structural units responsible for antiviral activity include the natural camphor skeleton, the presence of an imino group, and an alcohol moiety (Sokolova et al., 2015).

A study demonstrated that CI and CM exhibited limited antifungal efficacy, whereas another study indicated that CM displayed superior antifungal properties (Youssef et al., 2020; Zhang et al., 2020). The discrepancy may be attributed to the different plant parts used for CM extraction; the former study utilized flowers, while the latter employed roots. Specifically, the latter study analyzed 12 cultivars of CM roots, revealing that the primary compounds in root extracts differ from those in flower extracts, which likely explains the varying antifungal effects observed. Additionally, differences in extraction methods and fungal strains examined between the studies may have contributed to these discrepancies. Regarding antiviral activity, CI showed a stronger inhibitory effect on specific viruses such as VSV, HAV, and HSV-1 (Youssef et al., 2020; Gu et al., 2013). However, some studies reported antimicrobial activity using only IC50 values without MIC or *vice versa*, potentially introducing bias into their results.

Furthermore, both CM and CI extracts exhibit anti-inflammatory properties. CM can regulate inflammation by modulating the AMPK-SIRT1 and TLR4 signaling pathways (Lee et al., 2021; Zeng et al., 2020). CI modulates inflammatory pathways, including the TLR4/MyD88-dependent NF-κB signaling pathway, and MAPKs and NF-κB-dependent pathway, as well as ASC phosphorylation independent of JNK phosphorylation (Yu et al., 2019; Wu et al., 2014; Cheon et al., 2009). Both CM and CI extracts reduce oxidative stress markers such as MDA and increase antioxidant enzyme activities, including SOD, CAT, and GPX (Lii et al., 2010; Zhan et al., 2022; Hao et al., 2021; Tian et al., 2019; Zhang et al., 2019; Kim et al., 2017). The anti-oxidative mechanism of CM involves the arginine and purine metabolic pathways, the PI3K/Akt-mediated Nrf2/HO-1 signaling pathway, and others (Lii et al., 2010; Zhan et al., 2022; Hao et al., 2021; Tian et al., 2019). CM polysaccharides have demonstrated immunomodulatory effects in multiple studies, potentially through the NF-κB/TLR4 and IL-6/JAK2/STAT3 pathways, as well as by balancing Th1/Th2 and Th17/Treg cells (Tao et al., 2018; Tao et al., 2017; Wang et al., 2022). CI can regulate the immune response, which may be attributed to its flavonoid content (Cheng et al., 2005).

In TCM, infectious diseases are often conceptualized as disruptions to the body's balance caused by pathogenic factors such as "heat", "dampness", and "wind" (Wu et al., 2023). To eliminate these influences, botanical drugs with properties that "clear heat" and "detoxify" are utilized (Xu et al., 2019; Fang et al., 2009). The objective is to restore balance and harmony within the body, thereby alleviating both the symptoms and underlying causes of the disease. Specifically, CM and CI are used for their heat-clearing and detoxifying attributes, which effectively eliminate these pathogenic factors (Commission CP, 2020). CM and CI are commonly employed in TCM to alleviate symptoms of infections, including fever, inflammation, swelling, and abscesses, which align with the TCM concepts of "heat" and "toxins". In contemporary pharmacological research, CM and CI extracts have been shown to effectively alleviate infection severity and prevent associated complications by modulating inflammatory responses, enhancing immune function, and mitigating oxidative stress. However, our review reveals that research on CI's antimicrobial and anti-inflammatory properties is likely more extensive compared to that on CM, indicating that CI may hold greater potential for treating infectious diseases. Additionally, the efficacy of CM and CI in TCM formulations warrants further attention. Sangju cough mixture, which includes CM, has

demonstrated therapeutic efficacy against colds. It can also alleviate symptoms of *mycoplasma* pneumoniae (MP), expedite the negative conversion time of MP-IgM antibodies, and facilitate patient recovery (Yang et al., 2024; Ji et al., 2019). In addition, Xiasangju is a well-known TCM formula for treating fever and influenza, and its composition includes CI. Increasing evidence suggests its various pharmacological effects on bacterial infections, immune system disorders, and other conditions (Wu et al., 2022). Overall, CM and CI serve as prime examples of how traditional botanical knowledge can be integrated into contemporary therapeutic practices, providing valuable treatments for infectious diseases through their heat-clearing and detoxifying properties.

Moreover, we have not identified any clinical study reports on the use of CM and CI. In TCM, treatments typically involve TCM formulas rather than single botanical drugs. Therefore, conducting clinical studies using only single botanical drug may present challenges. Future research could focus on the application of traditional Chinese medicinal formulas that include CM and CI for treating infectious diseases (Yang et al., 2024; Ji et al., 2019; Wu et al., 2022).

However, comprehensive comparative studies between CM and CI are imperative. Rigorous investigations are required to elucidate the precise molecular mechanisms underlying their antimicrobial, anti-inflammatory, immunomodulatory, and antioxidant effects, including the interactions of specific compounds with cellular targets and signaling pathways. Furthermore, potential synergistic effects among different compounds within CM and CI warrant exploration. Additionally, both CM and CI extracts have demonstrated promising effects in preliminary studies, and further investigations, such as pharmacokinetic studies, could enhance our understanding of their bioavailability. Finally, establishing robust quality control measures and standardization protocols for CM and CI extracts will ensure consistent efficacy and safety in therapeutic applications, ultimately aiding in the fight against infectious diseases.

Author contributions

YL: Writing–original draft. TL: Writing–review and editing. DW: Writing–review and editing. QL: Writing–review and editing.

Funding

The author(s) declare that financial support was received for the research and/or publication of this article. This study was supported by the Innovation Team Project of the State Administration of traditional Chinese medicine (No. ZYYCXTD-D-202201).

Acknowledgments

Acknowledgement for the data support from Plant Data Center of Chinese Academy of Sciences (https://www.plantplus.cn) (Figure 2).

Conflict of interest

The authors declare that the research was conducted in the absence of any commercial or financial relationships that could be construed as a potential conflict of interest.

Generative AI statement

The author(s) declare that no Generative AI was used in the creation of this manuscript.

Publisher's note

All claims expressed in this article are solely those of the authors and do not necessarily represent those of their affiliated organizations, or those of the publisher, the editors and the reviewers. Any product that may be evaluated in this article, or claim that may be made by its manufacturer, is not guaranteed or endorsed by the publisher.

Supplementary material

The Supplementary Material for this article can be found online at: https://www.frontiersin.org/articles/10.3389/fphar.2025.1538311/full#supplementary-material

References

Akihisa, T., Franzblau, S. G., Ukiya, M., Okuda, H., Zhang, F., Yasukawa, K., et al. (2005). Antitubercular activity of triterpenoids from Asteraceae flowers. *Biol. Pharm. Bull.* 28 (1), 158–160. doi:10.1248/bpb.28.158

Ashique, S., Mishra, N., Mantry, S., Garg, A., Kumar, N., Gupta, M., et al. (2025). Crosstalk between ROS-inflammatory gene expression axis in the progression of lung disorders. *Naunyn Schmiedeb. Arch. Pharmacol.* 398 (1), 417–448. doi:10.1007/s00210-024-03392-1

Astani, A., Reichling, J., and Schnitzler, P. (2011). Screening for antiviral activities of isolated compounds from essential oils. *Evid. Based Complement. Altern. Med.* 2011, 253643. doi:10.1093/ecam/nep187

Boudou, F., Belakredar, A., Keziz, A., Aissani, L., Alsaeedi, H., Cronu, D., et al. (2024). Therapeutic potential of Curcuma longa against monkeypox: antioxidant, anti-inflammatory, and computational insights. *Front. Chem.* 12, 1509913. doi:10.3389/fchem.2024.1509913

Chen, J., Zhou, Z., Wu, N., Li, J., Xi, N., Xu, M., et al. (2024). Chlorogenic acid attenuates deoxynivalenol-induced apoptosis and pyroptosis in human keratinocytes via activating Nrf2/HO-1 and inhibiting MAPK/NF-κB/NLRP3 pathways. *Biomed. Pharmacother.* 170, 116003. doi:10.1016/j.biopha.2023.116003

Chen, W., Vermaak, I., and Viljoen, A. (2013). Camphor--a fumigant during the Black Death and a coveted fragrant wood in ancient Egypt and Babylon--a review. *Molecules* 18 (5), 5434–5454. doi:10.3390/molecules18055434

Chen, X., Wang, H., Yang, X., Jiang, J., Ren, G., Wang, Z., et al. (2020). Small-scale alpine topography at low latitudes and high altitudes: refuge areas of the genus Chrysanthemum and its allies. *Hortic. Res.* 7, 184. doi:10.1038/s41438-020-00407-9

Chen Caiying, C. D., Zhao, Y., and Han, Z. (2015). Textual research on medicine origin of wild Chrysanthemum. *J. Hunan Univ. Chin. Med.* 35 (5), 69–72. doi:10.3969/j.issn.1674-070X.2015.05.023

Cheng, W., Li, J., You, T., and Hu, C. (2005). Anti-inflammatory and immunomodulatory activities of the extracts from the inflorescence of Chrysanthemum indicum Linné. *J. Ethnopharmacol.* 101 (1-3), 334–337. doi:10.1016/j.jep.2005.04.035

Cheon, M. S., Yoon, T., Lee, D. Y., Choi, G., Moon, B. C., Lee, A. Y., et al. (2009). Chrysanthemum indicum Linné extract inhibits the inflammatory response by suppressing NF-kappaB and MAPKs activation in lipopolysaccharide-induced RAW 264.7 macrophages. *J. Ethnopharmacol.* 122, 3.473–477. doi:10.1016/j.jep.2009.01.034

Commission CP (2020). Pharmacopoeia of the people's Republic of China. Available online at: https://ydz.chp.org.cn/#/item?bookId=1&entryId=496 (Accessed April 01, 2024).

Committee FoCE (1983). Flora reipublicae popularis sinicae. Available online at: https://www.plantplus.cn/info/Dendranthema%20morifolium?t=z (Accessed May 12, 2024).

Committee FoCE (2011). Flora of China. Available online at: https://www.plantplus.cn/cn/sp/Chrysanthemum%20indicum?t=foc (Accessed May 10, 2024).

Costa, J. P., Sousa, S. A., Galvão, A. M., Mata, J. M., Leitão, J. H., and Carvalho, M. (2021). Key parameters on the antibacterial activity of silver camphor complexes. *Antibiot. (Basel)* 10, 135. doi:10.3390/antibiotics10020135

D'Acquisto, F., Iuvone, T., Rombolà, L., Sautebin, L., Di Rosa, M., and Carnuccio, R. (1997). Involvement of NF-kappaB in the regulation of cyclooxygenase-2 protein expression in LPS-stimulated J774 macrophages. *FEBS Lett.* 418 (1-2), 175–178. doi:10.1016/s0014-5793(97)01377-x

Esposito, S., De Simone, G., Boccia, G., De Caro, F., and Pagliano, P. (2017). Sepsis and septic shock: new definitions, new diagnostic and therapeutic approaches. *J. Glob. Antimicrob. Resist* 10, 204–212. doi:10.1016/j.jgar.2017.06.013

Fang, J., Wan, J., Tang, J., Wang, W., and Liu, Y. (2009). Radix isatidis and infectious diseases caused by viruses. *Zhongguo Zhong Yao Za Zhi* 34 (24), 3169–3172.

Gamal El-Din, M. I., Youssef, F. S., Ashour, M. L., Eldahshan, O. A., and Singab, A. N. B. (2018). Comparative analysis of volatile constituents of Pachira aquatica Aubl. and Pachira glabra Pasq., their anti-mycobacterial and anti-helicobacter pylori activities and their metabolic discrimination using chemometrics. *J. Essent. Oil Bear. Plants*, 21. 1550–1567. doi:10.1080/0972060X.2019.1571950

Gao, M. H., Li, H., Zhang, L., and Xiao, S. X. (2008). Studies on chemical constituents from flowers of Chrysanthemum indicum. *Zhong Yao Cai* 31 (5), 682–684.

Gu, Q. C. Y., Cui, H., Huang, D., Zhou, J. W., Wu, T. Z., Chen, Y. P., et al. (2013). Chrysanolide A, an unprecedented sesquiterpenoid trimer from the flowers of Chrysanthemum indicum L. *RSC Adv.* 3, 10168–10172. doi:10.1039/c3ra23172k

Guo, Q., Fang, H., and Shen, H. (2010). Determination of chlorogenic acid, caffeic acid and linarin in Flos Chrysanthemi Indici from different places by RP-hPLC. *Zhongguo Zhong Yao Za Zhi* 35 (9), 1160–1163. doi:10.4268/cjcmm20100917

Hamad, R. S., El Sherif, F., Al Abdulsalam, N. K., and Abd El-Moaty, H. I. (2023). Chlorogenic acid derived from Moringa oleifera leaf as a potential antiinflammatory agent against cryptosporidiosis in mice. *Trop. Biomed.* 40 (1), 45–54. doi:10.47665/tb.40.1.010

Han, J. M., Song, H. Y., Seo, H. S., Byun, E. H., Lim, S. T., Kim, W. S., et al. (2021). Immunoregulatory properties of a crude extraction fraction rich in polysaccharide from Chrysanthemum zawadskii Herbich var. latilobum and its potential role as a vaccine adjuvant. *Int. Immunopharmacol.* 95, 107513. doi:10.1016/j.intimp.2021.107513

Han, X., Wu, Y. C., Meng, M., Sun, Q. S., Gao, S. M., and Sun, H. (2018). Linarin prevents LPS-induced acute lung injury by suppressing oxidative stress and inflammation via inhibition of TXNIP/NLRP3 and NF-κB pathways. *Int. J. Mol. Med.* 42 (3), 1460–1472. doi:10.3892/ijmm.2018.3710

Hao, Y., Li, Y., Liu, J., Wang, Z., Gao, B., Zhang, Y., et al. (2021). Protective effect of Chrysanthemum morifolium cv. Fubaiju hot-water extracts against ARPE-19 cell oxidative damage by activating PI3K/Akt-Mediated Nrf2/HO-1 signaling pathway. *Front. Nutr.* 8, 648973. doi:10.3389/fnut.2021.648973

Hara, H., Tsuchiya, K., Kawamura, I., Fang, R., Hernandez-Cuellar, E., Shen, Y., et al. (2013). Phosphorylation of the adaptor ASC acts as a molecular switch that controls the formation of speck-like aggregates and inflammasome activity. *Nat. Immunol.* 14, 12.1247–1255. doi:10.1038/ni.2749

Ji, S., He, D. D., Su, Z. Y., Du, Y., Wang, Y. J., Gao, S. K., et al. (2019). P450 enzymes-based metabolic interactions between monarch drugs and the other constituent herbs: a strategy to explore compatibility mechanism of Sangju-Yin. *Phytomedicine* 58, 152866. doi:10.1016/j.phymed.2019.152866

Jiang, D., Liang, J., and Noble, P. W. (2011). Hyaluronan as an immune regulator in human diseases. *Physiol. Rev.* 91 (1), 221–264. doi:10.1152/physrev.00052.2009

Kang, S. C., Lim, S. Y., and Song, Y. J. (2013). Lupeol is one of active components in the extract of Chrysanthemum indicum Linne that inhibits LMP1-induced NF-κB activation. *PLoS One* 8 (11), e82688. doi:10.1371/journal.pone.0082688

Kim, I. H., Lee, T. K., Cho, J. H., Lee, J. C., Park, J. H., Ahn, J. H., et al. (2017). Pre-treatment with Chrysanthemum indicum Linné extract protects pyramidal neurons from transient cerebral ischemia via increasing antioxidants in the gerbil hippocampal CA1 region. *Mol. Med. Rep.* 16 (1), 133–142. doi:10.3892/mmr.2017.6591

Kim, J. E., Jun, S., Song, M., Kim, J. H., and Song, Y. J. (2012). The extract of Chrysanthemum indicum Linne inhibits EBV LMP1-induced NF-κB activation and the viability of EBV-transformed lymphoblastoid cell lines. *Food Chem. Toxicol.* 50, 5.1524–1528. doi:10.1016/j.fct.2012.02.034

Kim, J. W., and Kim, C. (2005). Inhibition of LPS-induced NO production by taurine chloramine in macrophages is mediated though Ras-ERK-NF-kappaB. *Biochem. Pharmacol.* 70, 9.1352–1360. doi:10.1016/j.bcp.2005.08.006

Kuang, C. L., Lv, D., Shen, G. H., Li, S. S., Luo, Q. Y., and Zhang, Z. Q. (2018). Chemical composition and antimicrobial activities of volatile oil extracted from Chrysanthemum morifolium Ramat. *J. Food Sci. Technol.* 55, 7.2786–2794. doi:10.1007/s13197-018-3203-1

Lee, D. Y., Choi, G., Yoon, T., Cheon, M. S., Choo, B. K., and Kim, H. K. (2009). Anti-inflammatory activity of Chrysanthemum indicum extract in acute and chronic cutaneous inflammation. *J. Ethnopharmacol.* 123 (1), 149–154. doi:10.1016/j.jep.2009.02.009

Lee, J. S., Kim, H. J., and Lee, Y. S. (2003). A new anti-HIV flavonoid glucuronide from Chrysanthemum morifolium. *Planta Med.* 69 (9), 859–861. doi:10.1055/s-2003-43207

Lee, Y., Lee, J., Lee, M. S., Chang, E., and Kim, Y. (2021). Chrysanthemum morifolium flower extract ameliorates obesity-induced inflammation and increases the muscle mitochondria content and AMPK/SIRT1 activities in obese rats. *Nutrients* 13, 3660. doi:10.3390/nu13103660

Li, H. (1993). *Chinese Chrysanthemum*. Nanjing: Jiangsu Scientific and Technological Publishing Co.

Li, L., Gu, L., Chen, Z., Wang, R., Ye, J., and Jiang, H. (2010). Toxicity study of ethanolic extract of Chrysanthemum morifolium in rats. *J. Food Sci.* 75 (6), T105–T109. doi:10.1111/j.1750-3841.2010.01702.x

Liang, X., Wu, H., and Su, W. (2014). A rapid UPLC-PAD fingerprint analysis of Chrysanthemum morifolium Ramat combined with chemometrics methods. *Food Anal. Methods* 7 (1), 197–204. doi:10.1007/s12161-013-9618-4

Lii, C. K., Lei, Y. P., Yao, H. T., Hsieh, Y. S., Tsai, C. W., Liu, K. L., et al. (2010). Chrysanthemum morifolium Ramat. reduces the oxidized LDL-induced expression of intercellular adhesion molecule-1 and E-selectin in human umbilical vein endothelial cells. *J. Ethnopharmacol.* 128 (1), 213–220. doi:10.1016/j.jep.2010.01.018

Lin, G. H., Lin, L., Liang, H. W., Ma, X., Wang, J. Y., Wu, L. P., et al. (2010). Antioxidant action of a Chrysanthemum morifolium extract protects rat brain against ischemia and reperfusion injury. *J. Med. Food* 13 (2), 306–311. doi:10.1089/jmf.2009.1184

Liu, G., Zheng, Q., Pan, K., and Xu, X. (2020). Protective effect of Chrysanthemum morifolium Ramat. ethanol extract on lipopolysaccharide induced acute lung injury in mice. *BMC Complement. Med. Ther.* 20 (1), 235. doi:10.1186/s12906-020-03017-z

Liu, L. L., Ha, T. K., Ha, W., Oh, W. K., Yang, J. L., and Shi, Y. P. (2017). Sesquiterpenoids with various carbocyclic skeletons from the flowers of Chrysanthemum indicum. *J. Nat. Prod.* 80 (2), 298–307. doi:10.1021/acs.jnatprod.6b00694

Liu, X. J., Li, Y., Su, S. L., Wei, D. D., Yan, H., Guo, S., et al. (2022). Comparative analysis of chemical composition andAntibacterial and anti-inflammatory activities of theEssential oils from Chrysanthemum morifolium ofDifferent flowering stages and different parts. *Evid. Based Complement. Altern. Med.* 2022, 5954963. doi:10.1155/2022/5954963

Looney, M. R., Su, X., Van Ziffle, J. A., Lowell, C. A., and Matthay, M. A. (2006). Neutrophils and their Fc gamma receptors are essential in a mouse model of transfusion-related acute lung injury. *J. Clin. Invest.* 116 (6), 1615–1623. doi:10.1172/jci27238

Meenu, M., Padhan, B., Patel, M., Patel, R., and Xu, B. (2023). Antibacterial activity of essential oils from different parts of plants against Salmonella and Listeria spp. *Food Chem.* 404, 134723. Pt B. doi:10.1016/j.foodchem.2022.134723

Miyazawa, M., and Hisama, M. (2003). Antimutagenic activity of flavonoids from Chrysanthemum morifolium. *Biosci. Biotechnol. Biochem.* 67, 10.2091–2099. doi:10.1271/bbb.67.2091

Moens, U., Kostenko, S., and Sveinbjørnsson, B. (2013). The role of mitogen-activated protein kinase-activated protein kinases (MAPKAPKs) in inflammation. *Genes (Basel)* 4 (2), 101–133. doi:10.3390/genes4020101

Park, M. Y., and Kang, D. H. (2021). Antibacterial activity of caffeic acid combined with UV-A light against *Escherichia coli* O157:H7, *Salmonella enterica* serovar typhimurium, and Listeria monocytogenes. *Appl. Environ. Microbiol.* 87 (15), e0063121. doi:10.1128/aem.00631-21

Peng, A., Lin, L., and Zhao, M. (2020). Screening of key flavonoids and monoterpenoids for xanthine oxidase inhibitory activity-oriented quality control of Chrysanthemum morifolium Ramat. 'Boju' based on spectrum-effect relationship coupled with UPLC-TOF-MS and HS-SPME-GC/MS. *Food Res. Int.* 137, 109448. doi:10.1016/j.foodres.2020.109448

Sander, W. J., Fourie, C., Sabiu, S., O'Neill, F. H., Pohl, C. H., and O'Neill, H. G. (2022). Reactive oxygen species as potential antiviral targets. *Rev. Med. Virol.* 32, 1.e2240. doi:10.1002/rmv.2240

Sangeetha Vijayan, P., Xavier, J., and Valappil, M. P. (2024). A review of immune modulators and immunotherapy in infectious diseases. *Mol. Cell Biochem.* 479 (8), 1937–1955. doi:10.1007/s11010-023-04825-w

Shao, Y., Sun, Y., Li, D., Chen, Y., and Chrysanthemum indicum, L. (2020). Chrysanthemum indicum L.: a comprehensive review of its botany, phytochemistry and pharmacology. *Am. J. Chin. Med.* 48 (4), 871–897. doi:10.1142/s0192415x20500421

Shen, J., Wang, G., and Zuo, J. (2018). Caffeic acid inhibits HCV replication via induction of IFNα antiviral response through p62-mediated Keap1/Nrf2 signaling pathway. *Antivir. Res.* 154, 154.166–173. doi:10.1016/j.antiviral.2018.04.008

Shibata, T., Fujimoto, K., Nagayama, K., Yamaguchi, K., and Nakamura, T. (2002). Inhibitory activity of brown algal phlorotannins against hyaluronidase. *Int. J. Food Sci. and Technol.* 37 (6), 703–709. doi:10.1046/j.1365-2621.2002.00603.x

Shunying, Z., Yang, Y., Huaidong, Y., Yue, Y., and Guolin, Z. (2005). Chemical composition and antimicrobial activity of the essential oils of Chrysanthemum indicum. *J. Ethnopharmacol.* 96 (1-2), 151–158. doi:10.1016/j.jep.2004.08.031

Sokolova, A. S., Yarovaya, C. O., Shernyukov, C. A., Pokrovsky, C. E., Pokrovsky, C. A., Lavrinenko, V. A., et al. (2013). New quaternary ammonium camphor derivatives and their antiviral activity, genotoxic effects and cytotoxicity. *Bioorg Med. Chem.* 21, 21.6690–6698. doi:10.1016/j.bmc.2013.08.014

Sokolova, A. S., Yarovaya, O. C., Korchagina, D. V., Zarubaev, V. V., Tretiak, T. S., Anfimov, P. M., et al. (2014). Camphor-based symmetric diimines as inhibitors of influenza virus reproduction. *Bioorg Med. Chem.* 22, 7.2141–2148. doi:10.1016/j.bmc.2014.02.038

Sokolova, A. S., Yarovaya, O. I., Shernyukov, A. V., Gatilov, Y. V., Razumova, Y. V., Zarubaev, V. V., et al. (2015). Discovery of a new class of antiviral compounds: camphor imine derivatives. *Eur. J. Med. Chem.* 105, 263–273. doi:10.1016/j.ejmech.2015.10.010

Sudha, P. N., and Rose, M. H. (2014). Beneficial effects of hyaluronic acid. *Adv. Food Nutr. Res.* 72, 137–176. doi:10.1016/b978-0-12-800269-8.00009-9

Sun, Y., Ma, X., and Liu, J. (2012). Compounds from fraction with cardiovascular activity of Chrysanthemum indicum. *Zhongguo Zhong Yao Za Zhi* 37 (1), 61–65.

Tao, J. H., Duan, J. A., Jiang, S., Feng, N. N., Qiu, W. Q., and Ling, Y. (2017). Polysaccharides from Chrysanthemum morifolium Ramat ameliorate colitis rats by modulating the intestinal microbiota community. *Oncotarget* 8, 46.80790–80803. doi:10.18632/oncotarget.20477

Tao, J. H., Duan, J. A., Zhang, W., Jiang, S., Guo, J. M., and Wei, D. D. (2018). Polysaccharides from Chrysanthemum morifolium Ramat ameliorate colitis rats via regulation of the metabolic profiling and NF-κ B/TLR4 and IL-6/JAK2/STAT3 signaling pathways. *Front. Pharmacol.* 9.746, 746. doi:10.3389/fphar.2018.00746

Termeer, C. C., Hennies, J., Voith, U., Ahrens, T., Weiss, J. M., Prehm, P., et al. (2000). Oligosaccharides of hyaluronan are potent activators of dendritic cells. *J. Immunol.* 165 (4), 1863–1870. doi:10.4049/jimmunol.165.4.1863

Tian, Z., Jia, H., Jin, Y., Wang, M., Kou, J., Wang, C., et al. (2019). Chrysanthemum extract attenuates hepatotoxicity via inhibiting oxidative stress *in vivo* and *in vitro*. *Food Nutr. Res.* 63, 63. doi:10.29219/fnr.v63.1667

Wang, J., Chen, D., Liang, L., Xue, P., and Tu, P. (2010). Chemical constituents from flowers of Chrysanthemum indicum. *Zhongguo Zhong Yao Za Zhi* 35 (6), 718–721. doi:10.4268/cjcmm20100613

Wang, X., Shen, Y., Thakur, K., Han, J., Zhang, J. G., Hu, F., et al. (2020). Antibacterial activity and mechanism of ginger essential oil against *Escherichia coli* and *Staphylococcus aureus*. *Molecules* 25, 3955. doi:10.3390/molecules25173955

Wang, Y., Chen, X., Zhao, P., Ren, L., Li, X., and Gao, W. (2022). Physicochemical characteristics and immunoregulatory activities of polysaccharides from five cultivars of Chrysanthemi Flos. *Food Sci. Nutr.* 10 (5), 1391–1400. doi:10.1002/fsn3.2720

Wang Xl, P. S., Liang, J. P., and Yu, K. B. (2006). (3β,5α,6β,7β,14β)-eudesmen-3,5,6,11-tetrol methanol solvate: a new sesquiterpenoid fromchrysanthemum indicuml. *Acta Crystallogr. Sect. E Struct. Rep. Online* 62 (8), o3570–o3571. doi:10.1107/s1600536806028522

Wu, S., Luo, H., Zhong, Z., Ai, Y., Zhao, Y., Liang, Q., et al. (2022). Phytochemistry, pharmacology and quality control of Xiasangju: a traditional Chinese medicine formula. *Front. Pharmacol.* 13, 930813. doi:10.3389/fphar.2022.930813

Wu, S., Su, W., Fan, Q., Shang, H., Xiao, W., and Wang, Y. (2023). Traditional Chinese medicine for the common cold: evidence and potential mechanisms. *Am. J. Chin. Med.* 51 (3), 487–515. doi:10.1142/s0192415x23500258

Wu, T., Jiang, C., Wang, L., Morris-Natschke, S. L., Miao, H., Gu, L., et al. (2015). 3,5-Diarylpyrazole derivatives obtained by ammonolysis of the total flavonoids from Chrysanthemum indicum extract show potential for the treatment of alzheimer's disease. *J. Nat. Prod.* 78 (7), 1593–1599. doi:10.1021/acs.jnatprod.5b00156

Wu, X. L., Feng, X. X., Li, C. W., Zhang, X. J., Chen, Z. W., Chen, J. N., et al. (2014). The protective effects of the supercritical-carbon dioxide fluid extract of Chrysanthemum indicum against lipopolysaccharide-induced acute lung injury in mice via modulating Toll-like receptor 4 signaling pathway. *Mediat. Inflamm.* 2014, 246407. doi:10.1155/2014/246407

Xie, Y. Y., Yuan, D., Yang, J. Y., Wang, L. H., and Wu, C. F. (2009). Cytotoxic activity of flavonoids from the flowers of Chrysanthemum morifolium on human colon cancer Colon205 cells. *J. Asian Nat. Prod. Res.* 11 (9), 771–778. doi:10.1080/10286020903128470

Xu, H., He, L., Chen, J., Hou, X., Fan, F., Wu, H., et al. (2019). Different types of effective fractions from Radix Isatidis revealed a multiple-target synergy effect against respiratory syncytial virus through RIG-I and MDA5 signaling pathways, a pilot study to testify the theory of superposition of traditional Chinese Medicine efficacy. *J. Ethnopharmacol.* 239, 111901. doi:10.1016/j.jep.2019.111901

Xue, G. M., Li, X. Q., Chen, C., Chen, K., Wang, X. B., Gu, Y. C., et al. (2018). Highly oxidized guaianolide sesquiterpenoids with potential anti-inflammatory activity from Chrysanthemum indicum. *J. Nat. Prod.* 81 (2), 378–386. doi:10.1021/acs.jnatprod.7b00867

Yamaguchi, T. (2022). Antibacterial effect of the combination of terpenoids. *Arch. Microbiol.* 204, 520. doi:10.1007/s00203-022-03142-y

Yang, P. F., Feng, Z. M., Yang, Y. N., Jiang, J. S., and Zhang, P. C. (2017). Neuroprotective caffeoylquinic acid derivatives from the flowers of Chrysanthemum morifolium. *J. Nat. Prod.* 80, 4.1028–1033. doi:10.1021/acs.jnatprod.6b01026

Yang, P. F., Yang, Y. N., Feng, Z. M., Jiang, J. S., and Zhang, P. C. (2019b). Six new compounds from the flowers of Chrysanthemum morifolium and their biological activities. *Bioorg Chem.* 82, 82.139–144. doi:10.1016/j.bioorg.2018.10.007

Yang, P. F., Yang, Y. N., He, C. Y., Chen, Z. F., Yuan, Q. S., Zhao, S. C., et al. (2019a). New caffeoylquinic acid derivatives and flavanone glycoside from the flowers of Chrysanthemum morifolium and their bioactivities. *Molecules* 24, 850. doi:10.3390/molecules24050850

Yang, X., Liu, Z., Liu, X., Li, Q., Huang, H., and Zhang, Z. (2024). Efficacy and influencing factors of Sangju cough mixture in the adjuvant treatment of adult patients with mycoplasma pneumoniae infection: a retrospective study. *Infect. Drug Resist* 17, 17.275–282. doi:10.2147/idr.S438202

Youssef, F. S., Eid, S. Y., Alshammari, E., Ashour, M. L., Wink, M., and El-Readi, M. Z. (2020). Chrysanthemum indicum and Chrysanthemum morifolium: chemical composition of their essential oils and their potential use as natural preservatives with antimicrobial and antioxidant activities. *Foods* 9, 1460. doi:10.3390/foods9101460

Yu, S. H., Sun, X., Kim, M. K., Akther, M., Han, J. H., Kim, T. Y., et al. (2019). Chrysanthemum indicum extract inhibits NLRP3 and AIM2 inflammasome activation via regulating ASC phosphorylation. *J. Ethnopharmacol.* 239, 111917. doi:10.1016/j.jep.2019.111917

Yu, Y. P., Lin, K. H., Shih, M. C., Chen, C. L., and Lu, C. P. (2023). Optimization of aqueous extraction of antioxidants from Chrysanthemum (C. morifolium Ramat and C. indicum L.) flowers and evaluation of their protection from glycoxidation damage on human αA-crystallin. *Exp. Eye Res.* 235, 109629. doi:10.1016/j.exer.2023.109629

Yuan, H., Jiang, S., Liu, Y., Daniyal, M., Jian, Y., Peng, C., et al. (2020). The flower head of Chrysanthemum morifolium Ramat. (Juhua): a paradigm of flowers serving as Chinese dietary herbal medicine. *J. Ethnopharmacol.* 261, 113043. doi:10.1016/j.jep.2020.113043

Zacchino, S. A., Butassi, E., Liberto, M. D., Raimondi, M., Postigo, A., and Sortino, M. (2017). Plant phenolics and terpenoids as adjuvants of antibacterial and antifungal drugs. *Phytomedicine* 37, 27–48. doi:10.1016/j.phymed.2017.10.018

Zeng, M., Li, M., Chen, Y., Zhang, J., Cao, Y., Zhang, B., et al. (2020). A new bisepoxylignan dendranlignan A isolated from Chrysanthemum Flower inhibits the production of inflammatory mediators via the TLR4 pathway in LPS-induced H9c2 cardiomyocytes. *Arch. Biochem. Biophys.* 690, 108506. doi:10.1016/j.abb.2020.108506

Zhan, G., Long, M., Shan, K., Xie, C., and Yang, R. (2022). Antioxidant effect of Chrysanthemum morifolium (chuju) extract on H(2)O(2)-treated L-O2 cells as revealed by LC/MS-Based metabolic profiling. *Antioxidants (Basel)* 11, 1068. doi:10.3390/antiox11061068

Zhang, D., Gao, W., Cui, X., Qiao, R., and Li, C. (2024). Caffeic acid and cyclen-based hydrogel for synergistic antibacterial therapy. *ACS Appl. Mater Interfaces* 16, 34.44493–44503. doi:10.1021/acsami.4c09037

Zhang, K., Jiang, Y., Zhao, H., Köllner, T. G., Chen, S., Chen, F., et al. (2020). Diverse terpenoids and their associated antifungal properties from roots of different cultivars of Chrysanthemum morifolium Ramat. *Molecules* 25, 2083. doi:10.3390/molecules25092083

Zhang, L., and Wang, C. C. (2014). Inflammatory response of macrophages in infection. *Hepatobiliary Pancreat. Dis. Int.* 13 (2), 138–152. doi:10.1016/s1499-3872(14)60024-2

Zhang, X., Wu, J. Z., Lin, Z. X., Yuan, Q. J., Li, Y. C., Liang, J. L., et al. (2019). Ameliorative effect of supercritical fluid extract of Chrysanthemum indicum Linnén against D-galactose induced brain and liver injury in senescent mice via suppression of oxidative stress, inflammation and apoptosis. *J. Ethnopharmacol.* 234, 44–56. doi:10.1016/j.jep.2018.12.050

Zheng, C., Dong, Q., Chen, H., Cong, Q., and Ding, K. (2015). Structural characterization of a polysaccharide from Chrysanthemum morifolium flowers and its antioxidant activity. *Carbohydr. Polym.* 130, 130.113–121. doi:10.1016/j.carbpol.2015.05.004

Zhou, H., Zhang, X., Li, B., and Yue, R. (2023). Fast and efficient identification of hyaluronidase specific inhibitors from Chrysanthemum morifolium Ramat. using UF-LC-MS technique and their anti-inflammation effect in macrophages. *Heliyon* 9 (2), e13709. doi:10.1016/j.heliyon.2023.e13709

Zielińska-Błajet, M., and Feder-Kubis, J. (2020). Monoterpenes and their derivatives-recent development in biological and medical applications. *Int. J. Mol. Sci.* 21, 7078. doi:10.3390/ijms21197078

frontiers | Frontiers in Pharmacology

TYPE Original Research
PUBLISHED 30 May 2025
DOI 10.3389/fphar.2025.1546652

Check for updates

OPEN ACCESS

EDITED BY
Quansheng Feng,
Chengdu University of Traditional Chinese Medicine, China

REVIEWED BY
Abeni Beshiru,
Federal Institute for Risk Assessment (BfR), Germany
Rosa Guillen Fretes,
National University of Asunción, Paraguay

*CORRESPONDENCE
Yong Tan,
tcmtanyong@126.com
Cheng Lu,
lv_cheng0816@163.com
Chunyan Jiang,
tcmjcy@126.com

†These authors share first authorship

RECEIVED 17 December 2024
ACCEPTED 12 May 2025
PUBLISHED 30 May 2025

CITATION
Zhang L, Feng X, An H, Yang W, Xia Y, Wen B, Zheng H, Chen Y, Cheng Y, Jiang C, Lu C and Tan Y (2025) Steamed panax notoginseng mitigates CA-MRSA USA300-induced necroptosis in human neutrophils. *Front. Pharmacol.* 16:1546652. doi: 10.3389/fphar.2025.1546652

COPYRIGHT
© 2025 Zhang, Feng, An, Yang, Xia, Wen, Zheng, Chen, Cheng, Jiang, Lu and Tan. This is an open-access article distributed under the terms of the Creative Commons Attribution License (CC BY). The use, distribution or reproduction in other forums is permitted, provided the original author(s) and the copyright owner(s) are credited and that the original publication in this journal is cited, in accordance with accepted academic practice. No use, distribution or reproduction is permitted which does not comply with these terms.

Steamed panax notoginseng mitigates CA-MRSA USA300-induced necroptosis in human neutrophils

Lulu Zhang[1†], Xiaoyu Feng[1†], Hongsa An[1†], Weifeng Yang[2], Yuwen Xia[1], Bo Wen[1], Haoran Zheng[1], Yihuan Chen[1], Yungchi Cheng[3], Chunyan Jiang[4*], Cheng Lu[1*] and Yong Tan[1*]

[1]Institute of Basic Research in Clinical Medicine, China Academy of Chinese Medical Sciences, Beijing, China, [2]Medical Experimental Center, China Academy of Chinese Medical Sciences, Beijing, China, [3]Department of Pharmacology, Yale University School of Medicine, New Haven, CT, United States, [4]Dermatological Department, Beijing Hospital of Traditional Chinese Medicine, Capital Medical University, Beijing, China

Background: Community-associated methicillin-resistant *Staphylococcus aureus* (CA-MRSA) disrupts innate immunity by inducing necroptosis in polymorphonuclear neutrophils (PMNs), a process linked to excessive inflammation and tissue damage. CA-MRSA releases virulence factors that enhance its pathogenicity by disrupting the host's innate immune response, particularly impairing the phagocytic function of PMNs. Steamed Panax notoginseng (S-PN), a traditional Chinese medicine (TCM), has demonstrated immune-regulatory and anti-inflammatory properties, showing promising therapeutic effects in alleviating the severe inflammatory responses induced by pathogenic microbial infections.

Objective: This study aims to investigate the pharmacological effects and mechanisms of S-PN alleviating CA-MRSA-induced PMN necroptosis by suppressing MRSA virulence factors and inhibiting the RIPK1/RIPK3/MLKL signaling pathway, thereby attenuating inflammatory damage.

Methods: A co-culture model of MRSA USA300 strain and PMNs isolated from healthy human blood was established to observe the changes in necroptosis marker HMGB1, PMNs counts, ROS, chemokine MCP-1 and pro-inflammatory cytokines IL-1β, IL-8, TNF-α. RNA-seq was employed to analyze the effects of S-PN on the transcriptional expression of pathogenesis-related genes of MRSA. RT-PCR was utilized to validate the expression of S-PN on MRSA virulence factors and PMNs necroptosis related genes.

Results: S-PN significantly inhibited HMGB1, ROS, MCP-1, IL-1β and IL-8 in MRSA-PMN co-cultures, the PMN count in the S-PN group was higher than that in the model group. S-PN downregulated MRSA pathogenic-associated *S. aureus* infection and quorum sensing signaling pathways, and significantly reduced the virulence factors PSM and PVL. S-PN suppressed the expression of genes associated with necroptosis ripk1, ripk3, and mlkl in PMNs.

Conclusion: S-PN alleviates CA-MRSA infection-induced immune damage through dual mechanisms: suppression of bacterial virulence factors (PSM and PVL) and inhibition of PMNs necroptosis. These findings underscore its potential

as a complementary therapeutic strategy against CA-MRSA infections, providing a theoretical foundation for integrating TCM into adjuvant treatments for drug-resistant bacterial infections.

KEYWORDS

steamed Panax notoginseng, CA-MRSA, virulence factors, polymorphonuclear neutrophils, necroptosis

1 Introduction

Community-acquired methicillin-resistant *Staphylococcus aureus* (MRSA) infections pose a significant threat to global public health (Palavecino, 2020). The incidence of CA-MRSA infections has been rising annually since the 1990s, with USA300 being the predominant strain in the United States (Ahmad-Mansour et al., 2021). CA-MRSA virulence factors, such as Panton-Valentine leukocidin (PVL), α-hemolysin (Hla), and phenol-soluble modulins (PSM), are critical to its pathogenicity and contribute to the impairment of innate immune responses (Tenover and Goering, 2009). The emergence of antibiotic resistance has further complicated the treatment of CA-MRSA, necessitate novel therapeutic strategies in clinical anti-infection research (Peacock and Paterson, 2015). Treatment that targets immune damage is an important part of the fight against MRSA infection.

MRSA can undermine the immune defense capacity of the host by disrupting the immune responses of immune cells (Chen et al., 2023). Clinical studies have shown that functional defects in polymorphonuclear neutrophils (PMNs) are closely associated with recurrent infections (Rungelrath and DeLeo, 2021; Warheit-Niemi et al., 2022). PMNs, as the first line of defense in innate immunity, are typically the first responders during MRSA infection, engaging in phagocytosis to eliminate the pathogen (Rungelrath and DeLeo, 2021). One of the key strategies by which MRSA disrupts the host immune response is by inducing necroptosis in PMNs. The virulence factors released by MRSA after being phagocytosed by PMNs are recognized to promote the lysis of these neutrophils (Rungelrath et al., 2021). Specifically, USA300 has been shown to induce rapid lysis of these cells, resulting in the release of damage-associated molecular patterns (DAMPs), such as HMGB1 (Irene H et al., 2015; Ludwig et al., 2023). This lysis process appears to differ from apoptosis and is characterized by features of programmed necrosis or necroptosis (Greenlee-Wacker et al., 2017; Rungelrath et al., 2021; Song et al., 2021). During this process, severe inflammatory responses and the accumulation of reactive oxygen species (ROS) are often observed, exacerbating host tissue damage (Liu et al., 2023). Developing pharmacological agents that reduce virulence factor-induced PMN necroptosis is critical to mitigate immune-mediated inflammation in CA-MRSA infections.

Traditional Chinese medicine (TCM) has been widely studied for its antibacterial effects (Yang et al., 2018; Huang et al., 2020; Zhang et al., 2021; Zhang et al., 2022). Ginseng, as a well-known TCM with clear immunoregulatory properties, has also attracted attention for its antibacterial potential (Wang et al., 2020). Asian ginseng (*Panax ginseng* C.A. Meyer), American ginseng (*Panax quinquefolius*), and *Panax notoginseng* (PN) are the three primary ginseng species globally (Wang et al., 2020). Extracts from Asian ginseng and American ginseng have demonstrated significant inhibitory effects on the growth, adhesion, and pathogenicity of *Pseudomonas aeruginosa* (*P. aeruginosa*), *S. aureus* (*S. aureus*), and *Propionibacterium acnes* (Alipour et al., 2011; Wang et al., 2013; Zhang et al., 2014). However, most of these studies focus on the direct effects on the pathogens themselves, with little attention paid to the interaction between bacterial virulence factors and immune cell responses. Unlike the other two types of ginsengs, PN, derived from the dried roots and rhizomes of the Araliaceae family plant *Panax notoginseng* (Burk.) F.H. Chen, does not exhibit significant inhibition on bacterial growth. However, PN extracts significantly inhibit on the quorum sensing system, reducing the area of flagella motility-dependent swarming in *P. aeruginosa* (Koh and Tham, 2011). At the same time, PN, a common anti-inflammatory agent in TCM, possesses immunoregulatory and antioxidant effects (Nian-Wu et al., 2012; Liu et al., 2020; Sheng-Yan et al., 2024; Yang et al., 2024). Steamed PN (S-PN) exhibits strong pro-apoptotic effects on PMNs, promoting non-lytic apoptosis and thus clearing PMNs with minimal release of immune stimulants (such as histones and extracellular DNA) (Wang et al., 2019; Xiong et al., 2022; Yang et al., 2024). This suggests that S-PN may be an effective agent for modulating PMN immune responses and inhibiting inflammation, potentially aiding in the treatment of MRSA infections. Using an MRSA-PMN co-culture model, this study investigates the effects of S-PN on inflammatory responses and ROS accumulation in this model. RNA-seq analysis evaluates the impact of S-PN on the transcriptional expression of virulence factors in CA-MRSA USA300. Furthermore, the study explores the inhibitory effect of S-PN on the apoptosis of PMNs induced by CA-MRSA USA300. This study establishes a theoretical foundation for the clinical application of S-PN in the treatment of infectious diseases.

2 Materials and methods

2.1 Experimental reagents, bacterial strains and cells

S-PN was manufactured by Yunnan Qidan Pharmaceutical Co., Ltd., Yunnan, China. (Production Batch No: 2309003). Its preparation was performed according to the provisions of the Yunnan Province Food and Drug Administration, China (Yun YPBZ-0193-2013). The dried roots and rhizomes of PN (Araliaceae, *Panax notoginseng* (Burk.) F.H. Chen) were selected, cleaned, and steamed for 3 h. Afterward, they were dried and ground into a fine powder. The resulting powder is light yellow or brownish-yellow in color. The product quality standard stipulates that the content of total saponins of panax notoginseng (ginsenoside Rb1, ginsenoside Rg1, and ginsenoside R1) should not be less than 4.5%

(Supplementary Figure S1; Supplementary Table S1). S-PN was dissolved in Dulbecco's Modified Eagle Medium (DMEM) to prepare a 10 mg/mL S-PN solution, which was subsequently filtered through a 0.22 μm filter membrane to remove bacteria.

The MRSA standard strain USA300 (Kansas, United States), hereafter referred to as MRSA, was purchased from American type culture collection (ATCC). The strain was stored at −80°C. The strains were cultured on Mueller–Hinton (MH) agar broth (CM0337, Batch No. 2989738, OXOID, Britain) before use. MRSA passaging culture was performed using MH broth (CM0405, Batch No. 2963434, OXOID, Britain), which was incubated in THZ-D Desktop Constant Temperature Oscillator (Peiving Experimental Equipment Co., Ltd, Suzhou, China) at 37°C and 280 r/min with shaking until the log-phase growth was reached (16–18 h), after which the culture was diluted to 5×10^6~1×10^7 CFU/mL using fresh medium.

The Ethics Committee of the Institute of Traditional Chinese Medicine Clinical and Basic Medical Sciences, China Academy of Chinese Medical Sciences approved all peripheral blood collection procedures. PMNs were isolated from the peripheral blood of healthy volunteers using a human peripheral blood neutrophil isolation solution kit (Batch No. P9402, Solarbio). The procedure involved adding 4 mL of neutrophil separation medium to a 10 mL sterile centrifuge tube, followed by carefully layering 10 mL of EDTA-anticoagulated peripheral blood along the wall of the tube to maintain separation. The sample was then centrifuged at 500 *g* for 30 min, resulting in six distinct layers, with neutrophils located in the fourth layer. The plasma, mononuclear cell layer, and separation medium were carefully removed, and the neutrophil layer was collected for subsequent use.

Trypsin-EDTA was purchased from Invitrogen (Carlsbad, California, United States). Tryptone (Batch No. LP0042) and yeast extracts (Batch No. LP0021) were obtained from Oxoid, United Kingdom. NaCl (Batch No. 10019318) was from Sinopharm Chemical Reagent Co., Ltd, China.

2.2 Cell viability assay

CCK-8 assay was recommended for viability test. In brief, PMNs (1×10^4) were plated into a 96-well plate. Following 24 h of incubation, the medium or prepared S-PN (concentration range of 0.0312-10 mg/mL) was added to the wells and incubated for 24 h. The medium was then replaced with 100 μL serum-free medium, and 10 μL CCK-8 solution (Solarbio, China) was dropped into each well for 4 h of incubation. Absorbance was measured by microplate reader at 450 nm.

2.3 MRSA-PMN co-culture model

An *in vitro* model of MRSA-PMN infection was established based on methods reported in the literature (Chen et al., 2015; Singh et al., 2022), with modifications tailored to this study. PMNs were adjusted to a density of 1×10^4 cells/well and uniformly seeded into plate wells. After 24 h of incubation at 37°C with 5% CO_2, the supernatant was discarded. MRSA was cultured in MH medium to 10^8–10^9 CFU/mL, harvested by centrifugation at 3,000 rpm for 5 min, and washed three times with PBS. The bacterial pellet was resuspended in antibiotic-free DMEM. Revived MRSA was added to the wells at multiplicity of infection (MOI) ratios of 1:5, 1:10, and 1:20 (PMN:MRSA), followed by coculture at 37°C with 5% CO_2 for 1, 4, and 18 h. The HMGB1 levels in the coculture supernatant were measured. MOI values and coculture durations that exhibited both elevated HMGB1 concentrations and statistically significant differences compared to other intervention conditions were selected as the optimal criteria for model establishment. Based on experimental results, an MOI of 1:10 and a 4 h coculture duration were selected as optimal parameters. For drug intervention, PMNs were pretreated with DMEM (MRSA-PMN group) or 10 mg/mL S-PN (S-PN-treated group) for 24 h prior to MRSA infection. The supernatant was then discarded, and MRSA-PMN coculture was performed as described above.

2.4 Enzyme-linked immunosorbent assay (ELISA)

ELISA was used to detect the secretion of HMGB1, IL-1β, IL-8, MCP-1, TNF-α in MRSA-PMN supernatants and PVL, PSM in MRSA. The sources of the kits were Human Interleukin 8 (IL-8) ELISA Kit (KQ110878), Human Tumor Necrosis Factor alpha (TNF-α) ELISA Kit (KQ102647), Human Interleukin 1β(IL-1β) ELISA Kit (KQ105768), Human Monocyte Chemotactic Protein 1 (MCP-1; CCL2) ELISA Kit (KQ110919), Human High Mobility Group Protein B1 (HMGB1) ELISA Kit (KQ105793), Bacterial phenol-soluble modulins (PSM) ELISA Kit (KQ141956) and Bacterial leucocytocide (PVL) ELISA kit (KQ141976) from Shanghai Keqiao Biotechnology Co., Ltd. Each sample was repeated three times.

2.5 Flow cytometry

Granulocyte counts were determined using BD FACSCalibur II™ Flow Cytometer. Granulocytes were identified and quantified by gating on the specific forward scatter (FSC) and side scatter (SSC) regions that correspond to their size and granularity. Intracellular ROS level was evaluated using the 2, 7-dichlorodihydrofluroresenin diacetate (DCFH-DA) (Cat.No. D399, Thermo). Cells were stained with 1 μL DCFH-DA for 60 min at 37°C, then washed and analyzed by flow cytometry. DCFH-DA fluorescence intensity (ex/em 488/525 nm) quantified intracellular ROS levels.

2.6 RNA extraction

Total RNA was extracted from three biological replicates of methicillin-resistant *S. aureus* (MRSA) in both control and S-PN-treated groups using TRIzol reagent (Invitrogen, CA, United States), followed by DNase I digestion (Takara, Japan) to eliminate genomic DNA. RNA integrity was rigorously verified through 1% agarose gel electrophoresis and Agilent 2,100 Bioanalyzer analysis (RIN ≥8.0; 28S/18S ratio >1.8), with quantification performed on a NanoDrop spectrophotometer (OD260/280 = 1.8–2.2).

2.7 RNA-seq

Sequencing libraries were constructed with NEBNext® Ultra™ RNA Kit (NEB) following poly-A selection and cDNA synthesis protocols, and sequenced on Illumina NovaSeq 6,000 (150 bp paired-end). Raw reads were preprocessed through adapter trimming (Trimmomatic; LEADING/TRAILING:20) and quality filtering (Phred score ≥ Q20), then aligned to the *S. aureus* USA300_TCH1516 reference genome (NCBI Assembly GCA_000017885.1) using STAR (v2.7.9a) with ≤1 mismatch. SNP calling was performed using GATK3 HaplotypeCaller after duplicate removal (Picard v1.41) and base quality recalibration.

2.8 Bioinformatics analysis

Gene expression quantification using HTSeq (v0.5.4) generated FPKM-normalized counts through union counting mode with reverse strand specificity. Differentially expressed genes (DEGs) were identified using DESeq (v1.10.1) with a negative binomial model, requiring |log2 (fold change)| ≥1 and Benjamini–Hochberg adjusted $P < 0.05$. Functional enrichment of differentially expressed genes was assessed by GOseq (v1.34.0) with Wallenius distribution-based length bias correction and KOBAS 3.0 using the *S. aureus* USA300 KEGG pathway database (sau00001), applying hypergeometric testing with Benjamini-Yekutieli FDR correction (FDR < 0.1).

2.9 Quantitative real-time PCR (qRT–PCR)

Total RNA was extracted using TRIzol reagent, and its quality was assessed with a NanoDrop spectrophotometer. cDNA was synthesized from 1 μg of RNA using HiScript III 1st Strand cDNA Synthesis Kit (+gDNA wiper) (R312-01, Nanjing Nuoweizan Biotechnology Co., Ltd). qRT-PCR was performed in a 20 μL reaction containing SYBR Green PCR Master Mix, primers (200 nM each), and cDNA template. The genes tested with MRSA as samples were *pvl*, *psmα1*, *psmα2*, *psmα3*, *psmα4* and the reference gene was 16s rRNA. The genes tested with PMNs as samples were ripk1, ripk3, mlkl, caspase-8, smac, spata2 and the reference gene was gapdh. The primer sequences used are shown in the Supplementary Table S2. The cycling conditions included an initial denaturation at 95°C for 10 min, followed by 40 cycles of 95°C for 15 s, annealing at the optimal temperature for 30 s, and extension at 72°C for 30 s. Gene expression was quantified using the ΔΔCt method, normalizing to reference gene.

2.10 Statistical analysis

Data are expressed as mean ± SD. Normality was assessed via Shapiro–Wilk test. For comparisons between two groups, unpaired Student's t-test (parametric) or Mann–Whitney U test (non-parametric) was applied. One-way ANOVA with Tukey's post-hoc test (parametric) or Kruskal–Wallis with Dunn's test (non-parametric) was used for multi-group comparisons. Adjusted P values <0.05 were considered significant. Analyses were performed using GraphPad Prism v10.0.

3 Results

3.1 Effects of S-PN on PMNs in MRSA-PMN Co-culture

HMGB1 levels increased significantly in MRSA-exposed PMNs versus uninfected controls. At an MOI of 1:10 and an infection duration of 4 h, the levels of HMGB1 were elevated to a greater extent compared to MOIs of 1:5 or 1:20, or infection durations of 1 h or 18 h. Based on these data, an MOI of 1:10 and an infection duration of 4 h were selected as the conditions for establishing the MRSA-PMN model in subsequent experiments (Supplementary Figure S2A).

The MIC and MBC assays revealed that S-PN does not exhibit inhibitory effects on the growth of MRSA (Supplementary Figure S2B,C). In the evaluation of drug effects on the cell viability of PMNs, it was observed that S-PN exhibits cytotoxicity at concentrations exceeding 1 mg/mL, with a cell growth inhibition rate greater than 10% (Figure 1A). Treatment with 1 and 0.5 mg/mL S-PN resulted in a significant reduction in HMGB1 level in the MRSA-PMN system post-infection, compared to the untreated Model (MRSA-PMN) group ($P < 0.05$). These results suggest that S-PN protected PMNs from MRSA-induced damage (Figure 1B). In subsequent experiments of this study, 0.5 mg/mL S-PN, which exhibits no significant cytotoxicity to PMNs and effectively suppresses the MRSA-induced elevation of HMGB1 under PMN damage, will be selected as the optimal experimental drug concentration.

3.2 Inhibition of MRSA-Induced PMN inflammatory response by S-PN

S-PN was investigated for its inhibitory effects on MRSA-induced PMN inflammatory responses by assessing PMN inflammatory marker levels. Compared to the Control group, the levels of IL-1β, IL-8, and MCP-1 were significantly elevated in the Model group. In the S-PN group, IL-1β and MCP-1 showed a decreasing trend (Figure 1C). There were no significant differences in TNF-α levels between the Model and S-PN groups compared to the Control group. These results indicate that S-PN has a certain inhibitory effect on PMN inflammatory damage, reducing the release of MRSA-induced PMN pro-inflammatory factors.

3.3 Alleviation PMN apoptosis and ROS accumulation by S-PN

The cell numbers of PMNs and intracellular ROS levels were assessed to further determine the effects of MRSA on PMN-induced cell death and oxidative damage. The results showed that the number of granulocytes in the Model group was significantly reduced compared to the Control group, but this reduction was reversed following S-PN intervention (Figures 1D,E; Supplementary Figure S3). Analysis using DCFH-DA revealed a significant increase in ROS levels in the Model group compared to the Control group, while the S-PN group exhibited a notable decrease in ROS levels (Figures 1F,G; Supplementary Figure S3). These findings suggest that S-PN effectively reverses MRSA-induced oxidative damage in PMNs.

10.3389/fphar.2025.1546652

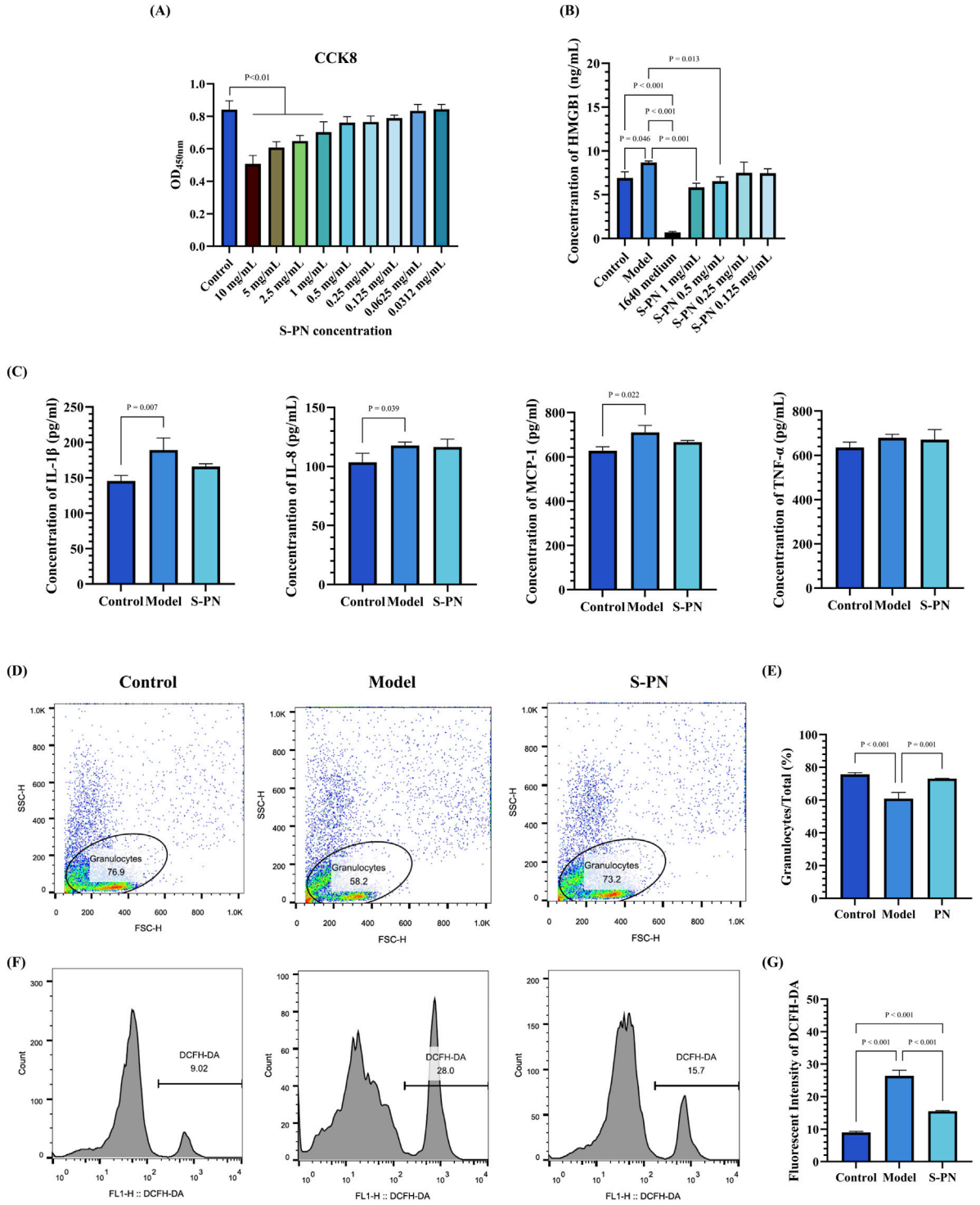


FIGURE 1
Effect of S-PN on PMNs. **(A)** Cytotoxicity of S-PN on PMNs. **(B)** Impact of S-PN on HMGB1 level released by PMNs in the MRSA-PMN model. **(C)** Expression levels of inflammatory cytokines in the MRSA-PMN model. **(D,E)** Flow cytometry analysis of the proportion of total PMNs in each group (n = 3). **(F,G)**. Flow cytometry analysis of ROS levels in each group (n = 3).

3.4 Inhibition of MRSA virulence factor-related pathways by S-PN

To determine whether the anti-inflammatory effect of S-PN on MRSA-induced inflammation in PMNs is associated with transcriptional suppression of MRSA genes, RNA-seq was performed to analyze the transcriptome of MRSA USA300 strain before and after S-PN intervention. A total of 2033 genes were detected. Among these, 1826 genes were common to both the Control and S-PN groups, 180 genes were exclusively found in

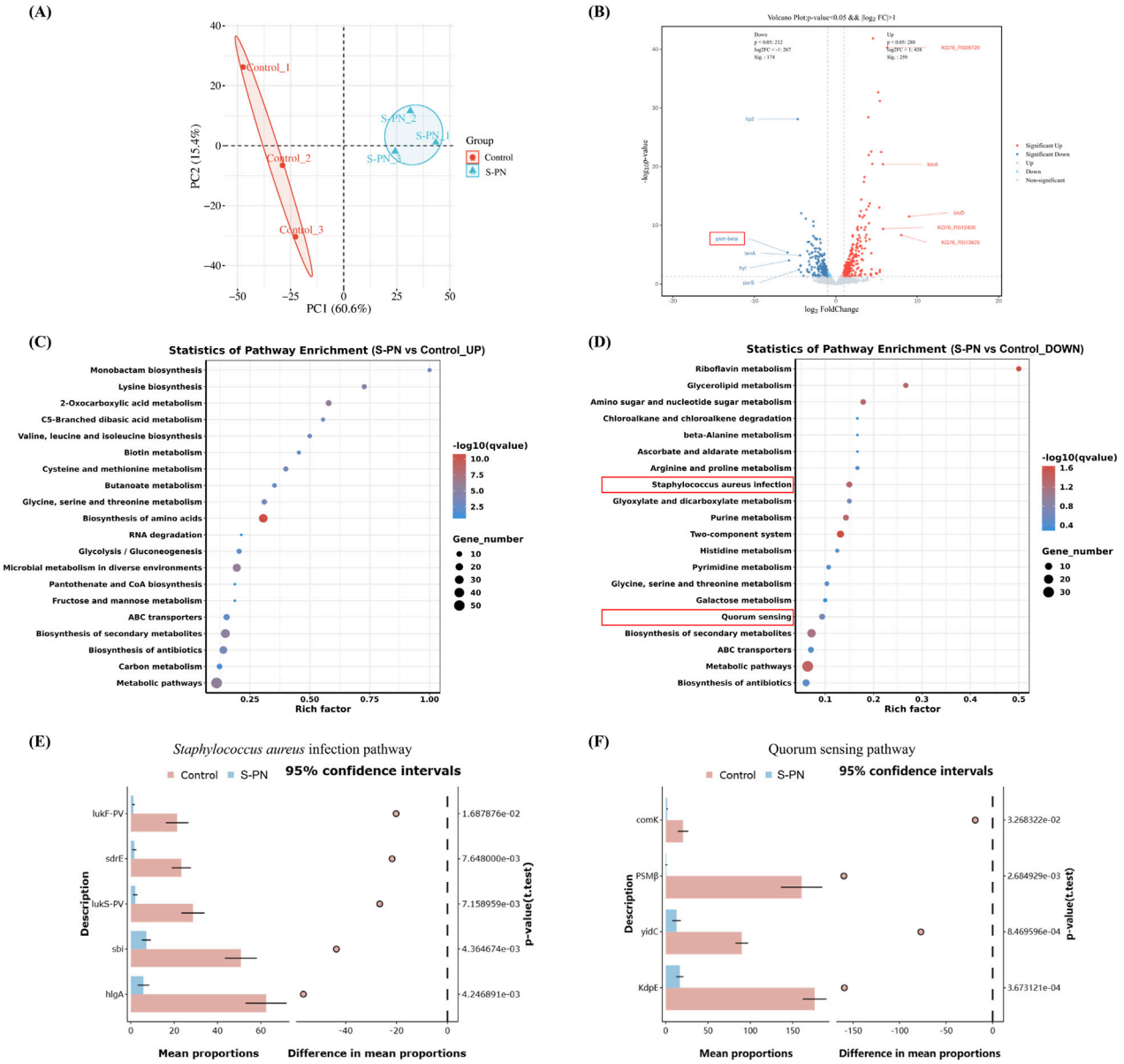


FIGURE 2
Effect of S-PN on MRSA Gene Transcription. **(A)** Principal Component Analysis (PCA) showing significant differences in gene transcription between MRSA with S-PN intervention (S-PN group) and MRSA without intervention (Control group). **(B)** The volcano plot. S-PN vs. Control, with red indicating significantly upregulated genes and blue indicating significantly downregulated genes ($P < 0.05$, $|\log_2 FC| > 1$). The top 10 genes with the most significant changes are labeled on the plot. **(C,D)**. KEGG pathway analysis showing significantly upregulated and downregulated pathways **(E,F)**. The difference expression levels of hub gene in each group in *Staphylococcus aureus* infection pathway and Quorum sensing pathway using STAMP.

the Control group, and 27 genes were unique to the S-PN group (Supplementary Figures S4A,B). Significant transcriptional differences between the two groups were observed, with 276 DEGs identified (Figure 2A; Supplementary Table S3). Following S-PN intervention, 161 DEGs such as *uspA*, *bioA*, *bioD*, and *ribU* were significantly upregulated, while 115 DEGs including *psm-beta* (*psmβ*), *lip2*, *tenA*, *hyl*, and *purS* were significantly downregulated (Figure 2B; Supplementary Figure S4B).

Gene Ontology (GO) enrichment analysis revealed that the upregulated DEGs were primarily associated with biological processes (e.g., oxidation-reduction processes, carboxylic acid metabolic processes, and oxygen-containing compound metabolic processes), cellular components (e.g., ribosomes), and molecular functions (e.g., oxidoreductase activity and ribosome structural constituent). In contrast, the downregulated DEGs were predominantly linked to biological processes (e.g., lipid biosynthesis processes, vitamin metabolic processes, and water-soluble vitamin metabolic processes) and molecular functions (e.g., 3-beta-hydroxy-delta5-steroid dehydrogenase activity and steroid dehydrogenase activity with CH-OH group donors and NAD or NADP as acceptors) (Supplementary Figures S4C,D; Supplementary Table S4).

KEGG pathway enrichment analysis indicated that the upregulated DEGs were significantly enriched in amino acid metabolism pathways (e.g., lysine biosynthesis, cysteine and methionine metabolism, and valine, leucine, and isoleucine biosynthesis), carbon and sugar metabolism pathways (e.g., glycolysis/gluconeogenesis and butyrate metabolism), and other specific metabolism pathways (e.g., 2-oxoacid metabolism and C5-branched dibasic acid metabolism). Conversely, the downregulated DEGs were primarily enriched in vitamin metabolism pathways (e.g., riboflavin metabolism), carbon and sugar metabolism pathways (e.g., glycerolipid metabolism and amino sugar and nucleotide sugar metabolism), as well as pathogen infection and signaling pathways (e.g., *S. aureus* infection and quorum sensing) (Figures 2C,D; Supplementary Table S5).

The genes enriched in these two pathways of pathogen infection and signaling are *lukF-PV*, *lukS-PV*, *sdrE*, *sbi*, *hlgA*, and *clfB* (*S. aureus* infection), as well as *psmβ*, *ribD*, *sspA*, *comK*, *KdpE*, and *yidC* (*Quorum sensing*) (Supplementary Figure S5). Functionally, these genes are associated with pathogenicity-related processes such as cytolysis [*psmβ* (Ebner et al., 2017), *LukF-PV* (Okolie et al., 2013), *LukS-PV*(Okolie et al., 2013), *hlgA* (Venkatasubramaniam et al., 2018)], immune interference [*sbi* (Gonzalez et al., 2019), *sspA* (Oscarsson et al., 2006)], and bacterial adhesion and colonization [*sdrE* (Paiva et al., 2023), *clfB* (Xue et al., 2012)], as well as non-pathogenicity-related processes including bacterial genetic metabolism [*comK* (Turgay et al., 1997), *yidC* (Li et al., 2014), *ribD* (Miao et al., 2024)] and osmotic regulation [*KdpE* (Freeman et al., 2013)].

We observed that following S-PN intervention, the expression levels of cytolytic virulence factor genes, including *psmβ* (log2FC = −5.92), *LukF-PV* (log2FC = −2.28), *LukS-PV* (log2FC = −1.85), and *hlgA* (log2FC = −1.83), were significantly downregulated (Supplementary Figure S3E,F; Supplementary Figures S5A,C). *LukF-PV* and *LukS-PV* encode the CA-MRSA hallmark virulence factor PVL, while *psmβ* encodes PSM. PSM has been shown to enhance the lytic activity of PVL against PMNs (Hongo et al., 2009), whereas *hlgA* is primarily associated with erythrocyte lysis. Based on these findings, this study focuses on investigating the impact of S-PN on PVL- and PSM-mediated PMN apoptosis during CA-MRSA infection.

3.5 Inhibition of MRSA virulence factors PSM and PVL expression by S-PN

The impact of S-PN on the expression of MRSA virulence factors PSM and PVL was assessed using PCR and ELISA. The mRNA transcription levels of *pvl*, *psm α1*, *α2*, *α3*, and *α4* in the S-PN group were significantly reduced compared to the Control group (Figure 3A). Similarly, the concentration levels of PVL and PSM in cells were markedly decreased in the S-PN group compared to the Control group (Figure 3B). These results indicate that S-PN exerts a suppressive effect on both the transcription and expression of MRSA virulence factors PSM and PVL. Therefore, S-PN may reduce the pathogenicity of MRSA by modulating its virulence factors.

3.6 Inhibitory effects of S-PN on the RIPK1/RIPK3/MLKL pathway induced by MRSA in PMNs

To further explore the specific mechanisms by which MRSA virulence factors induce damage in PMNs, we examined the expression levels of genes associated with RIPK1/RIPK3/MLKL necroptotic signaling pathway in PSM-induced PMNs. Necrostatin-1s (Nec-1s), an RIPK1 inhibitor, was used as a control (Supplementary Figure S2D). Both the S-PN and Nec-1s groups exhibited similar inhibitory effects on HMGB1 compared to the Control group, indicating that suppression of the necroptotic pathway can mitigate PMN damage (Figure 4A). In terms of gene expression related to the necroptotic pathway, the mRNA levels of ripk1, ripk3, and mlkl were significantly elevated in the model group, suggesting that MRSA induces necroptosis in PMNs. Following S-PN intervention, the mRNA levels of ripk1, ripk3, and mlkl were significantly reduced, with ripk1 and ripk3 levels comparable to those in Nec-1s group (Figure 4B). These results suggest that S-PN may regulate PMN necroptosis by inhibiting the transcription of ripk1, ripk3, and mlkl mRNA.

This finding was further corroborated by analyzing the mRNA expression of relevant regulators of the RIPK1/RIPK3/MLKL pathway, including caspase-8, smac, and spata2 (Figure 4B). Compared to the Control group, the expression of smac and spata2 was significantly decreased in the Model group, while caspase-8 expression also showed a decreasing trend (Figure 4B). The decreased expression of caspase-8 suggests that MRSA may promote necroptotic signaling by reducing the ability of Caspase-8 to dissociate the RIPK1/RIPK3 complex, thereby maintaining the complex and facilitating necroptosis. The decreased spata2 expression in the Model group suggests that necroptotic signaling in PMNs is not activated by MRSA through the enhancement of SPATA2-mediated RIPK1 deubiquitination. The S-PN group showed a trend of increased smac expression and similar levels of caspase-8 expression compared to the Model group, suggesting that S-PN may enhance SMAC-mediated activation of Caspase, though this activation does not appear to target caspase-8. The exact mechanism warrants further investigation.

4 Discussion

CA-MRSA spreads rapidly and has increasingly become predominant in community infections across various regions worldwide (Tenover and Goering, 2009). Its pathogenicity largely depends on its virulence factors. CA-MRSA virulence factors directly suppress host immune responses. As the first line of innate immunity, PMNs are particularly vulnerable to MRSA virulence factors like PSM, which can inhibit their phagocytic and bactericidal activities while inducing necroptosis (Peschel and Otto, 2013). S-PN, a commonly used anti-inflammatory agent in TCM, exhibits clear necroptosis inhibition (Hu et al., 2022). In this study, using an MRSA-PMNs co-culture model, we observed that S-PN suppressed the inflammatory response and ROS accumulation in the model. Furthermore, S-PN significantly inhibits the transcription of CA-MRSA USA300 virulence factors, including

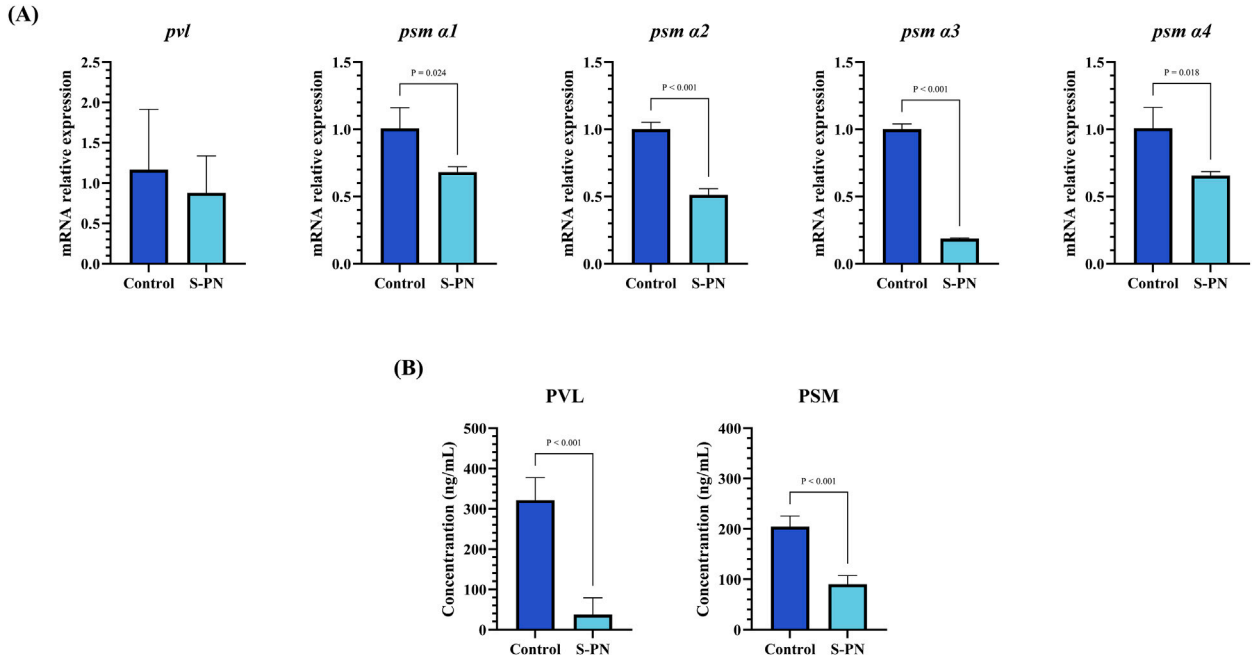


FIGURE 3
Effect of S-PN on MRSA virulence factors PSM and PVL expression. **(A)** The mRNA expression levels of MRSA virulence factors *psm α1, psm α2, psm α3, psm α4* and *pvl*. **(B)** The protein expression levels of MRSA virulence factors PSM and PVL.

PSM and PVL, and reduces the expression of pathogen infection-related pathways, including quorum sensing. This leads to the suppression of necroptotic signaling pathways induced by PSM in PMNs.

PMNs are the most abundant white blood cells in the circulatory system, and their phagocytic activity is crucial for the clearance of invading MRSA. The surface Toll-like receptors (TLRs) on PMNs recognize various surface-associated or freely secreted molecules produced by MRSA, thereby activating phagocytosis of MRSA (Hayashi et al., 2003). Intracellular ROS disrupt bacterial redox homeostasis, inducing lethal oxidative stress (Valko et al., 2007). However, excessive ROS can also be released into the extracellular environment, leading to localized tissue damage at the infection site (Figure 5). Research has demonstrated that ROS can induce permanent changes in the expression of inflammatory genes through redox signaling (Wright et al., 2010). Additionally, ROS can activate the NLRP3 inflammasome, leading to the cleavage of inflammatory cytokine precursors pro-IL-1β and pro-IL-18 into their active forms (IL-1β, IL-18) (Zhou et al., 2010). To prevent severe inflammatory responses and damage to host cells and tissues caused by excessive ROS accumulation, regulating the balance of ROS within PMNs is crucial for effective anti-infection therapy (Figure 5). S-PN demonstrates potent free radical scavenging (Xiong et al., 2019). Our findings confirm its antioxidative efficacy in combating CA-MRSA infection, with significantly reduced ROS accumulation levels observed in MRSA-PMN following S-PN intervention.

Current studies have confirmed that reducing excessive ROS production in glioblastoma cells can decrease pro-inflammatory factors IL-8 and MCP-1, thereby preventing the establishment of a harmful pro-inflammatory tumor microenvironment (Tewari et al., 2009). MCP-1 regulates immune cell recruitment (PMNs, monocytes, lymphocytes) to damaged tissues (Deshmane et al., 2009). It is primarily produced by early-infiltrating PMNs during infection. Inhibition of this chemokine can block the recruitment of immune cells to the infection site, thereby reducing excessive inflammatory responses (Yoshimura and Takahashi, 2007; Deshmane et al., 2009). In this study, MRSA caused significant damage to PMNs, with notable increases in the pro-inflammatory factors IL-1β, IL-8, and MCP-1. The anti-inflammatory efficacy of PN has been well-established in scientific literature. However, our results demonstrated only modest downregulation of inflammatory mediators following S-PN intervention. This attenuated effect may be attributed to alterations in bioactive components during PN processing (Xiong et al., 2019). While ginsenoside 20(S)-Rg3 has been identified as the primary bioactive component responsible for S-PN's anti-inflammatory effects, its content in S-PN is comparatively lower than unprocessed PN-derived anti-inflammatory constituents such as notoginsenoside R1, ginsenosides Rg1, Re, and Rb1 (Zhang et al., 2019). Although the intervention with S-PN did not significantly downregulate inflammatory factors. Reduced HMGB1, elevated granulocytes, and suppressed ROS collectively indicate that S-PN provides protective effects for PMNs (Figure 5).

Current research on the regulation of PMN immune function by PN primarily focuses on pathological conditions such as myocardial infarction (Li et al., 2022), ischemia-reperfusion (Rong et al., 2009), and inflammation (Xiong et al., 2022). However, the regulatory effect of S-PN on PMNs during infectious diseases, where external pathogens invade the body, has not been thoroughly explored. In the process of CA-MRSA infection, its strategy to counteract host immune defense relies on its functional agr quorum sensing

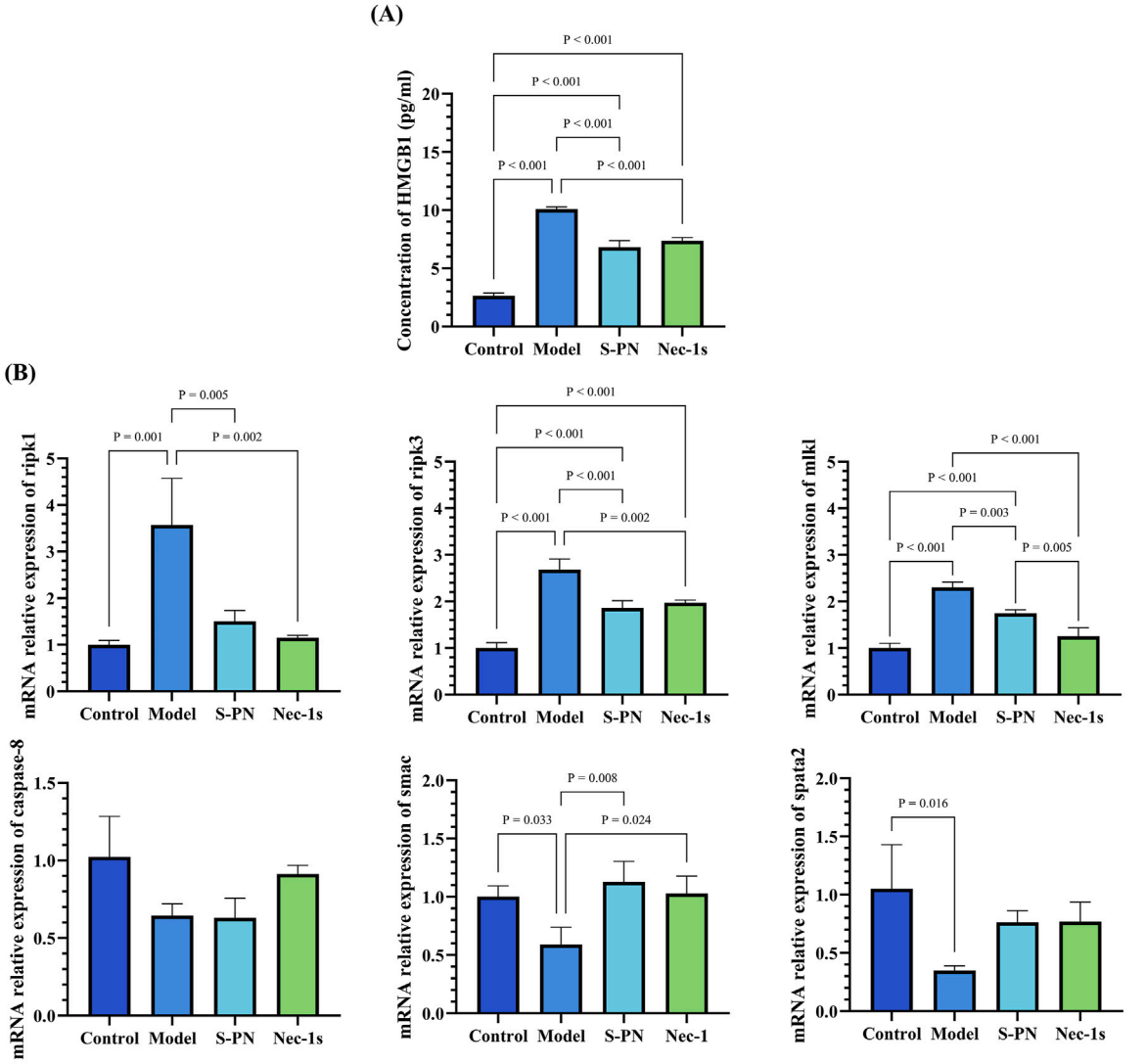


FIGURE 4
Effects of S-PN on the Necroptotic Apoptosis Pathway in MRSA-PMNs. **(A)** Expression levels of HMGB1 in MRSA-PMNs. **(B)** Expression levels of genes associated with the necroptotic apoptosis pathway in PMNs.

system (Cheung et al., 2021; Cella et al., 2023). The high virulence phenotype exhibited by CA-MRSA USA300 is intricately linked to the activation of the agr system. The quorum sensing system regulates the production of virulence factors that can evade PMN-mediated killing and lead to rapid destruction of these host cells (Matsumoto et al., 2021). Our study demonstrates that S-PN significantly downregulates the quorum sensing pathway in the MRSA-PMN model, suggesting that S-PN may influence the production of virulence factors regulated by this pathway. Consequently, we further investigated the virulence factors of USA300. Traditional programmed cell death is characterized by non-lytic processes. During cell death, 'eat me' signals attract phagocytes to clear the dead cells without triggering an inflammatory response (Newton et al., 2024). In contrast, lytic apoptosis, including necroptosis, involves cell rupture during death, releasing cellular contents and triggering an inflammatory response (Newton et al., 2024). PVL, a two-component toxin composed of LukF-PV and LukS-PV, has been shown to induce PMN lysis, impair host defenses, and facilitate the clearance of infected tissues (Jhelum et al., 2024). PVL-containing CA-MRSA strains typically cause tissue necrosis and leukopenia (Hofstee et al., 2024). PVL can activate the mitochondrial pathway of caspases to induce spontaneous apoptosis in PMNs (Genestier et al., 2005). However, there have been no clear reports indicating that PVL is associated with the necroptotic pathway in PMNs.

Another critical virulence factor of USA300, PSM, is an amphipathic α-helical peptide with strong hemolytic activity, considered a key factor in enhancing CA-MRSA virulence (Kim et al., 2020). Different types of PSM exhibit varied effects on PMNs (Hu Z. et al., 2022). PSMα3, in particular, has notable pro-inflammatory activity, stimulating PMN chemotaxis and inducing IL-8 release (Matsumoto et al., 2021). PSMα1, PSMα2, and PSMα3 contribute to the enhanced cell-lytic activity of CA-MRSA. Compared to PSMα gene knockout mutants, wild-type

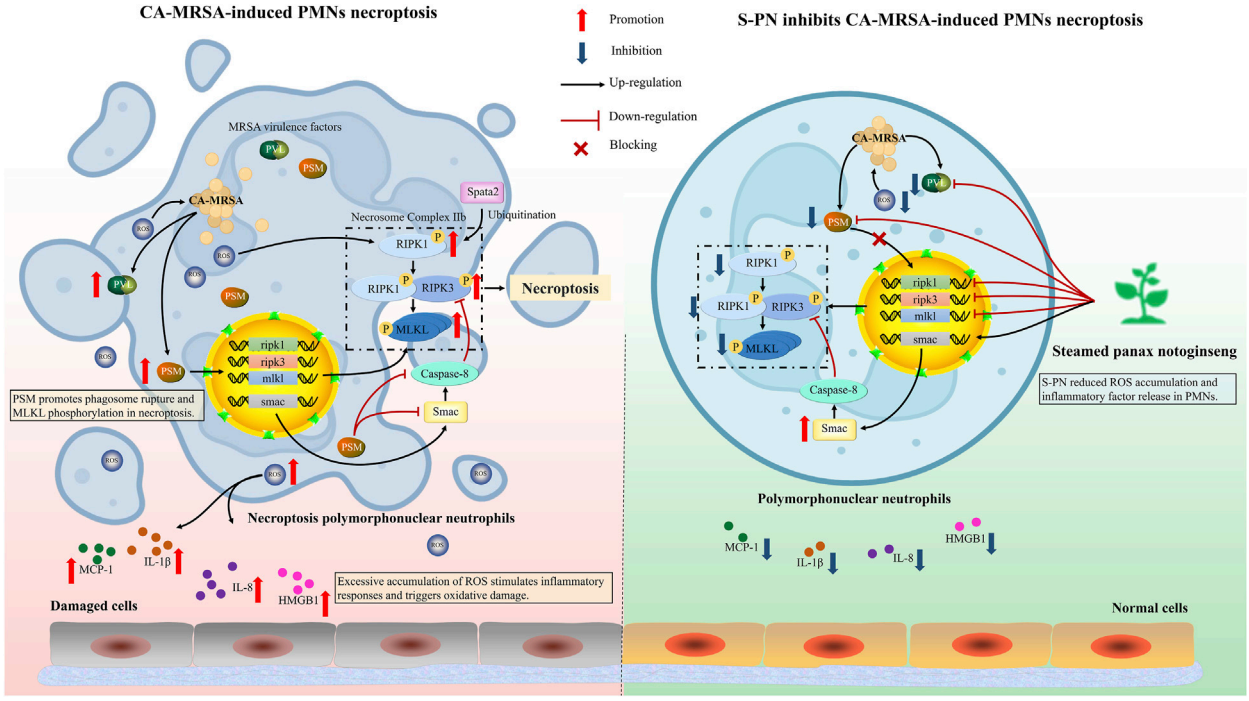


FIGURE 5
Schematic of the mechanism of S-PN inhibits CA-MRSA-induced necroptosis in PMNs. *(Left panel)* Upon MRSA phagocytosis by PMNs, robust ROS production facilitates bacterial clearance; however, MRSA counteracts this defense through secretion of virulence factors PVL and PSMs, which activate PSM-mediated necroptosis pathways in PMNs, ultimately triggering neutrophil lysis and exacerbating inflammatory responses. *(Right panel)* S-PN intervention suppresses MRSA virulence factor release, thereby abrogating PMN necroptosis and mitigating pathological inflammation. PVL, Panton-Valentine Leukocidin; PSM, Phenol Soluble Modulin; ROS, Reactive Oxygen Species; RIPK1, Receptor-Interacting Protein Kinase 1; RIPK3, Receptor-Interacting Protein Kinase 3; MLKL, Mixed-Lineage Kinase Domain-Like; SMAC, Second Mitochondria-Derived Activator of Caspases; SPATA2, Spermatogenesis Associated 2; IL-8, Interleukin-8; IL-1β, Interleukin-1 Beta; HMGB1, High Mobility Group Box 1; MCP-1, Monocyte Chemoattractant Protein-1. Image created by Figdraw.

strains exhibit significantly higher lytic activity against PMNs and monocytes (Wang et al., 2007). Research reports indicate that after phagocytosing *S. aureus*, PMNs undergo dissolution, accompanied by characteristics of both apoptosis and necrosis (Chen H. et al., 2022). This is due to PSMα1, α2, and α3 inducing MLKL phosphorylation, leading to necroptotic apoptosis in PMNs (Zhou et al., 2018). The necroptosis pathway primarily involves the RIPK1 and RIPK3 proteins, which interact to activate the apoptotic program (Figure 5). RIPK complex-mediated MLKL phosphorylation drives its oligomerization and membrane translocation, where it interacts with phosphatidylinositol, triggering membrane permeabilization and cell destruction (Rickard et al., 2014; Wang et al., 2014; Chen et al., 2017). S-PN suppresses the formation of lytic programmed cell death mechanisms, such as neutrophil extracellular traps (NETosis) (Chen Z. et al., 2022). In this study, experiments were conducted to investigate whether S-PN blocks CA-MRSA-induced necroptosis, a similarly lytic form of cell death. The results demonstrated that S-PN suppresses the expression of PVL and PSM. This indicates that S-PN interferes with the induction and activation of the necroptosis pathway in PMNs by PSM through downregulating the quorum sensing pathway in USA300. Specifically, this activation is confirmed to enhance the transcription of key genes ripk1, ripk3, and mlkl, which is reversed by S-PN (Figure 5). The inhibitory effects on ripk1 and ripk3 align with those of the RIPK1 inhibitor Nec-1s, while the suppression of mlkl is slightly weaker compared to Nec-1s. Nec-1s directly binds to the RIPK1 protein and inhibits its phosphorylation, thereby reducing MLKL activation (Jhun et al., 2019). Regarding the impact on necroptosis pathway-related proteins, based on existing studies, we hypothesize that PSM induces MLKL phosphorylation, promotes MLKL interaction with cell membranes, and triggers cell lysis. By suppressing PSM expression in USA300, S-PN reduces PSM-mediated MLKL phosphorylation and blocks PMN lysis. Notably, S-PN not only exhibits anti-necroptotic effects comparable to Nec-1s but also directly targets the pathogen by inhibiting the quorum sensing pathway and virulence factor expression in CA-MRSA.

Necroptosis is regulated by multiple intracellular factors. The inhibition of necroptosis is controlled by Caspase-8, which mediates the classical apoptotic pathway by cleaving RIPK1 protein to suppress its kinase activity, thereby blocking necroptosis (Weinlich et al., 2017). Smac, a caspase activator, facilitates the activation of downstream caspases and assists the Caspase-8 complex in inducing apoptosis and suppressing necrosis (Figure 5) (He et al., 2009; Green, 2022). Studies have shown that S-PN is enriched with bioactive components such as ginsenoside Rh4 and 20(S)-Rg3, which induce apoptosis in PMNs at amputation sites in zebrafish larvae (Xiong et al., 2022; Yang et al., 2024). However, our experimental results revealed that although S-PN significantly enhances smac transcription, it does not

increase caspase-8 expression, indicating that S-PN does not inhibit the necroptosis pathway via Caspase-8-mediated RIPK1 cleavage. Further studies demonstrate that active components in S-PN, including ginsenoside F4 and ginsenoside Rg6, exert significant regulatory effects on the mitochondria-dependent apoptotic protein Bax and the anti-apoptotic protein Bcl-2 (Chen and Jia, 2013; Chen et al., 2013). We hypothesize that S-PN may activate the classical apoptotic pathway by upregulating Bax and suppressing Bcl-2, thereby inhibiting necroptosis. Additionally, Spata2, a deubiquitinating enzyme for M1 ubiquitin chains of RIPK1, promotes necroptosis by enhancing RIPK1 kinase activity (Wei et al., 2017). MRSA suppresses spata2 transcription, suggesting that its promotion of PMN necroptosis does not rely on modulating RIPK1 ubiquitination. Nevertheless, whether MRSA or its virulence factor PSM directly regulates RIPK1 requires further investigation.

5 Conclusion

The induction of PMN necroptosis by CA-MRSA virulence factors is one of the key challenges in treating MRSA infections. During CA-MRSA infection, severe inflammatory responses caused by ROS accumulation in PMNs also contribute to tissue damage. S-PN reduces ROS levels in PMNs, inhibits the release of inflammatory cytokines IL-1β and IL-8, and suppresses the production of the chemokine MCP-1. By downregulating the quorum sensing system, S-PN inhibits the production of CA-MRSA virulence factors PVL and PSM, thereby blocking PSM-induced necroptosis in PMNs. This results in reduced expression of ripk1, ripk3, and mlkl, ultimately diminishing CA-MRSA's pro-necroptotic effects on PMNs. This study demonstrates that S-PN protects host immune defenses by suppressing CA-MRSA virulence factor release, thereby preserving PMN-mediated immune functions and mitigating tissue injury caused by excessive inflammation. Future research will focus on validating S-PN's therapeutic efficacy against CA-MRSA infections in in vivo models. Our findings provide a theoretical foundation for the clinical application of traditional Chinese medicine in antibacterial therapy.

Data availability statement

The data presented in the study are deposited in the Gene Expression Omnibus (GEO) database, accession number GSE284429.

Ethics statement

The studies involving humans were approved by the Ethics Committee of the Institute of Traditional Chinese Medicine Clinical and Basic Medical Sciences, China Academy of Chinese Medical Sciences. The studies were conducted in accordance with the local legislation and institutional requirements. The participants provided their written informed consent to participate in this study.

Author contributions

LZ: Conceptualization, Data curation, Methodology, Writing – original draft. XF: Conceptualization, Methodology, Writing – review and editing. HA: Formal Analysis, Investigation, Writing – original draft. WY: Supervision, Validation, Writing – review and editing. YX: Resources, Writing – review and editing. BW: Project administration, Writing – review and editing. HZ: Software, Writing – review and editing. YiC: Visualization, Writing – review and editing. YuC: Supervision, Writing – review and editing. CJ: Conceptualization, Supervision, Writing – review and editing. CL: Conceptualization, Investigation, Supervision, Writing – review and editing. YT: Conceptualization, Funding acquisition, Supervision, Writing – original draft.

Funding

The author(s) declare that financial support was received for the research and/or publication of this article. This work was supported by the scientific and technological innovation project of China Academy of Chinese Medical Sciences (CI2021B003, CI2021A00704-2, CI2023C065YLL); and the fundamental research funds for the central public welfare research institutes of China [Z0735].

Conflict of interest

The authors declare that the research was conducted in the absence of any commercial or financial relationships that could be construed as a potential conflict of interest.

Generative AI statement

The author(s) declare that no Generative AI was used in the creation of this manuscript.

Publisher's note

All claims expressed in this article are solely those of the authors and do not necessarily represent those of their affiliated organizations, or those of the publisher, the editors and the reviewers. Any product that may be evaluated in this article, or claim that may be made by its manufacturer, is not guaranteed or endorsed by the publisher.

Supplementary material

The Supplementary Material for this article can be found online at: https://www.frontiersin.org/articles/10.3389/fphar.2025.1546652/full#supplementary-material

References

Ahmad-Mansour, N., Loubet, P., Pouget, C., Dunyach-Remy, C., Sotto, A., Lavigne, J. P., et al. (2021). Staphylococcus aureus toxins: an update on their pathogenic properties and potential treatments. *Toxins (Basel)* 13 (10), 677. doi:10.3390/toxins13100677

Alipour, M., Omri, A., and Suntres, Z. E. (2011). Ginseng aqueous extract attenuates the production of virulence factors, stimulates twitching and adhesion, and eradicates biofilms of *Pseudomonas aeruginosa*. *Can. J. Physiology Pharmacol.* 89 (6), 419–427. doi:10.1139/y11-057

Cella, M. A., Coulson, T., MacEachern, S., Badr, S., Ahmadi, A., Tabatabaei, M. S., et al. (2023). Probiotic disruption of *quorum* sensing reduces virulence and increases cefoxitin sensitivity in methicillin-resistant Staphylococcus aureus. *Sci. Rep.* 13 (1), 4373. doi:10.1038/s41598-023-31474-2

Chen, B., and Jia, X.-B. (2013). Apoptosis-inducing effect of ginsenoside Rg6 on human lymphocytoma JK cells. *Mol. Basel, Switz.* 18 (7), 8109–8119. doi:10.3390/molecules18078109

Chen, B., Shen, Y.-P., Zhang, D.-F., Cheng, J., and Jia, X.-B. (2013). The apoptosis-inducing effect of ginsenoside F4 from steamed notoginseng on human lymphocytoma JK cells. *Nat. Prod. Res.* 27 (24), 2351–2354. doi:10.1080/14786419.2013.828290

Chen, H., Wang, B., Zhao, R., Gao, D., Guan, M., Zheng, L., et al. (2015). Coculture with low-dose SWCNT attenuates bacterial invasion and inflammation in human enterocyte-like Caco-2 cells. *Small Weinheim Der Bergstrasse, Ger.* 11 (34), 4366–4378. doi:10.1002/smll.201500136

Chen, H., Zhang, J., He, Y., Lv, Z., Liang, Z., Chen, J., et al. (2022a). Exploring the role of *Staphylococcus aureus* in inflammatory diseases. *Toxins* 14 (7), 464. doi:10.3390/toxins14070464

Chen, S., Lv, X., Hu, B., Shao, Z., Wang, B., Ma, K., et al. (2017). RIPK1/RIPK3/MLKL-mediated necroptosis contributes to compression-induced rat nucleus pulposus cells death. *Apoptosis* 22 (5), 626–638. doi:10.1007/s10495-017-1358-2

Chen, Y., Liu, Z., Lin, Z., Lu, M., Fu, Y., Liu, G., et al. (2023). The effect of Staphylococcus aureus on innate and adaptive immunity and potential immunotherapy for S. aureus-induced osteomyelitis. *Front. Immunol.* 14, 1219895. doi:10.3389/fimmu.2023.1219895

Chen, Z., Wang, G., Xie, X., Liu, H., Liao, J., Shi, H., et al. (2022b). Ginsenoside Rg5 allosterically interacts with P2RY12 and ameliorates deep venous thrombosis by counteracting neutrophil NETosis and inflammatory response. *Front. Immunol.* 13, 918476. doi:10.3389/fimmu.2022.918476

Cheung, G. Y. C., Bae, J. S., and Otto, M. (2021). Pathogenicity and virulence of Staphylococcus aureus. *Virulence* 12 (1), 547–569. doi:10.1080/21505594.2021.1878688

Deshmane, S. L., Kremlev, S., Amini, S., and Sawaya, B. E. (2009). Monocyte chemoattractant protein-1 (MCP-1): an overview. *J. Interferon Cytokine Res.* 29 (6), 313–326. doi:10.1089/jir.2008.0027

Ebner, P., Luqman, A., Reichert, S., Hauf, K., Popella, P., Forchhammer, K., et al. (2017). Non-classical protein excretion is boosted by psmα-induced cell leakage. *Cell Rep.* 20 (6), 1278–1286. doi:10.1016/j.celrep.2017.07.045

Freeman, Z. N., Dorus, S., and Waterfield, N. R. (2013). The KdpD/KdpE two-component system: integrating K^+ homeostasis and virulence. *PLoS Pathog.* 9 (3), e1003201. doi:10.1371/journal.ppat.1003201

Genestier, A.-L., Michallet, M.-C., Prévost, G., Bellot, G., Chalabreysse, L., Peyrol, S., et al. (2005). Staphylococcus aureus Panton-Valentine leukocidin directly targets mitochondria and induces Bax-independent apoptosis of human neutrophils. *J. Clin. Investigation* 115 (11), 3117–3127. doi:10.1172/JCI22684

Gonzalez, C. D., Ledo, C., Cela, E., Stella, I., Xu, C., Ojeda, D. S., et al. (2019). The good side of inflammation: Staphylococcus aureus proteins SpA and Sbi contribute to proper abscess formation and wound healing during skin and soft tissue infections. *Biochimica Biophysica Acta. Mol. Basis Dis.* 1865 (10), 2657–2670. doi:10.1016/j.bbadis.2019.07.004

Green, D. R. (2022). The mitochondrial pathway of apoptosis Part II: the BCL-2 protein family. *Cold Spring Harb. Perspect. Biol.* 14 (6), a041046. doi:10.1101/cshperspect.a041046

Greenlee-Wacker, M. C., Kremserová, S., and Nauseef, W. M. (2017). Lysis of human neutrophils by community-associated methicillin-resistant Staphylococcus aureus. *Blood* 129 (24), 3237–3244. doi:10.1182/blood-2017-02-766253

Hayashi, F., Means, T. K., and Luster, A. D. (2003). Toll-like receptors stimulate human neutrophil function. *Blood* 102 (7), 2660–2669. doi:10.1182/blood-2003-04-1078

He, S., Wang, L., Miao, L., Wang, T., Du, F., Zhao, L., et al. (2009). Receptor interacting protein kinase-3 determines cellular necrotic response to TNF-alpha. *Cell* 137 (6), 1100–1111. doi:10.1016/j.cell.2009.05.021

Hofstee, M. I., Siverino, C., Saito, M., Meghwani, H., Tapia-Dean, J., Arveladze, S., et al. (2024). Staphylococcus aureus Panton-Valentine Leukocidin worsens acute implant-associated osteomyelitis in humanized BRGSF mice. *JBMR Plus* 8 (2), ziad005. doi:10.1093/jbmrpl/ziad005

Hongo, I., Baba, T., Oishi, K., Morimoto, Y., Ito, T., and Hiramatsu, K. (2009). Phenol-soluble modulin alpha 3 enhances the human neutrophil lysis mediated by Panton-Valentine leukocidin. *J. Infect. Dis.* 200 (5), 715–723. doi:10.1086/605332

Hu, Y., Lei, H., Zhang, S., Ma, J., Kang, S., Wan, L., et al. (2022a). Panax notoginseng saponins protect Brain microvascular endothelial cells against oxygen-glucose deprivation/resupply-induced necroptosis via suppression of RIP1-RIP3-MLKL signaling pathway. *Neurochem. Res.* 47 (11), 3261–3271. doi:10.1007/s11064-022-03675-0

Hu, Z., Kopparapu, P. K., Ebner, P., Mohammad, M., Lind, S., Jarneborn, A., et al. (2022b). Phenol-soluble modulin α and β display divergent roles in mice with staphylococcal septic arthritis. *Commun. Biol.* 5 (1), 910. doi:10.1038/s42003-022-03839-2

Huang, X., Wang, P., Li, T., Tian, X., Guo, W., Xu, B., et al. (2020). Self-assemblies based on traditional medicine berberine and cinnamic acid for adhesion-induced inhibition multidrug-resistant *Staphylococcus aureus*. *ACS Appl. Mater. and Interfaces* 12 (1), 227–237. doi:10.1021/acsami.9b17722

Irene, H. H., Simon, D. P., Carin, L., Harold, G. d.B., G Jan, Z., Hester, v.d.V., et al. (2015). Cigarette smoke-induced damage-associated molecular pattern release from necrotic neutrophils triggers proinflammatory mediator release. *Am. J. Respir. Cell Mol. Biol.* 52 (5), 554–562. doi:10.1165/rcmb.2013-0505OC

Jhelum, H., Čerina, D., Harbort, C. J., Lindner, A., Hanitsch, L. G., Leistner, R., et al. (2024). Panton-Valentine leukocidin-induced neutrophil extracellular traps lack antimicrobial activity and are readily induced in patients with recurrent PVL + -Staphylococcus aureus infections. *J. Leukoc. Biol.* 115 (2), 222–234. doi:10.1093/jleuko/qiad137

Jhun, J., Lee, S. H., Kim, S.-Y., Ryu, J., Kwon, J. Y., Na, H. S., et al. (2019). RIPK1 inhibition attenuates experimental autoimmune arthritis via suppression of osteoclastogenesis. *J. Transl. Med.* 17 (1), 84. doi:10.1186/s12967-019-1809-3

Kim, D.-R., Lee, Y., Kim, H.-K., Kim, W., Kim, Y.-G., Yang, Y.-H., et al. (2020). Phenol-soluble modulin-mediated aggregation of community-associated methicillin-resistant Staphylococcus aureus in human cerebrospinal fluid. *Cells* 9 (3), 788. doi:10.3390/cells9030788

Koh, K. H., and Tham, F.-Y. (2011). Screening of traditional Chinese medicinal plants for *quorum*-sensing inhibitors activity. *J. Microbiol. Immunol. Infect. = Wei Mian Yu Gan Ran Za Zhi* 44 (2), 144–148. doi:10.1016/j.jmii.2009.10.001

Li, H., Zhu, J., Xu, Y.-W., Mou, F.-F., Shan, X.-L., Wang, Q.-L., et al. (2022). Notoginsenoside R1-loaded mesoporous silica nanoparticles targeting the site of injury through inflammatory cells improves heart repair after myocardial infarction. *Redox Biol.* 54, 102384. doi:10.1016/j.redox.2022.102384

Li, Z., Boyd, D., Reindl, M., and Goldberg, M. B. (2014). Identification of YidC residues that define interactions with the sec apparatus. *J. Bacteriol.* 196 (2), 367–377. doi:10.1128/JB.01095-13

Liu, H., Lu, X., Hu, Y., and Fan, X. (2020). Chemical constituents of Panax ginseng and Panax notoginseng explain why they differ in therapeutic efficacy. *Pharmacol. Res.* 161, 105263. doi:10.1016/j.phrs.2020.105263

Liu, J., Han, X., Zhang, T., Tian, K., Li, Z., and Luo, F. (2023). Reactive oxygen species (ROS) scavenging biomaterials for anti-inflammatory diseases: from mechanism to therapy. *J. Hematol. and Oncol.* 16 (1), 116. doi:10.1186/s13045-023-01512-7

Ludwig, N., Thörner-van Almsick, J., Mersmann, S., Bardel, B., Niemann, S., Chasan, A. I., et al. (2023). Nuclease activity and protein A release of *Staphylococcus aureus* clinical isolates determine the virulence in a murine model of acute lung infection. *Front. Immunol.* 14, 1259004. doi:10.3389/fimmu.2023.1259004

Matsumoto, M., Nakagawa, S., Zhang, L., Nakamura, Y., Villaruz, A. E., Otto, M., et al. (2021). Interaction between Staphylococcus Agr virulence and neutrophils regulates pathogen expansion in the skin. *Cell Host and Microbe* 29 (6), 930–940.e4. doi:10.1016/j.chom.2021.03.007

Miao, Y., Shuang, W., Qianwei, Q., Xin, L., Wei, P., Hai, Y., et al. (2024). Proteomic study of the inhibitory effects of tannic acid on MRSA biofilm. *Front. Pharmacol.* 15, 1413669. doi:10.3389/fphar.2024.1413669

Newton, K., Strasser, A., Kayagaki, N., and Dixit, V. M. (2024). Cell death. *Cell*, 187 (2), 235–256. doi:10.1016/j.cell.2023.11.044

Nian-Wu, H., Yan, Z., Ling, G., Jun, S., and Xing-Bin, Y. (2012). Antioxidant, antiproliferative, and pro-apoptotic activities of a saponin extract derived from the roots of Panax notoginseng (Burk.) F.H. Chen. *J. Med. Food* 15 (4), 350–359. doi:10.1089/jmf.2011.1801

Okolie, C. E., Cockayne, A., Penfold, C., and James, R. (2013). Engineering of the LukS-PV and LukF-PV subunits of *Staphylococcus aureus* Panton-Valentine leukocidin for diagnostic and therapeutic applications. *BMC Biotechnol.* 13, 103. doi:10.1186/1472-6750-13-103

Oscarsson, J., Tegmark-Wisell, K., and Arvidson, S. (2006). Coordinated and differential control of aureolysin (aur) and serine protease (sspA) transcription in *Staphylococcus aureus* by sarA, rot and agr (RNAIII). *Int. J. Med. Microbiol. IJMM* 296 (6), 365–380. doi:10.1016/j.ijmm.2006.02.019

Paiva, T. O., Geoghegan, J. A., and Dufrêne, Y. F. (2023). High-force catch bonds between the *Staphylococcus aureus* surface protein SdrE and complement regulator factor H drive immune evasion. *Commun. Biol.* 6 (1), 302. doi:10.1038/s42003-023-04660-1

Palavecino, E. L. (2020). Clinical, epidemiologic, and laboratory aspects of methicillin-resistant *Staphylococcus aureus* infections. *Methods Mol. Biol. Clift. N.J.* 2069, 1–28. doi:10.1007/978-1-4939-9849-4_1

Peacock, S. J., and Paterson, G. K. (2015). Mechanisms of methicillin resistance in Staphylococcus aureus. *Annu. Rev. Biochem.* 84, 577–601. doi:10.1146/annurev-biochem-060614-034516

Peschel, A., and Otto, M. (2013). Phenol-soluble modulins and staphylococcal infection. *Nat. Rev. Microbiol.* 11 (10), 667–673. doi:10.1038/nrmicro3110

Rickard, J. A., O'Donnell, J. A., Evans, J. M., Lalaoui, N., Poh, A. R., Rogers, T., et al. (2014). RIPK1 regulates RIPK3-MLKL-driven systemic inflammation and emergency hematopoiesis. *Cell* 157 (5), 1175–1188. doi:10.1016/j.cell.2014.04.019

Rong, L., Chen, Y., He, M., and Zhou, X. (2009). Panax notoginseng saponins attenuate acute lung injury induced by intestinal ischaemia/reperfusion in rats. *Respirol. Carlt. Vic.* 14 (6), 890–898. doi:10.1111/j.1440-1843.2009.01586.x

Rungelrath, V., and DeLeo, F. R. (2021). Staphylococcus aureus, antibiotic resistance, and the interaction with human neutrophils. *Antioxidants and Redox Signal.* 34 (6), 452–470. doi:10.1089/ars.2020.8127

Rungelrath, V., Porter, A. R., Malachowa, N., Freedman, B. A., Leung, J. M., Voyich, J. M., et al. (2021). Further insight into the mechanism of human PMN lysis following phagocytosis of Staphylococcus aureus. *Microbiol. Spectr.* 9 (2), e0088821. doi:10.1128/Spectrum.00888-21

Sheng-Yan, H., Wen, L., Chu-Man, H., Hui-Mei, H., Qi-Long, C., Yun-Xiao, L., et al. (2024). Enhancing antioxidant levels and mitochondrial function in porcine oocyte maturation and embryonic development through notoginsenoside R1 supplementation. *Reprod. Domest. Anim.* 59 (6), e14631. doi:10.1111/rda.14631

Singh, A. K., Praharaj, M., Lombardo, K. A., Yoshida, T., Matoso, A., Baras, A. S., et al. (2022). Re-engineered BCG overexpressing cyclic di-AMP augments trained immunity and exhibits improved efficacy against bladder cancer. *Nat. Commun.* 13 (1), 878. doi:10.1038/s41467-022-28509-z

Song, H.-S., Bhatia, S. K., Choi, T.-R., Gurav, R., Kim, H. J., Lee, S. M., et al. (2021). Increased antibiotic resistance of methicillin-resistant Staphylococcus aureus USA300 Δpsm mutants and a complementation study of Δpsm mutants using synthetic phenol-soluble modulins. *J. Microbiol. Biotechnol.* 31 (1), 115–122. doi:10.4014/jmb.2007.07034

Tenover, F. C., and Goering, R. V. (2009). Methicillin-resistant Staphylococcus aureus strain USA300: origin and epidemiology. *J. Antimicrob. Chemother.* 64 (3), 441–446. doi:10.1093/jac/dkp241

Tewari, R., Sharma, V., Koul, N., Ghosh, A., Joseph, C., Hossain, Sk U., et al. (2009). Ebselen abrogates TNFalpha induced pro-inflammatory response in glioblastoma. *Mol. Oncol.* 3 (1), 77–83. doi:10.1016/j.molonc.2008.10.004

Turgay, K., Hamoen, L. W., Venema, G., and Dubnau, D. (1997). Biochemical characterization of a molecular switch involving the heat shock protein ClpC, which controls the activity of ComK, the competence transcription factor of Bacillus subtilis. *Genes and Dev.* 11 (1), 119–128. doi:10.1101/gad.11.1.119

Valko, M., Leibfritz, D., Moncol, J., Cronin, M. T., Mazur, M., and Telser, J. (2007). Free radicals and antioxidants in normal physiological functions and human disease. *Int. J. Biochem. Cell Biol.* 39 (1), 44–84. doi:10.1016/j.biocel.2006.07.001

Venkatasubramaniam, A., Kanipakala, T., Ganjbaksh, N., Mehr, R., Mukherjee, I., Krishnan, S., et al. (2018). A critical role for HlgA in Staphylococcus aureus pathogenesis revealed by A switch in the SaeRS two-component regulatory system. *Toxins (Basel)* 10 (9), 377. doi:10.3390/toxins10090377

Wang, H., Sun, L., Su, L., Rizo, J., Liu, L., Wang, L. F., et al. (2014). Mixed lineage kinase domain-like protein MLKL causes necrotic membrane disruption upon phosphorylation by RIP3. *Mol. Cell* 54 (1), 133–146. doi:10.1016/j.molcel.2014.03.003

Wang, L., Huang, Y., Yin, G., Wang, J., Wang, P., Chen, Z.-Y., et al. (2020). Antimicrobial activities of Asian ginseng, American ginseng, and notoginseng. *Phytotherapy Res. PTR* 34 (6), 1226–1236. doi:10.1002/ptr.6605

Wang, L., Yang, X., Yu, X., Yao, Y., and Ren, G. (2013). Evaluation of antibacterial and anti-inflammatory activities of less polar ginsenosides produced from polar ginsenosides by heat-transformation. *J. Agric. Food Chem.* 61 (50), 12274–12282. doi:10.1021/jf404461q

Wang, P., Hou, Y., Zhang, W., Zhang, H., Che, X., Gao, Y., et al. (2019). Pseudoginsenoside-F11 attenuates lipopolysaccharide-induced acute lung injury by suppressing neutrophil infiltration and accelerating neutrophil clearance. *Inflammation* 42 (5), 1857–1868. doi:10.1007/s10753-019-01047-5

Wang, R., Braughton, K. R., Kretschmer, D., Bach, T. H., Queck, S. Y., Li, M., et al. (2007). Identification of novel cytolytic peptides as key virulence determinants for community-associated MRSA. *Nat. Med.* 13 (12), 1510–1514. doi:10.1038/nm1656

Warheit-Niemi, H. I., Edwards, S. J., SenGupta, S., Parent, C. A., Zhou, X., O'Dwyer, D. N., et al. (2022). Fibrotic lung disease inhibits immune responses to staphylococcal pneumonia via impaired neutrophil and macrophage function. *JCI Insight* 7 (4), e152690. doi:10.1172/jci.insight.152690

Wei, R., Xu, L. W., Liu, J., Li, Y., Zhang, P., Shan, B., et al. (2017). SPATA2 regulates the activation of RIPK1 by modulating linear ubiquitination. *Genes Dev.* 31 (11), 1162–1176. doi:10.1101/gad.299776.117

Weinlich, R., Oberst, A., Beere, H. M., and Green, D. R. (2017). Necroptosis in development, inflammation and disease. *Nat. Rev. Mol. Cell Biol.* 18 (2), 127–136. doi:10.1038/nrm.2016.149

Wright, H. L., Moots, R. J., Bucknall, R. C., and Edwards, S. W. (2010). Neutrophil function in inflammation and inflammatory diseases. *Rheumatology* 49 (9), 1618–1631. doi:10.1093/rheumatology/keq045

Xiong, Y., Chen, L., Man, J., Hu, Y., and Cui, X. (2019). Chemical and bioactive comparison of Panax notoginseng root and rhizome in raw and steamed forms. *J. Ginseng Res.* 43 (3), 385–393. doi:10.1016/j.jgr.2017.11.004

Xiong, Y., Halima, M., Che, X., Zhang, Y., Schaaf, M. J. M., Li, M., et al. (2022). Steamed panax notoginseng and its saponins inhibit the migration and induce the apoptosis of neutrophils in a zebrafish tail-fin amputation model. *Front. Pharmacol.* 13, 946900. doi:10.3389/fphar.2022.946900

Xue, T., You, Y., Shang, F., and Sun, B. (2012). Rot and Agr system modulate fibrinogen-binding ability mainly by regulating clfB expression in *Staphylococcus aureus* NCTC8325. *Med. Microbiol. Immunol.* 201 (1), 81–92. doi:10.1007/s00430-011-0208-z

Yang, C., Qu, L., Wang, R., Wang, F., Yang, Z., and Xiao, F. (2024). Multi-layered effects of Panax notoginseng on immune system. *Pharmacol. Res.* 204, 107203. doi:10.1016/j.phrs.2024.107203

Yang, W., Liu, J., Blažeković, B., Sun, Y., Ma, S., Ren, C., et al. (2018). *In vitro* antibacterial effects of Tanreqing injection combined with vancomycin or linezolid against methicillin-resistant *Staphylococcus aureus*. *BMC Complement. Altern. Med.* 18 (1), 169. doi:10.1186/s12906-018-2231-8

Yoshimura, T., and Takahashi, M. (2007). IFN-gamma-mediated survival enables human neutrophils to produce MCP-1/CCL2 in response to activation by TLR ligands. *J. Immunol.* 179 (3), 1942–1949. doi:10.4049/jimmunol.179.3.1942

Zhang, J., Sun, Y., Wang, Y., Lu, M., He, J., Liu, J., et al. (2014). Non-antibiotic agent ginsenoside 20(S)-Rh2 enhanced the antibacterial effects of ciprofloxacin *in vitro* and *in vivo* as a potential NorA inhibitor. *Eur. J. Pharmacol.* 740, 277–284. doi:10.1016/j.ejphar.2014.07.020

Zhang, L., Wen, B., Bao, M., Cheng, Y., Mahmood, T., Yang, W., et al. (2021). Andrographolide sulfonate is a promising treatment to combat methicillin-resistant *Staphylococcus aureus* and its biofilms. *Front. Pharmacol.* 12, 720685. doi:10.3389/fphar.2021.720685

Zhang, L., Yang, W., Chu, Y., Wen, B., Cheng, Y., Mahmood, T., et al. (2022). The inhibition effect of linezolid with reyanning mixture on MRSA and its biofilm is more significant than that of linezolid alone. *Front. Pharmacol.* 12, 766309. doi:10.3389/fphar.2021.766309

Zhang, Z., Chen, L., Cui, X., Zhang, Y., Hu, Y., Wang, C., et al. (2019). Identification of anti-inflammatory components of raw and steamed Panax notoginseng root by analyses of spectrum-effect relationship. *RSC Adv.* 9 (31), 17950–17958. doi:10.1039/c9ra00906j

Zhou, R., Tardivel, A., Thorens, B., Choi, I., and Tschopp, J. (2010). Thioredoxin-interacting protein links oxidative stress to inflammasome activation. *Nat. Immunol.* 11 (2), 136–140. doi:10.1038/ni.1831

Zhou, Y., Niu, C., Ma, B., Xue, X., Li, Z., Chen, Z., et al. (2018). Inhibiting PSMα-induced neutrophil necroptosis protects mice with MRSA pneumonia by blocking the agr system. *Cell Death Dis.* 9 (3), 362. doi:10.1038/s41419-018-0398-z

frontiers | Frontiers in Pharmacology

TYPE Review
PUBLISHED 31 July 2025
DOI 10.3389/fphar.2025.1592458

Check for updates

OPEN ACCESS

EDITED BY
Marcello Iriti,
University of Milan, Italy

REVIEWED BY
Quansheng Feng,
Chengdu University of Traditional Chinese Medicine, China
omali Y El-khawaga,
Mansoura University, Egypt

*CORRESPONDENCE
Aidong Yang,
aidongy@126.com
Bo Tan,
tbot@163.com

†These authors have contributed equally to this work

RECEIVED 12 March 2025
ACCEPTED 07 July 2025
PUBLISHED 31 July 2025

CITATION
Wang J, Yan Z, Zhang X, Wang S, Jiao L, Zhu B, Tan B and Yang A (2025) Exploring the pathogenesis of acute lung injury and its treatment through Traditional Chinese Medicine: a state-of-the-art review. *Front. Pharmacol.* 16:1592458. doi: 10.3389/fphar.2025.1592458

COPYRIGHT
© 2025 Wang, Yan, Zhang, Wang, Jiao, Zhu, Tan and Yang. This is an open-access article distributed under the terms of the Creative Commons Attribution License (CC BY). The use, distribution or reproduction in other forums is permitted, provided the original author(s) and the copyright owner(s) are credited and that the original publication in this journal is cited, in accordance with accepted academic practice. No use, distribution or reproduction is permitted which does not comply with these terms.

Exploring the pathogenesis of acute lung injury and its treatment through Traditional Chinese Medicine: a state-of-the-art review

Jiayun Wang[1†], Zhiqiang Yan[2†], Xinxin Zhang[3], Shun Wang[1], Liangbo Jiao[1], Binghua Zhu[4], Bo Tan[2*] and Aidong Yang[1*]

[1]The Research Center for Traditional Chinese Medicine, Shanghai Institute of Infectious Diseases and Biosecurity, School of Traditional Chinese Medicine, Shanghai University of Traditional Chinese Medicine, Shanghai, China, [2]Clinical Pharmacokinetic Laboratory, Shuguang Hospital Affiliated to Shanghai University of Traditional Chinese Medicine, Shanghai, China, [3]Department of Oncology, Baoshan Branch, Shuguang Hospital Affiliated to Shanghai University of Traditional Chinese Medicine, Shanghai, China, [4]Department of Emergency & Intensive Care Unit, Shuguang Hospital Affiliated to Shanghai University of Traditional Chinese Medicine, Shanghai, China

Acute Lung Injury (ALI) is a severe and progressive condition characterized by hypoxic respiratory failure, often triggered by multiple contributing factors. It is associated with high morbidity and mortality rates and can advance to Acute Respiratory Distress Syndrome (ARDS) in severe cases. The pathogenesis of ALI involves a complex interplay of pathological mechanisms, including immune-inflammatory responses, disruption of the alveolar-capillary barrier, damage to mesenchymal stem cell organelles, metabolic dysregulation, ferroptosis, and alterations in gut microbiota. From the perspective of Traditional Chinese Medicine (TCM), the development of ALI is primarily attributed to the invasion of toxic pathogens, which result in lung dysfunction. TCM treatment strategies, which emphasize heat-clearing, detoxification, promoting blood circulation, and resolving stasis, have demonstrated promising clinical efficacy. This paper provides a comprehensive analysis of the pathogenesis of ALI and explores the therapeutic mechanisms of TCM compounds and bioactive monomers with potential therapeutic benefits. The goal is to establish a solid theoretical foundation for the clinical application of TCM in ALI treatment and to further validate its scientific rationale.

KEYWORDS

acute lung injury, pathogenesis, treatment, Traditional Chinese Medicine, bioactive compounds

1 Introduction

ALI is characterized by decreased lung volume, reduced lung compliance, and an imbalance in the ventilation-perfusion ratio, which leads to clinical syndromes such as diffuse pulmonary interstitial edema and pulmonary edema. These conditions are primarily caused by lung infections (both bacterial and viral), as well as intrapulmonary or extrapulmonary factors, including lung contusion and sepsis, circulatory disorders associated with extracorporeal circulation, and immune system metabolic dysfunction. The underlying pathological mechanisms involve inflammation of the alveolar and

pulmonary parenchyma, damage to the alveolar-capillary membrane, increased vascular permeability, and neutrophil recruitment (Dong et al., 2024; Mokrá, 2020). Clinically, ALI manifests as severe hypoxemia, changes in pulmonary function due to increased alveolar capillary membrane permeability, pulmonary edema, and respiratory failure.

From the perspective of Traditional Chinese Medicine (TCM), ALI is classified under the categories of "sudden asthma" and "out of the syndrome" with pathogenic factors including heat, toxins, phlegm, and blood stasis. These factors often result from external pathogenic invasions affecting the lungs, internal phlegm accumulation, and subsequent impairment of lung qi, leading to symptoms such as coughing, sputum production, constipation, and irritability. A summary of the common etiology, pathogenesis, and pathological characteristics of ALI from an integrated Chinese and Western medicine perspective is provided in Table 1.

The current treatment landscape for ALI remains limited, with conventional therapies primarily comprising protective mechanical ventilation, glucocorticoid therapy, and fluid management. However, these approaches are often accompanied by significant side effects. For example, glucocorticoids can suppress the hypothalamic-pituitary-adrenal (HPA) axis, potentially leading to osteoporosis and other adverse effect (Schäcke et al., 2002). Similarly, mechanical ventilation, particularly when administered at high pressures or volumes, can aggravate ALI (Del Sorbo et al., 2011). In contrast, TCM offers a promising alternative, with a long-standing history in treating ALI, and has shown unique therapeutic benefits (Zhang et al., 2021; Jiang N. et al., 2021).

Recent years have seen an increase in research exploring the role of TCM in preventing and treating ALI. However, most existing reviews predate 2022 and do not incorporate the latest findings from the past 2 years (Liu Y. et al., 2024; Zhang, 2020). This paper aims to address this gap by providing a comprehensive review of significant advancements in ALI research over the past 5 years, with particular focus on recent discoveries related to its pathogenesis and molecular mechanism. Special attention is given to the pharmacological mechanisms and clinical application research of TCM in treating ALI since 2022, as well as the clinical efficacy of newly identified TCM formulations and their active components. By integrating the latest insights from both traditional Chinese and Western medicine, this review seeks to offer innovative strategies and perspectives for the holistic treatment of ALI.

2 Mechanisms of ALI pathogenesis

The pathogenesis of ALI is highly complex, involving a variety of physiological and pathological processes, including immune cell disfunction, alterations in cytokine profiles, disruption of the alveolar gas-blood barrier, organelle dysfunction, and ferroptosis. While classical mechanisms such as oxidative stress and inflammatory responses have been extensively discussed (Su et al., 2012), this review will briefly summarize these fundamental aspects while highlighting recent advancements and novel insights in ALI research over the past 5 years.

2.1 Dynamic alterations in immune cell composition and functionality

Dysregulation of the inflammatory response is a pivotal factor in ALI pathogenesis, encompassing not only aberrant expression of inflammatory factors but also intricate alterations in immune cell phenotypes and functions. Recent advances in cutting-edge technologies, such as single-cell sequencing, spatial transcriptomics, and spatial metabolomics, have enabled researchers to analyze the dynamic changes in cell types, migration patterns, and complex interaction networks within the lung microenvironment with unprecedented precision (Yu Y. et al., 2024; Wang Y. et al., 2024). These breakthroughs have significantly enhanced our understanding of ALI's pathological mechanisms and provided novel directions for developing precision treatment strategies. This sections reviews recent progress on lung immune cell lineages in ALI, focusing on functional changes, underlying mechanisms, and their implications for disease progression.

2.1.1 Alveolar macrophages

As the primary innate immune effector cells in the lung, alveolar macrophages play a critical role in ALI. Upon pathogen invasion, they promote the secretion of pro-inflammatory cytokines, which polarize neutrophils and mononuclear macrophages, and activating effector T cells. In the early stages of ALI, intratracheal administration of lipopolysaccharide (LPS) induces necrosis of alveolar macrophages and releases IL-1α, compromising the integrity of pulmonary endothelial cells (PEC) and facilitating neutrophil extravasation, thus exacerbating ALI progression (Dagvadorj et al., 2015). Macrophage polarization enhances the expression of pro-inflammatory cytokines (e.g., TNF-α, IL-6, IL-12) and chemokines (e.g., CCL8, IL-23), as well as oxidative stress factors like COX-2 and iNOS, all of which contribute to lung injury (Chen et al., 2020). Additionally, macrophages activate the NLRP3 inflammasome by upregulating key enzymes in the glycolysis signaling pathway, including HK1 and PKM2, which accelerate pyroptosis (Luo et al., 2022). Myeloid cells also express triggering receptor 1 (TREM-1), which reprograms macrophage metabolism, enhances glycolytic activity, activates the NLRP3 inflammasome, and triggers an inflammatory response in ALI (Zhong, 2023). The process of panoptosis in macrophages during ALI is regulated by the ZBP1 transcription factor. Knockdown of ZBP1 reduces key markers of inflammation and cell death (e.g., Caspase-3 p17/19, Caspase-1 p20, GSDMD p35, and Phospho-MLKL), thereby alleviating ALI in septic mice (Sun, 2024).

2.1.2 Neutrophils

In ALI, capillary endothelial and epithelial cells sustain significant damage, while alveolar macrophages are activated to release cytokines (e.g., TNF-α, IL-1β) and chemokines, recruiting neutrophils into the lungs (Bhatia et al., 2012). Infiltrating neutrophils degranulate, releasing bactericidal proteins and pro-inflammatory cytokines, further exacerbating the inflammatory response (Aulakh, 2018). External stimuli can activate neutrophils, leading to the formation of neutrophil extracellular traps (NETs) and the release of reactive oxygen species (ROS) and proteases. This process activates the NLRP3 inflammasome, releasing inflammatory mediators and aggravating lung tissue

injury (Li et al., 2018; Lin and Fessler, 2021; Lefrançais et al., 2018). In LPS-induced ALI models, Glycoprotein VI (GPVI) promotes neutrophil recruitment, platelet-neutrophil complexes and NETs, which subsequently trigger an inflammatory response (Burkard et al., 2023). The interaction between protein and fibrinogen in serum, via β-integrin on neutrophil surfaces, induces degranulation, abnormal neutrophil aggregation, and increased vascular permeability, contributing to ALI development (Soehnlein et al., 2008).

2.1.3 T lymphocytes

T cells are pivotal in ALI pathogenesis. Regulatory T cells (Tregs) suppress the proliferation and differentiation of lung fibroblasts during LPS-induced lung inflammation (Tan et al., 2019; Seyran et al., 2023). Th17 cells, a subset of T helper cells, contribute significantly to host defense by secreting pro-inflammatory cytokines (e.g., IL-17A/F, IL-21, and IL-22) (Sakaguchi et al., 2016). At the molecular level, upregulation of IL-10 expression and inhibition of IL-35, RAGE, and Caspase-1 expression can attenuate T cells differentiation and mitigate ALI (Xie et al., 2021). In sepsis-induced ALI patients, elevated plasma nicotinamide phosphoribosyl transferase (NAMPT) levels induce T cells pyroptosis and immune dysfunction, which can be alleviated by the NAMPT inhibitor FK886 (Zheng, 2020).

2.1.4 Other immune cells

Eosinophils, derived from bone marrow hematopoietic stem cells, play a role in immune regulation and allergic responses. Reduced eosinophil levels increase the risk of lung inflammation and mortality (Grisaru-Tal and Rothenberg, 2022). Conversely, IL-33-induced eosinophilia can mitigate the inflammatory response associated with *Staphylococcus aureus* lung infections (Krishack et al., 2021). Additionally, Natural killer (NK) lymphocytes can significantly alleviate inflammatory cell infiltration in lung immune injury and reduce the expression of IFN-γ expression in bronchoalveolar lavage fluid (Li et al., 2012).

2.2 Abnormal immune cytokines

2.2.1 Interleukins and tumor necrosis factor

In ALI and ARDS, inflammatory mediators such as TNF-α, IL-1β, and IL-6 play a central role by mediating Cytidine monophosphate kinase 2 (CMPK2) (Chen D. S., 2022; Wang et al., 2021). IL-10 and IL-18 are critical in lung infections, compromising cell membrane integrity, stimulating alveolar neutrophils to produce chemokines, and promoting fibrosis via TGF-β and SMAD4 activation. This leads to production of pro-fibrotic proteins (e.g., ZO-1, MUC2) and fibroblast markers (e.g., FGF-1, αSMA) in epithelial cell, resulting in mesenchymal transformation and extracellular matrix collagen accumulation (Wang K. et al., 2022; Kandikattu et al., 2023). IL-33 induces neutrophil infiltration, increases alveolar endothelial barrier permeability and triggers alveolar epithelial cell death (Zou et al., 2023).

2.2.2 Cell chemokines

Chemokines LCN2 and CCN3 regulate inflammatory responses in ALI. LCN2 enhances M2-type macrophage proportions via IL-6 and TNF-α (Zheng, 2023), while CCN3 promotes NF-κB p65, TGF-β1, TGF-βRII, and p-Smad2/3 expression, increasing IL-6 and TNF-α production (Zhu et al., 2020). Knockdown of CCL2 reduces mononuclear macrophage recruitment and increases neutrophil expression, mitigating viral-induced lung injury (Lai et al., 2017). The CRTH2 receptor antagonist CT-133 improves macrophage and neutrophil infiltration, inhibits pulmonary vascular permeability, and suppresses inflammatory factor expression (Hussain et al., 2019).

2.2.3 Other factors

Interferon (IFN) inhibits inflammatory responses to bacterial and viral infections and associated ALI (Verma et al., 2022). Inflammatory mediators activate the NLRP3 inflammasome in polymorphonuclear neutrophils (PMNs) and alveolar macrophages (AMs) (Cui et al., 2024). Heat shock protein HSP70 promotes lung inflammation in ALI mice but reduces CD36 receptor expression (Chen Y., 2022).

2.3 Impaired alveolar gas-blood barrier

In ALI, the alveolar-capillary barrier's function is compromised, increasing capillary permeability and protein leakage into alveoli (Esquivel-Ruiz et al., 2021). Apoptosis plays a key role in this process; modulation of apoptotic genes (e.g., Caspase-3, Caspase-8) can enhance cell viability and mitigates inflammation (Yang et al., 2021; Ju et al., 2018; Li X. et al., 2019). The pulmonary intravascular glycocalyx, composed of hyaluronan (HA), heparan sulfate proteoglycan (HSPG), Syndecan-1, and Glypican-1, degrades during ALI, reducing lung surface protein expression (e.g., VE-Cadherin, Occludin, VCAM-1, E-selectin) (Chen et al., 2021; Cao et al., 2023). Alveolar epithelial cell apoptosis disrupts barrier integrity via the DAPK1 ligand pathway (Wang Y. et al., 2020). Cytoskeletal protein stability is crucial for barrier maintenance, facilitating intracellular signaling, tight junctions, and alveolar permeability (Yang et al., 2023). Inhibition of MMP-9 degradation, stabilization of endothelial cytoskeletal proteins, and Rho kinase pathway-mediated cytoskeletal remodeling have been shown to alleviate lung injury (Müller et al., 2019; Wu et al., 2016).

2.4 Mesenchymal stem cells (MSCs)

Mesenchymal stem cells (MSCs) have emerged as a promising therapeutic avenue for ALI due to their self-renewal capacity, multidirectional differentiation potential, and ability to modulate inflammation and fibrosis. Exosomes derived from bone marrow-derived MSCs (BM-MSCs) have been shown to inhibit several key inflammatory proteins, such as p65, IKKβ, p-IκBα, p-IκBβ, Caspase-1, GSDMD, and NLRP3, thereby suppressing macrophage pyroptosis (Xiao et al., 2020; Liu P. et al., 2024). Human placental MSCs (hPMSCs) protect the alveolar epithelial barrier through the ACE2/Ang (1–7) axis, downregulating TNF-α, IL-1, IL-6, and IL-10 levels, and alleviating endothelial injury (Yu W. et al., 2024; Xu et al., 2020). Human umbilical cord MSCs

(hUC-MSCs) promote Trem2 expression, inhibit the NRF2/NF-κB/NLRP3 pathway, and reduce the release of TNF-α, IL-6, and IL-1β (Che et al., 2024). Overall, MSCs show considerable potential in the treatment of ALI, particularly in terms of protecting the alveolar barrier, modulating inflammatory responses, and exerting anti-fibrotic effects. Future research will aim to optimize MSC-based therapies, enhancing their efficacy and safety for clinical application.

2.5 Abnormal organelle function

2.5.1 Endoplasmic reticulum stress (ERS)

Endoplasmic reticulum stress (ERS) has been recognized as a significant contributor to ALI pathogenesis (Mo and Hu, 2019). ERS can induce M1 macrophage polarization, disrupting the balance between M1 and M2 macrophages and driving excessive inflammation. Specifically, the IRE-1/XBP-1 signaling pathway activated by ERS, leads to lung epithelial cell death and NLRP3 inflammasome activation, thereby accelerating ALI progression (Zhao et al., 2020; Uddin and Barabutis, 2019).

2.5.2 Abnormal mitochondrial function

Mitochondrial dysfunction plays a central role in ALI, with mitochondrial autophagy, dynamic imbalance, and metabolic dysfunction contributing to disease progression (Zong et al., 2024). This section focuses on mitochondrial autophagy and dynamic imbalance, while mitochondrial metabolic abnormalities are addressed in Section 2.7.

2.5.2.1 Mitochondrial autophagy

Mitochondrial autophagy, or mitophagy, is essential for maintaining cellular homeostasis and preventing inflammation by removing damaged mitochondria. Disruption of mitophagy can lead to release of mitochondrial DNA (mtDNA), which activates Toll-like receptor 9 (TLR9), triggering inflammation. Elevated mitophagy, induced by deficiency in serine-activated protein kinase 3 (MMK3), enhances histone deacetylase activity and exacerbates lung injury (Tan and Chen, 2020). The PINK1/PARKIN pathway is pivotal in mitophagy regulation, where NLRP3 upregulates PINK1 expression, promoting mitophagy. However, inhibition of PINK1 abolishes this effect. PARKIN-mediated degradation of PARIS increases PGC-1α expression, promoting mitochondrial biogenesis and offering protection against hyperoxia-induced damage (Um and Yun, 2017).

2.5.2.2 Mitochondrial dynamic imbalance

Imbalance between mitochondrial fusion and fission also contribute to ALI. In LPS-induced ALI models, fusion proteins Mfn1/2 and OPA1 are downregulated, while fission proteins Drp1 and Fis1 are upregulated, disrupting mitochondrial function and morphology (Shi et al., 2021). Additionally, activation of the Panx1 gene triggers the CAN-DRP1 signaling pathway, inducing mitochondrial dynamic imbalance, disrupting tight junctions, and promoting apoptosis, all of which contribute to ALI (Xu, 2023).

2.6 Iron death (ferroptosis)

Ferroptosis, an iron-dependent form of cell death characterized by lipid peroxidation, exacerbates ALI by causing oxidative damage to the alveolar membrane. In LPS-induced ALI models, elevated Fe^{2+} levels, decreased expression of ferroptosis markers (SLC7A11, GPX4), and increased lipid peroxidation (measured by propylene glycol) are observed in bronchial epithelial cells (Cai et al., 2022a). In sepsis-induced ALI, reduced GPX4 expression and increased MDA and Fe^{2+} levels further worsen lung injury (Cao et al., 2022; Long et al., 2020). Conversely, silencing mixed lineage kinase 3 (MLK3) mitigates LPS-induced epithelial damage by inhibiting p53-mediated ferroptosis (Liu et al., 2020). Furthermore, deficiency in the UTX/UTY protein family alleviates LPS-induced ALI by blocking ferroptosis in alveolar epithelia through NRF2 activation (Peng et al., 2021).

2.7 Metabolic disorders

Metabolic dysregulation plays a crucial role in ALI and ARDS, with altered sugar, lipid, amino acid, and glutathione metabolism being key contributors to disease progression (He et al., 2024).

2.7.1 Sugar metabolism

During M1-type macrophage polarization, hexokinase (HK) transitions from the low-affinity isoform HK4 to the high-affinity isoform HK2, which exhibits enhanced catalytic activity (Bustamante and Pedersen, 1977). HK2 binds to mitochondrial voltage-dependent anion channels (VDAC), localizing to the outer mitochondrial membrane (Wang et al., 2014). Polyunsaturated fatty acids (PUFAs) inhibit HK2 binding to VDAC (Colquhoun, 2002), acting as anti-inflammatory agents that promote the conversion from the M1 to the M2 phenotype (Kawano et al., 2019). HK2 expression correlated with the SLC7A11/GPX4 axis, and HK2 deficiency results in increased macrophage death (Tan et al., 2022). PKM2, upregulated in M1 macrophages, regulates the Warburg effect by translocating to the nucleus and binding HIF-1α, promoting the inflammatory metabolic response that exacerbates lung injury (Yu et al., 2021; Christofk et al., 2008; Wang J. et al., 2022). Reducing PKM2 activity enhances the Warburg effect, further driving lung injury (Li et al., 2021). Nrf2 is a key regulator of glucose metabolism, and its knockdown reduces the expression of glycolytic genes, inhibiting the glycolytic pathway (Osburn et al., 2006; Zhang et al., 2018).

2.7.2 Lipid metabolism

Phospholipid hydroperoxides, derived from PUFAs, are key products of lipid peroxidation and play a significant role in ALI. Fatty acyl-CoA synthase long-chain family member 4 (ACSL4) participates in lipid biosynthesis and catalyzes the conversion of PUFAs to PUFA-PLS, compromising plasma membrane integrity (Wang Y. et al., 2022). HIF-1α binds to the ACSL4 promoter and negatively regulates its transcription, while activating Nrf2 to enhance glycolysis (Li et al., 2024). Some hydroperoxides, along with free PUFAs, act as substrates for lipid signaling. The esterification of PUFAs to acyl-CoA by long-chain acyl-CoA

TABLE 1 Etiology, Pathogenesis and pathological Characteristics of ALI from an Integrated Chinese and Western Medicine Perspective.

Etiological categorization	Specific causes	Pathogenesis in traditional Chinese medicine	Pathology in western medicine	Document source
Infectious agent	Bacteria, Virus	Pathogenic factors such as wind-cold or wind-heat enter the body through the mouth and nose, invading the lungs. This disrupts the lung's functions of dispersing and descending qi, leading to qi stagnation and impaired distribution of body fluids. Over time, this results in the production of phlegm, which obstructs the lungs, further exacerbating respiratory dysfunction	Viral infections and bacterial proliferation in the lungs lead to the release of metabolites, which initiate inflammatory responses and cause subsequent tissue damage	McKelvey et al. (2024)
	Pyemia	Internal deficiency of vital qi, accumulation of toxic heat, obstruction of qi circulation, and the formation of blood stasis	The body becomes susceptible to external infections, resulting in an imbalanced inflammatory response and weakened immune function	Zeng (2019), Van der Poll et al. (2017)
Non-infectious Factor	Hemorrhagic shock induced by mechanical trauma	/	Pulmonary vascular protein leakage, neutrophil recruitment, and overexpression of proinflammatory factors, among other pathophysiological changes, lead to persistent and severe hypoxemia	Hao (2023)
The perfusion of the extracorporeal circulation system is compromised	Reperfusion following ischemic events	/	The imbalance between SOD and MDA in lung tissue led to the release and accumulation of oxygen free radicals within mitochondria, consequently increasing pulmonary vascular permeability and resulting in pulmonary edema, hypoxemia, and pulmonary hypertension	Shen et al. (2019)
Metabolic dysfunction within the immune system	Septicemia	The invasion of exogenous pathogens results in blood stasis and obstruction, internal accumulation of heat-toxin, and qi-yin deficiency	Bacterial toxins multiply in the bloodstream and spread systemically, causing toxic alterations in various tissues and organs. These alterations include pulmonary cellular turbidity, focal necrosis, and infiltration of inflammatory cells	Wang and Wang (2023), Xu Y. et al. (2024)

synthetase and their subsequent incorporation into membrane phospholipids contributed to ALI pathogenesis by activating toll-like receptors, thereby exacerbating inflammation (Zou et al., 2019; Imai et al., 2008).

2.7.3 Amino acid and glutathione metabolism

Glutathione (GSH), an important antioxidant, plays a crucial role in reducing reactive oxygen species (ROS) and preventing oxidative damage (Xie et al., 2016). GSH synthesis depends on the cystine/glutamate antiporter system, which exchanges extracellular cystine for intracellular glutamate, a precursor for GSH synthesis. Under the catalytic activity of GPX4, GSH reduces lipid hydroperoxides to non-toxic alcohols, with its depletion leading to increased oxidative stress and cell death (Yang et al., 2014). Fatty acid-binding proteins derived from glutathione can mitigate ALI by modulating inflammatory responses and inhibiting Grx1 expression (Guo Y. et al., 2021).

2.7.4 Mitochondrial metabolism disorder

Mitochondria are central to cellular energy metabolism, and their dysfunction contributes significantly to ALI. Pathological mitochondrial changes, such as shrinkage, altered membrane density, and compromised membrane integrity, are common in ALI. Inhibition of Mucin-1 dimerization disrupts mitochondrial function by downregulation GPX4, GSH and SOD expression, leading to lipid peroxide accumulation and mitochondrial damage. Targeted mitochondrial antioxidants, such as MitoQ, can reduce mitochondrial ROS, inhibit ferroptosis, and alleviate ALI (Kufe, 2020; Wang Y. M. et al., 2022; Zhan et al., 2022; Bock and Tait, 2020).

2.7.5 Other regulatory mechanisms

Exosome, small vesicles containing RNA and proteins, serve as important mediators of intracellular communication, immune responses, and cellular regulation (Wang and Zhu, 2019; Jiang et al., 2019; Tavasolian et al., 2021). In ALI, exosomes derived from alveolar macrophages have been shown to regulate the Hippo signaling pathway via tRNA-derived fragments, participating in LPS-induced ALI (Wang W. et al., 2022).

2.8 Intestinal bacteria factor

The intestinal microbiota, comprising bacteria like *Escherichia coli* and *Lactobacillus*, plays a critical role in immune modulation (Zhou et al., 2020). Disruption of the gut microbiota can lead to

systemic inflammation, contributing to ALI. Research suggests that the TLR-endoplasmic reticulum stress-ROS signaling pathway, activated by intestinal barrier dysfunction with gut microbiota, exacerbates lung injury by promoting systemic inflammatory responses (Gong et al., 2022).

3 Study on mechanism of TCM treatment of ALI

3.1 Compounds

Recent studies on the use of TCM for ALI have largely focused on therapies aimed at clearing heat and detoxifying, regulating fu-organs, and resolving blood stasis. Over the past 3 years, a significant body of clinical research has emerged in investigating TCM compound treatments for ALI (Gasmi et al., 2024; Ren, 2020; Li and Liang, 2019; Guo J. et al., 2021). These studies have helped to deepen our understanding of the mechanisms through which TCM influences ALI, establishing a foundation for evaluating the clinical efficacy of TCM-based therapies and supporting the development of novel therapeutic agents in the future.

3.1.1 Heat clearance and detoxification

The development of ALI is closely linked to the accumulation of pathogenic heat, which invades the lungs, cause fluid injury, depletes qi, and obstructs lung qi. Therefore, heat-clearing prescriptions are a key therapeutic approach in TCM for treating ALI (Lu et al., 2020). Studies have demonstrated that TCM formulas like Shenlian and Retong Fang markedly reduced mRNA levels of inflammatory factors (IL-6, IL-18 and MCP-1) and decrease protein levels of CD68, SP-A, and CC16 in rat lung tissue with ALI (Yang et al., 2022; Zhang et al., 2010).

The Wenqing Decoction has been found to inhibit the PI3K/AKT signaling pathway, reducing levels of TNF-α, IL-6, IL-1β, RAGE, and various phosphorylated proteins (PI3K, AKT, p-PI3K, p-AKT) (Xie et al., 2024). Chaihuqingwen and Zukamu Granules have also proven effective by inhibiting phosphorylation of NLRP3, TLR4, NF-κBp65, and IκBα in rat lung tissue, along with caspase-1 mRNA and protein expression, thus modulating inflammatory responses (Zhou et al., 2023; Yu C. et al., 2024).

The Qingfeilitan Formula reduces mRNA levels of TNF-α, IL-6, IL-1β, and MDA in alveolar lavage fluid, while increasing the activity of antioxidants like SOD and GSH-Px, providing anti-inflammatory and antioxidant effects (Diao et al., 2022). Similarly, Qingfei Paidu Decoction inhibits macrophage polarization, downregulates IL-6, TNF-α, MIP-2, MCP-1, upregulates IL-10, and reduces nuclear translocation of key inflammatory mediators (TAK1, IKK, and p65) (Ye et al., 2023).

Additionally, some formulas like Yindan Jiedu Capsule, Xuanfei Baidu Decoction and Tanreqing target various inflammatory pathways, including the MAPK/NF-κB and NF-κB signaling pathways, offering broad anti-inflammatory effects (Feng et al., 2022; Li et al., 2023; Hu et al., 2022). Shufengjiedu Capsule prevents macrophage apoptosis by increasing A2A adenosine receptor expression and inhibiting NF-κB phosphorylation (Cai et al., 2022b). Maxingshigan Decoction has been found to reduce lung inflammation, enhance antioxidant activity, and regulate key inflammatory pathways including MAPK/NF-κB pathway (Hou et al., 2023).

Qingjie Huagong Formula has shown promise in improving lung and pancreatic and lung tissue pathology in SAP-ALI rat models, inhibiting the PI3K/AKT1 signaling pathway (Feng et al., 2024). Gegen Qinlian Decoction has been found to reduce lung inflammation, enhance antioxidant activity, and suppress C3, C5a, and IL-17 expression (Li W. et al., 2022).

3.1.2 The catharsis category of promoting bowel clearance and pulmonary Detoxification (Tongfu)

The Tongfu approach, known for its cathartic properties, is crucial in managing ALI. Tongfu Formula, in particular, inhibits the expression of pro-inflammatory cytokines (IL-6, IL-1β, IL-18), STING pathway components (p-STING, STING) and inflammasome proteins (NLRP3, ASC) in mice with sepsis-induced ALI (Huo and Yue, 2024). Similarly, Tongfu Xiefei Enema Solution reduces mRNA expression of TNF-α, IL-1β, and p38 MAPK, as well as the protein expression of p38, p-MLC/MLC2, and MLCK, contributing to improved ALI outcomes (Ma et al., 2024).

Tingli Dazao Xiefei Decoction and Xuanbai Chengqi Decoction demonstrate efficacy in reducing inflammation by regulating the PI3K, mTOR, HIF-1α, and p-AKT/AKT pathways, while also inhibiting glycolysis in lung tissue (Zhang et al., 2023; Wang S. et al., 2024; Zhu et al., 2021). Research into lung-intestinal co-treatment for ALI has shown that the Dachengqi Decoction alleviates inflammation by regulating the NF-κB/NLRP3 signaling pathway (Kou et al., 2022).

3.1.3 Enhancing blood circulation and resolving blood stasis

TCM formulas aimed at enhancing blood circulation and resolving blood stasis, such as Huoxue Huayu Decoction, play a significant role in treating ALI by activating qi and promoting blood flow. These formulas help mitigate lung damage and enhance the expression of tight junction proteins (ZO-1, Occludin, AQP-1, AQP-5) in the lung gas-blood barrier (Qin et al., 2025).

Qidong Huoxue Yin inhibits apoptosis in lung epithelial cells and reduces inflammatory cytokines like TNF-α, IL-6, and chemokines in mice with ALI (Zheng et al., 2021). Xuebijing Injection mitigates inflammatory infiltration in ALI by antagonizing neutrophils and other immune cells (Zheng and Zhang, 2024). Other formulas, such as Qilongtian Capsule and Mailuo Yin regulate the NF-κB pathway and suppress inflammation by reducing the phosphorylation of MyD88, IκBα, and NF-κB (Luo et al., 2024; Miao et al., 2022).

3.1.4 Other formulas

Formulas like Xiaoxuming Decoction, traditionally used for stroke treatment, have shown potential in alleviating lung inflammation associated with ALI (Pei et al., 2023). Research indicates that Xiaoxuming decoction reduces levels of TNF-α, IL-1β and IL-8 in LPS-induced cells and mitigates pyroptosis by inhibiting key inflammasome proteins (USP9X, NLRP3, IL-1β, Caspase-1) (Xiang et al., 2022; Xiang et al., 2021).

Similarly, both Jiegeng Decoction and Compound Houttuynia mixture reduce oxidative stress and inflammatory responses by

inhibiting ROS production, mitochondrial membrane potential polarization, and the expression of inflammatory mediators, apoptotic proteins (Cleaved Caspase 3, Bax, Bcl2) and pyrogenic proteins (p-NF-κB,NLRP3, ASC, Cleaved-Caspase 1 and Cleaved-GSDMD) (Li, 2023; Wei, 2024). Further details are provided in Table 2, Figure 1.

3.2 Monomer components

This section systematically investigates the effects of monomer components with clinical therapeutic potential for treating ALI. These monomers have demonstrated diverse mechanisms of action, suggesting their promise as effective treatments for ALI.

3.2.1 Tanshinone IIA

Tanshinone IIA, when combined with carvedilol and simvastatin, is commonly used to treat cardiovascular diseases such as coronary heart disease and heart failure (Shao et al., 2022). Recent research has shown that tanshinone IIA can mitigate ALI by inhibiting key signaling molecules, including ROCK2, NF-κB, Pro-caspase, P65, and IκBα, all of which play roles in inflammation and cell death (Liu J. et al., 2022).

3.2.2 Artemisinin

Known for its broad therapeutic potential against conditions like tumors, rheumatoid arthritis, and skin inflammation (Zhao et al., 2024; Liu Y. J. et al., 2022), artemisinin has also shown promise in ALI treatment. Studies suggest it alleviates lung injury by suppressing inflammatory factors, myeloperoxidase (MPO), malondialdehyde (MDA), and other oxidative stress markers. Additionally, it reduces the expression of p-AKT and HO-1 proteins, contributing to its protective effects on the lung injury (Ji et al., 2023).

3.2.3 Glycyrrhizin

Glycyrrhizin, and its derivatives, have been shown to reduce serum inflammatory markers and transaminase levels in viral hepatitis (Guo, 2024). In ALI, glycyrrhizin helps by inhibiting ROS production in LPS-induced cells, downregulating p-PI3K and p-AKT protein levels, and reducing the formation of NLRP3 inflammasome. These actions help protect against ALI by mitigating oxidative stress and inflammation (Wang K. et al., 2020).

3.2.4 Andrographolide

Primarily used to treat bacterial pneumonia and other inflammatory conditions (Xu, 2016; Song, 2022), andrographolide has been shown to inhibit NLRP3 inflammasome activation, reducing inflammatory factor and alleviating lung epithelial cell damage (Qin et al., 2024).

3.2.5 Huperzine-A

Typically used in the treatment of neurodegenerative diseases like Alzheimer's disease and vascular dementia (Wang et al., 2023; Lu et al., 2021), huperzine-A also exhibits nti-inflammatory effects in ALI. It reduces levels of IL-6, MDA, and ROS, while increasing SOD levels, which contribute to its therapeutic effects in lung injury (Shi et al., 2024).

3.2.6 Cepharanthine

Although primarily used to treat leukopenia in cancer patients undergoing chemotherapy, cepharanthine has shown potential in treating ALI by improving immune function and reducing inflammation (Ge et al., 2023). Stephanolin, a related compound, has been shown to reduce viral RNA and virus production, suggesting its potential in viral-induced ALI (Fan et al., 2020).

3.2.7 Chloroquine

As a 4-aminoquinoline antimalarial drug, chloroquine is alsoused to treat autoimmune diseases like rheumatoid arthritis. It works by improving lysosomal pH, inhibiting autophagosome-lysosome fusion, and enhancing CXCR4 expression, thereby reducing inflammation and alleviating ALI (Yan et al., 2013).

3.2.8 Total paeony glycosides

These compounds inhibit mitochondrial ROS (mtROS) oxidative stress and block NLRP3 inflammasome activation. This significantly contributes to the treatment of ALI by reducing inflammation and cellular damage (Xu Y. J. et al., 2024).

3.2.9 Diacerein

As a derivative of rhein, diacerein is commonly used for degenerative joint diseases. Recently, diacerein has demonstrated potential in treating ALI by reducing the Sphk1/S1P axis and inhibiting GSK-3β, STAT3, and Caspase-3. It also increases BCL-2 protein expression, which plays a role in cell survival and inflammation regulation (Youssef et al., 2022). Further details are provided in Table 3, Figure 2.

4 Clinical research on the treatment of acute lung injury with Traditional Chinese Medicine

4.1 The significance and current status of clinical research

The application progress of traditional Chinese medicine (TCM) in the clinical treatment of acute lung injury (ALI) is substantial, demonstrating promising therapeutic potential. As research advances from cell culture to clinical trials, findings from basic studies are increasingly being translated into clinical practice. Randomized controlled trials (RCTs) serve as a critical methodology for evaluating the efficacy of TCM interventions in ALI. These trials provide valuable evidence and a scientific foundation for understanding the potential benefits of TCM in managing ALI (Zheng et al., 2024).

In recent years, a growing number of high-quality clinical studies have demonstrated the notable efficacy of traditional Chinese medicine (TCM) in treating acute lung injury (ALI). Particularly within an integrated treatment framework combining both TCM and Western medicine, this approach has been shown to effectively alleviate clinical symptoms, modulate inflammatory responses, improve oxygenation function, and significantly reduce patient mortality rates.

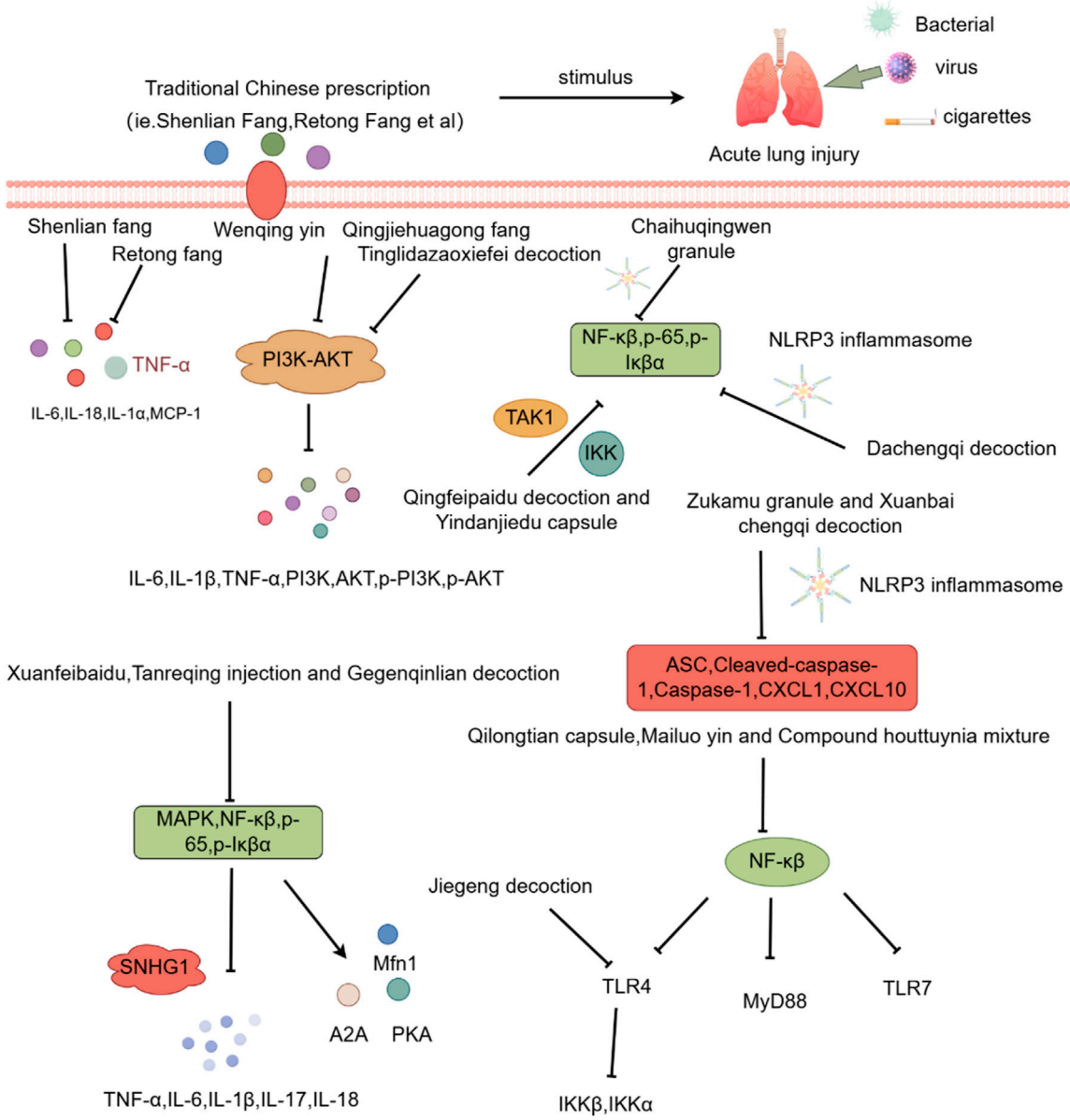


FIGURE 1
Investigation into the mechanism of TCM Compound in treating ALI.

4.2 Clinical evidence of integrated traditional Chinese and Western medicine in treatment

4.2.1 Clinical application of compound preparations

4.2.1.1 Baofeijiejiong mixture

A randomized controlled study involving 60 patients with acute lung injury (ALI) caused by sepsis demonstrated that the integration of traditional Chinese and Western medicine treatments—specifically Pulmonary Protective and Baofeijiejiong mixture—significantly reduced the 7-day mortality rate among ALI patients compared to treatment with Western medicine alone. Furthermore, this integrative approach enhanced the overall efficacy of Western medical treatment. Following the intervention, notable improvements were observed in traditional Chinese medicine (TCM) symptom scores, including symptoms such as fever, dyspnea, and sputum production. Inflammatory markers, such as IL-8 and TNF-α, showed a marked decrease, while organ function indicators, including SOFA and APACHE II scores, significantly improved. Additionally, levels of biomarkers such as white blood cell count, C-reactive protein (CRP), and procalcitonin (PCT) were also reduced. Importantly, this therapeutic strategy decreased the need for invasive mechanical ventilation, thereby lowering the incidence of acute respiratory distress syndrome (ARDS) and multiple organ dysfunction syndrome (MODS) in patients with sepsis-induced ALI (Su, 2015).

4.2.1.2 Dachengqi Decoction

In a clinical study involving 68 patients with acute lung injury (ALI), administration of Dachengqi Decoction via nasogastric feeding

TABLE 2 Summary of TCM Compounds for the prevention and treatment of ALI.

Principles of TCM	Herb/ Compound	Signal pathway	Dose	Index detection	Constitution
Heat Clearance and Detoxification	Shenlian Fang	/	8.64 g/kg	IL-6, IL-18, IL-1α, MCP-1, SP-A, CC16↓	*Panax ginseng* C. A. Mey., *Coptis chinensis* Franch., *Setaria italica* (L.) Beauv., *Citrus reticulata* Blanco, *Nelumbo nucifera* Gaertn., *Poria cocos* (Schw.)Wolf, et al.
	Retong Fang	/	1 g/kg	TNF-α, IL-6, IL-18, IL-1α↓	*Arnebia euchroma* (Royle) Johnst., *Eschenbachia blinii* (H.Lév.) Brouillet, *Gentiana macrophylla* Pall., et al.
	Wenqing Yin	PI3K/AKT	10.8 g/kg	TNF-α, IL-6, IL-1β, RAGE, PI3K, p-PI3K, AKT, p-AKT↓	*Angelica sinensis* (Oliv.)Diels, *Paeonia lactiflora* Pall., *Ligusticum chuanxiong* Hort., *Coptis chinensis* Franch., et al.
	Chaihuqingwen Granule	TLR4/NF-κB/NLRP3	8 g/kg	TLR4, NLRP3, NF-κB p65, p-IκBα↓	*Bupleurum chinense* DC., *Astragalus membranaceus* (Fisch.) Bge., *Lonicera japonica* Thunb., *Coix lacryma-jobi L.var.mayuen* (Roman.) Stapf, et al.
	Zukamu Granule	NLRP3/Caspase-1/GSDMD	2.34 g/kg	NLRP3, ASC, Caspase-1, Cleaved-caspase-1 p20, IL-1β, IL-18↓	*Rheum palmatum* L., *Glycyrrhiza uralensis* Fisch., *Mentha haplocalyx* Briq., et al.
	Qingfeilitan Formula	TNF-α,Toll-Like	10 mg/mL	TNF-α, IL-6, IL-1β↓; SOD, GSH-Px↑	*Gypsum* Fibrosum, *Scutellaria baicalensis* Georgi, *Trichosanthes kirilowii* Maxim., et al.
	Qingfei Paidu Decoction	TAK1/IKK/NF-κB	/	IL-6, TNF-α, MIP-2, MCP-1, TAK1, IKK p-p65↓; IL-10↑	*Ephedra sinica* Stapf, *Prunus armeniaca* L.var.ansu Maxim., *Poria cocos* (Schw.)Wolf, *Bupleurum chinense* DC., et al.
	Yindan Jiedu Capsule	NF-κB	30% medicated serum	IκBα/p-IκBα, p65, TNF-α, IL-6, IL-1β, NO↓	*Morus alba* L., *Scutellaria baicalensis* Georgi, *Descurainia Sophia* (L.)Webb. ex Prantl., *Lonicera japonica* Thunb., *Scrophularia ningpoensis* Hemsl., et al.
	Xuanfei baidu Decoction	MAPK/NF-κB	0.5 mg/mL; 2.16 g/kg	p-IKKα, p-NF-κB, p-IκBα, p-p38, p-Erk, TNF-α, IL-6, IL-1β, PGC-1α, LC3B, Nrf1, JC-1, NLRP1, NLRP3, Caspase11↓; Mfn1, Mfn2, ATP↑	*Ephedra sinica* Stapf, *Prunus armeniaca L.var.ansu* Maxim., *Gypsum* Fibrosum, *Coix lacryma-jobi L.var.mayuen* (Roman.)Stapf, *Atractylodes lancea* (Thunb.)DC., et al.
	Tanreqing	HMGB1/NF-κB/SNHG1	4 mL/kg	p-p65, p-p38, HMGB1, SNHG1, TNF-α, IL-6, IL-1β, IL-18, MCP-1, ROS↓	*Scutellaria baicalensis Georgi*, *Selenarctos thibetanus* (*G. Cuvier*), *Capra hircus* L
	Shufeng Jiedu Capsule	A2A/NF-κB	0.5 mg/mL	A2A, p-IκB/IκB, p-p65/p65, Cc3, Bax/Bcl-2↓; PKA↑	*Polygonum cuspidatum Sieb. et* Zucc., *Forsythia suspensa* (Thunb.)Vahl, *Isatis indigotica Fort., Bupleurum chinense.*DC, *Dahurian* Patrinia, *Verbena officinalis* L.,*Phragmites communis* Trin., *Glycyrrhiza uralensis* Fisch
	Maxingshigan Decoction	MAPK/NF-κB	5.4 g/kg	IL-1β, IL-6, TNF-α, p38MAPK, JNK, ERK1/2↓; MDA, SOD, GSH↑	*Prunus armeniaca L.var.ansu* Maxim., *Gypsum* Fibrosum, *Polygonum cuspidatum* Sieb. et Zucc., *Glycyrrhiza uralensis* Fisch
	Qingjie Huagong Formula	PI3K/AKT1	4.5 g/kg	TNF-α, IL-1β, IL-6↓	*Bupleurum chinense* DC., *Scutellaria baicalensis* Georgi, *Salvia miltiorrhiza* Bge., et al.
	Gegenqinlian Decoction	MAPK/NF-κB	1.25 g/kg	TNF-α, IL-6, IL-1β, C3, C5a,IL-17↓	*Pueraria lobata* (Willd.)Ohwi, *Coptis chinensis* Franch., *Glycyrrhiza uralensis* Fisch., et al.

(Continued on following page)

TABLE 2 (*Continued*) Summary of TCM Compounds for the prevention and treatment of ALI.

Principles of TCM	Herb/ Compound	Signal pathway	Dose	Index detection	Constitution
The Catharsis Category of Promoting Bowel Clearance and Pulmonary Detoxification (Tongfu)	Tongfu Formula	mtDNA-STING-NLRP3	9.9 g/kg	IL-6, IL-1β, IL-18, p-STING, STING, NLRP3, ASC mRNA and protein ↓	*Rheum palmatum* L., *Prunus persica* (L.) Batsch, *Paeonia lactiflora* Pall., et al.
	Tongfu Xiefei Enema Solution	p38 MAPK/MLCK	7.37 g/kg	TNF-1α, IL-1β, p38 MAPK mRNA and p38, p-MLC/ MLC2 MLCK protein↓	*Ephedra sinica* Stapf, *Prunus armeniaca L.var.ansu* Maxim., *Trichosanthes kirilowii* Maxim., et al.
	Tingli dazao xiefei Decoction	PTEN/PI3K/AKT	5.85 g/kg	IL-6, TNF-α, STAT3, SOC3, PI3K, AKT, p-AKT, PTEN↓	*Descurainia Sophia* (L.) *Webb*.ex, Prantl., *Ziziphus jujuba* Mill
	Xuanbai Cheng Qi Decoction	NLRP3 inflammasome	9 g/kg	NLRP3, Cleaved-Caspase1, GSDMD-N, IL-1β, pro-IL-1β, CXCL1, CXCL10, TNF-α, NLRP3, NF-κB P65 mRNA↓	*Gypsum* Fibrosum, *Rheum palmatum* L.,*Prunus armeniaca L.var.ansu* Maxim., et al.
	Dachengqi Decoction	NF-κB/NLRP3	5 g/kg	p-p65/p65, p-IκBα/IκBα, NLRP3, TNF-α, IL-6, IL-1β↓	*Rheum palmatum* L., *Magnolia officinalis Rehd.et* Wils., *Citrus aurantium* L., et al.
Enhancing blood circulation and resolving blood stasis	Huoxue Huayu Decoction	ZO-1/Occludin	7.2 g/kg	ZO-1, Occludin, AQP-1, AQP-5↑	*A.membranaceus* (Fisch.)Bge., *Codonopsis pilosula* (Franch.) Nannf., *Angelica sinensis* (Oliv.) Diels., et al.
	Qidong Huoxue Yin	iRhom2/TACE	8 mL/kg	iRhom2, TACE, TNF-α, IL-6↓	*A.membranaceus* (Fisch.)Bge., *Angelica sinensis* (Oliv.)Diels, *Rheum palmatum* L., et al.
	Xuebijing Injection	FPRs/NLRP3	12 mL/kg	FPR1, FPR2, NLRP3, IL-1β, IL-6, TNF-α↓	*Carthamus tinctorius* L., *Paeonia lactiflora* Pall., *Ligusticum chuanxiong* Hort., *Angelica sinensis* (Oliv.)Diels., et al.
	Qilongtian Capsule	TLR4/NF-κB	0.35 g/kg	TNF-α, IL-6, IL-1β, TLR4, NF-κBP65, NLRP3, MyD88 IκBα, NF-κBP65↓; IκBα↑	*Rhodiola crenulata* (Hook. f. et Thoms.) H. Ohba, *Panax notoginseng* (Burk.)F. H.Chen, *Pheretima aspergillum* (E.Perrier)
	Mailuo Yin	TLR4/NF-κB	1.25 μL/mL; 7.5 mL/kg	TLR4, MyD88, p-p65, p65, p-IκBα, TNF-α, IL-6, IL-1β, MPO↓	*Lonicera japonica* Thunb., *Achyranthes bidentata* BL., *Scrophularia ningpoensis* Hemsl., *Dendrobium nobile* Lindl
Others	Xiaoxuming Decoction	USP9X/NLRP3/Caspase-1/ Pro Caspase-1	10 mg/L	USP9X, NLRP3, IL-1β, Pro-IL-1β, Caspase-1, Pro-Caspase-1↓	*Ephedra sinica* Stapf, *Panax ginseng* C. A.Mey., *Scutellaria baicalensis* Georgi., et al.
	Jiegeng Decoction	/	250 mg/kg	TLR4, p-IKKβ, p-IKKα and p-IκBα↓	*Platycodon grandiflorum* (Jacq.) A.DC., *Glycyrrhiza uralensis* Fisch
	Compound Houttuynia mixture	TLR7/MyD88/NF-κB	5.46 g/kg; 87.4 mg/mL	TRAF6, IRF7, MyD88↓	*Houttuynia cordata* Thunb., *Scutellaria baicalensis* Georgi, *Isatis indigotica* Fort., et al.

demonstrated significant efficacy in reducing the Traditional Chinese Medicine (TCM) syndrome score of Yangming Fu in postoperative ALI patients, thereby effectively alleviating clinical symptoms such as profuse sweating, abdominal distension, and pain. Laboratory analyses revealed that following treatment, levels of C-reactive protein (CRP), interleukin-1 (IL-1) and interleukin-6 (IL-6) were markedly decreased, while the alveolar-arterial oxygen pressure difference P $(Aa)o_2$ improved significantly. Additionally, the duration of mechanical ventilation was notably shortened (Li Y. et al., 2022).

4.2.1.3 Yiqihuoxuexiezhuo formula

Professor Chao Enxiang, a master of traditional Chinese medicine, formulated a therapeutic regimen aimed at tonifying qi, resolving turbidity, and promoting blood circulation. This formula demonstrated significant efficacy in a randomized controlled trial involving 60 patients with acute lung injury. In the study, patients were randomly assigned to either the control group, which received standard Western medical treatment (including lung-protective ventilation strategies), or the experimental group, which received the same standard treatment supplemented with the TCM formula. The results indicated that following treatment, the experimental group exhibited marked improvements in oxygenation-related parameters, including heart rate, arterial partial pressure of oxygen, and Sao_2 levels. Additionally, biomarkers such as white blood cell count, C-reactive protein, and procalcitonin

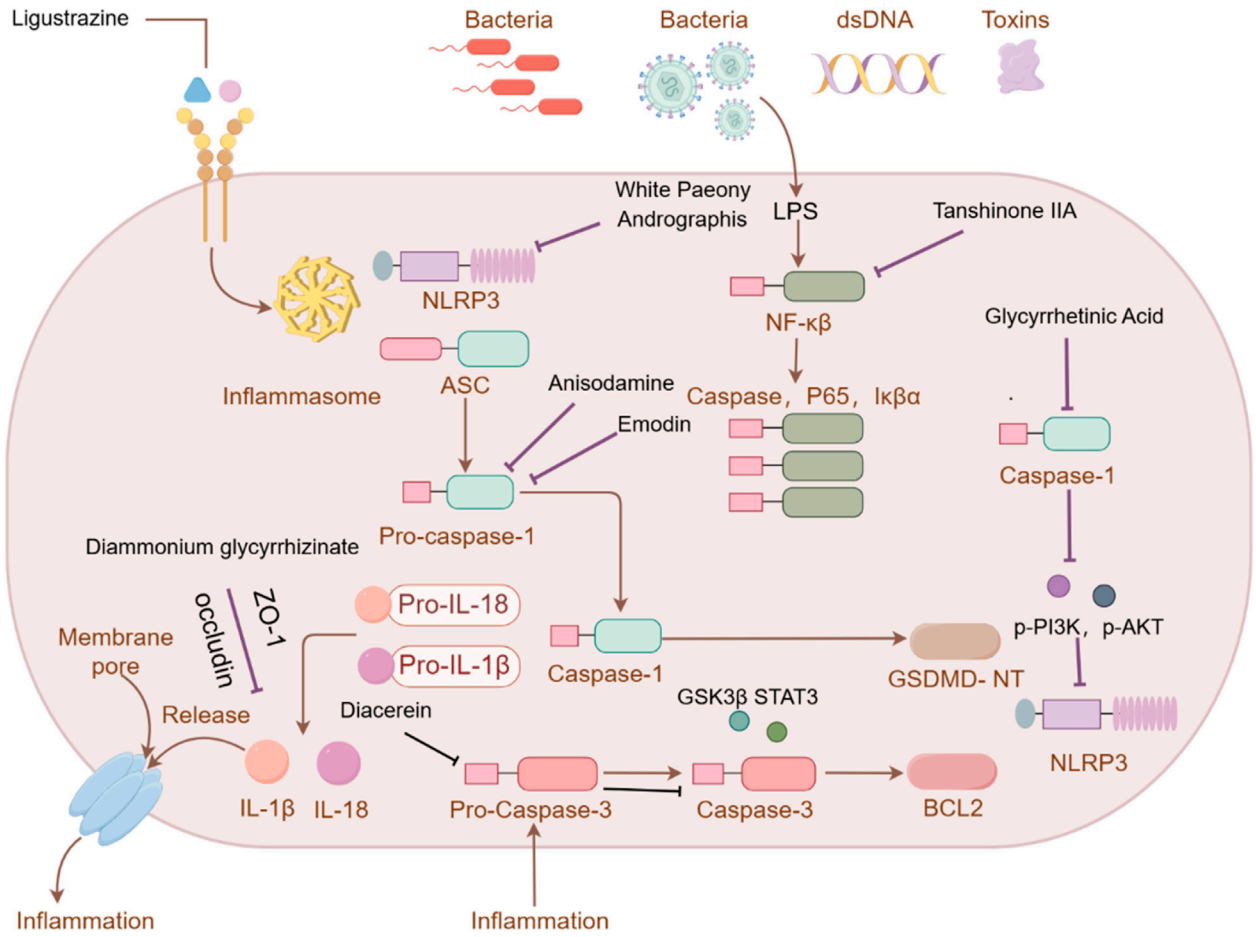


FIGURE 2
Investigation into the targets of TCM monomers and derivatives for the treatment of ALI.

showed notable reductions, while levels of inflammatory cytokines—including TNF-α, IL-6, and IL-8—decreased significantly. These findings provide strong evidence supporting the clinical application of the qi-tonifying, turbidity-resolving, and blood-circulation-promoting formula in the management of acute lung injury (Ren, 2020).

4.2.1.4 Tongfu Xiefei Formula

A study involving 40 patients with acute lung injury caused by phlegm-heat congestion syndrome revealed that Tongfu Xiefei Formula could effectively reduce the partial pressure of carbon dioxide ($Paco_2$), significantly increase the oxygenation index, and simultaneously decrease levels of DAO, MDA, NO, and inflammatory cytokines such as TNF-α and IL-6, thereby demonstrating a therapeutic effect on acute lung injury (Cheng, 2020).

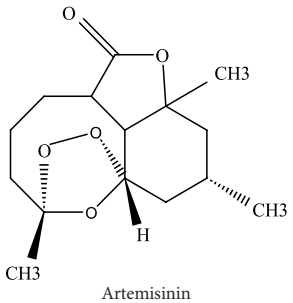
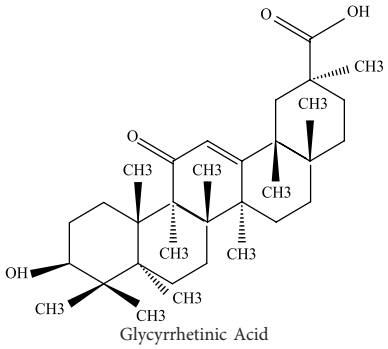
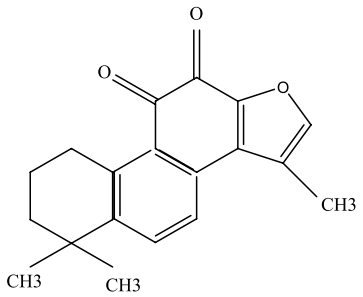
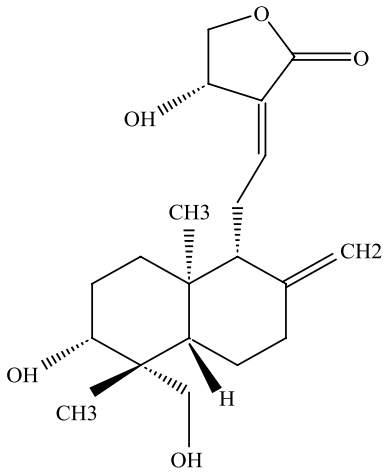
4.2.1.5 Qingwen Badu Yin

A randomized controlled trial conducted on 70 patients indicated that the addition of Qingwen Badu Yin to conventional treatment resulted in increased arterial partial pressure of oxygen (Pao_2) and oxygenation index (Pao_2/Fio_2) compared to baseline measurements. Additionally, $Paco_2$ levels were reduced after treatment, with more pronounced improvements observed in the treatment group ($P < 0.05$). Furthermore, serum levels of PCT, IL-6, TNF-α, and CRP were significantly decreased, and scores on the SOFA, APACHE II, and Murray lung injury scales were notably improved (Xu A. P. et al., 2024).

4.2.1.6 Shengjiang Lifei Decoction

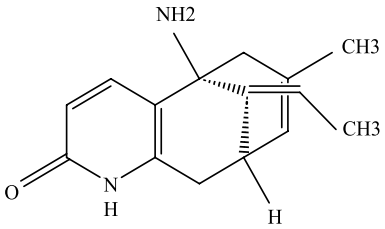
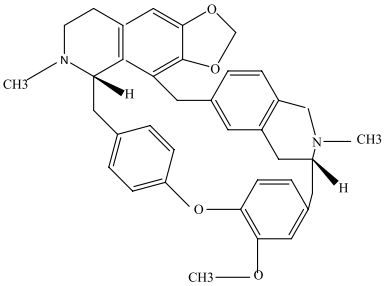
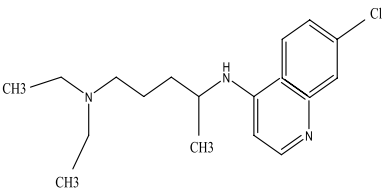
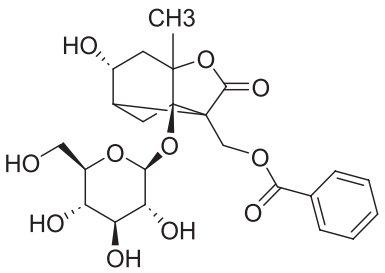
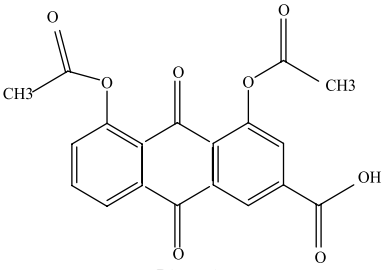
In a randomized controlled trial involving 60 patients, the treatment group received Shengjiang Lifei Decoction in conjunction with standard Western medical therapy. Following a seven-day treatment period, both groups exhibited improvements in Pao_2, $PaCo_2$, and oxygenation index compared to pre-treatment values, with greater therapeutic effects observed in the treatment group. Moreover, the duration of mechanical ventilation and ICU length of stay were shorter in the treatment group than in the control group. No adverse reactions were reported in either group throughout the treatment period, confirming that Shengjiang Lifei Decoction can enhance pulmonary function and alleviate clinical symptoms in patients with sepsis-induced ARDS, with favorable safety profile (Li G. C. et al., 2019).

TABLE 3 Investigation into the mechanism of monomer components in the treatment of ALI.

Monomer compounds	CAS	Molecular formula	*In vivo* and *in vitro* models	Pertinent pharmacological targets	Investigation of the relevant mechanism
 Artemisinin	63968–64-9	$C_{15}H_{22}O_5$	Ischemia-reperfusion modeling	TNF-a, IL-6, IL-1β, MDA, MPO, p-AKT, HO-1↓	Artemisinin has the potential to suppress the expression of inflammatory responses, thereby mitigating ALI.
 Glycyrrhetinic Acid	471–53-4	$C_{30}H_{46}O_4$	Intraperitoneal administration of LPS at a dose of 10 mg/kg	ROS, p-PI3K, p-AKT, Cleaved Caspase-1 and NLRP3 ↓	Glycyrrhizic acid and its derivatives mitigate the production of reactive oxygen species (ROS) in LPS-induced cells, downregulate the protein levels of phosphorylated phosphatidylinositol 3-kinase (p-PI3K) and phosphorylated AKT (p-AKT), reduce the expression of cleaved Caspase-1 and NLRP3, and inhibit the formation of NLRP3 inflammasomes, thereby providing protection against ALI.
 Tanshinone IIA	568–72-9	$C_{19}H_{18}O_3$	LPS was used to induce RLE-6TN cells. The sepsis model was established through cecal ligation and puncture (CLP)	ROCK2, TNF-α, IL-1β, IL-6, Caspase, pro-caspase, P65, IkBα↓	TIIA improved sepsis-induced lung injury by downregulating ROCK2 and further inactivating the NF-κB signaling pathway *in vivo* and *in vitro*
 Andrographis	5508–58-7	$C_{20}H_{30}O_5$	CLP mouse model	TNF-α, IL-1β↓	Andrographis suppresses the activation and release of inflammasomes, consequently inhibiting the secretion of inflammatory cytokines, which is beneficial for the treatment of ALI.
	102518–79-6	$C_{15}H_{18}NO_2$	Intratracheal administration of	IL-6, MDA, ROS↓; SOD↑	Huperzine A can decrease the concentrations of IL-6,

(Continued on following page)

TABLE 3 (*Continued*) Investigation into the mechanism of monomer components in the treatment of ALI.

Monomer compounds	CAS	Molecular formula	*In vivo* and *in vitro* models	Pertinent pharmacological targets	Investigation of the relevant mechanism
 Huperzine A			LPS at a dose of 5 mg/kg		MDA, and ROS while increasing the concentration of SOD, thereby contributing to the treatment of ALI.
 Cepharanthine	481–49-2	$C_{37}H_{38}N_2O_6$	/	/	Cepharanthine tablets significantly decrease viral RNA levels and inhibit viral replication, thereby mitigating acute lung injury
 Chloroquine	54–05-7	$C_{18}H_{26}ClN_3$	Infection with the H5N1 influenza virus	PH, CXCR4↑	Chloroquine elevates lysosomal pH, inhibits the fusion between autophagosomes and lysosomes, degrades lysosomal proteins, upregulates the expression of CXCR4 *in vivo*, thereby alleviating ALI.
 White Paeony	39011–90-0	$C_{23}H_{28}O_{11}$	Intratracheal administration of LPS at a dose of 50 ng/mL	IL-1β, IL-18, IL-6, TNF-α, ASC, NLRP3↓	Total paeony glycosides capsules may ameliorate ALI in mice through the inhibition of NLRP3 inflammasome activation
 Diacerein	13739–02-1	$C_{19}H_{12}O_8$	Intraperitoneal injection of LPS at 5 mg/kg	Sphk1/S1P, GSK-3β, STAT3, Caspase-3↓; BCL-2↑	Diacerein can modulate the Sphk1/S1P axis, reduce the levels of GSK-3β, STAT3, and Caspase-3, while increasing the expression of BCL-2 protein, thereby contributing to the treatment of acute lung injury

4.2.2 Clinical application of Traditional Chinese Medicine injections

4.2.2.1 Shenfu Injection

In a randomized controlled trial involving 50 patients with acute lung injury (ALI), treatment with Shenfu Injection led to a significant reduction in levels of inflammatory markers, including C-reactive protein (CRP), interleukin-6 (IL-6), and tumor necrosis factor-alpha (TNF-α). Additionally, prothrombin time was shortened, and D-dimer levels were markedly decreased compared to baseline (Zhang et al., 2022).

4.2.2.2 Xuebijing Injection

As one of the most widely prescribed traditional Chinese medicine (TCM) injections in current clinical practice, Xuebijing Injection has demonstrated notable therapeutic efficacy in managing ALI. Clinical evidence indicates that following intervention with Xuebijing Injection, multiple clinical and physiological parameters showed significant improvement. These include Traditional Chinese Medicine syndrome scores, Acute Physiology and Chronic Health Evaluation II (APACHE II) scores, Sequential Organ Failure Assessment (SOFA) scores, Murray Lung Injury scores, plateau pressure, and driving pressure (ΔP). Furthermore, levels of inflammatory biomarkers such as C-reactive protein, procalcitonin, interleukin-6, heparin-binding protein, white blood cell count, neutrophil count, neutrophil-to-lymphocyte ratio, and D-dimer were significantly reduced. Concurrently, pulmonary function indices—including arterial oxygen partial pressure (Pao2), oxygenation index (Pao2/Fio2), and static lung compliance—as well as immune function indicators such as $CD3^+$, $CD4^+$, and the CD4+/CD8+ ratio were notably elevated (Ding et al., 2024).

4.2.2.3 Reduning Injection

Clinical investigations have revealed that Reduning Injection can substantially enhance cellular immune function in patients. The treatment group exhibited higher levels of $CD3^+$, $CD4^+$, and CD4+/CD8+ compared to the control group. The short-term overall effective rate in the treatment group reached 90.91%, significantly surpassing the 68.18% observed in the control group. More importantly, during a six-month follow-up period, the survival rate in the treatment group was 67.50%, compared to 56.67% in the control group, indicating sustained clinical benefits (Li et al., 2020).

4.2.3 Clinical applications of monomers derived from Traditional Chinese Medicine and their derivatives

TCM monomers and their derivatives are diverse in nature, with complex structures and a broad range of pharmacological activities. Recent studies have increasingly highlighted the significant potential of these monomers and their combinations (i.e., component-based TCM) in treating ALI, offering safer and more effective therapeutic options for clinical use. While several reviews have extensively explored the mechanisms and clinical applications of TCM monomers in preventing and treating ALI, this paper aims to provide a deeper analysis by focusing specifically on the clinical applications of these monomers and their derivatives.

Although most studies on the efficacy of TCM monomers in treating ALI is still in the preclinical stage, their therapeutic potential is being reevaluated for both prevention and treatment, whether as individual monomers or in synthetic formulations. The primary objective of this section is to investigate the mechanisms through which these TCM monomers act in ALI treatment, thus laying a scientific foundation for their future clinical applications. Several TCM monomers have shown promising results in treating ALI, demonstrating their potential to modulate immune responses, reduce inflammation, and improve lung function.

4.2.3.1 Ligustrazine

This compound has been shown to reverse macrophage polarization, reduce pyroptosis, and exert anti-ALI effects (Jiang R. et al., 2021). Clinical studies indicate that tetramethylpyrazine injection, which contain ligustrazine, significantly improve patients' Pao_2/Fio_2 ratios and respiratory rates. It also reduces systemic inflammatory response syndrome (SIRS) and lowers APACHE II scores, as along with decreasing levels of IL-6, C-reactive protein (CRP), nitric oxide (NO). These effects help alleviate ALI symptoms and promote recovery (Liu et al., 2019).

4.2.3.2 Diammonium glycyrrhizinate

This compound mitigates LPS-induced ALI by improving vascular endothelial barrier function (Liu et al., 2021). When combined with Astragalus injection, diammonium glycyrrhizinate significantly increases Po_2/Fio_2 ratios in patients, while also markedly reducing lactate (Lac), CRP, lung injury scores, APACHE-II scores, and SIRS scores (Li et al., 2020).

4.2.3.3 Anisodamine

Preclinical studies suggest that anisodamine inhibits inflammasome activation, thereby suppressing macrophage pyroptosis (Zhang et al., 2024). In a clinical study involving 78 patients who developed ALI after lung cancer surgery, intravenous administration of anisodamine over 48 h reduce the levels of TNF-α, IL-6, high-sensitivity C-reactive protein (hs-CRP), and procalcitonin (PCT). Additionally, it improves lung compliance, Pao_2, and oxygenation indices, demonstrating its protective effects against ALI following thoracotomy for lung cancer (Du et al., 2017).

4.2.3.4 Diacerein

Through randomized, double-blind clinical trials, it was demonstrated that Diacerein can inhibit the secretion of IL-1β on the surface of human neutrophils during viral replication and downregulate the expression levels of NLRP3, Caspase-1, and GSDMD (Carmo et al., 2024). According to the World Clinical Trial Database, a study involving 40 patients with COVID-19 was conducted using diacerein as an intervention. Serum samples collected 10 days after treatment were analyzed for changes in biomarkers such as IL-1β, IL-8, IL-6, C-reactive protein and troponin. However, the results of this trial have not yet been disclosed (Fundação de Amparo à Pesquisa do Estado de São, 2022). Further details are provided in Table 4.

5 Discussion

According to the theory of Traditional Chinese Medicine (TCM), acute lung injury (ALI) can be categorized under syndromes such as "asthma syndrome" and "sudden asthma". Its etiology primarily involves pathological changes including deficiency of vital energy and accumulation of pathogenic toxins in the lungs. Consequently, clinical treatment strategies emphasize replenishing qi, nourishing Yin, clearing heat, and detoxifying (Xie et al., 2008). The pathogenesis of ALI involves a complex interplay of multiple pathophysiological mechanisms. Key pathogenic processes include excessive inflammatory response, disruption of the alveolar-capillary barrier, oxidative

stress, and apoptosis. During the initial phase of lung injury—triggered by factors such as infection, trauma, or aspiration—pathogen-associated molecular patterns (PAMPs) or damage-associated molecular patterns (DAMPs) activate alveolar macrophages and neutrophils, resulting in the release of substantial amounts of pro-inflammatory cytokines, such as TNF-α, IL-1β, and IL-6. These cytokines further recruit additional immune cells, leading to an inflammatory cascade (Vora et al., 2021). Concurrently, activated neutrophils secrete proteases, including elastase, along with reactive oxygen species (ROS), which directly damage alveolar epithelial and vascular endothelial cells. This results in the degradation of tight junction proteins, such as ZO-1 and Occludin, increased vascular permeability, and the development of pulmonary edema (Yu L. C. et al., 2024). Moreover, dysfunction and apoptosis of alveolar type II epithelial cells (AT2) impair surfactant production, thereby exacerbating alveolar collapse. Recent studies have also indicated that cellular metabolic reprogramming, mitochondrial dysfunction, endoplasmic reticulum stress, and regulated cell death pathways like ferroptosis and pyroptosis are not mere consequences but are central drivers of ALI progression, modulating apoptotic and autophagic pathways (Wang et al., 2025; Taheri et al., 2024). These mechanisms interact synergistically, forming a self-amplifying cycle that culminates in impaired gas exchange and respiratory failure.

Although significant progress has been made in the clinical and experimental research on TCM for ALI, there are still many issues worthy of in-depth exploration. Firstly, the quintessential strength of TCM lies in its holistic regulation and personalized treatment based on syndrome differentiation. Therapeutic principles such as clearing heat and resolving phlegm, or promoting blood circulation to unblock meridians, do not merely suppress excessive inflammatory responses but also aim to improve microcirculation and promote tissue repair. This multi-target, systematic approach contrasts sharply with the single-target interventions often prioritized in Western medicine. However, a critical gap remains: most current studies focuses on the mechanisms of single herbs or monomer components, while the synergistic effects arising from the complex interplay of components within a formula—governed by the principles of "sovereign, minister, assistant, and messenger" — are poorly understood. Bridging this gap is essential to elucidating the material basis of TCM efficacy. Secondly, while the anti-inflammatory and antioxidant mechanisms of certain TCM monomers (such as artemisinin and tanshinone IIA) have been well-characterized, translating these findings into clinical practice requires overcoming significant hurdles, such as optimizing dosage for a precise therapeutic window that balances efficacy with safety, and developing novel drug delivery systems to improve bioavailability at the target site.

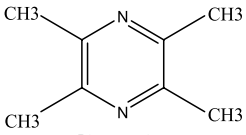
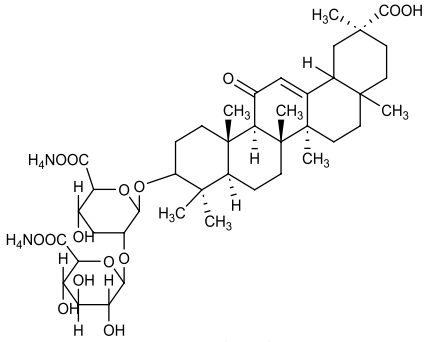
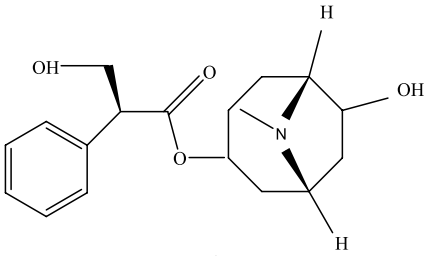
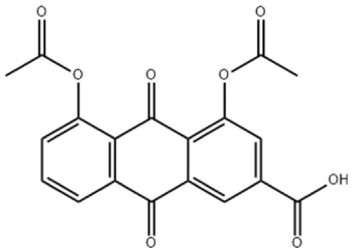
The rapid evolution of multi-omics technologies presents a paradigm-shifting opportunity for TCM pharmacology. An integrated multi-omics analysis, combining genomics, transcriptomics, proteomics, and metabolomics, can provide an unbiased, panoramic view of the body's response to TCM interventions. This approach allows us to move beyond a one-molecule-one-target framework and instead map the complex interaction network through which TCM components modulate the genome, transcriptome, and proteome, thus revealing the multi-level regulatory landscape of TCM. Network pharmacology, as a computational method, further helps to deconstruct this complexity by identifying core targets and pathways, providing a robust theoretical basis for clinical applications (Wang Z. Y. et al., 2022). Furthermore, the combination of cutting-edge technologies, such as single-cell technology and spatial omics technology, has brought new opportunities and challenges to dissect the mechanism of TCM in modulating cellular and spatial heterogeneity (Chen et al., 2022). Through these technologies, we can pinpoint how specific TCM formulas regulate distinct cell populations (e.g., macrophage subtypes, endothelial cells) within the lung microenvironment and understand the spatial distribution of key proteins, thereby offering a more comprehensive explanation of TCM's therapeutic mechanisms. This is a key direction for future work.

TCM compound prescriptions are the cornerstone of clinical TCM practice. However, due to the complex chemical composition of medicinal materials used in these formulations and the influence of multiple factors—including the origin of raw materials, processing methods of decoction pieces, and production techniques—the quality control of TCM faces significant challenges, often summarized as "uncertain efficacy and imprecise dosage". This has become a major bottleneck for modernization, industrialization, and internationalization of TCM (Sun et al., 2017). Therefore, it is imperative to establish a multi-dimensional quality control system. This system should integrate qualitative and quantitative dual-standards, spectroscopic-effect relationship analyses, network pharmacology- and metabolomics-based identification of quality markers (Q-markers), and the combination of multi-component quantification with bioactivity assays. Only through such a comprehensive quality evaluation system can we ensure the consistency and reliability of TCM preparations (Lu et al., 2024).

In the management of ALI, an integrative model combining TCM and Western medicine holds immense untapped potential. Western medicine provides objective, quantifiable biomarkers and rapid, life-sustaining interventions. In contrast, TCM emphasizes individualized treatment and holistic regulation, which can be highly beneficial for alleviating symptoms and improving quality of life (Yu et al., 2023). However, a significant challenge lies in reconciling their different diagnostic and therapeutic philosophies within the rigid framework of conventional randomized controlled trials (RCTs). The "one-size-fits-all" design of RCTs often conflicts with the personalized nature of TCM syndrome differentiation, potentially masking the true efficacy of a formula when applied to a heterogeneous patient population. Thus, future clinical trial designs should incorporate biomarker-guided patient stratification or adaptive designs that allow for treatment adjustments based on TCM pattern diagnosis. Merging TCM's holistic and individualized approach with Western medicine's precise and emergency care models represents the most promising path forward for optimizing patient outcomes in ALI (Li et al., 2025).

Finally, conventional pharmacokinetics, which focuses on systemic drug exposure, often overlooks the critical role of the gut. Many TCM components have low oral bioavailability and

TABLE 4 Clinical applications of monomeric components in the treatment of ALI.

Monomer species	CAS	Molecular formula	Case	Appropriate clinical evaluation metrics	Clinical research
 Ligustrazine	1124–11-4	$C_8H_{12}N_2$	55	SIRS, APACHEⅡ score, IL-6, C-protein, NO↓	Ligustrazine can decrease the incidence of lung injury and improve patients' respiratory rates
 Diammonium glycyrrhizinate	79165–06-3	$C_{42}H_{65}NO_{16}$	60	Lac, CRP, lung injury score, APACHE-Ⅱ, SIRS↓	Diammonium glycyrrhizinate can enhance the PO2/FiO2 ratio while reducing lactate (Lac), C-reactive protein (CRP), lung injury score, APACHE-II score, and SIRS score
 Anisodamine	55869–99-3	$C_{17}H_{23}NO_3$	78	TNF-α, IL-6, hs-CRP, PCT↓	Anisodamine reduces the expression of hs-CRP, and PCT while enhancing lung compliance, PaO2 levels, and the oxygenation index
 Diacerein	13739–02-1	$C_{19}H_{12}O_8$	40	IL-1β, IL-6, IL-8, C-reactive protein	/

exert their effects by modulating the gut microbiota or being transformed into active metabolites by it. Therefore, it is essential to investigate the "substance-effect" relationship within the intestinal lumen, clarifying how TCM components and their gut microbial metabolites interact to produce therapeutic effects or adverse reactions. This will provide a more complete picture of the multi-target interaction profiles of TCM and enhance the safety and efficacy of its clinical application (Zhu et al., 2024).

6 Conclusion

In conclusion, this review has systematically summarized the multifaceted pathogenesis of ALI and highlighted the significant therapeutic potential of TCM, acting through multi-component, multi-target, and multi-pathway mechanisms. While promising, the translation of TCM from bench to bedside requires a concerted effort to address existing challenges. Future efforts should prioritize the accumulation of high-quality clinical evidence through innovatively designed multicenter, international collaborations to achieve broader recognition from the mainstream medical community. Clinically, integrating TCM syndrome differentiation with modern diagnostic biomarkers can enable a more personalized and precise application of therapies, creating a synergistic effect that offers more comprehensive treatment for ALI patients. Mechanistically, the application of multi-omics and systems biology approaches is crucial for elucidating the complex pharmacological basis of TCM's efficacy. Additionally, exploring the novel therapeutic potential of existing TCM components and strengthening evidence-based research on integrative medicine will

not only elevate therapeutic outcomes but also enhance the scientific rigor and validation of TCM, providing a more reliable foundation for clinical decision-making in the fight against ALI.

Author contributions

JW: Writing – original draft, Writing – review and editing. ZY: Conceptualization, Writing – review and editing. XZ: Writing – original draft. SW: Investigation, Software, Writing – review and editing. LJ: Data curation, Investigation, Software, Validation, Writing – review and editing. BZ: Validation, Visualization, Writing – review and editing. BT: Supervision, Validation, Visualization, Writing – review and editing. AY: Supervision, Validation, Visualization, Writing – review and editing.

Funding

The author(s) declare that financial support was received for the research and/or publication of this article. The present research was supported from the Shanghai Municipal Science and Technology Major Project (No. ZXS004R4-1, No. ZD2021CY001), the Shuguang Hospital Research Funding Project (SG3915) and the Shanghai University of Traditional Chinese Medicine Budget Project (2021LK075).

Conflict of interest

The authors declare that the research was conducted in the absence of any commercial or financial relationships that could be construed as a potential conflict of interest.

Generative AI statement

The author(s) declare that no Generative AI was used in the creation of this manuscript.

Publisher's note

All claims expressed in this article are solely those of the authors and do not necessarily represent those of their affiliated organizations, or those of the publisher, the editors and the reviewers. Any product that may be evaluated in this article, or claim that may be made by its manufacturer, is not guaranteed or endorsed by the publisher.

References

Aulakh, G. K. (2018). Neutrophils in the lung: the first responders. *Cell Tissue Res.* 371 (3), 577–588. doi:10.1007/s00441-017-2748-z

Bhatia, M., Zemans, R. L., and Jeyaseelan, S. (2012). Role of chemokines in the pathogenesis of acute lung injury. *Am. J. Respir. Cell Mol. Biol.* 46 (5), 566–572. doi:10.1165/rcmb.2011-0392TR

Bock, F. J., and Tait, S. W. (2020). Mitochondria as multifaceted regulators of cell death. *Nat. Rev. Mol. Cell Biol.* 21 (2), 85–100. doi:10.1038/s41580-019-0173-8

Burkard, P., Schonhart, C., Vögtle, T., Köhler, D., Tang, L., Johnson, D., et al. (2023). A key role for platelet GPVI in neutrophil recruitment, migration, and NETosis in the early stages of acute lung injury. *Blood* 142 (17), 1463–1477. doi:10.1182/blood.2023019940

Bustamante, E., and Pedersen, P. L. (1977). High aerobic glycolysis of rat hepatoma cells in culture: role of mitochondrial hexokinase. *Proc. Natl. Acad. Sci. U. S. A.* 74 (9), 3735–3739. doi:10.1073/pnas.74.9.3735

Cai, J., Wang, Y. L., Sheng, X. D., Zhang, L., and Lv, X. (2022b). Shufeng jiedu capsule inhibits inflammation and apoptosis by activating A2AAR and inhibiting NF-κB to alleviate LPS-induced ALI. *J. Ethnopharmacol.* 298, 115661. doi:10.1016/j.jep.2022.115661

Cai, J., Xu, G., Lin, Y., Zhou, B., Luo, Z., Yu, S., et al. (2022a). Inhibition of TRPV4 attenuates ferroptosis against LPS-induced ALI via $Ca2^{+}$ pathway. *Turk J. Biol.* 46 (6), 465–474. doi:10.55730/1300-0152.2632

Cao, J., Ding, C., Huang, J., Chen, Y., and Chen, Y. (2023). Pulmonary vascular endothelial glycocalyx degradation contributes to acute lung injury in experiencing heatstroke. *Shock* 59 (6), 966–972. doi:10.1097/SHK.0000000000002130

Cao, Z., Qin, H., Huang, Y., Zhao, Y., Chen, Z., Hu, J., et al. (2022). Crosstalk of pyroptosis, ferroptosis, and mitochondrial aldehyde dehydrogenase 2-related mechanisms in sepsis-induced lung injury in a mousemodel. *Bioengineered* 13 (3), 4810–4820. doi:10.1080/21655979.2022.2033381

Carmo, H. R. P., Castillo, A. R., Bonilha, I., Gomes, E. I. L., Barreto, J., Moura, F. A., et al. (2024). Diacerein reduces inflammasome activation and SARS-CoV-2 virus replication: a proof-of-concept translational study. *Front. Pharmacol.* 15, 1402032. doi:10.3389/fphar.2024.1402032

Che, J., Wang, H., Dong, J., Wu, Y., Zhang, H., Fu, L., et al. (2024). Human umbilical cord mesenchymal stem cell-derived exosomes attenuate neuroinflammation and oxidative stress through the NRF2/NF-κB/NLRP3 pathway. *CNS Neurosci. Ther.* 30 (3), e14454. doi:10.1111/cns.14454

Chen, D. S. (2022). Research on the mechanism of CMPK2 regulating TNF-α affecting acute lung injury in sepsis. *Zhejiang: Chin. People's lib. Army Navy Mil. Med. Univ.* doi:10.26998/d.cnki.gjuyu.2022.000218

Chen, J., Luo, P., Wang, C., Yang, C., Bai, Y., He, X., et al. (2022). Integrated single-cell transcriptomics and proteomics reveal cellular-specific responses and microenvironment remodeling in aristolochic acid nephropathy. *JCI Insight* 7 (16), e157360. doi:10.1172/jci.insight.157360

Chen, J. D., Gong, D., Yi, Y. H., and Chen, Y. (2021). The role of vascular endothelial glycocalyx in the pathological mechanism, diagnosis and treatment of sepsis-related acute lung injury. *Med. J. People's Liberation Army* 46 (04), 398–403. doi:10.11855/j.issn.0577-7402.2021.04.13

Chen, X., Tang, J., Shuai, W., Meng, J., Feng, J., and Han, Z. (2020). Macrophage polarization and its role in the pathogenesis of acute lung injury/acute respiratory distress syndrome. *Inflamm. Res.* 69 (9), 883–895. doi:10.1007/s00011-020-01378-2

Chen, Y. (2022). *Heat shock protein 70 promotes pulmonary inflammatory response in mice with acute lung injury*. Anhui: Bengbu medical college. doi:10.26925/d.cnki.gbbyc.2022.000141

Cheng, L. (2020). "Clinical and experimental research on the treatment of sepsis-related acute respiratory distress syndrome with tongfu xiefei formula,". Jiangsu: Nanjing University of Chinese medicine. doi:10.27253/d.cnki.gnjzu.2020.000256

Christofk, H. R., Vander, H. M. G., Harris, M. H., Ramanathan, A., Gerszten, R. E., Wei, R., et al. (2008). The M2 splice isoform of pyruvate kinase is important for cancer metabolism and tumour growth. *Nature* 452 (7184), 230–233. doi:10.1038/nature06734

Colquhoun, A. (2002). Gamma-linolenic acid alters the composition of mitochondrial membrane subfractions, decreases outer mitochondrial membrane binding of hexokinase and alters carnitine palmitoyltransferase I properties in the walker 256 rat tumour. *Biochim. Biophys. Acta* 1583 (1), 74–84. doi:10.1016/s1388-1981(02)00162-2

Cui, A. F., Shao, Y. Y., Wang, H. D., Song, J. Y., and Wang, Y. (2024). Immune cells and cytokines in the research progress in the treatment of acute lung injury. *J. Of Clin. Med. Pract.* 33 (02), 114–117. doi:10.16047/j.cnki.cn14-1300/r.2024.02.005

Dagvadorj, J., Shimada, K., Chen, S., Jones, H. D., Tumurkhuu, G., Zhang, W., et al. (2015). Lipopolysaccharide induces alveolar macrophage necrosis via CD14 and the P2X7 receptor leading to interleukin-1α release. *Immunity* 42 (4), 640–653. doi:10.1016/j.immuni.2015.03.007

Del Sorbo, L., Goffi, A., and Ranieri, V. M. (2011). Mechanical ventilation during acute lung injury: current recommendations and new concepts. *Presse Med.* 40, 569–583. doi:10.1016/j.lpm.2011.05.028

Diao, Y., Ding, Q., Xu, G., Li, Y., Li, Z., Zhu, H., et al. (2022). Qingfei litan decoction against acute lung injury/acute respiratory distress syndrome: the potential roles of anti-

inflammatory and anti-oxidative effects. *Front. Pharmacol.* 13, 857502. doi:10.3389/fphar.2022.857502

Ding, W. C., Chen, J., Ye, Y., Sun, Z. R., and Nie, S. N. (2024). The clinical efficacy of xuebijing injection in the treatment of patients with pulmonary blood stasis syndrome in sepsis-related acute respiratory distress syndrome. *Chin. Herb. Med.* 55 (19), 6645–6654. doi:10.7501/j.issn.0253-2670.2024.19.018

Dong, J., Liu, W., Liu, W., Wen, Y. Q., Liu, Q. G., Wang, H. T., et al. (2024). Acute lung injury: a view from the perspective of necroptosis. *Inflamm. Res.* 73 (6), 997–1018. doi:10.1007/s00011-024-01879-4

Du, N., Wang, M., Zhang, Y. F., Sun, X., Ren, H., and Liu, D. P. (2017). The protective effect of anisodamine on acute lung injury after thoracotomy for lung cancer. *Mod. Oncol. Med.* 25 (23), 3770–3772. doi:10.3969/j.issn.1672-4992.2017.23.012

Esquivel-Ruiz, S., González-Rodríguez, P., Lorente, J. A., Pérez-Vizcaíno, F., Herrero, R., and Moreno, L. (2021). Extracellular vesicles and alveolar epithelial-capillary barrier disruption in acute respiratory distress syndrome: pathophysiological role and therapeutic potential. *Front. Physiol.* 12, 752287. doi:10.3389/fphys.2021.752287

Fan, H. H., Wang, L. Q., Liu, W. L., An, X. P., Liu, Z. D., He, X. Q., et al. (2020). Repurposing of clinically approved drugs for treatment of coronavirus disease 2019 in a 2019-novel coronavirus-related coronavirus model. *Chin. Med. J.* 133 (09), 1051–1056. doi:10.1097/CM9.0000000000000797

Feng, M. C., Luo, F., Tang, X. P., Li, K., Zhu, X. D., and Zhang, B. Y. (2024). The therapeutic effect and mechanism of qingjie huagong formula on acute lung injury in rats with severe acute pancreatitis model. *Chin. J. Pharmacol.* 40 (05), 975–983. doi:10.12360/CPB202308016

Feng, Y., Zhu, B., Liu, Y., Liu, Y., Zhou, G., Yang, L., et al. (2022). Yindan jiedu granules exhibit anti-inflammatory effect in patients with novel coronavirus disease (COVID-19) by suppressing the NF-κB signaling pathway. *Phytomedicine* 95, 153784. doi:10.1016/j.phymed.2021.153784

Fundação de Amparo à Pesquisa do Estado de São (2022). *Study design of the diacerein effect on inflammatory response in patients with Covid-19: a randomized, placebo-controlled, double-blind trial*, Editor P. Fundação de Amparo à Pesquisa do Estado de São (Brazil).

Gasmi, A., Gasmi, A., Tippairote, T., Mujawdiya, P. K., Menzel, A., Lysiuk, R., et al. (2024). Traditional Chinese medicine as the preventive and therapeutic remedy for COVID-19. *Curr. Med. Chem.* 31 (21), 3118–3131. doi:10.2174/0929867330666230331084126

Ge, Z., Xia, Z. J., and Ma, K. (2023). Reusing old drugs: scopolamine - a typical case of clinical off-indication application. *Chin. J. Ration. Drug Use Explor.* 20 (07), 26–28. doi:10.3969/j.issn.2096-3327.2023.07.008

Gong, H., Chen, Y., Chen, M., Li, J., Zhang, H., Yan, S., et al. (2022). Advanced development and mechanism of sepsis-related acute respiratory distress syndrome. *Front. Med. (Lausanne)* 9, 1043859. doi:10.3389/fmed.2022.1043859

Grisaru-Tal, S. M. E., and Rothenberg, M. E. (2022). Eosinophil-lymphocyte interactions in the tumor microenvironment and cancer immunotherapy. *Nat. Immunol.* 23 (9), 1309–1316. doi:10.1038/s41590-022-01291-2

Guo, J., Zhu, J., Wang, Q., Wang, J., and Jia, Y. (2021). Comparative efficacy of seven kinds of Chinese medicine injections in acute lung injury and acute respiratory distress syndrome: a network meta-analysis of randomized controlled trials. *Front. Pharmacol.* 12, 627751. doi:10.3389/fphar.2021.627751

Guo, X. Q. (2024). Comparison of clinical effects of magnesium isoglycyrrhizinate and diammonium glycyrrhizinate combined with shuganning in the treatment of viral hepatitis. *Clin. Ration. Drug Use* (35), 11–14. doi:10.15887/j.cnki.13-1389/r.2024.35.003

Guo, Y., Liu, Y., Zhao, S., Xu, W., Li, Y., Zhao, P., et al. (2021). Oxidative stress-induced FABP5 S-glutathionylation protects against acute lung injury by suppressing inflammation in macrophages. *Nat. Commun.* 12 (1), 7094. doi:10.1038/s41467-021-27428-9

Hao, J. D. (2023). *The role of NLRP3 in estrogen-mediated alleviation of intestinal lymph fluid-induced lung injury following hemorrhagic shock*. Hebei: Hebei North University. doi:10.27767/d.cnki.ghbbf.2023.000047

He, Y. T., Huang, W., Liu, S. T., Xie, W. P., and Kong, H. (2024). The mechanism and research progress of ferroptosis in acute lung injury. *J. Clin. Pulmonol.* 29 (12), 1906–1912.

Hou, W. Q., Liu, D. L., Hai, Y., Liu, X. F., Dong, J. Q., Su, J., et al. (2023). Maxing shigan decoction alleviates the inflammatory response of LPS-induced acute lung injury by regulating the MAPK/NF-κB pathway. *Clin. Pharmacol. Chin. Med.* 39 (3), 1–7. doi:10.13412/j.cnki.zyyl.20230220.002

Hu, C., Li, J., Tan, Y., Liu, Y., Bai, C., Gao, J., et al. (2022). Tanreqing injection attenuates macrophage activation and the inflammatory response via the lncRNA-SNHG1/HMGB1 axis in lipopolysaccharide-induced acute lung injury. *Front. Immunol.* 13, 820718. doi:10.3389/fimmu.2022.820718

Huo, Y., and Yue, D. (2024). Effect of anti-inflammatory tongfu formula on mtDNA-STING-NLRP3 signaling pathway in sepsis-induced acute lung injury rats. *Chin. J. Emerg. Med.* 44 (04), 323–329. doi:10.3969/j.issn.1002-1949.2024.04.008

Hussain, M., Xu, C., Wu, X., Lu, M., Tang, L., Wu, F., et al. (2019). A CRTH2 antagonist, CT-133, suppresses NF-κB signalling to relieve lipopolysaccharide-induced acute lung injury. *Eur. J. Pharmacol.* 854, 79–91. doi:10.1016/j.ejphar.2019.03.053

Imai, Y., Kuba, K., Neely, G. G., Yaghubian-Malhami, R., Perkmann, T., van Loo, G., et al. (2008). Identification of oxidative stress and toll-like receptor 4 signaling as a key pathway of acute lung injury. *Cell* 133 (2), 235–249. doi:10.1016/j.cell.2008.02.043

Ji, T., Chen, M., Liu, Y., Jiang, H., Li, N., and He, X. (2023). Artesunate alleviates intestinal ischemia/reperfusion induced acute lung injury via up-regulating AKT and HO-1 signal pathway in mice. *Int. Immunopharmacol.* 122, 110571. doi:10.1016/j.intimp.2023.110571

Jiang, L., Gu, Y., Du, Y., and Liu, J. (2019). Exosomes: diagnostic biomarkers and therapeutic delivery vehicles for cancer. *Mol. Pharm.* 16 (8), 3333–3349. doi:10.1021/acs.molpharmaceut.9b00409

Jiang, N., Li, Z., Luo, Y., Jiang, L., Zhang, G., Yang, Q., et al. (2021). Emodin ameliorates acute pancreatitis-induced lung injury by suppressing NLRP3 inflammasome-mediated neutrophil recruitment. *Exp. Ther. Med.* 22 (2), 857. doi:10.3892/etm.2021.10289

Jiang, R., Xu, J., Zhang, Y., Zhu, X., Liu, J., and Tan, Y. (2021). Ligustrazine alleviate acute lung injury through suppressing pyroptosis and apoptosis of alveolar macrophages. *Front. Pharmacol.* 12, 680512. doi:10.3389/fphar.2021.680512

Ju, M., Liu, B., He, H., Gu, Z., Liu, Y., Su, Y., et al. (2018). MicroRNA-27a alleviates LPS-Induced acute lung injury in mice via inhibiting inflammation and apoptosis through modulating TLR4/MyD88/NF-κB pathway. *Cell Cycle* 17 (16), 2001–2018. doi:10.1080/15384101.2018.1509635

Kandikattu, H. K., Upparahalli Venkateshaiah, S., Kumar, S., Yadavalli, C. S., and Mishra, A. (2023). IL-18-mediated neutrophil recruitment promotes acute lung injury in inflammation-mediated chronic pancreatitis. *Mol. Immunol.* 155, 100–109. doi:10.1016/j.molimm.2023.01.012

Kawano, A., Ariyoshi, W., Yoshioka, Y., Hikiji, H., Nishihara, T., and Okinaga, T. (2019). Docosahexaenoic acid enhances M2 macrophage polarization via the p38 signaling pathway and autophagy. *J. Cell Biochem.* 120 (8), 12604–12617. doi:10.1002/jcb.28527

Kou, Y. L., Wang, W. B., Yan, S. G., Li, J. T., Shi, J., and Hui, Y. (2022). Mechanism of lung and intestine combination therapy in treatment of acute lung injury by inhibiting inflammatory response based on NF-κB/NLRP3 signaling pathway and alveolar macrophage activation. *China J. Chin. Materia Medica* 47 (1), 151–158. doi:10.19540/j.cnki.cjcmm.20211027.401

Krishack, P. A., Hollinger, M. K., Kuzel, T. G., Decker, T. S., Louviere, T. J., Hrusch, C. L., et al. (2021). IL-33-mediated eosinophilia protects against acute lung injury. *Am. J. Respir. Cell Mol. Biol.* 64 (5), 569–578. doi:10.1165/rcmb.2020-0166OC

Kufe, D. W. (2020). MUC1-C in chronic inflammation and carcinogenesis; emergence as a target for cancer treatment. *Carcinogenesis* 41 (9), 1173–1183. doi:10.1093/carcin/bgaa082

Lai, C., Wang, K., Zhao, Z., Zhang, L., Gu, H., Yang, P., et al. (2017). C-C motif chemokine ligand 2 (CCL2) mediates acute lung injury induced by lethal influenza H7N9 virus. *Front. Microbiol.* 8, 587. doi:10.3389/fmicb.2017.00587

Lefrançais, E., Mallavia, B., Zhuo, H., Calfee, C. S., and Looney, M. R. (2018). Maladaptive role of neutrophil extracellular traps in pathogen-induced lung injury. *JCI Insight* 3 (3), e98178. doi:10.1172/jci.insight.98178

Li, F., Zhu, H., Sun, R., Wei, H., and Tian, Z. (2012). Natural killer cells are involved in acute lung immune injury caused by respiratory syncytial virus infection. *J. Virol.* 86 (4), 2251–2258. doi:10.1128/jvi.06209-11

Li, G. C., Tian, Z. Y., Zhang, F. H., Hao, H., and Kong, L. (2019). Clinical study on the treatment of sepsis-associated acute respiratory distress syndrome with shengxia lifei decoction. *Chin. J. Acute Med.* 28 (08), 1321–1323. doi:10.3969/j.issn.1004-745X.2019.08.002

Li, H., Zhou, X., Tan, H., Hu, Y., Zhang, L., Liu, S., et al. (2018). Neutrophil extracellular traps contribute to the pathogenesis of acid-aspiration-induced ALI/ARDS. *Oncotarget* 9 (2), 1772–1784. doi:10.18632/oncotarget.22744

Li, J., Wang, M., Xie, Y., Li, S., Yu, X., Li, F., et al. (2025). A randomized, double-blinded, placebo-controlled study of the use of traditional Chinese medicine for treating patients with mild/moderate chronic obstructive pulmonary disease. *J. Evid. Based Med.* 18 (2), e70023. doi:10.1111/jebm.70023

Li, M., Zhao, S., Liu, Y., Wang, Q., Chen, Y., and Zhou, Y. (2024). Pathological characteristics of ferroptosis in kidney tissues in type 2 diabetic patients with diabetic kidney disease. *Dis. Diabetes Metab. Syndr. Obes.* 17, 4105–4113. doi:10.2147/DMSO.S489536

Li, M. H. (2023). "*Investigation on the mechanism of quality markers of jiejing decoction in pedicting and improving acute lung injury*,". Jilin: Jilin agricultural university. doi:10.27163/d.cnki.gjlnu.2023.000920

Li, W., Ding, Z., Chen, Y., Wang, Y., Peng, M., Li, C., et al. (2022). Integrated pharmacology reveals the molecular mechanism of gegen qinlian decoction against lipopolysaccharide-induced acute lung injury. *Front. Pharmacol.* 13, 854544. doi:10.3389/fphar.2022.854544

Li, W. Q., Wu, S., and Qiu, C. H. (2020). Clinical effect of redu ning injection in the treatment of acute respiratory distress syndrome caused by sepsis. *Contemp. Chin. Med.* 27 (19), 57–60.

Li, X., Jamal, M., Guo, P., Jin, Z., Zheng, F., Song, X., et al. (2019). Irisin alleviates pulmonary epithelial barrier dysfunction in sepsis-induced acute lung injury via activation of AMPK/SIRT1 pathways. *Biomed. and Pharmacother.* 118, 109363. doi:10.1016/j.biopha.2019.109363

Li, X. N., Yang, S. Q., Li, M., Li, X. S., Tian, Q., Xiao, F., et al. (2021). Formaldehyde induces ferroptosis in hippocampal neuronal cells by upregulation of the warburg effect. *Toxicology* 448, 152650. doi:10.1016/j.tox.2020.152650

Li, Y., Tang, T. T., and Geng, Y. (2022). The influence of dachengqi decoction combined with basic treatment on inflammatory indicators and prognosis in patients with lung injury caused by sepsis. *Chin. J. Acute Med.* 31 (03), 443–446. doi:10.3969/j.issn.1004-745X.2022.03.018

Li, Z., Huang, H., Chen, F. K., Huang, K. G., Liang, Y. Y., Qiu, W. Y., et al. (2020). Study on the lung-protective effects of diammonium glycyrrhizinate and astragalus injection on acute lung injury. *World Comb. traditional Chin. West. Med. Mag.* 8 (10), 1025–1027. doi:10.13935/j.carolcarrollnkiSJZX.2013.10.030

Li, Z., Pan, H., Yang, J., Chen, D., Wang, Y., Zhang, H., et al. (2023). Xuanfei baidu formula alleviates impaired mitochondrial dynamics and activated NLRP3 inflammasome by repressing NF-κB and MAPK pathways in LPS-induced ALI and inflammation models. *Phytomedicine* 108, 154545. doi:10.1016/j.phymed.2022.154545

Li, Z. Y., and Liang, Q. (2019). Clinical observation on the treatment of acute lung injury in sepsis with chemical Fiber capsules. *World J. Integr. Traditional Chin. West. Med.* 14 (03), 403–406. doi:10.13935/j.cnki.sjzx.190327

Lin, W. C., and Fessler, M. B. (2021). Regulatory mechanisms of neutrophil migration from the circulation to the airspace. *Cell Mol. Life Sci.* 78 (9), 4095–4124. doi:10.1007/s00018-021-03768-z

Liu, J., Wu, Y. H., Zhang, Z. L., and Li, P. (2022). Tanshinone IIA improves sepsis-induced acute lung injury through the ROCK2/NF-κB axis. *Toxicol. Appl. Pharmacol.* 446, 116021. doi:10.1016/j.taap.2022.116021

Liu, M. M., Zhou, J., Ji, D., Yang, J., Huang, Y. P., and Wang, Q. (2021). Diammonium glycyrrhizinate lipid ligand ameliorates lipopolysaccharide-induced acute lung injury by modulating vascular endothelial barrier function. *Exp. Ther. Med.* 21 (4), 303. doi:10.3892/etm.2021.9734

Liu, P., Feng, Y., Li, H., Chen, X., Wang, G., Xu, S., et al. (2020). Ferrostatin-1 alleviates lipopolysaccharide-induced acute lung injury via inhibiting ferroptosis. *Cell Mol. Biol. Lett.* 25, 10–14. doi:10.1186/s11658-020-00205-0

Liu, P., Yang, S., Shao, X., Li, C., Wang, Z., Dai, H., et al. (2024). Mesenchymal stem cells-derived exosomes alleviate acute lung injury by inhibiting alveolar macrophage pyroptosis. *Stem Cells Transl. Med.* 13 (4), 371–386. doi:10.1093/stcltm/szad094

Liu, W. B., Jiang, X. H., and Xia, Y. F. (2019). Clinical efficacy study of ligustrazine injection in the treatment of acute lung injury. *Mod. Med. Health* 35 (15), 2363–2364. doi:10.3969/j.issn.1009-5519.2019.15.034

Liu, Y., Wang, X., Chen, Y., Zhou, L., Wang, Y., Li, L., et al. (2024). Pharmacological mechanisms of traditional Chinese medicine against acute lung injury: from active ingredients to herbal formulae. *Phytomedicine* 135, 155562. doi:10.1016/j.phymed.2024.155562

Liu, Y. J., Li, X., Liu, F., and Li, Y. (2022). Research progress on the antiangiogenic mechanism and clinical application of artemisinin and its derivatives,28(08),148–153. doi:10.13862/j.cn43-1446/r.2022.08.033

Long, W., Xu, L. H., Cheng, Y., and Wang, R. (2020). Ferroptosis involved in sepsis-associated acute lung injury in mice. *Southwest Natl. Def. Med.* 30 (08), 725–728. doi:10.3969/j.issn.1004-0188.2020.08.007

Lu, X. K., Li, D. W., Song, T. Q., Ding, X. Q., Feng, W. G. J., and Li, J. (2021). Observation on the therapeutic effect of huperzine A tablets combined with butylphthalide soft capsules on cognitive function in patients with mild alzheimer's disease. *J. BeiHua Univ. Nat. Sci. Ed.* 22 (01), 62–64. doi:10.11713/j.issn.1009-4822.2021.01.012

Lu, Y., Cheng, W. Q., Niu, K. J., Yu, H. J., and Wang, Y. F. (2024). Research review on quality evaluation of traditional Chinese medicine compound preparations based on multidimensional integration strategy. *Chin. Herb. Med.* 55 (22), 7847–7856. doi:10.7501/j.issn.0253-2670.2024.22.027

Lu, Y., Zhang, P. P., Wang, D. Q., and Li, Z. J. (2020). Discussion on pathogenesis and pathogenesis of acute lung injury. *Chin. J. Acute Med.* 29 (02), 280–282. doi:10.3969/j.issn.1004-745X

Luo, R., Li, X., and Wang, D. (2022). Reprogramming macrophage metabolism and its effect on NLRP3 inflammasome activation in sepsis. *Front. Mol. Biosci.* 9, 917818. doi:10.3389/fmolb.2022.917818

Luo, W., Ruan, Z. L., Yuan, C. F., Li, W. Y., Xia, Y. B., Qian, C., et al. (2024). Based on the TLR4/NF-κB signaling pathway, the mechanism by which qilongtian capsules reduce the polarization of M1 macrophages and inhibit the inflammatory response in acute lung injury was investigated. *Chin. Herb. Med.* 47 (9), 2345–2349. doi:10.13863/j.issn1001-4454.2024.09.034

Ma, M., Wang, K., Yang, Y. H., Yue, M. R., Ren, Q. N., Chen, Y. H., et al. (2024). Influence of tongfu xiefei guanchang solution on intestinal barrier and intestinal flora of rats with acute lung injury based on p38 MAPK/MLCK signaling pathway. *Chin. J. traditional Chin. Med.* 49 (21), 5919–5931. doi:10.19540/j.cnki.cjcmm.20240802.707

McKelvey, M., Uddin, M. B., Palani, S., Shao, S., and Sun, K. (2024). IL-10 counteracts IFN-γ to alleviate acute lung injury in a viral-bacterial superinfection model. *Am. J. Respir. Cell Mol. Biol.* 71 (1), 110–120. doi:10.1165/rcmb.2023-0437OC

Miao, J., Shen, J., Yan, C., Ren, J., Liu, H., Qiao, Y., et al. (2022). The protective effects of mai-luo-ning injection against LPS-induced acute lung injury via the TLR4/NF-κB signalling pathway. *Phytomedicine* 104, 154290. doi:10.1016/j.phymed.2022.154290

Mo, X., and Hu, R. C. (2019). Role of endoplasmic reticulum stress in respiratory diseases. *J. Clin. Pathological Sci.* 39 (10), 2281–2287. doi:10.3978/j.issn.2095-6959.2019.10.028

Mokrá, D. (2020). Acute lung injury - from pathophysiology to treatment. *Physiol. Res.* 69 (Suppl. 3), 353–366. doi:10.33549/physiolres.934602

Müller, M. T., Schempp, R., Lutz, A., Felder, T., Felder, E., Miklavc, P., et al. (2019). Interaction of microtubules and actin during the post-fusion phase of exocytosis. *Sci. Rep.* 9 (1), 11973. doi:10.1038/s41598-019-47741-0

Osburn, W. O., Wakabayashi, N., Misra, V., Nilles, T., Biswal, S., Trush, M. A., et al. (2006). Nrf2 regulates an adaptive response protecting against oxidative damage following diquat-mediated formation of superoxide anion. *Arch. Biochem. Biophys.* 454 (1), 7–15. doi:10.1016/j.abb.2006.08.005

Pei, X. T., Peng, L., and Chen, W. D. (2023). Research progress on the historical evolution, effective components, pharmacological effects and clinical application of xiaoxuming decoction. *J. liaoning Univ. traditional Chin. Med.* 25 (10), 120–124. doi:10.13194/j.issn.1673-842x.2023.10.024

Peng, J., Fan, B., Bao, C., and Jing, C. (2021). JMJD3 deficiency alleviates lipopolysaccharide-induced acute lung injury by inhibiting alveolar epithelial ferroptosis in a Nrf2-dependent manner. *Mol. Med. Rep.* 24 (5), 807. doi:10.3892/mmr.2021.12447

Qin, L., Xiang, Y., Li, H., Li, M., and Qi, X. R. (2025). Effects of yiqi huoxue formula on pulmonary Qi-blood barrier function in rats with acute lung injury induced by lipopolysaccharide. *J. Beijing Univ. Chin. Med.* 47 (12), 1702–1709. doi:10.3969/j.issn.1006-2157.2024.12.010

Qin, Y., Li, W., Liu, J., Wang, F., Zhou, W., Xiao, L., et al. (2024). Andrographolide ameliorates sepsis-induced acute lung injury by promoting autophagy in alveolar macrophages via the RAGE/PI3K/AKT/Mtor pathway. *Int. Immunopharmacol.* 139, 112719. doi:10.1016/j.intimp.2024.112719

Ren, Y. (2020). *Qi xie turbidity qi and the prevention and treatment of acute lung injury (ALI) clinical research*. Guangzhou: Guangzhou university of Chinese medicine. doi:10.27044/d.cnki.ggzzu.2020.000464

Sakaguchi, R., Chikuma, S., Shichita, T., Morita, R., Sekiya, T., Ouyang, W., et al. (2016). Innate-like function of memory Th17 cells for enhancing endotoxin-induced acute lung inflammation through IL-22. *Int. Immunol.* 28 (5), 233–243. doi:10.1093/intimm/dxv070

Schäcke, H., Döcke, W. D., and Asadullah, K. (2002). Mechanisms involved in the side effects of glucocorticoids. *Pharmacol. Ther.* 96 (1), 23–43. doi:10.1016/s0163-7258(02)00297-8

Seyran, M., Melanie, S., Philip, S., Amiq, G., and Fabian, B. (2023). Allies or enemies? The effect of regulatory T cells and related T lymphocytes on the profibrotic environment in bleomycin-injured lung mouse models. *Clin. Exp. Med.* 23 (4), 1075–1088. doi:10.1007/s10238-022-00945-7

Shao, H., Fang, C., Huang, Y., Ye, Y., and Tong, R. (2022). Sodium tanshinone ⅡA sulfonate injection as adjunctive therapy for the treatment of heart failure: a systematic review and meta-analysis. *Phytomedicine* 95, 153879. doi:10.1016/j.phymed.2021.153879

Shen, J. Y., Zhang, E. Y., and Hu, J. (2019). Research progress on acute lung injury and lung protective strategies by cardiopulmonary bypass. *Chin. J. Clin. Thorac. Cardiovasc. Surg.* 26 (02), 186–191. doi:10.7507/1007-4848.201805007

Shi, J., Chen, W., Tang, J., Zhang, C., Qi, M., Zheng, X., et al. (2024). Huperzine A protected against ferroptosis via activating PI3K/Akt signaling in lipopolysaccharide induced acute lung injury. *Eur. J. Pharmacol.* 983, 177004. doi:10.1016/j.ejphar.2024.177004

Shi, J., Yu, T., Song, K., Du, S., He, S., Hu, X., et al. (2021). Dexmedetomidine ameliorates endotoxin-induced acute lung injury *in vivo* and *in vitro* by preserving mitochondrial dynamic equilibrium through the HIF-1a/HO-1 signaling pathway. *Redox Biol.* 41, 101954. doi:10.1016/j.redox.2021.101954

Soehnlein, O., Oehmcke, S., Ma, X., Rothfuchs, A. G., Frithiof, R., van Rooijen, N., et al. (2008). Neutrophil degranulation mediates severe lung damage triggered by streptococcal M1 protein. *Eur. Respir. J.* 32 (2), 405–412. doi:10.1183/09031936.00173207

Song, J. (2022). Clinical effect and pharmacological study of andrographolide dispersible tablets in the treatment of acute periodontitis with wind-heat syndrome in the upper jiao. *Chin. J. Pract. Med.* 17 (22), 141–143. doi:10.14163/j.cnki.11-5547/r.2022.22.043

Su, C. F., Kao, S. J., and Chen, H. I. (2012). Acute respiratory distress syndrome and lung injury: pathogenetic mechanism and therapeutic implication. *World J. Crit. Care Med.* 1 (2), 50–60. doi:10.5492/wjccm.v1.i2.50

Su, Y. J. (2015). *Clinical research on the treatment of acute lung injury caused by sepsis with baofei jiejiong mixture*. Sichuan: ChengDu University of Traditional Chinese Medicine.

Sun, T. T., Ma, X. H., Li, X. X., Zhang, L. H., Li, X. Q., and Yu, F. (2017). Discussion on research status and development ideas of biopotency for Chinese materia medica. *Chin. Herb. Med.* 48 (09), 1906–1911. doi:10.11656/j.issn.1673-9043.2023.03.16

Sun, Z. J. (2024). *Down-regulation of SP1 inhibits ZBP1-induced pan-apoptosis of alveolar macrophages and alleviates sepsis lung injury*. Jiangxi: Nanchang university. doi:10.27232/d.cnki.gnchu.2024.004392

Taheri, P., Dave, D. D., Dash, R. K., Sharma, G. P., Clough, A. V., Jacobs, E. R., et al. (2024). Mitochondrial function in lungs of rats with different susceptibilities to hyperoxia-induced acute lung injury. *J. Appl. Physiol.* 137 (2), 233–253. doi:10.1152/japplphysiol.00243.2024

Tan, P., Li, M., Liu, Z., Li, T., Zhao, L., and Fu, W. (2022). Glycolysis-related LINC02432/hsa-miR-98–5p/HK2 axis inhibits ferroptosis and predicts immune infiltration, tumor mutation burden, and drug sensitivity in pancreatic adenocarcinoma. *Front. Pharma* 13, 937413. doi:10.3389/fphar.2022.937413

Tan, S. Y., and Chen, S. (2020). Progress in research on mitophagy and pulmonary diseases. *J. Basic Med. Clin.* 40 (6), 842–846. doi:10.16352/j.issn.1001-6325.2020.06.024

Tan, W., Zhang, C., Liu, J., and Miao, Q. (2019). Regulatory T-cells promote pulmonary repair by modulating T helper cell immune responses in lipopolysaccharide-induced acute respiratory distress syndrome. *Immunology* 157 (2), 151–162. doi:10.1111/imm.13060

Tavasolian, F., Hosseini, A. Z., Rashidi, M., Soudi, S., Abdollahi, E., Momtazi-Borojeni, A. A., et al. (2021). The impact of immune cell-derived exosomes on immune response initiation and immune system function. *Curr. Pharm. Des.* 27 (2), 197–205. doi:10.2174/1381612826666201207221819

Uddin, M. A., and Barabutis, N. (2019). P53: the endothelium defender. *J. Cell Biochem.* 120 (7), 10952–10955. doi:10.1002/jcb.28511

Um, J. H., and Yun, J. (2017). Emerging role of mitophagy in human diseases and physiology. *BMB Rep.* 50 (6), 299–307. doi:10.5483/bmbrep.2017.50.6.056

Van der Poll, T., Van de Veerdonk, F. L., Scicluna, B. P., and Netea, M. G. (2017). The immunopathology of sepsis and potential therapeutic targets. *Nat. Rev. Immunol.* 17 (7), 407–420. doi:10.1038/nri.2017.36

Verma, A. K., McKelvey, M., Uddin, M. B., Palani, S., Niu, M., Bauer, C., et al. (2022). IFN-γ transforms the transcriptomic landscape and triggers myeloid cell hyperresponsiveness to cause lethal lung injury. *Front. Immunol.* 13, 1011132. doi:10.3389/fimmu.2022.1011132

Vora, S. M., Lieberman, J., and Wu, H. (2021). Inflammasome activation at the crux of severe COVID-19. *Nat. Rev. Immunol.* 21 (11), 694–703. doi:10.1038/s41577-021-00588-x

Wang, H., Wang, S., and Huang, S. (2021). MiR-494-3p alleviates acute lung injury through regulating NLRP3 activation by targeting CMPK2. *Biochem. Cell Biol.* 99 (3), 286–295. doi:10.1139/bcb-2020-0243

Wang, J., Yang, P., Yu, T., Gao, M., Liu, D., Zhang, J., et al. (2022). Lactylation of PKM2 suppresses inflammatory metabolic adaptation in pro-inflammatory macrophages. *Int. J. Biol. Sci.* 18 (16), 6210–6225. doi:10.7150/ijbs.75434

Wang, K., Wang, M., Liao, X., Gao, S., Hua, J., Wu, X., et al. (2022). Locally organised and activated Fth1(hi) neutrophils aggravate inflammation of acute lung injury in an IL-10-dependent manner. *Nat. Commun.* 13 (1), 7703. doi:10.1038/s41467-022-35492-y

Wang, K., Zhang, Y., Cao, Y., Shi, Z., Lin, Y., Chen, Y., et al. (2020). Glycyrrhetinic acid alleviates acute lung injury by PI3K/AKT suppressing macrophagic Nlrp3 inflammasome activation. *Biochem. Biophys. Res. Commun.* 532 (4), 555–562. doi:10.1016/j.bbrc.2020.08.044

Wang, L., Xiong, H., Wu, F., Zhang, Y., Wang, J., Zhao, L., et al. (2014). Hexokinase 2-mediated warburg effect is required for PTEN-and p53-deficiency-driven prostate cancer growth. *Cell Rep.* 8 (5), 1461–1474. doi:10.1016/j.celrep.2014.07.053

Wang, P., Li, H., and Wu, W. (2025). Anti-inflammatory effects of esomeprazole in septic lung injury by mediating endoplasmic reticulum stress. *J. Bioenerg. Biomembr.* 57 (2-3), 173–182. doi:10.1007/s10863-025-10055-0

Wang, S., Lin, F., Zhang, C., Gao, D., Qi, Z., Wu, S., et al. (2024). Xuanbai chengqi decoction alleviates acute lung injury by inhibiting NLRP3 inflammasome. *J. Ethnopharmacol.* 319, 117227. doi:10.1016/j.jep.2023.117227

Wang, W., Zhu, L., Li, H., Ren, W., Zhuo, R., Feng, C., et al. (2022). Alveolar macrophage-derived exosomal tRF-22-8BWS7K092 activates hippo signaling pathway to induce ferroptosis in acute lung injury. *Int. Immunopharmacol.* 107, 108690. doi:10.1016/j.intimp.2022.108690

Wang, X. H., Wang, L., Chang, S., Chen, H. N., and Cui, X. L. (2023). Clinical research of huperzine A tablets combined with oxiracetam capsules in the treatment of vascular cognitive impairment after cerebral infarction. *Chin. Med.* 18 (11), 1642–1646. doi:10.3760/j.issn.1673-4777.2023.11.010

Wang, Y., Han, Q., Liu, L., Wang, S., Li, Y., Qian, Z., et al. (2024). Natural hydrogen gas and engineered microalgae prevent acute lung injury in sepsis. *Mater Today Bio* 28, 101247. doi:10.1016/j.mtbio.2024.101247

Wang, Y., Yang, Y., Chen, L., Xiong, W., Song, L., Li, B., et al. (2020). Death-associated protein kinase 1 mediates ventilator-induced lung injury in mice by promoting alveolar epithelial cell apoptosis. *Anesthesiology* 133 (4), 905–918. doi:10.1097/ALN.0000000000003464

Wang, Y., Zhang, M., Bi, R., Su, Y., Quan, F., Lin, Y., et al. (2022). ACSL4 deficiency confers protection against ferroptosis-mediated acute kidney injury. *Redox Biolo* 51, 102262. doi:10.1016/j.redox.2022.102262

Wang, Y. M., Gong, F. C., Qi, X., Zheng, Y. J., Zheng, X. T., Chen, Y., et al. (2022). Mucin 1 inhibits ferroptosis and sensitizes vitamin E to alleviate sepsis-induced acute lung injury through GSK3β/Keap1-Nrf2-GPX4 pathway. *Oxid. Med. Cell Longev.* 2022 (1), 2405943. doi:10.1155/2022/2405943

Wang, Z., and Wang, Z. (2023). The role of macrophages polarization in sepsis-induced acute lung injury. *Front. Immunol.* 14, 1209438. doi:10.3389/fimmu.2023.1209438

Wang, Z. W., and Zhu, X. (2019). Exosomal miR-19b-3p communicates tubular epithelial cells and M1 macrophage. *Cell Death Dis.* 10 (10), 762. doi:10.1038/s41419-019-2008-0

Wang, Z. Y., Wang, X., Zhang, D. Y., Hu, Y. J., and Li, S. (2022). Pharmacology of traditional chinese medicine network:development in the new era under the guidance of the guidelines. *Chin. J. Traditional Chin. Med.* 47 (01), 7–17. doi:10.19540/j.cnki.cjcmm.20210914.702

Wei, H. L. (2024). *Research on the efficacy and mechanism of compound houttuynia cordata mixture against H3N2 influenza virus*. Jiangsu: Yangzhou university. doi:10.27441/d.cnki.gyzdu.2024.001188

Wu, L., Ramirez, S. H., Andrews, A. M., Leung, W., Itoh, K., Wu, J., et al. (2016). Neuregulin1-β decreases interleukin-1β-induced RhoA activation, myosin light chain phosphorylation, and endothelial hyperpermeability. *J. Neurochem.* 136 (2), 250–257. doi:10.1111/jnc.13374

Xiang, Y., Cai, M., Li, X., Bao, X., and Cai, D. (2021). Protective effect of xiao-xu-ming Decoction-mediated inhibition of ROS/NLRP3 axis on lipopolysaccharide-induced acute lung injury *in vitro* and *in vivo*. *Evid. Based Complement. Altern. Med.* 2021, 8257495. doi:10.1155/2021/8257495

Xiang, Y. J., Cai, D. F., Wang, P., Yu, J. W., Cai, M., and Li, X. T. (2022). Study on the mechanism of xiaoxuming Decoction's intervention in acute lung injury by down-regulating USP9X to regulate NLRP3 ubiquitination levels. *Shanghai J. Traditional Chin. Med.* 56 (03), 48–55. doi:10.16305/j.1007-1334.2022.2105105

Xiao, K., He, W., Guan, W., Hou, F., Yan, P., Xu, J., et al. (2020). Mesenchymal stem cells reverse EMT process through blocking the activation of NF-κB and hedgehog pathways in LPS-induced acute lung injury. *Cell Death Dis.* 11 (10), 863. doi:10.1038/s41419-020-03034-3

Xie, K., Chen, Y. Q., Chai, Y. S., Lin, S. H., Wang, C. J., and Xu, F. (2021). HMGB1 suppress the expression of IL-35 by regulating naïve CD4+ T cell differentiation and aggravating caspase-11-dependent pyroptosis in acute lung injury. *Int. Immunopharmacol.* 91, 107295. doi:10.1016/j.intimp.2020.107295

Xie, L., Zhang, G., Wu, Y., Hua, Y., Ding, W., Han, X., et al. (2024). Protective effects of wenqingyin on sepsis-induced acute lung injury through regulation of the receptor for advanced glycation end products pathway. *Phytomedicine* 129, 155654. doi:10.1016/j.phymed.2024.155654

Xie, Y., Hou, W., Song, X., Yu, Y., Huang, J., Sun, X., et al. (2016). Ferroptosis: process and function. *Cell Death Differ.* 23 (3), 369–379. doi:10.1038/cdd.2015.158

Xie, Y. B., Liang, Z. J., and Huang, W. Q. (2008). Progress in traditional Chinese medicine treatment of acute lung injury. *J. Pract. Clin. Med.* (03), 113–114+118. Available online at: https://kns.cnki.net/kcms2/article/abstract?v=0YYC1NNgyEC98QcSjp0tLGKNxj9iEbQ9aq6uYMEMkkvrqlWFKp7zvihfcNmJIpE2RvE3aul_qz88sNvQ1mwWOQXti6Kf5X5Qu0n7NghjU3RyYuB2ST-bhf9eYF7ebEA-v8ILpm_JG2fX8e74_6Or-v0-aKWpWPPGk24l5M80f-Pl_F8C7zA9ng==&uniplatform=NZKPT&language=CHS.

Xu, A. P., He, X. L., and You, S. (2024). Clinical observation of qingwen badu decoction in the treatment of sepsis-associated acute respiratory distress syndrome. *Hebei J. Traditional Chin. Med.* 46 (06), 932–935.

Xu, G. R. (2016). Evaluation of the therapeutic effect of andrographolide dropping pills in the treatment of 85 cases of sore throat caused by upper respiratory tract infection. *Chin. J. Mod. Med.* 26 (07), 104–107. doi:10.3969/j.issn.1005-8982.2016.07.024

Xu, M., Li, X., Ma, C., Lü, Y., Ma, X., Ma, X., et al. (2020). Effect of human placental mesenchymal stem cells transplantation on pulmonary vascular endothelial permeability and lung injury repair in mice with acute lung injury. *Chin. J. Reparative Reconstr. Surg.* 34 (3), 387–392. doi:10.7507/1002-1892.201909070

Xu, Q. C. (2023). *Research on the role and mechanism of Pannexin1 in regulating mitochondrial dynamics in acute lung injury caused by sepsis*. Wu han: Wu Han University. doi:10.27379/d.cnki.gwhdu.2023.000365

Xu, Y., Xin, J., Sun, Y., Wang, X., Sun, L., Zhao, F., et al. (2024). Mechanisms of sepsis-induced acute lung injury and advancements of natural small molecules in its treatment. *Pharm. (Basel)* 17 (4), 472. doi:10.3390/ph17040472

Xu, Y. J., Wang, X. L., Mu, W. Q., Wen, J. C., Wang, Y., Xiu, Y., et al. (2024). Mechanism of total glucosides of white paeony capsules in ameliorating acute lung injury based on NLRP3 inflammasome. *ZhongGuo Zhong Yao Za Zhi* 49 (10), 2754–2765. doi:10.19540/j.cnki.cjcmm.20240202.703

Yan, Y., Zou, Z., Sun, Y., Li, X., Xu, K. F., Wei, Y., et al. (2013). Anti-malaria drug chloroquine is highly effective in treating Avian influenza A H5N1 virus infection in an animal model. *Cell Res.* 23 (2), 300–302. doi:10.1038/cr.2012.165

Yang, Q., Xu, H. R., Xiang, S. Y., Zhang, C., Ye, Y., Shen, C. X., et al. (2021). Resolvin conjugates in tissue regeneration 1 promote alveolar fluid clearance by activating alveolar epithelial sodium channels and Na, K-ATPase in lipopolysaccharide-induced acute lung injury. *J. Pharmacol. Exp. Ther.* 379 (2), 156–165. doi:10.1124/jpet.121.000712

Yang, S., Qin, H. L., Li, Y. X., Wang, X., Zhang, R. T., and Yang, J. (2023). Research progress on traditional Chinese medicine in prevention and treatment of alveolar-capillary barrier dysfunction. *Chin. Herb. Med.* 54 (15), 5075–5087. doi:10.7501/j.issn.0253-2670.2023.15.031

Yang, W. S., SriRamaratnam, R., Welsch, M. E., Shimada, K., Skouta, R., Viswanathan, V. S., et al. (2014). Regulation of ferroptotic cancer cell death by GPX4. *Cell* 156 (1), 317–331. doi:10.1016/j.cell.2013.12.010

Yang, Y. M., Qu, S. Q., Chen, L. N., Deng, S. Q., Zhang, Y, and Zheng, Z. Y. (2022). Protective effect of Shenlian prescription on acute lung injury induced by particulate matter exposure in rats. *Chin. J. Exp. Formulas Chin. Med.* 28 (20), 37–44. doi:10.13422/j.cnki.syfjx.20221405

Ye, X. L., Tian, S. S., Tang, C. C., Jiang, X. R., Liu, D., Yang, G. Z., et al. (2023). Cytokine storm in acute viral respiratory injury: role of qing-fei-pai-du decoction in inhibiting the infiltration of neutrophils and macrophages through TAK1/IKK/NF-[Formula: see text]B pathway. *Am. J. Chin. Med.* 51 (05), 1153–1188. doi:10.1142/S0192415X23500532

Youssef, N. S., Elzaitony, A. S., and Baky, N. A. A. (2022). Diacerein attenuate LPS-induced acute lung injury via inhibiting ER stress and apoptosis: impact on the crosstalk between SphK1/S1P, TLR4/NFκB/STAT3, and NLRP3/IL-1β signaling pathways. *Life Sci.* 308, 120915. doi:10.1016/j.lfs.2022.120915

Yu, C., Li, Y., Li, Y., Li, S., Zeng, F., Yu, J., et al. (2024). A novel mechanism for regulating lung immune homeostasis: zukamu granules alleviated acute lung injury in mice by inhibiting NLRP3 inflammasome activation and regulating Th17/Treg cytokine balance. *J. Ethnopharmacol.* 324, 117831. doi:10.1016/j.jep.2024.117831

Yu, H., Bai, Y., Qiu, J., He, X., Xiong, J., Dai, Q., et al. (2021). *Pseudomonas aeruginosa* PcrV enhances the nitric oxide-mediated tumoricidal activity of tumor-associated macrophages via a TLR4/PI3K/AKT/mTOR-glycolysis-nitric oxide circuit. *Front. Oncol.* 11, 736882. doi:10.3389/fonc.2021.736882

Yu, L. C., He, R., Wang, D. X., and Qi, D. (2024). Activated Clec4n(hi) neutrophils aggravate lung injury in an endothelial IGFBP7-dependent manner. *Am. J. Respir. Cell Mol. Biol.* 71 (1), 66–80. doi:10.1165/rcmb.2024-0017OC

Yu, W., Lv, Y., Xuan, R., Han, P., Xu, H., Ma, X., et al. (2024). Human placental mesenchymal stem cells transplantation repairs the alveolar epithelial barrier to alleviate lipopolysaccharides-induced acute lung injury. *Biochem. Pharmacol.* 229, 116547. doi:10.1016/j.bcp.2024.116547

Yu, Y., Li, Y., Zhou, L., Cheng, X., and Gong, Z. (2024). Hepatic stellate cells promote hepatocellular carcinoma development by regulating histone lactylation: novel insights from single-cell RNA sequencing and spatial transcriptomics analyses. *Cancer Lett.* 604, 217243. doi:10.1016/j.canlet.2024.217243

Yu, Y. J., Zhou, Z. Y., Lv, L., Jin, X. Y., Wang, Z. Q., Liu, Y. Y., et al. (2023). Discussion of traditional chinese medicine and western medicine treatment of pulmonary nodules. *J. Tianjin Univ. Of Traditional Chin. Med.* 42 (03), 366–374.

Zeng, Y. (2019). *The characteristics and evolutionary features of TCM syndrome elements in sepsis resulting from pulmonary infection*. Beijing: Beijing university of traditional Chinese medicine.

Zhan, P., Lu, X., Li, Z., Wang, W. J., Peng, K., Liang, N. N., et al. (2022). Mitoquinone alleviates bleomycin-induced acute lung injury via inhibiting mitochondrial ROS-dependent pulmonary epithelial ferroptosis. *Int. Immunopharmacol.* 113, 109359. doi:10.1016/j.intimp.2022.109359

Zhang, B., Luo, L., Xiong, S., Xiao, Y., Zhang, T., and Xiang, T. (2024). Anisodamine hydrobromide ameliorates acute lung injury via inhibiting pyroptosis in murine sepsis model. *Immunopharmacol. Immunotoxicol.* 46 (5), 662–671. doi:10.1080/08923973.2024.2386331

Zhang, C. (2020). *Omics method screening for the reuse of old drugs against highly pathogenic avian influenza virus and research on immune response and lung injury in COVID-19 patients (doctoral dissertation)*. Anhui: University of Science and Technology of China. doi:10.27517/d.cnki.gzkju.2020.001129

Zhang, C., Li, X., Gao, D., Zhu, H., Wang, S., Tan, B., et al. (2023). Network pharmacology and experimental validation of the anti-inflammatory effect of tingli dazao xiefei decoction in acute lung injury treatment. *J. Inflamm. Res.* 16, 6195–6209. doi:10.2147/JIR.S433840

Zhang, C., Wang, X., Wang, C., He, C., Ma, Q., Li, J., et al. (2021). Qingwenzhike prescription alleviates acute lung injury induced by LPS via inhibiting TLR4/NF-kB pathway and NLRP3 inflammasome activation. *Front. Pharmacol.* 12, 790072. doi:10.3389/fphar.2021.790072

Zhang, G. M., Li, F. A., and Tong, L. (2010). The protective effect of pretreatment with the hot pain formula on endotoxin-induced lung injury in rats. *Chin. J. Exp. formulas Chin. Med.* 16 (15), 129–131. doi:10.13422/j.cnki.syfjx.2010.15.049

Zhang, H., Hu, P. P., Wang, Z. L., Liu, Y. J., and Jin, Q. F. (2022). The influence of shenfu injection on the levels of inflammatory factors and coagulation function in patients with septic lung injury undergoing mechanical ventilation. *Chin. Foreign Med.* 41 (6), 17–21. doi:10.16662/j.carolcarrollnki.1674-0742.2022.06.017

Zhang, H. S., Du, G. Y., Zhang, Z. G., Zhou, Z., Sun, H. L., Yu, X. Y., et al. (2018). NRF2 facilitates breast cancer cell growth via HIF1α-mediated metabolic reprogramming. *Int. J. Biochem. Cell Biol.* 95, 85–92. doi:10.1016/j.biocel.2017.12.016

Zhao, Y., Jiang, Y., Chen, L., Zheng, X., Zhu, J., Song, X., et al. (2020). Inhibition of the endoplasmic reticulum (ER) stress-associated IRE-1/XBP-1 pathway alleviates acute lung injury via modulation of macrophage activation. *J. Thorac. Dis.* 12 (3), 284–295. doi:10.21037/jtd.2020.01.45

Zhao, Y. T., Zhang, H. Y., Cao, Y. J., Li, J. D., Yin, X. D., and Wang, P. R. (2024). Research progress on the role and mechanism of artemisinin and its derivatives in skin diseases. *Clin. Med. World* 45 (6), 575–582. doi:10.13683/j.wph.2024.06.002

Zheng, J. S., Qian, J. L., Jiang, N., Wei, Y., He, H. D., Ma, C. F., et al. (2021). The effect of qidong huoxue yin on the iRhom2/TACE signaling pathway in alveolar macrophages of mice with acute lung injury. *J. zhejiang Univ. Chin. Med.* 45 (05), 530–536. doi:10.16466/j.issn1005-5509.2021.05.018

Zheng, Q. (2020). Research on the role and mechanism of NAMPT regulating pyroptosis of T lymphocytes in immunosuppression of traumatic sepsis. Zhejiang: Huazhong university of science and technology. doi:10.27157/d.cnki.ghzku.2020.002090

Zheng, W. W., and Zhang, Z. B. (2024). The effect of xuebijing injection combined with ulinastatin injection in the treatment of sepsis complicated with acute lung injury and its influence on the HMGB1/TLR4/NF-Kb signaling pathway. *J. Transl. Med.* 13 (02), 259–263. doi:10.3969/j.issn.2095-3097.2024.02.021

Zheng, X. (2023). *Investigation on the effect of LCN2 on macrophage polarization in severe hypothermia acute lung injury based on RNA-seq*. Anhui: Anhui Medical University. doi:10.26921/d.cnki.ganyu.2023.000720

Zheng, Y., Liu, Y., Ye, C., Ming, L., and Wanru, C. (2024). Effectiveness and safety of qidong huoxue decoction in treatment of acute lung injury and acute respiratory distress syndrome: a randomized, controlled trial. *J. Tradit. Chin. Med.* 44 (2), 381–387. doi:10.19852/j.cnki.jtcm.2024.02.003

Zhong, W. J. (2023). *Research on the role and mechanism of TREM-1 mediating macrophage inflammation and prognosis in acute lung injury*. Hunan: Central south university. doi:10.27661/d.cnki.gzhnu.2023.000764

Zhou, B., Yuan, Y., Zhang, S., Guo, C., Li, X., Li, G., et al. (2020). Intestinal flora and disease mutually shape the regional immune system in the intestinal tract. *Front. Immunol.* 11, 575. doi:10.3389/fimmu.2020.00575

Zhou, Y., Li, Q. X., Liao, Z. Z., Liu, Y, Ouyang, Y., Jiang, W. J., et al. (2023). Anti-inflammatory effect and component analysis of Chaihu Qingwen granules. *J. Ethnopharmacol.* 317, 116763. doi:10.1016/j.jep.2023.116763

Zhu, H., Wang, S., Shan, C., Li, X., Tan, B., Chen, Q., et al. (2021). Mechanism of protective effect of xuan-bai-cheng-qi decoction on LPS-induced acute lung injury based on an integrated network pharmacology and RNA-sequencing approach. *Respir. Res.* 22 (1), 188. doi:10.1186/s12931-021-01781-1

Zhu, H. P., Huang, H. Y., Wu, D. M., Dong, N., Dong, L., Chen, C. S., et al. (2020). Regulatory mechanism of NOV/CCN3 in the inflammation and apoptosis of lung epithelial alveolar cells upon lipopolysaccharide stimulation. *Mol. Med. Rep.* 21 (4), 1872–1880. doi:10.3892/mmr.2019.10655

Zhu, L. J., He, Z. R., Wang, C. Y., Lu, D. Y., Yang, J. L., Jia, W. W., et al. (2024). Development history and frontier research progress of pharmacokinetics of traditional chinese medicine. *J. GuangZhou Univ. Chin. Med.* 41 (10), 2746–2757. doi:10.13359/j.cnki.gzxbtcm.2024.10.034

Zong, Y., Li, H., Liao, P., Chen, L., Pan, Y., Zheng, Y., et al. (2024). Mitochondrial dysfunction: mechanisms and advances in therapy. *Signal Transduct. Target Ther.* 9 (1), 124. doi:10.1038/s41392-024-01839-8

Zou, L., Dang, W., Tao, Y., Zhao, H., Yang, B., Xu, X., et al. (2023). The Il-33/St2 axis promotes acute respiratory distress syndrome by natural killer T cells. *Shock* 59 (6), 902–911. doi:10.1097/shk.0000000000002114

Zou, Y., Palte, M. J., Deik, A. A., Li, H., Eaton, J. K., Wang, W., et al. (2019). A GPX4-dependent cancer cell state underlies the clear-cell morphology and confers sensitivity to ferroptosis. *Nat. Commun.* 10 (1), 1617. doi:10.1038/s41467-019-09277-9

frontiers | Frontiers in Pharmacology

TYPE Original Research
PUBLISHED 03 September 2025
DOI 10.3389/fphar.2025.1586334

Check for updates

OPEN ACCESS

EDITED BY
Dâmaris Silveira,
University of Brasilia, Brazil

REVIEWED BY
Chandrabose Selvaraj,
Amet University, India
Omar Estrada,
Instituto Venezolano de Investigaciones Científicas (IVIC), Venezuela
Kameswara Rao Badri,
Morehouse School of Medicine, United States

*CORRESPONDENCE
Shyh-Shyun Huang,
sshuang@mail.cmu.edu.tw
Jung Chao,
jungchao@mail.cmu.edu.tw

†These authors have contributed equally to this work and share first authorship

RECEIVED 02 March 2025
ACCEPTED 18 July 2025
PUBLISHED 03 September 2025

CITATION
Chi M-H, Ko C-Y, Chi T-W, Huang C-R, Lin J-G, Chao J and Huang S-S (2025) Ethnobotanical survey of herbal medicines for anti-COVID-19 used by traditional Chinese medicine pharmacies in Taiwan.
Front. Pharmacol. 16:1586334.
doi: 10.3389/fphar.2025.1586334

COPYRIGHT
© 2025 Chi, Ko, Chi, Huang, Lin, Chao and Huang. This is an open-access article distributed under the terms of the Creative Commons Attribution License (CC BY). The use, distribution or reproduction in other forums is permitted, provided the original author(s) and the copyright owner(s) are credited and that the original publication in this journal is cited, in accordance with accepted academic practice. No use, distribution or reproduction is permitted which does not comply with these terms.

Ethnobotanical survey of herbal medicines for anti-COVID-19 used by traditional Chinese medicine pharmacies in Taiwan

Min-Han Chi[1†], Chien-Yu Ko[1†], Ting-Wei Chi[2], Chi-Ruei Huang[3], Jaung-Geng Lin[4], Jung Chao[5*] and Shyh-Shyun Huang[1,6*]

[1]School of Pharmacy, China Medical University, Taichung, Taiwan, [2]Department of Rehabilitation, Far Eastern Memorial Hospital, New Taipei City, Taiwan, [3]School of Medicine, Tzu Chi University, Hualien, Taiwan, [4]School of Chinese Medicine, College of Chinese Medicine, China Medical University, Taichung, Taiwan, [5]Department of Chinese Pharmaceutical Sciences and Chinese Medicine Resources, Master Program for Food and Drug Safety, Chinese Medicine Research Center, China Medical University, Taichung, Taiwan, [6]Department of Food Nutrition and Health Biotechnology, Asia University, Taichung, Taiwan

Introduction: Traditional Chinese medicine (TCM) pharmacies in Taiwan have been a vital healthcare resource in Chinese communities, with generations of accumulated TCM knowledge playing a crucial role in infectious disease prevention and treatment. However, as proprietors age and the industry declines, this valuable ethnomedicinal knowledge faces the risk of being lost. Therefore, documenting and analyzing the knowledge used by Taiwanese TCM pharmacies in combating COVID-19 is essential for the preservation and application of ethnomedicine.

Methods: This study employed a stratified sampling method to survey 106 TCM pharmacies in Taiwan, collecting 61 TCM formulae against COVID-19. The medicinal materials were compiled, and analysis were conducted using relative frequency of citation (RFC) and the Phi correlation coefficient to examine the relationships among TCMs. Furthermore, cluster analysis was applied to establish TCM combination patterns.

Results: This study recorded a total of 70 medicinal materials and identified 30 commonly used ones, categorizing them into four major groups: Group A (heat-clearing and detoxifying): As similar as NRICM101, suitable for moderate to severe cases. Group B (heat-clearing and tonifying): Suitable for mild cases, with both antiviral and immune-boosting effects. Group C (symptom relief): Primarily used for relieving cough, expelling phlegm, and alleviating discomfort. Group D (tonifying and strengthening): Suitable for uninfected individuals to enhance immunity.

Discussion: This study successfully documented and analyzed the TCM usage patterns of Taiwanese TCM pharmacies in combating COVID-19, revealing their alignment with modern TCM theories. The findings not only contribute to the preservation of ethnobotanical knowledge but also serve as a reference for

developing herbal prevention strategies and healthcare products, ensuring that traditional medical wisdom can play a greater role within the modern healthcare system.

KEYWORDS

SARS-CoV-2, COVID-19, traditional Chinese medicine, ethnobotany, Taiwan

1 Introduction

Coronavirus Disease 2019 (COVID-19) first emerged in Wuhan, China, in early December 2019 (Ahn et al., 2020; Zhou P. et al., 2020; Zhu et al., 2020). Research identified the pathogen as a novel coronavirus, named SARS-CoV-2 (Coronaviridae Study Group of the International Committee on Taxonomy of Viruses, 2020). According to statistics from the World Health Organization (WHO), as of 2 February 2025, the global number of confirmed COVID-19 cases has exceeded 770 million, with more than 7 million deaths (World Health Organization, 2024). Although the COVID-19 pandemic has gradually subsided with the increase in vaccination rates, studies have indicated that COVID-19 infection significantly raises the risk of cardiovascular complications and chronic kidney disease (Del Vecchio et al., 2024). Therefore, the search for potential drugs to prevent and treat COVID-19 infection remains important and necessary. According to the COVID-19 treatment guidelines published by the National Institutes of Health (NIH), recommended drugs for non-hospitalized adult patients include glucocorticoids (e.g., Dexamethasone), 3C-like protease inhibitors [e.g., Nirmatrelvir/ritonavir (Paxlovid®)], Nucleoside Analogues (e.g., Molnupiravir), and RNA-dependent RNA polymerase inhibitors (e.g., Remdesivir) (COVID-19 Treatment Guidelines Panel, 2024). The most used therapeutic drug in clinical settings is Paxlovid®. Although studies have shown that Paxlovid® can reduce the severity of COVID-19 symptoms, its high cost and potential for multiple drug interactions still make it unaffordable and intolerable for many patients with chronic diseases (Marzolini et al., 2022). In addition, the development of other new drugs takes a long time, which is not a quick solution. As a result, there has been an international effort to explore the therapeutic and preventive effects of traditional Chinese herbal medicine for COVID-19.

As countries worldwide strive to control the COVID-19 pandemic, the development of new drugs is time-consuming and cannot provide an immediate solution. Therefore, drug repurposing has become the primary strategy for using existing Western medicines to treat COVID-19 (Singh et al., 2020; Zhou Y. et al., 2020; Asselah et al., 2021; Yousefi et al., 2021). However, the side effects of many Western medicines are often difficult for patients to tolerate, and the therapeutic effects of drug repurposing remain limited. As a result, there has been a growing international effort to explore the therapeutic and preventive effects of traditional Chinese herbal medicine for COVID-19. A previous study tracked 782 patients who were treated with the traditional Chinese herbal formula—Qingfei Paidu Decoction (QFPDD)—for COVID-19. The findings revealed that early use of QFPDD significantly shortened the disease recovery period and hospitalization duration (Shi et al., 2020). Another systematic review found that the disease cure rate in the combined Chinese and Western medicine group was higher than that in the Western medicine-only group. Additionally, it was observed that the integration of Chinese and Western medicine significantly reduced the length of hospital stay for patients (Liu M. et al., 2020). In summary, the use of traditional Chinese herbal medicine alone or in combination with Western medicine can effectively shorten the COVID-19 recovery period. Therefore, exploring potential effective herbal medicines for the prevention and treatment of COVID-19 holds significant promise.

Previous studies have indicated that the annual prevalence of over-the-counter traditional Chinese medicine (TCM) purchases among the Taiwanese population is as high as 74.8% (Hu et al., 2020). According to statistics from the Ministry of Health and Welfare (MOHW) of Taiwan, as of the end of 2020, there were 8,348 TCM pharmacies across Taiwan (Ministry of Health and Welfare, 2024). On average, there are 0.231 TCM pharmacies per square kilometer, making them highly accessible. As a result, TCM pharmacies remain the primary channel for the Taiwanese public to purchase herbal medicines. These pharmacies have existed in Taiwanese society long before the introduction and development of Western medicine, with generations of accumulated TCM knowledge serving as a crucial tool for combating diseases in Chinese communities. Even today, despite the rapid advancement of Western medicine, the knowledge preserved in TCM pharmacies continues to play a vital role in disease prevention and health maintenance within Chinese society. Today, TCM pharmacies in Taiwan serve as rich repositories of TCM knowledge. However, the average age of TCM pharmacy proprietors has exceeded 60 years, and the number of pharmacies is decreasing annually. Therefore, exploring and preserving the extensive TCM knowledge passed down through these pharmacies has become an urgent task.

In this study, we conducted fieldwork to community TCM pharmacies in Taiwan, collecting the herbal formulae they offered for COVID-19 treatment. We analyzed these formulae, identified candidate medicinal materials used against COVID-19, and applied statistical analysis to examine the relationships between these medicinal materials. By doing so, we uncovered the selection patterns of medicinal materials used by TCM pharmacies in combating COVID-19. Ultimately, the findings of this study aim to provide clinical practitioners with reference data for COVID-19 treatment prescriptions and support the development and application of health products.

2 Materials and methods

2.1 Ethical review

This study was conducted from July 2021 to June 2022 and was approved by the Central Regional Research Ethics Committee of China Medical University and Hospital (Approval No. CMUH110-REC2-115) (Supplementary Figure S1).

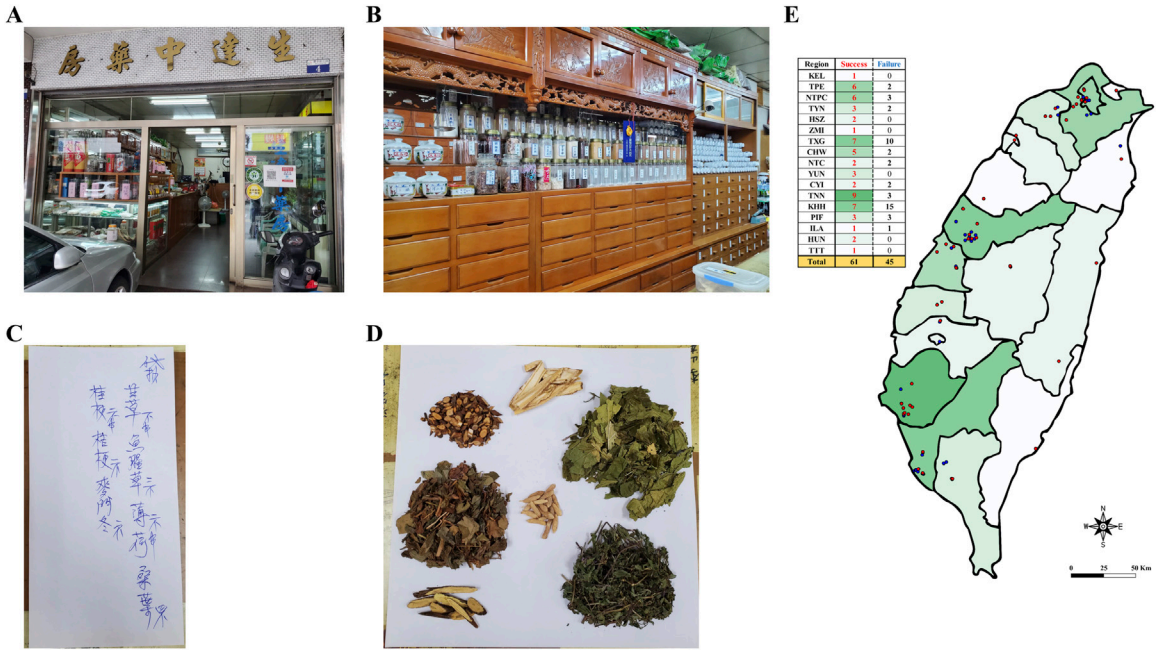


FIGURE 1
Photograph of TCM pharmacy **(A)** Appearance of TCM pharmacy **(B)** TCM cabinet **(C)** Anti-COVID-19 handwritten prescription **(D)** Anti-COVID-19 formula **(E)** Distribution map of 106 TCM pharmacies. Note: The red dots represent the locations of successful collection pharmacies; the blue dots represent the locations of failed collection pharmacies. KEL, Keelung City; TPE, Taipei City; NTPC, New Taipei City; TYN, Taoyuan City; HSZ, Hsinchu County; ZMI, Miaoli County; TXG, Taichung City; CHW, Changhua County; NTC, Nantou County; YUN, Yunlin County; CYI, Chiayi County; TNN, Tainan City; KHH, Kaohsiung City; PIF, Pingtung County; ILA, Yilan County; HUN, Hualien County; TTT, Taitung County.

2.2 Study area and formulae collection

The study area for this research is Taiwan, a spindle-shaped island located in the western Pacific Ocean, positioned between the Republic of the Philippines and the Ryukyu Islands. To the west, Taiwan is separated from the People's Republic of China by the Taiwan Strait. According to the Taiwan Geodetic Datum 1997 (TWD97) coordinate system, the geographic reference point of Taiwan is (23°58′N, 120°58′E), with a total land area of approximately 36,000 km^2.

The sampling data for this study were based on the official statistics published by the Department of Statistics at the MOHW in Taiwan (Ministry of Health and Welfare, 2024), using the data on the number of licensed TCM pharmacies operating under Article 103 of the Pharmaceutical Affairs Act as of the end of 2020, and stratified by county and city. The number of sampled pharmacies in each county and city was determined according to the distribution ratio presented in the official statistics (Supplementary Table S1).

After determining the sample size, the pharmacies in each county and city were visited to purchase the anti-COVID-19 formulae and the purchase information was recorded in detail (Figure 1). After reaching the estimated number of formulae to be collected in each county and city, the formulae were taken to the laboratory for disassembly.

2.3 Medicinal material identification and information sorting

In this study, the macroscopical identification method was used during formulae disassembly and medicinal materials recognition (Supplementary Figure S2). Firstly, the identification of medicinal materials was conducted through visual, olfactory, gustatory, and tactile examination (Zhao et al., 2011). Secondly, image authentication was carried out against the "Taiwan Herbal Pharmacopeia Database" (Department of Chinese Medicine and Pharmacy, 2024) and the "Color Atlas for the Authentic and Superior Chinese Material Medica" (Xian-Zhe, 2007). Thirdly, the results of the secondary authentication were provided to a review panel consisting of three PhDs in traditional Chinese medicine and two practitioners in Chinese medicine industry. These five experts conducted tertiary authentication by double-checking the results of the secondary authentication, and authentication report was compiled to confirm the correct origin of the medicinal materials. Afterwards, the medicinal materials were then photographed using a smartphone, and detailed information for each formula was compiled into a digital report (PDF file) for recordkeeping. Finally, each formula was ultimately packed into a separate bag, with the purchase location and date handwritten on the bag, and stored at the specimen storage area in the China Medical University.

In order to include information about all the medicinal materials collected in this study, the study referred to the *Taiwan Herbal Pharmacopeia fourth Edition* (Taiwan Herbal Pharmacopeia 4th Edition Committee, 2021), the *Pharmacopoeia of the People's Republic of China 2020 Edition* (Chinese Pharmacopoeia Commission, 2020), and *Chinese Materia Medica* (National Administration of Traditional Chinese Medicine "Chinese Materia Medica" Editorial Board, 1999) for medicinal material data collection. The collected information included kingdom,

family, local name, scientific name, part used, traditional use, and property and flavor. If discrepancies exist among the three references, the hierarchy of information, from highest to lowest authority, is as follows: the *Taiwan Herbal Pharmacopeia fourth Edition*, the *Pharmacopoeia of the People's Republic of China 2020 Edition*, and *Chinese Materia Medica*. For medicinal materials with differing family classifications and scientific names across different references, verification and standardization were conducted using World Flora Online database (Royal Botanic Gardens and Garden, 2024).

2.4 Data analysis

The data collected in this study were analyzed and visualized using Microsoft Office 365 Excel, GraphPad Prism (Version 10.2.2), Adobe Illustrator (Version 28.5.0.132), and RStudio (Version 2024.04.2). For quantitative analysis, two parameters were applied: relative frequency of citation (RFC) and the Phi coefficient. Referring to the RFC formula definition from previous studies (Ahmad et al., 2017), the formula was modified to fit this study, as shown below:

$$\mathrm{RFC} = \frac{\text{the number of one medicinal material mentioned in total formulae}}{\text{the total number of collected formulae}}$$

For the Phi coefficient, a contingency table was first created to record the occurrence frequency of any two medicinal materials. Then, referring to the Phi coefficient formula from previous studies (Chytrý et al., 2002; Cui et al., 2016), it was modified to fit this study, as shown below:

$$\text{phi coefficient } (\varphi) = \frac{(a \times d) - (b \times c)}{\sqrt{(a+b) \times (c+d) \times (a+c) \times (b+d)}}$$

In this formula, "a" represents the number of formulae in which both TCM-A and TCM-B appear; "b" represents the number of formulae in which TCM-A appears but TCM-B does not; "c" represents the number of formulae in which TCM-A does not appear but TCM-B does; and "d" represents the number of formulae in which neither TCM-A nor TCM-B appear. The Phi coefficient ranges from −1 to +1, with higher values indicating stronger associations between the medicinal materials. The calculated Phi coefficient values were then combined with cluster analysis to generate a network graph, which was used to explore the combination patterns of medicinal materials in Taiwan TCM pharmacies for combating COVID-19.

3 Results

3.1 Results of anti-COVID-19 formulae and medicinal material information collection

According to the data published by the Department of Statistics at MOHW in Taiwan at the end of 2020, there were a total of 8,348 TCM pharmacies in Taiwan, operating in accordance with Article 103 of the Pharmaceutical Affairs Act. Among these, Kaohsiung City had the highest number of pharmacies, with 1,350, while Taitung County had the fewest, with only 48 (Supplementary Table S1). This study conducted stratified sampling based on counties and cities, with the sample size determined according to the proportion of TCM pharmacies in each area. A total of 106 pharmacies were randomly selected for fieldwork. As a result, 61 anti-COVID-19 formulae were successfully collected. Additionally, 45 pharmacies reported that they did not sell any anti-COVID-19 formula (Figure 1).

Differences in taxonomic methods and the specific versions applied during the compilation of different pharmacopeias have led to inconsistencies in classification. Therefore, for the families and scientific names, this study uses the content recorded in World Flora Online as the standard to correct and integrate the plant information from each pharmacopeia (Royal Botanic Gardens and Garden, 2024). In this study, among the 61 formulae, a total of 70 medicinal materials were identified. Of these, 1 medicinal material belongs to the Fungi kingdom (1.43%), while the remaining 69 medicinal materials belong to the Plantae kingdom (98.57%). These 70 medicinal materials are distributed across 40 families, with the most common families being the Lamiaceae (n = 8, 11.43%), Apiaceae (n = 6, 8.57%), Fabaceae (n = 4, 5.71%), and Compositae (n = 4, 5.71%). Statistical results of the parts used suggested that 17 medicinal parts are used, with the radix being the most common (n = 19, 27.14%), followed by the rhizoma (n = 11, 15.71%) (Supplementary Figure S3).

3.2 Properties, flavors, and traditional uses of medicinal materials against COVID-19

Each medicinal material may possess multiple medicinal flavors, but it will only have one medicinal property. Medicinal properties can be classified as hot, warm, neutral, cool, or cold; medicinal flavors can be classified as sour, bitter, sweet, pungent, salty, bland, and astringent. This study consolidates pharmacopeial information for 70 medicinal materials, with cold properties (41.43%) and warm properties (40.00%) being the most prevalent (Figure 2A). The medicinal flavors are predominantly sweet (34.86%), bitter (33.03%), and pungent (23.85%) (Figure 2B). When both medicinal flavors and properties are considered together, the most common combinations are bitter and cold (18.35%), pungent and warm (17.43%), and sweet and cold (15.60%) (Figure 2C). In terms of traditional uses, among the 70 medicinal materials consolidated in this study, the top three most common traditional uses are "Qi-tonifying" (14.29%), "Heat-clearing and detoxicating" (11.43%), and "Pungent-warm exterior-releasing" (11.43%) (Figure 2D).

3.3 Correlation of medicinal materials against COVID-19

To determine the usage frequency of each medicinal material, this study calculated the RFC values for the 70 medicinal materials and excluded those with RFC values below 0.05 from the correlation statistics. Among the 70 medicinal materials, 30 had RFC values greater than 0.05 (referred to as commonly used medicinal materials), in descending order of *Glycyrrhiza uralensis* Fisch.

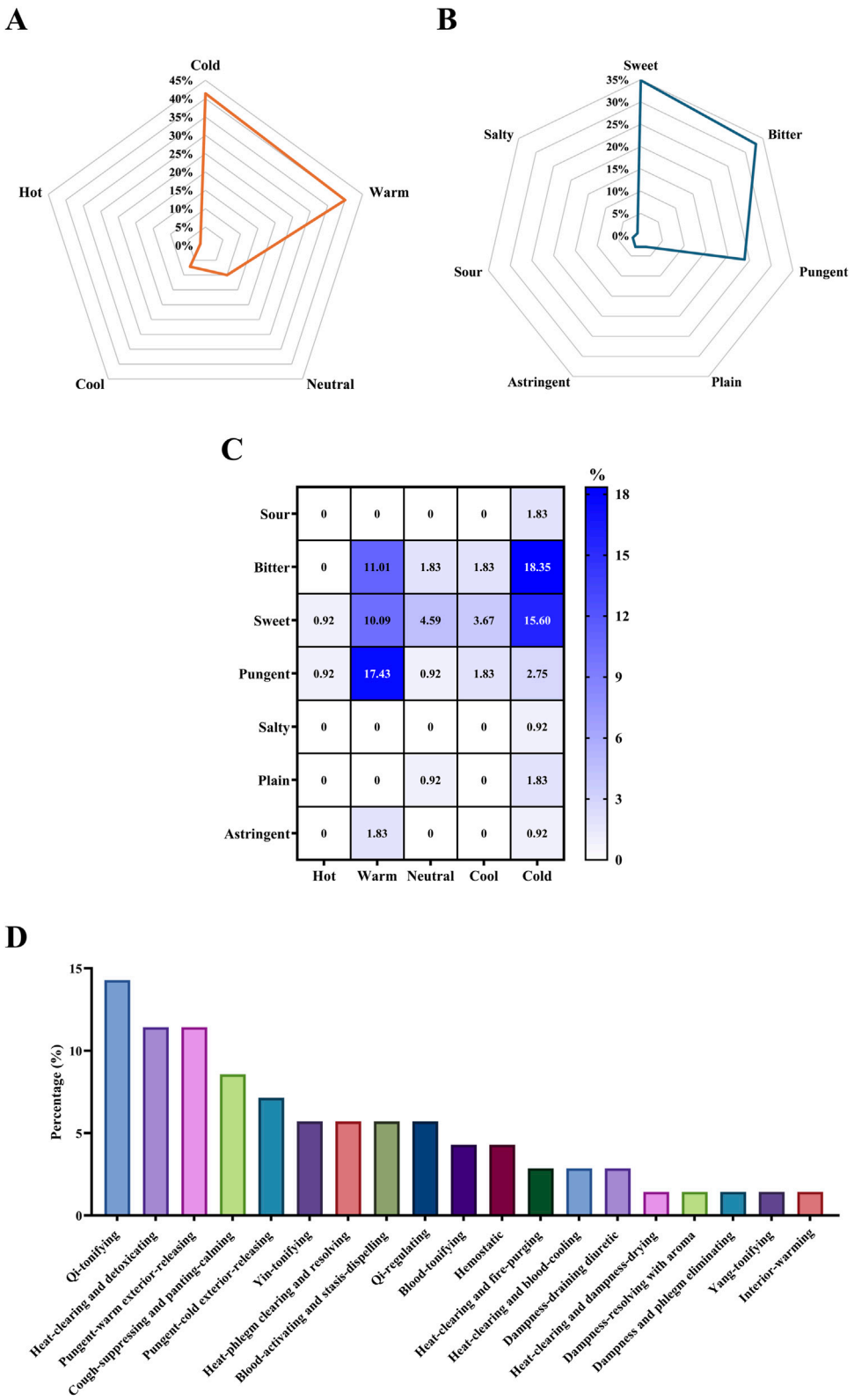


FIGURE 2
Flavor, property and traditional use statistics analysis charts of 70 medicinal materials combating COVID-19 **(A)** Radar plot of properties **(B)** Radar plot of flavors **(C)** Correlation heat map of flavors and properties **(D)** Bar chart of traditional uses.

TABLE 1 Information on 70 medicinal materials used in anti-COVID-19 formulae.

No	Latin name	Local name	Scientific name	Code	Family	Part used	RFC	Traditional use	Flavors/ Properties	Dosage[a]
1	Glycyrrhiza radix et rhizoma	Kan ts'ao 甘草	*Glycyrrhiza uralensis* Fisch	GLY	Fabaceae	Rhizoma et radix	0.574	Qi-tonifying	Sweet/Neutral	1.5–30 g
2	Houttuyniae herba	Yü hsing ts'ao 魚腥草	*Houttuynia cordata* Thunb	HNH	Saururaceae	Herba	0.475	Heat-clearing and detoxicating	Pungent/Mild cold	3–30 g
3	Jujubae fructus	Ta tsao 大棗	*Ziziphus jujuba* Mill	JJB	Rhamnaceae	Fructus	0.459	Qi-tonifying	Sweet/Warm	2–71 g
4	Menthae herba	Po hê 薄荷	*Mentha canadensis* L	MTH	Lamiaceae	Herba	0.361	Pungent-cold exterior-releasing	Pungent/Cool	1.5–40.5 g
5	Lycii fructus	Kou ch'i tzu 枸杞子	*Lycium chinense* Mill	LCF	Solanaceae	Fructus	0.361	Yin-tonifying	Sweet/Neutral	3.75–45 g
6	Astragali radix	Huang ch'i 黃耆	*Astragalus mongholicus* Bunge	AGR	Fabaceae	Radix	0.328	Qi-tonifying	Sweet/Mild warm	3.75–49 g
7	Hedysari radix	Hung ch'i 紅耆	*Hedysarum polybotrys* Hand.-Mazz	HDR	Fabaceae	Radix	0.311	Qi-tonifying	Sweet/Mild warm	6–40.5 g
8	Mori folium	Sang yeh 桑葉	*Morus alba* L	MRF	Moraceae	Folium	0.279	Pungent-cold exterior-releasing	Sweet, Bitter/Cold	5.75–33.75 g
9	Lonicerae japonicae flos	Chin yin hua 金銀花	*Lonicera japonica* Thunb	LJF	Caprifoliaceae	Flos	0.230	Heat-clearing and detoxicating	Sweet/Cold	1.5–19.5 g
10	Ophiopogonis radix	Mai mên tung 麥門冬	*Ophiopogon japonicus* (Thunb.) Ker Gawl	OPR	Asparagaceae	Radix	0.197	Yin-tonifying	Sweet, Mild bitter/Mild cold	2–15.5 g
11	Saposhnikoviae radix et rhizoma	Fang fêng 防風	*Saposhnikovia divaricata* (Turcz.) Schischk	SKE	Apiaceae	Radix et Rhizoma	0.180	Pungent-warm exterior-releasing	Pungent, Sweet/Mild warm	3–19 g
12	Cinnamomi ramulus	Kuei chih 桂枝	*Cinnamomum cassia* (L.) J.Presl	CMR	Lauraceae	Ramulus	0.180	Pungent-warm exterior-releasing	Pungent, Sweet/Warm	2–61.875 g
13	Platycodonis radix	Chieh kêng 桔梗	*Platycodon grandiflorus* (Jacq.) ADC.	PCR	Campanulaceae	Radix	0.180	Heat-phlegm clearing and resolving	Bitter, Pungent/Neutral	1–20 g
14	Nepetae herba	Ching chieh 荊芥	*Nepeta tenuifolia* Benth	NPH	Lamiaceae	Herba	0.164	Pungent-warm exterior-releasing	Pungent/Mild warm	3–17 g
15	Perillae folium	Tzu su yeh 紫蘇葉	*Perilla frutescens* (L.) Britton	PLF	Lamiaceae	Folium	0.148	Pungent-warm exterior-releasing	Pungent/Warm	3.75–15 g
16	Chrysanthemi flos	Chü hua 菊花	*Chrysanthemum morifolium* Ramat	CSF	Compositae	Flos	0.131	Pungent-cold exterior-releasing	Sweet, Bitter/Mild cold	3.5–10.5 g

(Continued on following page)

10.3389/fphar.2025.1586334

TABLE 1 (*Continued*) Information on 70 medicinal materials used in anti-COVID-19 formulae.

No	Latin name	Local name	Scientific name	Code	Family	Part used	RFC	Traditional use	Flavors/ Properties	Dosage[a]
17	Codonopsis radix	Tang san 黨參	*Codonopsis pilosula* (Franch.) Nannf	CSR	Campanulaceae	Radix	0.131	Qi-tonifying	Sweet/Neutral	3.75–22 g
18	Atractylodis macrocephal rhizoma	Pai chu 白朮	*Atractylodes macrocephala* Koidz	AMR	Compositae	Rhizoma	0.115	Qi-tonifying	Bitter, Sweet/Warm	1–16.5 g
19	Angelicae sinensis radix	Tang kuei 當歸	*Angelica sinensis* (Oliv.) Diels	ASR	Apiaceae	Radix	0.115	Blood-tonifying	Sweet, Pungent/Warm	3–15 g
20	Scutellapiae radix	Huang ch'in 黃芩	*Scutellaria baicalensis* Georgi	STR	Lamiaceae	Radix	0.098	Heat-clearing and dampness-drying	Bitter/Cold	2–12.5 g
21	Panacis quinquefolii radix	Hsi yang shên 西洋參	*Panax quinquefolius* L	PQR	Araliaceae	Radix	0.098	Qi-tonifying	Sweet, Mild bitter/Cool	3–21 g
22	Zingiberis rhizoma recens	Shêng chiang 生薑	*Zingiber officinale* Roscoe	ZGB	Zingiberaceae	Rhizoma	0.098	Pungent-warm exterior-releasing	Pungent/Warm	2–30 g
23	Trichosanthis fructus	Kua lou 栝蔞	*Trichosanthes kirilowii* Maxim	TSF	Cucurbitaceae	Fructus	0.082	Heat-phlegm clearing and resolving	Sweet, Mild bitter/Cold	4–20.5 g
24	Isatidis radix	Pei pan lan kên 北板藍根	*Isatis tinctoria* L	ITR	Brassicaceae	Radix	0.082	Heat-clearing and detoxicating	Bitter/Cold	1–11 g
25	Chuanxiong rhizoma	Ch'uan ch'iung 川芎	*Ligusticum striatum* DC.	CXR	Apiaceae	Rhizoma	0.082	Blood-activating and stasis-dispelling	Pungent/Warm	4.7–11.25 g
26	Agastachis herba	Huo hsiang 藿香	*Agastache rugosa* (Fisch. and C.A.Mey.) Kuntze	ATH	Lamiaceae	Herba	0.082	Dampness-resolving with aroma	Pungent/Mild warm	12–20 g
27	Phragmitis rhizoma	Lu kên 蘆根	*Phragmites australis* (Cav.) Trin. ex Steud	PMR	Poaceae	Rhizoma	0.082	Heat-clearing and fire-purging	Sweet/Cold	3–8.67 g
28	Ginseng radix et rhizoma	Jên shên 人參	*Panax ginseng* C.A.Mey	GSG	Araliaceae	Radix et Rhizoma	0.082	Qi-tonifying	Sweet, Mild bitter/Mild warm	3.75–8.5 g
29	Strobilanthii cusiae rhizoma et radix	Nan pan lan kên 南板藍根	*Strobilanthes cusia* (Nees) Kuntze	SCR	Acanthaceae	Rhizoma et radix	0.066	Heat-clearing and detoxicating	Bitter/Cold	10.5–21 g
30	Citri reticulatae pericarpium	Chü p'i 橘皮	*Citrus reticulata* Blanco	CRP	Rutaceae	Pericarpium	0.066	Qi-regulating	Bitter, Pungent/Warm	2–13.5 g
31	Salviae miltiorrhizae radix et rhizoma	Tan shên 丹參	*Salvia miltiorrhiza* Bunge	SME	Lamiaceae	Radix et rhizoma	0.049	Blood-activating and stasis-dispelling	Bitter/Mild cold	8–18.75 g

(Continued on following page)

10.3389/fphar.2025.1586334

TABLE 1 (*Continued*) Information on 70 medicinal materials used in anti-COVID-19 formulae.

No	Latin name	Local name	Scientific name	Code	Family	Part used	RFC	Traditional use	Flavors/ Properties	Dosage[a]
32	Glehniae radix	Pei sha shên 北沙參	*Glehnia littoralis* F.Schmidt ex Miq	GNR	Apiaceae	Radix	0.049	Yin-tonifying	Sweet, Mild bitter/Mild cold	10–21 g
33	Bupleuri radix	Ch'ai hu 柴胡	*Bupleurum chinense* DC.	BPR	Apiaceae	Radix	0.049	Pungent-cold exterior-releasing	Pungent/Bitter/Mild cold	4–12.5 g
34	Puerariae radix	Kê kên 葛根	*Pueraria montana* var. *chinensis* (Ohwi) Sanjappa and Pradeep	PRR	Fabaceae	Radix	0.049	Pungent-cold exterior-releasing	Sweet, Pungent/Cool	0.493–2 g
35	Armeniacae semen amarum	K'u hsing jên 苦杏仁	*Prunus sibirica* L	ASA	Rosaceae	Semen amarum	0.049	Cough-suppressing and panting-calming	Bitter/Warm	3.75–11.5 g
36	Magnolia cortex	Hou p'o 厚朴	*Magnolia officinalis* Rehder and E.H.Wilson	MNC	Magnoliaceae	Cortex	0.033	Qi-regulating	Bitter, Pungent/Warm	3–8.5 g
37	Angeliga dahurica radix	Pai chih 白芷	*Angelica dahurica* (Hoffm.) Benth. and Hook.f. ex Franch. and Sav	ADR	Apiaceae	Radix	0.033	Pungent-warm exterior-releasing	Pungent/Warm	9–12.5 g
38	Lilii bulbus	Pai hê 百合	*Lilium lancifolium* Thunb	LBS	Liliaceae	Bulbus	0.033	Yin-tonifying	Sweet/Mild cold	9.5 g
39	Fritillariae thunbergii bulbus	Chê pei mu 浙貝母	*Fritillaria thunbergii* Miq	FTB	Liliaceae	Bulbus	0.033	Heat-phlegm clearing and resolving	Bitter/Cold	8–17.5 g
40	Poria	Fu ling 茯苓	*Poria cocos* (Schwein.) F.A. Wolf	POR	Polyporaceae	Poria	0.033	Dampness-draining diuretic	Sweet, Plain/Neutral	1–18.5 g
41	Forsythiae fructus	Lien ch'iao 連翹	*Forsythia suspensa* (Thunb.) Vahl	FSR	Oleaceae	Fructus	0.033	Heat-clearing and detoxicating	Bitter/Mild cold	7.5–8 g
42	Perillae caulis	Tzu su kêng 紫蘇梗	*Perilla frutescens* (L.) Britton	PLC	Lamiaceae	Caulis	0.033	Qi-regulating	Pungent/Warm	12.5–19 g
43	Siraitiae fructus	Lo han kuo 羅漢果	*Siraitia grosvenorii* (Swingle) C.Jeffrey ex A.M.Lu and Zhi.Y.Zhang	STF	Cucurbitaceae	Fructus	0.033	Cough-suppressing and panting-calming	Sweet/Cool	16–25 g
44	Taraxaci herba	P'u kung ying 蒲公英	*Taraxacum mongolicum* Hand.-Mazz	TXH	Compositae	Herba	0.016	Heat-clearing and detoxicating	Bitter, Sweet/Cold	18.5 g
45	Dioscoreae rhizoma	Shan yao 山藥	*Dioscorea oppositifolia* L	DSR	Dioscroeaceae	Rhizoma	0.016	Qi-tonifying	Sweet/Neutral	3 g
46	Pinelliae rhizoma	Pan hsia 半夏	*Pinellia ternata* (Thunb.) Makino	PLR	Araceae	Rhizoma	0.016	Dampness and phlegm eliminating	Pungent/Warm	9 g
47	Scrophulariae radix	Hsüan shên 玄參	*Scrophularia ningpoensis* Hemsl	SPR	Scrophulariaceae	Radix	0.016	Heat-clearing and blood-cooling	Sweet, Bitter, Salty/ Mild cold	7.5 g

(Continued on following page)

10.3389/fphar.2025.1586334

TABLE 1 (*Continued*) Information on 70 medicinal materials used in anti-COVID-19 formulae.

No	Latin name	Local name	Scientific name	Code	Family	Part used	RFC	Traditional use	Flavors/ Properties	Dosage[a]
48	Bletillae rhizoma	Pai chi 白及	*Bletilla striata* (Thunb.) Rchb.f	BTR	Orchidaceae	Rhizoma	0.016	Hemostatic	Bitter, Sweet, Astringent/Mild cold	7.5 g
49	Paeoniae radix alba	Pai shao 白芍	*Paeonia lactiflora* Pall	PRA	Paeoniaceae	Radix	0.016	Blood-tonifying	Bitter, Sour/Mild cold	6 g
50	Imperatae rhizoma	Pai mao kên 白茅根	*Imperata cylindrica* (L.) Raeusch	IPR	Poaceae	Rhizoma	0.016	Hemostatic	Sweet/Cold	8 g
51	Stemonae radix	Pai pu 百部	*Stemona sessilifolia* (Miq.) Miq	SNR	Stemonaceae	Radix	0.016	Cough-suppressing and panting-calming	Sweet, Bitter/Mild warm	9.5 g
52	Cinnamomi cortex	Jou kuei 肉桂	*Cinnamomum cassia* (L.) J.Presl	CMC	Lauraceae	Cortex	0.016	Interior-warming	Pungent, Sweet/ Highly hot	3 g
53	Reynoutriae multiflorae radix	Hê shou wu 何首烏	*Reynoutria multiflora* (Thunb.) Moldenke	RMR	Polygonaceae	Radix	0.016	Blood-tonifying	Bitter, Sweet, Astringent/Mild warm	20 g
54	Eucommiae cortex	Tu chung 杜仲	*Eucommia ulmoides* Oliv	EMC	Eucommiaceae	Cortex	0.016	Yang-tonifying	Sweet/Warm	18 g
55	Acanthopanacis senticosi radix et rhizoma seu caulis	Tz'u wu chia 刺五加	*Eleutherococcus senticosus* (Rupr. and Maxim.) Maxim	ASE	Araliaceae	Radix et Rhizoma seu Caulis	0.016	Qi-tonifying	Pungent, Mild bitter/ Warm	16 g
56	Eriobotryae folium	P'i p'a yeh 枇杷葉	*Eriobotrya japonica* (Thunb.) Lindl	EBF	Rosaceae	Folium	0.016	Cough-suppressing and panting-calming	Bitter/Mild cold	9 g
57	Aurantii fructus Immaturus	Chih shih 枳實	*Citrus* × *aurantium* L	AFI	Rutaceae	Fructus immaturus	0.016	Qi-regulating	Bitter, Pungent, Sour/ Mild cold	6 g
58	Scaphii semen	P'ang ta hai 胖大海	*Scaphium affine* (Mast.) Pierre	SPS	Malvaceae	Semen	0.016	Heat-phlegm clearing and resolving	Sweet, Cold	19.5 g
59	Helminthostachydis radix et rhizoma	Tao ti wu kung 倒地蜈蚣	*Helminthostachys zeylanica* (L.) Hook	HCE	Ophioglossaceae	Radix et Rhizoma	0.016	Heat-clearing and detoxicating	Sweet, Bitter/Cool	18.75 g
60	Iris rhizoma	Yeh kan 射干	*Iris domestica* (L.) Goldblatt and Mabb	ISR	Iridaceae	Rhizoma	0.016	Heat-clearing and detoxicating	Bitter/Cold	14 g
61	Mori cortex	Sang pai p'i 桑白皮	*Morus alba* L	MRC	Moraceae	Cortex	0.016	Cough-suppressing and panting-calming	Sweet/Cold	18.5 g
62	Lophatheri herba	Tan chu yeh 淡竹葉	*Lophatherum gracile* Brongn	LOP	Poaceae	Herba	0.016	Heat-clearing and fire-purging	Sweet, Plain/Cold	4.4 g
63	Asari radix	Hsi hsin 細辛	*Asarum heterotropoides* F.Schmidt	ARR	Aristolochiaceae	Radix	0.016	Pungent-warm exterior-releasing	Pungent/Warm	2 g
64	Nelumbinis folium	Hê yeh 荷葉	*Nelumbo nucifera* Gaertn	NBF	Nymphaeaceae	Folium	0.016	Hemostatic	Bitter/Neutral	11.6 g

(Continued on following page)

10.3389/fphar.2025.1586334

10.3389/fphar.2025.1586334

TABLE 1 (*Continued*) Information on 70 medicinal materials used in anti-COVID-19 formulae.

No	Latin name	Local name	Scientific name	Code	Family	Part used	RFC	Traditional use	Flavors/ Properties	Dosage[a]
65	Ephedrae herba	Ma huang 麻黄	*Ephedra sinica* Stapf	EDH	Ephedraceae	Herba	0.016	Pungent-warm exterior-releasing	Pungent, Mild bitter/ Warm	6.5 g
66	Asteris radix et rhizoma	Tzu wan 紫菀	*Aster tataricus* L.f	ARE	Compositae	Radix et Rhizoma	0.016	Cough-suppressing and panting-calming	Pungent, Bitter/Warm	5 g
67	Rehmanniae radix	Ti huang 地黄	*Rehmannia glutinosa* (Gaertn.) DC.	RNR	Plantaginaceae	Radix	0.016	Heat-clearing and blood-cooling	Sweet, Bitter/Cold	6.875 g
68	Alismatis rhizoma	Tsê hsieh 澤瀉	*Alisma plantago-aquatica subsp. orientale* (Sam.) Sam	ALI	Alismataceae	Rhizoma	0.016	Dampness-draining diuretic	Sweet, Plain/Cold	4 g
69	Lycopi herba	Tsê lan 澤蘭	*Lycopus lucidus* var. *hirtus* Regel	LPH	Lamiaceae	Herba	0.016	Blood-activating and stasis-dispelling	Bitter, Pungent/Mild warm	15.8 g
70	Curcumae longae rhizoma	Chiang huang 薑黃	*Curcuma longa* L	CLR	Zingiberaceae	Rhizoma	0.016	Blood-activating and stasis-dispelling	Pungent, Bitter/Warm	7 g

[a]The dosage range is from the minimum to the maximum of formulae.

(RFC = 0.574), *Houttuynia cordata* Thunb. (RFC = 0.475), *Ziziphus jujuba* Mill. (RFC = 0.459), *Mentha canadensis* L. (RFC = 0.361), *Lycium chinense* Mill. (RFC = 0.361), *Astragalus mongholicus* Bunge (RFC = 0.328), *Hedysarum polybotrys* Hand.-Mazz. (RFC = 0.311), *Morus alba* L. (RFC = 0.279), *Lonicera japonica* Thunb. (RFC = 0.230), *Ophiopogon japonicus* (Thunb.) Ker Gawl. (RFC = 0.197), *Saposhnikovia divaricata* (Turcz.) Schischk. (RFC = 0.180), *Cinnamomum cassia* (L.). J.Presl (RFC = 0.180), *Platycodon grandiflorus* (Jacq.) A.DC. (RFC = 0.180), *Nepeta tenuifolia* Benth. (RFC = 0.164), *Perilla frutescens* (L.). Britton (RFC = 0.148), *Chrysanthemum morifolium* Ramat. (RFC = 0.131), *Codonopsis pilosula* (Franch.) Nannf. (RFC = 0.131), *Atractylodes macrocephala* Koidz. (RFC = 0.115), *Angelica sinensis* (Oliv.) Diels (RFC = 0.115), *Scutellaria baicalensis* Georgi (RFC = 0.098), *Panax quinquefolius* L. (RFC = 0.098), *Zingiber officinale* Roscoe (RFC = 0.098), *Trichosanthes kirilowii* Maxim. (RFC = 0.082), *Isatis tinctoria* L. (RFC = 0.082), *Ligusticum striatum* DC. (RFC = 0.082), *Agastache rugosa* (Fisch. and C.A.Mey.) Kuntze (RFC = 0.082), *Phragmites australis* (Cav.) Trin. ex Steud. (RFC = 0.082), *Panax ginseng* C.A.Mey. (RFC = 0.082), *Strobilanthes cusia* (Nees) Kuntze (RFC = 0.066), and *Citrus reticulata* Blanco (RFC = 0.066) (Table 1).

The Phi coefficient is a parameter used to measure the correlation between two binary variables. In this study, the occurrence of medicinal materials is considered a binary variable (either present or not present). To clarify the correlation between any two medicinal materials, this study calculates the occurrence of any two medicinal materials among the 30 commonly used medicinal materials in 61 medicinal formulae, constructs a frequency contingency table (Supplementary Table S2), and then calculates the Phi coefficient based on the results of the contingency table. Next, the Phi coefficient was combined with cluster analysis to create a network diagram (Figure 3). The results of the cluster analysis divided the 30 commonly used medicinal materials into four groups: Group A (N = 9) included *G. uralensis*, *H. cordata*, *M. canadensis*, *M. alba*, *S. divaricata*, *N. tenuifolia*, *S. baicalensis*, *T. kirilowii*, and *S. cusia*; Group B (N = 8) included *A. mongholicus*, *L. japonica*, *C. cassia*, *A. macrocephala*, *Z. officinale*, *I. tinctoria*, *A. rugosa*, and *C. reticulata*; Group C (N = 5) included *O. japonicus*, *P. grandiflorus*, *P. frutescens*, *C. morifolium*, and *P. australis*; Group D (N = 8) included *Z. jujuba*, *L. chinense*, *H. polybotrys*, *C. pilosula*, *A. sinensis*, *P. quinquefolius*, *L. striatum*, and *P. ginseng*.

3.4 Dosage of medicinal materials against COVID-19

In this study, based on the calculation results of Louvain community detection model, the 30 commonly used medicinal materials against COVID-19 were divided into four groups (Figure 4). In Group A, the dosage distribution ranged from 1.5 g to 45.0 g. The highest average dosage was *S. cusia* (15.3 g), while the lowest average dosage was *N. tenuifolia* (9.3 g). The medicinal material with the largest dosage range was *M. canadensis* (3.8 g–45.0 g). In Group B, the dosage distribution ranged from 1.0 g to 61.9 g. The highest average dosage was *A. mongholicus* (17.9 g), while the lowest average dosage was *A. rugosa* (5.8 g). The medicinal material with the largest dosage range was *C. cassia* (2.0 g–61.9 g). In Group C, the dosage distribution ranged

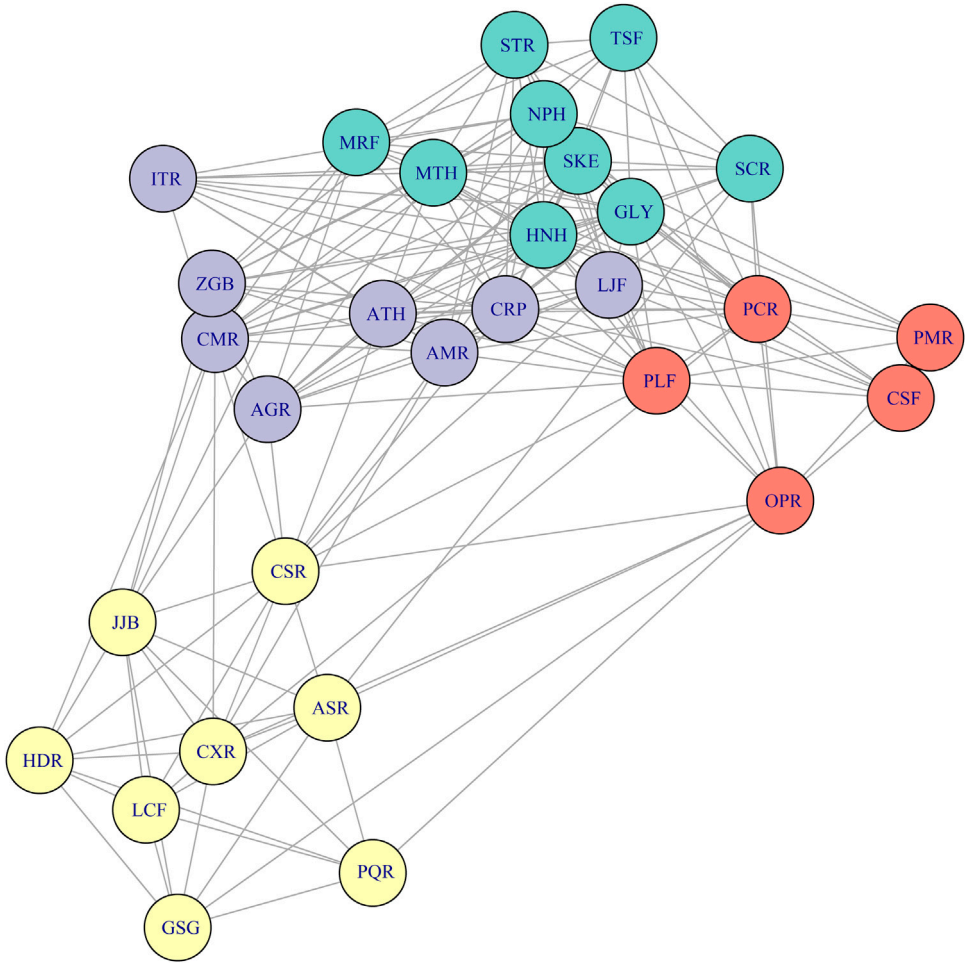


FIGURE 3
Network diagram of 30 commonly used medicinal materials against COVID-19. Note, The lines indicate a positive Phi coefficient between two medicinal materials. Different colors represent different groups in the cluster analysis. AGR, *A. mongholicus*; AMR, *A. macrocephala*; ASR, *A. sinensis*; ATH, *A. rugosa*; CMR, *C. cassia*; CRP, *C. reticulata*; CSF, *C. morifolium*; CSR, *C. pilosula*; CXR, *L. striatum*; GLY, *Glycyrrhiza uralensis*; GSG, *P. ginseng*; HDR, *H. polybotrys*; HNH, *H. cordata*; ITR, *Isatis tinctoria*; JJB, *Z. jujuba*; LCF, *L. chinense*; LJF, *L. japonica*; MRF, *M. alba*; MTH, *M. canadensis*; NPH, *Nepeta tenuifolia*; OPR, *Ophiopogon japonicus*; PCR, *P. grandiflorus*; PLF, *P. frutescens*; PMR, *P. australis*; PQR, *P. quinquefolius*; SCR, *S. cusia*; SKE, *S. divaricata*; STR, *S. baicalensis*; TSF, *Trichosanthes kirilowii*; ZGB, *Z. officinale*.

from 1.0 g to 20.0 g. The highest average dosage was *O. japonicus* (9.3 g), while the lowest average dosage was *P. australis* (6.0 g). The medicinal material with the largest dosage range was *P. grandiflorus* (1.0 g–20.0 g). In Group D, the dosage distribution ranged from 1.0 g to 71.0 g. The highest average dosage was *Z. jujuba* (25.5 g), while the lowest average dosage was *L. striatum* (5.7 g). The medicinal material with the largest dosage range was *Z. jujuba* (2.0 g–71.0 g).

4 Discussion

TCM pharmacies existed even before the introduction of Western medicine in Taiwan. Over generations, they have accumulated countless folk formulae and TCM knowledge. These formulae were practiced during early medical deprivation in Taiwan, serving as pioneers of evidence-based medicine. This highlights that TCM pharmacies have become a vital repository for the ethnobotanical knowledge in Taiwan. However, as the older generation of owners ages and the younger generation is reluctant to take over, this valuable ethnobotanical knowledge is gradually disappearing. Therefore, documenting and preserving the folk formulae and TCM selection strategies accumulated by these pharmacies has become a key issue in the preservation of ethnobotanical knowledge in Taiwan.

The rapid global spread of the COVID-19 pandemic and the slow pace of new drug development have made the repurposing of existing medications, along with the use of Chinese herbal medicine and folk formulae, a feasible alternative solution (Fan et al., 2020). In this study, the most widely distributed plant families among the 70 medicinal materials were Lamiaceae, Apiaceae, and Fabaceae. Previous studies have mentioned that compounds such as terpenes, phenylpropanoids, and alkaloids can inhibit viral spike proteins, thus combating coronavirus infections (Babaeekhou et al., 2021; Boozari and Hosseinzadeh, 2021; Ma et al., 2021; Wang et al., 2022; Yi et al., 2022). These three plant families are rich in various terpenes,

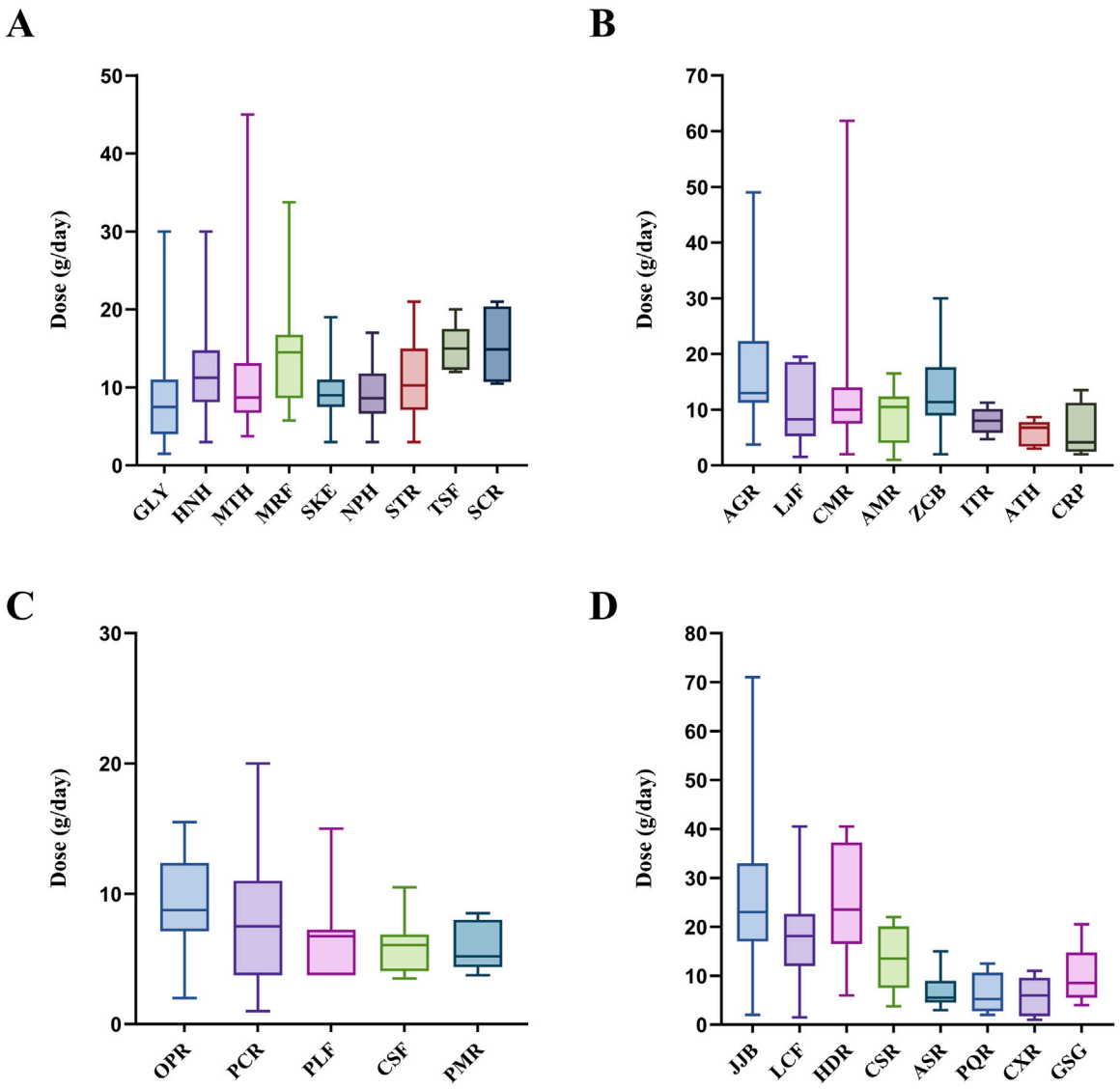


FIGURE 4
Boxplot of dosages for commonly used medicinal materials against COVID-19 **(A)** Group A (N = 9) **(B)** Group B (N = 8) **(C)** Group C (N = 5) **(D)** Group D (N = 8). AGR, *A. mongholicus*; AMR, *A. macrocephala*; ASR, *A. sinensis*; ATH, *A. rugosa*; CMR, *C. cassia*; CRP, *C. reticulata*; CSF, *C. morifolium*; CSR, *C. pilosula*; CXR, *L. striatum*; GLY, *Glycyrrhiza uralensis*; GSG, *P. ginseng*; HDR, *H. polybotrys*; HNH, *H. cordata*; ITR, *Isatis tinctoria*; JJB, *Z. jujuba*; LCF, *L. chinense*; LJF, *L. japonica*; MRF, *M. alba*; MTH, *M. canadensis*; NPH, *Nepeta tenuifolia*; OPR, *Ophiopogon japonicus*; PCR, *P. grandiflorus*; PLF, *P. frutescens*; PMR, *P. australis*; PQR, *P. quinquefolius*; SCR, *S. cusia*; SKE, *S. divaricata*; STR, *S. baicalensis*; TSF, *Trichosanthes kirilowii*; ZGB, *Z. officinale*.

phenylpropanoids, and alkaloids, which may provide multi-target inhibition of viral infections (Kulkarni et al., 2020; Boozari and Hosseinzadeh, 2021; Liana and Phanumartwiwath, 2022). Furthermore, due to the uneven distribution of effective compounds within the plant, the choice of part used varies (Masumbu et al., 2023). In this study, the majority of the 70 medicinal materials belong to the radix and rhizoma. While the radix and rhizoma may contain the highest concentration of active compounds, harvesting them often results in the death of the plant, which is not in line with the United Nations' Sustainable Development Goal—Life on Land (Department of Economic and Social Affairs, 2025). Therefore, future research should focus on studying the distribution of effective compounds within plants to identify alternative part used that can support sustainable resource development.

According to previous studies, common clinical manifestations of COVID-19 include fever, cough, systemic inflammatory and sputum production (An et al., 2021). The treatment strategy for COVID-19 in TCM focuses on expelling pathogenic factors and strengthening the body's vitality (Wang et al., 2020). The former refers to eliminating pathogens and the inflammation they cause, often using heat-clearing and exterior-dispersing medicinal materials; the latter aims to enhance immunity, prevent and treat pathogen invasion, commonly through tonifying medicinal materials. In this study, the 70 medicinal materials are primarily characterized by bitter-cold, pungent-warm, and sweet-cold properties, with traditional uses focused on Qi-tonifying, heat clearing and detoxifying, and dispersing exterior pathogens. According to previous research, sweet-tasting medicinal materials

are often rich in glycosides and amino acids, which mainly function to clear heat and tonify. Bitter-cold medicinal materials typically contain alkaloids and primarily serve to clear heat, with significant anti-inflammatory effects. Pungent-tasting medicinal materials contain terpenes and are known for their exterior-dispersing properties (Tie-jun and Liu, 2015; Wang et al., 2018). Other studies have found that bitter-cold medicinal materials can exert anti-inflammatory and angiogenic effects by inhibiting the NF-κB pathway and regulating IL1B, VEGF, and TNF (Zhang et al., 2013). The glycoside components found in sweet-tasting medicinal materials have shown immune-modulating effects in modern studies (Zhang Jing-ya et al., 2016). In summary, the selection of bitter-cold, pungent, and sweet medicinal materials by TCM pharmacies for anti-inflammatory and immune-regulating purposes is a rational combination for combating COVID-19.

The Louvain community detection model uses modularity to partition network nodes into communities with high internal cohesion and low external connections. It employs a hierarchical clustering method to gradually merge nodes, improving accuracy and efficiency (Traag et al., 2019). In this study, medicinal materials with an RFC greater than 0.05 were defined as commonly used medicinal materials. Each commonly used medicinal material represents one node, the number of positive Phi coefficient between any two medicinal materials is created as edges, and the Phi coefficient value is defined as edge weight in the Louvain community detection model. During the calculation, nodes were aggregated into communities to identify common medicinal material combinations used in TCM pharmacies for combating COVID-19. The results of this study indicate that the medicinal material combinations used in TCM pharmacies for combating COVID-19 can be categorized into four groups: Group A-D. Group A consists of 9 medicinal materials, corresponding to the formula *NRICM101* (Figure 5) [Composition: *G. uralensis* (7.5 g), *H. cordata* (18.75 g), *M. canadensis* (11.25 g), *M. alba* (11.25 g), *S. divaricata* (7.5 g), *N. tenuifolia* (11.25 g), *S. baicalensis* (11.25 g), *T. kirilowii* (18.75 g), *I. tinctoria* (18.75 g), and *Magnolia officinalis* (11.25 g)]. Previous research has shown that *NRICM101* has multi-target effects such as inhibiting the coronavirus spike protein, counteracting immune storms, and blocking viral replication, confirmed by assays such as the inhibition of 3CL protease, SARS-CoV-2 infection, and cytokine inhibition (Tsai et al., 2021). In addition, some studies have shown that *NRICM101* shortened the hospitalization duration, reduced the duration of COVID-19 positive status, and decreased the number of days on mechanical ventilation in initially severe cases (Tsai et al., 2021; Chang et al., 2024). This study found that TCM pharmacies tend to use lower average dosages of each medicinal material compared to *NRICM101*. A possible reason is that the Group A contains many cold property medicinal materials (*H. cordata*, *M. canadensis*, *M. alba*, *S. baicalensis*, *T. kirilowii*, and *S. cusia*). Previous studies have suggested that *NRICM101* may significantly increase the incidence of diarrhea (Chang et al., 2024), and excessive use of cold property medicinal materials can lead to cold-related symptoms such as diarrhea, cold limbs, and loss of appetite (Liu J. et al., 2020). Therefore, it is hypothesized that TCM pharmacies may reduce the dosage to minimize the occurrence of these side effects. Group B consists of 8 medicinal materials, with four herbs categorized as heat-clearing and exterior-releasing agents (*L. japonica*, *C. cassia*, *Z. officinale*, and *I. tinctoria*), and two herbs classified as tonifying agents (*A. mongholicus* and *A. macrocephala*). The selection of these medicinal materials aligns with TCM treatment strategies for COVID-19 (Wang et al., 2020). Previous studies have indicated that *L. japonica*, *I. tinctoria*, and *A. mongholicus* can inhibit M protein and spike protein on SARS-CoV-2, preventing viral entry into cells and replication (Mandal et al., 2021; Yeh et al., 2021). Meanwhile, *C. cassia*, *Z. officinale*, *A. rugosa*, and *C. reticulata* are rich in volatile compounds such as terpenes and phenolic compounds, which have been confirmed to possess antiviral activity in various studies (Astani et al., 2010; Wink, 2020; Elsebai and Albalawi, 2022). In addition, some studies have shown that *Z. officinale* can accelerate clinical recovery in mild and moderate COVID-19 cases and reduce pulmonary infiltrates (Singh et al., 2023; Ameri et al., 2024). Moreover, when considering the average dosages of the 8 medicinal materials in Group B, it was found that the dosage of *C. cassia* is higher than the standard dosage specified in the *Taiwan Herbal Pharmacopeia fourth Edition*, while the dosage of *I. tinctoria* is lower than the standard dosage (Taiwan Herbal Pharmacopeia 4th Edition Committee, 2021). Group C consists of five medicinal materials, all of which are symptomatic treatments. Medicinal materials such as *O. japonicus*, *P. grandiflorus*, *P. frutescens*, and *C. morifolium* are known for their antitussive, expectorant, and antipyretic effects (Zhang et al., 2015; Chen et al., 2016; Ahmed, 2018; Liu et al., 2024). *Phragmites australis* has been clinically proven to shorten the duration of fever in patients (Fang et al., 2024). In addition, previous study has shown that *P. frutescens* extract not only inhibits SARS-CoV-2 replication but also exhibits a synergistic effect when used in combination with remdesivir which is a Western medicine used to treat COVID-19 (Tang et al., 2021). Moreover, the average dosage of these five medicinal materials in Group C revealed that the dosage of *P. australis* is lower than the standard dosage specified in the *Taiwan Herbal Pharmacopeia fourth Edition*. Group D consists of 8 medicinal materials, 7 of which are tonifying herbs (*Z. jujuba*, *L. chinense*, *H. polybotrys*, *C. pilosula*, *A. sinensis*, *P. quinquefolius*, and *P. ginseng*). Previous research has highlighted the significant role of tonifying medicinal materials in the COVID-19 pandemic, as they regulate immunity, helping to prevent immune storms that could harm the body, while also boosting immune function to enhance the body's ability to fight viral infections (Sun et al., 2003; Yang et al., 2022). In addition, one study has shown that taking *P. ginseng* can enhance and maintain the effectiveness of COVID-19 vaccines, with particularly significant effects observed in individuals over the age of 50 (Yoon et al., 2023). Moreover, among the 8 medicinal materials in Group D, the dosage of *L. chinense* is higher than the standard dosage specified in the *Taiwan Herbal Pharmacopeia fourth Edition*. Furthermore, several of the 30 commonly used medicinal materials identified in this study have been reported to contain bioactive compounds with validated anti-COVID-19 activity. Notable examples include licoricesaponin A3 and glycyrrhetinic acid from *G. uralensis*; kuwanon C and mulberrofuran G from *M. alba*; quercetin and luteolin from *L. japonica* and *P. frutescens*; platycodin D from *P. grandiflorus*; baicalin and baicalein from *S. baicalensis*; ginsenoside compound K from *P. ginseng*; and obacunone, limonin, and nomilin from *C. reticulata* (Song et al., 2020; Kim et al., 2021; Liu et al., 2021; Magurano et al., 2021; Dissook et al., 2022; Kim et al., 2022a;



FIGURE 5
Photograph of *NRICM101* medicinal material composition.

Kim et al., 2022b; Yi et al., 2022; Boopathi et al., 2023; Gao et al., 2023). These compounds are primarily classified as terpenoids or polyphenols, indicating that future phytochemical screening for anti-COVID-19 candidates may be most fruitful when focused on these two classes of natural products.

In summary, the medicinal material combinations used in TCM pharmacies to combat COVID-19 can be categorized into four groups. Group A consists mainly of heat-clearing herbs, which are more suitable for moderate to severe COVID-19 patients to combat persistent high fever and inflammatory responses caused by viral infections. Group B is a mix of heat-clearing and tonifying herbs, making it suitable for mild COVID-19 patients as it combats the systemic inflammatory and boosts immunity simultaneously. Group C includes symptomatic treatments, which are appropriate for patients experiencing related symptoms such as cough and sputum production, or as an adjunct treatment in Group A and Group B therapies. Group D consists mainly of tonifying herbs, making it suitable for the public who have not yet contracted COVID-19, serving as an immunity-boosting regimen. Additionally, the dosages of the 30 commonly used medicinal materials vary across different pharmacies, and some of the average dosages do not conform to the standard dosages outlined in the *Taiwan Herbal Pharmacopeia fourth Edition*. This phenomenon reflects the unique approach TCM pharmacies take in selecting medicinal material dosages.

This study has several limitations. Firstly, the research is based on previous studies and makes pharmacological inferences regarding the commonly used anti-COVID-19 medicinal materials in TCM pharmacies. However, from a formulaic perspective, while the efficacy of Group A has been validated by research, Groups B-D still lack sufficient experimental evidence to support the effectiveness and safety of their formulae. Secondly, the doses of medicinal materials such as *C. cassia*, *I. tinctoria*, *P. australis*, and *L. chinense* mentioned in this study do not conform to the standard dosages outlined in the *Taiwan Herbal Pharmacopeia fourth Edition*, and thus their safety requires further research.

Despite these limitations, the results of this study not only provide numerous candidate medicinal materials and formulae for future anti-coronavirus treatments, but also contribute to the documentation of the ethnobotanical knowledge in combating COVID-19 from TCM pharmacy in Taiwan, thus supporting the achievement of the United Nations Sustainable Development Goals.

5 Conclusion

This study is the first ethnobotanical research on folk formulae for Anti-COVID-19 in Taiwan. It consolidates the use of 70 medicinal materials selected by TCM pharmacies for the prevention and treatment of COVID-19, with 30 commonly used medicinal materials categorized into four distinct formula groups, each targeting different stages of the disease. More importantly, this study employs an ethnobotanical research approach to not only identify potential herbs and formulae for combating COVID-19 but also to document and digitize traditional knowledge, ensuring its preservation in line with the United Nations Sustainable Development Goals. In the future., a “disease course-oriented specialized prescription model” will be adapted with reference to international literature and the development of COVID-19 symptoms reported by NIH. Different combinations of medicinal materials will be formulated in response to the rapid development of

the disease, providing the clinical outcome with a reference for the selection of prescriptions for different stages of the disease.

Data availability statement

The original contributions presented in the study are included in the article/Supplementary Material, further inquiries can be directed to the corresponding authors.

Ethics statement

The studies involving humans were approved by Research Ethics Committee China Medical University and Hospital, Taichung, Taiwan. The studies were conducted in accordance with the local legislation and institutional requirements. The ethics committee/institutional review board waived the requirement of written informed consent for participation from the participants or the participants' legal guardians/next of kin because Non-interventional studies (e.g., observational studies of behavior or nutrition).

Author contributions

M-HC: Conceptualization, Data curation, Formal Analysis, Investigation, Methodology, Project administration, Software, Visualization, Writing – original draft, Writing – review and editing. C-YK: Conceptualization, Investigation, Methodology, Project administration, Writing – original draft, Writing – review and editing. T-WC: Conceptualization, Investigation, Software, Visualization, Writing – review and editing. C-RH: Conceptualization, Investigation, Writing – review and editing. J-GL: Conceptualization, Investigation, Methodology, Project administration, Writing – review and editing. JC: Conceptualization, Investigation, Supervision, Validation, Writing – review and editing. S-SH: Conceptualization, Investigation, Methodology, Supervision, Validation, Writing – review and editing.

Funding

The author(s) declare that financial support was received for the research and/or publication of this article. This research was funded by the Tsuzuki Institute for Traditional Medicine, Grant numbers 108727B8, 109727B8 and 110727B8; China Medical University, Grant numbers CMU108-MF-116, CMU108-SR-101, CMU108-N-22, CMU109-MF-95, CMU109-MF-109 and CMU111-MF-75; the Ministry of Science and Technology, Grant number MOST 107-2320-B-039-030-MY3, 109-2320-B-039-026, 109-2813-C-039-061-B and 110-2320-B-039-021. The China Medical University under the Higher Education Sprout Project and Teaching Practice Research Program, Grant number 1077170A, of the Ministry of Education of Taiwan.

Acknowledgments

The authors thank the herbarium of China Medical University for providing us with space to store the medicinal materials for this study. Also, we would like to thank the 64th and 61st pharmacy students of China Medical University for their assistance in this study. Finally, we sincerely appreciate Shengda TCM pharmacy for providing us with a location for photography.

Conflict of interest

The authors declare that the research was conducted in the absence of any commercial or financial relationships that could be construed as a potential conflict of interest.

Generative AI statement

The author(s) declare that no Generative AI was used in the creation of this manuscript.

Publisher's note

All claims expressed in this article are solely those of the authors and do not necessarily represent those of their affiliated organizations, or those of the publisher, the editors and the reviewers. Any product that may be evaluated in this article, or claim that may be made by its manufacturer, is not guaranteed or endorsed by the publisher.

Supplementary material

The Supplementary Material for this article can be found online at: https://www.frontiersin.org/articles/10.3389/fphar.2025.1586334/full#supplementary-material

References

Ahmad, K. S., Hamid, A., Nawaz, F., Hameed, M., Ahmad, F., Deng, J., et al. (2017). Ethnopharmacological studies of indigenous plants in Kel village, Neelum Valley, Azad Kashmir, Pakistan. *J. Ethnobiol. Ethnomed* 13 (1), 68. doi:10.1186/s13002-017-0196-1

Ahmed, H. M. (2018). Ethnomedicinal, phytochemical and pharmacological investigations of *Perilla frutescens* (L.) britt. *Molecules* 24 (1), 102. doi:10.3390/molecules24010102

Ahn, D. G., Shin, H. J., Kim, M. H., Lee, S., Kim, H. S., Myoung, J., et al. (2020). Current status of epidemiology, diagnosis, therapeutics, and vaccines for novel coronavirus disease 2019 (COVID-19). *J. Microbiol. Biotechnol.* 30 (3), 313–324. doi:10.4014/jmb.2003.03011

Ameri, A., Farashahinejad, M., Davoodian, P., Safa, O., Hassaniazad, M., Parsaii, M., et al. (2024). The efficacy and safety of ginger (*Zingiber officinale*) rhizome extract in outpatients with COVID-19: a randomized double-blind placebo-control clinical trial. *Med. Baltim.* 103 (22), e38289. doi:10.1097/md.0000000000038289

An, X., Duan, L., Zhang, Y. H., Jin, D., Zhao, S., Zhou, R. R., et al. (2021). The three syndromes and six Chinese patent medicine study during the recovery phase of COVID-19. *Chin. Med.* 16 (1), 44. doi:10.1186/s13020-021-00454-x

Asselah, T., Durantel, D., Pasmant, E., Lau, G., and Schinazi, R. F. (2021). COVID-19: discovery, diagnostics and drug development. *J. Hepatol.* 74 (1), 168–184. doi:10.1016/j.jhep.2020.09.031

Astani, A., Reichling, J., and Schnitzler, P. (2010). Comparative study on the antiviral activity of selected monoterpenes derived from essential oils. *Phytother. Res.* 24 (5), 673–679. doi:10.1002/ptr.2955

Babaeekhou, L., Ghane, M., and Abbas-Mohammadi, M. (2021). *In silico* targeting SARS-CoV-2 spike protein and main protease by biochemical compounds. *Biol. Bratisl.* 76 (11), 3547–3565. doi:10.1007/s11756-021-00881-z

Boopathi, V., Nahar, J., Murugesan, M., Subramaniyam, S., Kong, B. M., Choi, S. K., et al. (2023). *In silico* and *in vitro* inhibition of host-based viral entry targets and cytokine storm in COVID-19 by ginsenoside compound K. *Heliyon* 9 (9), e19341. doi:10.1016/j.heliyon.2023.e19341

Boozari, M., and Hosseinzadeh, H. (2021). Natural products for COVID-19 prevention and treatment regarding to previous coronavirus infections and novel studies. *Phytother. Res.* 35 (2), 864–876. doi:10.1002/ptr.6873

Chang, W. K., Wang, C. J., Tsai, T. H., Sun, F. J., Chen, C. H., Kuo, K. C., et al. (2024). The clinical application of traditional Chinese medicine NRICM101 in hospitalized patients with COVID-19. *Expert Rev. Anti Infect. Ther.* 22 (7), 587–595. doi:10.1080/14787210.2024.2313054

Chen, M. H., Chen, X. J., Wang, M., Lin, L. G., and Wang, Y. T. (2016). Ophiopogon japonicus--A phytochemical, ethnomedicinal and pharmacological review. *J. Ethnopharmacol.* 181, 193–213. doi:10.1016/j.jep.2016.01.037

Chinese Pharmacopoeia Commission (2020). *Pharmacopoeia of People's Republic of China*. Beijing, China: China Medical Science Press.

Chytrý, M., Tichý, L., Holt, J., and Botta-Dukát, Z. (2002). Determination of diagnostic species with statistical fidelity measures. *J. Veg. Sci.* 13 (1), 79–90. doi:10.1658/1100-9233(2002)013[0079:dodsws]2.0.co;2

Coronaviridae Study Group of the International Committee on Taxonomy of Viruses (2020). The species severe acute respiratory syndrome-related coronavirus: classifying 2019-nCoV and naming it SARS-CoV-2. *Nat. Microbiol.* 5 (4), 536–544. doi:10.1038/s41564-020-0695-z

COVID-19 Treatment Guidelines Panel (2024). *Coronavirus disease 2019 (COVID-19) treatment guidelines*. State of Maryland, United States: N.I.o. Health.

Cui, Y., Wang, S., and Yan, S. (2016). Evaluating the applicability of Phi coefficient in indicating habitat preferences of Forest soil fauna based on a single field Study in subtropical China. *PLoS One* 11 (3), e0150380. doi:10.1371/journal.pone.0150380

Del Vecchio, L., Balafa, O., Dounousi, E., Ekart, R., Fernandez, B. F., Mark, P. B., et al. (2024). COVID-19 and cardiovascular disease in patients with chronic kidney disease. *Nephrol. Dial. Transpl.* 39 (2), 177–189. doi:10.1093/ndt/gfad170

Department of Chinese Medicine and Pharmacy (2024). Taiwan herbal Pharmacopeia database. Available online at: https://www.cmthp.mohw.gov.tw/English/index (Accessed July 29, 2024).

Department of Economic and Social Affairs (2025). Sustainable development: the 17 goals. Available online at: https://sdgs.un.org/goals ([Accessed Febrary 21, 2025).

Dissook, S., Umsumarng, S., Mapoung, S., Semmarath, W., Arjsri, P., Srisawad, K., et al. (2022). Luteolin-rich fraction from *Perilla frutescens* seed meal inhibits spike glycoprotein S1 of SARS-CoV-2-induced NLRP3 inflammasome lung cell inflammation *via* regulation of JAK1/STAT3 pathway: a potential anti-inflammatory compound against inflammation-induced long-COVID. *Front. Med. (Lausanne)* 9, 1072056. doi:10.3389/fmed.2022.1072056

Elsebai, M. F., and Albalawi, M. A. (2022). Essential oils and COVID-19. *Molecules* 27 (22), 7893. doi:10.3390/molecules27227893

Fan, A. Y., Gu, S., Alemi, S. F., and Research Group for Evidence-based Chinese Medicine (2020). Chinese herbal medicine for COVID-19: current evidence with systematic review and meta-analysis. *J. Integr. Med.* 18 (5), 385–394. doi:10.1016/j.joim.2020.07.008

Fang, M., Kong, L. Y., Ji, G. H., Pu, F. L., Su, Y. Z., Li, Y. F., et al. (2024). Chinese medicine *Phragmites communis* (Lu Gen) for acute respiratory tract infections: a systematic review and meta-analysis of randomized controlled trials. *Front. Pharmacol.* 15, 1242525. doi:10.3389/fphar.2024.1242525

Gao, B., Zhu, L., Liu, Z., Li, Y., He, X., Wu, X., et al. (2023). Chemical composition of honeysuckle (*Lonicerae japonicae*) extracts and their potential in inhibiting the SARS-CoV-2 spike protein and ACE2 binding, suppressing ACE2, and scavenging radicals. *J. Agric. Food Chem.* 71 (15), 6133–6143. doi:10.1021/acs.jafc.3c00584

Hu, F. P., Liao, C. C., Chen, T. L., Yeh, C. C., Shi, L., and Shih, C. C. (2020). Prevalence, expenditures, and associated factors of purchasing non-prescribed Chinese herbal medicine in Taiwan. *PLoS One* 15 (10), e0240311. doi:10.1371/journal.pone.0240311

Kim, T. Y., Jeon, S., Jang, Y., Gotina, L., Won, J., Ju, Y. H., et al. (2021). Platycodin D, a natural component of *Platycodon grandiflorum*, prevents both lysosome- and TMPRSS2-driven SARS-CoV-2 infection by hindering membrane fusion. *Exp. Mol. Med.* 53 (5), 956–972. doi:10.1038/s12276-021-00624-9

Kim, Y. S., Kim, B., Kwon, E. B., Chung, H. S., and Choi, J. G. (2022a). Mulberrofuran G, a mulberry component, prevents SARS-CoV-2 infection by blocking the interaction between SARS-CoV-2 spike protein S1 receptor-binding domain and human angiotensin-converting enzyme 2 receptor. *Nutrients* 14 (19), 4170. doi:10.3390/nu14194170

Kim, Y. S., Kwon, E. B., Kim, B., Chung, H. S., Choi, G., Kim, Y. H., et al. (2022b). Mulberry component kuwanon C exerts potent therapeutic efficacy *in vitro* against COVID-19 by blocking the SARS-CoV-2 spike S1 RBD:ACE2 receptor interaction. *Int. J. Mol. Sci.* 23 (20), 12516. doi:10.3390/ijms232012516

Kulkarni, S. A., Nagarajan, S. K., Ramesh, V., Palaniyandi, V., Selvam, S. P., and Madhavan, T. (2020). Computational evaluation of major components from plant essential oils as potent inhibitors of SARS-CoV-2 spike protein. *J. Mol. Struct.* 1221, 128823. doi:10.1016/j.molstruc.2020.128823

Liana, D., and Phanumartwiwath, A. (2022). Leveraging knowledge of Asian herbal medicine and its active compounds as COVID-19 treatment and prevention. *J. Nat. Med.* 76 (1), 20–37. doi:10.1007/s11418-021-01575-1

Liu, H., Ye, F., Sun, Q., Liang, H., Li, C., Li, S., et al. (2021). Scutellaria baicalensis extract and baicalein inhibit replication of SARS-CoV-2 and its 3C-like protease *in vitro*. *J. Enzyme Inhib. Med. Chem.* 36 (1), 497–503. doi:10.1080/14756366.2021.1873977

Liu, J., Feng, W., and Peng, C. (2020a). A Song of ice and fire: cold and hot properties of traditional Chinese medicines. *Front. Pharmacol.* 11, 598744. doi:10.3389/fphar.2020.598744

Liu, M., Gao, Y., Yuan, Y., Yang, K., Shi, S., Zhang, J., et al. (2020b). Efficacy and safety of integrated traditional Chinese and Western Medicine for Corona Virus disease 2019 (COVID-19): a systematic review and meta-analysis. *Pharmacol. Res.* 158, 104896. doi:10.1016/j.phrs.2020.104896

Liu, Y., Lu, C., Zhou, J., Zhou, F., Gui, A., Chu, H., et al. (2024). Chrysanthemum morifolium as a traditional herb: a review of historical development, classification, phytochemistry, pharmacology and application. *J. Ethnopharmacol.* 330, 118198. doi:10.1016/j.jep.2024.118198

Ma, L. L., Liu, H. M., Liu, X. M., Yuan, X. Y., Xu, C., Wang, F., et al. (2021). Screening S protein - ACE2 blockers from natural products: strategies and advances in the discovery of potential inhibitors of COVID-19. *Eur. J. Med. Chem.* 226, 113857. doi:10.1016/j.ejmech.2021.113857

Magurano, F., Sucameli, M., Picone, P., Micucci, M., Baggieri, M., Marchi, A., et al. (2021). Antioxidant activity of citrus limonoids and investigation of their virucidal potential against SARS-CoV-2 in cellular models. *Antioxidants (Basel)* 10 (11), 1794. doi:10.3390/antiox10111794

Mandal, A., Jha, A. K., and Hazra, B. (2021). Plant products as inhibitors of coronavirus 3CL protease. *Front. Pharmacol.* 12, 583387. doi:10.3389/fphar.2021.583387

Marzolini, C., Kuritzkes, D. R., Marra, F., Boyle, A., Gibbons, S., Flexner, C., et al. (2022). Recommendations for the management of drug-drug interactions between the COVID-19 antiviral Nirmatrelvir/Ritonavir (Paxlovid) and comedications. *Clin. Pharmacol. Ther.* 112 (6), 1191–1200. doi:10.1002/cpt.2646

Masumbu, F. F. F., Mwamatope, B., Tembo, D., Mwakikunga, A., and Kamanula, J. (2023). Ethnobotanical survey of medicinal plants claimed by traditional herbal practitioners to manage cancers in Malawi. *J. Herb. Med.* 42, 100796. doi:10.1016/j.hermed.2023.100796

Ministry of Health and Welfare (2024). *The administration of pharmaceutical affairs*. Taipei, Taiwan: D. o. Statistics.

National Administration of Traditional Chinese Medicine "Chinese Materia Medica" Editorial Board (1999). *Chinese Materia medica*. Shanghai: Scientific and Technical Publishers.

Royal Botanic Gardens, K., and Garden, M. B. (2024). World flora online. Available online at: http://www.worldfloraonline.org/(Accessed July 02, 2024).

Shi, N., Liu, B., Liang, N., Ma, Y., Ge, Y., Yi, H., et al. (2020). Association between early treatment with Qingfei *Paidu decoction* and favorable clinical outcomes in patients with COVID-19: a retrospective multicenter cohort study. *Pharmacol. Res.* 161, 105290. doi:10.1016/j.phrs.2020.105290

Singh, H., Yadav, B., Rai, A. K., Srivastava, S., Saiprasad, A., Jameela, S., et al. (2023). Ashwagandha (*Withania somnifera*) and Shunthi (*Zingiber officinale*) in mild and moderate COVID-19: an open-label randomized controlled exploratory trial. *Complement. Ther. Med.* 76, 102966. doi:10.1016/j.ctim.2023.102966

Singh, T. U., Parida, S., Lingaraju, M. C., Kesavan, M., Kumar, D., and Singh, R. K. (2020). Drug repurposing approach to fight COVID-19. *Pharmacol. Rep.* 72 (6), 1479–1508. doi:10.1007/s43440-020-00155-6

Song, J. W., Long, J. Y., Xie, L., Zhang, L. L., Xie, Q. X., Chen, H. J., et al. (2020). Applications, phytochemistry, pharmacological effects, pharmacokinetics, toxicity of *Scutellaria baicalensis* Georgi. and its probably potential therapeutic effects on COVID-19: a review. *Chin. Med.* 15, 102. doi:10.1186/s13020-020-00384-0

Sun, A., Chia, J. S., Chang, Y. F., and Chiang, C. P. (2003). Levamisole and Chinese medicinal herbs can modulate the serum interleukin-6 level in patients with recurrent aphthous ulcerations. *J. Oral Pathol. Med.* 32 (4), 206–214. doi:10.1034/j.1600-0714.2003.00096.x

Taiwan Herbal Pharmacopeia 4th Edition Committee (2021). *Taiwan herbal pharmacopeia*. 4th Edition. Taipei, Taiwan: Department of Chinese Medicine and Pharmacy, Ministry of Health and Welfare.

Tang, W. F., Tsai, H. P., Chang, Y. H., Chang, T. Y., Hsieh, C. F., Lin, C. Y., et al. (2021). Perilla (*Perilla frutescens*) leaf extract inhibits SARS-CoV-2 *via* direct virus inactivation. *Biomed. J.* 44 (3), 293–303. doi:10.1016/j.bj.2021.01.005

Tie-jun, Z., and Chang-xiao, L. (2015). Identification of Chinese materia medica and its chemical biology characterization path on five taste theory. *Chin. Traditional Herb. Drugs* 46 (1), 1–6. doi:10.7501/j.issn.0253-2670.2015.01.001

Traag, V. A., Waltman, L., and van Eck, N. J. (2019). From Louvain to Leiden: guaranteeing well-connected communities. *Sci. Rep.* 9 (1), 5233. doi:10.1038/s41598-019-41695-z

Tsai, K. C., Huang, Y. C., Liaw, C. C., Tsai, C. I., Chiou, C. T., Lin, C. J., et al. (2021). A traditional Chinese medicine formula NRICM101 to target COVID-19 through multiple pathways: a bedside-to-bench study. *Biomed. Pharmacother.* 133, 111037. doi:10.1016/j.biopha.2020.111037

Wang, C., Ming, H., Jia, W., Su, W., Zhan, L. R., Luo, D., et al. (2020). Analysis of medication regularity and pharmacodynamic characteristics of traditional Chinese medicine treatment in 444 severe cases of COVID-19. *Zhongguo Zhong Yao Za Zhi* 45 (13), 3007–3012. doi:10.19540/j.cnki.cjcmm.20200427.501

Wang, W. J., Chen, Y., Su, W. C., Liu, Y. Y., Shen, W. J., Chang, W. C., et al. (2022). Peimine inhibits variants of SARS-CoV-2 cell entry *via* blocking the interaction between viral spike protein and ACE2. *J. Food Biochem.* 46 (10), e14354. doi:10.1111/jfbc.14354

Wang, Z., Xia, Q., Liu, X., Liu, W., Huang, W., Mei, X., et al. (2018). Phytochemistry, pharmacology, quality control and future research of *Forsythia suspensa* (Thunb.) vahl: a review. *J. Ethnopharmacol.* 210, 318–339. doi:10.1016/j.jep.2017.08.040

Wink, M. (2020). Potential of DNA intercalating alkaloids and other plant secondary metabolites against SARS-CoV-2 causing COVID-19. *Diversity* 12 (5), 175. doi:10.3390/d12050175

World Health Organization (2024). WHO COVID-19 dashboard. Available online at: https://data.who.int/dashboards/covid19/cases (Accessed 28May, 2024).

Xian-Zhe, Z. (2007). *Color Atlas for the authentic and superior Chinese material medica*. Taichung, Taiwan: China Medical University.

Yang, F., Zhang, X., Zhang, Z., Lu, H., Li, J., Bai, N., et al. (2022). Efficacy and safety of Qi and blood tonic Chinese medicines in the treatment of COVID-19: a protocol for systematic review and meta-analysis. *Med. Baltim.* 101 (49), e32136. doi:10.1097/md.0000000000032136

Yeh, Y. C., Doan, L. H., Huang, Z. Y., Chu, L. W., Shi, T. H., Lee, Y. R., et al. (2021). Honeysuckle (*Lonicera japonica*) and Huangqi (*Astragalus membranaceus*) suppress SARS-CoV-2 entry and COVID-19 related cytokine storm *in vitro*. *Front. Pharmacol.* 12, 765553. doi:10.3389/fphar.2021.765553

Yi, Y., Li, J., Lai, X., Zhang, M., Kuang, Y., Bao, Y. O., et al. (2022). Natural triterpenoids from licorice potently inhibit SARS-CoV-2 infection. *J. Adv. Res.* 36, 201–210. doi:10.1016/j.jare.2021.11.012

Yoon, J., Park, B., Kim, H., Choi, S., and Jung, D. (2023). Korean red ginseng potentially improves maintaining antibodies after COVID-19 vaccination: a 24-week longitudinal study. *Nutrients* 15 (7), 1584. doi:10.3390/nu15071584

Yousefi, H., Mashouri, L., Okpechi, S. C., Alahari, N., and Alahari, S. K. (2021). Repurposing existing drugs for the treatment of COVID-19/SARS-CoV-2 infection: a review describing drug mechanisms of action. *Biochem. Pharmacol.* 183, 114296. doi:10.1016/j.bcp.2020.114296

Zhang, B., Wang, X., and Li, S. (2013). An integrative platform of TCM network pharmacology and its application on a herbal formula, qing-luo-yin. *Evid. Based Complement. Altern. Med.* 2013, 456747. doi:10.1155/2013/456747

Zhang, L., Wang, Y., Yang, D., Zhang, C., Zhang, N., Li, M., et al. (2015). *Platycodon grandiflorus* - an ethnopharmacological, phytochemical and pharmacological review. *J. Ethnopharmacol.* 164, 147–161. doi:10.1016/j.jep.2015.01.052

Zhang Jing-ya, C. H., Su-xiao, G., Jun, X., Yan-qi, H., Tie-jun, Z., and Chang-xiao, L. (2016). Expression of sweet-taste of Chinese materia medica and its application in clinical compatibility. *Chin. Traditional Herb. Drugs* 47 (4), 533–539. doi:10.7501/j.issn.0253-2670.2016.04.001

Zhao, Z., Liang, Z., and Ping, G. (2011). Macroscopic identification of Chinese medicinal materials: traditional experiences and modern understanding. *J. Ethnopharmacol.* 134 (3), 556–564. doi:10.1016/j.jep.2011.01.018

Zhou, P., Yang, X. L., Wang, X. G., Hu, B., Zhang, L., Zhang, W., et al. (2020a). A pneumonia outbreak associated with a new coronavirus of probable bat origin. *Nature* 579 (7798), 270–273. doi:10.1038/s41586-020-2012-7

Zhou, Y., Wang, F., Tang, J., Nussinov, R., and Cheng, F. (2020b). Artificial intelligence in COVID-19 drug repurposing. *Lancet Digit. Health* 2 (12), e667–e676. doi:10.1016/s2589-7500(20)30192-8

Zhu, N., Zhang, D., Wang, W., Li, X., Yang, B., Song, J., et al. (2020). A novel coronavirus from patients with pneumonia in China, 2019. *N. Engl. J. Med.* 382 (8), 727–733. doi:10.1056/NEJMoa2001017

Glossary

ADR	*Angelica dahurica* (Hoffm.) Benth. and Hook.f. ex Franch. and Sav.
AFI	*Citrus* × *aurantium* L.
AGR	*Astragalus mongholicus* Bunge
ALI	*Alisma plantago-aquatica subsp. orientale* (Sam.) Sam.
AMR	*Atractylodes macrocephala* Koidz.
ARE	*Aster tataricus* L.f.
ARR	*Asarum heterotropoides* F.Schmidt
ASA	*Prunus sibirica* L.
ASE	*Eleutherococcus senticosus* (Rupr. and Maxim.) Maxim.
ASR	*Angelica sinensis* (Oliv.) Diels
ATH	*Agastache rugosa* (Fisch. and C.A.Mey.) Kuntze
BPR	*Bupleurum chinense* DC.
BTR	*Bletilla striata* (Thunb.) Rchb.f.
CLR	*Curcuma longa* L.
CMC	*Cinnamomum cassia* (L.) J.Presl **(Cortex)**
CMR	*Cinnamomum cassia* (L.) J.Presl **(Ramulus)**
COVID-19	Coronavirus Disease 2019
CRP	*Citrus reticulata* Blanco
CSF	*Chrysanthemum morifolium* Ramat.
CSR	*Codonopsis pilosula* (Franch.) Nannf.
CXR	*Ligusticum striatum* DC.
DSR	*Dioscorea oppositifolia* L.
EBF	*Eriobotrya japonica* (Thunb.) Lindl.
EDH	*Ephedra sinica* Stapf
EMC	*Eucommia ulmoides* Oliv.
FSR	*Forsythia suspensa* (Thunb.) Vahl
FTB	*Fritillaria thunbergii* Miq.
GLY	*Glycyrrhiza uralensis* Fisch.
GNR	*Glehnia littoralis* F.Schmidt ex Miq.
GSG	*Panax ginseng* C.A.Mey.
HCE	*Helminthostachys zeylanica* (L.) Hook.
HDR	*Hedysarum polybotrys* Hand.-Mazz.
HNH	*Houttuynia cordata* Thunb.
IPR	*Imperata cylindrica* (L.) Raeusch.
ISR	*Iris domestica* (L.) Goldblatt and Mabb.
ITR	*Isatis tinctoria* L.
JJB	*Ziziphus jujuba* Mill.
LBS	*Lilium lancifolium* Thunb.
LCF	*Lycium chinense* Mill.
LJF	*Lonicera japonica* Thunb.
LOP	*Lophatherum gracile* Brongn
LPH	*Lycopus lucidus* var. *hirtus* Regel
MNC	*Magnolia officinalis* Rehder and E.H.Wilson
MOHW	the Ministry of Health and Welfare
MRC	*Morus alba* L. **(Cortex)**
MRF	*Morus alba* L. **(Folium)**
MTH	*Mentha canadensis* L.
NBF	*Nelumbo nucifera* Gaertn.
NIH	National Institutes of Health
NPH	*Nepeta tenuifolia* Benth.
OPR	*Ophiopogon japonicus* (Thunb.) Ker Gawl.
PCR	*Platycodon grandiflorus* (Jacq.) A.DC.
PLC	*Perilla frutescens* (L.) Britton **(Caulis)**
PLF	*Perilla frutescens* (L.) Britton **(Folium)**
PLR	*Pinellia ternata* (Thunb.) Makino
PMR	*Phragmites australis* (Cav.) Trin. ex Steud.
POR	*Poria cocos* (Schwein.) F.A. Wolf
PQR	*Panax quinquefolius* L.
PRA	*Paeonia lactiflora* Pall.
PRR	*Pueraria montana* var. *chinensis* (Ohwi) Sanjappa and Pradeep
QFPDD	Qingfei Paidu Decoction
RFC	Relative frequency of citation
RMR	*Reynoutria multiflora* (Thunb.) Moldenke
RNR	*Rehmannia glutinosa* (Gaertn.) DC.
SCR	*Strobilanthes cusia* (Nees) Kuntze
SKE	*Saposhnikovia divaricata* (Turcz.) Schischk.
SME	*Salvia miltiorrhiza* Bunge
SNR	*Stemona sessilifolia* (Miq.) Miq.
SPR	*Scrophularia ningpoensis* Hemsl.
SPS	*Scaphium affine* (Mast.) Pierre
STF	*Siraitia grosvenorii* (Swingle) C.Jeffrey ex A.M.Lu and Zhi.Y.Zhang
STR	*Scutellaria baicalensis* Georgi
TCM	traditional Chinese medicine
TSF	*Trichosanthes kirilowii* Maxim.
TWD97	the Taiwan Geodetic Datum 1997
TXH	*Taraxacum mongolicum* Hand.-Mazz.
WHO	World Health Organization
ZGB	*Zingiber officinale* Roscoe

frontiers | Frontiers in Pharmacology

TYPE Systematic Review
PUBLISHED 28 October 2025
DOI 10.3389/fphar.2025.1588586

Check for updates

OPEN ACCESS

EDITED BY
Quansheng Feng,
Chengdu University of Traditional Chinese Medicine, China

REVIEWED BY
Swayam Prakash,
University of California, Irvine, United States
Yong Xu,
Nanjing University of Chinese Medicine, China

*CORRESPONDENCE
Fan Wu,
wufan200610@126.com

RECEIVED 06 March 2025
ACCEPTED 24 September 2025
PUBLISHED 28 October 2025

CITATION
Jiang J, Zhang S, Wang H, Zhang L, Li Z, Tong J and Wu F (2025) Oral commercial Chinese polyherbal preparations combined with conventional biomedicine for pulmonary tuberculosis: network meta-analysis.
Front. Pharmacol. 16:1588586.
doi: 10.3389/fphar.2025.1588586

COPYRIGHT
© 2025 Jiang, Zhang, Wang, Zhang, Li, Tong and Wu. This is an open-access article distributed under the terms of the Creative Commons Attribution License (CC BY). The use, distribution or reproduction in other forums is permitted, provided the original author(s) and the copyright owner(s) are credited and that the original publication in this journal is cited, in accordance with accepted academic practice. No use, distribution or reproduction is permitted which does not comply with these terms.

Oral commercial Chinese polyherbal preparations combined with conventional biomedicine for pulmonary tuberculosis: network meta-analysis

Jiankang Jiang[1], Siqi Zhang[2], Hui Wang[1], Lu Zhang[1], Zegeng Li[3,4], Jiabing Tong[1,3,4,5] and Fan Wu[1,3,5]*

[1]School of Traditional Chinese Medicine, Anhui University of Chinese Medicine, Hefei, China, [2]Anhui Xinhua University, Hefei, China, [3]Anhui Provincial Key Laboratory of Applied Transformation for Prevention and Treatment of Major Pulmonary Diseases with Traditional Chinese Medicine, Hefei, China, [4]The First Affiliated Hospital of Anhui University of Chinese Medicine, Hefei, China, [5]Institute of Prevention and Treatment of Respiratory Diseases, Anhui Provincial Academy of Chinese Medical Sciences, Hefei, China

Background: Despite therapeutic interventions, tuberculosis (TB) remains a persistent challenge. Combination therapy integrating Traditional Chinese Medicine (TCM) with conventional anti-TB medications demonstrates therapeutic benefits, necessitating a meta-analysis evaluating the adjunctive use of oral commercial Chinese polyherbal preparation (CCPP).
Objectives: This study aims to evaluate the efficacy and safety of different oral TCMs combined with biomedicine for tuberculosis treatment, utilizing network meta-analysis techniques.
Methods: A computer-based search was conducted across various databases including the China National Knowledge Infrastructure (CNKI), Wanfang Database, VIP Database, SinoMed, PubMed, EMbase, Web of Science, and the Cochrane Library, covering records from database inception to 22 January 2025. Data analysis utilized Stata 18.0, R software (version 4.4.1), and Review Manager 5.4.
Results: A total of 100 randomized controlled trials (RCTs) were included, with a total sample size of 12,747 participants (6,639 in the experimental group and 6,108 in the control group), evaluating 12 distinct interventions. Network meta-analysis revealed the following optimal combinations: FeiJieHe Pill combined with standard biomedicine demonstrated superior efficacy for clinical response rate improvement (OR = 8.43, 95% CI [1.79, 39.69]). KangLao Pill combined with standard biomedicine was the most effective for negative conversion rate (OR = 11.55, 95% CI [3.04, 43.93]). Bu Jin Tablet combined with standard biomedicine demonstrated superior efficacy for lesion absorption rate (OR = 7.46, 95% CI [3.32, 16.75]). FeiJieHe Pill combined with standard biomedicine was the most effective for cavity absorption (OR = 5.11, 95% CI [2.04, 12.85]). JieHe Pill combined with conventional biomedicine yielded the greatest improvement in both $CD3^+$ T lymphocyte response (OR = 5.6, 95% CI [3.4, 7.8]) and $CD4^+$ T lymphocyte response (OR = 5.1, 95% CI [2.9, 7.3]).

Conclusion: Combination therapy utilizing oral CCPP alongside conventional biomedicine has a significant enhanced efficacy relative to conventional biomedicine monotherapy across multiple tuberculosis treatment metrics, including clinical efficacy rate, negative conversion rate, lesion absorption rate, cavity absorption rate, and improvement rates of $CD3^+$ and $CD4^+$ T lymphocyte levels.

Systematic Review Registration: https://www.crd.york.ac.uk/prospero/display_record.php?ID=CRD42024589122, identifier CRD42024589122.

KEYWORDS

pulmonary tuberculosis, oral commercial Chinese polyherbal, biomedicine, combination therapy, network meta-analysis, randomized controlled trials

1 Introduction

Tuberculosis (TB), an airborne infectious disease caused by *Mycobacterium tuberculosis*, persists as a major global health threat in 21st century and remains one of the key infectious diseases controlled in China. According to the World Health Organization's 2023 report (Wei and LiuYuhon, 2024), global TB incidence reached 10.6 million new cases in 2022, including 748,000 cases in China, ranking the third among high-burden nations. *Bacillus* Calmette-Guérin (BCG) vaccination programs and standardized modern pharmaceutical interventions render the TB epidemic both preventable and controllable. However, the emergence of drug-resistant strains, particularly multidrug-resistant tuberculosis, poses new challenge to TB control (Hui et al., 2020). Currently, biomedicine primarily treats TB with oral anti-TB medications, emphasizing early, combined, appropriate, regular, and full-course use. The conventional 2HRZE/4HR regimen comprises 2-month of therapy with Isoniazid, Rifampicin, Pyrazinamide, and Ethambutol followed by 4 months of Isoniazid and Rifampicin. While demonstrating clinical efficacy, long-term use of this regimen carries potential multi-organ toxicity risks (Shah et al., 2020; Prasad et al., 2019). Furthermore, treatment discontinuation secondary to adverse drug effects in newly diagnosed patients may predispose to develop drug-resistant TB development. A study by Zou Xia-li et al. (Xiali et al., 2017) identified a 2.38-fold increased risk of drug resistance development among TB patients experiencing anti-TB drug-related adverse reactions during initial treatment, with this the risk increased to 4.20-fold in individuals with prior treatment-associated adverse reactions. Correspondingly, Wei et al. (Wei et al., 2015) determined that anti-TB drug adverse reactions constitute the primary cause of treatment discontinuation in this patient population. Improving the efficacy of anti-TB drugs and reducing their side effects has become an urgent issue in modern TB management.

TB corresponds to the "pulmonary tuberculosis" classification within Traditional Chinese Medicine (TCM). Specialized texts such as Shí Yào Shén Shū (Ten Medicines Divine Book) of the Yuan Dynasty (Ge, 2019) documented early therapeutic approaches. The treatment principles of "tonifying the deficiency" and "killing parasites" established in Yīxué Zhèng Zhuàn (The Correct Transmission of Medicine) of the Ming Dynasty remain clinically relevant. TCM posits pulmonary tuberculosis as a chronic infectious disease caused by vital energy deficiency and infection of "consumption worms" that invade the lungs. Previous studies demonstrate that synergistic integration of TCM and biomedicine enhances the efficacy of anti-TB drugs, shortens treatment time, and mitigates side effects. Zhang Zhi-jie et al. (Zhijie, 2018) found that compared with simply using biomedicine, Qinghao Biejia Tang significantly improved the cure rate for drug-resistant TB. Similarly, Kang Guannan et al. (Guannan et al., 2023) observed higher cure rate, negative conversion rate, and cavity improvement rate following Kangfuxin Liquid combination therapy relative to anti-TB drugs alone, while also alleviating hemoptysis symptoms and reducing side effects.

Although multiple studies support enhanced treatment outcomes and reduced toxicity from adjunctive administration of oral traditional commercial Chinese polyherbal preparation (CCPP) alongside anti-TB biomedicine, the optimal therapeutic profile and comparative advantages of specific formulations remain undetermined. This study conducts a network meta-analysis comparing the efficacy of different oral CCPP as adjunctive therapy to anti-TB drugs, aiming to provide better treatment options for clinical practice.

2 Materials and methods

This study protocol received registration on the PROSPERO platform with the registration number CRD42024589122.

2.1 Literature search

To perform literature search, we have used multiple databases like China National Knowledge Infrastructure (CNKI) (https://oversea.cnki.net/index/), Wanfang (http://www.wanfangdata.com/), VIP Full Text Journals Database (https://www.fjlib.net/English/digitalresources/201804/t20180414_349923.htm), SinoMed (https://www.sinomed.com/), PubMed (https://pubmed.ncbi.nlm.nih.gov/), Embase (https://www.embase.com), Web of Science (https://www.

Abbreviations: T, Experimental group; C, Control group; Bio, biomedicine; —, Not reported; BL, Bailing Capsule; BFHX, Bu Fei HuoXue Capsule; BJ, Bu Jin Tablet; FJH, FeiJieHe Pill; FT, Fei Tai Capsule; JPRF, Jian Pi Run Fei Pill; JHL, Jie He Ling Tablet; JHW, Jie He Pill; KF, KangFu Xin Liquid; KL, KangLao Pill; QJLFJN, QiJia LiFei Capsule; YFZKJN, YiFei ZhiKe Capsule.

webofscience.com), and Cochrane Library (https://www.cochranelibrary.com/). The databases were screen up to 22 January 2025, based on a robust literature screening and data extraction strategy. The languages considered were Chinese and English.

2.2 Literature screening and data extraction

Three researchers participated in the literature screening and data extraction, with one designated as the group leader. In the event of any disagreement during the screening process, the group leader was responsible for making the final decision. According to the diagnostic criteria for pulmonary tuberculosis (Chuanjun et al., 2023; Guofang and Xiwei, 2020; Radiology, 2018), a confirmed diagnosis required meeting at least one of the following conditions, along with mandatory fulfillment of condition C:

A. Persistent cough and sputum production lasting for 2 weeks or more, with or without hemoptysis, blood-streaked sputum, or systemic symptoms.
B. Radiographic findings suggestive of pulmonary tuberculosis.
C. Detection of *Mycobacterium tuberculosis* in sputum or other specimens, confirmed by smear microscopy, culture, or molecular biological methods.

There were no restrictions regarding gender, age, prior treatment history (initial treatment or retreatment), or drug resistance status.

The control group received a standard anti-tuberculosis monotherapy regimen or monotherapy combined with adjunctive treatments such as hepatoprotective or hemostatic agents to alleviate complications. The experimental group was administered a single oral Chinese patent medicine in addition to the control regimen. The total treatment duration was the same for both groups.

Studies were excluded if they met any of the following criteria: non-randomized controlled trials (non-RCTs), narrative reviews, systematic reviews, conference abstracts, clinical guidelines, studies with undefined treatment durations, animal or *in vitro* experiments, academic theses, or topics for which fewer than three relevant studies were available.

The outcome indicators collected included the following: A. Clinical efficacy rate; B. Sputum conversion rate; C. Lesion absorption rate; D. Cavity closure rate; E. Improvement rate of $CD3^+$ T lymphocytes; F. Improvement rate of $CD4^+$ T lymphocytes; G. Incidence of adverse reactions.

2.3 Literature quality assessment

Methodological quality evaluation of included RCTs utilized Cochrane Handbook standards (Higgins et al., 2023) assessing dimensions of randomization method, allocation concealment, blinding of participants and staff, blinding of outcome assessors, completeness of data, selective reporting of outcomes, and other biases. If there were any disagreements during the evaluation, consensus was reached through in-depth discussion with the group leader. Each evaluation item was classified as "low risk", "unclear", or "high risk". All results were systematically documented within RevMan 5.4 software (Cochrane Collaboration, 2020), facilitating generation of corresponding risk of bias visualizations.

2.4 Statistical analysis

A network meta-analysis was conducted using the "netmeta" package (Rücker et al., 2024) in R (version 4.4.1) (R Core Team, 2024), and forest plots were generated.Binary outcomes employed odds ratio (OR) as the effect size measure, while continuous outcomes utilized standardized mean difference (MD), with reported 95% confidence intervals (CI). If the 95% CI for a binary variable does not include 1, or the 95% CI for a continuous variable does not include 0, statistical significance between groups was considered to be present. Evidence network were constructed using Stata 18.0 (StataCorp, 2023), featuring nodes proportional to intervention-specific sizes and interconnecting. To rank the effectiveness of different interventions, the Surface Under the Cumulative Ranking Curve (SUCRA) was used, with higher SUCRA values indicating a greater probability of being among the most effective treatments. No fixed SUCRA threshold was applied. This interpretation follows established methodological guidance in network meta-analysis (Salanti et al., 2011; Rücker and Schwarzer, 2015). Additionally, comparison-corrected funnel plots were drawn to examine publication bias in the included studies. Additional details are provided in the Supplementary Material (Supplementary Files 1–3).

3 Results

3.1 Literature search

A total of 15,036 articles were identified, with 100 articles meeting final inclusion criteria as exclusively two-arm RCTs. For multiple reports of the same study (such as clinical trial registration records and journal articles), the version with the most comprehensive or recent iteration was retained, and related studies were merged before data extraction. The literature screening flowchart is shown in Figure 1.

3.2 Characteristics of included literature

The 100 included articles (Jian, 2002; Yanpei and Shuyu, 2002; Ming, 2004; Wei et al., 2004; Donghua and Ganhong, 2005; Liuxing, 2005; Mengqiu et al., 2006; Lidong and Shuqing, 2007; Wulu et al., 2007; Xuewen, 2007; Yujuan, 2007; Ge et al., 2009; Kai, 2009; Shouyue, 2009; Xian, 2009; Xiuxia, 2009; Fuyuan and MeiMingxing, 2010; Guiqiu, 2010, Jun, 2010; Bing and Yuanai, 2011; Shiqi, 2011; Fengyan, 2012; Xinhua, 2012; Dan et al., 2013; Hualiang, 2013; Hunxi and Zhanqi, 2013; Lidong et al., 2013; Wenge et al., 2013; Xuhua et al., 2013; Zhongming, 2013; Long et al., 2014; Qianxin et al., 2014; Qing and Wengfang, 2014; Xiue et al., 2014; Jinghua et al., 2015; Min-shuang et al., 2015; Tianfeng, 2015; Yunxiao and Guosheng, 2015; Yuxia, 2015; Juan et al., 2016; Junguo

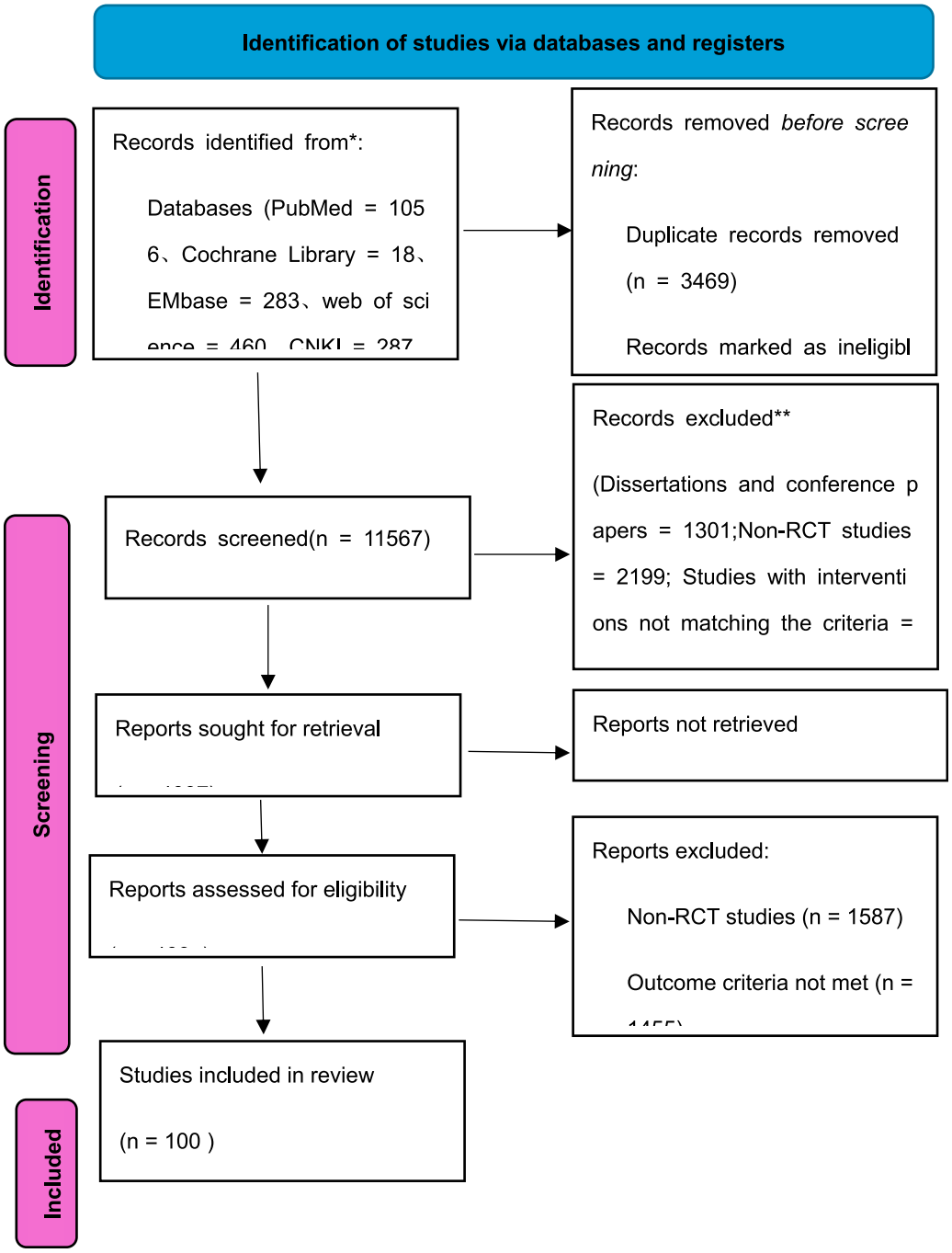


FIGURE 1
PRISMA flow diagram of the studies selection process.

et al., 2016; Shiming et al., 2016; Shuang, 2016; Shuhua and Fujian, 2016; Wei, 2016; Zhenru, 2016; Ji et al., 2017; Jun et al., 2017; Xing et al., 2017; Yongyi et al., 2017; Junjie, 2018; Lingwei, 2018; Liping, 2018; Xiaoni, 2018; Xiaoru et al., 2018; Di et al., 2019; Guizhen, 2019; Hai-xian et al., 2019; Junmei et al., 2019; Meng, 2019; Qingfeng, 2019; Zhibo et al., 2019; Bin, 2020; Guannan et al., 2020; Hui et al., 2020; Shuangli et al., 2020; Weiyong et al., 2020; Xian-hui and Shu-lin, 2020; Qiang, 2021; Qiong et al., 2021; Wei-wei, 2021; Chenyong et al., 2022; Jiafu and Lanhua, 2022; Juan, 2022; Qihuang, 2022; Jun et al., 2022; Xiaohua, 2022; Xuehu et al., 2022; Xueyun, 2022; Chang et al., 2022; Guannan et al., 2023; Chuanjun et al., 2023; Junguo, 2023; Qiaoe et al., 2023; Yawei et al., 2023; Yuxia, 2023; Peiqian et al., 2024; Xinlei and Rong, 2024; Yuelian, 2024) were all two-arm experiments, with a total sample size of 12,747 participants: 6,639 in the experimental group and 6,108 in the control group. These studies involved 12 different interventions:

- Bai Ling Capsule: seven studies (Yanpei and Shuyu, 2002; Donghua and Ganhong, 2005; Ge et al., 2009; Juan et al., 2016; Shuhua and Fujian, 2016; Hui et al., 2020; Shuangli et al., 2020)

TABLE 1 Characteristics of the included randomized controlled trials.

Included in study	Sample size		Age (years)		Interventions		Treatment course	Outcome measures
	T	C	T	C	T	C		
Jian (2002)	31	28	—	—	BJ+Bio	Bio	9	①②
Yanpei and Shuyu (2002)	48	30	60–86	60–84	BL+Bio	Bio	3	①②⑤
Ming (2004)	50	50	14–60	16–59	FJH+Bio	Bio	6	①
Wei et al. (2004)	64	64	18–76	18–74	YFZK+Bio	Bio	6	①②
Donghua and Ganhong (2005)	62	60	26–67	25–66	BL+Bio	Bio	6	①②④
Liuxing (2005)	128	64	—	—	YFZK+Bio	Bio	6	①④
Pu et al. (2005)	38	15	—	—	FT+Bio	Bio	6	①②③
Mengqiu et al. (2006)	168	85	—	—	FT+Bio	Bio	8	①②③⑤⑥⑦
Xuewen (2007)	64	64	18–76	18–74	YFZK+Bio	Bio	6	①③④⑤
Lidong and Shuqing (2007)	75	75	—	—	JHL+Bio	Bio	6	①③⑤
Wulu et al. (2007)	241	100	—	—	JPRF+Bio	Bio	2	①②④⑤
Yujuan (2007)	67	65	—	—	YFZK+Bio	Bio	9	①②③⑤
Shuqin et al. (2008)	70	70	18–65	18–65	JHL+Bio	Bio	8	①③④⑤
Shouyue (2009)	168	85	18–72	18–72	JPRF+Bio	Bio	8	①③④⑤
Kai (2009)	53	52	—	—	YFZK+Bio	Bio	6	①②
Xian (2009)	30	30	19–65	25–68	BJ+Bio	Bio	3	①④
Xiuxia (2009)	132	130	21–68	20–70	YFZK+Bio	Bio	21	①②⑤
Ge et al. (2009)	123	121	16–67	18–66	BL+Bio	Bio	6	①②④⑤
Fuyuan and Meimingxing (2010)	90	90	X70	X70	JPRF+Bio	Bio	6	①②⑤
Guiqiu (2010)	36	38	—	—	JH+Bio	Bio	3	①②③⑤
Jun (2010)	26	22	—	—	BJ+Bio	Bio	6	①②③
Shiqi (2011)	30	26	60–87	61–88	JH+Bio	Bio	3	①
Bing and Yuanai (2011)	100	100	25–71	23–70	JPRF+Bio	Bio	8	①②③⑤
Xinhua (2012)	50	50	—	—	FJH+Bio	Bio	6	①②③④
Fengyan (2012)	32	32	—	—	FJH+Bio	Bio	12	①②⑤
Lidong et al. (2013)	50	50	—	—	JH+Bio	Bio	3	①②④

(Continued on following page)

10.3389/fphar.2025.1588586

TABLE 1 (*Continued*) Characteristics of the included randomized controlled trials.

Included in study	Sample size		Age (years)		Interventions		Treatment course	Outcome measures
	T	C	T	C	T	C		
Wen-ge et al. (2013)	63	57	24–57	27–56	KF+Bio	Bio	6	①③⑤
Dan et al. (2013)	39	38	—	—	JH+Bio	Bio	6	①③④⑤
Hunxi and Zhanqi (2013)	100	90	11–75	19–68	JPRF+Bio	Bio	6	①⑤
Zhongming (2013)	75	75	—	—	JHL+Bio	Bio	6	①⑤
Hualiang (2013)	60	57	—	—	FT+Bio	Bio	6	①②④
Xuhua et al. (2013)	22	22	—	—	JH+Bio	Bio	3	①④⑤
Qing and Wengfang (2014)	40	40	—	—	FJH+Bio	Bio	6	①②⑤
Long et al. (2014)	50	50	—	—	QJLF+Bio	Bio	9	①④
Qianxin et al. (2014)	92	90	—	—	JH+Bio	Bio	2	①②⑤
Xiue et al. (2014)	97	98	31.6 ± 2.4	32.1 ± 2.1	QJLF+Bio	Bio	8	①②③⑥⑦
Jian and Li (2014)	24	24	68.5 ± 6.2	67.2 ± 5.7	JH+Bio	Bio	6	①⑥⑦
Jinghua et al. (2015)	53	53	21–73	20–73	KL+Bio	Bio	3	①
Xiang (2015)	50	58	22–87	23–88	KF+Bio	Bio	6	①④
Min-shuang et al. (2015)	56	58	42.18 ± 6.34	43.08 ± 6.63	JH+Bio	Bio	18	①⑤⑥⑦
Tianfeng (2015)	43	42	30–58	31–58	BFHX+Bio	Bio	3	①④
Yunxiao and Guosheng (2015)	40	40	—	—	BJ+Bio	Bio	6	①②③⑤
Yuxia (2015)	45	45	18–66	18–65	JH+Bio	Bio	2	①②⑤
Shuhua and Fujian (2016)	60	60	18–80	16–78	BL+Bio	Bio	6	①②
Shiming et al. (2016)	51	50	18–64	29–65	QJLF+Bio	Bio	18	①②③⑤
Qi et al. (2016)	150	150	—	—	BL+Bio	Bio	8	①②④⑤
Juan et al. (2016)	56	53	—	—	QJLF+Bio	Bio	8	①②③⑤
Wei (2016)	48	48	13–74	16–72	JPRF+Bio	Bio	6	①⑤
Zhenru (2016)	34	34	20–62	21–61	JH+Bio	Bio	6	②⑥⑦
Liping and Chun (2016)	42	28	—	—	FT+Bio	Bio	6	①②
Junguo et al. (2016)	40	38	18–65	17–64	JH+Bio	Bio	6	①②⑤
Qi (2016)	56	56	45.2 ± 3.4		JH+Bio	Bio	12	①②

(Continued on following page)

10.3389/fphar.2025.1588586

TABLE 1 (*Continued*) Characteristics of the included randomized controlled trials.

Included in study	Sample size		Age (years)		Interventions		Treatment course	Outcome measures
	T	C	T	C	T	C		
Shuang (2016)	40	38	—	—	JHL+Bio	Bio	6	①②④
Yongyi et al. (2017)	55	55	19–66	17–67	JH+Bio	Bio	6	①②④⑤
Ji et al. (2017)	58	55	—	—	FT+Bio	Bio	6	①②③⑤
Xing et al. (2017)	185	175	—	—	JH+Bio	Bio	12	①②③⑤
Jun et al. (2017)	56	53	—	—	QJLF+Bio	Bio	8	①②③⑤
Xu et al. (2018)	90	90	45.6 ± 9.9	42.8 ± 10.5	BFHX+Bio	Bio	6	①②③
Liping (2018)	43	43	18.3–76.5	18.1–76.9	JH+Bio	Bio	6	①②⑤⑥⑦
Lingwei (2018)	60	60	—	—	JH+Bio	Bio	6	②④
Junjie (2018)	57	57	19–63	20–62	QJLF+Bio	Bio	9	①⑤
Xiaoru et al. (2018)	54	54	33.8 ± 5.7	33.7 ± 5.3	KF+Bio	Bio	6	①
Xiaoni (2018)	50	50	24–63	25–65	KL+Bio	Bio	6	①④
Di et al. (2019)	35	35	19–58	18–60	FJH+Bio	Bio	6	②
Zhibo et al. (2019)	68	67	35.9 ± 10.5	36.3 ± 10.1	KF+Bio	Bio	6	①②③⑤
Meng (2019)	40	40	13–74	12–75	JH+Bio	Bio	6	①⑤
Junmei et al. (2019)	41	41	22–68	21–69	BFHX+Bio	Bio	4	①⑤⑦
Hai-xian et al. (2019)	30	30	33–59	31–61	KF+Bio	Bio	6	①③⑤
Guizhen (2019)	55	50	25–66	29–63	JH+Bio	Bio	9	①③④⑤
Qin (2019)	53	53	24–77	23–78	FT+Bio	Bio	6	①②③⑤
Qingfeng (2019)	30	30	32–69	33–68	KL+Bio	Bio	6	①
Guannan et al. (2020)	158	158	72.87 ± 7.12	73.91 ± 7.37	KF+Bio	Bio	6	①③④⑤
Hui et al. (2020)	220	180	48.82 ± 6.94	49.46 ± 6.95	BL+Bio	Bio	12	①②③⑤⑦
Weiyong et al. (2020)	50	50	—	—	KL+Bio	Bio	6	①④
Xian-hui and Shu-lin (2020)	75	75	32–60	36–65	FT+Bio	Bio	6	①②③④⑤
Bin (2020)	50	50	25–76	22–75	JH+Bio	Bio	6	①②④⑤
Shuangli et al. (2020)	90	90	18–60	18–58	BL+Bio	Bio	3	①②③④⑤⑥⑦
Qiong et al. (2021)	101	101	17–75	16–72	JH+Bio	Bio	6	①

(Continued on following page)

10.3389/fphar.2025.1588586

TABLE 1 (*Continued*) Characteristics of the included randomized controlled trials.

Included in study	Sample size		Age (years)		Interventions		Treatment course	Outcome measures
	T	C	T	C	T	C		
Wei-wei (2021)	62	62	60–81	60–76	JH+Bio	Bio	6	①⑥⑦
Qiang (2021)	60	60	49.14 ± 10.66	48.85 ± 10.27	JH+Bio	Bio	6	①②③④⑤
Qihuang (2022)	37	37	35–71	32–72	JH+Bio	Bio	3	①④⑤
Xuehu et al. (2022)	60	60	19–65	20–64	KF+Bio	Bio	3	①②③⑤
Yan et al. (2022)	56	56	32–67	30–68	JH+Bio	Bio	6	①②③④
Jia (2022)	50	50	25–67	24–69	JH+Bio	Bio	2	①
Jiafu and Lanhua (2022)	38	38	25–73	24–72	JH+Bio	Bio	6	②⑤
Xueyun (2022)	60	60	37.62 ± 6.91	38.15 ± 7.11	KF+Bio	Bio	6	①②③④⑤
Xiaohua (2022)	34	34	23–64	24–66	KF+Bio	Bio	6	①⑤⑥⑦
Juan (2022)	100	100	57.83 ± 5.09	52.17 ± 6.07	JH+Bio	Bio	9	①②③
Chenyong et al. (2022)	41	39	6–15	7–16	JPRF+Bio	Bio	3	①②③④⑤
Tao and Fei (2022)	40	40	26–75	24–75	JH+Bio	Bio	6	①②③④⑤
Yawei et al. (2023)	76	76	39–75	35–75	BFHX+Bio	Bio	6	①⑤
Guannan et al. (2023)	94	94	24–68	19–70	KF+Bio	Bio	6	①②③⑤
Qiaoe et al. (2023)	100	100	23–74	22–74	JH+Bio	Bio	6	①④
Junguo (2023)	30	30	70.48 ± 2.61	70.44 ± 2.23	JH+Bio	Bio	6	②⑤⑦
Yan et al. (2023)	35	35	55.61 ± 11.12	52.47 ± 10.49	KL+Bio	Bio	6	③⑥⑦
Yuxia (2023)	38	38	19–80	19–80	JH+Bio	Bio	6	①⑤
Hu et al. (2023)	68	68	41.87 ± 11.35	42.82 ± 11.02	BFHX+Bio	Bio	5	= 1 * GB3 ①②③④⑤⑥⑦
Peiqian et al. (2024)	49	49	15–17	15–18	JH+Bio	Bio	6	⑤⑥⑦
Xinlei and Rong (2024)	104	103	49.44 ± 12.79	50 ± 15.01	JH+Bio	Bio	6	= 2 * GB3 ②④⑤
Yuelian (2024)	49	49	52.97 ± 7.05	54.11 ± 6.83	JH+Bio	Bio	6	②③④⑥⑦

10.3389/fphar.2025.1588586

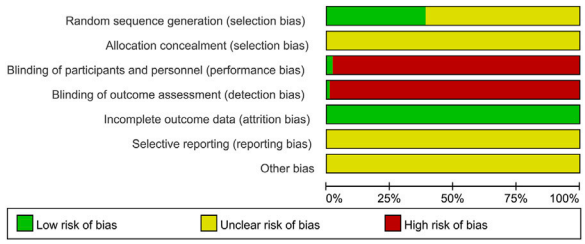


FIGURE 2
Percentages of items with risks of bias of included articles. In the domain of random sequence generation, 38 studies reported specific methods of randomization, while 62 studies merely mentioned randomization without providing details of the method used. For allocation concealment, none of the included studies reported any information. Regarding blinding of participants and personnel, one study reported a double-blind design, and another study adopted a single-blind design. In terms of blinding of outcome assessment, only one study reported using a double-blind approach. All included studies had complete outcome data. None of the studies mentioned selective reporting or other sources of bias. The term "other biases" refers to potential sources of bias such as funding-related bias, selective reporting bias, data collection bias, and study design bias.

- Bu Fei Huo Xue Capsule: five studies (Tianfeng, 2015; Xiaoru et al., 2018; Junmei et al., 2019; Chuanjun et al., 2023; Yawei et al., 2023)
- Bu Jin Tablet: four studies (Jian, 2002; Xian, 2009; Jun, 2010; Yunxiao and Guosheng, 2015)
- FeiJieHe Pill: five studies (Ming, 2004; Fengyan, 2012; Xinhua, 2012; Qing and Wengfang, 2014; Di et al., 2019)
- Fei Tai Capsule: seven studies (Donghua and Ganhong, 2005; Mengqiu et al., 2006; Hualiang, 2013; Junguo et al., 2016; Ji et al., 2017; Hai-xian et al., 2019; Xian-hui and Shu-lin, 2020)
- Jian Pi Run Fei Pill: seven studies (Wulu et al., 2007; Shouyue, 2009; Fuyuan and MeiMingxing, 2010; Bing and Yuanai, 2011; Hunxi and Zhanqi, 2013; Wei, 2016; Chenyong et al., 2022)
- Jie He Ling Tablet: four studies (Lidong and Shuqing, 2007; Zhongming, 2013; Shuang, 2016)
- Jie He Pill: 34 studies (Guiqiu, 2010; Shiqi, 2011; Dan et al., 2013; Lidong et al., 2013; Xuhua et al., 2013; Hunxi and Zhanqi, 2013; Qianxin et al., 2014; Min-shuang et al., 2015; Yuxia, 2015; Junguo et al., 2016; Juan et al., 2016; Zhenru, 2016; Xing et al., 2017; Yongyi et al., 2017; Lingwei, 2018; Liping, 2018; Guizhen, 2019; Meng, 2019; Bin, 2020; Chenyong et al., 2022; Jiafu and Lanhua, 2022; Juan, 2022; Jun et al., 2022; Chang et al., 2022; Junguo, 2023; Qiaoe et al., 2023; Yuxia, 2023; Peiqian et al., 2024; Xinlei and Rong, 2024; Yuelian, 2024)
- Kangfuxin Liquid: 10 studies (Wen-ge et al., 2013; Min-shuang et al., 2015; Xiaoru et al., 2018; Hai-xian et al., 2019; Zhibo et al., 2019; Guannan et al., 2020; Xiaohua, 2022; Xuehu et al., 2022; Xueyun, 2022; Guannan et al., 2023)
- KangLao Pill: five studies (Jinghua et al., 2015; Xiaoni, 2018; Qingfeng, 2019; Weiyong et al., 2020; Chenyong et al., 2022)
- Qi Jia Li Fei Capsule: six studies (Long et al., 2014; Xiue et al., 2014; Juan et al., 2016; Shiming et al., 2016; Jun et al., 2017; Junjie, 2018)
- Yi Fei Zhi Ke Capsule: six studies (Wei et al., 2004; Liuxing, 2005; Xuewen, 2007; Yujuan, 2007; Kai, 2009; Xiuxia, 2009)

The baseline characteristics of the two groups were comparable. The basic information of the included literature is shown in Table 1.

3.3 Literature quality assessment

All 100 included articles documented randomization procedures, with 28 employing random number tables (Mengqiu et al., 2006; Hualiang, 2013; Hunxi and Zhanqi, 2013; Xiue et al., 2014; Min-shuang et al., 2015; Juan et al., 2016; Zhenru, 2016; Ji et al., 2017; Jun et al., 2017; Xiaoru et al., 2018; Junmei et al., 2019; Hai-xian et al., 2019; Bin, 2020; Guannan et al., 2020; Weiyong et al., 2020; Qiang, 2021; Qihuang, 2022; Xiaohua, 2022; Xueyun, 2022; Guannan et al., 2023; Chuanjun et al., 2023; Qiaoe et al., 2023; Chenyong et al., 2022; Yawei et al., 2023; Yuxia, 2023; Peiqian et al., 2024; Xinlei and Rong, 2024; Yuelian, 2024), one utilizing random pairing (Jun, 2010), one applying random ordering (Wen-ge et al., 2013), two implementing random sampling (Juan et al., 2016; Jun et al., 2022), one adopting randomized controlled design (Chang et al., 2022), one using stratified block randomization (Guannan et al., 2020), two applying computer randomization (Xian-hui and Shu-lin, 2020; Juan, 2022); one implementing random parallel design (Chenyong et al., 2022), one using pathogen number draw (Yongyi et al., 2017), all rated as low risk. Studies mentioning randomization without methodological specification received unclear risk ratings. The investigation by Liu Xing et al. (Xing et al., 2017) implemented double-blind method and was rated as low risk, whereas Gao Mengqiu et al. (Mengqiu et al., 2006) applied single-blind method without specifying personnel responsible for implementation. All the included studies had complete data, with no evidence of selective reporting or other biases documented. Detailed risk of bias assessments are presented in Figure 2.

3.4 Evidence network

Fifty-three studies reported clinical efficacy rates, resulting in 12 direct comparisons, while 78 studies reported negative conversion rates yielding 12 direct comparisons. Evaluation of lesion absorption rates occurred across 56 studies generating 11 direct comparisons., with cavity absorption rates assessed in 42 studies forming 11 direct comparisons. 13 studies quantified $CD3^+$ T lymphocyte improvement rates forming seven direct comparisons, complemented by 16 studies examining $CD4^+$ T lymphocyte improvement rates forming seven direct comparisons. No closed loops were formed between the outcome indicators, so inconsistency tests were not conducted, with the complete evidence network structure depicted in Figure 3.

3.5 Network meta-analysis

3.5.1 Clinical efficacy rate

Assessment of clinical efficacy across 53 studies reported clinical efficacy rate, incorporating 13 interventions, including 12 types of oral TCMs, enrolled 6,625 participants. The network meta-analysis demonstrated significantly enhanced clinical efficacy for

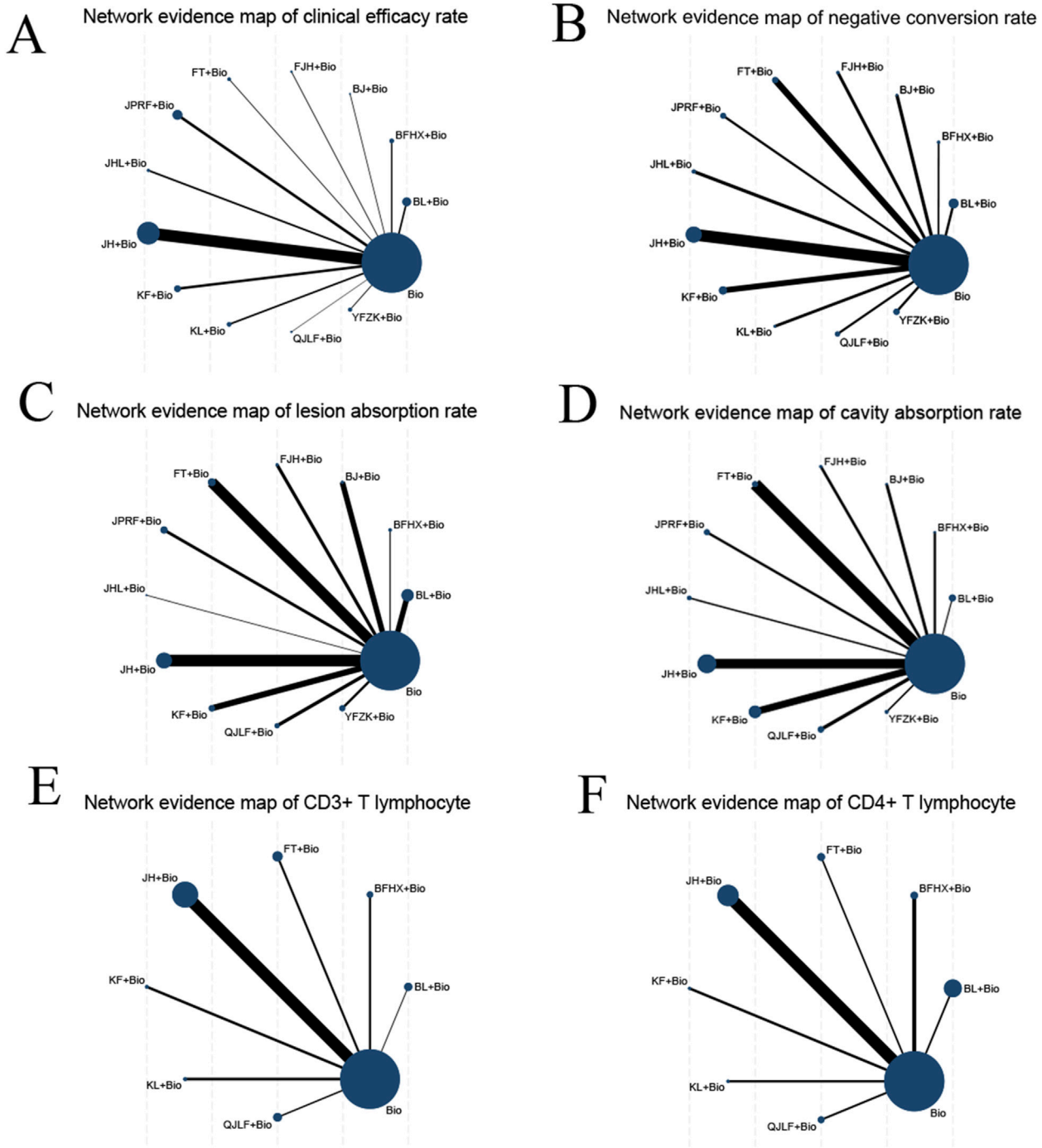


FIGURE 3
Network evidence maps comparing different outcomes: **(A)** network evidence map for clinical efficacy rate; **(B)** network evidence map for negative conversion rate; **(C)** network evidence map for lesion absorption rate; **(D)** network evidence map for cavity absorption rate; **(E)** network evidence map for improvement rate of $CD3^+$ T lymphocytes; **(F)** network evidence map for improvement rate of $CD4^+$ T lymphocytes.

combinations of standard biomedicine with: FeiJieHe Pill (OR = 8.43,95% CI [1.79, 39.7]), Yi Fei Zhi Ke Capsule (OR = 4.88, 95% CI [2.72, 8.74]), Kangfuxin Liquid (OR = 2.60, 95% CI [1.79, 3.78]), Qi Jia Li Fei Capsule (OR = 2.56, 95% CI [1.02, 6.46]), Bu Fei Huo Xue Capsule (OR = 2.54, 95% CI [1.58, 4.10]), Jian Pi Run Fei Pill (OR = 2.49, 95% CI [1.67, 3.71]), Fei Tai Capsule (OR = 2.48, 95% CI [1.46, 4.23]), KangLao Pill (OR = 2.16, 95% CI [1.42, 3.28]), Bai Ling Capsule (OR = 2.11, 95% CI [1.47, 3.03]), and Jie He Pill (OR = 2.14, 95% CI [1.77, 2.58]), all relative to biomedicine monotherapy. SUCRA ranking for clinical efficacy revealed the following hierarchy of therapeutic combinations: FeiJieHe Pill with standard biomedicine (SUCRA = 90.9%) exhibited the highest

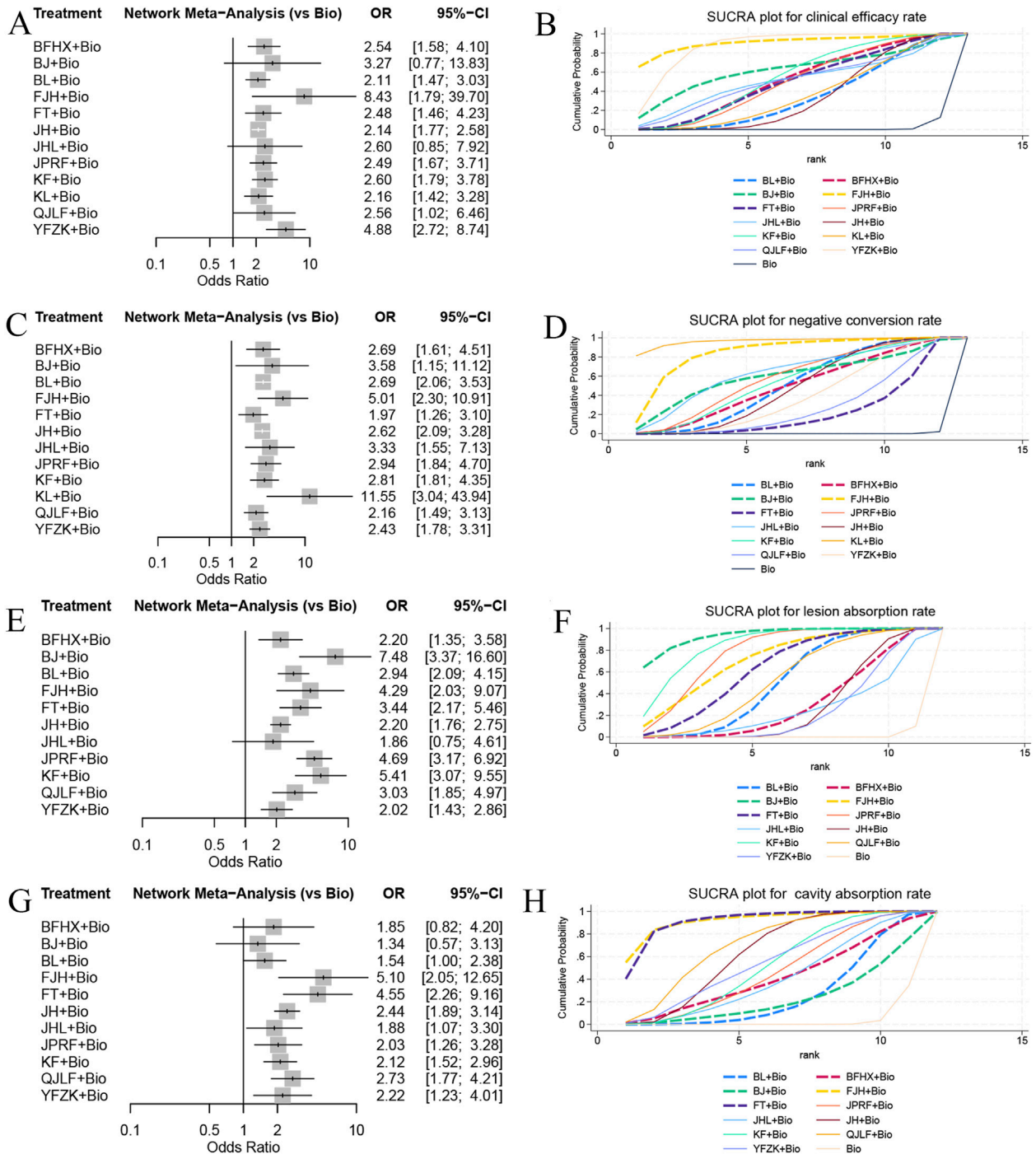


FIGURE 4
Forest plots and SUCRA ranking charts showing comparative effects on clinical efficacy rate, negative conversion rate, lesion absorption rate, and cavity absorption rate: **(A)** Forest plot of clinical efficacy rate; **(B)** SUCRA ranking chart for clinical efficacy rate; **(C)** Forest plot of negative conversion rate; **(D)** SUCRA ranking chart for negative conversion rate; **(E)** Forest plot of lesion absorption rate; **(F)** SUCRA ranking chart for lesion absorption rate; **(G)** Forest plot of cavity absorption rate; **(H)** SUCRA ranking chart for cavity absorption rate.

probability of superiority, followed sequentially by Yi Fei Zhi Ke Capsule (SUCRA = 87.2%), Bu Jin Tablet (SUCRA = 61.5%), Kangfuxin Liquid (SUCRA = 54.3%), Bu Fei Huo Xue Capsule (SUCRA = 51.3%), Jie He Ling Tablet (SUCRA = 50.7%), Qi Jia Li Fei Capsule (SUCRA = 50.3%), Jian Pi Run Fei Pill (SUCRA = 49.7%), Fei Tai Capsule (SUCRA = 49.2%), KangLao Pill (SUCRA = 36.2%), Bai Ling Capsule (SUCRA = 34%), and Jie He Pill (SUCRA = 33.7%), with all relative to standard biomedicine monotherapy (SUCRA = 1.1%). In summary, the combination of FeiJieHe Pill with standard biomedicine potentially represents the optimal approach for improving clinical efficacy, as visually summarized in Figures 4A,B.

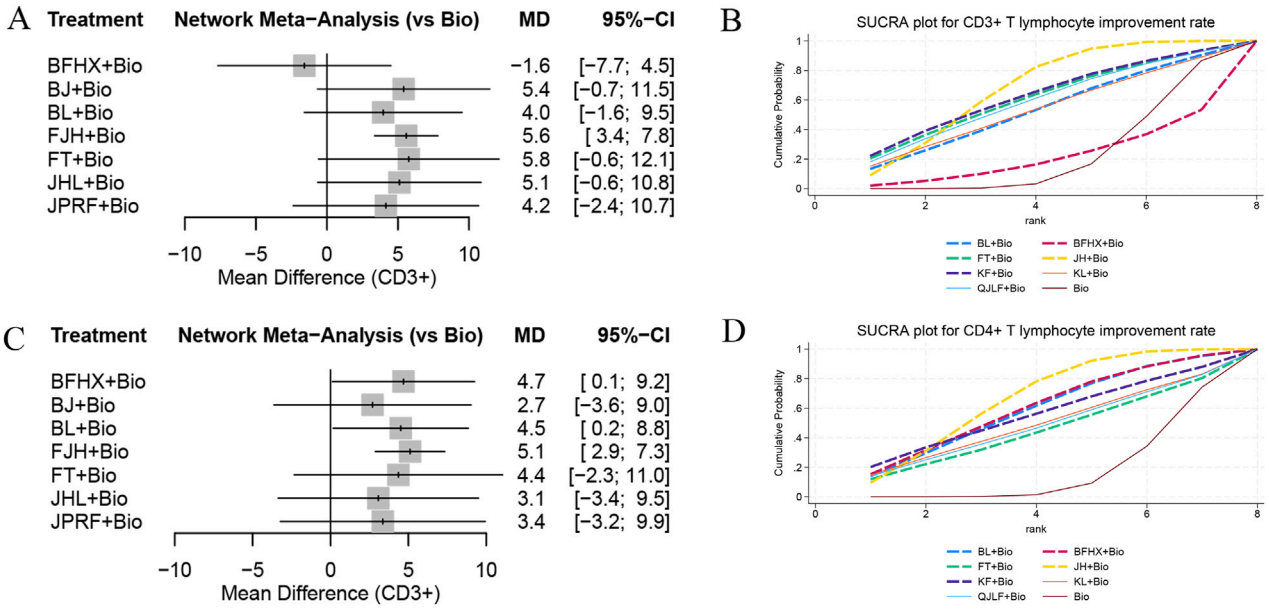


FIGURE 5
Forest plots and SUCRA ranking charts for CD3⁺ T lymphocyte improvement rate and CD4⁺ T lymphocyte improvement rate: **(A)** forest plot of CD3⁺ T lymphocyte improvement rate; **(B)** SUCRA ranking chart for CD3⁺ T lymphocyte improvement rate; **(C)** forest plot of CD4⁺ T lymphocyte improvement rate; **(D)** SUCRA ranking chart for CD4⁺ T lymphocyte improvement rate.

3.5.2 Negative conversion rate

A total of 78 studies reported the negative conversion rate, involving 13 interventions, including 12 types of oral TCMs, with 9,955 participants. The network meta-analysis results demonstrated significantly greater negative conversion rate for combination of standard biomedicine with: KangLao Pill (OR = 11.55, 95% CI [3.04, 43.93]), FeiJieHe Pill (OR = 5.01, 95% CI [2.30,10.91]), Jie He Ling Tablet (OR = 3.33, 95% CI [1.55, 7.13]), Bu Jin Tablet (OR = 3.58, 95% CI [1.15,11.12]), Jian Pi Run Fei Pill (OR = 2.94, 95% CI [1.84, 4.70]), Kangfuxin Liquid (OR = 2.81, 95% CI [1.81, 4.35]), Bai Ling Capsule (OR = 2.69, 95% CI [2.06, 3.53]), Bu Fei Huo Xue Capsule (OR = 2.69, 95% CI [1.61, 4.51]), Jie He Pill (OR = 2.62, 95% CI [2.09, 3.28]), Yi Fei Zhi Ke Capsule (OR = 2.43, 95% CI [1.78, 3.31]), Qi Jia Li Fei Capsule (OR = 2.16, 95% CI [1.49, 3.13]), and Fei Tai Capsule (OR = 1.97, 95%CI [1.26, 3.10]), all relative to standard biomedicine monotherapy. SUCRA ranking for negative conversion rate established a probabilistic hierarchy wherein KangLao Pill combined with standard biomedicine (SUCRA = 96.5%) showed the highest superiority probability, followed sequentially by FeiJieHe Pill (SUCRA = 84.2%), Jie He Ling Tablet (SUCRA = 63.3%), Bu Jin Tablet (SUCRA = 59.7%), Jian Pi Run Fei Pill (SUCRA = 57.4%), Kangfuxin Liquid (SUCRA = 53.8%), Bai Ling Capsule (SUCRA = 50.2%), Bu Fei Huo Xue Capsule (SUCRA = 49.2%), Jie He Pill (SUCRA = 47.3%), Yi Fei Zhi Ke Capsule (SUCRA = 38.7%), Qi Jia Li Fei Capsule (SUCRA = 28%), and Fei Tai Capsule (SUCRA = 21.6%), all benchmarked against standard biomedicine monotherapy (SUCRA = 0.2%). In summary, KangLao Pill combined with standard biomedicine potentially represents the optimal approach for improving negative conversion rates, as visualized in Figures 4C,D.

3.5.3 Lesion absorption rate

A total of 56 studies reported lesion absorption rate, involving 12 interventions, including 11 types of oral TCMs, with a total of 7,676 patients. The network meta-analysis showed a higher lesion absorption rate for the combinations of standard biomedicine with: Bu Jin Tablet (OR = 7.48, 95% CI [3.37,16.60]), Kangfuxin Liquid (OR = 5.41, 95% CI [3.07, 9.55]), Jian Pi Run Fei Pill (OR = 4.69, 95% CI [3.17, 6.62]), FeiJieHe Pill (OR = 4.29, 95% CI [2.03, 9.07]), Fei Tai Capsule (OR = 3.44, 95% CI [2.17, 5.46]), Qi Jia Li Fei Capsule (OR = 3.03, 95% CI [1.85, 4.97]), Bai Ling Capsule (OR = 2.94, 95% CI [2.09, 4.15]), Bu Fei Huo Xue Capsule (OR = 2.20, 95% CI [1.35,3.58]), Jie He Pill (OR = 2.20, 95% CI [1.76, 2.75]), and Yi Fei Zhi Ke Capsule (OR = 2.02, 95% CI [1.43, 2.86]), than using biomedicine monotherapy. SUCRA ranking for clinical efficacy revealed the following hierarchy of therapeutic combinations of Bu Jin Tablet with standard biomedicine (SUCRA = 93.4%) exhibited the highest lesion absorption rate, followed sequentially by Kangfuxin Liquid (SUCRA = 84.5%), Jian Pi Run Fei Pill (SUCRA = 77.3%), FeiJieHe Pill (SUCRA = 71.5%), Fei Tai Capsule (SUCRA = 63.5%), Qi Jia Li Fei Capsule (SUCRA = 52.3%), Bai Ling Capsule (SUCRA = 50%), Bu Fei Huo Xue Capsule (SUCRA = 30%), Jie He Pill (SUCRA = 23.7%), Jie He Ling Tablet (SUCRA = 25.3%), Yi Fei Zhi Ke Capsule (SUCRA = 24.1%) all relative to standard biomedicine monotherapy (SUCRA = 0.9%). In summary, the combination of Bu Jin Tablet with standard biomedicine may be the best approach for improving lesion absorption rate, as visually summarized in Figures 4E,F.

3.5.4 Cavity absorption rate

A total of 42 studies reported cavity absorption rate, involving 12 interventions, including 11 types of TCMs, enrolled 5,148 patients. The network meta-analysis results showed

TABLE 2 Adverse reactions reported in the included randomized controlled trials.

Included in study	Interventions		Adverse reactions	
	T	C	T	C
Junmei et al. (2019)	BFHX+Bio	Bio	2 cases of gastrointestinal reactions, 1 case of skin allergy, 1 case of gout, and 2 cases of liver function impairment.	2 cases of gastrointestinal reactions, 2 cases of skin allergies, 1 case of gout, and 3 cases of liver function impairment.
Yawei et al. (2023)	BFHX+Bio	Bio	3 cases of dizziness, 2 cases of liver function impairment, 5 cases of gastrointestinal reactions, 1 case of peripheral neuritis, 2 cases of rash.	2 cases of dizziness, 1 case of liver function impairment, 6 cases of gastrointestinal reactions, and 2 cases of rash.
Hu (2023)	BFHX+Bio	Bio	5 cases of abnormal liver function, and 2 cases of dry mouth.	10 cases of abnormal liver function, and 6 cases of gastrointestinal reactions.
Yunxiao and Guosheng (2015)	BJ+Bio	Bio	2 cases of abnormal liver function.	5 cases of abnormal liver function.
Yanpei and Shuyu (2002)	BL+Bio	Bio	9 cases of adverse reactions.	17 cases of adverse reactions.
Ge et al. (2009)	BL+Bio	Bio	12 cases of abnormal liver function.	31 cases of abnormal liver function.
Qi et al. (2016)	BL+Bio	Bio	15 cases of abnormal liver function, 1 case of kidney function injury, 13 cases of dizziness and tinnitus, and 7 cases of blood system reactions.	17 cases of abnormal liver function, 7 cases of kidney function injury, 16 cases of dizziness and tinnitus, and 19 cases of blood system reactions.
Hui et al. (2020)	BL+Bio	Bio	29 cases of gastrointestinal reactions, 3 cases of abnormal kidney function, 5 cases of abnormal liver function, 9 cases of hypothyroidism, 10 cases of blood system abnormalities, and 7 cases of neurological dysfunction.	35 cases of gastrointestinal reactions, 12 cases of abnormal kidney function, 16 cases of abnormal liver function, 13 cases of hypothyroidism, 22 cases of blood system abnormalities, and 12 cases of neurological dysfunction.
Shuangli et al. (2020)	BL+Bio	Bio	11 cases of gastrointestinal reactions, 1 case of abnormal kidney function, 2 cases of abnormal liver function, 4 cases of blood system injuries, and 3 cases of neurological injuries.	17 cases of gastrointestinal reactions, 6 cases of abnormal kidney function, 8 cases of abnormal liver function, 11 cases of blood system injuries, and 6 cases of neurological injuries.
Fengyan (2012)	FJH+Bio	Bio	2 cases of abnormal liver function, and 1 case of gastrointestinal reaction.	3 cases of abnormal liver function.
Qing and Wenfang (2014)	FJH+Bio	Bio	2 cases of abnormal liver function.	3 cases of abnormal liver function.
Mengqiu et al. (2006)	FT+Bio	Bio	1 case of elevated transaminase levels, and 1 case of Achilles tendon pain caused by levofloxacin.	Not reported.
Ji et al. (2017)	FT+Bio	Bio	3 cases of gastrointestinal reactions, 1 case of allergic reaction, 4 cases of liver injury, 3 cases of leukopenia (reduced white blood cells), 2 cases of gout, and 1 case of other conditions.	3 cases of gastrointestinal reactions, 2 cases of allergic reactions, 5 cases of liver injury, 4 cases of leukopenia (reduced white blood cells), 1 case of gout, and 1 case of other conditions.
Qingfeng (2019)	FT+Bio	Bio	2 cases of gastrointestinal reactions, 3 cases of functional impairment, 2 cases of leukopenia (reduced white blood cells), 1 case of gout, and 1 case of other conditions.	3 cases of gastrointestinal reactions, 6 cases of functional impairment, 5 cases of leukopenia (reduced white blood cells), 2 cases of gout, and 1 case of other conditions.
Xian-hui and Shu-lin (2020)	FT+Bio	Bio	4 cases of gastrointestinal reactions, 1 case of allergic reaction, 5 cases of abnormal liver function, 4 cases of leukopenia, 2 cases of gout.	3 cases of gastrointestinal reactions, 3 cases of allergic reactions, 4 cases of abnormal liver function, 3 cases of leukopenia (reduced white blood cells), and 1 case of gout.
Lidong and Shuqing (2007)	JHL+Bio	Bio	1 case of mildly abnormal liver function, and 2 cases of gastrointestinal reactions.	Not reported.
Shuqin et al. (2008)	JHL+Bio	Bio	2 cases of mild liver function impairment.	Not reported.
Zhongming (2013)	JHL+Bio	Bio	1 case of gastrointestinal reaction, and 1 case of liver function impairment.	Not reported.
Guiqiu (2010)	JH+Bio	Bio	2 cases of gastrointestinal reactions, and 1 case of liver function impairment.	Not reported.
Dan et al. (2013)	JH+Bio	Bio	6 cases of adverse reactions.	7 cases of adverse reactions.

(Continued on following page)

10.3389/fphar.2025.1588586

TABLE 2 (*Continued*) Adverse reactions reported in the included randomized controlled trials.

Included in study	Interventions		Adverse reactions	
	T	C	T	C
Xuhua et al. (2013)	JH+Bio	Bio	4 cases of gastrointestinal reactions, 1 case of abnormal liver function, and 1 case of abnormal kidney function.	8 cases of gastrointestinal reactions, 5 cases of abnormal liver function, 1 case of abnormal kidney function, and 2 cases of rash.
Qianxin et al. (2014)	JH+Bio	Bio	6 cases of abnormal liver function.	19 cases of abnormal liver function.
Min-shuang et al. (2015)	JH+Bio	Bio	3 cases of gastrointestinal reactions.	5 cases of gastrointestinal reactions.
Yuxia (2015)	JH+Bio	Bio	1 case of abnormal liver function.	5 cases of abnormal liver function.
Junguo et al. (2016)	JH+Bio	Bio	1 case of abnormal liver function.	4 cases of abnormal liver function.
Yongyi et al. (2017)	JH+Bio	Bio	3 cases of abnormal liver function.	6 cases of abnormal liver function.
Xing et al. (2017)	JH+Bio	Bio	5 cases of adverse reactions.	8 cases of adverse reactions.
Liping (2018)	JH+Bio	Bio	1 case of abnormal liver function, 2 cases of gastrointestinal reactions, and 1 case of abnormal kidney function.	2 cases of abnormal liver function, 4 cases of gastrointestinal reactions, and 3 cases of abnormal kidney function.
Meng (2019)	JH+Bio	Bio	2 cases of gastrointestinal reactions, and 1 case of abnormal liver function.	4 cases of gastrointestinal reactions, 3 cases of abnormal liver function, and 3 cases of abnormal kidney function.
Guizhen (2019)	JH+Bio	Bio	3 cases of leukopenia (reduced white blood cells), 7 cases of gastrointestinal reactions, and 6 cases of liver function impairment.	10 cases of leukopenia (reduced white blood cells), 18 cases of gastrointestinal reactions, 16 cases of liver function impairment, and 6 cases of joint pain.
Bin (2020)	JH+Bio	Bio	2 cases of gastrointestinal reactions, and 1 case of joint pain.	2 cases of gastrointestinal reactions, 1 case of joint pain, and 1 case of abnormal liver and kidney function.
Qiang (2021)	JH+Bio	Bio	5 cases of abnormal liver function, 11 cases of gastrointestinal reactions, 5 cases of allergic reactions, 2 cases of vision impairment, and 3 cases of other reactions.	4 cases of abnormal liver function, 13 cases of gastrointestinal reactions, 4 cases of allergic reactions, 3 cases of vision impairment, and 2 cases of other reactions.
Qihuang (2022)	JH+Bio	Bio	5 cases of gastrointestinal reactions, and 1 case of neuritis.	2 cases of gastrointestinal reactions, and 1 case of neuritis.
Jiafu and Lanhua (2022)	JH+Bio	Bio	1 case of gastrointestinal reaction, and 1 case of headache.	3 cases of gastrointestinal reactions, and 2 cases of headaches.
Tao and Fei (2022)	JH+Bio	Bio	3 cases of abnormal liver function, 7 cases of gastrointestinal reactions, 3 cases of allergic reactions, and 1 case of vision impairment.	2 cases of abnormal liver function, 8 cases of gastrointestinal reactions, 3 cases of allergic reactions, and 2 cases of vision impairment.
Junguo (2023)	JH+Bio	Bio	2 cases of gastrointestinal issues, and 1 case of abnormal liver and kidney function.	3 cases of gastrointestinal issues, and 1 case of dizziness.
Yuxia (2023)	JH+Bio	Bio	5 cases of gastrointestinal reactions, 1 case of abnormal liver function, and 2 cases of peripheral neuritis.	5 cases of gastrointestinal reactions, 2 cases of abnormal liver function, 1 case of reduced vision, and 3 cases of peripheral neuritis.
Peiqian et al. (2024)	JH+Bio	Bio	2 cases of gastrointestinal reactions, 1 case of liver and kidney injury, 1 case of dizziness, and 1 case of rash.	2 cases of gastrointestinal reactions, and 1 case of rash.
Xinlei and Rong (2024)	JH+Bio	Bio	3 cases of gastrointestinal dysfunction, 1 case of liver function impairment, 1 case of neurological damage, and 2 cases of rash.	15 cases of gastrointestinal discomfort, 2 cases of liver function impairment, 3 cases of neurological damage, and 7 cases of rash.
Wulu et al. (2007)	JPRF+Bio	Bio	4 cases of mild liver function impairment, and 2 cases of gastrointestinal reactions.	A total of 5 cases including liver function impairment, gastrointestinal reactions, neurological symptoms, and leukopenia (reduced white blood cells).
Shouyue (2009)	JPRF+Bio	Bio	12 cases of adverse reactions.	69 cases of adverse reactions.

(Continued on following page)

10.3389/fphar.2025.1588586

TABLE 2 (*Continued*) Adverse reactions reported in the included randomized controlled trials.

Included in study	Interventions		Adverse reactions	
	T	C	T	C
Fuyuan and Meimingxing (2010)	JPRF+Bio	Bio	4 cases of mild liver function impairment, and 2 cases of gastrointestinal reactions.	4 cases of severe side effects, and 14 cases of mild side effects.
Bing and Yuanai (2011)	JPRF+Bio	Bio	1 case of allergic reaction, 7 cases of gastrointestinal reactions, 10 cases of abnormal liver function, and 1 case of abnormal urinalysis.	3 cases of allergic reactions, 23 cases of gastrointestinal reactions, 29 cases of abnormal liver function, and 4 cases of abnormal urinalysis.
Hunxi and Zhanqi (2013)	JPRF+Bio	Bio	9 cases of adverse reactions.	26 cases of adverse reactions.
Wei (2016)	JPRF+Bio	Bio	4 cases of adverse reactions.	11 cases of adverse reactions.
Chenyong et al. (2022)	JPRF+Bio	Bio	1 case of gastrointestinal reaction, 1 case of peripheral neuritis, and 1 case of rash.	2 cases of gastrointestinal reactions, 1 case of peripheral neuritis, 3 cases of rash, and 2 cases of abnormal liver function.
Wen-ge et al. (2013)	KF+Bio	Bio	5 cases of gastrointestinal reactions, 4 cases of abnormal liver function, and 2 cases of rash.	6 cases of gastrointestinal reactions, 4 cases of abnormal liver function, and 2 cases of rash.
Zhibo et al. (2019)	KF+Bio	Bio	10 cases of adverse reactions.	12 cases of adverse reactions.
Hai-xian et al. (2019)	KF+Bio	Bio	5 cases of elevated uric acid, 3 cases of liver function impairment, 3 cases of gastrointestinal reactions, and 1 case of knee joint pain.	3 cases of elevated uric acid, 4 cases of liver function impairment, 10 cases of gastrointestinal reactions, and 1 case of knee joint pain.
Guannan et al. (2020)	KF+Bio	Bio	9 cases of leukopenia (reduced white blood cells), 6 cases of gastrointestinal reactions, 6 cases of abnormal liver function, and 5 cases of elevated bilirubin levels.	8 cases of leukopenia (reduced white blood cells), 11 cases of gastrointestinal reactions, 6 cases of abnormal liver function, and 5 cases of elevated bilirubin levels.
Xuehu et al. (2022)	KF+Bio	Bio	4 cases of gastrointestinal reactions.	Not reported.
Xueyun (2022)	KF+Bio	Bio	1 case of allergic reaction, 1 case of liver injury, 1 case of gastrointestinal reaction, and 3 cases of gout.	2 cases of allergic reactions, 2 cases of liver injuries, 3 cases of gastrointestinal reactions, and 3 cases of gout.
Xiaohua (2022)	KF+Bio	Bio	1 case of gastrointestinal reaction, and 1 case of thrombocytopenia (reduced platelets).	4 cases of gastrointestinal reactions, 2 cases of leukopenia (reduced white blood cells), 2 cases of thrombocytopenia (reduced platelets), and 1 case of abnormal liver function.
Guannan et al. (2023)	KF+Bio	Bio	1 case of gastrointestinal reaction, 1 case of allergic reaction, 2 cases of liver injuries, 2 cases of leukopenia (reduced white blood cells), and 1 case of gout.	8 cases of gastrointestinal reactions, 3 cases of allergic reactions, 2 cases of liver injuries, 3 cases of leukopenia (reduced white blood cells), and 2 cases of gout.
Shiming et al. (2016)	QJLF+Bio	Bio	5 cases of abnormal liver function, 5 cases of gastrointestinal reactions, and 1 case of hypokalemia (low blood potassium).	4 cases of abnormal liver function, 4 cases of gastrointestinal reactions, 2 cases of dizziness, and 2 cases of tinnitus.
Juan et al. (2016)	QJLF+Bio	Bio	2 cases of gastrointestinal reactions, 10 cases of elevated uric acid, 2 cases of abnormal liver function, and 1 case of joint pain.	8 cases of elevated uric acid, and 3 cases of abnormal liver function.
Jun et al. (2017)	QJLF+Bio	Bio	2 cases of gastrointestinal reactions, 10 cases of elevated uric acid, 2 cases of abnormal liver function, and 1 case of joint pain.	8 cases of elevated uric acid, and 3 cases of abnormal liver function.
Junjie (2018)	QJLF+Bio	Bio	4 cases of elevated uric acid, 2 cases of abnormal liver function, and 3 cases of gastrointestinal reactions.	2 cases of elevated uric acid, 2 cases of abnormal liver function, and 2 cases of joint pain.
Xuewen (2007)	YFZK+Bio	Bio	8 cases of mild liver function impairment, and 5 cases of gastrointestinal reactions.	7 cases of mild liver function impairment, and 5 cases of gastrointestinal reactions.
Yujuan (2007)	YFZK+Bio	Bio	10 cases of adverse reactions.	12 cases of adverse reactions.
Xiuxia (2009)	YFZK+Bio	Bio	10 cases of gastrointestinal reactions, 8 cases of liver function impairment, and 5 cases of rash.	38 cases of gastrointestinal reactions, 16 cases of liver function impairment, and 4 cases of rash.

10.3389/fphar.2025.1588586

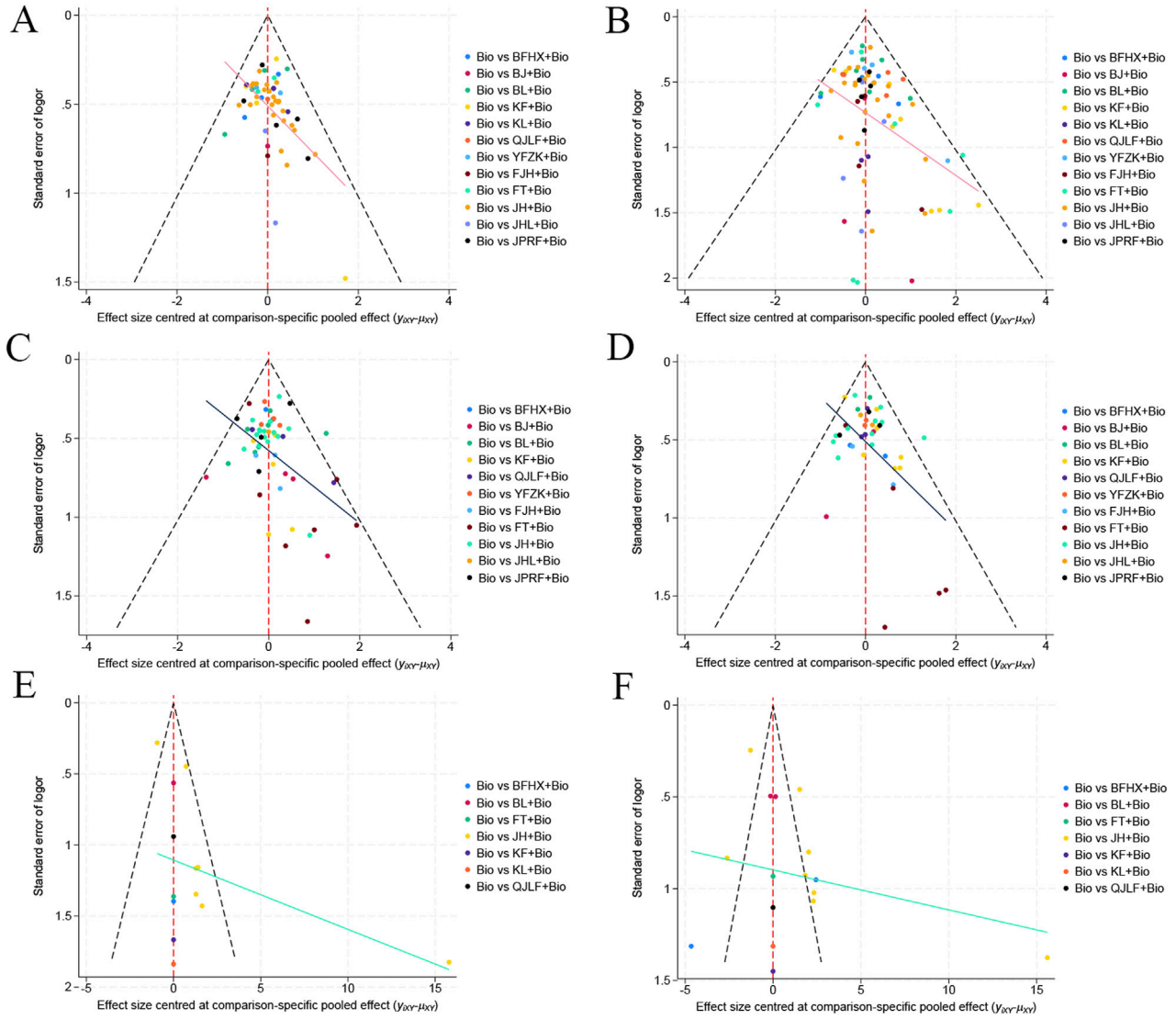


FIGURE 6
Comparison of various outcome indicators shown through adjusted funnel Plots: **(A)** Network evidence map of clinical efficacy rate; **(B)** Network evidence map of negative conversion rate; **(C)** Network evidence map of lesion absorption rate; **(D)** Network evidence map of cavity absorption rate; **(E)** Network evidence map of $CD3^+$ T lymphocyte improvement rate; **(F)** Network evidence map of $CD4^+$ T lymphocyte improvement rate.

significantly greater cavity absorption rate for combination of standard biomedicine with: FeiJieHe Pill (OR = 5.10, 95% CI [2.05, 12.65]), Fei Tai Capsule (OR = 4.55, 95% CI [2.26, 9.16]), Qi Jia Li Fei Capsule (OR = 2.73, 95% CI [1.77, 4.21]), Jie He Pill (OR = 2.44, 95% CI [1.89, 3.14]), Yi Fei Zhi Ke Capsule (OR = 2.22, 95% CI [1.23, 4.01]), Kangfuxin Liquid (OR = 2.12, 95% CI [1.52, 2.96]), Jian Pi Run Fei Pill (OR = 2.03, 95% CI [1.26, 3.28]), and Jie He Ling Tablet (OR = 1.88, 95% CI [1.07, 3.30]), all relative to biomedicine monotherapy. SUCRA ranking for cavity absorption rate established a probabilistic hierarchy wherein FeiJieHe Pill combined with standard biomedicine (SUCRA = 91.9%) showed the highest superiority probability, followed by Fei Tai Capsule (SUCRA = 91.1%), Qi Jia Li Fei Capsule (SUCRA = 69.9%), Jie He Pill (SUCRA = 62.7%), Yi Fei Zhi Ke Capsule (SUCRA = 53.5%), Kangfuxin Liquid (SUCRA = 51.1%), Jian Pi Run Fei Pill (SUCRA = 46.1%), Jie He Ling Tablet (SUCRA = 41.2%), Bu Fei Huo Xue Capsule (SUCRA = 40.5%), Bai Ling Capsule (SUCRA = 26.1%), Bu Jin Tablet (SUCRA = 22.4%), all benchmarked against standard biomedicine monotherapy (SUCRA = 3.4%). In summary, the combination of FeiJieHe Pill with standard biomedicine may be the best approach for improving cavity absorption rate, as visualized in Figures 4G,H.

3.5.5 $CD3^+$ T lymphocyte and $CD4^+$ T lymphocyte improvement rate

A total of 13 studies involving 1,519 participants across eight interventions, comprising seven types of oral TCMs, reported $CD3^+$ T lymphocyte improvement rates. The network meta-analysis revealed superior improvement rate of $CD3^+$ T lymphocytes for JieHe pill combined with conventional biomedicine (OR = 5.6, 95% CI [3.4, 7.8]) than monotherapy. Separately, 16 studies encompassing 2,057 participants under eight interventions

(including seven oral TCM types) documented $CD4^+$ T lymphocyte improvement rate. The network meta-analysis results show that the improvement rate of $CD4^+$ T lymphocytes was significantly enhanced outcomes for the combination of conventional biomedicine with JieHe pill (OR = 5.1, 95% CI [2.9, 7.3]), Bu Fei Huo Xue Capsule (OR = 4.7, 95% CI [0.1, 9.2]), and Bai Ling Capsule (OR = 4.5, 95% CI [0.2, 8.8]) compared to biomedicine monotherapy. SUCRA ranking for $CD3^+$ T lymphocyte improvement rate indicated the following hierarchy: the combination of standard biomedicine with Jie He Pill demonstrated superiority over Kangfuxin Liquid combination therapy (SUCRA = 67.6%), followed by Kangfuxin Liquid (SUCRA = 63.5%), Fei Tai Capsule (SUCRA = 60.7%), Qi Jia Li Fei Capsule (SUCRA = 59.2%), KangLao Pill (SUCRA = 53%), Bai Ling Capsule (SUCRA = 52.8%), standard biomedicine monotherapy (SUCRA = 22%), and Bu Fei Huo Xue Capsule (SUCRA = 21.3%), as shown in Figures 5A,B. For $CD4^+$ T lymphocyte improvement rate, the probability ranking positioned Jie He Pill combined with standard biomedicine (SUCRA = 66.5%) first, followed by Bu Fei Huo Xue Capsule (SUCRA = 60.4%), Bai Ling Capsule (SUCRA = 58.7%), Kangfuxin Liquid (SUCRA = 56.3%), KangLao Pill (SUCRA = 48.9%), Qi Jia Li Fei Capsule (SUCRA = 47.1%), and Fei Tai Capsule (SUCRA = 44.9%), each outperforming standard biomedicine monotherapy (SUCRA = 17.2%), as shown in Figures 5C,D.

3.6 Adverse reactions

Safety assessment across 61 encompassing 8,573 participants (4,496 in the experimental group and 4,077 in the control group) The majority of adverse reactions in both groups were related to the digestive system, characterized by mild, self-limiting manifestations. The experimental group reported 586 adverse reactions (approximate incidence 13%), compared with 1,022 adverse reactions (approximate incidence 25%) in controls. Since the types of adverse reactions reported in the included studies varied, only a descriptive analysis is provided here, as detailed in Table 2.

3.7 Publication bias assessment

This study conducted a publication bias assessment for the included literature and created a comparison-adjusted funnel plot. Due to the poor symmetry of the generated comparison-adjusted funnel plot using Egger's test, which demonstrated statistically significant publication bias for the following outcomes: clinical efficacy (P = 0.001), negative conversion rate (P < 0.001), lesion absorption (P = 0.004), cavity absorption (P = 0.001), $CD3^+$ T lymphocyte improvement rate (P = 0.049), and $CD4^+$ T lymphocyte improvement rate (P = 0.027), as visualized in Figure 6.

4 Discussion

Mycobacterium tuberculosis, a Gram-positive *bacillus* characterized by a unique lipid-rich, utilizes this structural feature for host survival and antimicrobial resistance (Gagneux, 2012). Following phagocytosis by alveolar macrophages during the initial infection, the bacterium replicates intracellularly due to their lipid membrane composition, thereby evading immune clearance (Pieters, 2008). In the pathological process of pulmonary tuberculosis, both the immune response and the direct toxic effects of the bacteria cause damage to lung tissue. Common tissue damage includes necrosis, fibrosis, and cavity formation. Although partial parenchymal repair may occur, persistent inflammation and fibrosis may lead to irreversible lung function impairment, ultimately affecting the quality of life among patients.

TCM classifies pulmonary tuberculosis as "lung tuberculosis", attributing its pathogenesis to dual mechanisms: deficiency of vital energy and invasion by the tuberculosis pathogen. The former refers to insufficient vital energy, while the latter refers to the invasion of the "tuberculosis insect", which damages the lung yin, leading to lung yin deficiency, and may progressively develop into both qi and yin deficiency. Progressive disease evolution may induce depletion of yin with yang transformation, potentially culminating in severe dual yin-yang deficiency without timely intervention (Cheng-Li et al., 2021). Therefore, TCM treatment for TB emphasizes both tonifying resistance and eliminating the pathogen: tonifying the body by strengthening the immune system, including methods like replenishing qi and blood, strengthening the spleen, and boosting energy; eliminating the pathogen involves targeting the removal of TB pathogens and their associated pathological changes, often using methods like nourishing the yin, moistening the lungs, generating body fluids, and detoxifying.

This study synthesizes 100 RCTs, including 12 types of oral TCMs, and analyzes six outcome indicators. Indirect comparisons among included oral TCMs suggest optimal therapeutic outcomes with combined oral TCM and standard biomedicine. The network meta-analysis indicates that the combination of FeiJieHe Pill with standard biomedicine shows strong effects in improving clinical efficacy and cavity absorption rates. FeiJieHe Pill contain threekey medicinal metabolites: Earthworm, *Bletilla striata*, and prepared *Polygonum multiflorum*. Modern pharmacological studies indicat the capacity of Earthworm to downregulate Bcl-2-associated X protein expression while upregulating B-cell lymphoma-2 protein expression, conferring a good immune-enhancing effect (Cheng-Li et al., 2021). *Bletilla striata* polysaccharides exhibit strong adhesion properties, forming a protective membrane on wound surfaces and adjusting the t-PA/PAI-1 ratio, restoring the balance of the coagulation system (Yuxuan et al., 2018; Jia, 2022). Prepared *Polygonum multiflorum*, a traditional tonic, demonstrates validated immunoenhancing activity in modern pharmacology (Ya et al., 2019; Donglin et al., 2021). In terms of improving negative conversion rates, KangLao Pill combined with standard biomedicine exhibited strong effects. KangLao Pill is primarily composed of two botanical drugs: Siegesbeckia orientalis and Morus root bark. Modern pharmacological studies reveal that the metabolites of Siegesbeckia orientalis (Chrysophanol I and II) exhibit strong inhibitory effects on*Mycobacterium tuberculosis* (Buhan et al., 1980), while Mulberry Root Bark Polysaccharides (PMA) are a unique plant polysaccharide that can regulate spleen lymphocytes in mice and enhance immune modulation (Kim et al., 2000). In parallel, Bu Jin Tablet combined with standard biomedicine exhibited optimal efficacy for lesion absorption rate

improvement. This formulation integrates traditional restorative agents: antler gelatin, silkworm, tortoise shell gelatin, red ginseng, polygonatum, Poria, and gecko, all traditional tonics. Modern pharmacological studies validate immune-enhancing or anti-aging effects of these botanical metabolites (Fang and Dao-Pei:, 2006; Xiue et al., 2014; Lili et al., 2018; Chen et al., 2020; Hongying et al., 2021; Ping et al., 2022). In terms of improving the improvement rate of $CD3^+$ T lymphocytes and $CD4^+$ T lymphocytes, the combination of Tuberculosis Pills with conventional biomedicine shows significant advantages. JieHe Pill incorporates three principalmetabolites: turtle shell, stem of hundred-leaf, and soft-shelled turtle shell. Modern pharmacological research has shown that turtle shell contains various active metabolites such as animal gelatin, collagen, protein, calcium, and phosphorus, which can enhance immunity through Th1 and Th2 cells modulation while exerting antibacterial and anti-inflammatory effects (Donglin et al., 2021). The stem of hundred-leaf contains multiple metabolites like stem alkaloids, proto-stem alkaloids, and deoxy-stem alkaloids, which can regulate anchor protein subtype 1 to relax smooth muscles, and have expectorant and antitussive effects (Chang et al., 2022). Soft-shelled turtle shell similarly contains animal gelatin, bone collagen, calcium, and phosphorus that can improve immunity, enhance hematopoietic function, and effectively reduce inflammation factor levels (Wenjia et al., 2023). Concerning adverse reactions, the addition of oral TCM to standard anti-TB drugs demonstrated no increased adverse reactions. On the contrary, among 60 studies reporting adverse reactions, the experimental group had fewer adverse reactions than the control group. However, the definitions and descriptions of adverse reactions varied among different studies, making quantitative evaluation difficult. Therefore, standardized reporting of adverse reactions to oral TCM is crucial for guiding clinical practice, assessing safety, and providing reliable decision-making support. Regarding publication bias, clinical efficacy, negative conversion rate, lesion absorption rate, cavity absorption rate, and $CD4^+$ T lymphocyte improvement rate all showed varying degrees of publication bias, potentially compromising the reliability of these findings.

This study has several limitations that should be acknowledged. First, the overall methodological quality of the included studies was moderate. None of the studies reported allocation concealment, and only one study employed a double-blind design while another used a single-blind design. The lack of blinding and allocation concealment may introduce selection bias and detection bias, thereby reducing the credibility of the results. Second, although all included CCPPs were labeled in the original studies as having adjuvant anti-tuberculosis effects, there is a lack of direct comparisons between different CCPPs. Consequently, the comparative results in this study are derived entirely from indirect evidence and should be interpreted with caution. Moreover, for immunological outcomes such as the improvement rates of $CD3^+$ and $CD4^+$ T lymphocytes, some intervention combinations demonstrated statistically significant effects; however, the wide confidence intervals suggest potential small-sample effects, which may undermine the stability of the findings. Third, most included studies did not report medication adherence or loss to follow-up, which may confound the assessment of treatment efficacy. Due to certain limitations inherent in studies on commercial Chinese polyherbal preparation, not all of the original publications provided detailed information on extraction processes or chemical fingerprinting. The available information was mainly obtained from drug package inserts or the Pharmacopoeia of the *Pharmacopoeia of the People's Republic of China* (Commission, 2020). Finally, there was inconsistency in the definition of "clinical efficacy rate" across studies, which may have introduced substantial heterogeneity in the pooled analysis and affected the robustness of the conclusions.

5 Conclusion

The integration of oral TCMs combined with standard biomedicine in the included studies demonstrated enhanced efficacy across at least one outcome measure. Among these regimens, FeiJieHe Pill combined with conventional biomedicine exhibits optimal efficacy for improving clinical efficacy and cavity absorption rate. JieHe Pill combined with conventional biomedicine similarly shows superior efficacy regarding the enhancement of the recovery rate of $CD3^+$ T lymphocytes and $CD4^+$ T lymphocytes. KangLao Pill combined with standard biomedicine achieves maximal improvement in negative conversion rates, while Bu Jin Tablet combined with standard biomedicine demonstrates the greatest effectiveness for lesion absorption rate improvement. The conclusions of this study also require verification through multi-center, large-sample, high-quality randomized controlled trials.

Author contributions

JJ: Conceptualization, Data curation, Formal Analysis, Investigation, Methodology, Visualization, Writing – original draft. SZ: Conceptualization, Methodology, Supervision, Writing – original draft. HW: Conceptualization, Data curation, Formal Analysis, Methodology, Supervision, Validation, Writing – original draft. LZ: Conceptualization, Data curation, Project administration, Software, Writing – review and editing. ZL: Funding acquisition, Supervision, Writing – review and editing. JT: Data curation, Formal Analysis, Methodology, Writing – review and editing. FW: Data curation, Funding acquisition, Methodology, Project administration, Supervision, Validation, Writing – review and editing.

Funding

The author(s) declare that financial support was received for the research and/or publication of this article. This work was supported by the National Natural Science Foundation of China (General Program, Grant No. 82374399); the Key Project of the Anhui Provincial Department of Education (Grant No. 2024AH050994); and the Hefei Comprehensive National Science Center, Institute of Health – Institute of Xin'an Medicine and Modernization of Traditional Chinese Medicine ("Jiebang Guashuai" Major Breakthrough Project, Grant No. 2023CXMMTCM005). No commercial funding was received. The funders had no role in study design, data collection and analysis, decision to publish, or preparation of the manuscript.

Conflict of interest

The authors declare that the research was conducted in the absence of any commercial or financial relationships that could be construed as a potential conflict of interest.

Generative AI statement

The author(s) declare that no Generative AI was used in the creation of this manuscript.

Any alternative text (alt text) provided alongside figures in this article has been generated by Frontiers with the support of artificial intelligence and reasonable efforts have been made to ensure accuracy, including review by the authors wherever possible. If you identify any issues, please contact us.

Publisher's note

All claims expressed in this article are solely those of the authors and do not necessarily represent those of their affiliated organizations, or those of the publisher, the editors and the reviewers. Any product that may be evaluated in this article, or claim that may be made by its manufacturer, is not guaranteed or endorsed by the publisher.

Supplementary material

The Supplementary Material for this article can be found online at: https://www.frontiersin.org/articles/10.3389/fphar.2025.1588586/full#supplementary-material

References

Bin, Z. (2020). Effect of jiehe pills on sputum negative conversion and levels of IFN-γ and IL-17 in initial treatment for patients with smear positive pulmonary tuberculosis. *New Chin. Med.* 52. doi:10.13457/j.cnki.jncm.2020.11.016

Bing, Z., and Yuanai, Z. (2011). Integrated traditional Chinese and Western medicine therapy for the treatment of 200 cases with recurrent sputum-positive pulmonary tuberculosis: a clinical study. *Guangming J. Chin. Med.* 26.

Buhan, H., Wenshen, C., and Yan, H. (1980). Study on the effective components of Ardisia japonica for antituberculosis activity. *Chin. Pharm. J.* 39.

Chang, L., Yanli, M., Shuang, L., Xiaoxi, W., Bo, W., Xin, W., et al. (2022). Effect of baibu (Radix Stemonae) on expression of cough factor TRPA1 in mice infected with Mycoplasma Pneumoniae. *Chin. Archives Traditional Chin. Med.* 40, 107-110+283–284.

Chen, Z., Liu, J., Kong, X., and Li, H. (2020). Characterization and immunological activities of polysaccharides from Polygonatum sibiricum. *Biol. Pharm. Bull.* 43, 959–967. doi:10.1248/bpb.b19-00978

Cheng-Li, B., Man-Jiao, F., Yan-Ke, L., Ke, Y., Li, Y., Li, Z., et al. (2021). Effect of Chinese medicine treatment on improving cellular immune status of patients with refractory extensive-drug-resistant tuberculosis. *J. Guangzhou Univ. Traditional Chin. Med.* 38, 1107–1112. doi:10.13359/j.cnki.gzxbtcm.2021.06.006

Chenyong, W., Xiaojiao, P., Zhiwei, Y., Lihong, Z., Yanbing, H., and Yanling, C. (2022). Efficacy of Jianpi Runfei pills combined with conventional antituberculosis drugs in the treatment of pediatric pulmonary tuberculosis and its impact on lung function. *Mod. J. Integr. Traditional Chin. West. Med.* 31.

Chuanjun, X., Puxuan, L., Yuling, H., Li, C., and Fang, W. (2023). Expert consensus on imaging diagnosis of drug-resistant pulmonary tuberculosis. *Electron. J. Emerg. Infect. Dis.* 8, 63–74. doi:10.19871/j.cnki.xfcrbzz.2023.05.013

Cochrane Collaboration, (2020). *Review Manager (RevMan), Version 5.4*. London, United Kingdom: Cochrane Collaboration.

Commission, C. P. (2020). *Pharmacopoeia of the People's Republic of China (Volume IV)*. Beijing: China Medical Science and Technology Press.

Dan, L., De-Bing, D., Chun-Qiao, X., Yuzhu, C., Zhijie, C., and Zhu, J. (2013). Clinical efficacy of Jie-he-wan as adjunctive therapy for with the MDR-TB and their effects on immunological functions. *China J. Mod. Med.* 23, 70–74.

Di, B., Yu, W., and Jing, A. (2019). Clinical effect analysis of Feijihe pills in adjuvant treatment of cavitary pulmonary tuberculosis. *China Pract. Med.* 14, 94–95. doi:10.14163/j.cnki.11-5547/r.2019.26.053

Donghua, L., and Ganhong, H. (2005). Curative effects of bailing capsule combined with antituberculotic on pulmonary tuberculosis: a report of 62 cases. *Chin. J. General Pract.* 3 (520), 474. doi:10.3969/j.issn.1674-4152.2005.06.027

Donglin, G., Ying, W., Jianbo, Y., Qi, W., Yue, L., Hongyu, J., et al. (2021). On the progress of the extraction, separation and structural analysis of polysaccharides from Polygonum multiflorum. *Chin. Pharm. Aff.* 35, 1166–1172. doi:10.16153/j.1002-7777.2021.10.012

Fang, L., and Dao-Pei, L. (2006). Preparation of placental-eluted gamma globulin and its immunosuppressive effect in vitro and in vivo. *J. Exp. Hematol.*, 529–534.

Fengyan, S. (2012). Clinical study of integrated traditional Chinese and Western medicine therapy for the treatment of multidrug-resistant pulmonary tuberculosis. *World Health Dig.* 9, 185–186. doi:10.3969/j.issn.1672-5085.2012.04.145

Fuyuan, C., and Meimingxing (2010). The effect observation of Jianpi Runfei pill adjuvant therapy of old patients with pulmonary tuberculosis in 90 cases. *Guide China Med.* 8. doi:10.15912/j.cnki.gocm.2010.21.022

Gagneux, S. (2012). Host-pathogen coevolution in human tuberculosis. *Philos. Trans. R. Soc. Lond B Biol. Sci.* 367, 850–859. doi:10.1098/rstb.2011.0316

Ge, K. (2019). Shi Yao Shen Shu. Fuzhou, China: Fujian Science and Technology Publishing House Co., Ltd.

Ge, Y., Ye, Y., Ying, X., and Qi, N. (2009). Curative efficacy on pulmonary tuberculosis with combined bailing capsule and anti-tuberculosis drug treatment: a 123 cases analysis. *China Mod. Dr.* 35–39.

Guannan, K., Lili, H., Qingyan, M., Shujun, G., Xiaofei, L., and Ping, D. (2020). Clinical study on the effect of Kangfuxin Liquid combined with second-line drugs on elder multidrug-resistant tuberculosis patients. *J. Xinjiang Med. Univ.*, 43.

Guannan, K., Lili, H., Xiaofei, L., Ping, D., Tao, S., and Yanqing, M. (2023). Effect of Kangfuxin liquid combined with standard chemotherapy scheme in the treatment of pulmonary tuberculosis and its effect on serum α1-acid glycoprotein and haptoglobin levels. *China Med.* 18.

Guiqiu, S. (2010). Efficacy observation of tuberculosis pills in the treatment of 36 cases with recurrent pulmonary tuberculosis. *China Health Care Nutrition* 19 (6), 2.

Guizhen, W. (2019). Efficacy observation of tuberculosis pills combined with antituberculosis chemotherapy in the treatment of pulmonary tuberculosis. *Chin. J. Conval. Med.* 28.

Guofang, D., and Xiwei, L. (2020). Expert consensus on a standard of activity judgment of pulmonary tuberculosis and its clinical implementation. *Chin. J. Antituberc.* 42, 301–307.

Hai-Xian, Q., Qi-Wen, H., Mei-Jin, H., Qinglan, P., and Fenlian, D. (2019). The curative effect of Kangfuxin liquid on cavitary pulmonary tuberculosis. *Trait Pharm. J.* 31.

Higgins, J. P. T., Thomas, J., Chandler, J., Cumpston, M., Li, T., Page, M. J., and Welch, V. A. (2023). *Cochrane handbook for systematic reviews of interventions*. London, United Kingdom: Cochrane.

Hongying, J., Su, W., Xiaochen, S., and Yanyan, Z. (2021). Research Progress Regarding Aging Mechanism and Anti-aging of Di huang Yin zi. *Liaoning J. Traditional Chin. Med.* 48, 248–252.

Hu, X., Wang, K., Liang, R. X., Cao, Y., Zhou, X. L., Zhao, Y., et al. (2023). Clinical observation of Bufei Huoxue Capsule combined with chemotherapy in treatment of rifampicin-susceptible retreated pulmonary tuberculosis (yin and yang deficiency type) and analysis of prognostic factors. *Chin. Tradit. Herb. Drugs* 54, 4245–4252.

Hualiang, L. (2013). Clinical observation of feitai capsules as an adjunctive therapy for recurrent pulmonary tuberculosis. *J. Emerg. Traditional Chin. Med.* 22, 954–964.

Hui, S., Jie, C., Yangbing, O., Yongrui, Y., Chichuan, L., Xin, L., et al. (2020). Efficacy of Bailing capsule combined with levofloxacin in the treatment of multidrug-resistant tuberculosis. *Med. J. West China* 32.

Hunxi, L., and Zhanqi, X. (2013). Clinical observation of Jianpi Runfei pills combined with Western medicine in the treatment of 100 cases of pulmonary tuberculosis. *Inn. Mong. J. Traditional Chin. Med.* 32.

Ji, W., Yan, Z., Jianfang, Z., and Malong, F. (2017). Efficacy observation of feitai capsules combined with 2HRZE/4HR chemotherapy in the treatment of initial sputum-positive pulmonary tuberculosis patients. *China Prev. Med. J.* 29.

Jia, L. (2022). Clinical efficacy observation of Chinese herbal tuberculosis pills as an adjunctive treatment for severe tuberculosis cases. *Chin. Sci. Technol. J. Database* (8), 3.

Jiafu, Q., and Lanhua, Z. (2022). Clinical analysis of tuberculosis pill combined with linezolid in the treatment of multi-drug resistant tuberculosis. *Clin. Med. Eng.* 29, 477–478.

Jian, W. (2002). Observation of the efficacy of a treatment regimen including bujin tablets for multidrug-resistant pulmonary tuberculosis. *Chin. Youjiang Med. J.* 30, 423. doi:10.3969/j.issn.1003-1383.2002.05.035

Jian, Z., and Li, L. (2014). Efficacy observation of Chinese herbal tuberculosis pills as an adjunctive therapy for elderly patients with pulmonary tuberculosis. *J. Clin. Pulm. Med.* 19, 366–368.

Jinghua, D., Jianchun, L., Xiaoju, W., and Aiming, W. (2015). Effect of Kanglao pill combined with Anti- tuberculosis Western medicine on Th17 cells and regulatory T cells balanced state of tuberculosis patients. *Chin. J. Traditional Med. Sci. Technol.* 22 (4), 371–372.

Juan, W. (2022). Clinical efficacy observation of tuberculosis pills as an adjunctive treatment for secondary pulmonary tuberculosis. *Chin. Sci. Technol. J. Database*.

Juan, W., Ru, G., Jing, W., and Qingfeng, W. (2016). Observation on the clinical efficacy of the Qijialifeiljiaonang for the retreatment pulmonary tuberculosis. *Chin. J. Antituberc*.

Jun, Z. (2010). Efficacy observation of chemotherapy combined with bujin tablets in the treatment of pulmonary tuberculosis. *Natl. Med. Front. China*.

Jun, W., Ru, G., Jing, W., and Qingfeng, W. (2017). Observation on the clinical efficacy of the QIJIALIFELJIAONANG for the re treatment pulmonary tuberculosis. *Chin. J. Antituberc*.

Jun, X., Yu-Tao, H., Xin, Y., Wei, X., Bingqi, Z., and Mengjiao, H. (2022). Pharmacological activity of traditional Chinese medicine Baiji and its application in new wound dressing. *Hainan Med. J.* 33, 371–373.

Junguo, Y. (2023). Clinical efficacy analysis of tuberculosis pills combined with antituberculosis drugs in the treatment of pulmonary tuberculosis. *Chin. Sci. Technol. J. Database*.

Junguo, Z., Liping, W., and Yan, S. (2016). Jiehewan adjuvant treatment of tuberculosis. *Jilin J. Chin. Med.* 36 (8), 790–792.

Junjie, W. (2018). Observation of the use of Qijia Lipei capsules as an adjunctive treatment for recurrent pulmonary tuberculosis. *J. Mod. Clin. Med.* 44.

Junmei, N., Zhengkui, L., and Bianfang, Z. (2019). Clinical efficacy of Bufei Huoxue capsules combined with 2HRZE/4HR regimen in treatment of pulmonary tuberculosis. *Med. J. Chin. People's Health* 31, 116–118.

Kai, L. (2009). Clinical observation of Yifei Zhike capsules as an adjunctive therapy for recurrent sputum-positive pulmonary tuberculosis. *Guide China Med.* 7, 70–71.

Kim, H. M., Han, S. B., Lee, K. H., Lee, C. W., Kim, C. Y., Lee, E. J., et al. (2000). Immunomodulating activity of a polysaccharide isolated from Mori Cortex Radicis. *Arch. Pharm. Res.* 23, 240–242. doi:10.1007/BF02976452

Lidong, F., and Shuqing, F. (2007). Efficacy observation of tuberculosis spirit tablets as an adjunctive therapy for sputum-positive pulmonary tuberculosis in initial treatment cases. *Chin. J. Prim. Med. Pharm.* 14.

Lidong, F., Lilei, F., and Ling, G. (2013). Observation on clinical efficacy of tuberculosis pills adjuvant therapy on retreatment smear positive pulmonary tuberculosis. *J. Med. Pest Control* 29, 570–571.

Lili, W., Bei, Z., Hao, C., Liting, F., and Jingui, H. (2018). Effects of different extract of Gekko gecko Linnaeus on immune function of aging model mice. *Chin. J. Geriatric Care* 16, 17–20.

Lingwei, L. (2018). Clinical efficacy observation of tuberculosis pills as an adjunctive treatment for multidrug-resistant pulmonary tuberculosis. *Electron. J. Clin. Med. Literature* 5, 167–168. doi:10.16281/j.cnki.jocml.2018.03.093

Liping, J. (2018). Efficacy observation of tuberculosis pills as an adjunctive treatment for newly diagnosed sputum-positive pulmonary tuberculosis patients. *J. Pract. Traditional Chin. Med.* 34.

Liping, W., and Chun, J. (2016). Clinical study on the Feitai capsule in the adjunctive treatment of new smear positive pulmonary tuberculosis. *Chinese Community Doctors* 32, 98–99.

Liuxing, S. (2005). Clinical efficacy observation of integrated traditional Chinese and Western medicine therapy for recurrent pulmonary tuberculosis: a study of 128 cases. *Henan Tradit. Chin. Med.*, 63–64. doi:10.16367/j.issn.1003-5028.2005.10.049

Long, J., Weihua, H., Mingxia, G., Xiuying, Z., and Lihua, W. (2014). Clinical observation of Qijia Lipei capsules as an adjunctive therapy for refractory pulmonary tuberculosis in traditional Chinese medicine. *J. Clin. Med. Pract.* 18.

Meng, L. (2019). Efficacy of Chinese herbal tuberculosis pills as an adjunctive treatment for newly diagnosed sputum-positive pulmonary tuberculosis patients. *Chin. J. Mod. Drug Appl.* 13.

Mengqiu, G., Lizhen, Z., Songlin, Y., Qingfeng, Z., Qing, Z., Ji, Y., et al. (2006). Observation of recent efficacy and safety of lung-tai capsules as an adjunctive therapy for recurrent pulmonary tuberculosis in a Chinese herbal medicine context. *Chin. J. Tuberc. Respir. Dis.* 29.

Min-Shuang, S., Chun-Xia, W., Hui, X., and Guomei, W. (2015). Clinical observation of Moxifloxacin combined with Jiehe pill in the treatment of multidrug-resistant tuberculosis. *China Pharm.* 26, 5092–5094.

Ming, L. (2004). Clinical observation of integrated traditional Chinese and Western medicine treatment for pulmonary tuberculosis in 50 cases. *Chin. J. Coal Industry Med.* 1231.

Peiqian, C., Zhigang, W., and Miaomiao, T. (2024). Clinical study on Jiehe pills combined with routine Western medicine for drug-resistant tuberculosis of yin deficiency resulting in vigorous fire type. *New Chin. Med.* 56, 61–65. doi:10.13457/j.cnki.jncm.2024.09.013

Pieters, J. (2008). Mycobacterium tuberculosis and the macrophage: maintaining a balance. *Cell Host Microbe* 3, 399–407. doi:10.1016/j.chom.2008.05.006

Ping, W., Yukun, W., Shangming, W., Tianming, Y., Daikui, Y., Liangliang, L., et al. (2022). Ffects of Poria polysaccharides on immune function in rats. *Shandong J. Animal Sci. Veterinary Med.* 43, 11–14+17.

Pu, W., Yongai, L., Xicheng, H., and Yun, Q. (2005). Combined use of Feitai capsule and antituberculosis agents in initial treatment of pulmonary tuberculosis. *J. Chongqing Med. Univ.*, 881–883.

Prasad, R., Singh, A., and Gupta, N. (2019). Adverse drug reactions in tuberculosis and management. *Indian J. Tuberc.* 66, 520–532. doi:10.1016/j.ijtb.2019.11.005

Qi, N., Lixuan, T., Ye, Y., Jin, Z., Yuhuan, D., and Zhidan, X. (2016). Clinical study of bailing capsules as an adjunctive treatment for first-time relapsed sputum-positive pulmonary tuberculosis patients. *Chin. J. Antituberc.* 38, 61–63.

Qi, Z. (2016). Efficacy observation of tuberculosis pills combined with western medicine in the treatment of multidrug-resistant pulmonary tuberculosis. *Shaanxi J. Tradit. Chin. Med.* 37, 434–435.

Qiang, L. (2021). Clinical study of tuberculosis pills combined with antituberculosis chemotherapy drugs in the treatment of initial sputum-positive pulmonary tuberculosis. *Harbin Med. J.* 41, 42–43.

Qianxin, W., Yuxian, Y., Jianhong, S., Chengxing, J., and Yangxing, J. (2014). Short-term efficacy observation of tuberculosis pills combined with chemotherapy in the initial treatment of sputum-positive cavitary pulmonary tuberculosis. *New Chin. Med.* 46, 52–53. doi:10.13457/j.cnki.jncm.2014.12.024

Qiaoe, X., Yongqiang, L., Man, Y., and Wenjun, Y. (2023). Clinical efficacy observation of tuberculosis pills combined with antituberculosis drugs in the treatment of recurrent refractory tuberculosis cases. *J. North Pharm.* 20, 43–45.

Qihuang, C. (2022). Exploration of the efficacy and value of integrated traditional Chinese and Western medicine treatment methods applied to pulmonary tuberculosis patients. *J. North Pharm.* 19.

Qin, X. (2019). Feitai capsule combined with linezolid in the treatment of extensively drug-resistant tuberculosis. *Shaanxi J. Tradit. Chin. Med.* 40, 469–471.

Qing, L., and Wengfang, G. (2014). Efficacy observation of feijie pills as an adjunctive therapy for initial treatment of sputum-positive pulmonary tuberculosis. *Chin. Med. J. Metallurgical Industry* 31, 620.

Qingfeng, Z. (2019). Clinical observation of antituberculosis pills as an adjunctive treatment for pulmonary tuberculosis. *J. Pract. Traditional Chin. Med.* 35, 1494–1495.

Qiong, H., Xiaodong, G., Xiaoqin, L., Haitao, H., Jianghong, L., Shijun, M., et al. (2021). Observation on clinical effects of tuberculosis pills combined with antituberculosis drugs in the treatment of recurrent refractory tuberculosis. *West. J. Traditional Chin. Med.* 34, 110–114.

Radiology, C. S. O. I. D. O. C. S. O. (2018). The expert consensus on imaging and grading diagnosis of tuberculosis. *Electron. J. Emerg. Infect. Dis.* 3, 118–127. doi:10.19871/j.cnki.xfcrbzz.2018.02.015

Rücker, G., and Schwarzer, G. (2015). Ranking treatments in frequentist network meta-analysis works without resampling methods. *BMC Med. Res. Methodol.* 15, 58. doi:10.1186/s12874-015-0060-8

Rücker, G. K. U., König, J., and Schwarzer, G. (2024). Netmeta: network meta-analysis using Frequentist methods. R. package version 2.0-1.

Salanti, G., Ades, A. E., and Ioannidis, J. P. (2011). Graphical methods and numerical summaries for presenting results from multiple-treatment meta-analysis: an overview and tutorial. *J. Clin. Epidemiol.* 64, 163–171. doi:10.1016/j.jclinepi.2010.03.016

Shah, I., Poojari, V., and Meshram, H. (2020). Multi-drug resistant and extensively-drug resistant tuberculosis. *Indian J. Pediatr.* 87, 833–839. doi:10.1007/s12098-020-03230-1

Shiming, L., Peng, Z., and Shuxiang, G. (2016). Clinical observation of Qijia-lifei capsule on the treatment of multi-drug resistant tuberculosis. *Hebei J. Traditional Chin. Med.* 38, 1240–1243.

Shiqi, W. (2011). Clinical efficacy of tuberculosis pills as an adjunctive therapy to antituberculosis drugs in treating 30 cases of pulmonary tuberculosis in the elderly. *Chin. J. Gerontology* 31, 698–699.

Shouyue, J. (2009). Clinical analysis of integrated traditional Chinese and Western medicine therapy for recurrent sputum-positive pulmonary tuberculosis. *Chin. J. Clin. Res.* 22, 483–484.

Shuang, Z. (2016). Evaluation on the effectiveness and safety of jiehelining tablets combined with chemotherapy in the treatment of primary smear-positive pulmonary tuberculosis. *Chin. Med. Mod. Distance Educ. China* 14 (21), 75–76.

Shuangli, Z., Meng, L., Hui, S., Jie, C., Xin, L., Chichuan, L., et al. (2020). Clinical efficacy of bailing capsule combined with Levofloxacin on multidrug-resistant tuberculosis. *Pharmacol. Clin. Chin. Materia Medica* 36, 223–226. doi:10.13412/j.cnki.zyyl.2020.03.034

Shuhua, G., and Fujian, Y. (2016). Efficacy observation of bailing capsules as an adjunctive treatment for pulmonary tuberculosis in 60 cases. *Hejiang J. Traditional Chin. Med.*

Shuqin, F., Lidong, F., and Lilei, F. (2008). Effect of combination of Jieheling and phthisical on retreated positive bacteria pulmonary tuberculosis. *Hebei J. Tradit. Chin. Med.* 30, 1085–1086.

StataCorp (2023). *Stata statistical software: release 18*. College Station, TX: StataCorp LLC.

R Core Team (2024). *R: a language and environment for statistical computing*. Vienna, Austria: R Foundation for Statistical Computing.

Tao, Y., and Fei, W. (2022). Clinical effect of tuberculosis pill combined with four anti-tuberculosis chemotherapy drugs in the treatment of pathogenic positive pulmonary tuberculosis. *Chin. J. Hemorheol.* 32, 83–85.

Tianfeng, S. (2015). Clinical report on the efficacy of bufeihuoxue capsules combined with conventional Western medicine in the treatment of drug-resistant pulmonary tuberculosis. *For all Health* 9, 91–92.

Wei, W. (2016). Clinical study on the efficacy of Jianpi Runfei pills combined with Western medicine in the treatment of pulmonary tuberculosis. *World Latest Med. Inf.* 16, 185+191.

Wei, S., and Liuyuhon (2024). Interpretation of WHO global tuberculosis report2023. *J. Tuberc. Lung Dis.* 5, 15–19. doi:10.19983/j.issn.2096-8493.2024006

Wei, Y., Hong-Wen, L., and Zhen-Jing, S. (2004). Yifeizhike capsules in treating secondarybacteria-discharging pulmonary tuberculosis. *J. Shandong Med. Coll.* 26.

Wei, X. L., Yin, J., Zou, G. Y., Zhang, Z. T., Walley, J., Harwell, J., et al. (2015). Treatment interruption and directly observed treatment of multidrug-resistant tuberculosis patients in China. *Int. J. Tuberc. Lung Dis.* 19, 413–419. doi:10.5588/ijtld.14.0485

Wei-Wei, L. (2021). Effects of adjuvant therapy with tuberculous pill on immune function and cytokines in elderly patients with pulmonary tuberculosis. *Shenzhen J. Integr. Traditional Chin. West. Med.* 31.

Weiyong, W., Hua, C., Jianhong, H., and Pingru, C. (2020). Clinical observation of antituberculosis pills combined with moxifloxacin in the treatment of pulmonary tuberculosis. *China Pract. Med.* 15, 131–133. doi:10.14163/j.cnki.11-5547/r.2020.03.063

Wen-Ge, H., Xiang-Yu, Y., Jing, W., and Lingling, Y. (2013). Clinical research on the efect of Kangfuxin liquid in the retreatment of bacteria positive pulmonary tuberculosis. *West China Med. J.*

Wenjia, L., Zongkai, L., Xiaosu, C., and Zhaidong, L. (2023). Network pharmacology-based discussion on molecular mechanism of "Different Treatment of the Same Disease" in the treatment of cancerous fever by Qinghao Bijia Tang and Buzhong Yiqi Tang. *West. J. Traditional Chin. Med.* 36, 20–26.

Wulu, L., Anqi, T., Genquan, Q., Li, L., and Changsheng, Z. (2007). Clinical study of Jianpi Runfei pills as an adjunctive therapy in short-course chemotherapy for tuberculosis. *Chin. J. Antituberc.*, 86–87.

Xiali, Z., Zhihong, D., and Shixiong, H. (2017). Risk factors of patients with drug resistant tuberculosis in Shaoyang, Hunan, 2014-2015. *China Trop. Med.* 17, 236–240. doi:10.13604/j.cnki.46-1064/r.2017.03.06

Xian, W. (2009). Clinical observation of integrated traditional Chinese and Western medicine therapy for pulmonary tuberculosis: a study of 30 cases. *Inf. Traditional Chin. Med.* 26, 51–52.

Xian-Hui, W., and Shu-Lin, Y. (2020). Clinical effect of Feitai Capsules combined with Western antituberculosis drug in the treatment of preliminary smear-positive pulmonary tuberculosis. *China Mod. Med.* 27, 137–140.

Xiang, L. (2015). Brief analysis of the clinical effectiveness of integrated traditional chinese and western medicine therapy in the treatment of 50 cases of tuberculosis. *Guide Chin. Med.* 13, 191.

Xiaohua, W. (2022). Efficacy observation of Kangfuxin liquid combined with the 2HRZE/4HR chemotherapy regimen in the treatment of initially treated sputum-positive pulmonary tuberculosis patients. *Jiangxi Med. J.* 57.

Xiaoni, Z. (2018). Clinical efficacy analysis of antituberculosis pills combined with moxifloxacin in the treatment of pulmonary tuberculosis. *World Latest Med. Inf.* 18, 99+102. doi:10.19613/j.cnki.1671-3141.2018.59.065

Xiaoru, W., Zhongping, W., Yunfei, H., Yi, X., and Wanfeng, T. (2018). Efficacy observation of Kangfuxin liquid as an adjunctive treatment for sputum-positive pulmonary tuberculosis. *Chin. J. Rural Med. Pharm.* 25.

Xing, L., Bing, O., Yan-Duo, L., Yalian, S., Changying, H., Lu, W., et al. (2017). Clinical efficacy of Jiehe pills combined with Levofloxacin such as anti-tuberculosis drugs in tuberculosis patients with multi-drug resistance. *Anti-Infection Pharm.* 14.

Xinhua, Z. (2012). Study on the efficacy of Feijie pill in the treatment of pulmonary tuberculosis and its effects on symptom improvement. *Contemp. Med. Symp.* 10, 704–705.

Xinlei, J., and Rong, S. (2024). The efficacy of tuberculosis pill adjuvant to conventional quadruple anti-tuberculosis therapy in the treatment of secondary pulmonary tuberculosis. *Chin. J. Med. Guide* 26, 804–807.

Xiue, X., Mingying, L., Xia, W., Zhenxuan, W., and Haozen, S. (2014). Efficacy and safety of Qijialifei capsule in adjuvant chemotherapy for retreatment pulmonary tuberculosis. *Chin. J. Antituberc.* 36 (11), 948–952.

Xiuxia, W. (2009). Clinical evaluation on the therapeutic effect of Yifeizhike capsules on drug resistant pulmonary tuberculosis. *China Mod. Med.* 16, 25–27.

Xuehu, D., Fei, D., and Xincan, C. (2022). Clinical study of Kangfuxin solution on treating initial smear positive tuberculosis patients. *J. Binzhou Med. Univ.* 45.

Xuewen, C. (2007). Clinical research on the curative effects of yifeizhike capsule on secondary bacteria-discharge pulmonary tuberculosis. *Hebei Med.*, 1268–1270.

Xueyun, T. (2022). Efficacy of Kangfuxin liquid combined with the 2HRZE/4HR regimen in the treatment of initially treated sputum-positive cavitary pulmonary tuberculosis patients with hemoptysis. *Med. Equip.* 35.

Xu, H., Yaomin, S., and Baochun, X. (2018). Clinical observation on 82 cases of initial pulmonary tuberculosis by adjuvant treatment of bufei huoxue capsule. *J. Tradit. Chin. Med.* 59, 1671–1673+1684.

Xuhua, W., Xiaobing, Z., and Qiang, X. (2013). Clinical observation of the treatment of relapsed sputum-positive pulmonary tuberculosis patients with Chinese herbal tuberculosis pills. *For All Health* 7, 27–28.

Ya, W., Li-Na, Y., Tian-Tian, S., Jiejie, H., Jia, L., Minghua, H., et al. (2019). Structural characterization of polysaccharide from Polygonum multiflorum and its immunomodulatory activity. *Chin. Traditional Herb. Drugs* 50, 2290–2295.

Yan, H., Xiangrong, Z., and Yi, L. (2022). Clinical efficacy of tuberculosis pill combined with standard chemotherapy for tuberculosis and its effect on IgG, IgA and IgM. *Chin. Arch. Tradit. Chin. Med.* 40, 255–258.

Yan, Z., Qianhong, W., Fan, W., Fengying, J., Zhen, Q., Yingxi, M., et al. (2023). Evaluation of the curative effect of the combination of traditional Chinese and Western medicine on retreated pulmonary tuberculosis. *Anhui Med. Pharm. J.* 27, 615–619.

Yanpei, Z., and Shuyu, G. (2002). Efficacy observation of bailing capsules as an adjuvant treatment for pulmonary tuberculosis in the elderly. *Zhejiang Clin. Med. J.* 4, 603–604. doi:10.3969/j.issn.1008-7664.2002.08.035

Yawei, C., Baocang, Z., Cunli, W., and Fenglu, C. (2023). Observation on efficacy of Bufei Huoxue capsules combined with anti-tuberculosis drugs in treatment of pulmonary tuberculosis. *Liaoning J. Traditional Chin. Med.* 50.

Yongyi, C., Yunhe, R., and Fen, D. (2017). Randomized parallel controlled study on the treatment of initial smear positive pulmonary tuberculosis with 2HRZE/4HR combined with tuberculosis. *J. Pract. Traditional Chin. Intern. Med.* 31, 52–54. doi:10.13729/j.issn.1671-7813.2017.07.20

Yuelian, T. (2024). Clinical efficacy of tuberculosis pills combined with conventional Western medicine in the treatment of recurrent pulmonary tuberculosis with Qi-Yin deficiency syndrome. *Chin. J. Clin. Ration. Drug Use* 17, 50–53. doi:10.15887/j.cnki.13-1389/r.2024.31.014

Yujuan, T. (2007). Clinical efficacy observation of Yifei Zhike capsules as an adjunctive therapy for multidrug-resistant pulmonary tuberculosis. *World Health Dig.* 4.

Yunxiao, W., and Guosheng, Y. (2015). Clinical efficacy observation of bujin tablets as an adjunctive treatment for initial sputum-positive pulmonary tuberculosis. *Chin. J. Clin. Ration. Drug Use* 8, 39–41. doi:10.15887/j.cnki.13-1389/r.2015.32.023

Yuxia, Z. (2015). Analysis of the efficacy of using Chinese herbal tuberculosis pills as an adjunctive treatment for newly diagnosed sputum-positive pulmonary tuberculosis patients. *Contemp. Med. Symp.*

Yuxia, Z. (2023). Clinical efficacy of tuberculosis pills combined with chemotherapy in the treatment of recurrent and refractory tuberculosis cases. *Renowned Dr.*, 171–173.

Yuxuan, L., He, XIAOMEI, Fucheng, Z., Fangli, G., Xingbang, H., and Yuhan, L. (2018). Research progress on the main bioactive compounds and pharmacological effects of Bletilla striata. *Hunan Agric. Sci.*, 107–109. doi:10.16498/j.cnki.hnnykx.2018.003.028

Zhenru, W. (2016). Efficacy of tuberculosis pills as an adjunctive therapy for multidrug-resistant pulmonary tuberculosis and its impact on immune function. *China Pract. Med.*

Zhibo, C., Pianpian, T., and Bohua, W. (2019). Clinical efficacy of Kangfuxin Liquid combined with standard chemotherapy regimen in the treatment of cavitary pulmonary tuberculosis complicated with hemoptysis. *Mod. Diagnosis Treat.*

Zhijie, Z. (2018). Clinical efficacy analysis of Qinghao Biejia decoction in the treatment of fever in patients with drug-resistant pulmonary tuberculosis. *Heilongjiang J. Traditional Chin. Med.* 47, 38–39.

Zhongming, L. (2013). Discussion on the efficacy of the Chinese patent medicine tuberculosis spirit tablets as an adjunctive therapy for initial treatment of sputum-positive pulmonary tuberculosis. *Pract. Clin. Med.* 14.

Frontiers in Pharmacology

Explores the interactions between chemicals and living beings

The most cited journal in its field, which advances access to pharmacological discoveries to prevent and treat human disease.

Discover the latest Research Topics

See more →



Frontiers

Avenue du Tribunal-Fédéral 34
1005 Lausanne, Switzerland
frontiersin.org

Contact us

+41 (0)21 510 17 00
frontiersin.org/about/contact